The interactions of apolipoprotein E and inflammation in human iPSC-derived astrocytes



Trinity College Dublin

The University of Dublin

Thesis submitted for the degree of

Ph.D. in Physiology

Sarah Frances McComish

2021

Supervised by Prof Maeve Caldwell

Department of Physiology, School of Medicine, TBSI

and

Trinity College Institute of Neuroscience, Lloyd Institute

Trinity College Dublin, Ireland

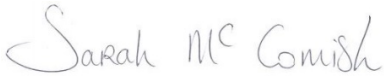
Declaration and Statement of Plagiarism

I declare that this thesis has not been submitted as an exercise for a degree at this or any other university and it is entirely my own work.

I agree to deposit this thesis in the University's open access institutional repository or allow the Library to do so on my behalf, subject to Irish Copyright Legislation and Trinity College Library conditions of use and acknowledgement.

I consent to the examiner retaining a copy of the thesis beyond the examining period, should they so wish (EU GDPR May 2018).

I have read and I understand the plagiarism provisions in the General Regulations of the University Calendar for the current year, found at: http://www.tcd.ie/calendar. I have also completed the Online Tutorial on avoiding plagiarism 'Ready, Steady, Write', located at http://tcd-ie.libguides.com/plagiarism/ready-steady-write

Signed: 

Date: 30.04.2020

This thesis is dedicated to my grandparents,

Bernadette and Patrick McComish,

And Paddy and Rosaleen O'Leary

Acknowledgements

First and foremost, I would like to express my sincere gratitude to my amazingly talented and supportive research supervisor Prof Maeve Caldwell. This thesis would not exist without the guidance and encouragement you have provided during my PhD. Thank you for choosing me to be your PhD student four years ago, I absolutely love being part of the Caldwell lab and am excited to get started on the next project!

I offer my sincere appreciation to Dr Jon Lane for welcoming me into his lab in order to train in iPSC culture, and to Dr Lucy Crompton and Dr Petros Stathakos for providing this training and their continued support since.

Thank you to the staff of the Department of Physiology and TCIN for helping me daily in many different ways, in particular I would like to thank Dr Noreen Boyle for providing indispensable advice and support with various practical aspects of my project.

To all undergrad and postgrad students, and summer interns of the Caldwell lab (Alanna, Alicia, Ibel, Lisa, Sadbh, Carmelia, Sarah, Laura, Cliona, Eva, Cian, Rebecca, Rachel, Conor, Adina, Aine and Aoife), thank you for the hard-work and dedication you put into your research and for helping to gather much of the data contained in this thesis.

I am especially grateful for all my amazing colleagues in TCIN and the Physiology department for making this PhD journey so enjoyable, it would not have been the same without you. And to my amazing office mates for making 3.09 the best office in the Lloyd. A special mention has to go to Kate, my partner in PhD crime and travel buddy. I couldn't have hoped for a better friend to share this experience with. Although our lab-based adventures have come to an end, the world awaits!!

To all my friends near and far, thank you for the coffee dates, dinners, nights out, video-calls, hikes and adventures, and for in general just being amazing friends. Thank you for revelling in the highs and helping me get through the lows these past 3.5 years.

Finally, I am extremely grateful to my mam Aileen, my dad Pat, and my brothers Craig, Keith and Conor for all their love and unwavering support they provided throughout my PhD journey.

Table of Contents

Declaration and Statement of Plagiarism ii

Acknowledgements iv

Table of Contents v

List of Figures xiv

List of Tables xix

List of Abbreviations xxi

Abstract xxvi

Lay Abstract xxviii

1. Main Introduction 2

1.1 Alzheimer's disease 2

1.1.1 Current therapies fail to manage disease progression 3

1.1.2 Amyloid-beta and amyloid pathology 4

1.1.3 Tau and tau pathology 5

1.1.4 Vascular impairment in Alzheimer's disease 6

1.1.5 Neuroinflammation in Alzheimer's disease 6

1.1.6 Alzheimer's disease genes 7

1.2 Apolipoprotein E 9

1.2.1 Apolipoprotein E – a multifunctioning protein 9

1.2.2 APOE receptors (in the CNS) 12

1.2.3 APOE has far reaching functions in the CNS 14

1.2.4 The APOE4 genotype has a profound effect on CNS response to disease and injury 14

1.3 Astrocytes – the main homeostatic regulators of the CNS 18

1.3.1 Astrocyte function in the healthy CNS 19

1.4 The role of astrocytes in neurodegeneration 22

1.4.1 Parkinson's disease 23
1.4.2 Amyotrophic lateral sclerosis 24
1.4.3 Huntington's disease 24
1.5 Reactive astrocytes in Alzheimer's disease 26
1.5.1 Do reactive astrocytes suffer a loss of function or gain of toxic function? 26
1.5.2 Non-cell-autonomous mechanisms 28
1.6 Modelling Alzheimer's disease 30
1.6.1 Murine models of Alzheimer's disease 30
1.6.2 There is a need for better disease modelling with regards to Alzheimer's disease 32
1.7 Pluripotent stem cells 33
1.7.1 Induced pluripotent stem cells 33
1.7.2 Neural differentiation drives iPSC towards a neural fate 36
1.8 Overarching aims and hypotheses 51
1.8.1 Aims 51
1.8.2 Hypotheses 51
2. Methods 53
2.1 Cell culture 53
2.1.1 iPSC maintenance and passaging 54
2.2 NPC cell culture 55
2.2.1 Neural induction for the generation of cortical neural progenitor cells .. 55
2.2.2 Expansion of NPC and plating for terminal differentiation 55
2.3 Astrocyte cell culture 57
2.3.1 Expansion of APC and plating for terminal differentiation 57
2.3.2 Cryopreservation of cells 58
2.3.3 Quality Control 58
2.4 Molecular biology methods 60

2.4.1 Analysis of gene expression by quantitative polymerase chain reaction 60
2.5 Protein analysis 63
2.5.1 Analysis of cytokine secretion by enzyme-linked immunosorbent assay (ELISA) 63
2.5.2 Immunocytochemistry 64
2.5.3 Western blotting 65
2.6 Statistical analysis 68
3. Neuroinflammatory astrocytes generated from fibroblast-derived human induced pluripotent stem cells 70
3.1 Introduction 70
3.1.1 Concept of A1 and A2 reactive astrocyte phenotypes 70
3.1.2 Alternative methods of characterising reactive astrocytes 72
3.1.3 Modelling the role of reactive astrocytes *in vitro* using human induced pluripotent stem cells 75
3.1.4 Aims 76
3.2 Materials and Methods 77
3.2.1 Cell lines 77
3.2.2 Cell culture and neural patterning 77
3.2.3 Cortical neuralisation of human iPSC 77
3.2.4 Characterisation of iPSC-derived neurons 81
3.2.5 Astrocyte progenitor differentiation 81
3.2.6 Characterisation of iPSC-derived astrocytes 84
3.2.7 Cell treatment for generation of reactive astrocytes 85
3.2.8 Cell treatment to demonstrate neurodegeneration 86
3.2.9 Analysis of gene expression by quantitative polymerase chain reaction 86
3.2.10 Analysis of cytokine secretion by enzyme-linked immunosorbent assay 87
3.2.11 Immunocytochemistry 88
3.2.12 Statistical analysis 90

3.3 Results 91
3.3.1 iPSC-derived neurons are positive for classical neuronal markers 91
3.3.2 iPSC-derived astrocytes are positive for classic astrocyte markers 93
3.3.3 Maturation factors BMP4 and hLIF significantly affect IL6 secretion in stimulated iPSC-derived astrocytes 94
3.3.4 Maturation factors BMP4 and hLIF did not significantly affect expression of classical and reactive astrocyte markers in stimulated iPSC-derived astrocytes. 95
3.3.5 iPSC-derived reactive astrocytes display morphological changes..... 98
3.3.6 iPSC-derived reactive astrocytes show increased expression IL6 and secretion of pro-inflammatory mediators 101
3.3.7 iPSC-derived reactive astrocytes show increased expression of genes associated with reactive astrogliosis 104
3.3.8 iPSC-derived reactive astrocyte conditioned media causes detrimental effects to iPSC-derived neurons..... 106
3.4 Discussion 108
3.4.1 iPSC-derived neurons and astrocytes are positive for classical markers 108
3.4.2 Withdrawal of maturation factors prior to stimulation ensures a mature quiescent-like astrocyte is achieved at baseline..... 109
3.4.3 Characterisation of astrocyte reactivity..... 110
3.4.4 iPSC-derived reactive astrocyte conditioned media compromises neuronal health 118
3.4.5 Concluding remarks 119
4. Delineation of the effect of apolipoprotein E genotype on astrocyte reactivity following an inflammatory insult..... 122
4.1 Introduction 122
4.1.1 APOE4 – evidence for a role in AD pathogenesis..... 122
4.1.2 Modelling genetic variants using human iPSC 127
4.1.3 Aims 128
4.2 Materials and Methods..... 129

4.2.1 Cell lines 129

4.2.2 Astrocyte progenitor cell culture and terminal differentiation 129

4.2.3 Astrocyte stimulation to examine reactivity in *E3E3* and *E4E4* astrocytes 129

4.2.4 Analysis of mRNA expression by qPCR 130

4.2.5 Analysis of cytokine secretion by ELISA 131

4.2.6 Immunocytochemistry 131

4.2.7 Analysis of GFAP protein expression by Western blotting 132

4.2.8 Statistical analysis 133

4.3 Results 134

4.3.1 iPSC-derived *E4E4* astrocytes are positive for classical astrocyte markers 134

4.3.2 iPSC-derived *E4E4* astrocytes are capable of responding to inflammatory insult and displaying a reactive phenotype 135

4.3.3 iPSC-derived *E4E4* reactive astrocytes do not display cytoskeletal alterations 138

4.3.4 *E4E4* astrocytes have greater base line secretion and expression of reactivity markers compared to *E3E3* astrocytes 140

4.3.5 *E4E4* iPSC-derived astrocytes show increased IL6 expression following inflammatory insult 143

4.3.6 *E4E4* iPSC-derived astrocytes show enhanced expression of some reactivity markers following inflammatory insult compared to *E3E3* iPSC-derived astrocytes 145

4.4 Discussion 149

4.4.1 *E4E4* astrocytes are capable of responding to inflammatory insult 149

4.4.2 *E4E4* astrocytes have a higher level of basal reactivity compared to *E3E3* astrocytes 151

4.4.3 *E4E4* astrocytes show an enhanced IL6 response to inflammatory insult 152

4.4.4 *E4E4* astrocytes show greater reactivity with regards to certain reactive astrocyte markers compared to *E3E3* astrocytes 153

4.4.5 Concluding remarks 154

5. Modulating astrocyte reactivity in a human iPSC-derived model of Alzheimer's disease 156

5.1 Introduction 156

5.1.1 Fibroblast growth factors constitute a large family of molecules..... 156

5.1.2 FGF genes and proteins are structurally comparable 157

5.1.3 FGF Receptors – There are four known FGF receptors 158

5.1.4 FGF plays numerous important roles in development..... 161

5.1.5 FGF and the CNS..... 161

5.1.6 Cannabidiol – a cannabinoid with the potential of modulating iPSC-derived astrocyte reactivity 165

5.1.7 Aims 169

5.2 Materials and Methods..... 170

5.2.1 Cell lines 170

5.2.2 Astrocyte progenitor cell culture and terminal differentiation 170

5.2.3 Astrocyte stimulation to examine the effect of FGF2 on astrocyte reactivity 170

5.2.4 Astrocyte stimulation to examine the effect of CBD on astrocyte reactivity 170

5.2.5 Analysis of astrocyte reactivity by qPCR 171

5.2.6 Analysis of astrocyte reactivity by ELISA 172

5.2.7 Statistical analysis 172

5.3 Results..... 173

5.3.1 FGF2 does not alter IL6 secretion and expression in *E3E3* astrocytes ... 173

5.3.2 FGF2 significantly attenuates the microglial factors induced expression of reactive astrocyte markers in *E3E3* astrocytes 175

5.3.3 FGF2 significantly attenuates the microglial factors induced expression of reactive astrocyte markers in *E4E4* astrocytes 178

5.3.4 CBD has varied effects on astrocyte basal reactivity 181

5.3.5 CBD tends to reduce astrocyte reactivity following inflammatory insult 183

5.4 Discussion 187

5.4.1 FGF2 holds promise as a modulator of astrocyte reactivity 187

5.4.2 The ability of CBD to modulate reactivity in astrocytes warrants further investigation 194

5.4.3 Concluding remarks 196

6. Glutamate dynamics in human iPSC-derived astrocytes is affected by APOE genotype 198

6.1 Introduction 198

6.1.1 Glutamate homeostasis – one of the key functions of astrocytes 198

6.1.2 Glutamate Transporters 200

6.1.3 Glutamate metabolism in astrocytes 203

6.1.4 Dysfunctional glutamate cycling and excitotoxicity in Alzheimer's disease 205

6.1.5 Role of APOE in astrocyte glutamate handling 206

6.1.6 Aims 207

6.2 Materials and Methods 208

6.2.1 Cell lines 208

6.2.2 Astrocyte progenitor cell culture and terminal differentiation 208

6.2.3 Astrocyte stimulation to examine the effect of astrocyte reactivity on glutamate dynamics 208

6.2.4 Astrocyte stimulation to examine the effect of FGF2 on glutamate transporter expression in iPSC-derived astrocytes 209

6.2.5 Analysis of glutamate transporter mRNA expression by qPCR 210

6.2.6 Analysis of glutamate transporter protein expression by Western blotting 210

6.2.7 Glutamate assay 211

6.2.8 Statistical analysis 213

6.3 Results 214

6.3.1 APOE3 and APOE4 homozygous astrocytes show differential expression of glutamate transporters, EAAT1 and EAAT2 214

6.3.2 Inflammatory insult affects glutamate transporter expression 217

6.3.3 FGF2 decreases glutamate transporter expression 221

6.3.4 APOE4 astrocytes show altered glutamate dynamics 227

6.3.5 Astrocyte reactivity state does not affect glutamate dynamics 230

6.3.6 *GLUL* expression in *E3E3* and *E4E4* astrocytes 235

6.4 Discussion 240

6.4.1 EAAT1 is more highly expressed than EAAT2 in human iPSC-derived astrocytes 240

6.4.2 APOE4 astrocytes have reduced glutamate transporter expression and altered glutamate dynamics 241

6.4.3 Reactive astrocytes display altered glutamate transporter expression which does not impact glutamate dynamics 246

6.4.4 FGF2 affects glutamate transporter expression 248

6.4.5 *GLUL* expression is increased in APOE4 and reactive astrocytes 249

6.4.6 Concluding remarks 251

7. Final discussion 253

7.1.1 Summary of findings 253

7.1.2 APOE4: Loss or Gain of Function? 254

7.1.3 Limitations 255

7.1.4 Data presented in this thesis may contribute to future therapeutic strategies259

7.1.5 Concluding remarks 260

8. Appendices 262
8.1 Appendix 1 – iPSC Characterisation 262
8.2 Appendix 2 – Materials 263
8.2.1 Molecular biology 263
8.2.2 Cell culture reagents 263
8.2.3 Primary and secondary antibodies for immunocytochemistry 264
8.2.4 Experimental treatments 264
8.2.5 Biological assays, chemicals and reagents 265
8.2.6 Laboratory equipment and consumables 265
8.3 Appendix 3 – Media Recipes 267
8.4 Appendix 4 – Solutions and Buffers 268
8.4.1 Solutions for general lab use 268
8.4.2 ELISA solutions 268
8.4.3 Western blotting buffers 268
8.4.4 Immunofluorescence buffers 271
8.5 Appendix 5 – Cell Counting 272
8.6 Appendix 6 – Three-way ANOVA with Bonferroni *post hoc* 273
8.7 Appendix 7 – Presentations and publications 282
8.7.1 Presentations 282
8.7.2 Publications 283
9. Bibliography 285

List of Figures

Figure 1.1.1. Aβ formation. 5
Figure 1.2.1. APOE3 and APOE4 protein structure. 10
Figure 1.4.1. Reactive astrocytes are involved in a range of pathologies. 22
Figure 2.2.1. NAS2 iPSC colonies ready for neural patterning. 55
Figure 2.4.1. Livak Method. 62
Figure 3.2.1. NAS2 iPSC colonies ready for neural patterning. 78
Figure 3.2.2. Original neuralisation timeline. 80
Figure 3.2.3. Optimised neuralisation timeline. 80
Figure 3.2.4. Differentiation timeline for generation of mature quiescent-like astrocytes. 83
Figure 3.2.5. Timeline for optimisation of astrocyte terminal differentiation protocol. . 84
Figure 3.2.6. Experimental timeline for generation of mature quiescent-like and reactive astrocytes. 85
Figure 3.2.7. Experimental timeline for characterisation of iPSC-derived neurons and effect of reactive astrocyte conditioned media on neurons. 86
Figure 3.2.8. Morphological analysis of iPSC-derived astrocytes. 89
Figure 3.2.9. Neuronal clusters may be characterised by size. 90
Figure 3.3.1. Neuralisation timeline and characterisation of iPSC-derived neurons. 91
Figure 3.3.2. iPSC-derived cortical neurons stain positive for classical neuronal and cortical markers. 92
Figure 3.3.3. iPSC-derived cortical astrocytes stain positive for classical astrocyte markers. 93
Figure 3.3.4. Maturation factors BMP4 and hLIF significantly affect IL6 secretion in stimulated iPSC-derived astrocytes. 96
Figure 3.3.5. Maturation factors BMP4 and hLIF do not affect mRNA expression in stimulated iPSC-derived astrocytes. 97
Figure 3.3.6. Stimulation with inflammatory microglial factors results in significant morphological changes in iPSC-derived cortical astrocytes. 99
Figure 3.3.7. Stimulation with inflammatory microglial factors does not affect GFAP fluorescence in iPSC-derived cortical astrocytes. 100
Figure 3.3.8. Inflammatory microglial factors significantly increase IL6 mRNA expression and secretion in iPSC-derived cortical astrocytes. 102

Figure 3.3.9. Inflammatory microglial factors significantly increase secretion of RANTES and GM-CSF in iPSC-derived cortical astrocytes. 102
Figure 3.3.10. Inflammatory microglial factors significantly increase IL6 secretion and expression in iPSC-derived cortical astrocytes. 103
Figure 3.3.11. Inflammatory microglial factors significantly increase expression of reactive genes in iPSC-derived cortical astrocytes. 105
Figure 3.3.12. Stimulation with reactive astrocyte conditioned media results in smaller and significantly less clusters of iPSC-derived cortical neurons. 107
Figure 3.4.1. Schematic of results. 120
Figure 4.2.1. Experimental timeline to test the effect of microglial factors on astrocyte reactivity in E4E4 astrocytes. 130
Figure 4.3.1. E4E4 iPSC-derived cortical astrocytes are positive for classical astrocyte markers. 134
Figure 4.3.2. Reactive E4E4 astrocytes show increased IL6 mRNA expression and secretion. 136
Figure 4.3.3. E4E4 reactive astrocytes show increased mRNA expression of reactive astrocyte markers. 137
Figure 4.3.4. Reactivity state does not affect morphology in E4E4 iPSC-derived astrocytes. 138
Figure 4.3.5. Reactivity does not affect GFAP expression in E4E4 iPSC-derived astrocytes. 139
Figure 4.3.6. E4E4 iPSC-derived astrocytes show increased baseline IL6 secretion and expression. 141
Figure 4.3.7. E4E4 iPSC-derived astrocytes show increased baseline GFAP expression. 141
Figure 4.3.8. E4E4 iPSC-derived astrocytes show increased baseline expression of reactivity markers. 142
Figure 4.3.9. E4E4 iPSC-derived astrocytes show increased IL6 expression following inflammatory insult. 144
Figure 4.3.10. GFAP mRNA and protein expression does not differ between E4E4 and E3E3 iPSC-derived reactive astrocytes. 146
Figure 4.3.11. E4E4 iPSC-derived astrocytes show increased expression of CXCL10 and C3 compared to E3E3 iPSC-derived astrocytes in response to inflammatory insult. 147
Figure 4.3.12. E4E4 iPSC-derived astrocytes show decreased expression of IL1β, LCN2 and PTX compared to E3E3 iPSC-derived astrocytes in response to inflammatory insult. ... 148

Figure 5.1.1. Biosynthesis of CBD. 167
Figure 5.2.1. Experimental timeline to test the effect of immunomodulatory agents on astrocyte reactivity. 171
Figure 5.3.1. FGF2 does not significantly attenuate the microglial factors induced expression and secretion of IL6 in E3E3 astrocytes. 174
Figure 5.3.2. FGF2 significantly attenuates the microglial factors induced expression of reactive astrocyte markers in E3E3 astrocytes. 176
Figure 5.3.3. FGF2 does not affect mRNA expression of inflammatory astrocyte markers IL1β, PTX3 and VIM in E3E3 astrocytes. 177
Figure 5.3.4. FGF2 significantly increases IL6 and IL1β mRNA expression in E4E4 reactive astrocytes. 179
Figure 5.3.5. FGF2 significantly attenuates inflammatory microglial factor induced expression of reactivity markers CXCL10, C3, LCN2 and PTX3 in E4E4 astrocytes..... 180
Figure 5.3.6. Effect of CBD on baseline reactivity in iPSC-derived astrocytes. 182
Figure 5.3.7. CBD tends to decrease reactive markers IL6, CXCL10 and C3 in iPSC-derived reactive astrocytes. 184
Figure 5.3.8. CBD does not affect mRNA expression of reactive markers LCN2, ICAM1 and PTX3 in iPSC-derived reactive astrocytes. 185
Figure 5.3.9. CBD does not affect mRNA expression of reactive markers GFAP and IL1β in iPSC-derived reactive astrocytes. 186
Figure 6.1.1. Healthy and dysfunctional astrocytes in AD. 199
Figure 6.1.2. Glutamate uptake and metabolism by astrocytes. 204
Figure 6.1.3. Dysfunctional glutamate cycling in Alzheimer's disease results in excitotoxicity. 206
Figure 6.2.1. Experimental timeline to test the effect of astrocyte reactivity on glutamate transporter expression and glutamate dynamics. 209
Figure 6.2.2. Glutamate assay mechanism. 212
Figure 6.3.1. SLC1A3 expression is greater than SLC1A2 mRNA expression in E3E3 and E4E4 astrocytes. 215
Figure 6.3.2. E4E4 astrocytes have significantly reduced glutamate transporter mRNA expression but no change in EAAT1 protein expression. 216
Figure 6.3.3. Inflammatory microglial factors affect SLC1A3 and SLC1A2 mRNA expression in E3E3 and E4E4 astrocytes. 218

Figure 6.3.4. Inflammatory microglial factors do not affect SLC1A3 mRNA expression but significantly increase SLC1A2 mRNA expression in E3E3 and E4E4 astrocytes..... 219
Figure 6.3.5. EAAT1 protein expression in E3E3 and E4E4 astrocytes following inflammatory insult. 220
Figure 6.3.6. FGF2 significantly decreases SLC1A3 and SLC1A2 mRNA expression in E3E3 and E4E4 astrocytes..... 222
Figure 6.3.7. FGF2 significantly reduces the factor-induced up-regulation of SLC1A3 and SLC1A2. 223
Figure 6.3.8. APOE genotype, astrocyte reactivity state and FGF2 treatment affects SLC1A3 expression..... 225
Figure 6.3.9. FGF2 treatment does not alter SLC1A2 expression. 226
Figure 6.3.10. APOE genotype affects glutamate dynamics in iPSC-derived astrocytes.228
Figure 6.3.11. Reducing extracellular glutamate does not alter the genotype effect on glutamate dynamics..... 229
Figure 6.3.12. Inflammatory microglial factors do not affect glutamate dynamics in iPSC-derived astrocytes. 231
Figure 6.3.13. Glutamate dynamics which are altered in E4E4 astrocytes is independent of reactivity state..... 232
Figure 6.3.14. Reducing extracellular glutamate does not alter the effect of inflammatory microglial factors on glutamate dynamics in iPSC-derived astrocytes. 233
Figure 6.3.15. Reducing extracellular glutamate does not alter the APOE dependent effect on glutamate dynamics. 234
Figure 6.3.16. E4E4 astrocytes have significantly increased baseline GLUL mRNA expression compared to E3E3 astrocytes..... 236
Figure 6.3.17. Inflammatory microglial factors significantly increase GLUL mRNA expression in E3E3 and E4E4 astrocytes..... 237
Figure 6.3.18. FGF2 attenuates the effect of reactivity on GLUL expression in iPSC-derived astrocytes. 238
Figure 6.3.19. FGF2 tends to attenuate the factor induced increase in GLUL mRNA expression..... 239
Figure 7.1.1. Characterisation of isogenic iPSC-derived neural progenitors..... 257
Figure 8.1.1. Generation of iPSC from E4E4 homozygous dermal fibroblasts and subsequent characterisation. 262
Figure 8.1.2. Characterisation of E4E4 iPSC..... 262

Figure 8.5.1. Diagram of a haemocytometer glass slide used to count cells. 272

List of Tables

Table 1.2.1. APOE isoforms differ at amino acid residues 112 and 158. 10

Table 1.2.2. APOE isoform frequencies in the general and AD populations. 11

Table 1.2.3. The major APOE receptors and their binding characteristics. 13

Table 1.2.4. The role of APOE4 in AD pathology. 17

Table 1.7.1. Human PSC-derived regional-specific neurons. 44

Table 1.7.2. Human PSC-derived regional specific astrocytes. 50

Table 2.1.1. iPSC donor information. 54

Table 3.2.1. Neural differentiation timeline showing media supplements and passaging days. 79

Table 3.2.2. Target primers used for qPCR analysis of astrocyte gene expression profile. 87

Table 3.2.3. Primary antibodies. 88

Table 3.2.4. Secondary antibodies. 88

Table 4.1.1. AD frequency has a positive correlation with number of APOE4 genes. 123

Table 4.2.1. Target genes used for qPCR analysis of E4E4 astrocyte reactivity profile. 131

Table 4.2.2. Primary antibodies. 131

Table 4.2.3. Secondary antibodies. 132

Table 4.2.4. Antibodies used for Western blotting analysis of GFAP expression. 132

Table 5.1.1. FGF chromosomal localisation in humans. 157

Table 5.1.2. Binding of the various members of the FGF family to the four FGF receptors. 160

Table 5.2.1. Target genes used for qPCR analysis of E4E4 astrocyte reactivity profile. 172

Table 6.1.1. Comparison of excitatory amino acid transporters 1 and 2. 201

Table 6.2.1. Target genes used for qPCR analysis of glutamate transporter and glutamine synthetase expression. 210

Table 6.2.2. Antibodies used for Western blotting analysis of EAAT1 expression. 210

Table 8.6.1. Three-way ANOVA analysis of SLC1A3 mRNA expression. 273

Table 8.6.2. Bonferroni post hoc of SLC1A3 mRNA expression. 275

Table 8.6.3. Three-way ANOVA analysis of SLC1A2 mRNA expression. 276

Table 8.6.4. Bonferroni post hoc of SLC1A2 mRNA expression. 278

Table 8.6.5. Three-way ANOVA analysis of GLUL mRNA expression. 279

Table 8.6.6. Bonferroni post hoc of GLUL mRNA expression. 281

List of Abbreviations

AA	Arachidonic acid
AA	Ascorbic acid
ABCA1	ATP-binding cassette A1
ACh	Acetylcholine
ACM	Astrocyte conditioned media
AD	Alzheimer's disease
ALDH1L1	Aldehyde dehydrogenase 1 family member L1
ALS	Amyotrophic lateral sclerosis
AMPA	α-amino 3-hydroxy-5-methyl-4-isoxazolepropionic acid
ANOVA	Analysis of variance
APC	Astrocyte progenitor cells
APOE	Apolipoprotein E
APOER2	APOE receptor 2
APP	Amyloid precursor protein
APS	Ammonium persulfate
AQP4	Aquaporin 4
Arg	Arginine
ATP	Adenosine triphosphate
Aβ	Amyloid-β
BBB	Blood-brain barrier
BCA	Bicinchoninic acid
BDNF	Brain-derived neurotrophic factor
BFCN	Basal forebrain cholinergic neurons
BMP	Bone morphogenic protein
BSA	Bovine serum albumin
C1q	Complement component 1 subcomponent q
C3aR	C3 receptor
CAA	Cerebral amyloid angiopathy
CaMKII	Calmodulin-dependent protein kinase II
Cas9	CRISPR-associated 9
CB1	Cannabinoid receptor 1
CB2	Cannabinoid receptor 2
CBD	Cannabidiol
CCL2	Chemokine C-C motif ligand 5
CCL5	Chemokine C-C motif ligand 5
CD4/8	Cluster of differentiation 4/8
cDNA	Complementary DNA
ChAT	Choline acetyltransferase

CLAC-P/collagen XXV	Collagen-like Alzheimer amyloid plaque component precursor/collagen type XXV
CNTF	Ciliary neurotrophic factor
CoA	Coenzyme A
Cpd E	Compound E
CRISPR	Clustered regularly-interspaced short palindromic repeat
CSF	Cerebrospinal fluid
Ct	Cycle threshold
CT1	Creatine transporter
CTCF	Corrected total cell fluorescence
Cx43	Connexin-43
CXCL2	Chemokine (C-X-C motif) ligand 2
CXCR3	Chemokine receptor 3
Cys	Cysteine
db-cAMP	Dibutyryl cyclic-AMP
DMSO	Dimethyl sulfoxide
DR	Diabetic retinopathy
E8	Essential 8^{TM} flex media
EAAT1	Excitatory amino acid transporter 1
EAAT2	Excitatory amino acid transporter 2
EB	Embryoid body
EDTA	Ethylenediaminetetraacetic acid
EGF	Epidermal growth factor
ELISA	Enzyme-linked immunosorbent assay
ERK	Extracellular signal-regulated kinase
ESC	Embryonic stem cells
FACS	Fluorescence-activated cell sorting
FDA	Food and Drug Administration
FGF	Fibroblast growth factor
FGFR	FGF receptor
GABA	γ-aminobutyric acid
GDNF	Glial cell-derived neurotrophic factor
GFAP	Glial fibrillary acidic protein
GLT1	Glutamate transporter 1
GM-CSF	Granulocyte-macrophage colony-stimulating factor
GPCR	G-protein coupled receptors
GPR55	G-protein coupled receptor 55
GS	Glutamine synthetase
HD	Huntington’s disease
hLIF	Human leukemia inhibitory factor

HSPG	Heparan sulfate proteoglycans
HTT	Huntingtin
ICAM1	Intercellular adhesion melcule-1
ICC	Immunocytochemistry
IFNγ	Interferon gamma
Ig	Immunoglobulin
IGF	Insulin-like growth factor
IL	Interleukin
IL6R	Interleukin 6 receptor
iPSC	Induced pluripotent stem cells
ISL1	Insulin gene enhancer protein
JAK	Janus kinase
LCN2	Lipocalin-2
LCN2	Lipocalin-2
LDL	Low density lipoprotein
LDLR	LDL receptor
LIF	Leukemia inhibitory factor
LPS	Lipopolysaccharide
LRP1	LDLR-related protein 1
LTP	Long-term potentiation
MAP2	Microtubule-associated protein 2
MAPK	Mitogen-activated protein kinase
MB	Midbrain
MCAO	Middle cerebral artery occlusion
MEGF10	Multiple EGF-like-domains 10
MERTK	C-mer proto-oncogene tyrosine kinase
mHTT	Mutant HTT
MN	Motoneuron
MNP	Motor neuron progenitor cells
mRNA	Messenger RNA
MS	Multiple Sclerosis
nAChR	Nicotinic acetylcholine receptors
NAS2	Non-affected sibling 2
NEAA	Non-essential amino acids
NFT	Neurofibrillary tangles
NGF	Nerve growth factor
NGS	Normal goat serum
NLRP3	NOD-, LRR- and pyrin domain-containing protein 3
NMDA	N-methyl-D-aspartate
NMM	Neural maintenance media
NO	Nitric oxide

NPC	Neural progenitor cells
NT-3/4	Neurotrophin 3/4
PAMP	Pathogen-associated molecular pattern
PBS	Phosphate buffered saline
PD	Parkinson's disease
PDGF	Platelet-derived growth factor
Pen/strep	Penicillin-streptomycin
PFA	Paraformaldehyde
PKC	Protein kinase C
PO	Polyornithine
PS	Presenilin
PSC	Pluripotent stem cells
PTX3	Pentraxin-3
qPCR	Quantitative polymerase chain reaction
RA	Retinoic acid
RAGE	Receptor for advanced glycation end-products
RANTES	Regulated upon activation, normal T cell expressed and presumably secreted
RGC	Retinal ganglion cells
ROS	Reactive oxygen species
RQ	Relative quantity
RT	Room temperature
SDS	Sodium dodecyl sulfate
SEM	Standard error of the mean
SerioEL	Serio culture medium supplemented with EGF and hLIF
SERPINA3	Serpin peptidase inhibitor clade A member-3
SGZ	Sub-granular zone
SHH	Sonic hedgehog
sIL6R	Soluble IL6 receptor
SNARE	Soluble NSF attachment protein receptor
SOD1	Superoxide dismutase
STAT	Signal transducer and activator of transcription
Strep-HRP	Streptavidin conjugated to horseradish peroxidase
SVZ	Sub-ventricular zone
TCA	Tricarboxylic acid
TGFβ	Transforming growth factor beta
Th	T-helper
TH	Tyrosine hydroxylase
THC	Tetrahydrocannabinol
TLR	Toll-like receptor
TMB	Tetramethylbenzidine
TNFα	Tumor necrosis factor alpha

TuJ1	Neuron-specific Class III β-tubulin
VAChT	Vesicular acetylcholine transporter
VLDL	Very low density lipoprotein
VLDLR	VLDL receptor
VR1/2	Vanilloid receptor 1/2
VTN	Vitronectin
ZFN	Zinc Finger Nuclease

Abstract

Alzheimer's disease (AD) is a devastating neurodegenerative disease characterised histologically by the presence of extracellular plaques and intracellular neurofibrillary tangles, and clinically by memory loss, cognitive decline and personality changes. Much of the research investigating AD to date has focused on the familial early-onset form of AD which accounts for <5% of cases. Most cases are sporadic with late-onset, with certain genes presenting a high risk. Apolipoprotein E (APOE) genotype is one of the major genetic risk factors for late-onset AD. There are three major APOE isoforms (*APOE2*, *APOE3* and *APOE4*), each differing by a single amino acid residue at the protein level and thus inferring different AD-risk. APOE2 contains cysteine at amino acid residues 112 and 158, APOE3 contains a cysteine at residue 112 and arginine at residue 158, while APOE4 contains arginine at both residue sites. APOE3 is most common in the general population and APOE4 associated with an increased AD risk. Emerging evidence supports a detrimental role of astrocytes in AD, with astrocytes developing a reactive phenotype upon exposure to inflammatory microglial factors. Furthermore, excitotoxicity has been well characterised in AD as a mechanism for neuronal death which may occur as a result of altered astrocyte function following activation. With this in mind, our study aimed to investigate the impact of *APOE* genotype on astrocyte reactivity and functionality using human induced pluripotent stem cell (iPSC)-derived astrocytes with homozygous *APOE3* and *APOE4* genotypes. Human iPSC homozygous for *APOE3* and *APOE4* were patterned towards a neural fate using dual SMAD inhibition to produce neural progenitor cells. Subsequently, astrocytes were derived using epidermal growth factor and human leukemia inhibitory factor to produce mature astrocytes after 90 days. Astrocytes were characterised by immunostaining for classic markers, then stimulated (IL1α, TNFα and C1q) to induce reactivity and a reactivity profile was generated via morphological, ELISA and qPCR analysis. The functional capacity of astrocytes was investigated via glutamate assay. iPSC-derived astrocytes are positive for astrocyte markers GFAP, S100β, Connexin-43 and EAAT1 confirming cell fate. Stimulation with microglial factors resulted in increased IL6, RANTES and GM-CSF secretion, coupled with increased expression of genes associated with reactivity including *IL6*, *ICAM1*, *LCN2* and *SERPINA3. APOE* genotype affected basal expression and secretion of IL6 as well as *IL1B*. Fibroblast growth factor 2 (FGF2) was capable of modulating some aspects of astrocyte reactivity while cannabidiol (CBD) did not. Glutamate dynamics were unaffected by stimulation, however *APOE4* astrocytes have altered glutamate flux relative to *APOE3* control. In conclusion, the ability

to produce reactive astrocytes derived from genotyped human cells *in vitro* provides a powerful model for researching the mechanisms underlying the detrimental role of astrocytes and the effect of *APOE* genotype in AD. *APOE* genotype appears to influence astrocyte reactivity and *APOE4* is strikingly detrimental to glutamate handling. While CBD did not successfully modulate astrocyte reactivity, FGF2 had some success modulating reactivity. This study presents the potential mechanisms which predispose *APOE4* carriers to AD and presents some therapeutic targets in order to manage AD risk.

Lay Abstract

Astrocytes are star-shaped brain cells that support and protect nerve cells. They do this by providing nutrients, maintaining water balance and preventing build-up of exciting signals. Astrocytes have recently gained much interest in the field of neurodegenerative disease research. It is now known that these cells play a role in inflammation in the brain. This increases nerve cell damage in diseases such as Alzheimer's disease. Astrocytes change in response to brain injury and disease, they lose their protective functions and gain harmful functions which causes nerve cell damage and death. We aimed to investigate why people with the *APOE4* gene in their DNA are at high risk for developing Alzheimer's disease.

Using stem cell technology which converts skin cells into astrocytes and other brain cells we made a "disease-in-a-dish" model of Alzheimer's disease. Astrocytes with the *APOE4* gene produced high levels of inflammatory indicators following inflammation. Astrocytes with the *APOE4* gene also lose their ability to prevent build-up of exciting signals. In the brain, these toxic functions would cause nerve cell damage. This might explain the risk for developing Alzheimer's disease linked to the *APOE4* gene.

This study shows that *APOE4* and astrocyte inflammation could be targeted with drugs to help treat Alzheimer's disease.

Chapter 1

Introduction

1. Main Introduction

1.1 Alzheimer's disease

Alzheimer's disease (AD) is a neurodegenerative disease characterised by the build-up of extracellular neuritic plaques formed from amyloid-β (Aβ) aggregates and intracellular neurofibrillary tangles (NFT) formed from hyperphosphorylated tau protein (Udan *et al.*, 2008). AD pathology results from a chronic imbalance in Aβ production and clearance leading to persistent increase in the levels of this protein (Reed-Geaghan *et al.*, 2009). At the phenotypic level, the disease presents as progressive loss of function in learning, memory and general cognition often accompanied later by altered thought, behaviour, and perception. This disease phenotype results from severe neuronal loss particularly from the hippocampus and basal forebrain. However, a precise diagnosis of the disease at the clinical stage can be illusive owing to the heterogeneity of symptoms and similarity of presentation to other dementias. It is classified into familial and sporadic forms associated with early (< 65 years) and late (> 65 years) onset respectively. Overall, around 95% of cases of AD are thought to be sporadic, with late-onset of disease (Barage & Sonawane, 2015).

AD was first discovered about 100 years ago but research into the disease origin and the biological changes which occur during pathogenesis only became recognised as an important area of research approximately 30 years ago. AD affects tens of millions globally and is expected to increase as the global population ages. It is the most common cause of dementia in elderly patients accounting for up to 70% of cases, and affects approximately 35.6 million people worldwide with this incidence projected to double every 20 years according to the World Health Organisation. An estimated 5.8 million people over the age of 65 in the US are currently affected by AD with numbers expected to rise to 13.8 million by 2050 in the US alone and up to 100 million worldwide (2020 Alzheimer's disease facts and figures, ALZHEIMER'S ASSOCIATION REPORT, (2020; Abdullah *et al.*, 2020)). Although much has been learned in the last 10 years, disease ethiology, why the disease progresses differently in some individuals and the exact manner in which to prevent, slow or stop disease progression is still unknown. Therefore, continued research into the underlying molecular mechanisms is of huge importance in order to identify novel therapeutic targets (2015 Alzheimer's disease facts and figures, Alzheimer's Association Report (Association, 2015)).

1.1.1 Current therapies fail to manage disease progression

Although much research has been dedicated to developing new therapeutics, AD patients do not have many therapeutic options; only five pharmacological agents have received approval for clinical treatment of AD by the Food and Drug Administration, these include the acetylcholinesterase inhibitors tacrine, donepezil, galantamine, rivastigmine, and the N-methyl-D-aspartate (NMDA) receptor antagonist memantine (Batarseh *et al.*, 2016). Loss of cholinergic tone following death of basal forebrain cholinergic neurons is a characteristic of early AD pathology, therefore acetylcholinesterase inhibitor classed drugs have been applied in order to increase acetylcholine levels at cholinergic synapses. Another feature of AD pathology is neuronal excitotoxicity due to high levels of excitatory neurotransmitter glutamate at glutamatergic synapses which results in death of the postsynaptic neuron. NMDA receptor antagonist class drugs such as memantine may help prevent excitotoxicity by blocking glutamate receptors on the postsynaptic neurons.

Solanezumab was a monoclonal antibody designed to increase the clearance of soluble Aβ peptides from the brain (Honig *et al.*, 2018). In preclinical research solanezumab reversed memory deficits in transgenic mice expressing amyloid precursor protein (APP). However, in clinical trials the drug did not significantly affect cognitive decline in patients with mild AD (Honig *et al.*, 2018). This emphasises the limitations of using animal models to study human biology. Similarly nilvadipine, a dihydropyridine calcium-channel blocker already licensed for the treatment of hypertension, showed promise in preclinical studies with reduced amyloid production, increased regional cerebral blood flow, and anti-inflammatory and anti-tau activity. However, results from the Phase III clinical trials in mild-to-moderate AD patients did not suggest benefit of nilvadipine as a treatment for AD (Lawlor *et al.*, 2018).

These pharmacological therapeutics only relieve symptoms without targeting the underlying pathology of AD. Moreover, the effectiveness of these agents varies among AD patients as evidenced by a moderate efficiency in no more than 20% of patients, and tolerance, non-compliance or side-effects in more than 60% of treated patients (Yang *et al.*, 2016b). The reason for this is potentially due to the fact that disease pathology begins decades prior to development of clinical symptoms, at which stage a significant amount of damage has already occurred and there is little to be done by way of therapeutic strategy. Given that AD pathology takes hold 10-15 years before development of clinical symptoms a means of early detection or determining those who are at risk of developing AD is hugely important for combating this disease.

1.1.2 Amyloid-beta and amyloid pathology

The predominant theory of AD pathogenesis is that of the Aβ cascade. To begin with, this consists of disturbed Aβ production followed by altered CNS Aβ uptake and clearance from the extracellular space, leading to Aβ peptide deposition and plaque formation (Barage & Sonawane, 2015). Extracellular Aβ plaques are the most recognised lesion of AD (Karran & De Strooper, 2016).

Aβ is a 40-42 amino acid protein residue derived from proteolysis of transmembrane APP by β-secretase to form sAPP-β and APP CTF99 which is subsequently cleaved by γ-secretase to form Aβ (Figure 1.1.1). Aβ monomers are non-toxic, however in AD when Aβ is produced at a rate greater than it can be cleared, these "sticky" monomers aggregate to form dimers, polymers, fibrils and finally the characteristic plaques seen in the brains of AD patients which are toxic to neurons (Udan *et al.*, 2008). Plaque formation is associated with direct synaptic toxicity, neuronal degeneration, microglial and astrocytic activation and general inflammation (Barage and Sonawane, 2015). Neurons are the main generators of Aβ but are also the most vulnerable to the toxicity of Aβ accumulation (Zhang *et al.*, 2016c). Aβ accumulation results in a multitude of pathological features in neurons including degradation of synapses, altered synaptic transmission and circuit activity and ultimately cell death (Palop & Mucke, 2010; De Strooper & Karran, 2016). Plaque formation begins in the hippocampus, an area of the brain associated with learning and memory, and so memory deficits correlate to the synaptic loss that occurs with plaque build-up (Jana *et al.*, 2008).

Owing to its role in APP processing, β-secretase has emerged as an attractive therapeutic target for the treatment of AD. However, β-secretase also cleaves non-amyloid substrates with important physiological functions, for example neuregulin is a BACE1 substrate involved in myelination of neuronal axons (Ben Halima *et al.*, 2016). As a result, widespread generalised inhibition of β-secretase is not a feasible therapeutic strategy. Research is now focusing on selective inhibition of β-secretase as an alternative approach (Ben Halima *et al.*, 2016).

Concerning NFTs, there is conflicting evidence about whether Aβ causes tau phosphorylation, or if they share a common upstream instigator (Wang *et al.*, 2018).

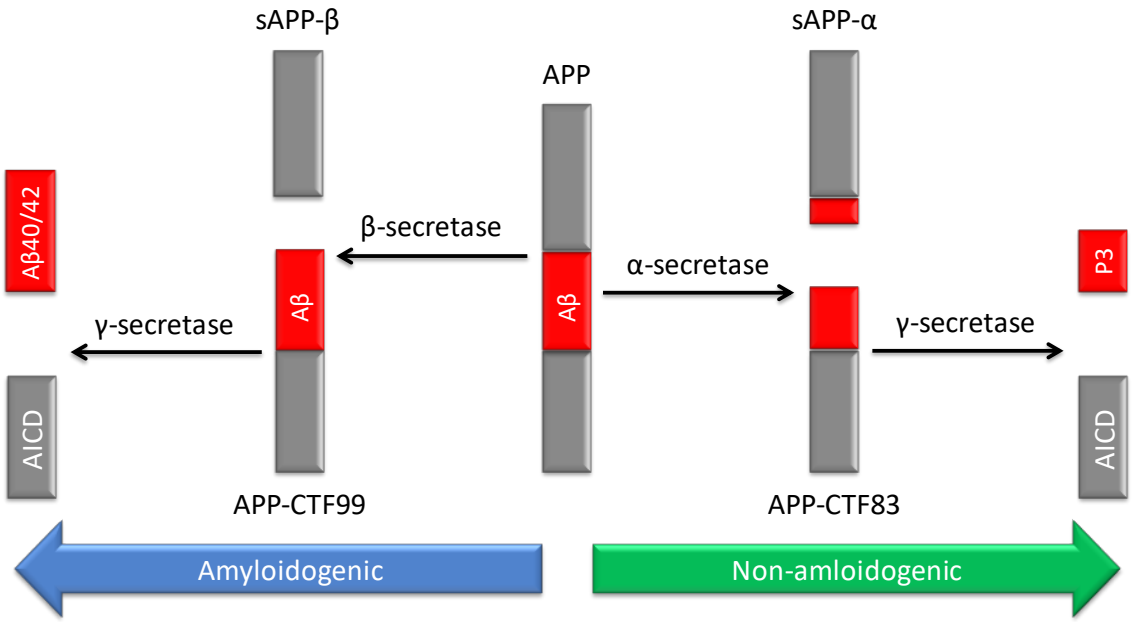


Figure 1.1.1. Aβ formation.

Proteolysis of APP by α-secretase forms sAPP-α and APP-CTF83, when subsequently cleaved by γ-secretase P3 and amyloid precursor protein intracellular domain (AICD) are formed which do not result in Aβ pathology. Proteolysis of APP by β-secretase forms sAPP-β and APP-CTF99, when subsequently cleaved by γ-secretase $Aβ_{40/42}$ and AICD are formed which results in Aβ pathology due to aggregation of the "sticky" Aβ peptides.

1.1.3 Tau and tau pathology

Another pathological feature of AD is intracellular NFT of hyperphosphorylated tau. Tau is a microtubule-associated protein that is abundant in axons (Essayan-Perez *et al.*, 2019). Tau is a phosphoprotein with 80 serine/threonine and 5 tyrosine phosphorylation sites. Under normal conditions, tau contains 2-3 moles of phosphate per mole of protein (Wang *et al.*, 2013). However, in AD tau is abnormally phosphorylated. In this hyperphosphorylated state, tau aggregates to form NFT.

In AD, hyperphosphorylated tau loses its ability to bind to microtubules and is mislocalised to the neuronal soma (Wang *et al.*, 2018). Aβ has been shown to up-regulate tau in mixed neuron and astrocyte cultures, and subsequently induced caspase-3-mediated cleavage of tau to a truncated form which rapidly aggregates (Garwood *et al.*, 2011). There is conflicting evidence pertaining to the Aβ and NFT timeline, where some studies indicate that Aβ pathology may subsequently drive tau pathology while other studies show that both pathologies run alongside each other.

1.1.4 Vascular impairment in Alzheimer's disease

Vascular impairment of the blood-brain barrier (BBB) has been widely reported in AD pathology as more than 80% of AD patients have mild cerebral amyloid angiopathy in which Aβ is deposited in the capillary walls leading to their degradation and subsequent BBB deterioration (Jellinger, 2002). This degradation results in decreased cerebral blood flow and inflammatory stimulation which is suggested to promote Aβ aggregation and neuronal death (Rius-Perez *et al.*, 2018). Thus, vascular dysfunction appears to exacerbate AD pathogenesis.

1.1.5 Neuroinflammation in Alzheimer's disease

In the last two decades, the role of neuroinflammation and its contribution to AD pathology has received much attention. There is still ongoing debate as to whether neuroinflammation is a causative factor or consequence of AD, in any case the current understanding of AD places the inflammatory component at the centre of the pathology (Zhang *et al.*, 2013; Barage & Sonawane, 2015). Consequently, more studies are investigating glial cell involvement in AD. Neuroinflammation in AD is typified by widespread activation of microglia and astrocytes which can modulate the development and/or progression of the disease (Garwood *et al.,* 2011). The severity of the activation of these glial cells correlates with the extent of brain atrophy and cognitive decline in AD (Garwood *et al.,* 2011).

There is evidence that astrocytic uptake of Aβ is impaired by exposure to inflammatory conditions (Liu *et al.*, 2016). This may represent a positive feedback loop which underlies chronic inflammation in AD. Another potential feedback loop is represented by the effects of CNS inflammation in the processing of APP, wherein inflammation causes an increase in APP and $A\beta_{42}$ production, prolonging the Aβ cascade (Sheng *et al.*, 2003).

Furthermore, Aβ itself may be considered a pro-inflammatory stimulus. Proof of this lies in the documented cases where an up-regulation of inflammatory markers, such as activated microglia and inflammatory cytokines, was recorded in the immediate areas surrounding Aβ plaques in the brains of AD patients (Udan *et al.*, 2008). Microglia are the resident immune cells of the CNS. Like macrophages of the periphery, microglia continuously survey the environment and become active upon detection of pathogens, tissue injury or Aβ as is the case in AD. Inflammation is a direct result of Aβ-mediated microglial activation (Costello *et al.*, 2015) and the resulting inflammatory environment

may be causative of the cognitive and behavioural deficits seen in AD patients. Several reports indicate that Aβ peptides are capable of binding to several cell surface receptors including the receptor for advanced glycation end-products (RAGE), the NMDA receptor, the P75 neurotrophin receptor, the collagen-like Alzheimer amyloid plaque component precursor/collagen type XXV (CLAC-P/collagen XXV), and the scavenger type A receptor (Jana *et al.*, 2008). Numerous other studies have reported a link between Aβ in AD and the toll-like receptor (TLR) family of receptors (Fassbender *et al.*, 2004; Liu *et al.*, 2005; Walter *et al.*, 2007; Jana *et al.*, 2008; Richard *et al.*, 2008; Udan *et al.*, 2008). Aβ acts as a pathogen-associated molecular pattern (PAMP)-like infectious agent causing TLR activation and pro-inflammatory cascade. Microglia have been shown to become active, proliferate and assemble at the sites of Aβ plaque build-up where they proceed to induce an inflammatory environment resulting in neuronal damage (Reed-Geaghan *et al.*, 2009; Liu *et al.*, 2012). Astrocytes have also been shown to become phagocytic and actively clear Aβ (Byun & Chung, 2018).

1.1.6 Alzheimer's disease genes

Numerous genes provide a strong genetic risk factor for developing AD. Genome wide association studies have associated *APP*, and the presenilins *PSEN1* and *PSEN2* with familial AD, and genes such as apolipoprotein E (*APOE*) have been linked to late-onset sporadic AD (Bertram *et al.*, 2008; Beecham *et al.*, 2014; Chung *et al.*, 2018).

1.1.6.1 The genetics of familial Alzheimer's disease

Most cases of AD are sporadic; however there are also familial forms which are genetic in origin. The genetic causes which have been implicated include mutations or variants in the *APP*, *PSEN1* and *PSEN2* genes (Duff, 2002). Historically, research focused on these autosomal dominant mutations since they occur in genes that affect Aβ plaque formation (Karran & De Strooper, 2016). PSEN1 and PSEN2 proteins influence multiple molecular pathways which play a role in the γ-secretase cleavage of type I transmembrane proteins including APP (Elder *et al.*, 2010). Most AD transgenic mouse models overexpress *APP* transgenes containing familial AD-associated mutations (Elder *et al.*, 2010; Fernandez *et al.*, 2019).

While early-onset familial AD has been the predominant focus of AD research to date it accounts for less than 5% of patients, with over 95% of AD patients presenting with the late-onset sporadic form of AD.

1.1.6.2 The genetics of sporadic Alzheimer's disease

APOE is a protein coding gene associated with late-onset sporadic AD. The *APOE* gene is located on chromosome 19, within an area of the genome that has already been strongly linked to familial AD (Poirier et al., 1993). It is highly expressed in the CNS, primarily by astrocytes (Holtzman *et al.*, 2012). The *APOE* gene has three isoforms, *APOE2*, *APOE3* and *APOE4*, each of which have different effects on the likelihood of developing AD later in life (Huang *et al.*, 2017). *APOE3* is the common isoform and is most prevalent in the population. The *APOE4* allele presents a risk factor for late-onset AD. Heterozygotes with one *APOE4* allele have a 3.7 times greater risk of developing AD compared to *APOE3* homozygotes, this risk increases to 12 times in *APOE4* homozygous individuals (Verghese *et al.*, 2013). *APOE2* is thought to lower the chance of developing AD (Huang *et al.*, 2017). While the APOE4 variant presents the greatest genetic risk factor for late-onset AD, many other genes have been identified through genome-wide association studies. Examples of such late-onset AD risk genes include *TREM2* (Guerreiro *et al.*, 2013; Jonsson *et al.*, 2013), *CR1* (Brouwers *et al.*, 2012), *CD33* (Hollingworth *et al.*, 2011; Naj *et al.*, 2011; Tai *et al.*, 2015), and *CLU* (Bagyinszky *et al.*, 2014). A recent genetic meta-analysis confirmed 20 previously identified risk loci, while also identifying five new genome-wide loci (*IQCK*, *ACE*, *ADAM10*, *ADAMTS1*, and *WWOX*). Pathway analysis implicated immunity, lipid metabolism, tau binding proteins, and APP metabolism (Kunkle *et al.*, 2019a). This new association data shows that genetic variants affecting APP and Aβ processing are not only associated with early-onset familial AD but also with sporadic AD.

1.2 Apolipoprotein E

1.2.1 Apolipoprotein E – a multifunctioning protein

APOE is one of the major human apolipoproteins, an abundant plasma protein that plays a major role in cholesterol transport. It interacts with low density lipoprotein (LDL) receptors and other proteins, participating in the transport of cholesterol and lipids (Mahley, 1988; Dorey *et al.*, 2014). This multifunctional protein also plays a role in BBB integrity, synaptic plasticity and cell signalling. In the CNS, APOE was previously believed to be expressed and secreted mainly by astrocytes (Zhang *et al.*, 2014; Zhang *et al.*, 2016c). Recent transcriptome analysis has indicated that APOE is also expressed by microglia and even in neurons under stress conditions (Lin *et al.*, 2018; Belloy *et al.*, 2019; Mathys *et al.*, 2019). APOE is a polymorphic protein with three common isoforms: *APOE2*, *APOE3* and *APOE4*. *APOE4* is the single greatest genetic risk factor for sporadic AD, with 65% of AD patients carrying a copy (Crompton *et al.*, 2017). Although it is a well-established risk factor, it remains understudied and the contribution of *APOE4* astrocytes to the development of AD needs to be elucidated.

1.2.1.1 APOE isoforms

The human APOE gene has five transcript variants resulting from different splicing and/or promotor usages. The three main human APOE isoforms are *APOE2*, *APOE3* and *APOE4* (Nickerson *et al.*, 2000; Crompton *et al.*, 2017). The resultant proteins differ by a single amino acid at residues 112 and 158 (Figure 1.2.1, Table 1.2.1). APOE2 has cysteine (Cys) residues at both positions, APOE3 has a Cys residue at 112 and an arginine (Arg) residue at 158, and APOE4 has Arg residues present at both positions (Weisgraber *et al.*, 1981; Wang *et al.*, 2018).

APOE3 is the most common variant, carried by 78% of the population (Table 1.2.2), and can thus be considered the normal “healthy” isoform (Belloy *et al.*, 2019). *APOE4* is less prevalent in the general population (14%) but those homozygous for *APOE4* are 14 times more likely to develop AD than an *APOE3* carrier (Crompton *et al.*, 2017; Belloy *et al.*, 2019). While isoform differences are subtle they have a profound effect on the risk of developing AD. This risk has been linked to their differential ability to stimulate neuronal Aβ production. APOE binding to APOE receptors activates dual leucine-zipper kinase thereby initiating a non-canonical mitogen-activated protein kinase (MAPK) pathway

leading to enhanced APP transcription and subsequently increased Aβ production. APOE4 is the most potent activator of this mechanism, while APOE2 is the least (Huang *et al.*, 2017).

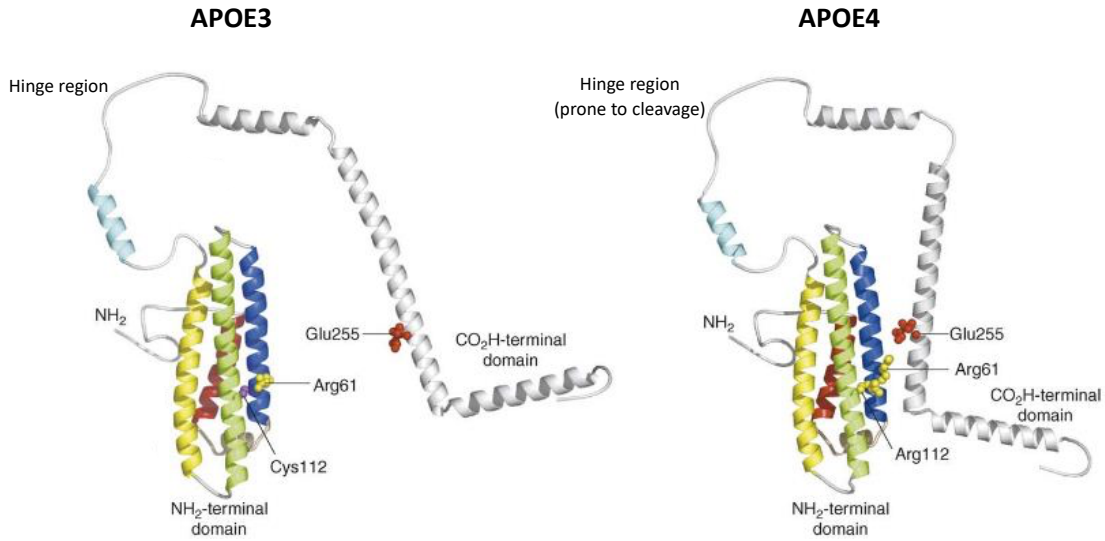


Figure 1.2.1. APOE3 and APOE4 protein structure.

The APOE protein consists of two separately folded domains, the N-terminal contains a receptor binding domain, the C-terminal contains the main lipid binding domain and a "hinge" region connects the two domains. In the APOE4 protein, the Arg residue at 112 interacts with the glutamic acid residue at 255 resulting in a conformational change. The APOE4 conformation leaves the hinge region prone to cleavage thereby compromising lipid binding capacity. Modified from Liu et al., 2013.

	Amino acids present at residues	
	112	**158**
APOE2	Cysteine	Cysteine
APOE3	Cysteine	Arginine
APOE4	Arginine	Arginine

Table 1.2.1. APOE isoforms differ at amino acid residues 112 and 158.

The three major APOE isoforms generate proteins which differ from each other at amino acid residues 112 and 158. APOE2 has a cysteine at both sites, APOE3 has a cysteine at 112 and an arginine at 158, and APOE4 has an arginine at both sites. Adapted from Liu et al., 2013.

	Isoform frequency in general and AD population (%)	
	General	**AD**
APOE2	8.4	3.9
APOE3	77.9	59.4
APOE4	13.7	36.7

Table 1.2.2. APOE isoform frequencies in the general and AD populations.

APOE3 is the most common isoform within the general population. APOE4 is more prevalent in the AD population compared to the general population. Adapted from Liu et al., 2013.

1.2.1.2 APOE biological and biochemical features

APOE is a glycoprotein consisting of two separately folded domains, the N-terminal contains a receptor binding domain, the C-terminal contains the main lipid binding domain and a "hinge" region connects the two domains (Dorey *et al.*, 2014) (Figure 1.2.1).

APOE is highly expressed in both the brain and the liver. In the periphery, APOE is produced predominantly by hepatocytes, as well as by macrophages and adipocytes. Within the CNS, APOE is highly expressed by astrocytes, but is also expressed by microglia, vascular mural cells, choroid plexus and neurons under conditions of stress or injury. In the periphery, APOE predominantly binds to very low density lipoprotein (VLDL) particles combined with other apolipoproteins, phospholipids and cholesterol. In the CNS, APOE tends to bind to HDL particles since VLDL are not present centrally (Bu, 2009). Circulating levels of APOE vary among the three isoforms in plasma, cerebrospinal fluid (CSF) and interstitial fluid where APOE2 levels are greater than APOE3 levels, which in turn are greater than APOE4 levels (Dorey *et al.*, 2014). Interestingly, APOE is not capable of crossing the BBB. Liver transplant studies have shown that the new liver produces the APOE protein corresponding to its genotype while the APOE within the CNS retains the phenotype corresponding to the genotype of the original liver (Linton *et al.*, 1991).

1.2.2 APOE receptors (in the CNS)

APOE binds to lipoprotein receptors and proteoglycans (Ji *et al.*, 1993). The major APOE receptors are from a class of metabolic receptors known as the LDL receptor (LDLR) family and includes LDLR itself, LDLR-related protein 1 (LRP1), VLDL receptor (VLDLR), and APOE receptor 2 (APOER2) amongst others. LDLR comprise a highly conserved family of transmembrane receptors responsible for the uptake and clearance of lipoproteins in plasma and CSF, as well as the regulation of lipid metabolism, and mediation of a wide range of cell signalling pathways (Dorey *et al.*, 2014). The seven receptors from the LDLR family share a common conserved structure: consisting of an intracellular domain which mediates signal transduction, a transmembrane domain and an extracellular domain where ligand binding and release occurs (Lane-Donovan & Herz, 2017). All members of the LDLR family are capable of interacting with APOE and as such are often referred to as the "APOE receptors" (Lane-Donovan & Herz, 2017). Table 1.2.3 describes the major APOE receptors and their characteristics. As well as the LDLR family, APOE is capable of binding to heparan sulfate proteoglycans (HSPG) present at the cell surface. There is evidence that HSPG is capable of forming a complex with LRP1, this mediates binding of APOE and is suggestive of a facilitative effect at the cell surface (Wilsie & Orlando, 2003).

Binding affinity is affected by APOE isoform and lipidation state, i.e. whether it is lipid bound or unbound. APOE must be appropriately lipidated in order for normal receptor binding to occur. APOE lipidation is facilitated by a cholesterol-efflux protein on the cell membrane known as the ATP-binding cassette A1 (ABCA1). ABCA1 is necessary for proper lipidation of APOE (Wahrle *et al.*, 2004). In knockout models, ABCA1 deficiency leads to a decrease in APOE levels in the CNS (Krimbou *et al.*, 2004). Poorly-lipidated APOE particles have an altered conformation, decreased stability in the CNS, and altered interactions with Aβ (Wahrle *et al.*, 2004; Dorey *et al.*, 2014).

Receptor	Binding Characteristics	Reference
LRP1	• Recombinant APOE • APOE aggregates • Prefers lipid-bound APOE • Recognises all isoforms	(Ruiz *et al.*, 2005)
LDLR	• Lipidated APOE • Strong affinity for APOE3 and APOE4 • Poor affinity for APOE2	(Ruiz *et al.*, 2005) (Dorey *et al.*, 2014)
VLDLR	• Lipid-free APOE • Recognises all isoforms	(Ruiz *et al.*, 2005)
HSPG	• Lipidated APOE • Non-lipidated APOE • Recognises all isoforms	(Ji *et al.*, 1993) (Saito *et al.*, 2003)

Table 1.2.3. The major APOE receptors and their binding characteristics.

APOE receptors show variable binding preferences across the APOE isoforms and is dependent on lipidation state.

1.2.2.1 Role of APOE isoform in receptor binding

APOE2 has a low binding affinity to LDLR compared to APOE3, this leads to an increased risk of developing type III hyperlipidaemia in individuals who are homozygous for APOE2 (Zhao *et al.*, 2018). The compromised binding of APOE which results leads to an increase in circulating cholesterol and triglycerides which is characteristic of this class of hyperlipidaemia. The VLDLR and HSPG receptors recognise all APOE isoforms with comparable affinity (Ruiz *et al.*, 2005).

In APOE4, domain interaction occurs between the carboxy and amino terminals owing to the effect of arginine at position 112. Arg-Cys interaction in APOE4 changes its conformation ultimately affecting binding affinities compared to the other isoforms (Dorey *et al.*, 2014). This domain interaction is a unique property of APOE4 and has been suggested to contribute to its detrimental effect in AD risk and pathogenesis as it influences its ability to bind to lipids, receptors and Aβ (Wang *et al.*, 2018). For example, APOE3 has a 5-fold higher binding affinity for Aβ than APOE4 (Tokuda *et al.*, 2000). This is important as astrocytes' ability to localise to Aβ plaques to degrade them requires APOE (Crompton *et al.*, 2017). Consequently, small molecule correctors which can structurally convert APOE4 to APOE3 are being pursued as a therapeutic target (Wang *et al.*, 2018).

1.2.3 APOE has far reaching functions in the CNS

APOE functions predominantly as a lipid transporter. Binding of APOE on lipid particles by APOE receptors facilitates transport of lipoproteins and lipid compounds into and throughout cells in the CNS, and regulates concentrations for different cellular compartments in isoform-dependent rates (Huang & Mahley, 2014).

APOE plays a key role in transporting cholesterol to plasma membranes which is essential for structure, synaptic formation and remodelling (Belloy *et al.*, 2019). Cholesterol plays a critical role in synaptic function, by helping maintain adequate curvature of the membrane. Cholesterol also facilitates soluble NSF attachment protein receptor (SNARE)-mediated membrane fusion. Cholesterol deficiency in neurons leads to impaired synaptic plasticity (Koudinov & Koudinova, 2002). Synaptic transmission can be significantly reduced by depleting cholesterol, then recovered by reintroducing cholesterol (Tong *et al.*, 2009; Linetti *et al.*, 2010). Astrocytes are the main producers of cholesterol in the CNS (Nieweg *et al.*, 2009), the synthesis of which is tightly regulated by means of an internal feedback loop. Low intracellular cholesterol triggers cholesterol synthesis by inducing proteolytic processes of sterol regulatory element-binding proteins and reducing cholesterol efflux (Benarroch, 2008; Jeong *et al.*, 2019). High intracellular cholesterol results in lipoprotein complex efflux following LXR/RXR-mediated transcription of cholesterol transport proteins (Jeong *et al.*, 2019). APOE also plays a role in BBB integrity, synaptic plasticity and cell signalling.

1.2.4 The APOE4 genotype has a profound effect on CNS response to disease and injury

APOE4 undergoes a profound structural shift due to the side-chain of arginine at position 112 interacting with the glutamine at position 255 as determined by x-ray crystallography (Hatters *et al.*, 2006). As a result, a ‘salt bridge’ forms between the C- and N-terminal domains which is believed to play a critical role in the functional differences between APOE4 and the other isoforms (Dorey *et al.*, 2014). The role of APOE in CNS disease and injury is summarised in Table 1.2.4.

1.2.4.1 Altered cholesterol homeostasis

Within the CNS, APOE functions as a lipid transporter, e.g. cholesterol, and in this manner aids neuronal homeostasis and synapse integrity. In AD, APOE has been shown to stimulate APP and Aβ production (Huang *et al.*, 2017), as well as compromise the neurotrophic function of astrocytes (Zhao *et al.*, 2017). APOE4 astrocytes have previously been demonstrated to have a more pronounced effect in contributing to AD pathogenesis in a number of ways including reduced efficiency in clearing $A\beta_{42}$ and reduced support of neuronal viability compared to their APOE3 counterparts (Zhao *et al.*, 2017; Lin *et al.*, 2018).

1.2.4.2 Compromised synaptic pruning

APOE4 decreases the rate of synapse pruning by astrocytes *in vivo* compared to APOE3 or APOE2 (Chung *et al.*, 2016). In a murine model where the *ApoE* gene was replaced with one of the three main human isoforms (*APOE2*, *APOE3* or *APOE4*) it was found that *APOE4* astrocytes had a reduced phagocytic capacity and increased senescent synapses (Chung *et al.*, 2016). This is consistent with a study carried out in human iPSC-derived neurons which demonstrated that *APOE4*-expressing neurons had an increased number of synapses compared to their *APOE3*-expressing counterparts (Lin *et al.*, 2018).

1.2.4.3 APOE4 plays a role in various aspects of AD pathology

APOE is known to have significant effects on AD pathology associated with Aβ production, clearance and plaque formation (Table 1.2.4). A critically important paper showed that astrocyte-secreted APOE stimulates a kinase cascade, promoting neuronal APP transcription and Aβ secretion in the order APOE4 > APOE3 > APOE2 (Huang *et al.*, 2017). APOE isoforms differentially increase Aβ aggregation and plaque formation independent of $A\beta_{40}$ and $A\beta_{42}$ levels and ratios in the order of APOE4 > APOE3 > APOE2 (Huang & Mahley, 2014). There is evidence that APOE is up-regulated in response to neuronal damage. However, there is evidence also that APOE is subject to proteolytic degradation, and that fragments of APOE4 are neurotoxic, and found in both NFT and Aβ plaques. This raises the possibility that APOE4 up-regulation could self-perpetuate and lead to chronic toxicity.

Following on from studies showing that the APOE4 isoform leads to Aβ pathology, studies have shown that APOE4 is also implicated in non-Aβ pathology surrounding AD, including effects on BBB permeability (Bell *et al.*, 2012), altering synapse integrity (Klein *et al.*, 2010), and independent involvement in exacerbating tau-mediated phosphorylation (Shi *et al.*, 2017c). The APOE4 isoform also impedes autophagy in astrocytes, with the clearance of soluble Aβ significantly less effective than in APOE3 astrocytes (Simonovitch *et al.*, 2016).

APOE plays an isoform-dependent role in inflammation. Shi and colleagues have demonstrated that APOE4 increases microglial and astrocytic activation (Shi *et al.*, 2017c). Interesting work by Theendakara and colleagues has provided evidence that APOE4 acts as a major mediator of the inflammatory response. They demonstrated that APOE4, but not APOE3, can translocate directly to the nucleus and bind promoter regions of AD-associated genes. Of these, genes which corresponded to an anti-inflammatory and anti-apoptotic phenotype were suppressed by APOE4 (Theendakara *et al.*, 2016). It was shown that APOE4 can bind double-stranded DNA at the SirT1 promotor sequence and act as a transcription factor with the effect of suppressing SirT1 promotor activity. It is yet unclear how APOE translocates to the nucleus, but it has also been implicated in the repression of four other genes – MADD, ADNP, COMMD6, and PPP2R5E – pointing to a potential role in transcription (Theendakara *et al.*, 2016; Theendakara *et al.*, 2018).

Role	Model Used	Main Finding	Reference
Aβ deposition and clearance	Human brain endothelial cells and transgenic mice	APOE isoform affects lipoprotein receptor shedding in the brain (APOE4 > APOE3 > APOE2).	(Bachmeier *et al.*, 2014)
	Rat neuroblastoma B103 cells	APOE4 increased Aβ production to a greater extent than APOE3 (60% vs 30%) due to more pronounced stimulation of APP recycling.	(Ye *et al.*, 2005)
	APOE-inducible mouse model	APOE4 enhanced Aβ deposition, neuritic dystrophy and gliosis.	(Liu *et al.*, 2017)
	Human iPSC	↑$A\beta_{42}$ secretion by APOE4 neurons. Impaired Aβ clearance by APOE4 astrocytes. ↓Aβ clearance by APOE4 microglia.	(Lin *et al.*, 2018)
Hyper-phosphorylation of tau and tauopathy	P301S tau transgenic mice with *APOE* KO or *APOE4* KI	APOE4 affects tau pathogenesis, neuroinflammation, and tau-mediated neurodegeneration independently of Aβ pathology.	(Shi *et al.*, 2017c)
	APOE transgenic mice	↑tau phosphorylation mediated by activation of Erk.	(Harris *et al.*, 2004)
	Post mortem AD brain tissue	There is a strong interaction between APOE4 expression and tau pathology in the presence of Aβ pathology.	(Farfel *et al.*, 2016)
BBB integrity	*In vitro* BBB model and *APOE3* and *APOE4* knock-in mice	BBB tight junction integrity is APOE isoform dependent. BBB permeability is greater in APOE4 vs APOE3.	(Nishitsuji *et al.*, 2011)
	APOE transgenic mice	APOE4 and APOE ablation result in reduced BBB integrity. Vascular defects result from activation of pro-inflammatory cyclophilin A/NF-κB pathways.	(Bell *et al.*, 2012)
Mitochondria dysfunction	Primary neurons from APOE transgenic mice and Neuro-2A neuroblastoma cells	Reduced expression of mitochondrial subunits in APOE4-expressing neurons and Neuro-2A cells. ↓Mitochondrial respiratory capacity in APOE4-expressing neurons and Neuro-2A cells.	(Chen *et al.*, 2011b)
Total APOE levels	Plasma and CSF samples from human AD and non-AD participants	↓plasma APOE in APOE4 carriers. Attributed to a decrease in the APOE4 isoform concentrations.	(Martinez-Morillo *et al.*, 2014)

Table 1.2.4. The role of APOE4 in AD pathology.

1.3 Astrocytes – the main homeostatic regulators of the CNS

Astrocytes are the most abundant cell type in the mammalian CNS (Azevedo *et al.*, 2009) and play a central role in the development and homeostasis of the healthy brain. In the human CNS, it is thought the glia to neuron ratio is 1:1 (Vasile *et al.*, 2017), and that astrocytes account for 30% of cells (Liddelow & Barres, 2017). A single astrocyte can contact up to a million different synapses (Halassa *et al.*, 2007b), as well as dendrites and blood vessels, owing to significant arborisation. Eight major processes give rise to hundreds of thousands of fine processes (Tyzack *et al.*, 2016). This highly connective property allows for cell-cell contact, the regulation of synaptic transmission and the release of neuromodulatory factors. Astrocytes maintain the CNS in a number of ways, providing trophic and structural support for neurons whilst also promoting neurogenesis. Neurogenesis is an ongoing process throughout adulthood, which is spatially restricted to the sub-granular zone (SGZ) of the hippocampus and sub-ventricular zone (SVZ) in the lateral ventricles (Gage, 2000). It has been demonstrated that both human and rodent astrocytes can promote the formation of synapses *in vitro* while also promoting neuronal survival (Chung *et al.*, 2013; Zhang *et al.*, 2016c). Further to this, astrocytes are involved in the management of neuronal networks through synaptic pruning, which involves the elimination of excess synapses and thus enhances the efficiency of active synapses (Clarke & Barres, 2013; Zhang *et al.*, 2016c). Their release of cytokine TNFα also acts to enhance synaptic efficiency by increasing the number of α-amino 3-hydroxy-5-methyl-4-isoxazolepropionic acid (AMPA) receptors on the cells surface (Eroglu & Barres, 2010).

Astrocytic transporters, excitatory amino acid transporter 1 and 2 (EAAT1/EAAT2) support the clearance of glutamate, avoiding excitotoxicity that can occur from high levels of synaptic glutamate (Dong *et al.*, 2009). They respond to neurotransmitters, e.g. glutamate (Porter & McCarthy, 1996), at the 'tripartite synapse' – an area where there is close association of astrocytes to pre- and post-synaptic neuronal terminals. When Ca^{2+} is elevated at tripartite synapses, astrocytes are activated and release neuromodulatory molecules such as nitric oxide (NO) and D-serine, which influence neuron excitability (Eroglu & Barres, 2010). Their release of D-serine is also necessary in neuronal synaptic plasticity as NMDA receptors require D-serine for long-term potentiation (LTP) (Yang *et al.*, 2003). As the key regulators of homeostasis within the CNS, astrocytes are indispensable for normal brain functioning.

1.3.1 Astrocyte function in the healthy CNS

In the developing brain astrocytes control the formation, maturation and elimination of synapses via a process known as synaptic pruning (Clarke & Barres, 2013; Allen, 2014). This process involves the removal of synapses in order to strengthen neural circuits, is mediated by the multiple EGF-like-domains 10 (MEGF10) and c-mer proto-oncogene tyrosine kinase (MERTK) phagocytic pathways, and is strongly dependent on neuronal activity (Chung *et al.*, 2013). In the adult brain, astrocytes' main function is to maintain a homeostatic environment that is optimal for neuronal health and function, they do this by maintaining the BBB, ion balance, neurotransmitter turnover and release of growth factors that aid synapse formation.

1.3.1.1 Astrocytes aid in the formation and maintenance of neuronal networks

Astrocytes are critical in brain development as contributors to neurogenesis, synaptogenesis and synaptic function (Baldwin & Eroglu, 2017; Casse *et al.*, 2018). Astrocytes promote synaptic formation via a number of secreted factors such as thrombospondins and brain-derived neurotrophic factor (BDNF) (Baldwin & Eroglu, 2017). A study carried out in 1995, using rat retinal ganglion cells, provided the first evidence for astrocyte involvement in synapse formation. It was found that astrocytes can control different synapse formation stages by secreting factors that can increase the synaptic numbers (Meyer-Franke *et al.*, 1995). It was later discovered *in vitro* that this also occurs in human neurons (Diniz *et al.*, 2012).

1.3.1.2 Astrocytes and the blood-brain barrier

The BBB is a specialised structure of the CNS that restricts immune cell migration and soluble molecule diffusion between the brain parenchyma and the blood travelling from the periphery, thus endowing a relative immune privilege upon the brain (Prat *et al.*, 2001). Astrocytes are a component of the BBB along with pericytes and endothelial cells. Here astrocytes regulate what substances may enter or leave the CNS, protecting the CNS from toxins, pathogens, injury, inflammation and disease. Tight junctions are present between the endothelial cells which form a diffusion barrier between the blood and brain (Abbott *et al.*, 2006). Astrocytic end feet firmly ensheath the blood vessels and are critical for maintaining this tight junction barrier (Ballabh, Braun and Nedergaard, 2004).

Astrocytes regulate the morphology and angiogenesis of endothelial cells and influence BBB phenotype under physiological and pathological conditions (Prat *et al.*, 2001). It has been shown *in vitro* that astrocytes are necessary for the correct association of endothelial cells and pericytes in tube-like structures (Ramsauer *et al.*, 2002). Astrocytes also mediate the permeability of the BBB by the activation of tight junction proteins through the NF-κB pathway (Brown *et al.*, 2003). BBB regulation is vital for neuroprotection and minimising the amount of infiltrating cells from the periphery which is characteristic of certain pathologies (Capani *et al.*, 2016).

Further to their role as a component of the BBB, astrocytes also function to regulate cerebral blood flow through the release of K^+ from astrocytic end feet in contact with blood vessels (Paulson & Newman, 1987). They also mediate blood vessel diameter via the production and release of prostaglandins, NO and arachidonic acid (AA) (Gordon *et al.*, 2007).

1.3.1.3 Astrocytes and the tripartite synapse

Protoplasmic and fibrous astrocytic end feet envelop the neuronal synaptic cleft and nodes of Ranvier respectively. Here astrocytes are involved in responding to synaptic activity and regulating synaptic transmission due to the presence and structure of the tripartite synapse – consisting of an astrocyte in contact with both a pre- and post-synaptic neuron (Araque *et al.*, 1999; Panatier *et al.*, 2011). Their envelopment of neurons allows for adequate uptake of K^+, glutamate and H_2O, which may be released from neurons during neurotransmission thus, playing a critical role in synapse regulation (Crompton *et al.*, 2017). Astrocytes regulate synaptic transmission at the tripartite synapse through release of synaptically active substances such as γ-aminobutyric acid (GABA), glutamate, purines and D-serine (Halassa *et al.*, 2007a). Astrocytes communicate with synapses through the regulation of Ca^{2+} increase in response to neurotransmitters released by neurons and other glial cells (Cornell-Bell *et al.*, 1990).

1.3.1.4 Astrocytes maintain energy supply in the CNS

In order to meet its high metabolic demands; the human brain has a critical dependence on a constant energy supply (almost exclusively from glucose). Astrocytes play a metabolic role in regulating this brain energy supply by producing lactate through

glutamate-mediated glycolysis (Brown & Ransom, 2007; Nortley & Attwell, 2017). This lactate is then used as an energy source by neurons and as such this process is known as the astrocyte-neuron lactate shuttle hypothesis. Overall, this hypothesis states that glutamate, released from activated neurons, stimulates glycolysis in nearby astrocytes and the lactate that is produced is released to provide a fuel source for neuronal metabolism (Mangia *et al.*, 2009). In astrocytes, glucose is mainly stored as glycogen. This glycogen is metabolised to pyruvate and lactate, which are transported by monocarboxylate transport proteins across the cell membrane where the lactate can then be used for neuronal metabolism (Magistretti & Pellerin, 1999). Both *in vivo* and *in vitro* animal studies have shown that lactate can sustain neuronal activity in times of glucose deprivation demonstrating a direct neuroprotective effect (Wyss *et al.*, 2011). Tight regulation of these homeostatic factors by astrocytes surmounts to an important role in maintaining optimal conditions within the CNS in order to maintain neuronal health and survival, and ultimately function.

1.3.1.5 Astrocytes maintain the extracellular environment for neuronal functioning

Astrocytes maintain extracellular levels of K^+, Cl^-, and Ca^{2+} ions, and cellular pH (Matias *et al.*, 2019). This function maintains neuron excitability. During neuronal activity, astrocytes take up excess extracellular K^+ via inward rectifying Kir 4.1 K^+ channels, or the Na^+/K^+ ATPase pump (Hertz & Chen, 2016). Water homeostasis is maintained via aquaporin 4 (AQP4) expressed on astrocyte end feet (Vandebroek & Yasui, 2020).

At the synapse, astrocytes also partake in neurotransmitter cycling via the rapid uptake of synaptically-released glutamate from the extracellular environment. This helps modulate both the spatial and temporal degree of glutamate signalling. The majority of this uptake occurs via Na^+-dependent EAAT1 and EAAT2 on astrocytes and helps protect against excitotoxicity caused by high levels of extracellular glutamate (Armbruster *et al.*, 2016). This glutamate can be converted to glutamine in astrocytes by glutamine synthetase then released to be used by neurons for the synthesis of glutamate or GABA.

1.4 The role of astrocytes in neurodegeneration

Neurodegeneration has traditionally focused primarily on autonomous cell death, before it was questioned whether neurodegeneration is an example of non-cell autonomous death (Di Giorgio *et al.*, 2007). This would imply that the interaction between neurons and other cell types, such as astrocytes, is responsible for neuronal degeneration as opposed to toxicity arising solely within vulnerable neurons (Lobsiger & Cleveland, 2007). Having traditionally been considered mere ancillary cells in the CNS there is now a body of literature to support a detrimental role for astrocytes in neurodegeneration (Lobsiger & Cleveland, 2007; Roybon *et al.*, 2013; Osborn *et al.*, 2016; Liddelow *et al.*, 2017). Much research is interested in trying to elucidate the signals present in the injured or diseased brain which compromise astrocyte function (Figure 1.4.1). Advances in techniques for culturing pure populations of astrocytes have elucidated that multiple reactive astrocyte phenotypes may exist and that these populations of cells may have differential effects on neurodegeneration.

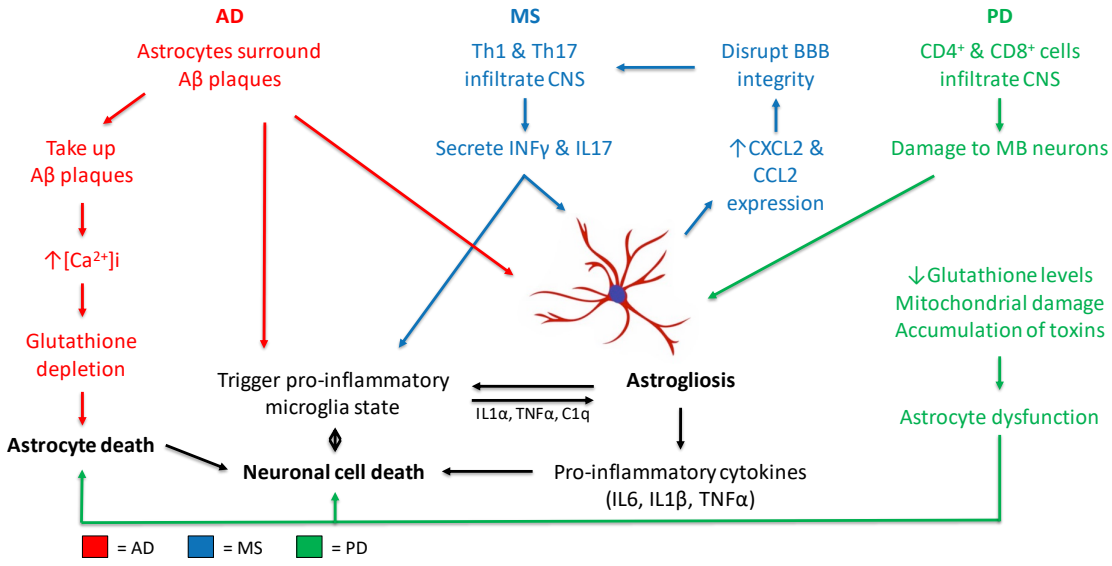


Figure 1.4.1. Reactive astrocytes are involved in a range of pathologies.

The reactive astrocyte phenotype arises from a range of pathological scenarios where astrogliosis leads to further pro-inflammatory cytokine production and thus, neuronal damage and death. Incidentally, astrocyte death leads to neuronal death due to the high level of dependence neurons have on astrocytes. Microglia and astrocytes drive each other in a feedback-like manner, where neuroinflammation appears to be simultaneously aiding and exacerbating neurodegeneration. Abbreviations: CCL2 = Chemokine (C-C motif) ligand 2, CD4 = Cluster of differentiation 4, CD8 = Cluster of differentiation 8, CXCL2 = Chemokine (C-X-C motif) ligand 2, IFNγ = interferon-gamma, IL17 = interleukin-17, MB = midbrain, Th1 = T-helper cell 1, Th17 = T-helper cell 17.

1.4.1 Parkinson's disease

Parkinson's disease (PD) is the second most common neurodegenerative disease and affects approximately 1% of the population over the age of 65 (Crompton *et al.*, 2017). It was first described in 1817 by James Parkinson in "An essay on the shaking palsy" (Parkinson, 2002). PD is characterised by the loss of dopaminergic neurons from the substantia nigra pars compacta of the striatum due to the toxic effects of abnormal α-synuclein protein aggregations known as Lewy bodies (Wakabayashi *et al.*, 2000). The disease phenotype presents as bradykinesia, tremor, rigidity and postural instability and is typically diagnosed on the basis of these clinical criteria (Jankovic, 2008). Similar to Aβ in AD, astrocytes internalise α-synuclein protein aggregates which is thought to compromise their ability to produce and release neurotrophic factors as well as hinder their role as a BBB component leading to "leakiness" (Yamamizu *et al.*, 2017). PD is a neuroinflammatory disorder, this inflammation is thought to be modulated by astrocytes via exocytosis of paracrine factors such as ICAM1 and IL6 which stimulate microglia migration (McGeer & McGeer, 2008). In the LPS rat model of PD, administration of the astrocyte toxin L-alpha-aminoadipic acid attenuated reactive astrogliosis, microglial activation and loss of dopamine neurons thereby indicating a key role of astrocytes in these processes (O'Neill *et al.*, 2019).

There is a genetic component to PD with mutations in 17 different genes such as *SNCA*, *Parkin*, *DJ-1* and *PINK1* linked to the disease (Hernandez *et al.*, 2016). DJ-1 encoded by the *PARK7* gene is the most studied PD mutation. In astrocytes, DJ-1 knockout impairs their ability to protect against neurotoxins such as rotenone (Mullett & Hinkle, 2011). Under conditions of oxidative stress or ischaemia, reactive astrocytes were found to up-regulate DJ-1 (Neumann *et al.*, 2004). A study from the Kahle laboratory found that DJ-1 knockout astrocytes produced 10 times more nitric oxide than littermate controls when treated with lipopolysaccharide (LPS), a TLR4 agonist (Waak *et al.*, 2009). Mutation of the *SNCA* gene is also associated with PD resulting in α-synuclein aggregation in astrocytes. Gu and colleagues, demonstrated that when *A53T* α-synuclein was selectively expressed in rodent astrocytes it lead to paralysis (Gu *et al.*, 2010). These results indicate both that astrocytes play a key role in PD.

1.4.2 Amyotrophic lateral sclerosis

Amyotrophic lateral sclerosis (ALS) is a neurodegenerative disorder which leads to the death of upper and lower motor neurons, and as such is often termed motor neuron disease. The contribution of astrocytes to neurodegeneration has been well characterised. It has been proposed that astrocytes play a role in disease progression following loss of the astrocyte glutamate transporter 1 (GLT1) (the rodent homolog of human EAAT2) which leads to excitotoxicity and subsequent neuronal loss (Rothstein *et al.*, 1995). Astrogliosis has been described in both white and grey matter in ALS brain and is now considered a hallmark of the disease (Yamanaka *et al.*, 2008; Lasiene & Yamanaka, 2011).

Approximately 25% of cases of genetically associated ALS are caused by mutations in superoxide dismutase (SOD1) (Di Giorgio *et al.*, 2007). The SOD1 mouse model of ALS shows considerable astrocyte atrophy (Rossi *et al.*, 2008) and microglial activation which is modulated by astrocytes (Yamanaka *et al.*, 2008). A study by Marchetto and colleagues found 50% loss of motor neurons when co-cultured with primary astrocytes overexpressing mutant SOD1, indicating a non-cell autonomous mechanism for degeneration. Significantly, this effect was found to be motor neuron specific, while other neuronal cell types such as GABAergic neurons were unaffected (Marchetto *et al.*, 2008). Mutations in the TARDBP gene, which encodes TDP43, were found to affect the survival of human iPSC neurons and astrocytes, indicating that the nuclear-cytoplasmic generation of TDP43 must be finely tuned in both cell types. However, neuron death was not correlated with a TARDBP mutation in astrocytes, indicating that cell death in this circumstance is mediated by cell autonomous mechanisms (Serio *et al.*, 2013).

1.4.3 Huntington's disease

Huntington's disease (HD) is a neurodegenerative disorder caused by a mutation in the huntingtin (HTT) gene. This involves an expansion in the CAG (cytosine, adenine & guanine) tri-nucleotide repeat and is characterised by the loss of medium spiny neurons. There is evidence to support the idea that astrocytes play a role in HD pathogenesis. Accumulation of mutant *HTT* (*mHTT*) in astrocytes has been seen in brain tissue of human and mouse HD subjects (Shin *et al.*, 2005). The expression of *mHTT* in astrocytes impairs astrocytic production of neurotrophic factors such as BDNF, which is produced by quiescent astrocytes. BDNF normally plays a key role in plasticity while promoting the

survival of neurons, however reduced levels of BDNF in HD and has been linked to a longer CAG repeat and duration of illness (Ciammola *et al.*, 2007). Further to this, astrocytes from HD mouse models have been shown to develop reactive astrogliosis, impaired glutamate reuptake (Faideau *et al.*, 2010) and down-regulation of K^+ channels (Zhang *et al.*, 2018b).

1.5 Reactive astrocytes in Alzheimer's disease

Original investigations into progressive degenerative disorders focused on neuronal dysfunction and loss, once thought to be the main players hence the term "neurodegeneration". There is now a growing body of literature to support a detrimental role for astrocytes, previously considered mere ancillary cells in the CNS, in neurodegeneration (Lobsiger & Cleveland, 2007; Roybon *et al.*, 2013; Osborn *et al.*, 2016; Liddelow *et al.*, 2017). Reactive astrocytes have been closely linked to the pathology of AD in recent years (Perez-Nievas & Serrano-Pozo, 2018). Aberrant calcium signalling, altered gliotransmission and an increase in GABA levels at the synapse have been reported in these astrocytes (Agulhon *et al.*, 2012; Shigetomi *et al.*, 2019). Increased GABA levels at the synapse inhibit neuronal activity and impairs memory retention in mouse models of AD (Jo *et al.*, 2014).

1.5.1 Do reactive astrocytes suffer a loss of function or gain of toxic function?

One theory poses that astrocytes lose their normal homeostatic functions in a disease scenario, while others theorise a gain of toxic function. It is also possible that a combination of both occurs, where astrocytes' normal functioning is compromised and toxic side effects ensue. The discovery of different reactive phenotypes in astrocytes in response to immune attack, chronic neurodegenerative disease or acute trauma has been termed "reactive astrogliosis" (Pekny *et al.*, 2014). Reactive astrogliosis involves a phenotypic change with many functional consequences.

Reactive astrocytes exhibit a biphasic effect in AD, with both beneficial and detrimental roles. Beneficial effects of reactive astrocytes are more prominent in the early stages of AD and include plaque degradation via phagocytosis and transportation out of the brain parenchyma, across the BBB (Pekny *et al.*, 2014). Another defensive role of astrocytes is the generation of antioxidants such as glutathione which protects against oxidative damage (Chun & Lee, 2018). As AD advances reactive astrocytes take on more detrimental characteristics, they begin to secrete pro-inflammatory cytokines and have altered gliotransmitter release (Chun & Lee, 2018). Astrocytes release pro-inflammatory cytokines such as interleukin (IL)-6, TNFα and IL1β which can augment Aβ plaque formation, promote phosphorylation of tau and contribute to neurodegeneration (Gonzalez-Reyes *et al.*, 2017; Kinney *et al.*, 2018).

1.5.1.1 Aβ internalisation compromises astrocyte function

Reactive astrocytes have been found to co-localise with Aβ plaques in AD, and are capable of internalising Aβ via APOE. Astrocytic uptake of Aβ was first seen in post mortem tissue samples where Aβ deposits were found in astrocytes in close proximity to Aβ plaques (Yamaguchi *et al.*, 1998). Internal build-up of Aβ is thought to disrupt the antioxidant abilities of astrocytes and as a result impair neuronal viability (Abramov *et al.*, 2003; Angelova & Abramov, 2014). The Inoue laboratory found accumulation of Aβ oligomers in astrocytes from patients with both a familial *APP* mutation and sporadic AD leading to endoplasmic reticulum and oxidative stress (Kondo *et al.*, 2013). The Noble laboratory similarly found that the presence of small numbers of astrocytes could exacerbate neuronal death associated with Aβ and caspase-3 activation. They found that inhibiting astrocytic activation with an anti-inflammatory agent such as minocycline could reduce the inflammatory response they associated with neuronal death (Garwood *et al.*, 2011). The authors also claimed in this study that astrocytes are essential for Aβ-induced tau phosphorylation which could be observed in primary neurons. Furthermore, astrocytes may also be involved in the build-up of Aβ as they alone are capable of secreting high levels of Aβ (Liao *et al.*, 2016).

1.5.1.2 Glutamate-mediated excitotoxicity

A primary role for astrocytes in the CNS is the removal of glutamate from the extracellular space, particularly the synaptic cleft (Mark *et al.*, 2001). Elevated levels of extracellular glutamate have been noted in AD patients which is thought to contribute to excitotoxicity-induced neurodegeneration (Perego *et al.*, 2000). In the hippocampus of AD mice, it was shown that excessive GABA released by reactive astrocytes resulted in memory impairments (Jo *et al.*, 2014). Glutamate is also released from reactive astrocytes which can activate extrasynaptic NMDA receptors resulting in synaptic depression and spine loss (Talantova *et al.*, 2013). Consistent with this finding, studies from post mortem AD patients have shown a significant reduction of EAAT1 and EAAT2 expression in the prefrontal cortex (Chen *et al.*, 2011b). Reactive astrocytes are believed to contribute to the increased levels of glutamate at the synapse via TNFα secretion which can cause glutamate release from astrocytes (Jensen *et al.*, 2013; Barateiro *et al.*, 2014). A seizure phenotype and abnormal cortical electroencephalogram activity in aged APOE4

transgenic mice suggests that APOE4 may contribute to increased glutamate concentrations at the synapse (Hunter *et al.*, 2012).

1.5.1.3 Astrocytes are key players in neuroinflammation

Astrocytes can undergo a phenotypic switch known as reactive astrogliosis. Astrogliosis is characterised genetically by up-regulation of reactive astrocyte genes, morphologically by the proliferation of reactive astrocytes with hypertrophied processes (Sofroniew & Vinters, 2010), and functionally by increased production and secretion of inflammatory mediators (Trindade *et al.*, 2020). Reactive astrogliosis has many functional consequences in conditions such as stroke, trauma, epilepsy and AD as well as other neurodegenerative diseases. It has been shown that not just disease and injury, but also normal aging, can induce reactive astrogliosis (Clarke *et al.*, 2018). RNA sequencing of astrocytes identified both age- and brain region-dependent transcriptional changes leading aged astrocytes to develop a reactive phenotype, typical of what has been characterised in disease and inflammation (Boisvert *et al.*, 2018; Heimann & Sirko, 2019). Further studies have shown that the Janus kinase (JAK)-signal transducer and activator of transcription (STAT) pathway is necessary and sufficient to induce and maintain reactivity in astrocytes. Inhibiting this pathway in mouse models of AD led to the reduction of amyloid deposits, the improvement in spatial learning and the restoration of synaptic deficits; hallmark features of the disease (Ceyzeriat *et al.*, 2018). Therefore, astrocytes are involved in non-cell-autonomous mechanisms of neuronal cell death in AD.

1.5.2 Non-cell-autonomous mechanisms

Neuronal cell death in neurodegenerative diseases is not solely as a result of the causative mutant protein, rather the effect of that mutant protein on the non-neuronal glia population. This toxicity derived from glia has been deemed a non-cell-autonomous mechanism of disease initiation and progression (Lobsiger & Cleveland, 2007). There is an abundance of evidence supporting this mechanism whereby both neuronal and non-neuronal cell populations are affected by the mutant protein for that particular disease (Di Giorgio *et al.*, 2008; Ilieva *et al.*, 2009; Chai & Kohyama, 2019; di Domenico *et al.*, 2019). Neurons subsequently degenerate as a result of their mutant protein and the toxicity of cells in their neighbouring environment. Three pathways for the involvement of glia in non-cell-autonomous neurodegeneration have been proposed: (i) affected

neurons induce damaging responses in nearby glia, (ii) mutant protein expressed in glia compromises their normal response to damage of nearby neurons, thereby exacerbating the damage to vulnerable neurons, and (iii) mutant protein expression in glia induces neurotoxicity, independent of signals produced by surrounding neurons.

1.6 Modelling Alzheimer's disease

Effective and efficient modelling has been a major focus of disease research since the discovery of pathology and although countless breakthroughs have been made over the years it is still arguably the limiting factor for translating therapies from "bench-to-bedside". Approaches to CNS research have utilised immortalised cell lines, e.g. HEK293 and SH5Y-5Y, however these immortalised cell lines have intrinsic flaws as they are often derived from cancers and may not be from the tissue affected by the disease in question (Avior *et al.*, 2016). Additionally cell lines are by definition highly proliferative and therefore do not provide adequate models for slowly proliferating cells such as neurons and microglia (Haenseler *et al.*, 2017). Primary cultures of neurons, astrocytes and microglia isolated from rodents are widely used but these primary cells have issues of their own as they can be difficult to maintain and expand in culture, particularly when isolated from an aged animal and are often contaminated with other cell types.

Another pathway for research utilises model organisms, often rodents which have been genetically modified to over express the relevant disease causing genes, for example the APP/PS1 mouse model of AD over expresses APP leading to the characteristic Aβ pathology associated with the disease (Carrera *et al.*, 2013). The mouse is the most prevalent animal model used in research today, despite the fact that there are many differences between mice and humans both genetically and phenotypically (Oberheim *et al.*, 2009; Avior *et al.*, 2016).

1.6.1 Murine models of Alzheimer's disease

Although *in vitro* experiments are required initially, the vast majority of what we know about AD today has come from the development of animal models which emulate the disease and allow for *in vivo* studies. Numerous mouse models have been engineered in an attempt to understand the ethiology and pathogenesis of AD, however while these models possess various aspects of the disease they fail to replicate complete AD pathology (Webster *et al.*, 2013). Many of these transgenic AD models have been engineered through the mutation of the genes which code for APP, PS or tau protein, therefore they replicate aspects of the disease but cannot explicitly mirror the disease as it presents in humans. In terms of testing therapeutics this does not exactly present a drawback, for example when testing a drug that potentially reduces Aβ production, a

model which over produces Aβ and presents with Aβ pathology is sufficient to determine the efficacy of the drug in question with human trials necessary at later stages.

Some excellent models of amyloidosis have been developed using transgenic mice which have contributed greatly to our current understanding of AD pathology. The PDAPP line was the first transgenic AD model. It was published in 1995 by the Exemplar/Athena Neuroscience group. This model was generated using platelet-derived growth factor-β (PDGFβ) as the promoter to drive a human APP minigene encoding mutant APP, hence the name PDAPP. The resulting transgenic mice developed many of the hallmarks of AD including Aβ deposition, neuritic plaque formation, synaptic loss, astrocytosis and microgliosis, making it the first transgenic model to develop AD pathology (Games *et al.*, 1995). In 1996, a second model (Tg2576) was created by Karen Hsiao and colleagues, this model also over expressed APP resulting in Aβ plaque formation and cognitive deficits similar to that which presents in the human form of the disease (Hsiao *et al.*, 1996). A Tg2576/PS1 double transgenic model was later produced which also possessed a mutation in the PS gene resulting in approximately twice as much Aβ plaque deposition (Duff, 2002); this solidified a role of the presenilin molecule in plaque formation. These early models allowed for the study of Aβ plaque formation and indicated a role for PS, they failed however to exhibit the behavioural and cognitive deficits combined with inflammation as seen in human AD, a feat that was rectified in the most widely used AD animal model today - the APP/PS1 mouse model.

1.6.1.1 APP/PS1 mouse model of Alzheimer's disease

Currently there are no existing models of AD which fully represent the chemical, pathological and behavioural changes as seen in humans with AD (Ferguson *et al.*, 2013), however the use of transgenic animals has significantly advanced our understanding of the disease and is crucial for the development of therapeutics. The APP/PS1 double transgenic mouse model of AD is the most widely used AD animal model today. This model has been programmed to express a chimeric mouse/human form of APP and a mutated form of PS1 resulting in the neuropathological hallmarks of AD (Carrera *et al.*, 2013). The APP/PS1 model exhibits considerable elevation in Aβ production and behavioural abnormalities consistent with AD pathology (Lok *et al.*, 2013). Other properties of the APP/PS1 model include an increase in oxidative stress and metabolic disturbances starting as early as 1-2 months of age, reduction of neuronal L-type calcium

channel activity in 14-month-old mice, impaired hippocampal LTP, and age-related increases in reactive gliosis and pro-inflammatory cytokine production (Webster *et al.*, 2013).

Webster and colleagues compared the APP/PS1 model with other AD mouse models with regards to the onset of AD-relevant impairments in motor function, anxiety-related behaviour, and cognition in order to clarify how the APP/PS1 model fits into the growing literature on modelling AD in rodents. They found that in comparison to other models the APP/PS1 model does not present with motor deficits while it does present with cognitive deficits at an earlier stage (Webster *et al.*, 2013). Another study examined behavioural changes in APP/PS1 mice compared to wild type mice and found that the transgenic mice exhibited significant spatial learning and memory deficits; they attributed this to substantial plaque build-up in the hippocampus and cortex (Ferguson *et al.*, 2013).

1.6.2 There is a need for better disease modelling with regards to Alzheimer's disease

Although model organisms have contributed to elucidating key pathological mechanisms there have been difficulties translating these into feasible therapies as certain therapeutics may be viable in one species and detrimental in another (McGonigle & Ruggeri, 2014; National Academies of Sciences *et al.*, 2017). The majority of drugs put forward for AD drug trials targeted Aβ having shown promise in animal models but then failed to produce results in human trials. A human model in theory would create a more realistic representation of human disease. And help bridge the gap between the laboratory and the clinic. Human pluripotent stem cells (PSC) present a means by which a human model can be created. Neuronal and astrocyte cultures may be differentiated from human PSC to provide a "disease in a dish" model of CNS disorders.

1.7 Pluripotent stem cells

PSC have the potential to differentiate into any cell type in the body. These cells have the ability to expand indefinitely and may be prompted with the appropriate factors to differentiate into a cell type of interest. Currently there are two sources of human PSC, firstly human embryonic stem cells (ESC) derived from cells isolated from the blastocyst and secondly, human induced pluripotent stem cells (iPSC) derived from adult somatic cells which are manipulated into a state of pluripotency.

ESC are derived from the inner cell mass of the blastocyst. They have many uses in research including investigating disease mechanisms, drug screening and regenerative medicine. However, obtaining human embryonic tissue is difficult, and there are many ethical controversies surrounding the use of human embryos in research, additionally it is difficult to generate disease- or patient-specific ESC. iPSC are providing an alternative approach thereby bypassing some of the limitations of ESC. They have the same differentiating abilities of ESC without the ethical issues associated with the use of human embryos and there is a reduced risk of rejection by the host following implantation (Zhao *et al.*, 2011; Araki *et al.*, 2013). Early protocols used mouse and human ESC to establish differentiating techniques [for review see (Petros *et al.*, 2011)] however iPSC are more commonly used today.

1.7.1 Induced pluripotent stem cells

Human iPSC are adult somatic cells which have been reprogrammed into a primordial state much like ESC, and thus in theory can give rise to any cell type of the body. They were first derived in 2006 in the laboratory of Shinya Yamanaka from mouse skin cells (Takahashi & Yamanaka, 2006) and the first human iPSC were derived in 2007 (Takahashi *et al.*, 2007; Yu *et al.*, 2007). This pioneering research has revolutionised disease modelling and is considered such a breakthrough that Shinya Yamanaka was awarded the Nobel Prize in Medicine in 2012. The real beauty of these cells is that they may be derived from any willing donor and a corresponding iPSC line containing the donor's genetic fingerprint can be produced and subsequently differentiated into the desired cell type, therefore disease- and patient-specific cell lines may be produced for modelling diseases which arise from genetic mutation. Human iPSC derived from tissue collected from AD patients will naturally contain any mutations that led to the development of AD in that individual, and thus bypass the need for transgenic induction of the disease.

Takahashi and colleagues showed that iPSC generated from mouse fibroblasts resembled ESC with regards to morphology, gene expression, proliferation and formation of teratomas - and can give rise to adult chimeras capable of germline transmission when transplanted into blastocysts (Takahashi *et al.*, 2007). With appropriate stimulation iPSC can give rise to multiple cell types such as neurons, astrocytes, cardiomyocytes, pancreatic cells and liver cells (Lai *et al.*, 2011; Sanal, 2011) making them extremely versatile in terms of modelling disease. As iPSC are derived from tissues from consenting adults this bypasses the ethical limitations of ESC and allows for the generation of disease- and patient-specific cell lines. They also have the advantages of a normal karyotype and continuous self-renewal allows them to survive in culture indefinitely. iPSC technology has shown many applications in the fields of drug development, disease modelling, organ synthesis and tissue repair. Therefore, the introduction of iPSC technology has helped overcome many limitations associated with the use of animal models and ESC thereby helping to bridge the "gap" that exists between bench and bedside.

1.7.1.1 Generation of iPSC is a finely tuned process

A number of steps are involved in the generation of iPSC prior to differentiation namely sample collection, parent cell isolation and expansion, transfection, culture, expansion and characterisation. iPSC may be derived from a number of sources including skin fibroblasts, mesenchymal stem cells from bone marrow, hair follicles, mononuclear cells from peripheral blood, or even exfoliated renal epithelial cells from urinary sediments. Skin fibroblasts are the traditional source of iPSC, as the method of isolation is minimally invasive (Zhang *et al.*, 2016a).

Skin fibroblasts are isolated by taking a dermal punch from the forearm of the participant, this skin section is then cultured to encourage growth of fibroblasts. Early protocols forced somatic cells into a pluripotent state by means of retroviral transduction, whereby embryonic transcription factors (*OCT3/4*, *c-MYC*, *SOX2* and *KLF4*) are introduced into the adult cells. Subtle changes to the Yamanaka group's original protocol have occurred over the years including the use of different vectors and reprogramming genes. The latest protocols use non-integrating episomal plasmid vector to introduce the embryonic gene cocktail and the non-transforming form of *c-MYC*, *L-MYC* (Okita *et al.*, 2011), is now used thereby reducing the concern of differentiated cells forming teratomas or becoming cancerous following implantation. Once transfected the cells are cultured until iPSC

colonies begin to appear in culture, these colonies are then isolated and expanded to produce a pure iPSC culture, free from fibroblast contamination. iPSC then undergo a series of tests to ensure they present with the characteristics of pluripotent cells. The necessary characterisation tests to prove pluripotency are as follows: (i) morphology and gene expression is examined and compared to ESC, (ii) silencing of the retroviral transgenes should occur after approximately four passages, (iii) iPSC form embryoid bodies with markers for all three germ layers demonstrated by immunostaining and RT-PCR, and (iv) injection of undifferentiated iPSC colonies into immunodeficient mice results in the formation of teratomas (Bilican *et al.*, 2012).

1.7.1.2 Yamanaka Factors

In 2007, Takahashi and colleagues successfully dedifferentiated the first human fibroblasts using retro-virus-mediated transfection of four transcription factors now called the "Yamanaka factors", *OCT4*, *SOX2*, *KLF4* and *c-MYC.* These genes code for proteins which reverse and suppress differentiation of cells (Takahashi & Yamanaka, 2006; Takahashi *et al.*, 2007).

OCT4 is a member of the POU transcription factor family. It is central to pluripotency, therefore aids maintenance of pluripotency in stem cells as well as re-establishment of stemness in somatic cells (Shi & Jin, 2010). *OCT4* is highly expressed during development in ESC and germline cells, then expression declines as cells begin to differentiate. *OCT4* is essential for early embryonic development, its absence results in death of the embryo (Nichols *et al.*, 1998). Steroidogenic factor-1 and oestrogen-related receptor activate *OCT4* transcription (Yang *et al.*, 2007; Zhang *et al.*, 2008). *OCT4* acts to maintain pluripotency by simultaneously promoting expression of self-renewal genes and inhibiting expression of differentiation promoters (Nichols *et al.*, 1998), and modulating Wnt/β-catenin signalling (Abu-Remaileh *et al.*, 2010). Together with *SOX2*, *OCT4* is considered a master regulator of pluripotency, and further is considered indispensible in pluripotency reprogramming.

SOX2 is a member of the *Sry* gene family. It is necessary for neural tube development, highly expressed during early neurodevelopment and later localised to the ventricular layer of the cortex. *SOX2* is highly expressed by neural stem cells and neural progenitor cells, and functions to maintain pluripotency and self-renewal, and inhibits differentiation. *SOX2* is predominantly a self-regulating gene, it regulates epidermal

growth factor (EGF) receptor expression which in turn regulates *SOX2*. *SOX2* also activates transcription of sonic hedgehog, while the downstream factor *GLI2* in turn regulates *SOX2* transcription. *SOX2* activates *Nestin* and *Tlx*, while it suppresses *NeuroD1*. As such it is an important regulator of some major signalling pathways involved in neural development (Shen *et al.*, 2015).

KLF4 has been shown to directly bind the Nanog promoter to aid *OCT4/SOX2* regulation of Nanog expression (Zhang *et al.*, 2010). Therefore, *KLF4* is another transcription factor critical to maintaining the pluripotent and self-renewal properties of ESC (Di Giammartino *et al.*, 2019). *MYC* also regulates self-renewal and pluripotency. It acts via microRNA to both inhibit differentiation and promote cell division (Lin *et al.*, 2009; Chappell & Dalton, 2013). *c-MYC* was used in the original somatic cell reprogramming protocols (Takahashi & Yamanaka, 2006; Takahashi *et al.*, 2007). However, the non-transforming L-*MYC* is now more widely used (Okita *et al.*, 2011). Expression of these pluripotency factors can induce pluripotency in adult cells, and conversely developmental ques can be utilised to drive differentiation.

1.7.2 Neural differentiation drives iPSC towards a neural fate

Over the last decade, the introduction of technologies capable of reprogramming human somatic cells into human iPSC has led to a novel approach to studying neurodegenerative diseases *in vitro,* and a greater understanding into the pathophysiology of numerous neurological disorders. Since the first protocol describing neural induction of iPSC (Chambers *et al.*, 2009), many new protocols have been established and it is now possible to generate a variety of defined neuronal phenotypes from iPSC, for example dopaminergic and cortical neurons and regionalised astrocyte populations (Crompton *et al.*, 2017; McComish & Caldwell, 2018). The advent of PSC technologies, in particular the generation of iPSC, has facilitated research on a cellular and molecular level that was unattainable previously.

Neural differentiation protocols have rapidly evolved over the years significantly improving efficiency and purity and allowing patterning of regionalised neural progenitor cells and subsequently subtype specific neural cells. PSC can be differentiated into defined neural subtypes by modulating exogenous levels of signalling molecules present in the brain at significant developmental time points such as bone morphogenic protein (BMP), Wnt, SHH and fibroblast growth factor (FGF) (Petros *et al.*, 2011). By mimicking

cues which guide neural development in the embryo it is possible to generate regional-specific neural progenitors that can then be matured into neurons and glial cells in order to model human development and disorders of the CNS.

Human PSC can be differentiated using a number of protocols, e.g. monolayer, on plastic ware and in defined chemical conditions. Two main protocols have been developed to parallel *in utero* mechanisms involved in neurogenesis: the neurosphere-based technique and the monolayer-based method. There is some debate within the community as to which protocol is more effective. There are advantages and limitations associated with both protocols. Neurospheres recapitulate the environment within the embryo, i.e. a 3D bundle of cells (Nilbratt *et al.*, 2010; Crompton *et al.*, 2013), allowing for greater cell-cell and cell-matrix interactions, which some argue demonstrates a better imitation of endogenous differentiation (Chandrasekaran *et al.*, 2016). However, this method is also associated with the formation of other cell types, presenting the risk of contamination (Crompton *et al.*, 2017). Monolayer systems, on the other hand, can often lead to easier differentiations and result in more homogenous populations (Crompton *et al.*, 2017).

In the embryo, the three germ layers – mesoderm, endoderm and ectoderm – give rise to the tissues in the body. Neural tissue derives from ectoderm and it's development is under inhibitory control in vertebrates. Activin and BMP signalling, members of the transforming growth factor-β (TGFβ) family, inhibit neuralisation by inducing mesoderm and endoderm differentiation respectfully (Wilson & Hemmati-Brivanlou, 1995). These pathways are almost indistinguishable, both acting through downstream effector SMAD proteins (Pauklin & Vallier, 2015). Thus by inhibiting SMAD signalling ectoderm differentiation may be induced. The Studer laboratory found that dual SMAD inhibition (using SB431542 and Noggin) allowed for efficient neural induction, where Noggin is used to inhibit BMP signalling while SB431542 inhibits the TGFβ pathway. This monolayer method allows for rapid and uniform neural conversion of human iPSC (Chambers *et al.*, 2009).

There is now an abundance of protocols available for the differentiation of regionalised neural populations. Regional patterning is achieved by mimicking signals present in the developing neural tube. The rostro-caudal axis is generated with increasing concentration of the caudalising agent retinoic acid (RA). The dorso-ventral axis is set up by driving dorsal signalling with BMP or ventral signalling with SHH (Crompton *et al.*, 2017). These regionalising factors may be utilised to derive cell subtypes specifically affected in neurological disorders, e.g. cholinergic and cortical neurons may be used in AD focused

studies (Shi *et al.*, 2012; Crompton *et al.*, 2013; Duan *et al.*, 2014; Nistor *et al.*, 2015), while midbrain populations are useful when studying PD (Devine *et al.*, 2011), and spinal cord neurons and astrocytes are required to study spinal cord injury (Roybon *et al.*, 2013; Kawabata *et al.*, 2016).

1.7.2.1 Basal forebrain cholinergic neurons

The basal forebrain is considered the major source of acetylcholine (Ach) within the CNS and the main source of cholinergic input to the cortex (Bissonnette *et al.*, 2011). Basal forebrain cholinergic neurons (BFCN) are the earliest population of neurons to be affected by tau pathology in AD, resulting in loss of cholinergic input to the cortex and subsequently cognitive decline (Bissonnette *et al.*, 2011; Duan *et al.*, 2014). Cognitive impairment in AD has been linked to a loss of nicotinic ACh receptors (nAChR) (Nilbratt *et al.*, 2010), and as such dysfunction of the cholinergic system. Therefore these neuronal subtypes provide an extremely useful model to analyse the efficacy of drugs designed to combat neuronal loss in AD. iPSC-derived from AD patients may be differentiated into BFCN and used to elucidate why this cell population is so vulnerable.

Factors present in the forebrain which result in BFCN development include RA, SHH, FGF8 and BMP9. These factors must be present in the right combination, at the right time and at the right concentrations in order to differentiate BFCN. The Kessler laboratory elucidated a mechanism of BFCN differentiation in 2011, whereby patterning factors (RA, SHH, FGF8, BMP9) result in the transcription of the genes *Lhx8* and *Gbx1*, subsequently leading to the production of a population of cells positive for the basal forebrain markers choline acetyltransferase (ChAT) and p75 (Table 1.7.1). Removal of BMP9, or addition at incorrect time points and knockdown of *Lhx8* or *Gbx1* resulted in the generation of a neuronal population positive for the neuronal marker MAP2 but none of the BFCN-specific markers (Bissonnette *et al.*, 2011). Functional cholinergic neurons will provide a source for the screening of drugs targeting the cholinergic system, or a useful model for diseases involving dysfunction of the cholinergic system.

1.7.2.2 Cortical neurons

Cortical neurons represent a population of cells vulnerable to AD pathology, with severe cortical atrophy associated with this disease (Braak *et al.*, 2006; Stranahan & Mattson, 2010). This cortical atrophy results in cognitive decline, a classical symptom of AD (Geula, 1998). The primate cortex is different from that of the rodent in the following ways: it is significantly larger relative to the rest of the CNS, it is more complex and there is greater diversity within the neuronal cell population (Shi *et al.*, 2012). Therefore, iPSC have the potential to overcome the challenges linked to the production of animal models of disease of the cortex, including AD and schizophrenia.

Some studies have found that cortical neuron fate is determined *in vitro* prior to implantation (Gaspard *et al.*, 2008), while other studies have found that implanted cortical neurons developed dendritic and axonal connections applicable to the transplant site indicating that their fate is influenced by the environment (Ideguchi *et al.*, 2010). Dual-SMAD inhibition has successfully been used to derive cortical neurons from human iPSC (Table 1.7.1).

1.7.2.3 Midbrain dopaminergic neurons

Dopamine neurons of the substantia nigra pars compacta are the most vulnerable cells in PD. Significant loss of dopamine neurons results in the characteristic motor symptoms of PD due to a loss of dopamine in the striatum (Rinaldi & Caldwell, 2013). Given that idiopathic and genetic PD result from multiple genetic mutations, iPSC are proving a powerful model following derivation of midbrain dopaminergic neurons to study the intricacies of this debilitating disorder (see Table 1.7.1 for derivation protocols).

1.7.2.4 Spinal motoneurons

Spinal motoneurons are the key effector cells of motor function, relaying signals generated in the motor cortices of the brain to the muscles. The loss of motor neurons has been associated with a number of movement disorders including ALS (Lee *et al.*, 2007). The generation of protocols to derive motoneurons from human iPSC has not only provided a model for diseases affecting this cell population but also allowed further probing of development of the CNS (Table 1.7.1).

Brain region	Initial differentiation	Neuralising and regionalising factors	Summary of differentiation protocol	Time required for mature neurons	Characterisation markers and yield	References
Basal forebrain	iPSC Neurosphere	RA FGF8 SHH bFGF EGF NGF	Treatment with bFGF, RA, EGF, FGF8 and SHH. Transfected with Lhx8/Gbx1-IRES-GFP, FACS sorted.	~24 d	~ 60% $ChAT^+$ $MAP2^+$ Lhx8 Gbx1 VAChT Nkx2.1	(Duan *et al.*, 2014)
	ESC iPSC Embryoid body	SB431542 FGF2 EGF	Colonies were chopped, plated in low-adherence plastic ware and allowed to form EB (4 d). SB added D4-12 for neural enrichment. Neurospheres expanded in FGF2 + EGF (+ SB, 10 d). Basal forebrain identity is the result of endogenous SHH secretion in EB.	~80 d	> 90% $TUJ1^+$ $ChAT^+$ > 90% $NESTIN^+$ $NKX2.1^+$ VAChT ISL1 FOXG1 $P75^{NTR}$ *Nkx2.1* *Lhx8* *SHH*	(Crompton *et al.*, 2013)
	ESC Neurosphere	RA SHH FGF8 BMP9 bFGF	Cells induced with bFGF, RA, FGF8 and SHH. BFCN were derived from NPC by addition of BMP9 or neucleofection with Lhx8, Gbx1.	35-40 d	94% $ChAT^+$ MAP^+ P75 *Lhx8* *Gbx1*	(Bissonnette *et al.*, 2011)
	ESC Neurosphere	NGF BDNF NT-3 CNTF EGF bFGF	1. Suspension culture: Neurospheres expanded in bFGF and EGF. 2. Adherent culture: Neurospheres dissociated,	> 70 d	76±1.8% *Nkx2.1* > 69% ChAT $P75^{NTR}$ *Gsh2* *Dlx1/2* *Gbx2*	(Nilbratt *et al.*, 2010)

		NT-4	plated and treated with BDNF, CNTF, NT-4 and NGF.		*Lhx6/8* Islet-1	
Cortical	ESC iPSC	Dorsomorphin/noggin SB431542 FGF2	SMAD inhibition (noggin/dorsomorphin and SB431542; 12 days). NSC expanded with N2 and B27. FGF2 added to neural rosettes. Neurons maintained for up to 80 days. Early projection neurons ~2-3 weeks after initiation of induction. Layer 2 neurons ~90 d.	> 80 d 45-50 d synapses appear 2-3 months neural networks appear	> 90% $Pax6^+$ Deep-layer: Tbr1 CTIP2 Upper-layer: Satb2 Cux1 Brn2	(Shi *et al.*, 2012)
Midbrain	PSC	SB431542 Noggin SHH-C24II CHIR99021 FGF8b BDNF AA GDNF DAPT db-cAMP	Dual SMAD inhibition (SB431542, noggin), SHH, CHIR and FGF8b (D9 only). From day 16+ NPC may be matured by plating and addition of BDNF, AA, GDNF, db-cAMP and DAPT.	~ 16 d for NPC > 40 d for mature neurons	~ 80% $LMX1^+$ $FOXA2^+$ ~ 95% $LMX1^+$ $OTX2^+$ TH EN1 MAP2	(Nolbrant *et al.*, 2017)
	iPSC Monolayer protocol	Noggin SB431542 Dorsomorphin SHH C24II Wnt1 Dkk1 blocking antibody FGF2 BDNF	SB, dorsomorphin, SHH C24II, Wnt1 and Dkk1 blocking antibody. NPC maintained in SHH, BDNF, AA and FGF8, and matured in BDNF, AA, GDNF, TGFβ3 and db-cAMP.	> 25 d	~ 30% TH^+ $TUJ1^+$ α-synuclein LMX1B *LMX1A* *NURR1* *TH* *DAT*	(Devine *et al.*, 2011)

		GDNF AA FGF8 TGFβ3 db-cAMP				
	ESC Monolayer	FGF8 SHH C24II LDN193189 SB431542 CHIR99021 Purmorphamine BDNF GDNF TGFβ3 AA db-cAMP DAPT	Cells induced with FGF8, SHH C24II, LDN193189, SB431542, CHIR99021 and purmorphamine. Expanded in media with CHIR, BDNF, GDNF, TGFβ3, AA, cAMP and DAPT.	~ 60 d	> 60 % TH^+	(Kriks *et al.*, 2011)
	iPSC	Noggin SB431542 SHH FGF8 BDNF AA GDNF TGFβ3 cAMP	Dual SMAD inhibition with noggin/SB431542. BDNF, AA, SHH and FGF8. Cells matured in BDNF, GDNF, AA, TGFβ1 and cAMP.	~19 d	82% $(HES5\text{-}GFP)^+$ TH	(Chambers *et al.*, 2009)
Striatal	ESC	LDN193189 SB431542 SHH DKK1 BDNF	LDN + SB D0-D12; SHH + DKK1 D5-D25; BDNF D25+.	50 d	~ 40% $PAX6^+$ after 15 d ~ 30% $CTIP2^+$ ~ 15% $CTIP2^+$ $DARPP32^+$ ~ 6% $CTIP2^+$ $DARPP32^+$ $GABA^+$	(Besusso *et al.*, 2020)

	iPSC Monolayer	SB431542 LDN193189 Dorsomorphin SHH Cyclopamine Activin A BDNF GDNF	Cells induced with SB, LDN, dorsomorphin, SHH, cyclopamine for 10 d. Activin A added at day 9. Neurons matured in BDNF, GDNF.	~ 40 d	> 50% CTIP2$^+$ > 50% GSX2$^+$ > 30% DARPP32$^+$ NKX2.1 MAP2	(Arber *et al.*, 2015)
	ESC iPSC	LDN193189 Noggin SB431542 Wnt3a CHIR99021 DKK1 XAV-939 SHH Cyclopamine BDNF db-cAMP Valpromide	Dual SMAD inhibition D0-10; Wnt3a + CHIR (or DKK1 + XAV) D1-20/28; SHH (or cyclopamine) D10-20/28; BDNF + db-cAMP + valpromide D20+.	60 d	40-70% MAP2$^+$ 15-30% MAP2$^+$ DARPP32$^+$ 15-25% MAP2$^+$ Calbindin$^+$ Calretinin CTIP2 FOXG1 FOXP1 DRD2 Sub P	(Nicoleau *et al.*, 2013)
Spinal cord	iPSC ESC	SB431542 Dorsomorphin N-acetylcysteine RA Purmorphamine bFGF BDNF GDNF Forskolin	Dual SMAD inhibition and RA. Cell expanded in purmorphamine and FGF. Neurons matured in BDNF, GDNF, and forskolin.	~ 70 d	> 80% Nestin$^+$ Sox1$^+$ ~ 50% HB9$^+$ SMI-32	(Bilican *et al*., 2012)
	iPSC	Noggin SB431542 SHH	Dual SMAD inhibition using noggin/SB431542, with BDNF, AA, SHH and RA.	~19 d	*ISL1* *HB9*	(Chambers *et al.*, 2009)

		RA BDNF AA				
	ESC Neural rosette	SHH RA Noggin AA BDNF	Cells induced MS5 stromal cells with SHH, RA, noggin. Cells maintained in media with AA, BDNF and GDNF.	> 60 d	20% $HB9^+$ Olig2	(Lee *et al.*, 2007)
	ESC Neural rosette to adherent monolayer	RA SHH cAMP FGF2 BDNF GDNF IGF1	Cells induced with RA, SHH and cAMP. Expanded with BDNF, GDNF and IGF1.	~ 50 d	~ 21% $HB9^+$ HoxC8 ChAT VAChT	(Li *et al.*, 2005)
Motor neurons	ESC iPSC	SB431542 DMH1 CHIR99021 RA Purmorphamine Compound E (Cpd E)	CHIR + SB + DMH for 6 d. CHIR + SB + DMH + RA + purmorphamine for a further 6 d generates MNP. RA + purmorphamine for 6 d. RA + purmorphamine + Cpd E for a further 10 d for MN.	12 d for MNP ~ 28 d for MN	> 90% $OLIG2^+$ 90±9% $MNX1^+$ 95±3% $ISL1^+$ > 90% $MAP2^+$ $ChAT^+$ SOX1 HOXA3 NKX2.2	(Du *et al.*, 2015)

Table 1.7.1. Human PSC-derived regional-specific neurons.

Neurons may be generated from iPSC by mimicking the signals present during embryonic development, and many protocols now exist to generate regionally defined neural progenitor cells which may subsequently be matured into neurons. Neuralising agents such as noggin, dorsomorphin and SB431542 drive ectoderm differentiation by inhibiting mesoderm and epithelial differentiation (i.e. SMAD inhibition) respectively to derive NPC. Regional patterning is achieved by mimicking signals present in the developing neural tube. The caudalising agent retinoic acid can be utilised to derive spinal cord astrocytes. The dorsoventral axis is set up by driving dorsal signalling with BMP or ventral signalling with SHH. Abbreviations: retinoic acid (RA), fibroblast growth factor (FGF) 8/2, sonic hedgehog (SHH), basic fibroblast growth factor (bFGF), epidermal growth factor

(EGF), nerve growth factor (NGF), fluorescence-activated cell sorting (FACS), choline acetyltransferase (ChAT), microtubule-associated protein 2 (MAP2), vesicular acetylcholine transporter (VAChT), Insulin gene enhancer protein (ISL1), embryoid body (EB), bone morphogenic protein 9 (BMP9), neural progenitor cell (NPC), brain-derived growth factor (BDNF), neurotrophin (NT)-3/4, ciliary neurotrophic factor (CNTF), glial cell-derived neurotrophic factor (GDNF), ascorbic acid (AA), transforming growth factor beta (TGFβ), dibutyryl cyclic-AMP (db-cAMP), tyrosine hydroxylase (TH), neuron-specific Class III β-tubulin (TUJ1), motoneuron (MN), Insulin-like growth factor 1 (IGF1), Compound E (Cpd E).

1.7.2.5 Human iPSC-derived regionalised astrocytes

Given that astrocytes represent up to 40% of brain cells (Crompton *et al.*, 2017) it is vital that they be included when modelling neurodegeneration to give a more representative disease model. Astrocytes are commonly isolated from rodent brain samples and cultures are typically contaminated with other cell types, such as microglia, therefore deriving astrocytes from iPSC is the most convenient method of attaining disease-specific astrocyte cultures of a high purity level. Astrocytes are a heterogeneous cell population (Matias *et al.*, 2019), and much like neurons have different subtypes related to location, morphology, etc. Morphologically human astrocytes are larger, structurally they are more complex, and functionally more diverse than their rodent counterparts (Oberheim *et al.*, 2012). It follows therefore that it is imperative that human astrocytes be used in studies attempting to understand their function in pathological circumstances. The isolation of primary human astrocytes is not trivial and requires post mortem brain tissue. These primary astrocytes are then difficult to grow in culture having been removed from their structurally supportive environment. As such alternative approaches to culturing human astrocytes have been pursued. The current go to method is deriving astrocytes from human iPSC.

The change from neurogenesis to gliogenesis requires Notch signalling, which activates the JAK/STAT3 pathway and acts to promote astrogliogenesis (Kamakura *et al.*, 2004). There are a number of current protocols that focus on this gliogenic switch, allowing for the differentiation of astrocytes (Roybon *et al.*, 2013; Chandrasekaran *et al.*, 2016). A significant study by Emdad described the production of astrocytes via human iPSC which were indistinguishable from those produced from human ESC (Emdad *et al.*, 2012). Serio and colleagues generated astrocytes from human iPSC neural progenitors using gliogenic cytokines EGF, leukemia inhibitory factor (LIF) and ciliary neurotrophic factor (CNTF). These transcriptional activators allow for differentiation of neural progenitor cells (NPC) towards an astrocytic fate. In this study, a high yield of glial fibrillary acidic protein (GFAP) positive cells were derived in a much shorter time period than required without (Serio *et al.*, 2013).

The ability to generate specific defined astroglial populations from iPSC allows for research to focus on the brain regions and specific cell types affected in neurological diseases. Due to regional differences it is important to characterise these astrocyte populations and use the appropriate region when modelling disease. Human astrocytes have been successfully generated from both ESC and iPSC with numerous established

protocols for differentiation existing in the literature today, however a paucity remains with regards to regional-specific protocols. Table 1.7.2 summaries protocols for the generation of PSC-derived astrocytes.

Brain region	Initial differentiation	Neuralising and regionalising factors	Astrogliogenic factors	Summary of differentiation protocol	Time required for mature astrocytes	Characterisation markers and yield	References
n/a	iPSC	Noggin PDGF-AA	FGF2 EGF hLIF	SMAD inhibition followed by JAK/STAT induction.	> 50 d	> 80% $CD44^+$ ~90% $S100\beta^+$ ~50% $ALDH1L1^+$ GFAP	(Santos *et al.*, 2017)
Cortical	iPSC-derived NPC Monolayer	FGF2 CNTF BMP2	EGF Insulin	Astrocyte differentiation was induced with medium modified from Shaltouki *et al*. (FGF2, CNTF and BMP2) (Shaltouki et al., 2013) and addition of EGF and insulin.	~30 d	> 95% $GFAP^+$ EAAT1 S100β GS	(Jones *et al.*, 2017)

n/a	iPSC Neurospheres and monolayer	SB431542 Dorsomorphin N-acetylcysteine RA Purmorphamine bFGF BDNF GDNF Forskolin	EGF LIF FGF CNTF	MN precursors generated as described *(Bilican et al*., 2012). Enriched for APC with EGF, LIF, Expanded in EGF, FGF2. Terminally differentiated with CNTF.	> 100 d	90.6±0.7% $GFAP^+$ 91.9±1.9% $S100\beta^+$ Vimentin NFIA EAAT1 *GFAP* *S100β*	(Serio *et al*., 2013)
n/a	ESC iPSC Embryonic body protocol	CT-1 JAG1 Noggin SB431542	FGF2 EGF CNTF	EB dissociated, treated with FGF2, EGF, and CNTF. Once neural rosettes formed noggin and SB431542 used for terminal differentiation.	~35 d	55-70% $GFAP^+$ *S100* *GLT-1*	(Emdad *et al*., 2012)
n/a	ESC Neurosphere	BMP4 LIF	FGF2 EGF	Neurospheres plated as a monolayer. Expanded in FGF2 and EGF; 2 months. Cells treated with BMP2, BMP4 and LIF for terminal differentiation.	> 60 d	95.7±3.1% $GFAP^+$ 79.4±1.0% $AQP4^+$ 90.1±2.0% $S100\beta^+$ 89.5±3.2% $EAAT1^+$	(Gupta *et al*., 2012)

n/a	PSC	FGF8 RA SHH	EGF FGF2	Cells treated with FGF8, RA or SHH for rosette formation. Rosettes patterned with EGF, FGF2. Matured with CNTF.	> 90 d	> 90% S100β$^+$ > 90% GFAP$^+$ CD44 Nkx2.1	(Krencik *et al.*, 2011)
n/a	Patient-derived iPSC	SB431542 DMH1 CHIR99021 RA Purmorphamine Compound E (Cpd E)	FBS	MNP were derived as per Du *et al*., 2015. MNP were further cultured in DMEM/GlutaMAX with 10% FBS to generate astrocytes.	> 16 d	100% GFAP$^+$	(Madill *et al.*, 2017)
Multiple	ESC iPSC	SB431542 LDN193189 XAV939	NFIA FGF2 EGF LIF	Dual SMAD for 8 d (PSC → NSC), + XAV939 (D0-D2) for anterior forebrain. Viral transduction of NFIA for 5 d (↑CD44). Expanded in LIF for 77 d to generate GFAP$^+$ APC.	~ 77 d	> 90% GFAP$^+$ CD44 NFIA SLC1A2 S100β	(Tchieu *et al.*, 2019)

Table 1.7.2. Human PSC-derived regional specific astrocytes.

Astrocytes may be generated from iPSC by mimicking the signals present during embryonic development, and many protocols now exist to generate astrocytes from regionally defined NPC. Regionalised NPC can then derive glia with addition of factors such as EGF, CNTF and hLIF. Abbreviations: platelet-derived growth factor (PDGF), human leukaemia inhibitory factor (hLIF), aldehyde dehydrogenase 1 family member L1 (ALDH1L1), glial fibrillary protein (GFAP), excitatory amino acid transporter 1 (EAAT1), glutamine synthetase (GS), astrocyte precursor cell (APC), creatine transporter (CT1), aquaporin (AQ)4, motor neuron progenitor cells (MNP).

1.8 Overarching aims and hypotheses

1.8.1 Aims

AD affects tens of millions globally and incidence is expected to increase as the global population continues to live longer. Although much resources are spent on developing new therapeutics, at the time of writing, only five drugs are available with FDA approval for the treatment of AD. Of these medications, none have the capability of halting or reversing disease pathogenesis. AD research exhibits a high failure rate in therapeutics at the clinical stage, owing to translational issues from animal models to human trials. This suggests that there are still large gaps in our fundamental understanding of AD at a cellular level, and further the role of the leading genetic risk factor *APOE4*.

The aims of this study are to build on research over the past decade which place astrocytes at the centre of AD pathology. Taking advantage of the latest PSC technologies, iPSC of known APOE genotypes will be used to generate astrocytes and neurons in order to investigate the interplay between neuroinflammation and APOE genotype on astrocyte reactivity and functionality.

1.8.2 Hypotheses

APOE4 is the largest genetic risk factor for sporadic AD but its role in pathology remains enigmatic. The aims of this study are to investigate the link between two molecular hallmarks of AD, namely neuroinflammation and disturbed glutamate dynamics, with respect to APOE genotype.

The hypotheses pertaining to these aims are:

1. iPSC can successfully be used to derive cortical astrocytes with APOE3 and APOE4 homozygous genotype to be used as the model system.
2. iPSC-derived astrocytes will respond to inflammatory insult resulting in generation of a reactive phenotype; APOE4 homozygous astrocytes are expected to be more inflammatory with respect to expression of reactive astrocyte markers.
3. iPSC-derived astrocytes will be functionally capable of glutamate uptake; reactivity and APOE4 genotype is expected to have a detrimental effect on astrocyte ability to uptake glutamate.

Chapter 2

Materials and Methods

2. Methods

2.1 Cell culture

The following cell lines were used throughout this research:

- A non-affected sibling 2 (NAS2) iPSC line kindly gifted by Dr Tilo Kunath (University of Edinburgh, UK). This line was generated as part of a PD study where it was used as the control for a PD patient line (Devine *et al.*, 2011). The NAS2 line was genotyped for APOE and found to be *E3E3* homozygous (Table 2.1.1). This iPSC cell line is now available to purchase via the European Bank for induced pluripotent Stem Cells under the cell line name EDi002-A (https://cells.ebisc.org/EDi002-A/).
- *E4E4* homozygous iPSC line derived from human dermal fibroblasts by episomal plasmid vector reprogramming as per Okita *et al*., 2011 were generated by Dr Lucy Crompton at the University of Bristol (Table 2.1.1. and Appendix 1). The *E4E4* homozygous participant donated skin cells after learning of their APOE genotype following a free genome screen via 23andMe. Genotype was confirmed by Dr Crompton using a Taqman PCR SNP genotyping kit.

All cell culture techniques were carried out in a sterile laminar flow hood (Nuaire, USA). All materials used were autoclaved and sterile to prevent bacterial or fungal contamination. Aseptic techniques were used throughout cell culture. Materials entering the laminar flow hood were sprayed with 70% ethanol to maintain sterile conditions. Cells were incubated in a humidified (37°C, 5% CO_2) incubator (Nuaire, USA).

	NAS2 (*E3E3*)	*E4E4*
Age	30-34	49
Sex	Female	Male
Ethnic Origin	Iowa kindred	Unknown
Medical History	Strong family history of Parkinson's disease due to autosomal dominant inheritance of *SNCA* triplication. This donor did not inherit the mutation.	No record of disease onset at time of cell donation.
Medication	Unknown	Unknown
Tissue Origin	Fibroblast of dermis	Dermal punch (anterior forearm) to isolate fibroblasts
Reprogramming methods	Retroviral transduction of the four Yamanaka reprogramming factors; *OCT4*, *SOX2*, *KLF4* and *c-MYC*	Episomal plasmid vector was used to introduce embryonic genes – *OCT4*, *SOX2*, *KLF4* and *l-Myc* – according to Okita *et al*. 2011

Table 2.1.1. iPSC donor information.

2.1.1 iPSC maintenance and passaging

iPSC were cultured in complete Essential 8^{TM} flex media (E8; Thermo Fisher Scientific, USA) on Vitronectin (VTN; 0.5 µg/cm^2; Thermo Fisher Scientific, USA) coated 6-well plates (Chen *et al.*, 2011a). Media was changed daily (2 mL) and cells were given extra media for weekend breaks (2 mL/day). Cells were passaged upon reaching 80% confluency following the E8 culture system protocol suggested by the manufacturer. Spent media was removed and discarded, cells were washed once with phosphate buffered saline (PBS; 1 mL; Thermo Fisher Scientific, USA), once with ethylenediaminetetraacetic acid (EDTA; 0.5 mM; 1 mL; Thermo Fisher Scientific, USA), and then cells were dissociated by incubation with EDTA (1 mL, 4 min, RT). EDTA was removed and cells washed once with fresh E8 (1 mL) to remove remaining EDTA which might affect adherence. Cells were then detached from the culture vessel with 2 mL of fresh E8 media, collected in a falcon tube and plated on a new VTN-coated plate at an appropriate split ratio. 1:4 is the classic split ratio for expanding iPSC, while lower densities are used on the passage before initiating the neural induction protocol.

2.2 NPC cell culture

2.2.1 Neural induction for the generation of cortical neural progenitor cells

Prior to neural induction iPSC should be passaged at a lower density such that 4 d following passage colonies are numerous but small with smooth defined edges. iPSC with these characteristics are ideal for neural induction (Figure 2.2.1).

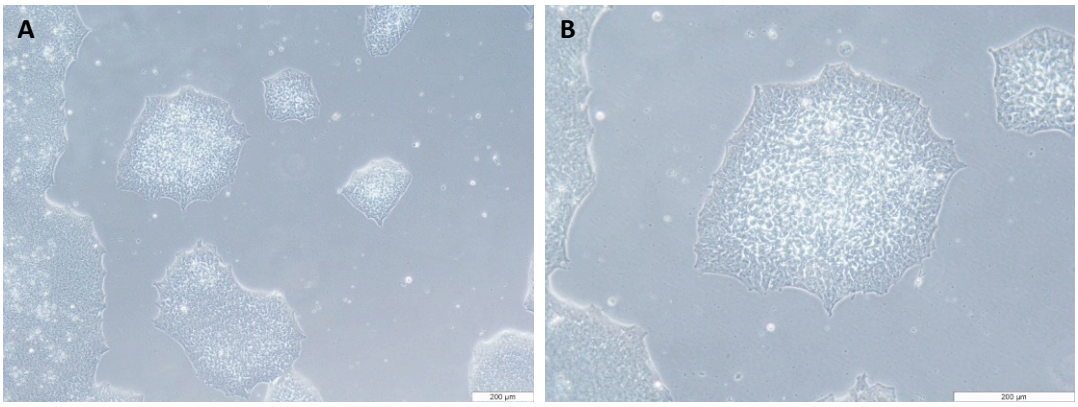


Figure 2.2.1. NAS2 iPSC colonies ready for neural patterning.

Colonies are small and well-spaced (A). Colonies have a dense centre with smooth edges (B). Images taken at passage 58. Scale bar represents 200 µm.

Neural induction, protocol optimisation and associated troubleshooting is described in full in Section 3.1.8 of this thesis.

2.2.2 Expansion of NPC and plating for terminal differentiation

From D11 onwards, NPC were cultured in neural maintenance media [NMM; 1:1 DMEM/F-12 + Glutamax and Neurobasal media, 1% non-essential amino acids (NEAA), 0.5% Glutamax, 1% penicillin-streptomycin (pen/strep), 0.5% N2, 1% B27, β-mercaptoethanol (75 µM), insulin (5 µg/mL)] on polyornithine (PO; 1 µg/cm^2; 1 h, 37°C; Sigma-Aldrich, UK) and laminin (1 µg/cm^2; Engelbreth-Holm-Swarm murine sarcoma basement membrane; 2 h, 37°C; Thermo Fisher, USA) coated 6-well plates (Nunc by Thermo Fisher Scientific, USA). Cells were fed every other day (2 mL) and extra media was given for weekend breaks (2 mL/day).

NPC were passaged upon reaching 100% confluency. Spent media was removed and discarded, cells were washed once with PBS, and then cells were dissociated by incubation with Accutase (1 mL, 3-4 min, RT; Thermo Fisher Scientific, USA). Accutase was removed, cells were washed once with NMM then lifted with NMM, collected in a falcon

tube and transferred onto a fresh PO/laminin coated plate at an appropriate split ratio (usually 1:3). RevitaCell (1:100; Thermo Fisher Scientific, USA) or ROCK inhibitor Y-27632 (10 µM; Bio-Techne, USA) was added after passaging to aid cell survival (Watanabe *et al.*, 2007).

NPC were plated on 24-well plates for maturation and subsequent treatment. Cells were dissociated as described for passaging and centrifuged (1000 rpm, 3 min, RT). Once pelleted, cells were resuspended in 1 mL NMM. The cell suspension was further diluted 1:10 with NMM, RevitaCell (1:100) added and cells were plated on PO/laminin coated coverslips at a density of 100 µL cells per coverslip. Cells were incubated overnight to adhere, with PBS between the wells to increase humidity. Next morning, wells were topped up with NMM (500 µL/well). NPC were left untouched for 3-5 d before characterisation or treatment.

2.3 Astrocyte cell culture

NPC may stimulated to induce differentiation into glial precursor cells. The astrocyte progenitor differentiation protocol, along with optimisation and troubleshooting steps will be discussed later in Section 3.1.10 of this thesis.

2.3.1 Expansion of APC and plating for terminal differentiation

Astrocyte progenitor cells (APC) were passaged upon reaching 100% confluency onto Geltrex (1X; 2 hr; 37°C) coated plates. Spent media was removed and discarded, cells were washed once with PBS, and then incubated with Accutase (1 mL, 3-4 min, RT; Thermo Fisher Scientific, USA). Accutase was removed and cells lifted with Serio, collected in a falcon tube and centrifuged (1000 rpm, 3 min). The supernatant was removed and discarded, and the cells resuspended in 1 mL and transferred onto a fresh Geltrex coated plate at an appropriate split ratio (usually 1:4). RevitaCell (1:100; Thermo Fisher Scientific, USA) or Y-27632 (10 µM; Bio-Techne, USA) was added after each passage to aid cell survival (Watanabe *et al.*, 2007). APC were expanded until D80 before plating for terminal differentiation and characterisation experiments (described later in Section 3.2.5).

APC were plated from D80 for terminal differentiation prior to characterisation and stimulation studies. Cells were dissociated and detached as for passaging. Once pelleted cell supernatant was removed and discarded, and the cell pellet resuspended in 1 mL fresh Serio media. Cells were prepared for counting by first taking a 10 µL aliquot of cell suspension, diluting 1:5 in Serio media and subsequently diluting 1:2 in trypan blue (0.4%; Thermo Fisher Scientific, USA) to give a final dilution factor of 10. Cells were counted using a haemocytometer. Cells were plated on oven autoclaved, Geltrex coated (10X; 2 h, 37°C) coverslips at a density of 5×10^4 cells per coverslip for immunofluorescence staining. Cells were plated on Geltrex coated (1X; 2 h, 37°C) 24-well plates at a cell density of 2×10^5 cells per well for qPCR analysis. Cells were incubated for 30 min to adhere, then wells were topped up with Serio (500 µL/coverslip or 1 mL/well). Once cells reached confluency media was changed to terminal differentiation media, Serio supplemented with BMP4 (20 ng/mL; R&D Systems, UK) and human LIF (hLIF; 20 ng/mL). Cells were matured for 7 d followed by 3 d in Serio media without factors prior to experimentation (Figure 2.4). Mature astrocytes may be used in experiments up to D120, after which they reach the end of their life span in culture.

2.3.2 Cryopreservation of cells

iPSC, NPC past D20 and APC may be cryopreserved in liquid nitrogen for long term storage. Cells are dissociated as per the appropriate passaging protocol, detached with media, collected in a 15 mL Falcon tube and centrifuged (1000 rpm, 3 min, RT). Media was removed, taking care not to disturb the cell pellet and cells resuspended in CryoStor cell cryopreservation media (500 µL; Sigma-Aldrich, USA). Resuspended cells were transferred into a re-labelled cryovial (Thermo Fisher Scientific, USA), which was then put in a Nalgene Mr Frosty cryo freezing container (Thermo Fisher Scientific, USA) containing propanol (200 mL) in the -80°C freezer to freeze at a rate of 1°C per minute. Once frozen, cryovials were transferred into liquid nitrogen for long term storage.

2.3.2.1 Recovery of frozen cell stocks

Cells were quickly defrosted by incubating in a water bath (37°C) until the contents are almost fully defrosted. The cryovial is transferred to a sterile culture hood to ensure cells are maintained under sterile conditions. Defrosted cells in CryoStor media are transferred to a 15 mL falcon tube and warm culture media is added (1:10) to dilute the dimethyl sulfoxide (DMSO) containing CryoStor media and prevent cytotoxicity. Media is added dropwise to prevent osmotic shock. Cells are centrifuged (1000 rpm, 3 min, RT), DMSO contaminated media is removed and discarded and cells are resuspended in fresh media and added to pre-coated plates (usually 1 cryovial = 1 well of a 6-well plate).

2.3.3 Quality Control

2.3.3.1 Mycoplasma testing

Mycoplasma is a genus of bacteria that lack a cell wall, providing them with resistance against antibiotics which target bacterial cell walls. Mycoplasma cells are approximately 1 µm in size meaning they cannot be visualised using an inverted light microscope. This characteristic combined with resistance to antibiotics commonly used in cell culture, i.e. penicillin and streptomycin, means that mycoplasma infection can go undetected without regular screening.

Cultures were regularly tested for mycoplasma infection using the PlasmoTest™ Mycoplasma Detection Kit (InvivoGen, USA) as per the manufacturer's instructions. Briefly, HEK-Blue™-2 cells were thawed and maintained in DMEM (high glucose)

supplemented with FBS (10%), pen/strep (1%) and Normocin™ (100 µg/mL). Media exposed to cell cultures for at least 24 h was collected (500 µL) and samples were heated (100°C, 15 min) prior to testing. HEK-Blue™ Detection solution was prepared by solubilising the powder in HEK-Blue™ water (50 mL) then filtering before use. Samples and positive control (50 µL) were loaded onto a 96-well plate. A cell suspension of HEK-Blue™-2 cells in HEK-Blue™ Detection medium was prepared, added to samples and controls (200 µL), and incubated (16-24 h, 37°C, 5% CO_2). Presence of mycoplasma contamination was assessed by examining the colour of the samples. The test is based off TLR2 signalling whereby mycoplasma binding to TLR2 results in a colour change which can be compared to a pre-prepared positive control; purple/blue indicates presence of mycoplasma, and pink indicates absence of mycoplasma.

2.4 Molecular biology methods

2.4.1 Analysis of gene expression by quantitative polymerase chain reaction

Messenger RNA (mRNA) expression was determined in cell lysates by quantitative polymerase chain reaction (qPCR) following RNA isolation and complementary DNA (cDNA) manufacture. Invented by Kary Mullis in 1983, PCR is a molecular biological technique used to study gene expression in a population of cells. By rapidly copying a DNA sample, a very small starting sample of DNA may be amplified enough to study its gene expression in detail. Since the original sample is mRNA isolated from the cell population of interest, PCR can be used to determine what genes are being expressed at the time of sample harvest.

2.4.1.1 Sample collection and preparation

Cells were lysed in lysis buffer consisting of RA1 lysis buffer (350 µL per sample) and β-mercaptoethanol (3.5 µL per sample) and lysates stored at -80°C prior to RNA isolation. All RNA isolation, cDNA manufacture and qPCR setup procedures were carried out in a designated molecular biology fume hood (Premier, Scotland) cleaned with 70% ethanol and RNase-away (VWR International, UK) to remove RNAase and DNases that breakdown RNA and DNA respectively.

2.4.1.2 RNA isolation

RNA was isolated using a NucleoSpin® total RNA isolation kit (Macherey-Nagel, Germany) as per the manufacturer's instructions. Each new kit was completed by reconstituting rDNase with RNase-free H_2O (550 µL) then dispensing into aliquots and storing at -20°C, and preparing RA3 buffer by adding molecular biology grade ethanol (ethyl alcohol, 200 proof; 48 mL; Sigma Aldrich, UK). Before each isolation, DNase reaction mixture was prepared by combining reconstituted rDNase (10 µL per sample) and reaction buffer (90 µL per sample), and 70% ethanol was prepared by adding ethyl alcohol (7 mL) to RNase-free H_2O (3 mL). Cell lysates were added to pink NucleoSpin® filter units in collection tubes and centrifuged (11000 x g, 1 min) to filter the lysate. The filter tubes were discarded and 70% ethanol (350 µL) was added to adjust RNA binding conditions and triturated. The lysates were loaded into blue NucleoSpin® RNA II columns in collection tubes to bind the RNA and centrifuged (11000 x g, 30 s). The columns were placed into new collection tubes,

membrane desalting buffer (350µL) was added to desalt the membrane and the tubes were centrifuged (11000 x g, 1 min). DNase reaction mixture (95 µL) was added to the centre of the column and incubated (15 min, RT) to digest DNA. RAW2 buffer (200 µL) was added to the column to inactivate the rDNase and centrifuged (11000 x g, 30 s). The blue columns were placed in new collection tubes. RA3 buffer (600 µL) was added to the column and centrifuged (11000 x g, 30 s). The blue columns were placed in new collection tubes. RA3 buffer (250 µL) was added to the column and centrifuged (11000 x g, 2 min) to dry the membrane. The columns were placed into nuclease-free micro centrifuge tubes (1.5 mL). RNase-free H_2O (40 µL) was added to the column and centrifuged (11000 x g, 1 min) to elute the RNA. The concentrations of RNA isolated from each sample were assessed using a NanoDrop 2000 Spectrophotometer (Thermo Scientific, USA) and then equalised to 40 ng/mL by adding the appropriate amount of RNase-free H_2O. Equalised RNA was stored at -80^oC prior to cDNA manufacture.

2.4.1.3 cDNA manufacture

Isolated RNA was reverse transcribed into cDNA using a High-Capacity cDNA manufacture kit (Applied Biosystems, USA) as per manufacturer's instructions. 2X RT reaction mix was prepared by adding 10X RT buffer (2 µL per reaction), 25X dNTP mix (100 mM, 0.8 µL per reaction), 10X RT random primers (2 µL per reaction), MultiScribe RT (1 µL per reaction) and nuclease-free H_2O (4.2 µL). 2X RT reaction mix (10 µL) was added to equalised RNA (10 µL), the tubes were centrifuged to mix the contents (1000 rpm, 1 min) and loaded in the thermal cycler (PTC-200 Peltier Thermal Cycler, MJ Research, USA) to run on the AB-cDNA program (25°C for 10 min, 37 °C for 120 min, 95 °C for 5 min, 4 °C for ∞). cDNA was diluted 1:4 with nuclease-free H_2O and stored at -20^oC prior to qPCR analysis.

2.4.1.4 Quantitative polymerase chain reaction

The manufactured cDNA was amplified using multi-target qPCR. PCR mastermix was prepared by adding target primer (0.5 µL per sample), endogenous primer (0.5 µL per sample), and Taqman mastermix (5 µL per sample). cDNA samples (4 µL) were loaded on a 96-well PCR fast plate (Thermo Fisher Scientific, USA) in an ice block. PCR mastermix (6 µL) was added and the plate centrifuged (1000 rpm, 1 min). The plate was then inserted into an ABI Prism 7300 Fast Track Sequence Detection System (v1.4.1, Applied Biosystems, USA). The Step One Real Time PCR System was run (Comparative Ct program)

using GAPDH (Hs02786624_g1, VIC) as the endogenous control with the following stages: holding stage 1, 50°C, 120 s; holding stage 2, 95°C, 20 s; cycling stage 95°C, 1 s and 60°C, 20 s for 40 cycles. Gene expression data was analysed using the Livak ΔΔCt method to produce a relative quantity (RQ) value of target gene expression relative to GAPDH expression as per formulae in Figure 2.4.1.

$$\Delta Ct = Ct_{TARGET} - Ct_{ENDOGENOUS}$$

$$\Delta\Delta Ct = \Delta Ct_{SAMPLE} - \Delta Ct_{CONTROL\ SAMPLE}$$

$$RQ = 2^{-\Delta\Delta Ct}$$

Figure 2.4.1. Livak Method.

Cycle threshold (Ct) values of target and endogenous gene expression were used to calculate relative quantity (RQ) against the control sample.

2.5 Protein analysis

2.5.1 Analysis of cytokine secretion by enzyme-linked immunosorbent assay (ELISA)

Enzyme-linked immunosorbent assay (ELISA; R&D Systems, USA) was used to assess the concentrations of IL6, RANTES (Regulated upon activation, normal T cell expressed and presumably secreted) and granulocyte-macrophage colony-stimulating factor (GM-CSF) secreted into the supernatant obtained from cultured astrocytes.

First described in 1971 by Engvall and Perlmann, the ELISA is a quantitative biochemical assay used to detect and quantify the presence of a ligand of interest in a liquid sample, e.g. protein, peptide, hormones, etc. ELISA uses a plate-based enzyme immunoassay and antibodies directed against the protein of interest to quantify the concentration within the sample. The antigen is first immobilised on a plate then complexed with an enzyme-linked antibody to produce a colour change dependent on the quantity of the antigen present.

2.5.1.1 Sample collection and preparation

Following stimulation, supernatants were collected, frozen and stored at -20°C prior to ELISA analysis.

2.5.1.2 ELISA protocol

Capture antibody (50 µL) was added to a 96-well ELISA plate (Nunc by Thermo Fisher Scientific, USA), the plate was covered with an adhesive strip and incubated at room temperature (RT) overnight. The plate was washed and aspirated three times with wash buffer (0.05% Tween-20 in PBS; Sigma Aldrich, UK). The plate was blocked with reagent diluent (150 µL; 1% bovine serum albumin (BSA) in PBS; 1 h, RT). The plate was washed as above, the standards (50 µL) and samples (50 µL, diluted 1:5 in reagent diluent for IL6 ELISA) were loaded, and the plate was incubated (2 h, RT). The plate was washed as before, detection antibody (50 µL) was applied to each well and incubated (2 h, RT). The plate was washed and aspirated as before, streptavidin conjugated to horseradish peroxidase (Strep-HRP; 1:40 in reagent diluent; 100 µL) was added and the plate was incubated (20 min, RT, in dark). The plate was washed, substrate solution

(tetramethylbenzidine; TMB; 100 µL; Sigma-Aldrich, UK) was added and the plate was incubated (20 min, RT, in the dark). The reaction was stopped by adding stop solution (1 M H_2SO_4; 50 µL). The plate was read at 450 nm absorbance using a microplate reader (Synergy HT, BioTek Instruments, USA) and the Gen 5 program, wavelength correction was set to 540 nm absorbance to maximise accuracy. Cytokine concentrations in samples were calculated from the standard curve produced.

2.5.2 Immunocytochemistry

Immunocytochemistry (ICC) is a laboratory technique widely used to anatomically visualise the specific protein or antigen localisation within cells. A protein specific primary antibody is used to bind to the protein of interest. A secondary antibody specific to the species of the primary antibody is then used to apply a colour via a conjugated fluorophore. The now immune-labelled protein may be visualised using the appropriate microscope. A fluorescent microscope is required to visualise fluorescently labelled proteins while a standard light microscope may be used to visualise proteins labelled with DAB, which forms a visible brown precipitate in its oxidised form.

2.5.2.1 Sample preparation

Cells on coverslips were fixed with 4% paraformaldehyde (PFA; 25 min, RT).

2.5.2.2 Immunostaining protocol

Cells were washed with PBS (3 x 5 min washes). Cells were blocked with 10% normal goat serum (NGS) and permeabilised with Triton X-100 (0.3% in PBS; PTx; Sigma-Aldrich) for 2 h. They were then stained with primary antibodies against the neuronal and astrocytic antigens of interest in NGS (2%) and PTx (0.06%) at 4°C overnight, a negative control without primary antibody was used as a control to reveal any non-specific staining. Cells were washed (3 x 10 min) with wash buffer (0.02% PTx) followed by incubation with species-specific secondary antibodies in PTx (0.02%) for 2 h in the dark. Cells were washed as before and nuclear stained with Hoechst (1:1000 in PBS, 30 min, RT; Cell Signalling Technology, USA). Cells were washed once with wash buffer and stored in PBS (500 µL) until mounting. Coverslips were mounted on slides in mounting media (5 µL; 1:1 PBS-glycerol), sealed with clear nail varnish and stored at 4°C in the dark.

2.5.2.3 Image acquisition

Cells were imaged using a fluorescent microscope (Carl Zeiss Axio Imager Z1 microscope, x20-x40 objectives) with attached camera (AxioCam HRm; Carl Zeiss, Germany). All images were taken at the same magnification and exposure times while collecting images for each experiment. Cells were counted manually using the ImageJ (ImageJ 1.50i) counting tool, and all analysis was performed on unmodified images.

2.5.3 Western blotting

Western blotting is an analytical technique used to detect specific proteins in a sample of tissue homogenate or extract. The samples, once equalised in terms of total protein concentration, undergo protein denaturation followed by gel electrophoresis in order to separate out the proteins in the sample by size. To make the proteins accessible for antibody detection, they are transferred from within the gel onto a nitrocellulose membrane. The membrane is then stained first with a protein-specific primary antibody and then with a secondary antibody which may be visualised to allow for indirect measurement of the target protein.

2.5.3.1 Sample preparation and protein equalisation

Following stimulation, media was removed and the cells washed with PBS (300 µL). Cells were lysed in RIPA lysis buffer (50 µL; Thermo Scientific, USA) containing a protease and phosphatase inhibitor cocktail (1%; Sigma-Aldrich, UK) to prevent degradation of the proteins of interest. Lysates were centrifuged (1000 rpm, 1 min, RT) and the resulting supernatant collected and stored at -20°C prior to protein quantification assay.

A bicinchoninic acid (BCA) assay was used to determine the concentration of total protein in each sample. Protein samples were first diluted (1:10 in dH_2O) to ensure they fell within the range of the standard curve. BSA (Sigma-Aldrich, UK) was used as the protein standard for generation of a standard curve, by preparing a top standard of 2 mg/mL and carrying out a serial dilution to 0.015625 mg/mL. RIPA lysis buffer (10% in dH_2O) was used as a blank standard. Pierce BCA reagent was prepared by mixing 50 parts of BCA reagent A (Thermo Scientific, USA) with 1 part BCA reagent B (Thermo Scientific, USA). Standards and diluted samples (25 µL) were loaded in duplicate on a 96-well plate (Bio-Sciences Ltd., Ireland), Pierce BCA reagent (200 µL) added, the plate was sealed with an adhesive

covering (Bio-Sciences Ltd., Ireland) and mixed thoroughly on an orbital plate shaker (1 min) followed by incubation (30 min, 37°C). Absorbance was measured at 562nm on a plate reader (Synergy HT, Biotek, USA) and the protein concentration of each sample was determined from the standard curve produced. Protein concentration was equalised to 15 µg/10 µL with RIPA lysis buffer.

Sample buffer was prepared by adding β-mercaptoethanol to protein loading dye (1:10, Appendix 4). Sample buffer (5 µL) was then added to each sample (25 µL) then samples were boiled (5 min, 85-95°C) on a heat block (VWR, USA) to denature the protein.

2.5.3.2 Gel electrophoresis and semi-dry transfer

Sodium dodecyl sulfate–polyacrylamide gel electrophoresis was used to separate proteins based on size. The gel electrophoresis apparatus was cleaned with dH_2O and 70% ethanol prior to use.

In the fume hood, separating gel (10% for proteins between 15-100 kDa; see Appendix 4) was prepared, and applied between two transfer glass plates (Bio-Rad, USA) assembled in a gate (Rio-Rad, USA) using a Pasteur pipette until it was approximately ¾ full. A layer of isopropanol (Hazardous Materials Facility TCD, Ireland) was placed over the gel to prevent dehydration and the gel allowed to set (30 min). Isopropanol was removed and any remnants rinsed with dH_2O. A 4% stacking gel (see Appendix 4) was prepared and layered on top of the stacking gel. A comb was placed into the gel to create wells and the gel was allowed to set (30 min). Once set the gels were transferred into the electrophoresis tank, the tank was flooded with 1X electrode running buffer (Appendix 4) and the samples were loaded (15 µL). A spectra multicolour broad range molecular weight marker was loaded for reference (7 µL; Thermo Scientific, USA). The gel was run (35 mÅ) until the dye front reached the bottom of the gel.

The resolved protein was then electrotransferred from the gel onto a nitrocellulose membrane (0.22 µm pore size; GE Healthcare Life Sciences, USA). Filter paper and the nitrocellulose membrane were soaked in dH_2O then transfer buffer (1X, see Appendix 4) prior to assembling the transfer sandwich. The transfer sandwich (filter paper, gel, nitrocellulose membrane, filter paper) was prepared from the positive anode base of the semi-dry transfer unit (Trans-blot SD cell; Bio-Rad, USA) and rolled to removed bubbles. The transfer sandwich was then soaked in transfer buffer (1X, see Appendix 4). The

negative cathode plate was placed on top of the sandwich, the transfer unit was closed and sealed and run (constant current 6V, 75 min).

2.5.3.3 Western blotting protocol

To prevent non-specific protein binding, the nitrocellulose membrane was blocked in 5% Marvel in PBS-T (10 mL, 1 h, RT; see Appendix 4) on a rocker (see-saw rocker SSL4; Stuart Scientific, USA). Primary antibody against the protein of interest was used to blot the membrane. Primary antibodies were diluted in 5% Marvel in PBS-T (overnight, 4°C). The membrane was washed with PBS-T (3 x 5 min). Horseradish peroxidase-conjugated secondary antibodies against the species of the primary antibody were used. Membranes were incubated with the appropriate secondary antibody diluted in 5% Marvel in PBS-T (5 mL, 1 h, RT). The membrane was washed again with PBS-T (3 x 5 min). Protein bands were visualised using chemiluminescent substrate (Western Blotting Detection kit) and images were captured using a FujiFilm intelligent dark box and LAS-3000 image reader (Fujifilm, Japan). Membranes were stored in PBS at 4°C in case of future re-probing. To strip a membrane, PBS was discarded and Reblot stripping buffer (5 mL, 10 min, RT; Thermo Scientific, USA) was applied. Following stripping, membranes were rinsed in PBS-T before probing for the next protein began, starting with the blocking step.

Densitometry analysis was carried out using Image Studio Lite (v 5.2) using B-actin as a loading control and normalising the signal to control.

2.6 Statistical analysis

Data is expressed as mean ± standard error of the mean (SEM). At least three neural induction and astrocyte differentiations (N) were performed per iPSC line. 'n' values denote experimental or biological replicates and are representative of different thaws or passage numbers, while 'reps' denotes technical replicates within each experimental group, i.e. cells from the same plate but separate wells.

Outliers were determined using the Grubb's test, also called the extreme studentised deviate method. Significant outliers were excluded from analysis.

Unpaired student t-test were used to analyse differences between two groups. One-way analysis of variance (ANOVA) was used for statistical analysis of means of more than two treatment groups with a single variable, followed by appropriate *post hoc* analysis if significance was inferred. Newman-Keuls *post hoc* was used for groups less than 5 and Tukey *post hoc* for more than 5 groups. Two-way ANOVA was used for statistical analysis when two experimental conditions were used, followed by Bonferroni *post hoc* if significance was inferred. Three-way ANOVA was used for statistical analysis when three experimental conditions were used, followed by Bonferroni *post hoc* if significance was inferred. Significance was set at $p < 0.05$. Statistical analysis was performed using GraphPad Prism 8 (GraphPad Software).

Chapter 3

Neuroinflammatory astrocytes generated from fibroblast-derived human induced pluripotent stem cells

3. Neuroinflammatory astrocytes generated from fibroblast-derived human induced pluripotent stem cells

3.1 Introduction

In response to CNS injury or disease, astrocytes can undergo a phenotypic change known as reactive astrogliosis. Reactive astrogliosis may be triggered by small molecules such as purines and transmitters, as well as large polypeptide growth factors and cytokines. Factors such as TGFα (Rabchevsky *et al.*, 1998), CNTF (Winter *et al.*, 1995), IL6, LIF and oncostatin M induce astrocyte activation *in vivo* (Pekny *et al.*, 2014). These factors act via the STAT3 signalling pathway (Sriram *et al.*, 2004). It is important to note that while these factors may act directly on astrocytes, they may also act on other cell types including neurons, microglia and endothelial cells. These other cells may, in turn, secrete factors which can activate astrocytes which complements the inflammatory cascade hypothesis of neuroinflammation. This evidence suggests that reactive astrogliosis is neither an all-or-nothing phenomenon nor the result of a simple on-off mechanism, but rather is regulated by a number of mechanisms in a context specific manner. This begs the question: how can reactive astrocytes be characterised relative to their quiescent counterparts?

3.1.1 Concept of A1 and A2 reactive astrocyte phenotypes

Reactive astrocytes may play a protective or detrimental role within the CNS. This is highly dependent on minute changes in the microenvironment associated with the area of damage. Stimulation of purified and genetically profiled mouse astrocytes with either LPS to induce an inflammatory response, or with middle cerebral artery occlusion (MCAO) as a method of simulating ischemic stroke, induced two distinct reactive phenotypes in astrocytes (Zamanian *et al.*, 2012).

Astrocyte activation and reactive gliosis may be beneficial and protective to the surrounding brain tissue via regulation of inflammation, promoting repair of damaged neurons and by the formation of glial scars to inhibit the axonal regeneration of injured neurons. Reactive astrocytes induced by ischemia, were shown to up-regulate expression of neurotrophic factors which promote neuronal outgrowth, including thrombospondins (Zamanian *et al.*, 2012) which are important in synapse formation and repair (Clarke & Barres, 2013). These phenotypically neuroprotective reactive astrocytes have been

classified by Liddelow and colleagues as displaying an "A2" phenotype (Liddelow *et al.*, 2017), analogous to previous characterisation of M1/M2 macrophages and microglia (Mills *et al.*, 2000; Mosser & Edwards, 2008; Murray *et al.*, 2014). However, if not resolved, in time reactive gliosis can have detrimental effects on several aspects of plasticity and regeneration. Maladaptive reactive astrocytes, which exacerbate damage, have been described as displaying an "A1" phenotype and may be triggered by a number of stimuli, e.g. the inflammatory mediator IL1α released from activated microglia (Liddelow *et al.*, 2017). The reactive astrocytes produced as a result of inflammation were shown to up-regulate the expression of factors, such as C1q which is known to be involved in synapse elimination (Fourgeaud & Boulanger, 2007). These neurotoxic astrocytes also secrete toxic materials which can induce cell death in neurons and oligodendrocytes (Satoh *et al.*, 2013).

Liddelow and colleagues described the mechanism by which A1 astrocytes could be generated, i.e. LPS caused increased secretion of cytokines IL1α, complement component 1q (C1q), and tumor necrosis factor alpha (TNFα) by activated microglia. They proposed that these microglia-secreted cytokines result in reactive astrogliosis and subsequently neuronal cell death. A highly pure population of A1 astrocytes was created using these three cytokine following refined immunopanning protocols (Liddelow *et al.*, 2017). Alternatively, the MCAO model of ischaemic stroke was found to produce a neuroprotective A2 phenotype (Liu & Chopp, 2016; Liddelow *et al.*, 2017; Tyzack *et al.*, 2017). They distinguished these polarised astrocyte phenotypes in terms of gene expression. An A1 neurotoxic phenotype associated with inflammation was linked to elevated levels of gene transcripts such as *Amigo2*, *Gbp2*, *Fbln5* and *Sgrn*, while the A2 neuroprotective phenotype showed elevated levels of genes including *Ptx3*, *Cd14*, *Clcf1* and *Emp1* (Zamanian *et al.*, 2012; Liddelow *et al.*, 2017).

In contrast to results generated in the Barres laboratory, the Angelo All laboratory found up-regulation of FGF2, BDNF and nerve growth factor (NGF), and down-regulation of axonal inhibitory molecules such as ROBO1/2, which shows that the reactive astrocyte profile has yet to be definitively characterised (Teh *et al.*, 2017). While this A1/A2 characterisation may be useful for *in vitro* studies, it is now accepted that such distinct phenotypes are unlikely to exist *in vivo*, with M1/M2 classification of activated microglia also accepted to be an oversimplification of the *in vivo* scenario.

3.1.2 Alternative methods of characterising reactive astrocytes

The heterogeneity described in astrocytes across brain regions is likely to persist in the reactive phenotype (Trias *et al.*, 2018) and as has already been determined *in vitro*, is highly influenced by the disease condition or cause of injury. As such astrocyte reactivity cannot be simply defined by two set phenotypes, rather a shifting continuum between quiescent and active states with varying degrees of reactivity is more likely and therefore characterisation should account for the whole astrocyte phenotype from morphology to function. Astrocyte activation is known to cause a change in morphology, function and production of secretory products, particularly of pro-inflammatory cytokines (Liddelow & Barres, 2017).

3.1.2.1 Proliferation and morphological changes are associated with astrogliosis

Excessive proliferation, loss of spatial domain exclusivity with process interdigitation, reorganisation of parenchymal architecture and disruption of astrocytic networks are associated with reactive astrogliosis. Considerable proliferation of astrocytes is seen after trauma as cells respond to produce a protective glial scar around the injury site (Anderson *et al.*, 2016). Several promoters of reactive astrocyte proliferation have been identified including EGF, FGF, endothelin 1 and adenosine triphosphate (ATP) (Ciccarelli *et al.*, 1994; Gadea *et al.*, 2008; Herrero-Gonzalez *et al.*, 2009).

Further to proliferation, the stellate morphology of astrocytes has been found to change in response to conditions of stress or degeneration. A well characterised feature of astrocyte activation is the increased production of intermediate filament proteins and remodelling of the filament system (Pekny *et al.*, 2014) in astrocytes leading to morphological changes. The most prominent morphological features of activated astrocytes are: hypertrophied astrocyte cellular processes and cell soma, coupled with up-regulation of intermediate filament proteins, e.g. GFAP, vimentin, nestin and S100β (Liddelow & Barres, 2017). The individual change in morphology is believed to be related to the expression of GFAP, the up-regulation of which depends on the nature of the damage, the distance between the astrocyte and site of injury and the time after injury (Becerra-Calixto & Cardona-Gomez, 2017). As a result increased GFAP expression has long been considered a marker of astrocyte reactivity. However, this characterisation of reactive astrocytes is flawed, as GFAP is also up-regulated during proliferation and glial

scar formation (Anderson *et al.*, 2016). It is therefore important to consider other genes which may be altered in response to injury or disease.

3.1.2.2 Altered gene expression may act as a readout of astrocyte activation

Astrocyte activation results in widespread changes in gene expression. Depending on the activating stimulus, astrogliosis has been linked with up-regulation of genes associated with repair and genes associated with inflammation. These altered transcripts may be one approach used to define the phenotype of activated astrocytes.

Activation via inflammatory insult leads to the production of a wide array of mediators of inflammation as well as transcriptional changes of a variety of genes, e.g. connexins, which are involved in cell-cell communication and *GFAP.* Combined exposure of mouse primary astrocytes to TGFβ1, LPS, and interferon-gamma (IFNγ) significantly altered astrocyte expression of > 6800 gene probes. Bioinformatics analyses revealed that these inflammatory stimuli up-regulate astrocyte molecular networks associated with immune and injury related functions including *Cxcl10*, *Tlr2*, *Myd88, IL6* and *Gp130* (Hamby *et al.*, 2012). *Cxcl10* encodes a pro-inflammatory chemokine (Koper *et al.*, 2018), *Tlr2* and *Myd88* are involved in TLR signalling pathways of the innate immune system (Hoffmann *et al.*, 2007; Liu *et al.*, 2012), and *IL6* and *Gp130* activate the JAK/STAT pathways with many resultant pro-inflammatory effects (Heinrich *et al.*, 1998; Sriram *et al.*, 2004).

Expression of *Serpina3N* and *Lipocalin-2* (*LCN2)* in astrocytes was induced by injury and could not be found in healthy brain sections (Liddelow *et al.*, 2017). Genes such as these may be useful for distinguishing between quiescent and activated astrocytes. *Pentraxin-3* (*PTX3*) is seen to be highly up-regulated 1 day after MCAO and remains elevated 7 days post infarction (Zamanian *et al.*, 2012). *PTX3*, a member of the pentraxin family, plays a role in acute immune response by facilitating pathogen recognition by macrophages. *PTX3* has been classified as an A2 specific marker (Liddelow *et al.*, 2017) although it has also been found highly expressed after treatment with IL1β (Skelly *et al.*, 2013) and is up-regulated in conjunction with *STEAP4* following exposure to nanoparticles (Hawkins *et al.*, 2018) so may act as a more general pan reactive marker of astrocyte activation. TNFα triggers reactivity in human PSC-derived spinal astrocytes resulting in increased expression of *RANTES*, *CXCL8*, and *LCN2.* In the same study IL1β stimulation also resulted in up-regulated expression of *LCN2* (Roybon *et al.*, 2013). A more rounded picture of astrocytic changes as a result of reactivity may be achieved by changes in gene expression.

3.1.2.3 The astrocyte secretome is altered following activation - IL6 as a marker of astrocyte reactivity

The increase in gene expression of inflammatory cytokines is often coupled with an increase in secretion of their respective immunomodulatory agents. It follows that with astrocyte activation comes altered cytokine secretion therefore the secretome may be utilised as a means to characterise reactive astrocytes. Stimulation with TNFα results in secretion of the pro-inflammatory cytokines IL1β, IL8, and IFNγ (Trindade *et al.*, 2020). In an AD model, it has been shown that Aβ species are capable of inducing the release of several pro-inflammatory agents from glial cells, including NO, IL1β, IL6 and TNFα (Gonzalez-Reyes *et al.*, 2017). Astrocytes are a major source of IL6 in the CNS (Van Wagoner *et al.*, 1999), therefore it is of interest how its secretion is altered in reactive astrocytes.

IL6 levels are commonly elevated in cases of injury, infection and inflammation (Van Wagoner & Benveniste, 1999), with increased secretion detected in human PSC-derived spinal astrocytes following stimulation with inflammatory mediators TNFα or IL1β (Roybon *et al.*, 2013). IL6 production may be high under inflammatory conditions due to its autocrine mechanism of action, whereby it stimulates its own production (Van Wagoner & Benveniste, 1999).

IL6 has been shown to act as both a pro- and anti-inflammatory cytokine. IL6 has two forms of signalling, classical and trans. Classic signalling acts via the IL6 receptor and is associated with regenerative and anti-inflammatory processes. Trans-signalling acts via the soluble IL6 receptor and is associated with pro-inflammatory processes (Scheller *et al.*, 2011). Classic IL6 signalling involves IL6 binding of the membrane bound IL6 receptor (IL6R) which associates with gp130. Gp130 then dimerises activating JAK which results in phosphorylation of tyrosine residues in the cytoplasmic portion of gp130. This engages Src which activates the Ras/Raf/MAPK pathway and subsequently STAT which translocates to the nucleus where it activates target genes (Scheller *et al.*, 2011). In trans-signalling gp130 interacts with IL6 bound to a soluble form of the IL6R (sIL6R). The soluble sIL6R is generated following proteolytic cleavage of a membrane bound precursor protein. Gp130 can be activated by sIL6R-ligand complex in an autocrine and paracrine manner (Scheller *et al.*, 2011), therefore IL6 is influential over numerous different cell types given the presence of the soluble receptor.

3.1.3 Modelling the role of reactive astrocytes *in vitro* using human induced pluripotent stem cells

The models available for the study of astrocytes have expanded greatly in recent years. Several avenues of research were previously explored including rodent models (Oberheim *et al.*, 2012; Chandrasekaran *et al.*, 2016), immortalised cell lines (Kaur & Dufour, 2012) and post-mortem disease tissue (Crompton *et al.*, 2017). However these were limited in their ability to faithfully represent living human tissue to an appropriate degree of integrity (Zhang *et al.*, 2016a). ESC were the first source of cultured PSC which laid the groundwork for modern day differentiation protocols (Chambers *et al.*, 2009). However, as they demand the destruction of the human embryo they have raised controversy on ethical grounds. Human iPSC represent an advantage over ESC as they can be derived from patient tissue thus rendering them invaluable as a source of personalised drug discovery; cells derived from patients suffering from a neurodegenerative disease may be grown *in vitro* and used for the testing of new treatments which otherwise could not be authorised for clinical trials. It is hoped in future years that they may be used for therapeutic purposes via autologous transplant (Singh *et al.*, 2015), with the first clinical trial using iPSC-derived cell transplants for neurodegenerative diseases currently underway in Japan (Morizane, 2019). In the meantime, these cells are providing an efficient *in vitro* human model. Once formed, iPSC can spontaneously differentiate in culture due to intrinsic signalling, however, by mimicking developmental cues iPSC may be used to derive a specific cell type for modelling a “disease in a dish”.

Most existing research regarding the role of reactive astrocytes in AD is largely based on animal model studies, specifically, rodent studies. Although rodent models and corresponding primary cultures have provided a valuable tool for studying neurodegenerative disease, the use of non-human models for human diseases presents a barrier, because human diseases such as AD, do not naturally occur in most model organisms. Furthermore, rodent astrocytes differ greatly from human astrocytes in morphology, such as number and thickness of branches, in their ratio to neurons and in their gene expression patterns (Chandrasekaran *et al.*, 2016). As such we here describe a human *in vitro* model of reactive astrogliosis, a key driving force in the progression of AD, which will offer important insight into the response of human iPSC-derived astrocytes to an inflammatory insult and the subsequent effect on surrounding neurons.

3.1.4 Aims

The objectives of this chapter can be separated into three primary aims:

1. To generate cortical neurons and astrocytes from human fibroblast-derived iPSC,
2. To stimulate iPSC-derived astrocytes with inflammatory microglial factors (IL-1α, TNFα and C1q) and characterise their response at the gene, protein and morphological level,
3. To assess the effect of reactive astrocyte conditioned media on human iPSC-derived cortical neurons.

The hypothesis pertaining to these aims are that using modified and optimised versions of already established and published protocols, it will be possible to derive regionally defined neurons and astrocytes from human iPSC. PCR, ELISA and immunocytochemical analysis will give insight into the reactivity profile of stimulated astrocytes and it follows from the literature that neurotoxic astrocytes will be detrimental to neuronal cells. The overarching premise of this study will address whether strict reactive astrocyte phenotypes exist and whether the induction of a neurotoxic phenotype by inflammation is partially responsible for cell death in neurodegeneration.

3.2 Materials and Methods

3.2.1 Cell lines

Characterisation experiments were carried out using the NAS2 iPSC line kindly gifted by the Kunath laboratory. This iPSC line was generated as part of a PD study where it served as the control for a PD patient with a triple α-synuclein mutation and as such the pluripotent nature of this iPSC line is well established (Devine *et al.*, 2011). For the purpose of this study the NAS2 iPSC line was genotyped by the Seth Loves laboratory group, University of Bristol, and found to be APOE3 homozygous, and so is considered the control genotype.

3.2.2 Cell culture and neural patterning

All cell culture techniques were carried out in a sterile laminar flow hood (Nuaire, USA). All materials used were autoclaved and sterile to prevent bacterial or fungal contamination. Aseptic techniques were used throughout cell culture. Materials entering the laminar flow hood were sprayed with 70% ethanol to maintain sterile conditions. Cells were incubated in a humidified (37°C, 5% CO_2) incubator (Nuaire, USA). NAS2 iPSC were expanded and passaged and stocks were banked as described in the main methods section of this thesis.

3.2.3 Cortical neuralisation of human iPSC

Prior to beginning the neural induction protocol iPSC were prepared by passaging at a lower density, e.g. using a split ratio of 1:5 instead of 1:4, and cultured for 4 d in E8 media without ROCK inhibitor. Once iPSC had reached a confluency of 70-80%, with numerous small colonies in culture rather than fewer larger colonies, and the colonies had defined smooth rounded edges (Figure 3.2.1) they were ready for neuralisation.

iPSC were patterned towards a cortical fate for 10 d in Neural Maintenance Media (NMM; 1:1 DMEM/F-12 + Glutamax and Neurobasal media, 1% NEAA, 0.5% Glutamax, 1% pen/strep, 0.5% N2, 1% B27, β-mercaptoethanol (75 µM), insulin (5 µg/mL)) supplemented with SB431542 (10 µM; Bio-Techne, USA) to inhibit pluripotency and LDN193189 (100 nM; Sigma-Aldrich, UK) to inhibit mesoderm differentiation. On day 10 (D10), cells were passaged onto PO/laminin coated 6-well plates as described in Section 2.2.2. NPC are maintained in NMM without SMAD inhibitors from D11 onwards.

This cortical neuralisation protocol is based on those published by Chambers *et al*. and Shi *et al*., with modifications made by Paul Nistor (past member of the Caldwell Laboratory Group) detailed in Nistor *et al*. (Chambers *et al.*, 2009; Shi *et al.*, 2012; Nistor *et al.*, 2015). Further modification to the neuralisation timeline with respect to passaging days was inspired by a protocol published by the Kirkeby group (Nolbrant *et al.*, 2017). Table 3.2.1 summarises the media changes and passaging days during neural differentiation of iPSC towards a cortical NPC state.

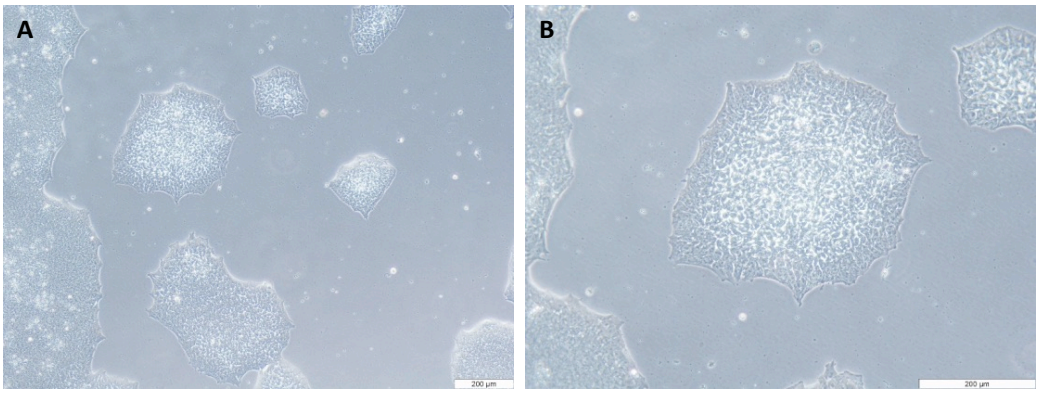


Figure 3.2.1. NAS2 iPSC colonies ready for neural patterning.

Colonies are small and well-spaced (A). Colonies have a dense centre with smooth edges (B). Images were taken at passage 58. Scale bar represents 200 µm.

Day	Media	Passage
-4	E8 Media	✓
-3	E8 Media	
-2	E8 Media	
-1	E8 Media	
0	NMM + SB431542 (10 µM) + LDN193189 (100 ng/mL)	
1	NMM + SB431542 (10 µM) + LDN193189 (100 ng/mL)	
2	NMM + SB431542 (10 µM) + LDN193189 (100 ng/mL)	
3	NMM + SB431542 (10 µM) + LDN193189 (100 ng/mL)	+ Laminin
4	NMM + SB431542 (10 µM) + LDN193189 (100 ng/mL)	
5	NMM + SB431542 (10 µM) + LDN193189 (100 ng/mL)	
6	NMM + SB431542 (10 µM) + LDN193189 (100 ng/mL)	+ Laminin
7	NMM + SB431542 (10 µM) + LDN193189 (100 ng/mL)	

8	NMM + SB431542 (10 µM) + LDN193189 (100 ng/mL)	
9	NMM + SB431542 (10 µM) + LDN193189 (100 ng/mL)	
10	NMM + SB431542 (10 µM) + LDN193189 (100 ng/mL)	✓
11	NMM	
12	NMM	
13	NMM	
14	NMM	✓
15	NMM	
16	NMM	*

Table 3.2.1. Neural differentiation timeline showing media supplements and passaging days.
iPSC were passaged at D-4 into E8 media in preparation for neural differentiation. Patterning factors SB431542 and LDN193189 were added to NMM from D0-D10 to induce neural differentiation of iPSC. Addition of laminin (10 µg/mL) at D3 and D6 aids cell adherence while over confluent. Cells must also be over confluent before passaging at D14. NPC can be terminally differentiated from D16 by plating in NMM, or cryopreserved and banked for future use (*).

3.2.3.1 Expansion of NPC and plating for terminal differentiation

From D11 onwards, NPC were cultured in NMM on PO/laminin coated 6-well plates (Nunc by Thermo Fisher Scientific, USA). Cells were fed every other day (2 mL) and extra media was given for weekend breaks (2 mL/day). NPC were passaged upon reaching 100% confluency as described in Section 2.2.2. From D20 onwards, NPC can be cryopreserved to generate stocks or plated for terminal differentiation and characterisation. Neural differentiation, NPC expansion and plating procedures required optimisation across several stages of the protocol as described in the following sections.

3.2.3.2 Optimisation of neuralisation timeline

iPSC were patterned towards a neural fate by addition of NMM supplemented with SB431542 and LDN193189 for 9 d. Media was changed daily to provide adequate nutrition as cells are highly proliferative and metabolic during the neural differentiation process. Cells were passaged on D3 and D7 as denoted in the timeline (Figure 3.2.2). It was noted that a significant amount of cell death occurred around D7 and continued through to D9, visualised as cell debris suspended in the media. Upon inspection under the light microscope, it was determined that this cell debris was likely due to the death of non-

neural cells, but suggested that passaging should be avoided at this time point while cells are at their most sensitive.

Following the publication of a neuralisation protocol by the Kirkeby laboratory, the neuralisation protocol was modified by increasing the length of patterning to 10 d as well as refraining from passaging during the neural patterning process (Nolbrant *et al.*, 2017). This optimised timeline is denoted in Figure 3.2.3 and improved NPC yield.

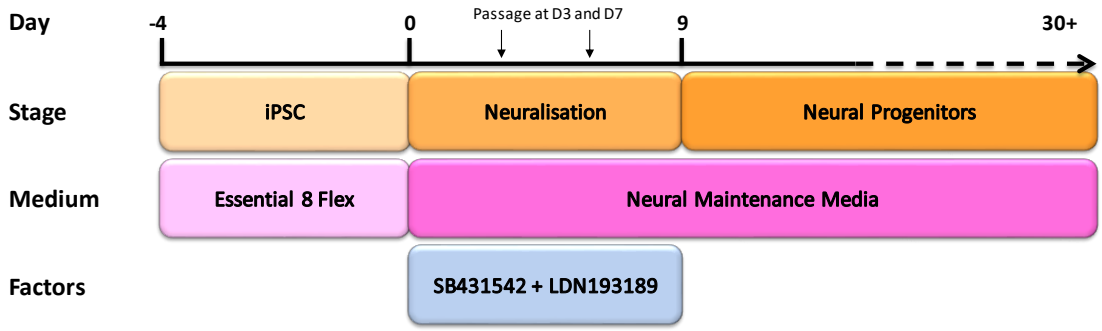


Figure 3.2.2. Original neuralisation timeline.

The initial neural patterning protocol involved addition of SB431542 and LDN193189 to NMM for 9 days with passaging at D3 and D7. Protocol modified from Chambers et al., 2009.

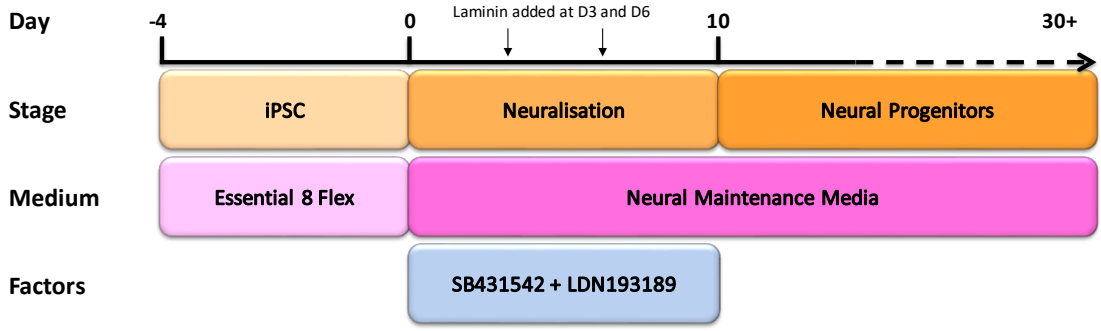


Figure 3.2.3. Optimised neuralisation timeline.

The optimised neural patterning protocol involved addition of SB431542 and LDN193189 to NMM for 10 days with no passaging until D10 and addition of laminin at D3 and D6 to aid cell adherence. Protocol modified from Nolbrant et al., 2017.

3.2.3.3 Troubleshooting cell adherence issues

Patterning for 10 d without passage resulted in issues relating to cell adherence due to high confluency. Cells began to lift from the edges of the well from D3. Laminin (10 µg/mL) was added to media when feeding on D3 and D6.

Plastic ware was changed from Corning (cat no. 10578911) to Nunc (cat no. 140675) to further aid cell adherence and neuralisation yield. iPSC were passaged onto Nunc 6-well plates on the passage before initiating the neuralisation protocol, i.e. D -4.

3.2.4 Characterisation of iPSC-derived neurons

Human iPSC-derived neurons were characterised by immunocytochemical staining for neuronal marker β-tubulin III and cortical marker TBR1 (Yan *et al.*, 2018). Refer to Section 2.5.2 for staining and imaging protocol.

3.2.5 Astrocyte progenitor differentiation

NPC were patterned towards a glial fate from D30 in modified 'Serio' media (Serio; Advanced DMEM/F-12 (Thermo Fisher Scientific, USA); 1% Glutamax ; 1% NEAA; 1% pen/strep; 0.2% B27; 1% N2) supplemented with EGF (20 ng/mL; Sigma-Aldrich, UK) a potent driver of glial cell differentiation and hLIF (20 ng/mL; PeproTech, UK) a strong mitogen to maintain cell proliferation during long-term culture (Serio *et al.*, 2013). Serio base media supplemented with EGF and hLIF will be referred to as SerioEL throughout. On the first passage after addition of SerioEL, differentiating APC were transitioned from PO/laminin coated 6-well plates to Geltrex coated 6-well plates.

Geltrex is a soluble basement membrane matrix derived from murine Engelbreth-Holm-Swarm tumors, with major components including laminin, collagen IV, entactin, and heparin sulfate proteoglycans making it ideal for a number of culture systems including iPSC culture. Differentiating APC were expanded on Geltrex (1X; Thermo Fisher Scientific, USA) coated 6-well plates in SerioEL. Standard Corning plastic ware is sufficient for expansion of APC. Cells were fed every other day by removing spent media and replacing with fresh SerioEL (2 mL); extra media was given for weekend breaks (2 mL/day).

3.2.5.1 Passaging for expansion of APC cultures

APC were passaged upon reaching 100% confluency onto Geltrex (1X; 2 hr; 37°C) coated plates. Spent media was removed and discarded, cells were washed once with PBS, and then incubated with Accutase (1 mL, 3-4 min, RT; Thermo Fisher Scientific, USA). Accutase was removed and cells lifted with Serio, collected in a falcon tube and centrifuged (1000 rpm, 3 min). The supernatant was removed and discarded, and the cells resuspended in 1 mL SerioEL and transferred onto a fresh Geltrex coated plate at an appropriate split ratio (usually 1:4). RevitaCell (1:100; Thermo Fisher Scientific, USA) or Y-27632 (10 µM; Bio-Techne, USA) was added after each passage to aid cell survival (Watanabe *et al.*, 2007). APC were then expanded until D80 before plating for terminal differentiation and characterisation experiments.

3.2.5.2 Plating and terminal differentiation

APC were plated from D80 for terminal differentiation prior to characterisation and stimulation studies. Cells were dissociated and detached as for passaging. Once pelleted cell supernatant was removed and discarded, and the cell pellet resuspended in 1 mL fresh Serio media. Cells were prepared for counting by first taking a 10 µL aliquot of cell suspension, diluting 1:5 in Serio media and subsequently diluting 1:2 in trypan blue (0.4%; Thermo Fisher Scientific, USA) to give a final dilution factor of 10. Cells were counted using a haemocytometer. Cells were plated on Geltrex coated (10X; 2 h, 37°C) coverslips for immunofluorescence staining at a density of 5×10^4 cells per coverslip in a 100 µL droplet. Cells were plated on Geltrex coated (1X; 2 h, 37°C) 24-well plates at a cell density of 2×10^5 cells per well for qPCR analysis. Cells were incubated for 30 min to adhere, then wells were topped up with SerioEL (500 µL/coverslip or 1 mL/well). Once cells reached confluency media was changed to terminal differentiation media, Serio supplemented with BMP4 (20 ng/mL; R&D Systems, UK) and hLIF (20 ng/mL). Cells were matured for 7 d followed by 3 d in Serio media without factors, to remove any potential priming effect of maturation factors (Tyzack *et al.*, 2017), prior to experimentation (Figure 3.2.4). Mature astrocytes may be used in experiments up to D120, after which they reach the end of their life span in culture.

Difficulties with cell adhesion on glass ware for immunocytochemical analysis meant that a number of different plating procedures were trialled during optimisation. These optimisation steps are described in the subsequent section.

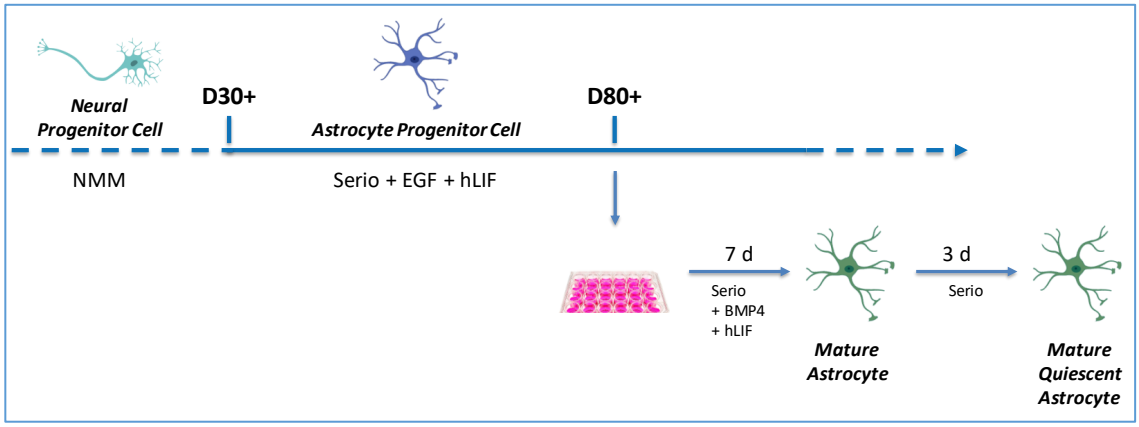


Figure 3.2.4. Differentiation timeline for generation of mature quiescent-like astrocytes.

APC are derived from NPC by addition of 'Serio' media supplemented with EGF (20 ηg/mL) and hLIF (20ηg/mL) from D30. APC may be terminally differentiated to mature astrocytes from D80 by plating in 'Serio' media supplemented with BMP4 (20 ηg/mL) and hLIF (20 ηg/mL) for 7 d followed by 72 h in Serio media without factors prior to experiments to generate a mature quiescent-like astrocyte. Mature astrocytes are optimal for use in experiments up to D120.

3.2.5.3 Optimisation of plating protocol and cell adherence for terminal differentiation and characterisation of astrocytes

iPSC-derived astrocytes were observed to have an aversion to seeding on glass coverslips. Plating on coverslips coated on Geltrex (1% in Serio media) was not sufficient to maintain astrocytes as an adherent monolayer for the duration of the maturation protocol, with astrocytes branching and clumping together and sometimes lifting completely from the coverslip. A number of alternative coating procedures were trialled in order to optimise seeding on coverslip for ICC, detailed as follows:

1. Coverslips were pre-coated with PO (1 µg/cm^2) followed by laminin (1 µg/cm^2)
2. Coverslips were pre-coated with PO (1 µg/cm^2) followed by Geltrex (1% in Serio media)
3. Coverslips were coated with Geltrex at 2%, 5% and 10% in Serio media

It was found that 2-5% Geltrex in Serio media was sufficient to maintain astrocytes on coverslips as a monolayer for the duration of the astrocyte maturation and ICC protocols, and this increased percent of Geltrex did not affect the quality and clarity of captured images.

Having resolved the issue of cell adhesion to glass coverslips, two terminal differentiation protocols were compared to determine which was most appropriate for the generation of mature quiescent-like astrocytes. The timelines are presented schematically in Figure 3.2.5 below.

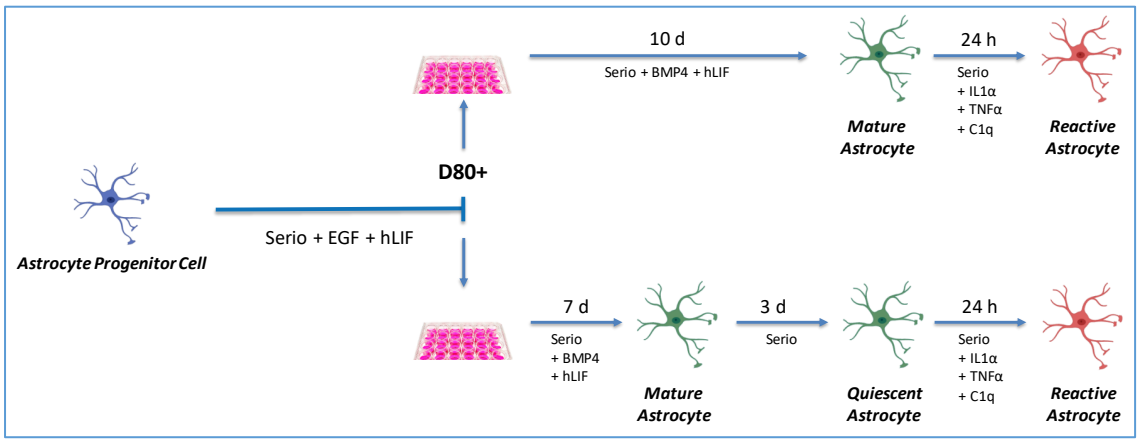


Figure 3.2.5. Timeline for optimisation of astrocyte terminal differentiation protocol.

APC are derived from NPC by addition of 'Serio' media supplemented with EGF (20 ηg/mL) and hLIF (20ηg/mL) from D30. APC may be terminally differentiated to mature astrocytes from D80 by plating in 'Serio' media supplemented with BMP4 (20 ηg/mL) and hLIF (20 ηg/mL). The initial terminal differentiation protocol involved maturation for 10 d prior to stimulation. This was optimised to maturation for 7 d followed by 72 h in Serio media without factors prior to experiments to generate a mature quiescent-like astrocyte, without any potential priming effect that may be induced by the maturation factors BMP4 and hLIF. Mature astrocytes are optimal for use in experiments up to D120.

3.2.6 Characterisation of iPSC-derived astrocytes

Human iPSC-derived astrocytes were characterised by immunocytochemical staining for classical astrocyte markers GFAP, Connexin-43, EAAT1 and S100β. Refer to Section 2.5.2 for staining and imaging protocol. Figure 3.2.6 denotes some important time points in the characterisation protocol.

3.2.7 Cell treatment for generation of reactive astrocytes

Astrocytes were stimulated with inflammatory microglial factors interleukin-1 alpha (IL1α; 3 ng/mL; PeproTech, UK), tumor necrosis factor alpha (TNFα; 30 ng/mL; Cell Signalling Technology, USA) and complement component 1q (C1q; 400 ng/mL; MyBioSource, USA) for 24 h. Concentrations of IL1α, TNFα and C1q were chosen based on a study carried out in mouse primary astrocytes (Liddelow et al., 2017), a 10-factor dilution of these concentrations was also used to test the sensitivity of iPSC-derived astrocytes to this inflammatory insult. These treatments are denoted as "Factors High" (Liddelow *et al.*, 2017) and "Factors Low" where appropriate.

Post stimulation, media was collected and stored at -20˚C. Cells were prepared for immunostaining (described in Section 2.5.2 – main methods) and qPCR (Section 2.4.1 – main methods).

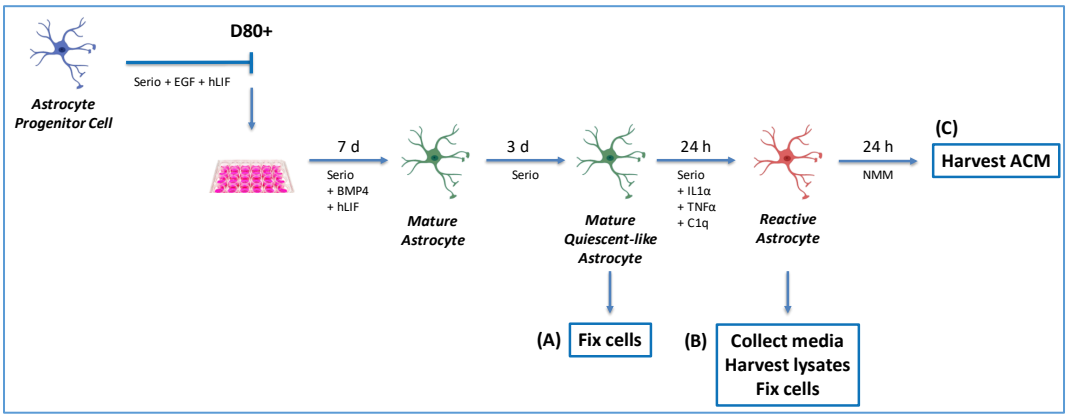


Figure 3.2.6. Experimental timeline for generation of mature quiescent-like and reactive astrocytes.

APC were expanded in Serio media supplemented with EGF and hLIF. From D80 APC are plated and terminally differentiated in Serio media supplemented with BMP4 and hLIF for 7 d. Factors where then withdrawn for 72 h to ensure a mature quiescent-like astrocyte. Mature astrocytes were fixed to confirm cell fate (A). Alternatively astrocytes are stimulated for 24 h in order to generate a reactive astrocyte. Media and lysates may be harvested to examine the reactive astrocyte profile or cells fixed for immunostaining (B). NMM may be added to reactive astrocytes for 24 h to collect conditioned media (C).

3.2.8 Cell treatment to demonstrate neurodegeneration

iPSC-derived astrocytes were stimulated with inflammatory microglial factors for 24 h, as described above. Post stimulation media was removed and the astrocytes were washed with PBS (1 mL, 1X) in order to remove remaining media containing microglial factors IL1α, TNFα and C1q. Following this wash step, the PBS was replaced with NMM for 24 h in order to collect astrocyte conditioned media (ACM) devoid of microglial factors, this media change ensures that ACM later applied to neurons contains only astrocyte secreted factors (Figure 3.2.6). ACM was stored at -20˚C. Conditioned media (100% ACM) from control and reactive astrocytes was applied to iPSC-derived *E3E3* neuronal cultures and incubated for 48 h (Figure 3.2.7). Post stimulation, cells were prepared for immunocytochemical staining (see Section 2.5.2 – main methods).

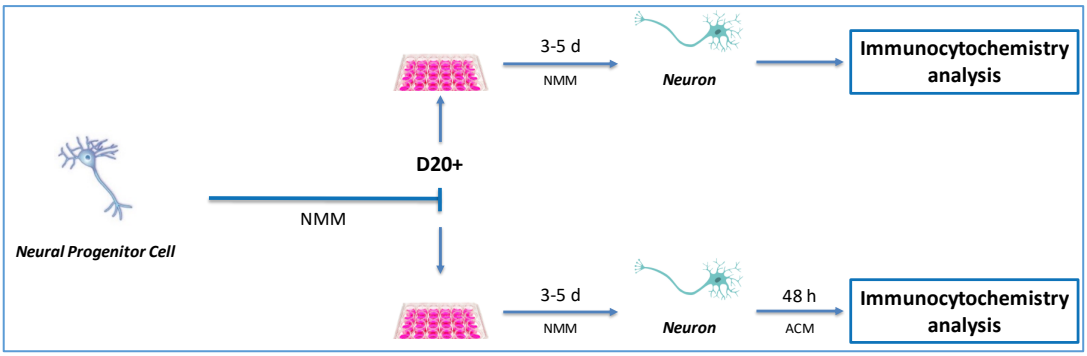


Figure 3.2.7. Experimental timeline for characterisation of iPSC-derived neurons and effect of reactive astrocyte conditioned media on neurons.

NPC were expanded in NMM until D20 when they were seeded on coverslip and subsequently left to settle for 3-5 d prior to fixation for characterisation or treatment with ACM.

3.2.9 Analysis of gene expression by quantitative polymerase chain reaction

Cells were lysed in lysis buffer consisting of RA1 lysis buffer (350 µL per sample) and β-mercaptoethanol (3.5 µL per sample) and lysates stored at -80°C prior to RNA isolation. mRNA expression was determined in cell lysates by quantitative polymerase chain reaction (qPCR) following RNA isolation and cDNA manufacture. All RNA isolation, cDNA manufacture and qPCR setup procedures were carried out in a designated molecular biology fume hood (Premier, Scotland) cleaned with 70% ethanol and RNase-away (VWR International, UK) to remove RNase and DNases that breakdown RNA and DNA respectively. RNA isolation, cDNA manufacture and qPCR protocols are detailed in

Chapter 2 (Section 2.4). Table 3.2.2 details the target primers used for gene expression analysis. GAPDH was used as the endogenous control reference.

Gene	Cat No.	Gene Code
C3	4453320	Hs00163811_m1
CXCL10	4453320	Hs00171042_m1
GFAP	4453320	Hs00909233_m1
ICAM1	4453320	Hs00164932_m1
IL1B	4453320	Hs01555410_m1
IL6	4453320	Hs00174131_m1
LCN2	4453320	Hs01008571_m1
PTX3	4453320	Hs00173615_m1
SERPINA3	4453320	Hs00153674_m1
VIM	4448892	Hs00958111_m1

Table 3.2.2. Target primers used for qPCR analysis of astrocyte gene expression profile.

3.2.10 Analysis of cytokine secretion by enzyme-linked immunosorbent assay

ELISA analysis (R&D Systems, USA) was used to assess the concentrations of IL6, RANTES and GM-CSF secreted into the supernatant obtained from cultured astrocytes. The ELISA protocol is detailed in Chapter 2 (Section 2.5.1).

3.2.11 Immunocytochemistry

Cells on coverslips were fixed with 4% paraformaldehyde (PFA; 25 min, RT) in preparation for immunocytochemistry (Chapter 2, Section 2.5.2). Primary and secondary antibodies are detailed in Tables 3.2.3 and 3.2.4 respectively.

Antigen	Dilution	Manufacturer
Chicken anti-GFAP	1:1000	DAKO, Denmark
Rabbit anti-Connexin-43	1:1500	Sigma-Aldrich, USA
Mouse anti-S100β	1:1000	Sigma-Aldrich, USA
Rabbit anti-EAAT1	1:1500	Novus Biologicals, USA
Hoechst	1:1000	Cell Signaling Technology, USA
Mouse anti-β-tubulin III	1:1000	Merck-Millipore, USA
Rabbit anti-TBR1	1:1500	Abcam, UK

Table 3.2.3. Primary antibodies.

Antigen	Dilution	Manufacturer
Alexa Fluor 488 donkey anti-mouse	1:500	Molecular Probes
Alexa Fluor 488 goat anti-chicken IgG	1:500	Life Technologies, USA
Alexa Fluor 568 donkey anti-rabbit IgG	1:500	Molecular Probes

Table 3.2.4. Secondary antibodies.

3.2.11.1 Quantification of GFAP expression

GFAP expression was determined by measuring its fluorescent signal in the acquired images. ImageJ software was used to carry out this densitometry analysis, whereby each individual cell was traced and the integrated density and cell area noted. Three measurements of background fluorescence were also used to calculate mean background fluorescence. GFAP expression was then calculated as corrected total cell fluorescence (CTCF).

$$\mathrm{CTCF} = \frac{\text{Integrated density}}{\text{Area of cell x Mean background fluorescence}}$$

3.2.11.2 Quantification of morphological changes via nuclear:cytoplasm ratio

Total cell and nuclear areas were measured in ImageJ by tracing the cell perimeter and nuclear perimeter respectively. Cytoplasm area was then calculated by subtracting the nuclear area of each cell from its total cell area. The nuclear:cytoplasm ratio was then calculated by dividing nuclear area by cytoplasm area for each cell. Morphological changes as a result of astrocyte reactivity will be reflected in altered nuclear:cytoplasm ratios.

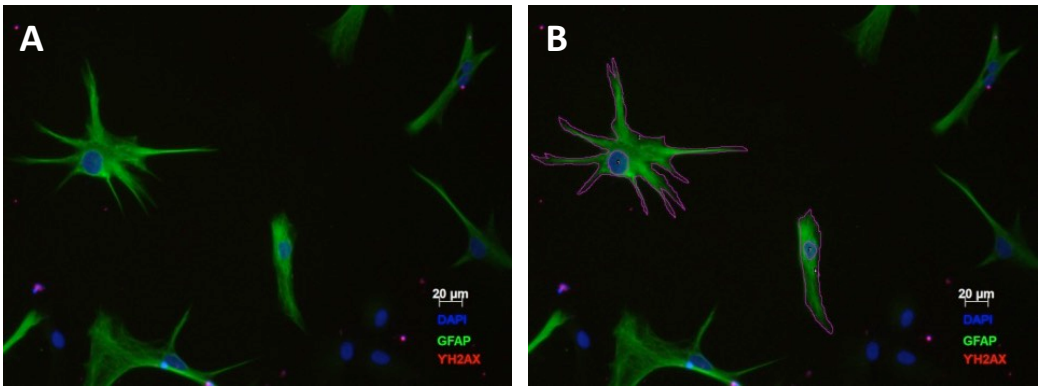


Figure 3.2.8. Morphological analysis of iPSC-derived astrocytes.

Images were acquired at x40 magnification (A). Cells were measured by tracing both the nucleus and cell membrane (B), and from this cytoplasm volume and nuclear:cytoplasm ratio were calculated.

3.2.11.3 Quantification of neuronal clusters

Cortical neurons tended to cluster rather than remaining on coverslips as a monolayer. Therefore, traditional manual total cell counting could not be used for quantification. Instead neuronal cultures were quantified by first characterising the clusters in terms of size by manually counting the number of nuclei visible on the surface of each cluster; small clusters consisted of < 10 cells, medium clusters have 10-50 cells, large clusters have 50-100 cells and extra-large clusters have more than 100 cells (Figure 3.2.9). Clusters were also characterised as having extending processes or not. Clusters were then quantified by counting the number of small, medium, large and extra-large clusters with and without extending processes across each treatment group (Park *et al.*, 2009; Tornero *et al.*, 2013).

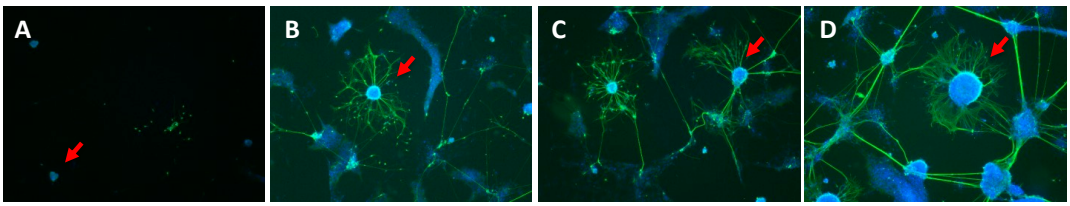


Figure 3.2.9. Neuronal clusters may be characterised by size.

Small clusters (A) have 10 or less cells, medium clusters (B) have 10-50 cells, large clusters (C) have 50-100 cells and extra-large (D) clusters have more than 100 cells. Images were taken at x5 magnification.

3.2.12 Statistical analysis

Data is expressed as mean ± SEM. At least three neural induction and astrocyte differentiations (N) were performed per iPSC line. 'n' values denote experimental or biological replicates and are representative of different thaws or passage numbers, while 'reps' denotes technical replicates within each experimental group, i.e. cells from the same plate but separate wells.

An unpaired student t-test was used for statistical analysis of the effect of microglial factors compared to control. One-way ANOVA was used when both low and high concentrations of factors were compared to control or each other, followed by Newman-Keuls *post hoc* if significance was inferred. Two-way ANOVA was used for analysis pertaining to the effect of astrocyte maturation factors on reactivity markers, with Bonferroni *post hoc* where appropriate. Two-way ANOVA was also applied to analysis of the effect of ACM on neuronal clusters with respect to size, with Bonferroni *post hoc*. Significance was set at $p < 0.05$. Statistical analysis was performed using GraphPad Prism 8 (GraphPad Software).

3.3 Results

3.3.1 iPSC-derived neurons are positive for classical neuronal markers

Cortical neurons were successfully derived from human iPSC. The neuralisation protocol used combined aspects of protocols originally published by the Studer and Livesey laboratories (Chambers *et al.*, 2009; Shi *et al.*, 2012), and modified by Paul Nistor, previously of the Caldwell Laboratory (Nistor *et al.*, 2015) (Figure 3.3.1). Cell fate was confirmed by immunofluorescent staining for classical neuronal marker β-tubulin III and cortical marker TBR1 (Figure 3.3.2).

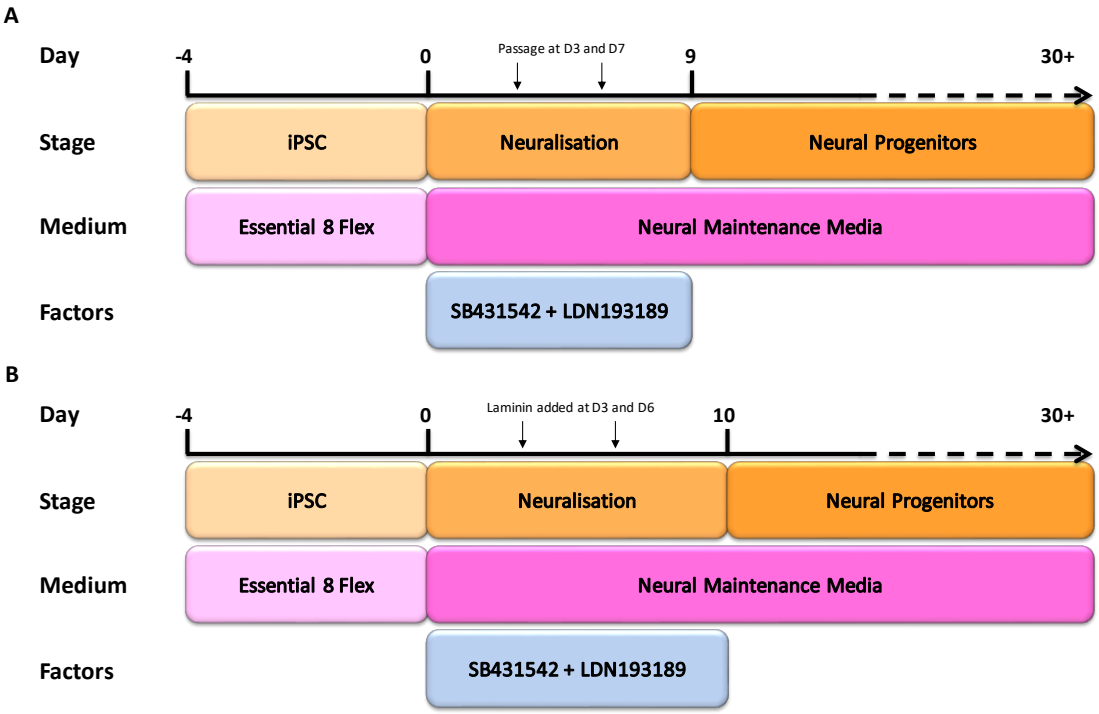


Figure 3.3.1. Neuralisation timeline and characterisation of iPSC-derived neurons.

The original (A) and optimised (B) neural patterning protocols involve addition of SB431542 and LDN193189 to NMM at D0. The protocol was optimised in terms of the number of days in patterning media, passaging and managing cell adherence.

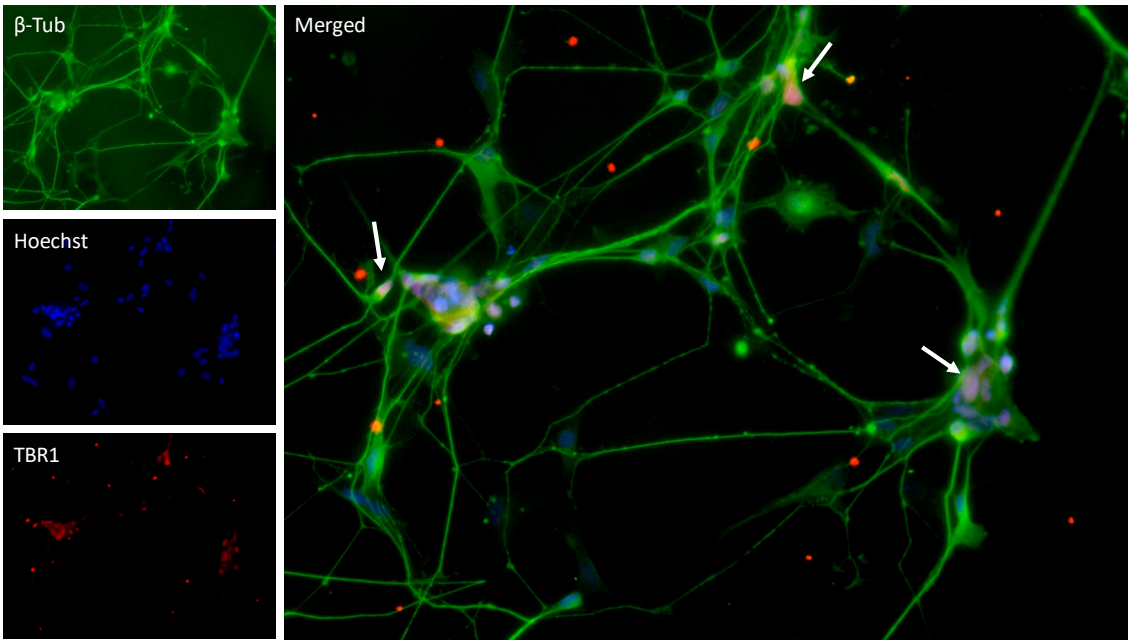


Figure 3.3.2. iPSC-derived cortical neurons stain positive for classical neuronal and cortical markers.

iPSC-derived cortical neurons stained positive for classical neuronal marker B-tubulin III (green channel) and cortical marker TBR1 (red channel). Nuclear stain hoechst also shown (blue channel). White arrows denote B-tub^{+} TBR1^{+}. Images shown are x20 magnification.

3.3.2 iPSC-derived astrocytes are positive for classic astrocyte markers

In order to confirm cell fate, iPSC-derived astrocytes were fluorescently-labelled with astrocytic markers GFAP, connexin-43 (Cx43), S100β and EAAT1 and the nuclear marker hoechst. iPSC-derived cortical astrocytes were positive for the markers GFAP and Cx43 (Figure 3.3.3. A), S100β and EAAT1 (Figure 3.3.3. B).

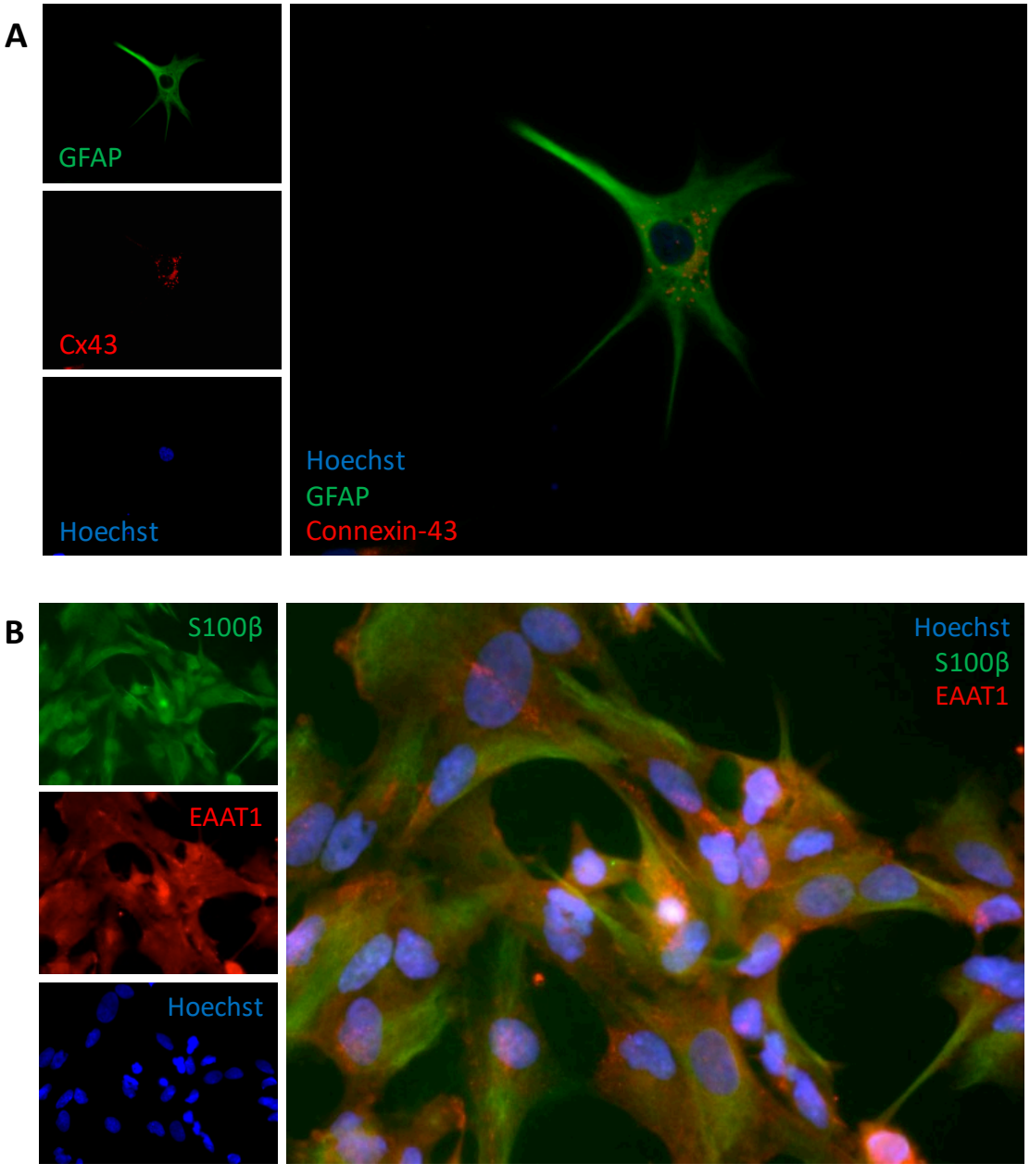


Figure 3.3.3. iPSC-derived cortical astrocytes stain positive for classical astrocyte markers.
iPSC-derived cortical astrocytes stained positive for classical astrocyte markers GFAP and Cx43 (A), and S100β and EAAT1 (B). Images shown are x40 magnification.

3.3.3 Maturation factors BMP4 and hLIF significantly affect IL6 secretion in stimulated iPSC-derived astrocytes

Once cell fate was confirmed, it was ensured that matured astrocytes were quiescent-like prior to stimulation. Basal reactivity was assessed following an indication that hLIF may induce reactivity via STAT3 (Tyzack *et al.*, 2017). In order to ascertain whether maturation factors were inducing any baseline reactivity in matured astrocytes, iPSC-derived cortical astrocyte progenitor cells were matured in Serio media supplemented with BMP4 and hLIF for either 10 d, or 7 d then changed to Serio only media for 72 h prior to stimulation with inflammatory microglial factors as per the timeline (Figure 3.3.4. A). iPSC-derived astrocytes responded robustly with significantly increased secretion of IL6, GM-CSF and RANTES ($p < 0.001$, Figure 3.3.4. B-D). With regards to the effect of maturing factors, BMP4 and hLIF withdrawal had a significant effect on IL6 secretion. Withdrawal of the maturing factors 72 h prior to stimulation led to significantly reduced secretion of IL6 following stimulation compared astrocytes matured in BMP4 and hLIF for 10 d ($p < 0.01$). The maturing factors BMP4 and hLIF did not affect the secretion of GM-CSF or RANTES at baseline or following stimulation (Figure 3.3.4. B-D).

3.3.4 Maturation factors BMP4 and hLIF did not significantly affect expression of classical and reactive astrocyte markers in stimulated iPSC-derived astrocytes

Expression at the mRNA level of reactive astrocyte marker *PTX3* tended to decrease when astrocytes were matured for 7 d compared to 10 d but this effect is not significant (Figure 3.3.5. A). *SERPINA3* and *AMIGO2* mRNA expression at baseline and following 24 h stimulation with inflammatory microglial factors were unaffected by astrocyte maturation protocol (Figure 3.3.5. B, C). Expression of astrocyte marker *GFAP* tended to increase when astrocyte maturation factors were withdrawn prior to simulation but this effect was not significant, maturation similarly have no effect on *GFAP* mRNA expression following stimulation (Figure 3.3.5. D). *VIM* mRNA expression was not affected by incubation time with maturation factors BMP4 and hLIF (Figure 3.3.5. E).

Taken together this data does not indicate that the astrocyte maturation protocols are drastically affecting basal reactivity or response to inflammation, however, BMP4 and hLIF may be having a priming effect with regards to IL6 secretion. This coupled with a trend for reduced *PTX3* following withdrawal indicated that the 7 d maturation followed by 3 d rest is best to ensure a quiescent-like mature astrocyte is produced prior to stimulation. As such this protocol was applied for the remainder of the study.

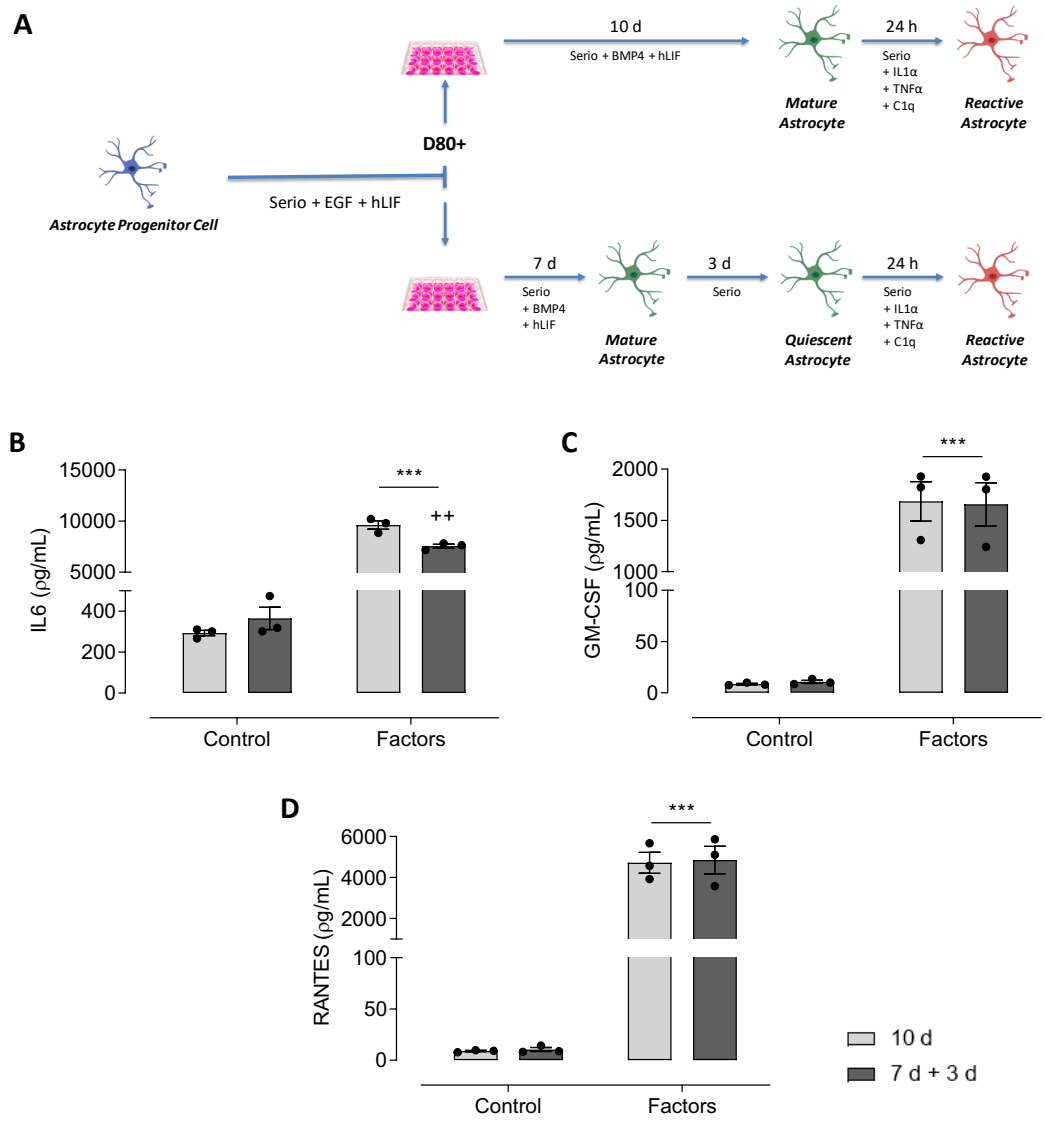


Figure 3.3.4. Maturation factors BMP4 and hLIF significantly affect IL6 secretion in stimulated iPSC-derived astrocytes.

*iPSC-derived cortical astrocyte maturation and stimulation timeline (A). IL6 secretion was significantly increased following stimulation with inflammatory microglial factors, this increase is significantly reduced as a result of withdrawing BMP4 and hLIF 72 h prior to stimulation (B). GM-CSF (C) and RANTES (D) secretion is significantly increased following stimulation with inflammatory microglial factors but is unaffected by maturation factors. Data expressed as mean ± SEM (N=3, n=3). *** $p < 0.001$ vs control $^{++}$ $p < 0.01$ vs 10 d maturation. IL6 effect of maturation factors $F(1, 8) = 19.65$, $p = 0.0022$; effect of factors $F(1, 8) = 1349$, $p = < 0.0001$; interaction effect $F(1, 8) = 22.59$, $p = 0.0014$. GM-CSF effect of maturation factors $F(1, 8) = 0.009043$, $p = 0.9266$; effect of factors $F(1, 8) = 135.8$, $p = < 0.0001$; interaction effect $F(1, 8) = 0.1224$, $p = 0.9146$. RANTES effect of maturation factors $F(1, 8) = 0.02441$, $p = 0.8797$; effect of factors $F(1, 8) = 128.6$, $p = < 0.0001$; interaction effect $F(1, 8) = 0.02331$, $p = 0.8824$ (Two-way ANOVA with Bonferroni post hoc).*

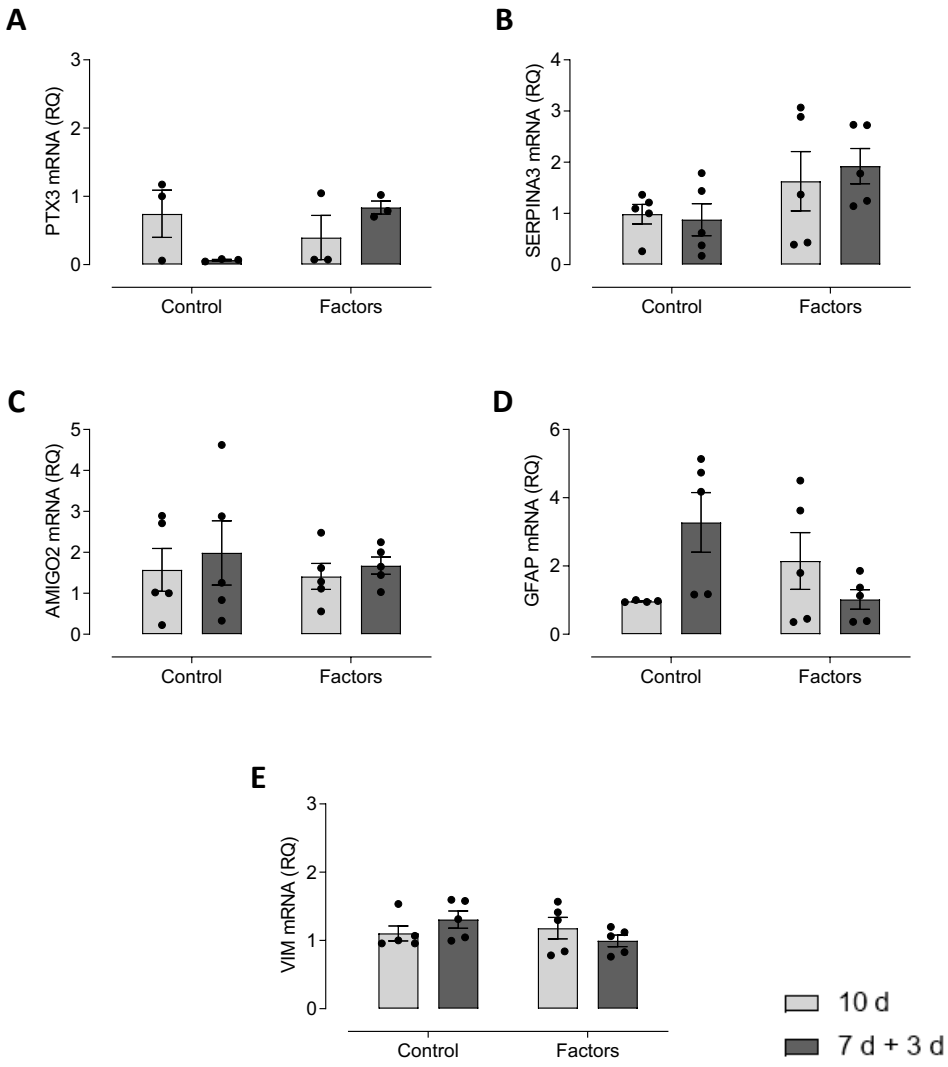


Figure 3.3.5. Maturation factors BMP4 and hLIF do not affect mRNA expression in stimulated iPSC-derived astrocytes.

Baseline levels of PTX3 (A) tended to decrease when astrocytes were matured for 7 d compared to 10 d but this effect is not significant. Expression of SERPINA3 (B) and AMIGO2 (C) were not affected by maturation factors. Expression of astrocyte markers GFAP (D) and VIM (E) were not affected by incubation time with maturation factors BMP4 and hLIF. Data expressed as mean ± SEM (N=3, n=3-5). PTX3 effect of maturation factors F(1, 8) = 0.2433, p = 0.6351; effect of factors F(1, 8) = 07692, p = 0.4060; interaction effect F(1, 8) = 5.351, p = 0.0494. SERPINA3 effect of maturation factors F(1, 16) = 0.06034, p = 0.8091; effect of factors F(1, 16) = 4.852, p = 0.0426; interaction effect F(1, 16) = 0.2753, p = 0.6070. AMIGO2 effect of maturation factors F(1, 16) = 0.4471, p = 0.5133; effect of factors F(1, 16) = 0.2137, p = 0.6501; interaction effect F(1, 16) = 0.02193, p = 0.8841. GFAP effect of maturation factors F(1, 15) = 0.8019, p = 0.3847; effect of factors F(1, 15) = 0.6587, p = 0.4297; interaction effect F(1, 15) = 6.756, p = 0.0201. VIM effect of maturation factors F(1, 16) = 0.005011, p = 0.9444; effect of factors F(1, 16) = 0.9159, p = 0.3528; interaction effect F(1, 16) = 2.513, p = 0.1325 (Two-way ANOVA with Bonferroni post hoc).

3.3.5 iPSC-derived reactive astrocytes display morphological changes

Morphological changes were quantitatively analysed as nuclear:cytoplasm ratio (Hallmann *et al.*, 2017). Nuclear area was quantified and found to be significantly decreased in reactive astrocytes ($p < 0.05$) compared to control astrocytes. Cytoplasm area was also reduced in reactive astrocytes compared to control ($p = 0.0525$). Subsequently, the nuclear:cytoplasm ratio was increased in reactive astrocytes (Figure 3.3.6).

In order to ascertain the effect of microglial factors on GFAP protein expression, a commonly used marker of astrocyte reactivity, densitometry analysis of GFAP fluorescence was carried out and presented as CTCF (Hawkins *et al.*, 2018). No significant difference in GFAP fluorescence was found in stimulated astrocytes compared to control (Figure 3.3.7).

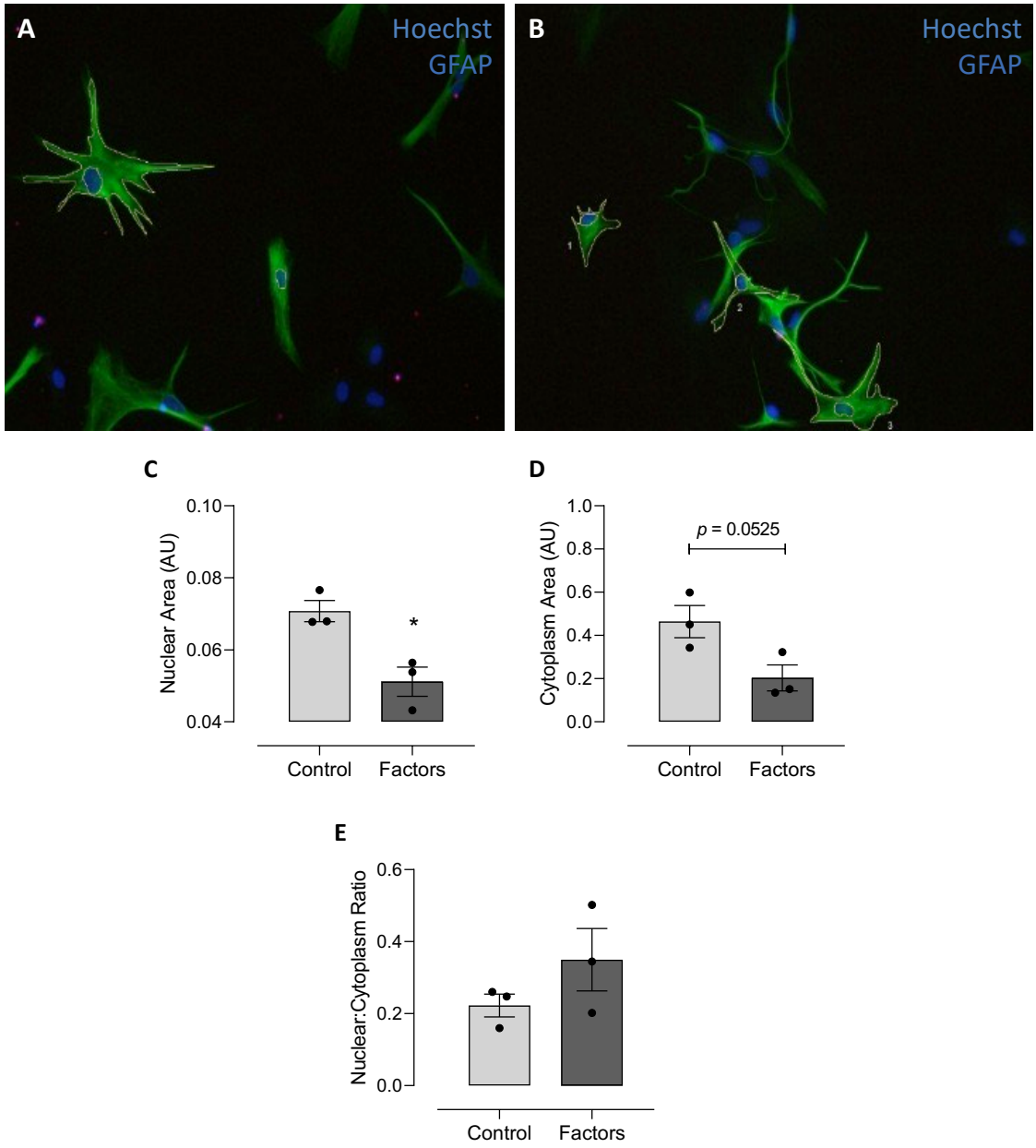


Figure 3.3.6. Stimulation with inflammatory microglial factors results in significant morphological changes in iPSC-derived cortical astrocytes.

*iPSC-derived astrocytes have significantly altered morphology following stimulation with inflammatory microglial factors. Nuclear area (C) is significantly reduced. Cytoplasm area (D) tends to decrease in stimulated astrocytes compared to control. Nuclear:cytoplasm ratio tends to increase in stimulated astrocytes compared to control (E). Representative images display control astrocytes (A) and stimulated astrocytes (B) at x40 magnification. Data expressed as mean ± SEM (N=3, n=3). * $p < 0.05$ vs control. Nuclear area $t = 3.924$, $df = 4$, $p = 0.0172$; cytoplasm area $t = 2.730$, $df = 4$, $p = 0.0525$; nuclear:cytoplasm area $t = 1.378$, $df = 4$, $p = 0.2402$ (Unpaired student t-test).*

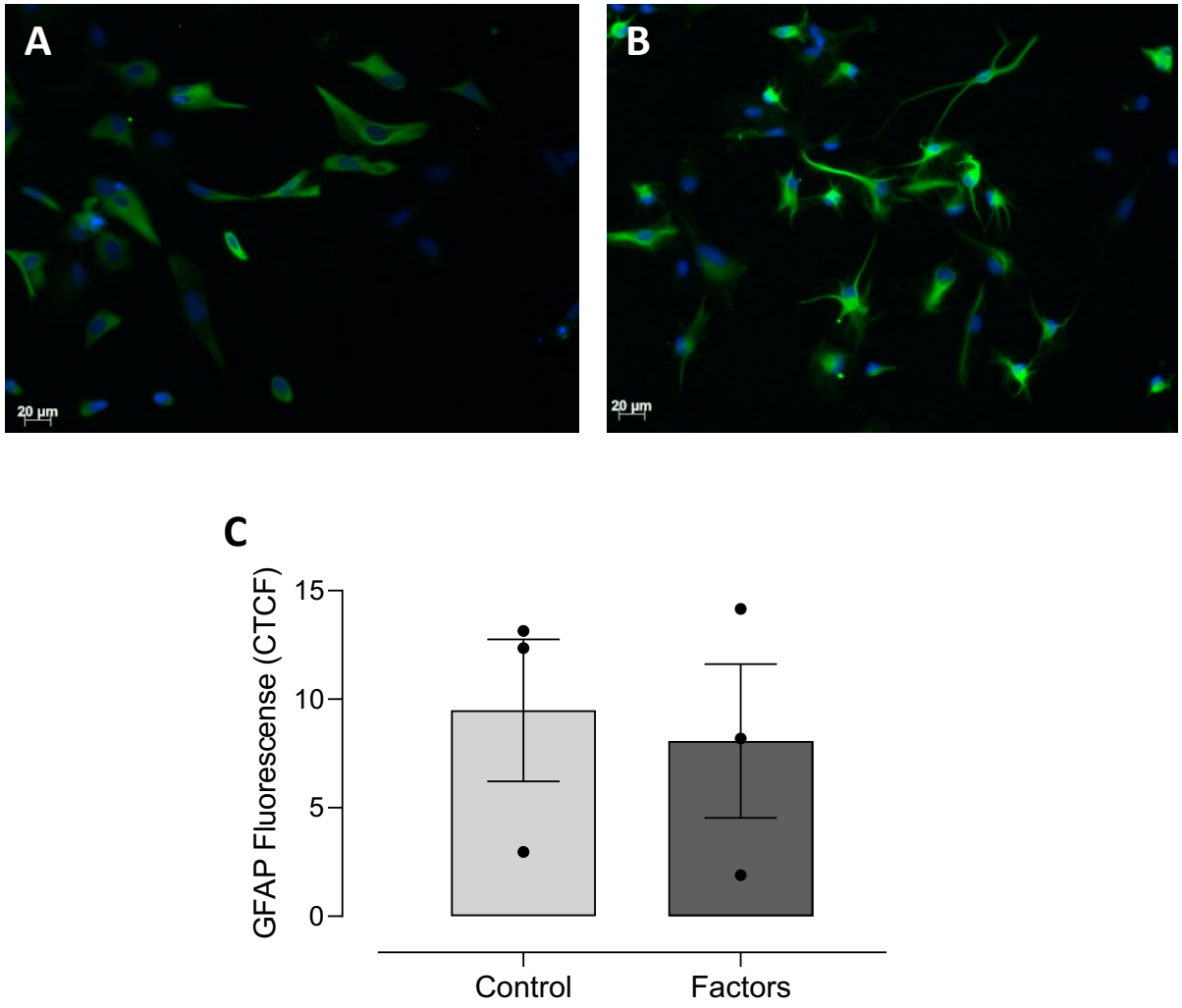


Figure 3.3.7. Stimulation with inflammatory microglial factors does not affect GFAP fluorescence in iPSC-derived cortical astrocytes.

Representative images shown for control quiescent astrocytes (A) and stimulated reactive astrocytes (B) imaged at x40 magnification. GFAP fluorescence is not significantly altered in reactive astrocytes compared to control (C). Data expressed as mean ± SEM (N=3, n=3). t = 0.2926, df = 4, p = 0.7844 (Unpaired student t-test).

3.3.6 iPSC-derived reactive astrocytes show increased expression IL6 and secretion of pro-inflammatory mediators

IL6 is a major cytokine associated with astrocytes, which has been shown to be a key player in astrocyte-mediated neurodegeneration (Hawkins *et al.*, 2018) and as such, it was important to show that human iPSC-derived astrocytes respond in the same fashion. iPSC-derived astrocytes were stimulated with inflammatory microglial factors (IL1α, 3 ng/mL; TNFα, 30 ng/mL; C1q, 400 ng/mL) and the subsequent effect on IL6 was examined via qPCR and ELISA.

IL6 mRNA expression is significantly increased ($p < 0.01$) as a result of microglial factor stimulation (Figure 3.3.8. A). Coupled with this, IL6 secretion is also significantly increased ($p < 0.001$) in astrocytes stimulated with inflammatory microglial factors (Figure 3.3.8. B).

This robust IL6 signal prompted further investigation of protein secretion in iPSC-derived reactive astrocytes. Levels of the inflammatory chemokine RANTES and the inflammatory cytokine GM-CSF secreted by stimulated astrocytes were examined via ELISA. Secretion of these proteins also significantly increased ($p < 0.01$) in response to inflammatory insult (Figure 3.3.9).

Cytokine levels ranging in the thousands of ρg/mL are extraordinarily high and as such the concentrations used for subsequent stimulation included at 10-fold titrated down stimulation for comparison (IL1α, 0.3 ng/mL; TNFα, 3 ng/mL; C1q, 40 ng/mL). Treatments are subsequently denoted as high (Liddelow *et al.*, 2017) and low (1:10 dilution of Liddelow factors). *IL6* mRNA expression is increased at both concentration of microglial factors but this increase is significant at the higher concentration only ($p < 0.001$). IL6 secretion is significantly increased in astrocytes stimulated with inflammatory microglial factors at both low and high concentrations ($p < 0.001$) (Figure 3.3.10).

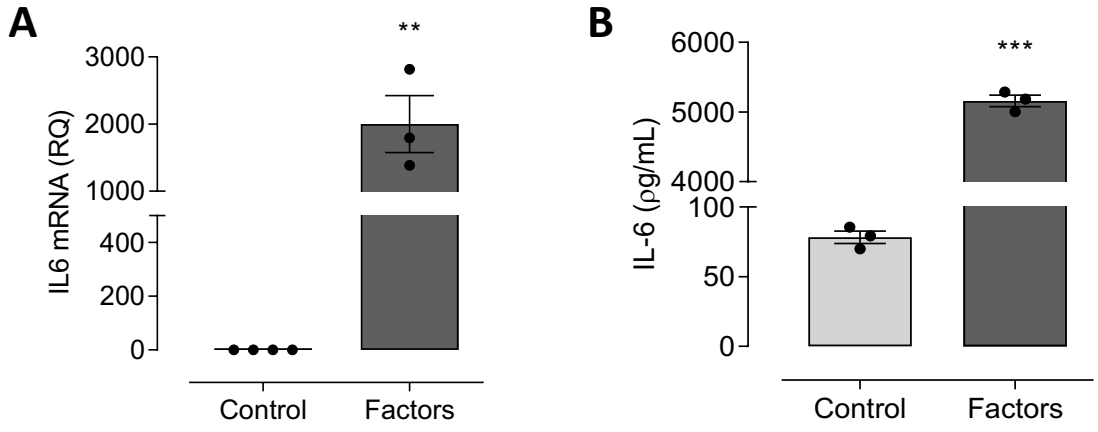


Figure 3.3.8. Inflammatory microglial factors significantly increase IL6 mRNA expression and secretion in iPSC-derived cortical astrocytes.

*Stimulation with inflammatory microglial factors significantly increases IL6 mRNA expression (A) and protein secretion (B). Data expressed as mean ± SEM (N=3, n=3-4). ** p < 0.01, *** p < 0.001 vs control. IL6 mRNA t = 5.612, df = 5, p = 0.0025; IL6 protein t = 61.10, df = 4, p = < 0.0001 (Unpaired t-test).*

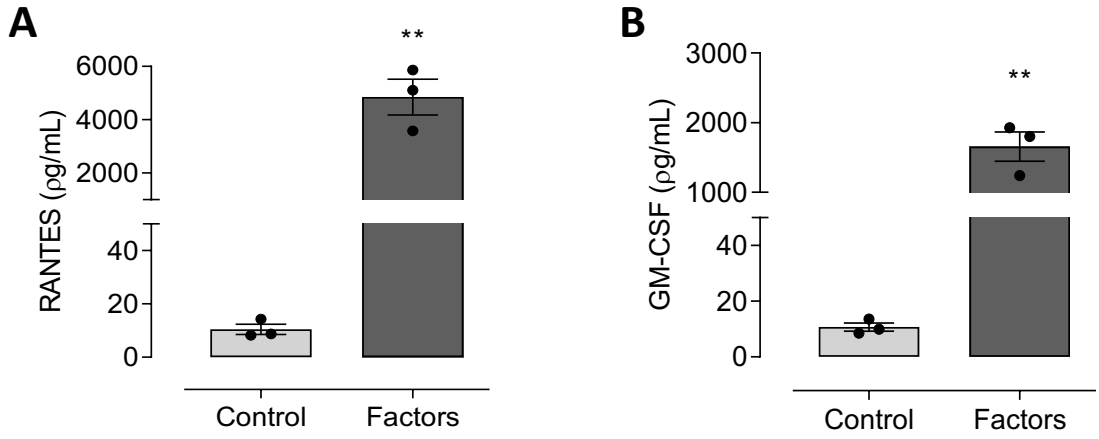


Figure 3.3.9. Inflammatory microglial factors significantly increase secretion of RANTES and GM-CSF in iPSC-derived cortical astrocytes.

*Secretion of inflammatory chemokine RANTES (A) and inflammatory cytokine GM-CSF (B) is significantly increased in astrocytes following stimulation with inflammatory microglial factors. Data expressed as mean ± SEM (N=3, n=3). *** p < 0.001 vs control. RANTES t = 7.215, df = 4, p = 0.0020; GM-CSF t = 7.795, df = 4, p = 0.0015 (Unpaired t-test).*

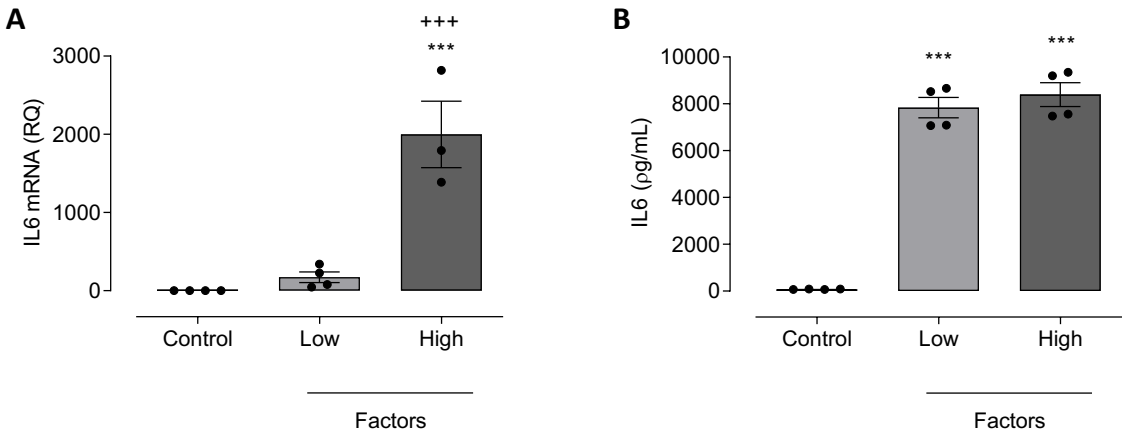


Figure 3.3.10. Inflammatory microglial factors significantly increase IL6 secretion and expression in iPSC-derived cortical astrocytes.

*IL6 mRNA expression is increased at both concentration of microglial factors but this increase is significant at the higher concentration only (A). IL6 secretion is significantly increased in astrocytes stimulated with inflammatory microglial factors at both low and high concentrations (B). Data expressed as mean ± SEM (N=3, n=3-4). *** p < 0.001 vs control, $^{+++}$ p < 0.001 vs factors low. IL6 mRNA F(2, 8) = 28.15, p = 0.0002; IL6 protein F(2, 9) = 144.1, p = < 0.0001 (One-way ANOVA with Newman-Keuls post hoc).*

3.3.7 iPSC-derived reactive astrocytes show increased expression of genes associated with reactive astrogliosis

The secretion of potent levels of inflammatory mediators seen here, combined with the previously discussed morphological changes complement the existing literature which shows that these inflammatory microglial factors IL1α, TNFα and C1q are sufficient to generate a reactive astrocyte (Zamanian *et al.*, 2012; Liddelow *et al.*, 2017). However, it is necessary to further consolidate this data by examining gene expression. A number of genes associated with reactive astrogliosis were chosen from the literature in order to construct a more rounded inflammatory profile for human iPSC-derived astrocytes.

Stimulation with microglial factors significantly increased mRNA expression of *IL1β* ($p < 0.01$), *CXCL10* ($p < 0.001$) and *ICAM1* ($p < 0.001$) at the high concentration only. C*3* ($p < 0.001$), *SERPINA3* ($p < 0.001$) and *LCN2* ($p < 0.01$, $p < 0.001$) mRNA expression were significantly induced at both concentrations. *PTX3* mRNA expression was significantly increased ($p < 0.05$) at the low concentration only. Stimulation with microglial factors significantly decreased mRNA expression of *GFAP* ($p < 0.001$) at both concentrations, but had no effect on *VIM* mRNA expression (Figure 3.3.11).

This data supports the hypothesis that IL1α, TNFα and C1q are sufficient to induce a reactive phenotype in iPSC-derived astrocytes.

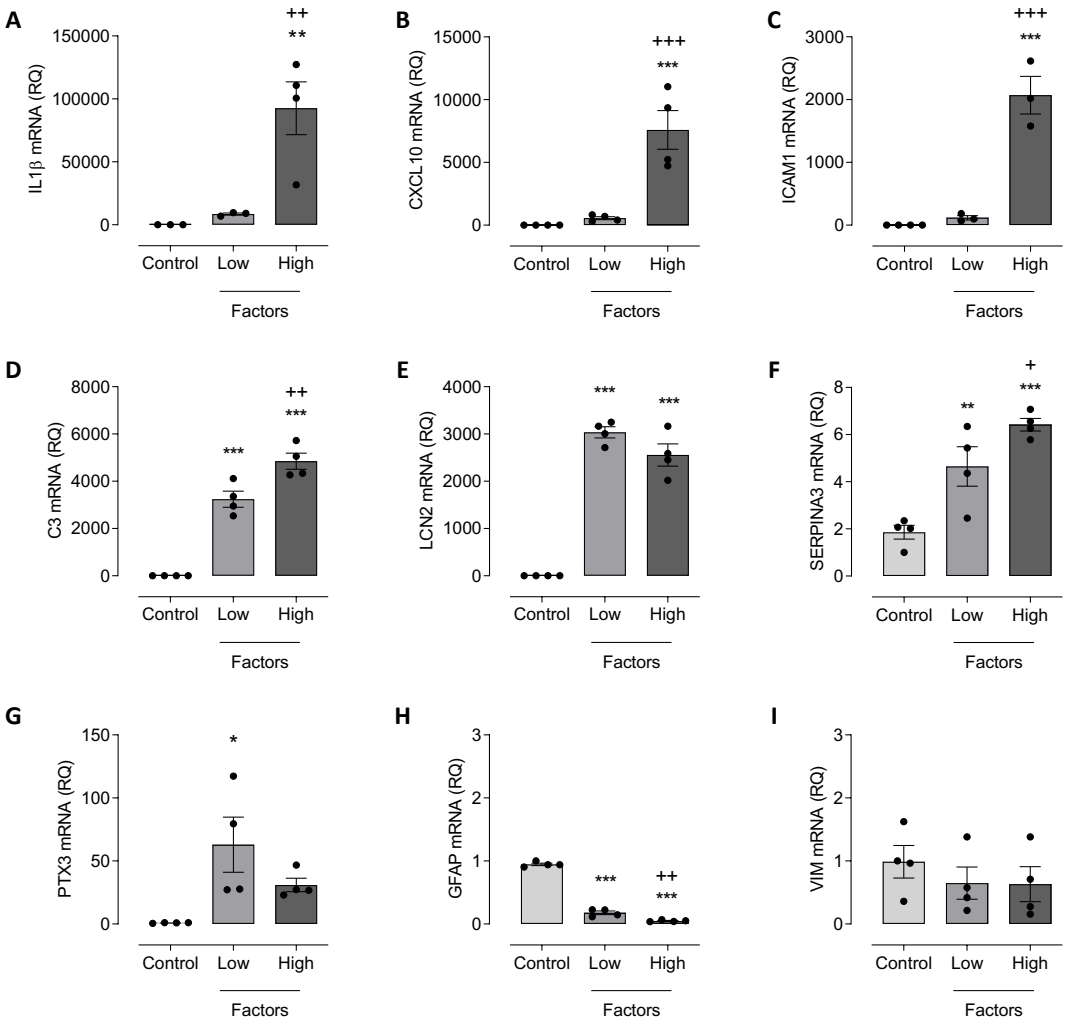


Figure 3.3.11. Inflammatory microglial factors significantly increase expression of reactive genes in iPSC-derived cortical astrocytes.

*Stimulation with microglial factors significantly increased mRNA expression of IL1β (A), CXCL10 (B) and ICAM1 (C) at the high concentration. Stimulation with inflammatory microglial factors significantly increased mRNA expression of C3 (D), LCN2 (E) and SERPINA3 (F) at both concentrations. PTX3 mRNA expression was significantly increased at the low concentration only (G). GFAP mRNA expression was significantly decreased upon stimulation (H). mRNA expression of VIM was unaffected (I). Data expressed as mean ± SEM (N=3, n=3-4). * $p < 0.05$, ** $p < 0.01$, *** $p < 0.001$ vs control; $^{+}$ $p < 0.05$, $^{++}$ $p < 0.01$, $^{+++}$ $p < 0.001$ vs factors low. IL1β $F(2, 7) = 12.40$, $p = 0.0050$; CXCL10 $F(2, 9) = 22.27$, $p = 0.0003$; ICAM1 $F(2, 7) = 54.96$, $p = < 0.0001$; C3 $F(2, 9) = 79.54$, $p = < 0.0001$; LCN2 $F(2, 9) = 114.2$, $p = < 0.0001$; SERPINA3 $F(2, 9) = 18.51$, $p = 0.0006$; PTX3 $F(2, 9) = 5.692$, $p = 0.0253$; GFAP $F(2, 9) = 565.5$, $p = < 0.0001$; VIM $F(2, 9) = 0.5780$, $p = 0.5806$ (One-way ANOVA with Newman-Keuls post hoc).*

3.3.8 iPSC-derived reactive astrocyte conditioned media causes detrimental effects to iPSC-derived neurons

Having shown that stimulation with microglial factors IL1α, TNFα and C1q generates a reactive astrocyte, it was next determined whether these reactive astrocytes were detrimental to neurons as is the case throughout much of the literature. Conditioned media from control and reactive astrocytes was applied to neurons for 48 h. The impact of reactive ACM was assessed via ICC and quantification of neuronal clusters in terms of total clusters, clusters with extending processes and cluster size.

Stimulation with ACM from reactive astrocytes resulted in a significant reduction in the total number of neuronal clusters ($p < 0.001$; Figure 3.3.12. D, E), a significant reduction in the number of clusters with extending processes ($p < 0.001$; Figure 3.3.12. F) as well as a reduced number of smaller and medium sized clusters ($p < 0.01$, $p < 0.001$; Figure 3.3.12. G).

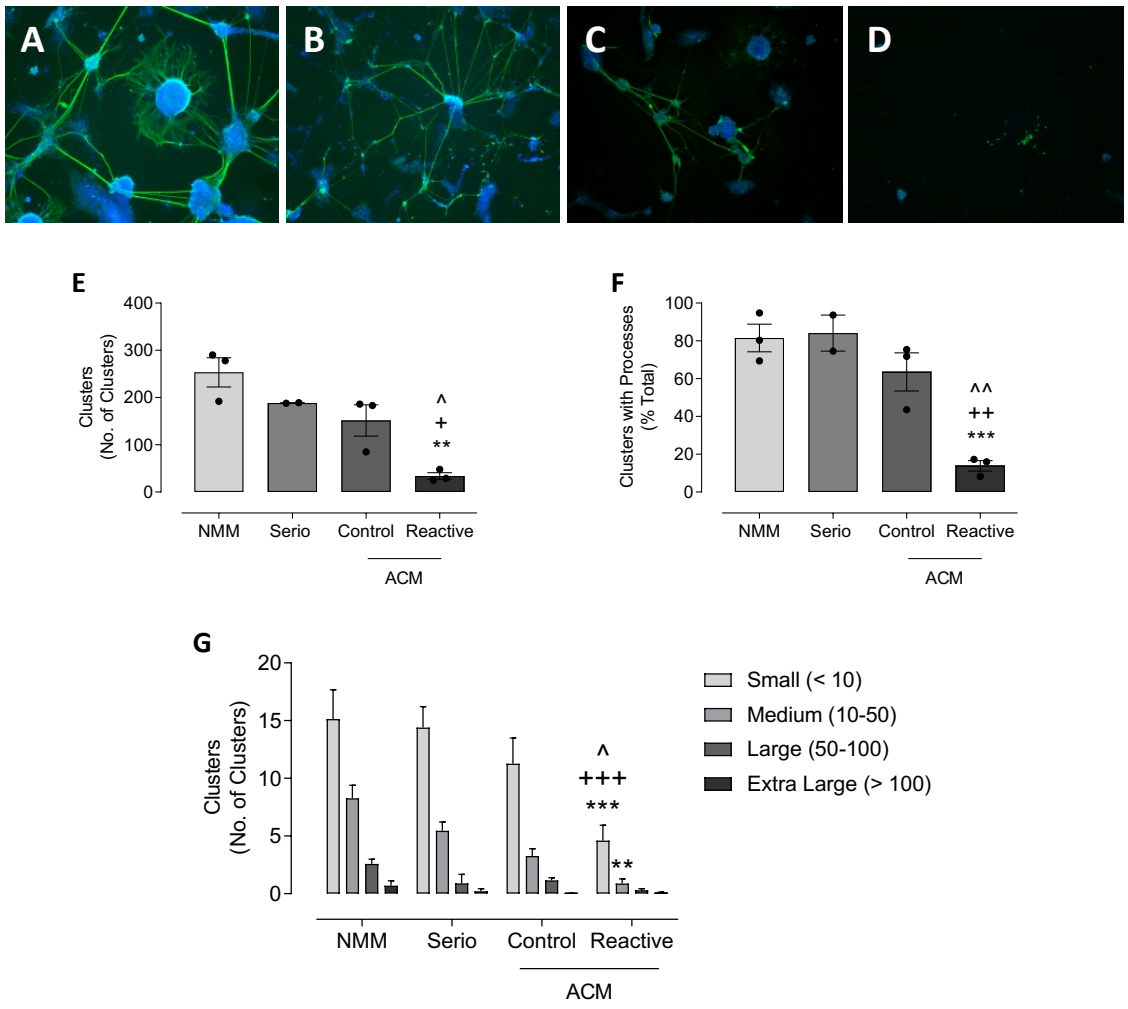


Figure 3.3.12. Stimulation with reactive astrocyte conditioned media results in smaller and significantly less clusters of iPSC-derived cortical neurons.

*Representative images from each treatment group NMM (A), Serio (B), ACM control (C) and reactive ACM (D) were captured at x5 magnification. Stimulation with astrocyte conditioned media from reactive astrocytes resulted in a significant reduction in the total number of neuronal clusters (D, E), a significant reduction in the number of clusters with extending processes (F). With regards to classification of clusters by size, reactive ACM resulted in a significant reduction in small and medium sized clusters compared to control (G). Data expressed as mean ± SEM (N=3, n=4). *** $p < 0.001$ vs NMM, $^{+++}$ $p < 0.001$ vs Serio, ^^ $p < 0.01$ vs ACM Control. Clusters $F(3, 7) = 13.90$, $p = 0.0025$; Clusters with processes $F(3, 7) = 18.03$, $p = 0.0011$ (One-way ANOVA with Newman-Keuls post hoc). Classification by size: effect of cluster size $F(3, 40) = 66.95$, $p = < 0.0001$; effect of ACM $F(3, 40) = 15.75$, $p = < 0.0001$; interaction effect $F(9, 40) = 3.636$, $p = 0.0022$ (Two-way ANOVA with Bonferroni post hoc).*

3.4 Discussion

Astrocytes are the homeostatic regulators of the CNS, but there is more and more evidence in the literature supporting a detrimental role of astrocytes in neurodegenerative diseases (Roybon *et al.*, 2013; Osborn *et al.*, 2016; Liddelow *et al.*, 2017). Many studies support a reactive astrocyte phenotype in disease, for example, the Barres laboratory group found significant C3 (a marker for reactive astrocytes) immunoreactivity in post mortem tissue from patients of AD, PD and HD, compared to healthy counterparts (Liddelow *et al.*, 2017). The same lab attempted to characterise activated astrocytes into two broad categories, A1 reactive astrocytes produced following an inflammatory insult and A2 protective astrocytes resulting from ischemic shock (Zamanian *et al.*, 2012). These astrocyte phenotypes were characterised via their gene expression profiles where genes related to inflammation were up-regulated in the A1 phenotype and genes related to repair were up-regulated in the A2 phenotype. This classification of activated phenotypes follows the previous characterisation of polarised macrophages and microglia (Kanazawa *et al.*, 2017), and while this may be an oversimplification of the *in vivo* environment it provides strong evidence for different reactive phenotypes in disease, thereby supporting the concept of an astrocytic functional switch in disease.

The aim of this study was to generate and characterise human iPSC-derived astrocytes and subsequently stimulate them to produce a reactive astrocyte phenotype representative of a disease state. Reactivity was characterised by examining astrocyte morphology, protein secretion and gene expression, and the effect of reactive astrocytes on neurons was examined.

3.4.1 iPSC-derived neurons and astrocytes are positive for classical markers

iPSC-derived neurons (D20+) stained positive for the classical neuronal marker β-tubulin III, and the cortical markers TBR1 confirming successful differentiation of the target cell population. β-tubulin III is a constituent of neuronal microtubules frequently used as a marker of neuronal populations (Prokosch *et al.*, 2019). During neurogenesis, β-tubulin III is neuron associated but also has transient expression in putative neuronal and glial cells (Vinores *et al.*, 1995). In the CNS, β-tubulin III is expressed by NPC as well as glial progenitor cells, however, in the adult CNS is almost exclusively neuron specific and expressed neither in adult glia nor vascular cells (Prokosch *et al.*, 2019). Besides specific

marker proteins that define cell type in the CNS, different regions of the CNS have specific expression patterns. The numerous areas and layers of the cerebral cortex are defined by specific genetic programs which are initiated in the relevant progenitor cells then implemented in post-mitotic neurons. One of these such genetic programs is TBR1, a transcription factor expressed in post-mitotic projection neurons (Bedogni *et al.*, 2010). TBR1 is therefore used as a deep cortical layer VI marker (Yan *et al.*, 2018).

Further to the characterisation of iPSC-derived neurons, iPSC-derived astrocytes stained positive for traditional astrocyte markers GFAP, Cx43, S100β and EAAT1. Integral to the astrocyte cytoskeleton, intermediate filament protein GFAP, involved in cell migration and motility, anchors the highly expressed glutamate transporter EAAT1 in the cell membrane (Hol & Pekny, 2015; Ghanavatinejad *et al.*, 2019). Cx43 is an astrocyte specific connexin, and the most widely and abundantly expressed gap junction protein in astrocytes (Almad *et al.*, 2016). S100β, a glial-specific calcium-binding protein, is primarily expressed in astrocytes, most commonly co-localised with GFAP (Shaltouki *et al.*, 2013). Furthermore, S100β is considered a mature astrocyte marker as it is highly expressed in the adult CNS (Raponi *et al.*, 2007). As well as expressing astrocyte associated markers, iPSC-derived astrocytes were observed to have a stellate morphology characteristic of this cell type (Matyash & Kettenmann, 2010). Taken together this confirms astrocyte cell fate.

3.4.2 Withdrawal of maturation factors prior to stimulation ensures a mature quiescent-like astrocyte is achieved at baseline

BMP4 is a member of the TGFβ superfamily, which mediates the suppression of neural fate acquisition by ectodermal cells (Wilson & Hemmati-Brivanlou, 1995). It has additionally been found to induce the elaboration and differentiation of the astroglial lineage (Gomes *et al.*, 2003). LIF is a member of the IL6 family of cytokines that has been shown to promote cell survival and influence cell fate. It acts through the JAK-STAT3 pathway (Majumder *et al.*, 2013) which is involved in mediating astrocyte reactivity and is activated in many models of neurodegenerative disease (Okada *et al.*, 2006). LIF is included in the protocol of astrocyte maturation as it prevents the fate transition of neural stem cells into neurons (Palm *et al.*, 2015).

It has recently been questioned if the presence of these factors in the astrocyte maturation protocol may increase the baseline reactivity of astrocytes. A 2017 publication

indicated that hLIF activates STAT3 signalling and may result in up-regulation of inflammatory mediators such as IL6 (Tyzack *et al.*, 2017). To ensure astrocytes were quiescent at the time of stimulation two terminal differentiation protocols were compared. iPSC-derived astrocytes were either matured for 10 d then stimulated or matured for 7 d followed by a 72 h rest period without any additional factors prior to stimulation. While gene expression of classical and reactive astrocyte markers were not significantly affected, baseline expression of *PTX3* mRNA tended to decrease when astrocytes were matured for 7 d followed by a 72 h "cooling-off" period. Subsequent to this, IL6 secretion was significantly reduced following stimulation with inflammatory microglial factors when maturation was carried out for only 7 d. Surprisingly, unlike IL6, secretion of GM-CSF and RANTES – direct targets of the NF-κB pathway like IL6 – was unaffected by withdrawal of the maturing factors BMP4 and hLIF prior to stimulation. Taken together, this data indicates that maturation for 7 d followed by a 72 h period without factors produces a more "quiescent-like" astrocyte at baseline. It was determined that this quiescent-like astrocyte was the more desirable control and as such the 7 d maturation protocol was followed for all subsequent experiments.

3.4.3 Characterisation of astrocyte reactivity

With the characterisation of reactive astrocytes as A1 or A2 phenotypes in terms of their gene expression now widely considered to be an oversimplification of *in vivo* scenarios, it is of interest to more thoroughly explore the reactive astrocyte phenotype from form to function.

3.4.3.1 GFAP, a classical astrocyte marker but flawed reactivity marker

GFAP is an intermediate filament protein constituent of astrocytes, widely used as an astrocytic marker and also as a common indicator of astrocyte reactivity. There is a body of literature which report significant increases in GFAP expression following astrocyte activation (Zamanian *et al.*, 2012; Anderson *et al.*, 2014; Ben Haim *et al.*, 2015; Anderson *et al.*, 2016). Furthermore, the density of GFAP fluorescence has been shown to be up-regulated in a post mortem HD study where GFAP co-localisation with mutant HTT protein was found in striatal astrocytes of HD patients (Faideau *et al.*, 2010). Measured as CTCF, no significant difference in GFAP fluorescence was found in microglial factor-stimulated CTX astrocytes compared to control. Subsequent to this, *GFAP* mRNA expression was

found to be down-regulated in human iPSC-derived astrocytes in response to an inflammatory insult. Down-regulation of GFAP was also recorded in human iPSC-derived astrocytes subjected to treatment with TNFα and IL1β (Hyvarinen *et al.*, 2019). Other research has reported similar findings, where different stimulators of astrocyte reactivity led to similar degrees of GFAP up-regulation while causing substantially different changes in transcriptome profiles and cell function (Anderson *et al.*, 2014), highlighting the unpredictability of GFAP as a marker of astrocyte reactivity. There is also great heterogeneity in GFAP expression in adjacent astrocytes in all brain regions under normal physiological conditions (John Lin *et al.*, 2017), there are even certain subpopulations of astrocytes which do not express GFAP at all (Walz & Lang, 1998). Taken together this suggests that GFAP is not a clear marker of astrocyte reactivity. Different stimuli which result in astrocyte reactivity and similar responses in GFAP can have notably different changes in gene expression and subsequently cell function. As such GFAP is no longer acceptable as a marker of astrocyte reactivity in its own right, but is rather considered one of many possible markers of reactivity.

3.4.3.2 Reactive astrocytes undergo morphology changes

Reactive astrogliosis is associated with significant morphological changes in the affected astrocyte population. In vivo, these morphological changes include hypertrophied processes and interdigitation (Anderson *et al.*, 2014). Control iPSC-derived astrocytes displayed the classic star-shaped morphology associated with this cell type, while reactive astrocytes had more pronounced longer and extending processes. Nuclear:cytoplasm ratio provides a quantitative evaluation of the morphological changes induced by microglial factors (Hallmann *et al.*, 2017). Following stimulation, a significant decrease in nucleus area coupled with a decrease in cytoplasm area compared to control resulted in a trend towards an increased nuclear:cytoplasm ratio. This converges from a similar study which observed increased nucleus and cytoplasm area following astrocyte stimulation (Hawkins *et al.*, 2018). Altered morphology may in turn alter function in astrocytes. Compromised astrocytic function has been proposed as a mechanism of neuronal death via astrocytes (Liddelow *et al.*, 2017).

3.4.3.3 The astrocyte secretome is a viable indicator of astrocyte reactivity

The inflammatory cytokine IL6 is considered a canonical marker of reactivity, associated with context-specific induced signalling which can result in deleterious pro-inflammatory processes or neuroprotective anti-inflammatory processes (Tyzack *et al.*, 2017). IL6 expression and secretion was significantly increased in iPSC-derived astrocytes following stimulation with inflammatory microglial factors IL1α, TNFα and C1q. This corresponds with a study carried out in rat astrocytes which showed that IL1β and TNFα have a strong induction on IL6 secretion (Benveniste *et al.*, 1990). Similarly, LPS-induced inflammation results in increased IL6 mRNA and secretion in glial cultures from adult rat brains, with aging having a significant effect on IL6 in its own right and in conjunction with LPS-induced inflammation (Xie *et al.*, 2003). Furthermore, IL1β and TNFα have independently been demonstrated to induce increased mRNA expression and secretion of numerous inflammatory associated cytokines including IL6 in embryonic brain-derived human astrocytes (Aloisi *et al.*, 1992). More recently it has been elucidated that IL6 can exert pro- and anti-inflammatory responses depending on its method of activation, with regenerative anti-inflammatory processes mediated by classical signalling via JAK/STAT pathways and pro-inflammatory processes mediated by trans signalling via a complex consisting of IL6 bound to sIL6R (Scheller *et al.*, 2011). IL6 can also induce its own production in an autocrine manner dependent on the presence of sIL6R (Van Wagoner *et al.*, 1999; Roybon *et al.*, 2013), this may explain the potent levels of IL6 secretion observed in iPSC-derived reactive astrocytes.

GM-CSF is a pro-inflammatory cytokine which signals via STAT3 and STAT5 to stimulate the production of monocytes, which may then migrate through the circulation and mature into macrophages in tissue, thus forming part of an inflammatory cascade (Fleetwood *et al.*, 2005; Choi *et al.*, 2014). GM-CSF is also a potent mitogen for microglia (Lee *et al.*, 1994; Fan *et al.*, 2018) dependent on p38 MAPK and NF-κB activation (Zaheer *et al.*, 2007), and has also been shown to prime microglia via the same ERK1/2 and p38 pathway (Parajuli *et al.*, 2012). As a result, an increase in GM-CSF secretion by astrocytes can drive microglia activation and proliferation, exacerbating inflammation and subsequently degeneration. While non-activated astrocytes and neurons have been shown to have low basal secretion levels of GM-CSF, increased GM-CSF has been linked to a number of neurodegenerative diseases including AD, PD and MS (Tarkowski *et al.*, 2001; Kempuraj *et al.*, 2016; Ifergan *et al.*, 2017). Furthermore, the GM-CSF-dependent secretion of a number of inflammatory cytokines, including IL1β and IL6, is cytotoxic to

neurons (Zaheer *et al.*, 2007). This study found significant GM-CSF secretion from iPSC-derived astrocytes upon inflammatory insult which corresponds to a study carried out in the human astrocyte Ntera2 cell-line which found increased secretion of GM-CSF following IL1β or TNFα stimulation (Burkert *et al.*, 2012). Taken together, our results combined with the literature may be indicative of a role for astrocytes in the recruitment and subsequent activation of microglia during the inflammatory response to neurodegeneration.

RANTES, also known as CCL5 (chemokine C-C motif ligand 5), is a chemokine which plays a role in the peripheral immune system as a chemoattractant molecule. In the CNS, RANTES is multifunctional with roles including the promotion of inflammation, insulin signalling, modulation of synaptic activity as well as providing protection against a variety of neurotoxins (Lanfranco *et al.*, 2017). RANTES expression is localised in oligodendrocytes, astrocytes and microglia (Lanfranco *et al.*, 2017). Its expression by astrocytes is of particular interest as RANTES is a potent chemoattractant of monocytes and $CD4^+$ T lymphocytes (Tokami *et al.*, 2013), which breach the BBB to enter the brain under neuroinflammatory conditions. The proposed mechanism for its chemoattractant abilities is via interaction with G-protein coupled receptors (GPCR): CCR1, CCR3, CCR4 and CCR5. An astrocytoma cell-line, as well as human and rat primary astrocytes, produce RANTES following stimulation with TNFα and IL1β (Barnes *et al.*, 1996). This corresponds with the significantly increased RANTES secretion detected in our iPSC-derived astrocytes following stimulation with inflammatory microglial factors (IL-1α, TNFα and C1q). Further evidence pertaining to a role for RANTES in neurodegeneration has been found in the MPTP mouse model of PD (Chandra *et al.*, 2016), as well as in PD where a study correlated elevated serum RANTES levels with Hoehn-Yahr score and disease duration (Tang *et al.*, 2014). A chemotactic role of RANTES has been suggested in MS (Barnes *et al.*, 1996) while elevated cytosolic RANTES levels have been seen in the brain of HD mouse models and human HD patients (Chou *et al.*, 2008). There is also some literature claiming high levels of RANTES are secreted in response to MCAO leading to a neuroprotective state (Tokami *et al.*, 2013), however, RANTES is more consistently characterised as an inflammatory chemokine (Choi *et al.*, 2014; Tarassishin *et al.*, 2014; Hennessy *et al.*, 2015).

3.4.3.4 Reactive astrocyte gene expression profile

A 2017 study characterised activated astrocytes into two categories, an A1 reactive astrocyte phenotype induced by inflammatory insult which is pro-inflammatory and an A2 neuroprotective astrocyte induced following ischemic stroke which is anti-inflammatory and reparative (Liddelow *et al.*, 2017). The astrocytes were characterised according to their gene expression profile following activation. Numerous genes were described as PAN reactive because their expression was up-regulated regardless of activated phenotype, these included *GFAP*, *STEAP4* and *VIM*. Further to this, a panel of genes were denoted as either A1-specific (e.g. *SERPING1*, *LIGP1* and *AMIGO2*) or A2-specific (e.g. *CLCF1*, *PTX3* and *CD14*). Given that this study was carried out in mouse primary astrocytes, it was of interest to determine whether a reactive phenotype could similarly be induced in human iPSC-derived astrocytes. From the extensive list of genes probed by Liddelow and colleagues, ten genes were selected and used as a panel of markers to verify that stimulated astrocytes were activated.

GFAP and *VIM* encode the intermediate filament proteins GFAP and vimentin respectively. They are both considered canonical astrocytic markers widely used in the literature to confirm astrocyte cell fate (Roybon *et al.*, 2013). *GFAP* and *VIM* are typically found to be up-regulated when astrocytes become reactive, and are thus regarded as pan-reactive markers (Liddelow *et al.*, 2017). In this study, *GFAP* mRNA expression was significantly decreased following stimulation with inflammatory microglial factors, while *VIM* mRNA was unchanged. While this result contrasts with the expected increase in GFAP in response to activation (Zamanian *et al.*, 2012; Ben Haim *et al.*, 2015), it does concur with the results of a fronto-temporal dementia study which also utilised iPSC-derived astrocytes (Hallmann *et al.*, 2017) as well as confirming the outcome of the densitometry analysis in this study where GFAP was unchanged in reactive astrocytes compared to control. Following microglial factor stimulation, the expression of *VIM* mRNA did not change in astrocytes compared to control. This differs from the expected result of increased expression as the intermediate filament system, which includes both GFAP and vimentin, is known to be up-regulated and rearranged during reactive astrogliosis (Hol & Pekny, 2015). However GFAP is also up-regulated in proliferating cells which clouds its ability to represent reactivity (Janeczko, 1993; Liddelow & Barres, 2017).

The remaining genes which were probed – *IL6*, *IL1β*, *CXCL10*, *ICAM1*, *C3*, *LCN2*, *SERPINA3* and *PTX3* – were all increased in stimulated astrocytes and therefore provide a useful panel for confirmation of astrocyte reactivity state.

IL6 mRNA expression was significantly increased following stimulation with inflammatory microglial facts. This complements the already discussed significant increase in IL6 secretion, a major astrocyte cytokine. Another cytokine whose transcript was induced is IL1β. IL1β is a pro-inflammatory cytokine and a key molecule in systemic immune responses in health and disease. IL1 has been associated with AD where a number of different polymorphisms associated with IL1α and IL1β are implicated in excessive synthesis, translation, and processing of neuronal APP as well as other plaque-associated proteins (Griffin *et al.*, 2000; Griffin & Mrak, 2002). *IL1β* mRNA expression was significantly induced in iPSC-derived astrocytes following stimulation with inflammatory microglial factors IL1α, TNFα and C1q. Increased *IL1β* expression has been associated with Multiple Sclerosis (MS) where patient peripheral immune cells were found to express significantly greater levels of *IL1β* mRNA compared to controls (Heidary *et al.*, 2014). IL1β is a product of NLRP3 (NOD-, LRR- and pyrin domain-containing protein 3) inflammasome activation and assembly. NLRP3 and its molecular components, as well as IL1β, have been found in spinal cord astrocytes of the SOD1 mouse model of ALS. Further, evidence for NLRP3 activation has been detected in ALS patient tissue suggesting that astroglial NLRP3 inflammasome complexes and IL1β are critically involved in neuroinflammation in ALS (Johann *et al.*, 2015).

CXCL10 is a chemokine responsible for attracting peripheral monocytes such as T-helper (Th) cells expressing chemokine receptor 3 (CXCR3), key examples being Th1 and Th17 cells which then proceed to breakdown cell debris at the site of induced inflammation (Groom & Luster, 2011). *CXCL10* mRNA expression was significantly increased in iPSC-derived astrocytes following inflammatory insult, corresponding with much of the related literature. *CXCL10* has been shown in many studies to be up-regulated in reactive astrocytes following stimulation with either LPS or microglial factors (Zamanian *et al.*, 2012; Clarke *et al.*, 2018). Additionally, *CXCL10* expression has previously been shown to be up-regulated at a higher rate in aged reactive astrocytes, when AD prominently occurs, and is also expressed at higher levels in mice hippocampal and striatal reactive astrocytes in comparison to cortical astrocytes (Clarke *et al.*, 2018). CXCL10 immunoreactivity was found to be markedly elevated in astrocytes in AD post-mortem brain samples compared to control, these $CXCL10^{+}$ astrocytes were found to be associated with senile plaques (Xia *et al.*, 2000). CXCL10 has also been shown to be elevated in the CSF of AD patients and subjects with mild cognitive impairment compared to healthy controls (Galimberti *et al.*, 2003). This high expression of *CXCL10*, coupled with BBB breakdown seen in AD and other

neurodegenerative disorders, could result in mass invasion of peripheral immune cells into the CNS and irreversible damage.

ICAM1 (intercellular adhesion molecule-1) is a cell surface glycoprotein which contributes to the mediation of cellular signalling through integrin binding. It is typically expressed on endothelial cells and cells of the immune system (Long, 2011). ICAM1 additionally forms part of the STAT3 signalling pathway (Hashioka *et al.*, 2011; Tyzack *et al.*, 2017) and so is associated with inflammation. *ICAM1* expression was significantly increased in iPSC-derived astrocytes following stimulation. This is congruent with the findings of studies in primary rat astrocytes (Shrikant *et al.*, 1994) and human astrocyte cultures (Aloisi *et al.*, 1992). Constitutively expressed by astrocytes, *ICAM1* expression is known to be up-regulated in an inflammatory environment (Shrikant *et al.*, 1994) and is aberrantly induced in CNS pathologies, including AD, with ligation of the molecule even leading to IL6 secretion (Lee *et al.*, 2000). Additionally, reactive astrocytes in the substantia nigra of PD and MPTP-treated monkeys have high levels of ICAM1, which is shown to be induced by secreted α-synuclein (Klegeris *et al.*, 2006).

C3 is a member of the complement system. In the developing CNS, C1q promotes activation of C3 which in turn marks subsets of synapses for pruning. However, inappropriate activation of this pathway by soluble Aβ has been linked to synaptic loss in AD (Hong *et al.*, 2016). More recently, C3 has been proposed as a new marker of astrocyte reactivity following detection of high levels of $C3^+$ astrocytes in post mortem brain samples from AD, PD and ALS patients (Liddelow *et al.*, 2017). *C3* mRNA expression was significantly induced in this study, which complements the existing literature pertaining to C3 as a reactive astrocyte marker. High levels of *C3* expression have also been reported in human iPSC-derived astrocytes following stimulation with microglial factors IL1β and TNFα (Hyvarinen *et al.*, 2019). The C3 receptor (C3aR) which is highly expressed by astrocytes and microglia in the CNS has been suggested as a target for therapies aiming to reduce reactive astrogliosis in neurodegeneration. A recent study demonstrated that C3aR deletion in the tau PS19 mouse model of AD resulted in the rescue of tau pathology and attenuation of neuroinflammation, synaptic deficits, and neurodegeneration (Litvinchuk *et al.*, 2018). However, this is contrasted in a mouse model of prion disease where abolishing A1 astrocytes led to an accelerated disease course (Hartmann *et al.*, 2019). So while C3 may act as a useful reactive astrocyte marker, its use as a therapeutic target requires further investigation.

Lipocalin-2 (LCN2) is a secretory protein involved in the regulation of diverse cellular processes including cell death and survival, cell migration and invasion, cell differentiation, inflammation, and tissue regeneration. LCN2 secreted by astrocytes under inflammatory conditions promotes apoptosis, morphological changes, and migration in astrocytes both *in vitro* and *in vivo* (Lee *et al.*, 2009; Lee *et al.*, 2015). LCN2 is an innate immunity-associated gene and inducible factor in reactive astrocytes which is selectively neurotoxic in neurodegenerative diseases (Bi *et al.*, 2013; Tong *et al.*, 2015), however, LCN2 has also been shown to serve as a potent protective factor in the CNS in response to systemic injury (Kang *et al.*, 2018). Up-regulation of LCN2 has previously been observed following stimulation with TNFα and IL1β amongst other inflammatory microglia secreted factors, while it is undetectable in quiescent astrocytes (Zamanian *et al.*, 2012; Roybon *et al.*, 2013; Liddelow *et al.*, 2017). LCN2 secreted under inflammatory conditions promotes morphology changes associated with reactive astrocytosis and apoptosis, further promoting astrocytic death (Lee *et al.*, 2015) so it was expected that LCN2 would be up-regulated in stimulated iPSC-derived astrocytes. As expected, *LCN2* mRNA expression was significantly induced in iPSC-derived astrocytes following inflammatory insult with microglial factors IL1α, TNFα and C1q.

SERPINA3, which codes for the expression of the protease-inhibitory glycoprotein serpin peptidase inhibitor clade A member-3 (SEPRINA3), was significantly increased in iPSC-derived astrocytes following stimulation with inflammatory microglial factors. According to the Barres laboratory, *SERPINA3* is highly up-regulated in both a MCAO and LPS model of trauma, indicating that it may be used as an indicator of pan-reactivity in astrocytes (Liddelow *et al.*, 2017). SERPINA3 has been proposed as a therapeutic target and indicator of prognosis for glioblastoma (Li *et al.*, 2018). Raised SERPINA3 has also been associated with neuroinflammation in schizophrenia (Trepanier *et al.*, 2016; Purves-Tyson *et al.*, 2019), has been proposed as an indicator of MS severity (Masvekar *et al.*, 2019), and is up-regulated in the motor cortex of sporadic ALS patients (Sanfilippo *et al.*, 2017).

PTX3 plays an acute role in the innate immune response binding apoptotic cells in order to regulate their clearance. The exact role of PTX3 in the CNS remains undetermined but several studies have linked its function in astrocytes with maintaining BBB integrity (Rodriguez-Grande *et al.*, 2014). It has also been hypothesised that PTX3 may contribute to preventing an autoimmune response in inflamed tissue (Rovere *et al.*, 2000). While *PTX3* has previously been characterised as an A2-specific marker of reactive astrocytes (Zamanian *et al.*, 2012; Liddelow *et al.*, 2017), there is evidence in the literature for its

increased expression and secretion following an inflammatory stimulus (Skelly *et al.*, 2013; Rodriguez-Grande *et al.*, 2014) which would support the findings of this study where low concentrations of the microglial factors were sufficient to significantly increase *PTX3* mRNA expression. This is in line with previous studies where *PTX3* has been shown to be induced by inflammatory signals including IL1β, IL6, TNFα, and LPS (Rovere *et al.*, 2000; Hughes *et al.*, 2010; Hennessy *et al.*, 2015). Interestingly, a previous study has linked increased PTX3 expression with a 20% increase in cognitive decline in elderly individuals across 1,315 participants, suggesting PTX3 may be a viable inflammatory biomarker for measuring cognitive decline (Sharma *et al.*, 2016).

Taken together this data, along with the previously discussed increased secretion of pro-inflammatory cytokines and chemokines (IL6, GM-CSF and RANTES), supports the hypothesis that IL1α, TNFα and C1q may be used in combination to induce reactivity in human iPSC-derived astrocytes in order to facilitate the study of astrocyte reactivity *in vitro*. In order to determine the impact of these astrocyte secreted produces on neuronal health, ACM was collected from control and reactive astrocytes and the effect on neuronal cultures was examined.

3.4.4 iPSC-derived reactive astrocyte conditioned media compromises neuronal health

After demonstrating that iPSC-derived astrocytes release inflammatory cytokines and chemokines following stimulation, it was key to investigate the effect of reactive astrocytes in our human iPSC-derived model of neuroinflammation. To estimate the possible neurodetrimental effect of activated astrocytes in our model, mature iPSC-derived neurons were incubated with reactive ACM. Neuronal cell viability was quantified by immunofluorescent labelling with the neuronal marker β-tubulin III and subsequently counting the number of neuronal clusters in culture (Park *et al.*, 2009; Belinsky *et al.*, 2013; Tornero *et al.*, 2013). Quantification of neuronal clusters confirmed that ACM from reactive astrocytes has a detrimental effect on neurons resulting in an overall reduction in the total number of clusters as well as the size of clusters, and the observed extension of processes. This result follows the abundance of literature pertaining to the neurotoxic effect of astrocytes in an inflammatory or disease environment.

Previously, it has been demonstrated in a murine model by the Barres laboratory group that astrocytes activated following inflammatory insult are detrimental to neuronal

viability. They found significant cell death across retinal ganglion cells (RGC), cortical neurons, and ESC, which was attributed to loss of astrocyte homeostatic functions or potential secretion of a neurotoxic agent (Liddelow *et al.*, 2017). Numerous other studies have demonstrated neurotoxic effects of reactive astrocytes (Lobsiger & Cleveland, 2007; Marchetto *et al.*, 2008). Subsequently, reactive astrocytes have been documented in post mortem brain tissue of numerous neuroinflammatory disorders including AD (Osborn *et al.*, 2016), PD (Teismann & Schulz, 2004), ALS (Almad *et al.*, 2016) and HD (Faideau *et al.*, 2010). Future studies should pursue the effects of IL6, RANTES and GM-CSF on neuronal health as these factors were potently secreted by iPSC-derived reactive astrocytes. Exogenous application of these astrocyte-secreted factors to neuronal cultures could provide some insight on whether these are neurodegeneration inducing factors.

It was interesting to find that ACM from control astrocytes did not exert trophic effects on neuronal cultures. The literature indicates that ACM from healthy astrocytes typically promotes neuronal survival and neurite outgrowth (Gray & Patel, 1992; Yoshida *et al.*, 1995; Dhandapani *et al.*, 2003; Cordero-Llana *et al.*, 2011; Yan *et al.*, 2013). It is positive to note that the ACM from our control astrocytes also had no detrimental effect on neurons. Perhaps collecting the ACM in neuron base media would yield a different result, or indeed incubating neurons in ACM for a longer period, e.g. 7 days, may have a greater effect on neuron survival and growth of processes. The impact of ACM on neuronal cell adherence and apoptosis could be examined by quantification of apoptotic markers such as caspase-3, this would consolidate our conclusions that reactive astrocyte ACM has a detrimental effect on the health of iPSC-derived neuronal cultures. Taken together, this study further validates the use of human iPSC-derived neurons and astrocytes as an *in vitro* model system of neuroinflammation.

3.4.5 Concluding remarks

The reactivity of astrocytes in response to brain insult or injury is now recognised as a key contributor to neurodegeneration. Generation of an effective astrocyte model of neurodegeneration will be invaluable in future neurodegenerative research to contribute to the identification of potential novel targets for the development of neurodegenerative disease therapies. This study has shown that iPSC-derived reactive astrocytes may be generated by stimulation with inflammatory microglial factors IL1α, TNFα and C1q (Figure 3.4.1). These reactive astrocytes may be characterised in terms of morphology,

presenting with an increased nuclear:cytoplasm ratio, as well as increased secretion of inflammatory mediators and increased expression of a number of genes associated with a reactive phenotype.

In conclusion, these iPSC-derived reactive astrocytes are representative of a disease condition where inflammation is a known factor and provide a useful "disease in a dish" model to further investigate the role of astrocytes in AD. By comparing the responses of astrocytes with different genotypes for the AD risk factor APOE, this model will be a useful means to elucidate the effect of APOE genotype on astrocyte reactivity.

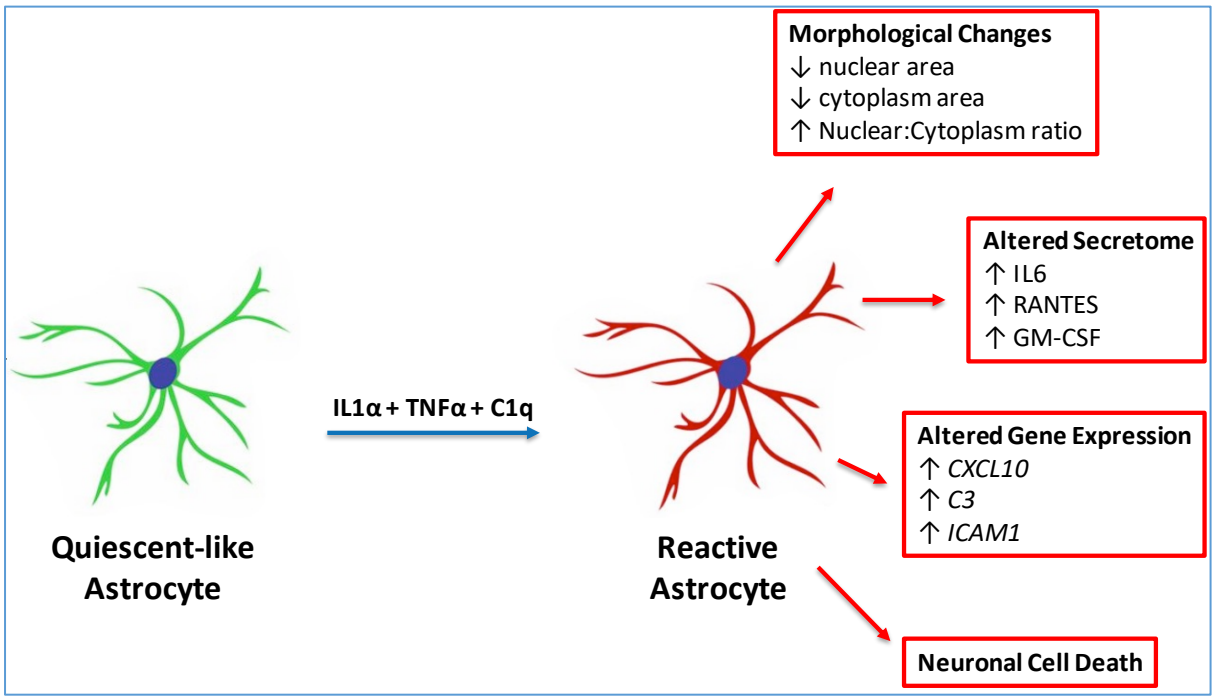


Figure 3.4.1. Schematic of results.

Inflammatory microglial factors IL1α, TNFα and C1q are sufficient to induce reactivity in iPSC-derived astrocytes to generate a "disease in a dish" model of astrogliosis. Reactive astrocytes can be characterised by their inflammatory profile which includes changes in morphology, protein secretion, gene expression and ultimately resulting in neuronal cell death.

Chapter 4

Delineation of the effect of apolipoprotein E genotype on astrocyte reactivity following an inflammatory insult

4. Delineation of the effect of apolipoprotein E genotype on astrocyte reactivity following an inflammatory insult

4.1 Introduction

AD was first described in 1907 by Alois Alzheimer (Penney *et al.*, 2020). Over 100 years later, our understanding of the disease has improved, although there is still much to uncover. In recent years, research has moved away from a neuron-centric approach to focus more on glial cell involvement in AD. While most research focuses on the less prevalent familial AD which is genetically inherited and associated with an earlier age of onset (< 65 years) (Essayan-Perez *et al.*, 2019), over 95% of AD patients suffer from late-onset sporadic AD (Lin *et al.*, 2018).

The current FDA approved drugs for AD target neuronal function which provide modest cognitive aid but do not alter the disease course or underlying neurodegeneration (Penney *et al.*, 2020). Additionally, the persistent failure of neuron-targeting therapeutics in AD clinical trials has seen a shift towards more research investigating the roles of glial cells, in particular astrocytes. Astrocytes are the most abundant glial cells in the human brain and are essential for maintaining brain homeostasis. In AD, astrocytes are believed to be instrumental to the pathology of AD and are thought to contribute to AD neurodegeneration via their reactivity and APOE genotype.

APOE4 is the single greatest genetic risk factor for sporadic AD. By age 85, ~11% of the general population will develop late-onset AD, compared to 25% of individuals heterozygous for APOE4 and 55% of those homozygous for APOE4 (Genin *et al.*, 2011). APOE is mainly expressed by astrocytes within the CNS, and yet the exact mechanisms underlying how APOE4 contributes to reactive astrogliosis and AD pathogenesis has not been established.

4.1.1 APOE4 – evidence for a role in AD pathogenesis

The *APOE* gene is located on chromosome 19, and within an area of the genome that has already been strongly linked to familial AD (Poirier *et al.*, 1993). While differences in terms of the primary structure of the three major APOE isoforms are extremely subtle, this has a marked effect on the risk of developing AD later in life. APOE3 is the most prevalent isoform in the general population (~78%), presents a neutral risk for developing AD and as such is considered the normal isoform (Liu *et al.*, 2013). APOE2 frequency is about 8%

and is considered neuroprotective, resulting in a lower than average risk of developing AD (Corder *et al.*, 1994; Liu *et al.*, 2013). GWAS studies have identified APOE4 as a major genetic risk factor for late-onset AD (Lambert *et al.*, 2013; Kunkle *et al.*, 2019b), present in 20% of the general population (Lane-Donovan & Herz, 2017; Jeong *et al.*, 2019). *APOE4* increases the risk of developing AD in a gene-dose dependent manner (Corder *et al.*, 1993), where people homozygous for *APOE4* are at a greater risk than those heterozygous for *APOE4* or non-carriers (Liu *et al.*, 2013). This increased AD frequency is coupled with a reduced average age of onset of clinical symptoms, whereby 91% of APOE4 homozygotes develop AD with a mean age at clinical symptom onset of 68 years (Table 4.1.1). In the 25 years since APOE4 was first associated with AD many studies have tried to unravel the reason why one amino acid difference between APOE4 and APOE3 can have such a profound effect on AD risk. However, recent data would suggest that APOE4 disrupts normal glial function alongside changes associated with the aging brain that may lead to neurodegeneration (Fernandez *et al.*, 2019), with links to disrupted cholesterol homeostasis, compromised Aβ handling and implications on glial reactivity.

	APOE4		
	Not present	**Heterozygous**	**Homozygous**
AD Frequency (%)	20	47	91
Age of Onset of Clinical Symptoms (year)	84	76	68

Table 4.1.1. AD frequency has a positive correlation with number of APOE4 genes.

APOE4 increases AD risk in a gene-dose dependent manner, this is coupled with a reduced age of clinical symptom onset. Adapted from Liu et al., 2013.

4.1.1.1 Brain cholesterol dysregulation by APOE4

Abnormal cholesterol metabolism by APOE4 could be linked to AD-associated pathology. Within the CNS, cholesterol is mainly transported from astrocytes to neurons by lipoprotein particles. APOE is a major component of these particles (Vance, 2012; Liu *et al.*, 2013), forming a lipoprotein complex with cholesterol and is secreted through the function of ABCA. Of the three APOE isoforms, APOE4 has a lower transport affinity and binding capacity for lipids (Hatters *et al.*, 2006; Vance, 2012), which may result in reduced cholesterol transport from astrocytes to neurons. This reduction in cholesterol delivery

to neurons may affect formation of neuronal lipid rafts which are cholesterol-rich microdomains within the plasma membrane. Such lipid rafts are thought to be important for cell adhesion, axon guidance, synaptic transmission and signal transduction (Tsui-Pierchala *et al.*, 2002).

Recent studies using human iPSC-derived astrocytes showed increased intracellular and extracellular cholesterol accumulation in APOE4 astrocytes compared to isogenic APOE3 control astrocytes (Lin *et al.*, 2018). With regards to cholesterol secretion, Lin and colleagues showed that APOE4 astrocytes had increased extracellular cholesterol as determined by measuring cholesterol levels in the culture media (Lin *et al.*, 2018). In contrast, the Goate laboratory associated APOE4 with increased lysosomal cholesterol and decreased cholesterol secretion which they postulated was due to a reduction in total APOE protein as well as reduced *Abca1* expression [(Tcw *et al.*) 2019 preprint]. Intracellular cholesterol accumulation in APOE4 astrocytes has also been proposed to be as a result of impaired efflux as well as increased expression of genes associated with cholesterol biosynthesis (Jeong *et al.*, 2019), however the precise mechanisms are unknown.

4.1.1.2 APOE and Aβ – production, clearance, deposition, aggregation and toxicity

The effects of APOE genotype on circulating Aβ, as well as CSF levels of Aβ is quite conflicting in the literature with some studies indicating an APOE-dependent effect (Lin *et al.*, 2018) and others showing an APOE-independent effect (Lautner *et al.*, 2014).

Aβ levels within the CNS are representative of the homeostatic balance of Aβ production and clearance. Aβ build-up may be indicative of overproduction, compromised clearance or a combination of both. There is increasing evidence in the literature to support a role for APOE and APOE receptors in these processes. Many of the APOE receptors interact with APP thereby affecting its processing. This affect is thought to be isoform specific, where APOE4 increases APP internalisation resulting in increased Aβ production via the LRP1 receptor interaction with APP (Ye *et al.*, 2005). A study in a rat neuroblastoma cell line showed that APOE4 increased Aβ production; blocking the LRP pathway and reducing LRP1 expression attenuated the APOE4 effect on Aβ production indicating this process may be LRP1-dependent. Amino acid replacement to disrupt domain interaction within the LRP1 receptor gave further proof that LRP1 is heavily involved (Ye *et al.*, 2005).

Increased Aβ production in the APOE4 phenotype has also been linked to the APOE-binding protein TMCC2 (Hopkins *et al.*, 2011). Huang and colleagues found differential APP transcription across APOE genotypes, with an *APOE4* > *APOE3* > *APOE2* potency rank order. They found that APOE activates a non-canonical MAPK signalling cascade which enhances APP transcription and subsequent Aβ synthesis (Huang *et al.*, 2017).

The APOE4 isoform is also associated with altered clearance of Aβ aggregates. APOE4 astrocytes are less efficient at clearing $A\beta_{42}$ which was shown to be a lysosome dependent effect (Lin *et al.*, 2018). APOE4 has less affinity for Aβ compared to APOE3 and this combined with reduced APOE secretion may contribute to the impaired Aβ clearance (Lin *et al.*, 2018). The research group also noted age-dependent and APOE4-dependent elevations of Aβ and phosphorylated tau which were found to correspond temporally to the appearance of astrocytes, indicating the critical importance of APOE to astrocytic function (Lin *et al.*, 2018). APOE4 has also been shown to form smaller lipoprotein complexes with reduced affinity for Aβ, as well as reduced binding affinity for APOE receptors, compared to APOE3 (Kim *et al.*, 2009).

Evidence from clinical studies have shown a positive correlation between APOE4 genotype and Aβ deposition (Kantarci *et al.*, 2012; Murphy *et al.*, 2013). Subsequent to this, Aβ deposition appears to begin earlier in individuals with at least one *APOE4* gene compared to non-carriers (Fleisher *et al.*, 2013). The results from these clinical studies support the hypothesis that APOE4 contributes to the risk of AD as a result of early initiation and accelerated deposition of Aβ. In contrast, APOE2 is thought to have a protective effect with reduced Aβ deposition (Corder *et al.*, 1994; Serrano-Pozo *et al.*, 2015). The mechanisms underlying the neuroprotective characteristics of APOE2 may be the key to understanding the compromised cognitive function and increased AD risk seen in APOE4 carriers, however they remain unknown due to its low incidence in the population therefore large scale APOE2 studies are few.

It has been suggested that Aβ metabolism is compromised in APOE4 carriers as it was demonstrated that AD brains from APOE4 homozygous individuals have 2.7 times more oligomeric Aβ compared to APOE3 counterparts (Hashimoto *et al.*, 2012). The aggregation of Aβ plaques is more abundant in APOE4 carriers than in either of the other two isoforms because it is less effective at clearing soluble Aβ from the extracellular space, due to its poorly lipidated structure (Hauser & Ryan, 2013). In cognitively normal individuals, and in transgenic mice, a differential rate of clearance and synthesis of Aβ in early life resulted in an APOE isoform-dependent rate of Aβ aggregation in later life, with

APOE4 showing the poorest ability to remove soluble Aβ from the interstitial fluid (Castellano *et al.*, 2011; Youmans *et al.*, 2012). The binding abilities of APOE3 and APOE4 have been compared and APOE3 has a 5-fold higher binding affinity for both $A\beta_{40}$ and $A\beta_{42}$, the two most common Aβ species seen in AD (Tokuda *et al.*, 2000). These observations suggest that APOE4 may further contribute to Aβ load in AD as a result of compromised clearance and breakdown.

4.1.1.3 APOE genotype – implications in tauopathy

Given that Aβ pathology is thought to drive tau pathology in AD, it is likely that APOE also plays a role in tauopathy. APOE has been shown to co-localise with and bind to tau *in vitro* (Strittmatter *et al.*, 1993; Strittmatter *et al.*, 1994), while *in vivo*, transgenic mice expressing neuron-specific human APOE resulted in hyperphosphorylation of tau in the manner of *APOE4* > *APOE3* (Brecht *et al.*, 2004). Lin and colleagues found increased Aβ accumulation coupled with elevated levels of phosphorylated tau in APOE4 iPSC-derived organoids compared to their APOE3 controls (Lin *et al.*, 2018). Shi and colleagues showed that APOE4 leads to accelerated hyperphosphorylation of tau and tau-mediated neurodegeneration in a transgenic mouse model of tauopathy. By co-culturing tau-expressing neurons with APOE4-expressing astrocytes they found a significant increase in TNFα secretion and subsequent decrease in neuron viability (Shi *et al.*, 2017b). TNFα is one of the factors shown to evoke reactivity in astrocytes (Liddelow *et al.*, 2017) and so it is highly likely that reactive astrogliosis is a contributing factor to this APOE4 induced pathology in AD.

4.1.1.4 APOE, astrocytes and neuroinflammation

The mechanisms underpinning APOE4 associated AD risk are not yet understood but it has been proposed to be a combination of a loss of neurotrophic functions as well as a gain of toxic function (Holtzman *et al.*, 2012; Liu *et al.*, 2017; Zhao *et al.*, 2017). Barger and Harmon found that soluble APP activated microglia. This effect was blocked by incubating microglia with exogenous APOE3 protein but not APOE4, indicating a potential lack of immunomodulation by APOE4 which in turn may result in chronic neuroinflammation (Barger & Harmon, 1997). Some studies have suggested that APOE4 astrocytes are more pro-inflammatory in nature compared to APOE3 astrocytes which could contribute to AD pathology (Dorey *et al.*, 2014). Another study demonstrated that

neurons co-cultured with APOE4 astrocytes expressed decreased amounts of neuronal and synaptic markers and had lower viability rates than neurons co-cultured with APOE3 isogenic astrocytes (Zhao *et al.*, 2017). This suggests that APOE4 astrocytes have a decreased ability to support neuronal and synaptic homeostasis. However, the evidence pertaining to the impact of APOE genotype on astrocyte reactivity is inconsistent and warrants further investigation. This confusion surrounding the narrative of the APOE inflammatory response amongst the literature has been suggested to arise from the lack of human APOE models available (Tai *et al.*, 2015).

4.1.2 Modelling genetic variants using human iPSC

Most existing research regarding the involvement of reactive astrocytes and APOE in AD is largely based on animal model studies, specifically rodent studies. Although rodent models and corresponding primary cultures have provided a valuable tool for studying neurodegenerative disease, the use of non-human models for human diseases presents a barrier to what we can learn. Furthermore, rodents possess only one APOE isoform which most closely resembles that of the human APOE3 isoform making it difficult to compare genotypes in rodent models (Raffai *et al.*, 2001; Fernandez *et al.*, 2019). The development of iPSC technology has become a vital tool for the generation of disease- and patient- specific *in vitro* models and subsequent analysis of genetic variants (Takahashi & Yamanaka, 2006; Takahashi *et al.*, 2007). Specifically, it has been shown that iPSC-derived astrocytes are a valid model for studying the effect of APOE genotype on astrocytic function.

Recently, several studies have used human iPSC-derived astrocytes to investigate the effects of APOE genotype on *in vitro* cultures. Zhao and colleagues found that APOE4 carrying astrocytes were less effective at supporting neuron growth and synaptogenesis compared to APOE3 carriers (Zhao *et al.*, 2017). In a comprehensive study carried out by Lin and colleagues, it was found that APOE4 affects transcription of hundreds of genes and leads to increased Aβ burden (Lin *et al.*, 2018). Wang and colleagues found they could use a small molecule corrector to re-conform APOE in human iPSC-derived astrocytes *in vitro* and ameliorate AD-associated pathology of cells (Wang *et al.*, 2018). To this author's knowledge, no human iPSC model has been used to investigate the impact of APOE genotype on astrocyte reactivity.

4.1.3 Aims

The objectives of this chapter can be separated into two primary aims:

1. To generate APOE4 homozygous cortical astrocytes from human iPSC,
2. To stimulate APOE3 and APOE4 homozygous iPSC-derived astrocytes with inflammatory microglial factors (IL1α, TNFα and C1q) and compare their reactivity profile at the gene, protein and morphological level in order to determine whether APOE genotype affects reactivity in our model.

The hypothesis pertaining to these aims are that APOE4 will be inherently reactive compared to APOE3 astrocytes at a basal level as well as following stimulation.

4.2 Materials and Methods

4.2.1 Cell lines

Human iPSC homozygous for APOE3 and APOE4 were used in this study to generate astrocytes and subsequently reactive astrocytes. *E3E3* astrocytes were derived from the NAS2 iPSC line previously described. *E4E4* astrocytes were derived from an APOE4 homozygous iPSC line generated by Dr Lucy Crompton of the Caldwell laboratory in the University of Bristol. The original fibroblasts were donated by a participant on the premise of receiving a free 23andMe genome screen, the APOE genotype was confirmed by Dr Crompton.

4.2.2 Astrocyte progenitor cell culture and terminal differentiation

Human *E3E3* and *E4E4* iPSC were patterned towards a neural fate and subsequently differentiated along a glial lineage as described in sections 3.2.8 and 3.2.10. APC were seeded from D80 onwards for terminal differentiation to produce mature astrocytes as described in section 3.2.5. Cell fate was confirmed by immunofluorescent staining.

4.2.3 Astrocyte stimulation to examine reactivity in *E3E3* and *E4E4* astrocytes

Astrocytes were stimulated with inflammatory microglial factors IL1α (3 ng/mL), TNFα (30 ng/mL) and C1q (400 ng/mL) for 24 h in order to generate reactive astrocytes. A 10-factor dilution of these concentrations was also used. These treatments are denoted as “Factors High” and “Factors Low” where appropriate. Post stimulation, media was collected and cells were lysed as appropriate for qPCR and Western blotting analysis of reactivity markers (see Figure 4.2.1 for timeline).

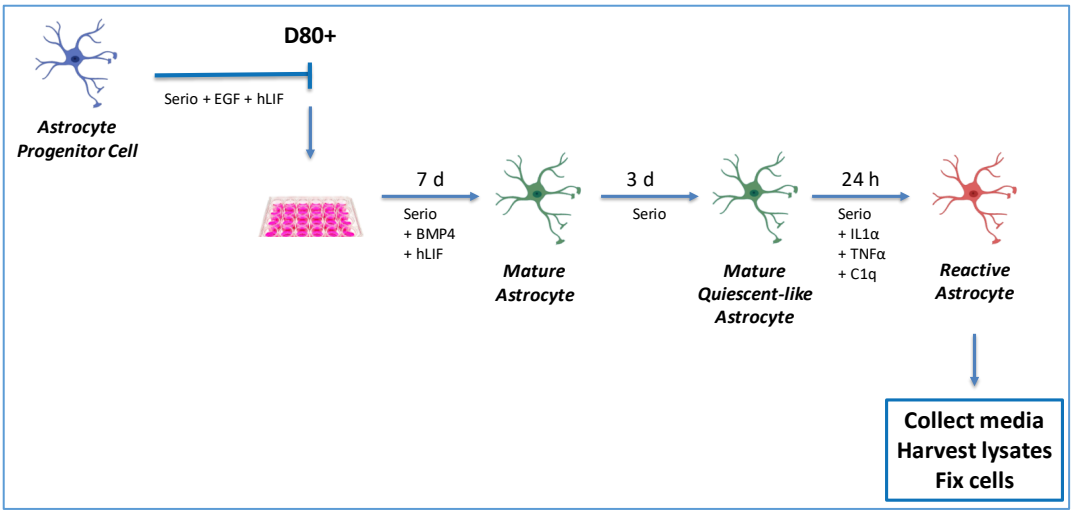


Figure 4.2.1. Experimental timeline to test the effect of microglial factors on astrocyte reactivity in E4E4 astrocytes.

APC were expanded in Serio media supplemented with EGF and hLIF. From D80 APC are plated and terminally differentiated for 7 d, followed by 3 d in Serio media without factors to ensure a quiescent-like astrocyte at time of stimulation. Astrocytes are stimulated for 24 h to generate a reactive astrocyte. Post-stimulation media was collected for ELISA analysis and cell lysates were harvested for qPCR and Western Blotting analysis.

4.2.4 Analysis of mRNA expression by qPCR

The mRNA expression of a panel of eight reactivity markers (*C3*, *CXCL10*, *GFAP*, *ICAM1*, *IL1β*, *IL6*, *LCN2* and *PTX3*) were assessed by qPCR (Table 4.2.1). Gene expression concentrations were analysed using the comparative Ct method. The target genes from each sample were compared with GAPDH, which acted as the endogenous control. The Ct values of each target gene and control gene were compared and expressed as a RQ. The full qPCR protocol is described in detail in the main methods section of this thesis (Sections 2.4.1).

Gene	Cat No.	Gene Code
C3	4453320	Hs00163811_m1
CXCL10	4453320	Hs00171042_m1
GFAP	4453320	Hs00909233_m1
ICAM1	4453320	Hs00164932_m1
IL1B	4453320	Hs01555410_m1
IL6	4453320	Hs00174131_m1
LCN2	4453320	Hs01008571_m1
PTX3	4453320	Hs00173615_m1

Table 4.2.1. Target genes used for qPCR analysis of E4E4 astrocyte reactivity profile.

4.2.5 Analysis of cytokine secretion by ELISA

ELISA analysis was used to assess the concentration of IL6 secreted into the supernatant obtained from cultured *E4E4* astrocytes. The ELISA protocol is detailed in Chapter 2 (Section 2.5.1).

4.2.6 Immunocytochemistry

Cells on coverslips were fixed with 4% PFA (500 µL, 25 min, RT) in preparation for immunocytochemistry (Chapter 2, Section 1.5.2). Primary and secondary antibodies are detailed in Tables 4.2.2 and 4.2.3 respectively.

Antigen	Dilution Factor	Manufacturer
Chicken anti-GFAP	1:1000	Abcam, UK
Goat anti-GFAP	1:1000	DAKO, Denmark
Rabbit anti-Connexin-43	1:1500	Sigma-Aldrich, USA
Mouse anti-S100β	1:1000	Sigma-Aldrich, USA
Rabbit anti-EAAT1	1:1500	Novus Biologicals, USA
Hoechst	1:1000	Cell Signaling Technology, USA

Table 4.2.2. Primary antibodies.

Antigen	Dilution Factor	Manufacturer
Alexa Fluor 488 donkey anti-mouse	1:500	Molecular Probes
Alexa Fluor 488 goat anti-chicken IgG	1:500	Life Technologies, USA
Alexa Fluor 568 donkey anti-rabbit IgG	1:500	Molecular Probes

Table 4.2.3. Secondary antibodies.

4.2.7 Analysis of GFAP protein expression by Western blotting

The protein expression of GFAP was assessed by Western blotting (Table 4.2.4). Densitometry analysis was carried out on protein bands using Image Studio Lite (v 5.2) with β-actin acting as a loading control. Densitometry signals for GFAP were divided by β-actin signals and then normalised to control in order to present data as fold change. The full Western blotting protocol is described in detail in the main methods section of this thesis (Sections 2.5.3).

Antibody	Dilution Factor	Manufacturer
Goat anti-GFAP	1:1000	DAKO, Denmark
Mouse anti-β-actin	1:2000	Sigma-Aldrich, USA
Goat anti-rabbit HRP-conjugated	1:2000	Thermo Scientific, USA
Goat anti-mouse HRP-conjugated	1:2000	Thermo Scientific, USA

Table 4.2.4. Antibodies used for Western blotting analysis of GFAP expression.

4.2.8 Statistical analysis

Data is expressed as mean ± SEM. At least three neural induction and astrocyte differentiations (N) were performed per iPSC line. 'n' values denote experimental or biological replicates and are representative of different thaws or passage numbers, while 'reps' denotes technical replicates within each experimental group, i.e. cells from the same plate but separate wells.

One-way ANOVA was used to analyse the effect of two concentrations of inflammatory microglial factors on markers of astrocyte reactivity, with Newman-Keuls *post hoc* analysis to decipher significance. An unpaired Student's t-test was used to compare baseline levels of reactive astrocyte markers in *E3E3* versus *E4E4* astrocytes. Two-way ANOVA was used for statistical analysis of the effect of inflammatory insult with respect to APOE genotype, followed by Bonferroni *post hoc* if significance was inferred. Significance was set at $p < 0.05$. Statistical analysis was performed using GraphPad Prism 8 (GraphPad Software).

4.3 Results

APOE is most highly expressed in the CNS by astrocytes. APOE3 is considered the normal genotype as it is expressed most prevalently in the general population, while the APOE4 genotype presents the greatest genetic risk for sporadic AD. The effects of APOE genotype on astrocyte response to an inflammatory stimulus remains incompletely understood, as such this study aimed to assess the response of inflammatory insult in APOE4 astrocytes and compare this to their APOE3 controls. Inflammatory insult was delivered via microglial factors IL1α, TNFα and C1q.

4.3.1 iPSC-derived *E4E4* astrocytes are positive for classical astrocyte markers

In order to confirm cell fate, iPSC-derived astrocytes were fluorescently-labelled with classical astrocytic markers. *E4E4* astrocytes are positive for GFAP, Cx43 and EAAT1 (Figure 4.3.1).

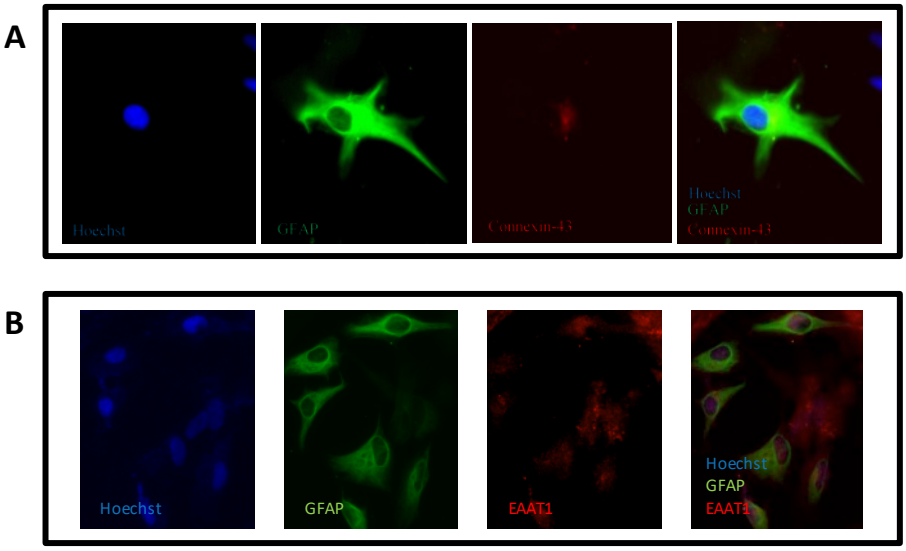


Figure 4.3.1. E4E4 iPSC-derived cortical astrocytes are positive for classical astrocyte markers. *E4E4 astrocytes show positive immunostaining for classical astrocyte markers GFAP and Connexin-43 (A), as well as EAAT1 (B). Images were taken at x40 magnification.*

Part 1: *E4E4* Astrocyte Reactivity Profile

4.3.2 iPSC-derived *E4E4* astrocytes are capable of responding to inflammatory insult and displaying a reactive phenotype

Prior to generating a reactivity profile, it was first determined that *E4E4* astrocytes were capable of responding to an inflammatory insult in the same manner as their *E3E3* counterparts as characterised in the previous chapter. Inflammatory insult was delivered as a combined dose of microglial factors IL1α (3 ng/mL), TNFα (30 ng/mL) and C1q (400 ng/mL) as per Liddelow *et al.*, 2017, denoted as "Factors High" and a lower dose IL1α (0.3 ng/mL), TNFα (3 ng/mL) and C1q (40 ng/mL), denoted as "Factors Low". As IL6 is the main cytokine produced and secreted by astrocytes it was analysed in media collected from reactive astrocytes. IL6 mRNA expression ($p < 0.001$) and secretion ($p < 0.01$) was significantly increased in a dose dependent manner in response to stimulation with inflammatory microglial factors (Figure 4.3.2).

Stimulation with inflammatory microglial factors also induced increased mRNA expression of reactive astrocyte markers *CXCL10* ($p < 0.001$), *C3* ($p < 0.001$), *LCN2* ($p < 0.001$), *IL1β* ($p < 0.001$), *ICAM1* ($p < 0.001$) and *PTX3* ($p < 0.001$; Figure 4.3.3. A-F). Interestingly, *GFAP* mRNA expression was significantly decreased in *E4E4* astrocytes following inflammatory insult ($p < 0.001$; Figure 4.3.3. G). This data indicates that *E4E4* astrocytes are capable of responding to inflammatory insult and generating a reactive phenotype much like their *E3E3* counterparts.

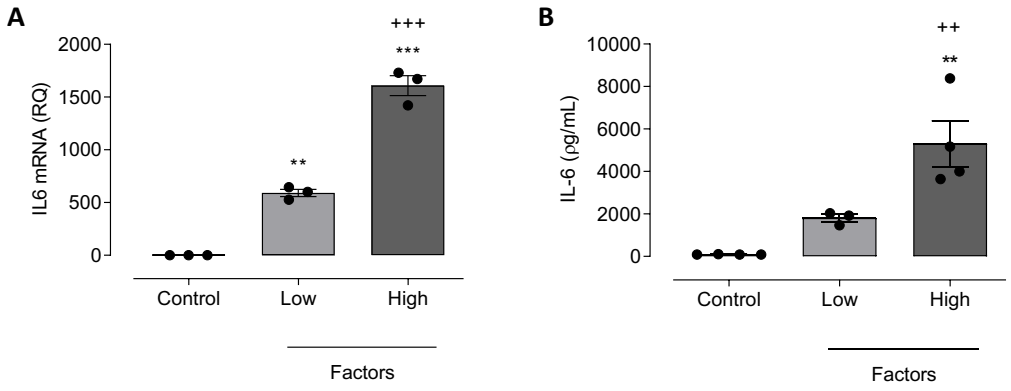


Figure 4.3.2. Reactive E4E4 astrocytes show increased IL6 mRNA expression and secretion.

*Stimulation with inflammatory microglial factors increased IL6 mRNA expression (A) and secretion (B) in E4E4 reactive astrocytes. Data expressed as mean ± SEM (N=3, n=3-4). ** $p < 0.01$, *** $p < 0.001$ vs control; $^{++}$ $p < 0.01$, $^{+++}$ $p < 0.001$ vs low concentration. IL6 mRNA $F(2, 6) = 196.0$, $p = < 0.0001$; IL6 protein $F(2, 8) = 15.83$, $p = 0.0017$ (One-way ANOVA with Newman-Keuls post hoc).*

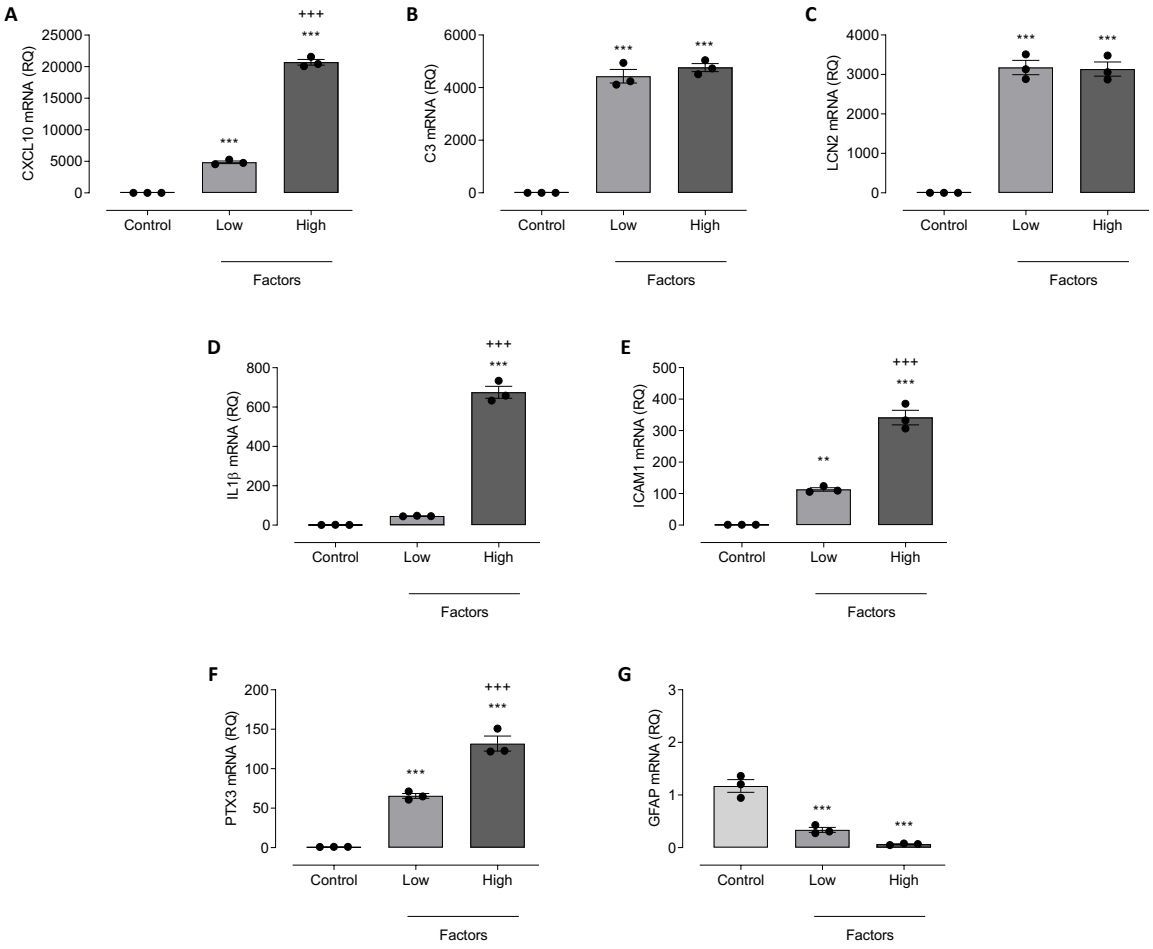


Figure 4.3.3. E4E4 reactive astrocytes show increased mRNA expression of reactive astrocyte markers.

*Stimulation with inflammatory microglial factors increased mRNA expression of reactive astrocyte markers CXCL10 (A), C3 (B), LCN2 (C), IL1β (D), ICAM1 (E) and PTX3 (F) in E4E4 reactive astrocytes. GFAP mRNA expression was significantly reduced in E4E4 reactive astrocytes compared to control (G). Data expressed as mean ± SEM (N=3, n=3). ** p < 0.01, *** p < 0.001 vs Control; $^{+++}$ p < 0.001 vs Low concentration. CXCL10 F(2, 6) = 1415, p = < 0.0001; C3 F(2, 6) = 236.3, p = < 0.0001; LCN2 F(2, 6) = 151.6, p = < 0.0001; IL1β F(2, 6) = 461.5, p = < 0.0001; ICAM1 F(2, 6) = 159.6, p = < 0.0001; PTX3 F(2, 6) = 128.7, p = < 0.0001; GFAP F(2, 6) = 58.69, p = 0.0001 (One-way ANOVA with Newman-Keuls post hoc).*

4.3.3 iPSC-derived *E4E4* reactive astrocytes do not display cytoskeletal alterations

The effect of astrocyte reactivity state on morphology of *E4E4* astrocytes was assessed as a measure of nuclear:cytoplasm ratio (Hallmann *et al.*, 2017). Both nuclear and cytoplasm areas were marginally but not significantly decreased in reactive astrocytes compared to control. As such nuclear:cytoplasm ratio was unaffected by astrocyte reactivity (Figure 4.3.4). This lack of significant morphological change in reactive astrocytes is mirrored in protein analysis of the cytoskeletal protein GFAP.

In order to ascertain the effect of microglial factors on GFAP protein expression, a commonly used marker of astrocyte reactivity, densitometry analysis of GFAP fluorescence was carried out and presented as CTCF (Hawkins *et al.*, 2018), as well as via Western blotting which is presented as fold change compared to control. No significant difference in GFAP protein was found compared to control (Figure 4.3.5). This data indicates that *E4E4* reactive astrocytes do not undergo the same cytoskeletal restructuring which was detected in *E3E3* astrocytes, and suggests differences in the reactivity profiles of the two genotypes.

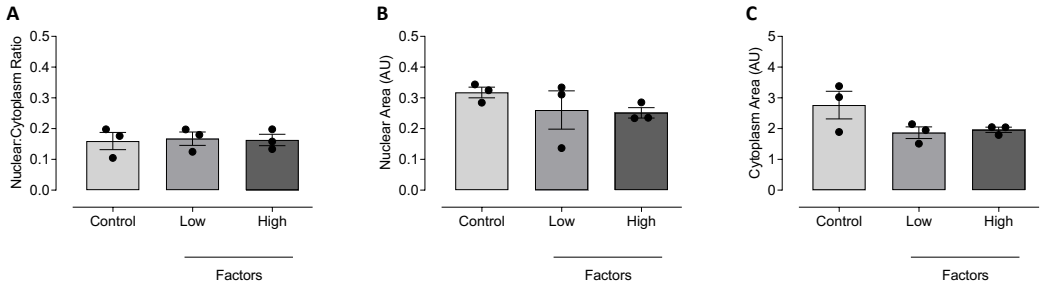


Figure 4.3.4. Reactivity state does not affect morphology in E4E4 iPSC-derived astrocytes.

Nuclear:cytoplasm ratio is unaffected by reactivity state in E4E4 astrocytes (A). Nuclear area (B) and cytoplasm area (C) are marginally decreased as a result of astrocyte reactivity but not significantly. Data expressed as mean ± SEM (N=3, n=3). N:C ratio F(2, 6) = 0.02774, p = 0.9728; Nuclear area F(2, 6) = 0.8638, p = 0.4681; Cytoplasm area F(2, 6) = 2.984, p = 0.1260 (One-way ANOVA).

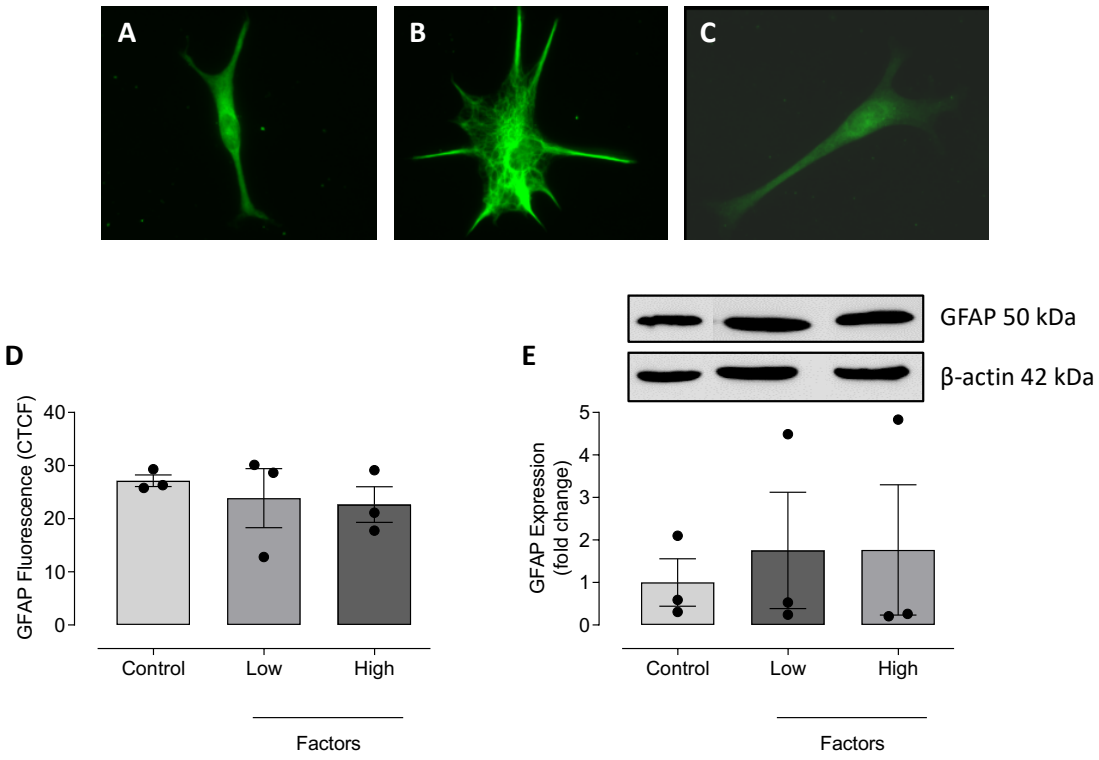


Figure 4.3.5. Reactivity does not affect GFAP expression in E4E4 iPSC-derived astrocytes.

Representative images of GFAP⁺ staining (x40 magnification) in control astrocytes (A), and following stimulation with inflammatory microglial factors at a low (B) and high (C) concentrations. GFAP protein levels as assessed by immunofluorescent staining were not affected by astrocyte reactivity state (A-D). Furthermore, GFAP densitometry as assessed by Western blotting was unchanged in reactive astrocytes compared to control (E). Data expressed as mean ± SEM (N=3, n=3). GFAP CTCF F(2, 6) = 0.3717, p = 0.7044. GFAP expression F(2, 6) = 0.1274, p = 0.8827 (One-way ANOVA).

Results Part 2: The effect of APOE genotype on iPSC-derived astrocyte baseline reactivity

E4E4 astrocytes are capable of responding to inflammatory insult and show increased expression of some key reactive astrocyte markers as a result. In order to more fully understand any effect APOE genotype may have on astrocyte reactivity, it is first important to consider whether *E4E4* astrocytes carry any basal reactivity which may have an effect much like priming on later insult. Increased basal inflammatory activation state could contribute to the increased AD risk for APOE4 carriers, therefore base line reactivity states of *E4E4* astrocytes were compared to *E3E3* astrocytes in order to determine whether APOE genotype impacted basal inflammatory states in these astrocytes.

4.3.4 *E4E4* astrocytes have greater base line secretion and expression of reactivity markers compared to *E3E3* astrocytes

E4E4 astrocytes display a heightened basal reactivity state in terms of IL6, with significantly increased resting levels of *IL6* mRNA expression ($p < 0.001$) coupled with increased IL6 secretion ($p < 0.05$) into media detected via ELISA (Figure 4.3.6).

GFAP is a commonly used astrocyte marker, also widely considered a reactive astrocyte marker. While its efficacy as a reactivity marker has been called in to question by many, basal levels of GFAP were compared between *E3E3* and *E4E4* astrocytes. *E4E4* astrocytes had significantly higher basal *GFAP* mRNA expression compared to *E3E3* astrocytes ($p < 0.01$), this increased GFAP at mRNA level did not however translate to increased GFAP protein as detected by Western blotting (Figure 4.3.7).

Following on from this the mRNA expression levels of six genes chosen from multiple astrocyte transcriptomic studies as indicative markers of astrocyte reactivity were compared in *E3E3* and *E4E4* astrocytes while in their unstimulated quiescent state. It was found that basal mRNA expression of *IL1β* ($p < 0.01$), *CXCL10* ($p < 0.001$), *C3* ($p < 0.01$) and *ICAM1* ($p < 0.01$) were significantly greater in *E4E4* astrocytes compared to *E3E3* astrocytes (Figure 4.3.8. A-D). *PTX3* ($p < 0.01$) mRNA expression was significantly lower in *E4E4* astrocytes while *LCN2* basal mRNA levels were not affected as a function of genotype (Figure 4.3.8. E, F). This data indicates that *E4E4* astrocytes have an increased basal inflammatory activation state. It was next assessed how this might affect their response to inflammatory stimulus.

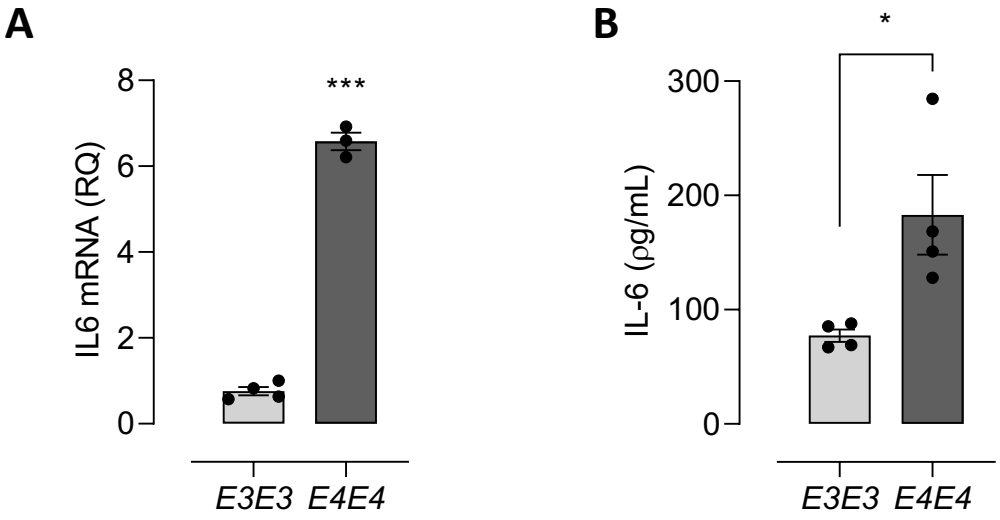


Figure 4.3.6. E4E4 iPSC-derived astrocytes show increased baseline IL6 secretion and expression.
*Baseline mRNA expression of IL6 is significantly greater in E4E4 astrocytes compared to E3E3 astrocytes (A). Baseline secretion of IL6 is greater in E4E4 astrocytes compared to E3E3 astrocytes (B). Data expressed as mean ± SEM (N=3, n=3-4). * p < 0.05, *** p < 0.001 vs E3E3 astrocytes. IL6 secretion t = 2.992, df = 6, p = 0.0243; IL6 mRNA t = 28.22, df = 5, p = < 0.0001 (Unpaired students t-test).*

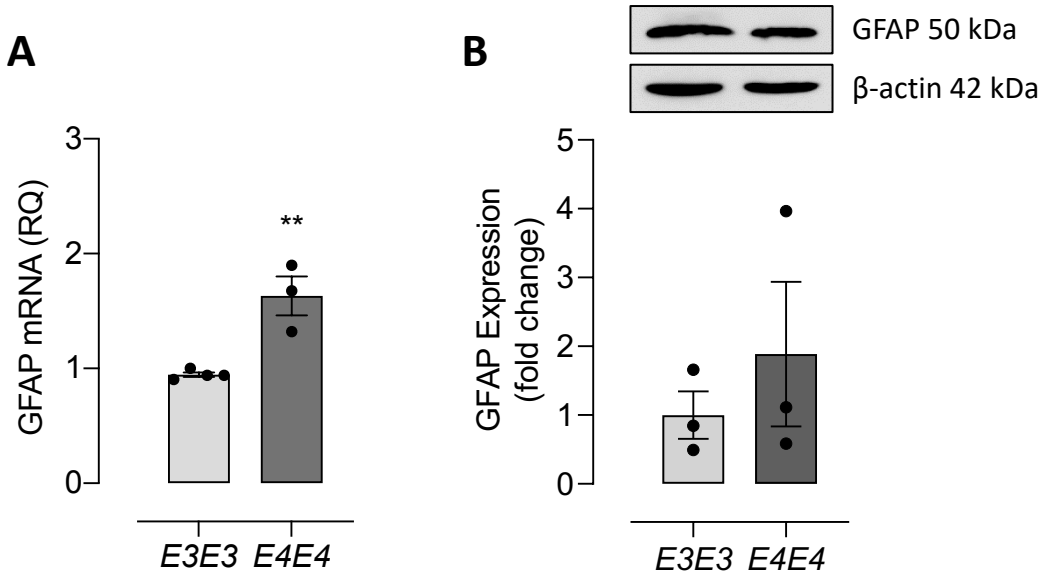


Figure 4.3.7. E4E4 iPSC-derived astrocytes show increased baseline GFAP expression.
*Baseline mRNA expression of GFAP is significantly greater in E4E4 astrocytes compared to E3E3 astrocytes (A). Baseline protein expression of GFAP is not different between genotypes at baseline (B). Data expressed as mean ± SEM (N=3, n=3-4). ** p < 0.01 vs E3E3 astrocytes. GFAP mRNA t = 4.790, df = 5, p = 0.0049; GFAP protein t = 0.8025, df = 4, p = 0.4672 (Unpaired students t-test).*

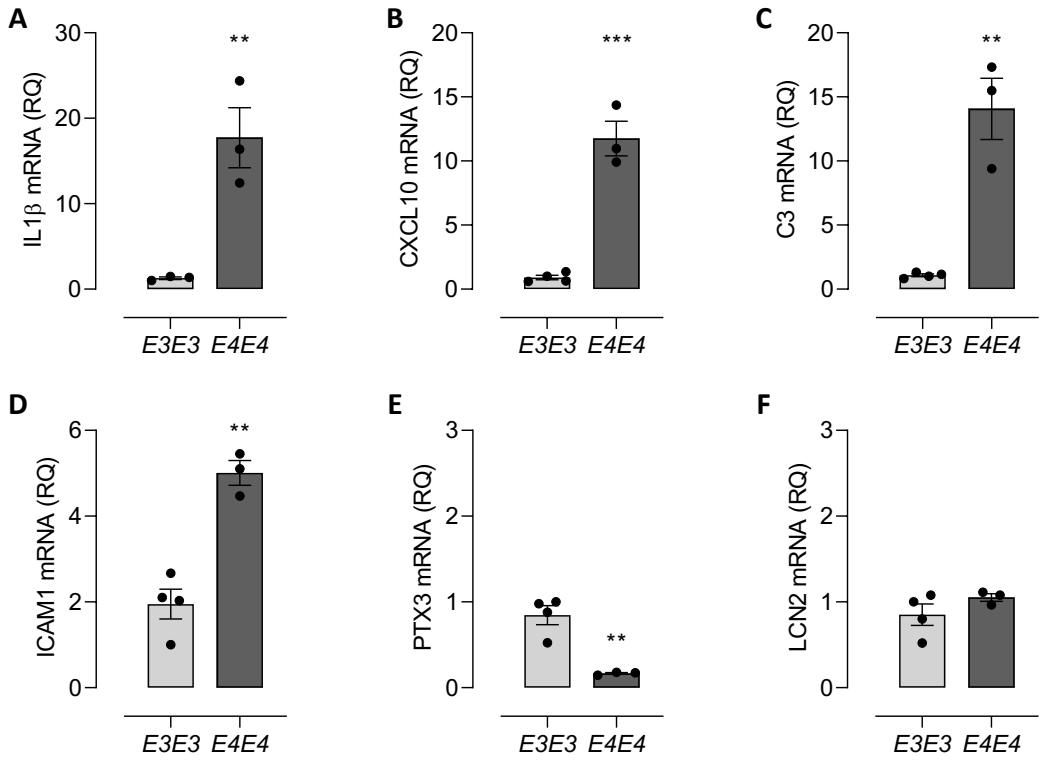


Figure 4.3.8. E4E4 iPSC-derived astrocytes show increased baseline expression of reactivity markers.

*E4E4 astrocytes have significantly increased basal mRNA expression of IL1β (A), CXCL10 (B), C3 (C) and ICAM1 (D) compared to E3E3 astrocytes. E4E4 astrocytes have significantly decreased PTX3 expression compared to E3E3 astrocytes (E). LCN2 mRNA expression does not differ between genotypes (F). Data expressed as mean ± SEM (N=3, n=3-4). ** p < 0.01, *** p < 0.001 vs E3E3 astrocytes. IL1β t = 4.673, df = 4, p = 0.0095; CXCL10 t = 9.483, df = 5, p = 0.0002; C3 t = 6.469, df – 5, p = 0.0013; ICAM1 t = 6.431, df = 5, p = 0.0014; PTX3 t = 5.204, df = 5, p = 0.0035; LCN2 t = 1.324, df = 5, p = 0.2428 (Unpaired students t-test).*

Results Part 3: The effect of APOE genotype on iPSC-derived astrocyte reactivity in response to an inflammatory signal

E4E4 astrocytes appear to be somewhat inflammatory at base line compared to their *E3E3* counterparts. Whether this translates to an exaggerated response to inflammatory insult is important to consider given the well-established role of neuroinflammation in AD pathogenesis. *E4E4* reactive astrocytes were generated by stimulating with inflammatory microglial factors IL1α, TNFα and C1q as previously described (Liddelow *et al.*, 2017) and their reactivity profile was examined and compared to that of *E3E3* astrocytes in order to more conclusively determine the effect of APOE genotype on astrocyte reactivity.

4.3.5 *E4E4* iPSC-derived astrocytes show increased IL6 expression following inflammatory insult

E4E4 astrocytes had significantly greater *IL6* mRNA expression in response to stimulation with inflammatory microglial factors compared to *E3E3* astrocytes ($p < 0.001$). With regards to the lower dose of microglial factors this exaggerated response was more than 10-fold greater in *E4E4* astrocytes compared to *E3E3* astrocytes, and 5-fold greater at the high dose of microglial factors (Figure 4.3.9. A). However, this drastic difference in *IL6* mRNA expression was not seen at the protein level as detected by ELISA. IL6 secretion was comparable across both APOE genotype and dose of factors (Figure 4.3.9. B).

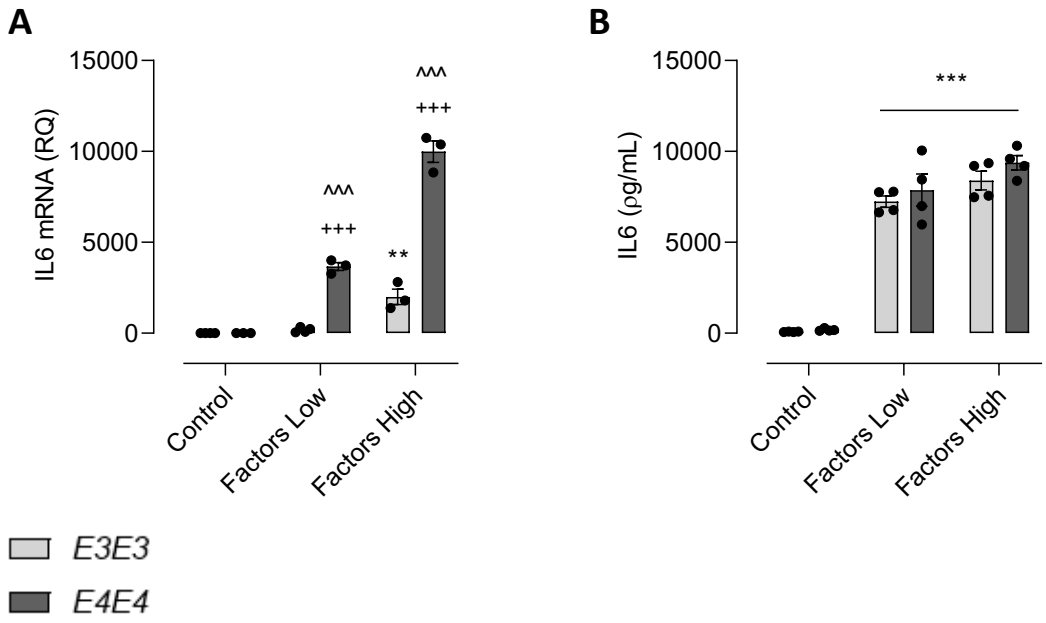


Figure 4.3.9. E4E4 iPSC-derived astrocytes show increased IL6 expression following inflammatory insult.

*IL6 mRNA expression is significantly greater in E4E4 astrocytes in response to inflammatory microglial factors compared to E3E3 astrocytes (A). E3E3 and E4E4 astrocytes secrete significantly greater IL6 compared to control with no difference between genotypes (B). Data expressed as mean ± SEM (N=3, n=3-4). ** p < 0.01, *** p < 0.001 vs E3E3 control; $^{+++}$ p < 0.001 vs E4E4 control; ^^^ p < 0.001 vs E3E3. IL6 mRNA: APOE effect F(1, 14) = 289.5, p = < 0.0001; factors effect F(2, 14) = 237.6, p = < 0.0001; interaction effect F(2, 14) = 102.6, p = < 0.0001. IL6 secretion: APOE effect F(1, 18) = 2.261, p = 0.1500; factors effect F(2, 18) = 205.5, p = < 0.0001; interaction effect F(2, 18) = 0.4464, p = 0.6468 (Two-way ANOVA with Bonferroni post hoc).*

4.3.6 *E4E4* iPSC-derived astrocytes show enhanced expression of some reactivity markers following inflammatory insult compared to *E3E3* iPSC-derived astrocytes

There is evidence in the literature indicating that APOE4 is inherently pro-inflammatory compared to APOE3, a characteristic which may contribute to the increased AD risk associated with APOE4 genotype. In order to test this in our model system, *E4E4* and *E3E3* astrocytes were exposed to inflammatory insult and their reactivity compared in order to determine whether APOE genotype affected astrocyte reactivity.

E4E4 astrocytes have significantly greater basal *GFAP* mRNA expression ($p < 0.001$) compared to *E3E3* astrocytes but this significant effect of genotype does not apply following stimulation, interestingly *GFAP* mRNA expression is significantly decreased as a result of stimulation. The trend for increased GFAP expression in *E4E4* astrocytes compared to *E3E3* astrocytes is apparent in the protein data, however no significant effect of genotype or stimulation was detected thereby calling to question its role as a reactive astrocyte marker (Figure 4.3.10).

E4E4 reactive astrocytes express significantly more *CXCL10* ($p < 0.001$) at the mRNA level compared to *E3E3* reactive astrocytes, a difference of almost 40-fold and 12-fold when stimulated at the low and high dose respectively (Figure 4.3.11. A). The same trend follows with regards to *C3* mRNA expression ($p < 0.001$), with *E4E4* astrocytes expressing at least 10-fold more *C3* compared to *E3E3* astrocytes (Figure 4.3.11. B). With regards to *ICAM1* mRNA expression, *E4E4* astrocytes tend to express more than *E3E3* astrocytes when stimulated with a low dose of inflammatory microglial factors, however the opposite is the case when stimulated with a high dose of factors (Figure 4.3.11. C). This data supports the theory that *E4E4* astrocytes are more reactive than *E3E3* astrocytes, but this striking trend is not the case for all reactivity markers analysed.

When mRNA expression levels of *IL1β*, *LCN2* and *PTX3* are considered, *E4E4* astrocytes have a relatively weak response to inflammatory insult compared to *E3E3* astrocytes. *E4E4* astrocytes express up to 10-fold less *IL1β* ($p < 0.01$), 2-fold less *LCN2* ($p < 0.001$) and 5-fold less *PTX3* compared to *E3E3* astrocytes (Figure 4.3.12). Taken together this data is indicative of a genotype effect on astrocyte reactivity state and gives weight to the hypothesis that *E4E4* astrocytes are pro-inflammatory compared to *E3E3* astrocytes with respect to several indicators of astrocyte reactivity.

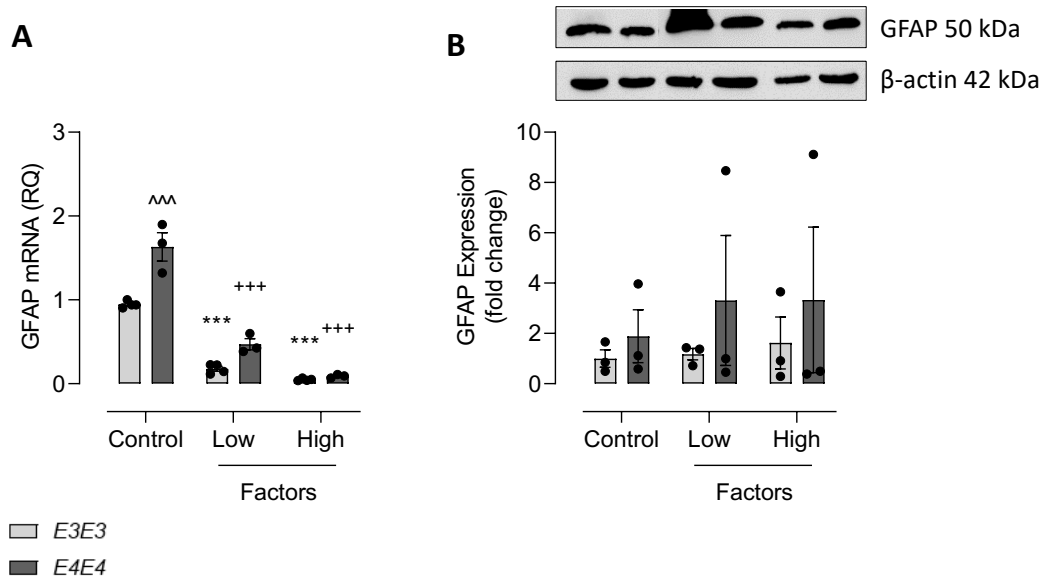


Figure 4.3.10. GFAP mRNA and protein expression does not differ between E4E4 and E3E3 iPSC-derived reactive astrocytes.

*GFAP mRNA expression is significantly greater in E4E4 astrocytes at base line, GFAP expression is reduced in response to stimulation but there is no effect of APOE genotype (A). GFAP protein expression is not significantly different in E3E3 and E4E4 reactive astrocytes (B). Data expressed as mean ± SEM (N=3, n=3-4). *** $p < 0.001$ vs E3E3 control; $^{+++}$ $p < 0.001$ vs E4E4 control; ^^^ $p < 0.001$ vs E3E3. GFAP mRNA APOE effect $F(1, 15) = 41.87$, $p = < 0.0001$; factors effect $F(2, 15) = 199.9$, $p = < 0.0001$; interaction effect $F(2, 15) = 12.79$, $p = 0.0006$. GFAP protein APOE effect $F(1, 12) = 1.289$, $p = 0.2783$; factors effect $F(2, 12) = 0.2024$, $p = 0.8195$; interaction effect $F(2, 12) = 0.06957$, $p = 0.9332$ (Two-way ANOVA with Bonferroni post hoc).*

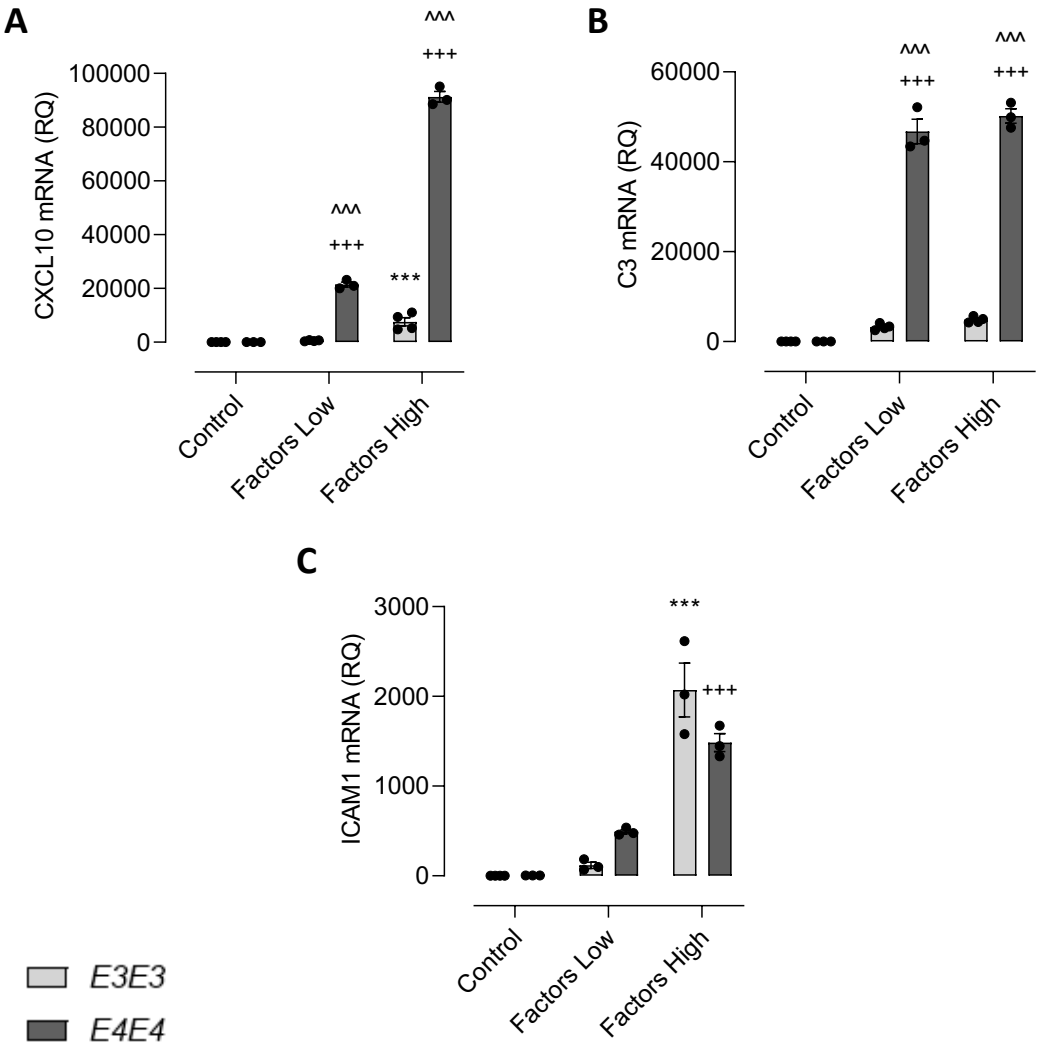


Figure 4.3.11. E4E4 iPSC-derived astrocytes show increased expression of CXCL10 and C3 compared to E3E3 iPSC-derived astrocytes in response to inflammatory insult.

*E4E4 astrocytes show an enhanced response to inflammatory microglial factors compared to E3E3 astrocytes in terms of CXCL10 (A) and C3 (B) mRNA expression. E4E4 astrocytes tend to have a greater increase in ICAM1 mRNA expression when stimulated with a low dose of microglial factors, while E3E3 astrocytes tend to have a greater increase in ICAM1 mRNA expression when stimulated with the high dose of microglia factors (C). Data expressed as mean ± SEM (N=3, n=3-4). *** p < 0.001 vs E3E3 control; $^{+++}$ p < 0.001 vs E4E4 control; ^^^ p < 0.001 vs E3E3. CXCL10: APOE effect F(1, 15) = 1618, p = < 0.0001; factors effect F(2, 15) = 1197, p = < 0.0001; interaction effect F(2, 15) = 842.6, p = < 0.0001. C3: APOE effect F(1, 15) = 1081, p = < 0.0001; factors effect F(2, 15) = 379.9, p = < 0.0001; interaction effect F(2, 15) = 270.4, p = < 0.0001. ICAM1: APOE effect F(1, 13) = 0.4938, p = 0.4946; factors effect F(2, 13) = 119.2, p = < 0.0001; interaction effect F(2, 13) = 7.525, p = 0.0067 (Two-way ANOVA with Bonferroni post hoc).*

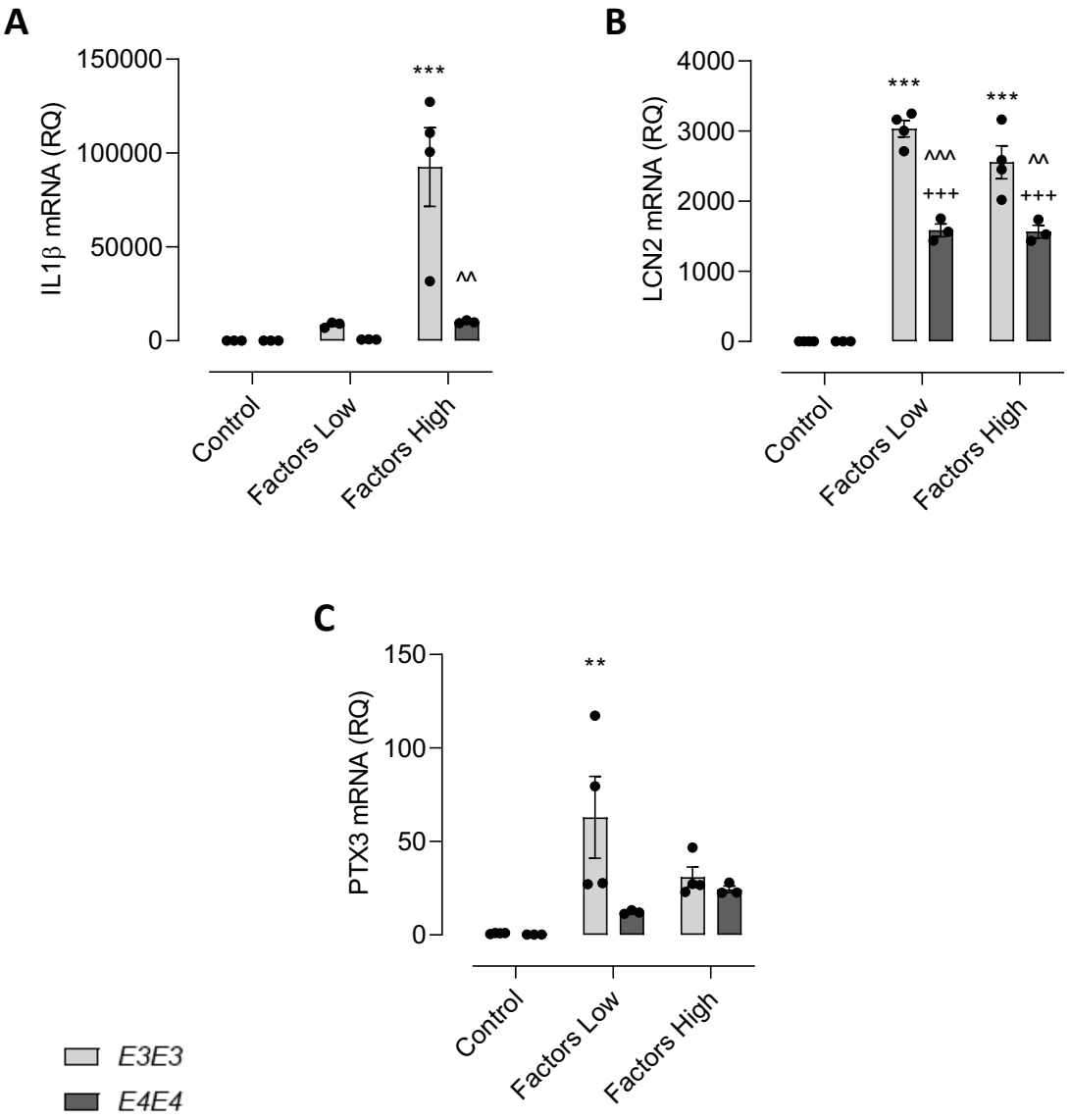


Figure 4.3.12. E4E4 iPSC-derived astrocytes show decreased expression of IL1β, LCN2 and PTX compared to E3E3 iPSC-derived astrocytes in response to inflammatory insult.

*E4E4 astrocytes do not respond as robustly as E3E3 astrocytes in terms of IL1β (A) and LCN2 (B) mRNA expression. There is no effect of APOE genotype on PTX3 mRNA expression in response to microglial factors, although E3E3 astrocytes tend to have greater PTX3 expression compared to E4E4 astrocytes following insult (C). Data expressed as mean ± SEM (N=3, n=3-4). ** p < 0.01, *** p < 0.001 vs E3E3 control; $^{+++}$ p < 0.001 vs E4E4 control; ^^ p < 0.01, ^^^ p < 0.001 vs E3E3. IL1β: APOE effect F(1, 13) = 10.43, p = 0.0066; factors effect F(2, 13) = 12.89, p = 0.0008; interaction effect F(2, 13) = 8.306, p = 0.0047. LCN2: APOE effect F(1, 15) = 54.40, p = < 0.0001; factors effect F(2, 15) = 176.5, p = < 0.0001; interaction effect F(2, 15) = 15.05, p = 0.0003. PTX3: APOE effect F(1, 15) = 4.709, p = 0.0465; factors effect F(2, 15) = 6.191, p = 0.0110; interaction effect F(2, 15) = 3.152, p = 0.0720 (Two-way ANOVA with Bonferroni post hoc).*

4.4 Discussion

The APOE4 genotype carries the greatest genetic risk for sporadic AD and the effect of APOE4 on glial response has been proposed as a potential mechanism, yet its involvement in the inflammatory response in astrocytes is not well defined. The elusive narrative of the APOE inflammatory response in the literature may be attributed in part to a lack of tractable human APOE models that may have clouded the effect of APOE on AD relevant inflammatory pathways (Tai *et al.*, 2015). Thus, this study aimed to examine the reactivity profile of *E4E4* astrocytes and compare it to that of *E3E3* astrocytes in order to discern any genotype effect on reactivity state. Reactivity was measured by examining alterations in IL6 mRNA expression and secretion as well as other previously established reactive astrocyte markers including *CXCL10*, *C3*, *ICAM1*, etc.

Astrocyte cell fate was confirmed via immunofluorescent staining for classical astrocyte markers GFAP, Cx43, S100β and EAAT1, all of which *E4E4* astrocytes were found to be positive for. Following confirmation of cell fate it was next established whether *E4E4* astrocytes are capable of responding to inflammatory insult delivered via microglial factors IL1α, TNFα and C1q. Base line reactivity was examined as a function of APOE genotype then astrocyte response to inflammatory insult was again assessed across both genotypes.

4.4.1 *E4E4* astrocytes are capable of responding to inflammatory insult

It was determined that *E4E4* astrocytes are capable of responding to inflammatory insult by stimulating with inflammatory microglial factors IL1α, TNFα and C1q (Liddelow *et al.*, 2017) and subsequently assessing reactivity markers. *E4E4* astrocytes responded with increased IL6 mRNA expression and secretion as well as up-regulation of reactivity genes *CXCL10*, *C3*, *LCN2*, *IL1β*, *ICAM1* and *PTX3* mRNA expression.

C3 has been identified as a key marker for reactive astrocytes in a variety of neurodegenerative diseases, including AD, where prefrontal cortex astrocytes are positive for C3 (Liddelow *et al.*, 2017). C3 is part of the complement system which enhances the body's ability to target and destroy pathogens (Ricklin *et al.*, 2016). Direct interaction of APOE4 and C3 has been shown in both CSF Aβ and phosphorylated tau aggregates resulting in the theory that a synergistic relationship exists between C3 and

APOE4 resulting in elevated AD associated neurodegeneration and in turn, Aβ regulates the effect of the complement cascade on tau pathology (Bonham *et al.*, 2016).

CXCL10 has previously been associated with early AD, where increased CSF levels of CXCL10 were found in individuals with mild cognitive impairment and mild AD but not those with severe AD (Galimberti *et al.*, 2006). This increased CXCL10 was specific to the CNS, as serum levels were not affected (Galimberti *et al.*, 2007) and could contribute to high levels of infiltrating peripheral immune cells. While Galimberti and colleagues did not assess the influence of APOE genotype, our data would suggest that it is a contributing factor to raised CXCL10 in AD. Similarly raised levels of CSF ICAM1 have been detected in patients with preclinical, prodromal and dementia stages of AD (Janelidze *et al.*, 2018). Therefore, ICAM1 has been flagged as a potential early biomarker for AD. ICAM1 has been linked to BBB breakdown, neuroinflammation and cognitive decline in AD (Bowman *et al.*, 2018).

The research pertaining to a link between APOE and LCN2 has been carried out with respect to atherosclerosis and cardiovascular disease models, i.e. the role of APOE in the periphery as opposed to the CNS. Serum LCN2 has been positively correlated with coronary artery disease severity and accelerates formation of atherosclerosis, an effect which is coupled with increased expression of *ICAM1*, *PTX3* and *NF-κB* and exacerbated in *Apoe* knockout mice (Shibata *et al.*, 2020). Interestingly, this effect is ameliorated by dietary curcumin via down-regulation of LCN2 (Wan *et al.*, 2016), this plant-derived polyphenol has also demonstrated anti-inflammatory effects on human immune cells (Campbell *et al.*, 2018; Campbell *et al.*, 2019). Successfully delivery of curcumin to the CNS in exosomes has ameliorated tau pathology in AD mice (Wang *et al.*, 2019). Our data now also provides evidence of a link between LCN2, neuroinflammation and APOE genotype.

IL1β is among the cytokines that display significant up-regulation in AD patients, and its potential role has been extensively researched and reviewed by Di Bona and colleagues (Di Bona *et al.*, 2008). IL1β and IL18 are downstream products of NLRP3 inflammasome activation where inflammasome assembly activates caspase-1 which in turn cleaves the pro/inactive form of these cytokines into their active secreted forms (Ojala *et al.*, 2009). Raised levels of IL1β, IL18 and caspase-1 were detected in the frontal cortex of AD brain samples compared to control, with no detected correlation with APOE genotype (Ojala *et al.*, 2009). Raised IL1β levels have also been found in the plasma of patients with late-onset AD, as well as those with vascular dementia and cerebrovascular disease in the

absence of dementia (Zuliani *et al.*, 2007). Overexpression of IL1β has been implicated in increased tau phosphorylation, neuritic plaque development and exacerbated cognitive decline (Ojala *et al.*, 2009).

High levels of pentraxins and pro-inflammatory cytokines are thought to contribute to the acceleration of disease progression in AD (Osera *et al.*, 2012). PTX3 specifically has been poorly studied in relation to AD, however its involvement in neurodegeneration is well characterised with Cunningham and colleagues noting its involvement in Prion disease (Cunningham *et al.*, 2005), and Liddelow and colleagues identifying PTX3 as a reactive astrocyte marker (Liddelow *et al.*, 2017). PTX3 has been associated with cognitive decline, presenting a 20% increased risk of cognitive decline in individuals with mild cognitive impairment. Although no association was found when APOE4 genotype was considered (Sharma *et al.*, 2016).

E4E4 astrocytes are capable of responding to an inflammatory insult and express reactive astrocyte markers much like their *E3E3* counterparts characterised in the previous chapter. It was next established whether quiescent *E4E4* astrocytes are more inflammatory at base line compared to *E3E3* astrocytes, and furthermore whether the *APOE4* genotype heightens astrocytic response to inflammatory insult.

4.4.2 *E4E4* astrocytes have a higher level of basal reactivity compared to *E3E3* astrocytes

The effect of APOE genotype on astrocyte reactivity is a growing topic of interest in the fight against AD. With astrocyte reactivity considered to be an important contributing factor to AD pathogenesis and APOE4 genotype a major genetic risk factor, it is worth considering that APOE4 may predispose astrocytes to becoming reactive in the AD brain. High base line expression of pro-inflammatory mediators in an *APOE4* carrier may over a lifetime contribute to chronic inflammation, which in turn may lead to irreversible cell damage or death and thus contribute to increased AD risk. As such, basal levels of astrocyte reactivity markers were assessed in *E4E4* astrocytes and compared to their *APOE3*-expressing counterparts.

In a quiescent state, *E4E4* astrocytes express genes associated with reactivity at a significantly higher level compared to their *E3E3* counterparts. Base line mRNA expression and protein secretion of IL6 were significantly greater in *E4E4* astrocytes. It was subsequently found that *E4E4* astrocytes also had exaggerated expression of *IL1β*,

CXCL10, *C3*, *ICAM1* and *GFAP* in their quiescent state. Taken together this would indicate that *E4E4* astrocytes have inherent inflammatory characteristics which may have profound effects in the AD brain and potentially explain why *APOE4* carriers have such a high risk of developing AD.

Literature pertaining to APOE genotype and astrocyte reactivity by in large supports the suggestion that *E4E4* astrocytes are pro-inflammatory compared to their *E3E3* counterparts. Exogenous human APOE has been shown to induce IL1β in rat glial cultures, with APOE4 inducing significantly greater levels compared to APOE3 (Guo *et al.*, 2004; Dorey *et al.*, 2014). In mice expressing either human APOE3 or APOE4 it was found that the *APOE4* isoform induced significantly greater central and peripheral levels of TNFα and IL6 in response to LPS insult delivered intravenously, indicating an isoform dependent inflammatory response. Interestingly, an APOE-mimetic peptide was capable of suppressing this response thereby indicating that targeting APOE may be viable therapeutically (Lynch *et al.*, 2003).

4.4.3 *E4E4* astrocytes show an enhanced IL6 response to inflammatory insult

Another pressing question in the characterisation of the APOE3 and APOE4 astrocyte inflammatory response debate is whether APOE4 astrocytes are less anti-inflammatory or more pro-inflammatory in response to reactive stimuli. To date, studies have examined inflammatory responses of the APOE3 and APOE4 astrocyte homologues with data suggesting that APOE4 may have pro-inflammatory or less effective anti-inflammatory functions compared to the APOE3 (Dorey *et al.*, 2014). However, some APOE knock-out models support an anti-inflammatory role. Exogenous APOE applied to microglia and macrophage cultures down-regulated their activation (Baitsch *et al.*, 2011).

With regards to IL6, *E4E4* astrocytes have increased basal expression and secretion compared to *E3E3* astrocytes. Furthermore, *E4E4* reactive astrocytes expressed greater levels of *IL6* mRNA compared to *E3E3* astrocytes which interestingly did not translate to the protein level. IL6 secretion by astrocytes at a basal level is thought to be neurotropic in the CNS, however, overexpression of IL6 has long been shown to have damaging effects on neurons (Van Wagoner *et al.*, 1999) with high serum IL6 associated with various astrocyte pathologies.

Since IL6 secretion by reactive astrocytes was not affected by APOE genotype it may be the case that this increase in IL6 is a general pro-inflammatory response rather than

APOE4 and AD specific. Raised plasma levels of IL6 have been found in patients with vascular dementia, at a significantly higher level to patients with late-onset AD (Zuliani *et al.*, 2007). Perhaps levels of other cytokines and chemokines may be altered in an APOE genotype-dependent manner, making them more specific to the AD condition. High plasma concentrations of pro-inflammatory cytokines and chemokines have previously been positively correlated with APOE genotype in AD patients. Specifically, AD patients expressing the *APOE4* genotype have been found to have elevated circulating IL18 levels compared to patients expressing the *APOE3* or *APOE2* genotypes (Reale *et al.*, 2012). Furthermore, the common p.D358A variant of the IL6R is associated with increased shedding of the receptor resulting in sIL6R and its associated pro-inflammatory trans signalling pathway. This variant and associated increase in sIL6R is enriched in APOE4^{+} AD populations and may form a part of the associated AD risk for APOE4 carriers (Haddick *et al.*, 2017). So while IL6 secretion was not affected by APOE genotype, perhaps its downstream effects are.

4.4.4 *E4E4* astrocytes show greater reactivity with regards to certain reactive astrocyte markers compared to *E3E3* astrocytes

The mRNA expression profile of *E4E4* reactive astrocytes compared to *E3E3* reactive astrocytes does little to settle the debate of which genotype is more inflammatory. *E4E4* reactive astrocytes dominate in terms of *CXCL10*, *C3* and *ICAM1* mRNA expression, while *E3E3* reactive astrocytes show enhanced expression of *IL1β*, *LCN2* and *PTX3*.

The literature surrounding the inflammatory response of APOE astrocytes is similarly ambiguous. The LPS-induced inflammatory response in an APOE targeted replacement mouse model showed that APOE3 > APOE4 for IL1β and IL6 expression (Maezawa *et al.*, 2006). However, APOE has also been demonstrated to act as an anti-inflammatory agent, as reactivity was reduced when exogenous APOE was added to microglia and macrophage cultures (Baitsch *et al.*, 2011). In a post-mortem study of AD brains, it was noted that there was no difference in the number of GFAP positive astrocytes between *APOE4* carriers and non-*APOE4* carriers, the authors also found no indication for APOE-dependent astrogliosis or interactions of astrocytes with plaques in an *APOE*-dependent fashion (Serrano-Pozo *et al.*, 2013).

However, a growing body of literature points to an APOE4 > APOE3 astrocyte inflammatory response (Dorey *et al.*, 2014; Tai *et al.*, 2015), with a 2008 study indicating

that non-steroidal anti-inflammatory drugs benefitting AD risk in APOE4 carriers (Szekely *et al.*, 2008). Tai and colleagues provide evidence from mixed glial *in vitro* cultures that for neuroinflammation, APOE4 involves a relative loss of positive function compared to the APOE3 cell types (Tai *et al.*, 2015). Specifically, TNFα secretion is significantly increased in the order of APOE knockout > APOE4 > APOE3, supporting the idea that APOE4 is anti-inflammatory compared to a total loss of APOE but less anti-inflammatory compared to APOE3 cells. A study carried out in APOE4 knock-in mice showed increased glial activation and greater secretion of pro-inflammatory cytokines following LPS administration compared to APOE3 or APOE2, and furthermore that APOE knockout yielded similar results prompting the authors to suggest that APOE4 protein may lack anti-inflammatory properties compared to the other genotypes (Zhu *et al.*, 2012). Shi and colleagues also found that APOE4 increased activation of glial cells (Shi *et al.*, 2017b).

Our data supports a pro-inflammatory phenotype for *E4E4* astrocytes with respect to some reactive astrocyte indicators and provides further insight into the potential role of this APOE genotype in AD pathology. This possibly reflects the heterogeneity observed in reactive astrocytes, which is often underappreciated (Anderson *et al.*, 2014). It is worth remembering that astrocyte reactivity is a graded and complex response, and undoubtedly contributes to our difficulty defining an inflammatory profile for APOE4 astrocytes.

4.4.5 Concluding remarks

Human iPSC-derived *E3E3* and *E4E4* astrocytes appear to exhibit different inflammatory profiles in response to pro-inflammatory microglial factors. The induction and characterisation of an inflammatory profile in response to these specific factors has recently been characterised for astrocytes (Liddelow *et al.*, 2017). However, to this author's knowledge, this study is the first to compare the high-risk APOE4 homologue to the APOE3 homologue in terms of astrocytic response to these factors in a human iPSC model. The data presented here begins to tease out some of the mechanisms which may contribute to its associated AD risk, with APOE4 astrocytes appearing inherently pro-inflammatory at basal levels and displaying some exaggerated responses to inflammation. In conclusion, astrocyte reactivity and importantly APOE4 astrocyte reactivity should be considered a therapeutic target for modulation which may prove useful in future attempts to augment its associated AD risk.

Chapter 5

Modulating astrocyte reactivity in a human iPSC-derived model of Alzheimer's disease

5. Modulating astrocyte reactivity in a human iPSC-derived model of Alzheimer's disease

5.1 Introduction

With reactive astrogliosis shown to play a prominent role in neurodegenerative diseases, particularly in AD, developing drug therapies that can target reactive astrocytes is of the utmost importance. Current AD therapies are limited and primarily target the cholinergic system (Ferreira-Vieira *et al.*, 2016), as well as some success with drugs targeting NMDA receptors (Olivares *et al.*, 2012; Zhang *et al.*, 2016b). Choosing appropriate astrocytic targets however has proved difficult, with some progress being made targeting S100β and activated cannabinoid receptors to reduce reactive astrogliosis (Zhang *et al.*, 2019).

5.1.1 Fibroblast growth factors constitute a large family of molecules

Fibroblast growth factor (FGF) and their receptors combine to create an elaborate signalling system which is involved in numerous developmental processes and repair. FGF is a growth factor and signalling protein which has been implicated in many diverse biological processes including limb and nervous system development, wound healing, and tumour growth (Guillemot & Zimmer, 2011). In the developing CNS, FGF plays a crucial role in processes including neurogenesis, axon growth and differentiation. In addition to their role in development, FGF are paramount for neuronal survival throughout adulthood with FGF1 playing a crucial role in regulation of synaptic plasticity, learning and memory, along with FGF2 which is paramount for adult neurogenesis.

FGF2 was the first member of the FGF family to be isolated in the 1980s (Abraham *et al.*, 1986) and as such is commonly referred to as basic FGF, it is the most studied FGF. Since then this family of signalling molecules has grown significantly in both number and complexity. To date there are 23 known members of the FGF family, 22 of which are expressed in humans (FGF15 has not been found in the human genome) and 10 of which have been found to be expressed in the brain (Reuss & von Bohlen und Halbach, 2003). Subsequent to FGF there are four FGF receptors (FGFR), FGFR1-4 (Ford-Perriss *et al.*, 2001). FGF is widely expressed throughout the CNS where FGF2 is expressed and synthesised predominantly by astrocytes, while other members of the FGF family such as FGF5, FGF8 and FGF9 are expressed by neurons (Reuss & von Bohlen und Halbach, 2003).

5.1.2 FGF genes and proteins are structurally comparable

All known FGF genes have the same basic structure, consisting of three coding exons with exon 1 containing the start codon. FGF2 and FGF3 have an additional 5' untranscribed regions while some of the FGF subfamilies have subdivisions in their exon 1, e.g. FGF8, with exon 1A containing the start codon in this case (Reuss & von Bohlen und Halbach, 2003). Localisation of the various FGF on the human chromosome are known for all members with the exception of FGF16 (Table 5.1.1).

FGF	Chromosome localisation
FGF1	5q31
FGF2	4q26-27
FGF3	11q13
FGF4	11q13
FGF5	4q21
FGF6	12p13
FGF7	5q15-21.1
FGF8	10q24
FGF9	13q11-q12
FGF10	5p12-p13
FGF11	17p13.1
FGF12	3q28
FGF13	Xq26
FGF14	13q34
FGF15	*
FGF16	Unknown
FGF17	8p21
FGF18	5q34
FGF19	11q13
FGF20	8p22
FGF21	19q13.1-qter
FGF22	19p13.3
FGF23	12p13

Table 5.1.1. FGF chromosomal localisation in humans.

** not expressed in humans. Modified from Ornitz & Itoh, 2001.*

FGF-like genes have also been found in certain viral DNA (Li *et al.*, 2002) but not in unicellular organisms such as *E. coli* and *S. cerevisiae* (Ornitz & Itoh, 2001; Itoh, 2007), and FGF-like genes have been found in the model systems *Drosophila* (Sutherland *et al.*, 1996) and *Caenorhabditis elegans* (Burdine *et al.*, 1997). With regards to vertebrates, twenty-two FGF genes have been identified in mice, four have been identified in zebrafish, six in *Xenopus* and seven in chicken (Reuss & von Bohlen und Halbach, 2003). Across these species FGF proteins share more than 90% homology, this gives some insight into the evolutionary development of the FGF family indicating that they likely evolved in invertebrates and as such are considered old molecules.

The FGF protein in vertebrates has a molecular weight range of 17-34 kDa. The general protein structure is consistent across all FGF molecules with two core domains separated by a spacer region which varies in length, similarly the C- and N-terminal regions vary in length. Some FGF, namely FGF2, FGF3 and FGF9 have alternative N-terminal splicing sites (Li & Murphy, 2000; Zhang *et al.*, 2007). Most FGF can be secreted from cells as a result of amino-terminal signal peptides; the FGF containing this signal peptide include FGF3-8, FGF10, FGF15, FGF17-19 and FGF21-23. Those lacking the conventional signal peptide are not readily secreted and include FGF1, FGF2, FGF9, FGF16 and FGF20; it is thought that alternative methods, e.g. exocytosis, are required for secretion of FGF1 and FGF2 for example which have extracellular roles, while secretion of FGF that act intracellularly may be indicative of cellular damage (Mignatti *et al.*, 1992; Ornitz & Itoh, 2001).

5.1.3 FGF Receptors – There are four known FGF receptors

Four FGF receptors have been identified to date (Reuss & von Bohlen und Halbach, 2003), these receptors come from the tyrosine kinase class of receptor. The structure of the FGFR family is homologous (Itoh & Ornitz, 2004), with three extracellular immunoglobulin (Ig)-like domains (IgI, IgII and IgIII), four acidic amino acids between IgI and IgII, a hydrophobic transmembrane domain, and two intracellular tyrosine kinase domains divided by a fourteen amino acid insert which allows for heparin binding (Reuss & von Bohlen und Halbach, 2003). Both heparin and heparin sulfate proteoglycans bind FGF and FGFR to enhance the signal by regulating the formation of the ligand-receptor complex (Loo *et al.*, 2001).

Binding affinity of the FGF ligands to their receptors is highly diverse with different ligands having different binding affinity or no affinity for each of the four identified receptors (see

Table 5.1.2). Ligand binding is dependent on heparin sulphate proteoglycans. These heparin compounds act as low affinity FGF receptors. A 14 amino acid insert in the tyrosine kinase domains of the FGF receptors is important for heparin binding and as such is required for receptor dimerisation (Olsen *et al.*, 2004). Specificity of FGFR is dependent on the third extracellular Ig-like domain, this part of the receptor complex is prone to structural variability across the FGFR family as a result of alternative splicing (Reuss & von Bohlen und Halbach, 2003; Farrell & Breeze, 2018). The effect the different FGF members exert is dependent on the structural and functional diversity of the FGF receptors. This diversity is as a result of alternative splice variants within the *FGFR* gene. The variant with the highest impact on receptor specificity relates to the IgIII domain which has three splice variants, namely IgIIIa, IgIIIb and IgIIIc. FGFR1 and FGFR2 have all three splice variants, while FGFR3 only has the IgIIIb and IgIIIc variants and FGFR4 only has the IgIIIc variant (Wang *et al.*, 1995; Olsen *et al.*, 2004).

FGFR binding results in the formation of a receptor complex containing two FGF molecules bound to a receptor with a heparin sulphate proteoglycan molecule linking the two FGF molecules. Complex formation leads to the activation of the receptor via phosphorylation and subsequent intracellular signal transduction following phosphorylation of intracellular signalling molecules. FGFR activation results in the initiation of several intracellular signalling cascades, including phosphorylation of src and PLCγ subsequently activating protein kinase C (PKC). It is thought that src and PLCγ signalling plays a role in cytoskeleton alteration (Wells, 2000; Davies *et al.*, 2008). Crk and Shc can also be activated in this manner, which may have a mitogenic effect (Hart *et al.*, 2001). Alternatively, PKC may be activated via SNT/FRS2 which also initiates the Ras signalling cascade (Reuss & von Bohlen und Halbach, 2003). The SNT1/FRS2 signalling pathway offers an alternative link between FGFR signalling and the Ras/MAPK signalling pathway in a tyrosine-phosphorylation-independent manner (Wang *et al.*, 1996; Kouhara *et al.*, 1997). This pathway is important for cell cycle progression, where SNT1/FRS2 activation recruits the adaptor protein Grb2/Sos which in turn recruits Ras. Activation of the Ras/MAPK signalling cascade is essential for growth factor-induced cell proliferation and differentiation (Kouhara *et al.*, 1997).

As members of the tyrosine kinase receptor family, FGFR propagate their signal via phosphotyrosine-induced activation of their target proteins. Given the homology of the FGFR family it is thought that the intracellular signalling cascade is the same, with the main difference lying in the transduction of the signal meaning that receptor binding

affects the same downstream molecules but to various degrees of strength in the signal (Raffioni *et al.*, 1999; Reuss & von Bohlen und Halbach, 2003). The Bradshaw laboratory group compared the intracellular responses of three FGFR chimeras (PRF1, PRF3 and PRF4) to ligand binding and found that all chimeras activated PLCγ, Shc, FRS2, and the MAP kinases, ERK1 and 2 in a PC cell line (Raffioni *et al.*, 1999) giving weight to the theory that the main difference between FGFR1, FGFR3 and FGFR4 is in the strength of the tyrosine kinase activity.

	FGFR1	**FGFR2**	**FGFR3**	**FGFR4**
FGF1	√	√	√	√
FGF2	√	√	√	√
FGF3	√	√		
FGF4	√	√	√	√
FGF5	√	√		
FGF6	√	√		√
FGF7		√		
FGF8	√	√	√	√
FGF9		√	√	√
FGF10		√		
FGF11	Unknown	Unknown	Unknown	Unknown
FGF12	Unknown	Unknown	Unknown	Unknown
FGF13	Unknown	Unknown	Unknown	Unknown
FGF14	Unknown	Unknown	Unknown	Unknown
FGF15	Unknown	Unknown	Unknown	Unknown
FGF16	Unknown	Unknown	Unknown	Unknown
FGF17		√	√	√
FGF18			√	√
FGF19	Unknown	Unknown	Unknown	Unknown
FGF20	Unknown	Unknown	Unknown	Unknown
FGF21	Unknown	Unknown	Unknown	Unknown
FGF22	Unknown	Unknown	Unknown	Unknown
FGF23	Unknown	Unknown	Unknown	Unknown

Table 5.1.2. Binding of the various members of the FGF family to the four FGF receptors.

Modified from Reuss & von Bohlen und Halbach, 2003.

5.1.4 FGF plays numerous important roles in development

The biological significance of this family of molecules and their receptors during development has been greatly advanced through the use of knockout animals. *Fgf10* and *Fgf18* knockout mice died shortly after birth, indicating a crucial developmental role of these molecules (Itoh, 2007). FGF10 is required for limb and lung development, hence a foetus is capable of developing to term but *Fgf10* knockout is lethal upon birth (Min *et al.*, 1998). FGF18 is required for normal skeletal development in vertebrates, appearing to promote osteogenesis and inhibit chondrogenesis (Ohbayashi *et al.*, 2002). Since FGF18 is a ligand for FGFR3, disruption of *Fgfr3* also results in skeletal defects (Liu *et al.*, 2002). *Fgf9* knockout also results in death shortly after birth. FGF9 plays a key role in embryonic testicular development with male-to-female sex reversal occurring in some *Fgf9* knockout models (Colvin *et al.*, 2001). Interestingly, loss of FGFR2 also results in partial sex reversal indicating that FGFR2 acts as a receptor for FGF9 in testes development (Bagheri-Fam *et al.*, 2008). In contrast, *Fgf4* and *Fgf8* knockout mice die during early embryonic development. FGF4 plays a role in cell proliferation of the inner cell mass, therefore knockout impairs development following implantation (Feldman *et al.*, 1995). FGF8 is required for gastrulation, therefore Fgf8 knockout results in failure of cell migration which is necessary for proper development of the germ layers (Sun *et al.*, 1999). *Fgf15* and *Fgf23* knockout mice are capable of developing to term but typically gradually die in the postnatal stages due to abnormal cardiac functioning, and growth retardation and compromised phosphate and vitamin D metabolism respectively (Itoh, 2007). The effects of knocking out FGF11, FGF13, FGF20 and FGF22 are currently unknown. Knockout of the remaining FGF molecules (FGF1-3, FGF5-7, FGF12, FGF14-17 and FGF21) result in viable mice with non-lethal developmental anomalies (Itoh, 2007).

5.1.5 FGF and the CNS

The major roles of FGF during neural development have been researched quite thoroughly. Out of the numerous molecules involved in neural development, FGF have possibly the most diverse roles in the formation of the complex CNS (Guillemot and Zimmer, 2011). During embryonic development FGF are vital for modulating cell proliferation, migration and differentiation (Ornitz & Itoh, 2001). In the developing brain, FGF plays a major role in developmental processes including neurogenesis, axon growth, differentiation, as well as neuronal survival (Reuss & von Bohlen und Halbach, 2003).

The effect of FGF molecules on differentiation is highly time dependent. In mouse, FGF2 along with EGF drive stem cell proliferation in the striatum. Findings from the Aebischer Laboratory suggest that insulin-like growth factor (IGF)-1 is a key factor in the regulation of NSC activation, and that EGF and FGF2 drive NSC proliferation in the striatum via distinct intracellular mechanisms (Arsenijevic *et al.*, 2001). Basic FGF, i.e. FGF2, is thought to play a role in astrocyte maturation after it was shown to up-regulate microRNA-134 in astrocytes via extracellular signal-regulated kinase and phosphatidylinositol 3-kinase signalling (Numakawa *et al.*, 2015).

In the adult brain, FGF is involved in adult neurogenesis, learning and memory processes, as well as having roles in areas such as synaptic functions, behaviours and neurological disorders (Guillemot & Zimmer, 2011; Turner *et al.*, 2012; Kang *et al.*, 2014a). Overall, in the adult brain it is believed that FGF act as homeostatic factors with roles in tissue repair and injury response (Ornitz & Itoh, 2001). Neurogenesis has been found to occur in the hippocampus and the subventricular zone of the forebrain of the adult CNS. Adult neurogenesis is highly dependent on FGF2 (Kuhn *et al.*, 1996; Reuss & von Bohlen und Halbach, 2003), which is not surprising when you consider its crucial role in CNS development. FGF2 has been implicated in adult neurogenesis as a result of evidence of changes in proliferation and differentiation of adult neural stem and progenitor cells (Rai *et al.*, 2007; Werner *et al.*, 2011). FGF1 and FGF2 are thought to be involved in modulating processes attributed to learning and memory (Reuss & von Bohlen und Halbach, 2003) as well as the regulation of synaptic plasticity both *in vitro* and *in vivo*. For example, when applied to cerebral cortical neurons of rats, FGF2 enhanced neurite growth (Morrison *et al.*, 1986).

5.1.5.1 FGF2 – a growth factor with the potential of modulating iPSC-derived astrocyte reactivity

The ability to ameliorate or decrease reactivity in neurotoxic astrocytes holds great potential as a therapeutic target in order to reduce the detrimental effect of reactive astrogliosis. A role for FGF in repair processes has been identified (Haynes, 1988) in particular following trauma to the CNS (Mocchetti & Wrathall, 1995), which highlights its therapeutic potential. FGF2 is a growth factor and signalling protein which has been implicated in many diverse biological processes including limb and nervous system development, wound healing, and tumour growth (Guillemot & Zimmer, 2011). FGF2

signalling is initiated upon the molecule binding to its receptor tyrosine kinase, which activates its downstream signal extracellular signal-regulated kinase 1/2 (ERK1/2), a member of the MAPK family (Johnson-Farley *et al.*, 2007).

Numerous studies have uncovered evidence that FGF signalling mediates morphological changes in reactive astrocytes. It has also been shown that FGF ligand or receptor expression is affected by various types of CNS injury (Reilly & Kumari, 1996; Goldshmit *et al.*, 2012; Kang *et al.*, 2014a; Kang *et al.*, 2014b). As a result of the many similarities between the processes of astrocyte glycogenesis and reactive astrocyte gliosis, there are also similarities in the molecules which modulate these processes, including FGF and STAT3 (Kang *et al.*, 2014a). Similarities between these processes are seen with regards to gene expression, mitotic responses, morphological changes and, electrophysiological properties. It has also been highlighted via genome-wide analysis of gene expression that over half of the genes expressed by dividing glial cells *in vitro* are also expressed in reactive astrocytes *in vivo* (Cahoy *et al.*, 2008).

The neuroprotective properties of FGF2 have been demonstrated over a wide range of neuronal phenotypes. Mouse primary astrocytes cultured in serum-free medium supplemented with FGF2 and EGF displayed enhanced glycolytic metabolism, higher glycogen content, lower GFAP expression, increased glutamine synthase and *Glt1* mRNA levels compared to astrocytes cultured in serum enriched DMEM, indicating a quiescent astrocyte was produced under these culture conditions (Prah *et al.*, 2019).

In terms of FGF2 ameliorating the negative effects of reactive astrocytes, this has been shown in several animal studies both *in vitro* and *in vivo*. The Hébert Laboratory demonstrated that FGF signallling could suppress astrocyte activaton in the healthy and injured brain. Loss- and gain-of-function genetics revealed that FGF signalling was necessary to maintain quiescent astrocytes in the unperturbed adult neocortex. It was further shown that FGF signalling delays the astrocytic response to insult, increases the rate of “deactivation”, and decreases glial scar size without affecting neuronal survival (Kang *et al.*, 2014b). In a study carried out in rats by Ye and colleagues, it was revealed that exogenous FGF2 attenuated astrocyte activation by reducing GFAP expression, as well as some other astrocytic markers such as neurocan and vimentin (Ye *et al.*, 2015). This study also showed a decrease in the expression of inflammatory cytokines, including IL6 and TNFα, potentially via the upstream TLR4/NF-κB signaling pathway. As a whole, this study provided strong evidence that FGF2 is capable of inhibiting excessive astrogliosis and glial scarring following CNS injury (Ye *et al.*, 2015).

Furthermore, Shi and colleagues examined the role of the FGF2/FGFR1 signalling pathway in an *in vitro* and *in vivo* model of infrasound exposure, whereby astrocytes were exposed to low frequency sound waves which have previously been shown to cause CNS injury via astrocyte activation (Shi *et al.*, 2018). They elucidated a role of FGF2 in infrasound-induced astrocyte activation and neurodegeneration as it counteracted the infrasound-induced decrease in FGFR1 expression and attenuated levels of pro-inflammatory cytokines TNFα, IL1β, IL18, IL6, and IFNγ both *in vitro* and *in vivo* (Shi *et al.*, 2018). FGF2 has also shown potential in an ischemic model. FGF2 overexpression improved neural stem cell survival and subsequently improved brain function in a mouse model of neonatal hypoxia-ischemia (Ye *et al.*, 2018), indicating a protective role of FGF following neural trauma. This protective role may extend to modulating astrocyte reactivity.

The ability to ameliorate or decrease reactivity of neurotoxic astrocytes could prove extremely beneficial for the management of conditions and diseases in which astrocytes play a detrimental role. Evidence in the literature pertaining to the role of FGF2 in altering astrocyte reactive state led us to believe it worth investigating in our human iPSC-derived reactive astrocyte model.

5.1.6 Cannabidiol – a cannabinoid with the potential of modulating iPSC-derived astrocyte reactivity

The cannabinoid system has recently gained traction in the fields of immunology and inflammatory disorders research. This system consists of two membrane bound cannabinoid receptors (CB1 and CB2), their endogenous ligands, and the agents involved in the synthesis and degradation of these receptors and ligands (Booz, 2011). Endogenous ligands include anandamide and 2-arachidonoylglycerol, while hundreds of exogenous ligands also exist with various affinities for the CB1 and CB2 receptors, a major source of which is the *Cannabis sativa* plant (Kozela *et al.*, 2017). Cannabidiol (CBD) and tetrahydrocannabinol (THC) are the main phytocannabinoids in *Cannabis*. THC is the main psychotomimetic component in *Cannabis*, while CBD is non-psychotomimetic. Both are on the market in various forms for the treatment and management of inflammatory disorders including MS. Epidiolex was the first Food and Drug Administration (FDA) approved drug derived from the *Cannabis* plant. This drug is CBD-based, and is approved for the treatment of the epileptic disorders Lennox-Gastaut and Dravet syndrome as it has shown success in reducing the frequency of epileptic seizures in patients (Devinsky *et al.*, 2018). Nabiximol, a combination therapeutic containing both CBD and THC, has been approved for the management of nausea and chronic pain as a result of chemotherapy in cancer patients, and has also been successful in management of neuropathic pain and spasticity relating to MS (Whiting *et al.*, 2015).

5.1.6.1 CBD and the cannabinoid receptors

CBD was first isolated from the *Cannabis* plant in 1940 by Roger Adams, with its structure later determined in 1963 (Burstein, 2015). The endogenous production of CBD (Figure 5.1.1) begins with the condensation of hexanoyl-coenzyme A (CoA) and three malonyl-CoA, catalysed by tetraketide synthase. Olivetoic acid cyclase completes the conversion of hexanoyl-CoA to olivetolic acid. Aromatic prenyltransferase with the addition of geranyldiphosphate converts olivetolic acid to cannabigerolic acid, which is further converted to cannabidiolic acid by cannabidiolic acid synthase. The final step in this pathway is the decarboxylation of cannabidiolic acid to CBD (Gagne *et al.*, 2012).

To date five cannabinoid receptors have been identified. In addition to CB1 and CB2 which share 44% homology (Console-Bram *et al.*, 2012), G-protein coupled receptor 55 (GPR55) (Yang *et al.*, 2016a), and vanilloid receptor 1 and 2 (VR1/2) also respond to cannabinoids

(Burstein, 2015). CBD has no affinity for CB1 due to its non-planar molecular conformation. However, several hydrogenated CBD analogs bind to CB1 with some affinity (Burstein, 2015). CBD is reported to act as a functional antagonist to the GPR55 receptor, a receptor with prominent roles in inflammatory pain, gut and bone physiology, as well as cancer. Through the antagonism of CBD it was found that GPR55 is pro-inflammatory (Chiurchiu *et al.*, 2015). CBD activates VR1 and VR2 at high micro molar concentrations thereby inhibiting uptake and degradation of anandamide. CBD exerts anti-hyperalgesia effects via the vanilloid receptor TRPV1 (Costa *et al.*, 2004), while vanilloid receptor TRPV2 is also activated by CBD (Qin *et al.*, 2008).

In addition CBD has been shown to act via hetero dimers of the CB2 and serotonin 1A receptors. In a hypoxic-ischaemic brain injury model, CBD provided neuroprotection by modulating inflammation, excitotoxicity and oxidative stress. Since these protective effects were counteracted with CB2 and serotonin 1A receptor antagonists, the authors proposed roles of these receptors which was confirmed via bioluminescence analysis in HEK-293T cells showing CB2 and serotonin 1A receptors form heteromers (Pazos *et al.*, 2013). It has also been reported that CBD enhances adenosine signalling by inhibiting uptake and therefore provides a CB receptor-independent mechanism by which CBD can decrease inflammation since adenosine agonists have anti-inflammatory effects (Carrier *et al.*, 2006; Castillo *et al.*, 2010).

CBD is devoid of direct CB1 and CB2 receptor activity, but exerts a number of important effects in the brain (Kozela *et al.*, 2017). Since CBD is lipophilic and therefore readily crosses the BBB (Cabral & Jamerson, 2014; Aparicio-Blanco *et al.*, 2019), it is of interest how this interacts with cells in the CNS and furthermore whether it has the potential to modulate astrocyte reactivity.

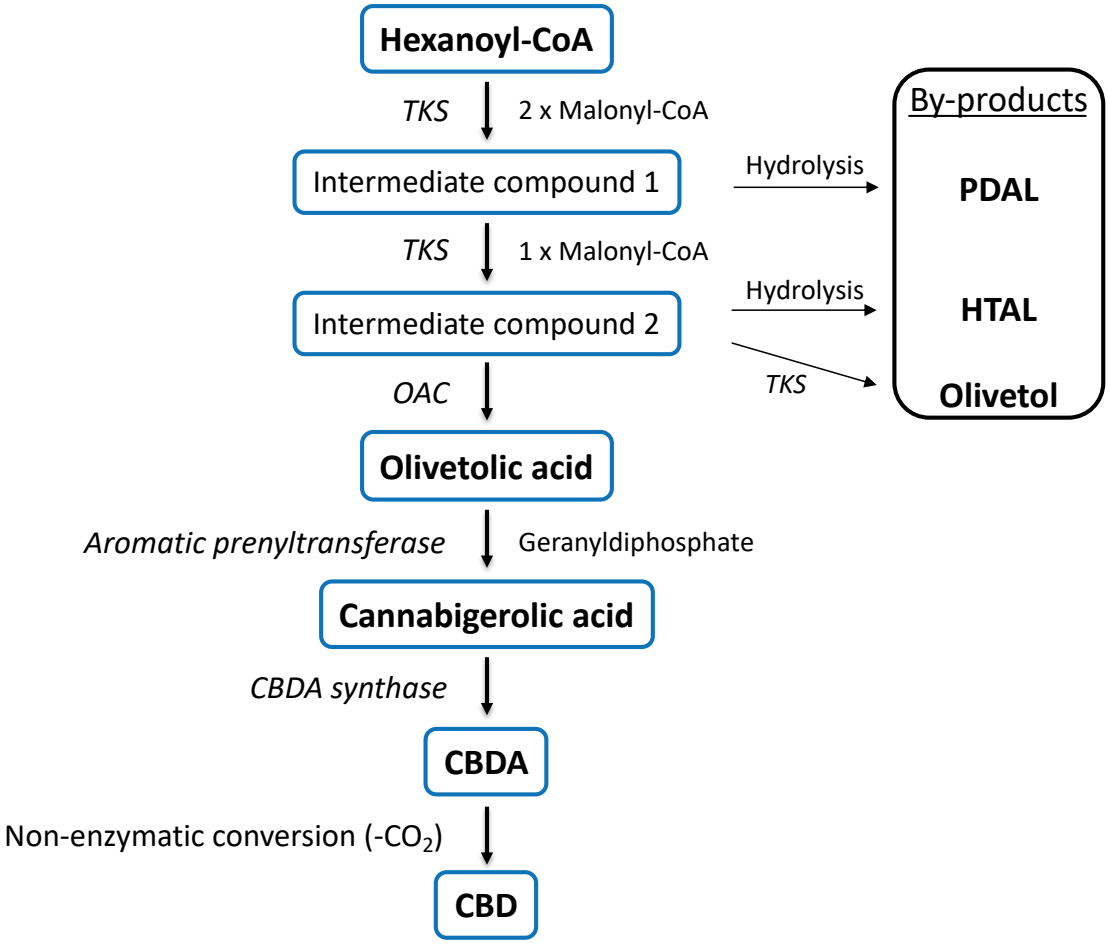


Figure 5.1.1. Biosynthesis of CBD.

The biosynthesis of CBD begins with the condensation of hexanoyl-CoA and two malonyl-CoA, catalysed by TKS, to yield intermediate compound 1. The hydrolysis of intermediate compound 1 yields the by-product PDAL. Intermediate compound 1 is further condensed with one malonyl-CoA, also catalysed by TKS, to yield intermediate compound 2. The hydrolysis of intermediate compound 2 yields the by-product HTAL, while olivetol is yielded is catalysed by TKS. OAC completes the conversion of hexanoyl-CoA to olivetolic acid. Aromatic prenyltransferase with the addition of geranyldiphosphate converts olivetolic acid to cannabigerolic acid, which is further converted to CBDA by CBDA synthase. The final step in this biosynthesis pathway is the non-enzymatic decarboxylation of CBDA to CBD. TKS: tetraketide synthase, PDAL: pentyl diacetic lactone, HTAL: hexanoyl triacetic acid lactone, OAC: olivetoic acid cyclase, CBDA: cannabidiolic acid, CBD: cannabidiol.

5.1.6.2 CBD in the CNS

The cannabinoid system and its ligands have been shown to interact with and affect the activities of astrocytes. CBD does not directly interact with CB1 or CB2 due to its molecular conformation but is capable of carrying out a number of important effects in the CNS (Kozela *et al.*, 2017). CBD has been show to affect microglia and astrocyte function.

Within the CNS, neurons express mainly CB1, microglia mainly express CB2 and astrocytes express both CB1 and CB2 (Kozela *et al.*, 2017). CB2 expression has been shown to be up-regulated in microglia and astrocytes under neuroinflammatory conditions (Shohami *et al.*, 2011). Since CB2 activation typically suppresses activity of immune cells this could be detrimental to immune management of infection but may prove beneficial for management of chronic neuroinflammation in diseases such as AD (Benito *et al.*, 2005; Cassano *et al.*, 2017). The literature pertaining to CBD and astrocyte reactivity shows that increased astrocyte activity is suppressed in the presence of CBD in models of ischemic stroke, AD-like and MS-like neurodegenerations, as well as in models of epilepsy and schizophrenia (Kozela *et al.*, 2017), indicating potential for this compound to modulate astrocyte reactivity.

5.1.6.3 CBD as a modulator of astrocyte reactivity

The endocannabinoid system and its associated ligands have been shown to interact and affect astrocyte activities (Kozela *et al.*, 2017). Moreover, CBD has been shown to decrease pro-inflammatory functions and signalling in astrocytes (Kozela *et al.*, 2017).

CBD has been shown to limit the harmful effects of an exacerbated inflammatory response in the TMEV mouse model of MS. CBD attenuated microglial activation and subsequent release of pro-inflammatory cytokines TNFα and IL1β (Mecha *et al.*, 2013). Iuvone and colleagues have shown that CBD decreases levels of Aβ-associated ROS and lipid peroxidation *in vitro* in PC12 cells and *in vivo* (Iuvone *et al.*, 2004). Neuroprotective effects of CBD have been further demonstrated in the PC12 rat cell line, stimulation with Aβ resulted in significant increase in nitrite production which was attenuated by CBD decreasing levels of p38 MAPK and NF-κB which are involved in the oxidative stress response (Esposito *et al.*, 2006). An expansion of this study found that CBD exerts anti-inflammatory actions in a mouse model of AD neuroinflammation induced by Aβ injection into the hippocampus. In a dose-dependent manner, CBD attenuated *GFAP* mRNA expression, iNOS and IL1β protein expression, and NO and IL1β release (Esposito *et al.*,

2007). More recently, CBD has been demonstrated to attenuate microglial activation in both *in vitro* and *in vivo* models of AD (Martin-Moreno *et al.*, 2011).

The bulk of the literature pertaining to the anti-inflammatory and immunosuppressive effects of CBD have utilised rodent models of peripheral and CNS inflammatory disorders, showing promising results in neurodegenerative and neuroinflammatory settings. Therefore it is of interest to examine the effect of CBD on human astrocytes. Given that CBD readily crosses the BBB to enter the CNS, it will be important to examine its effects on quiescent astrocytes, and furthermore examine whether it is capable of modulating reactivity in astrocytes following inflammatory insult.

5.1.7 Aims

While there is currently an abundance of literature pertaining to the neuroprotective role of FGF2 in rodents, there is limited literature supporting this role translates into the human CNS.

Human iPSC provide a valuable model system for the investigation of the effect neuroprotective agents on human cells, therefore the objectives of this chapter can be separated into two primary aims:

1. To investigate the ability of FGF2 to modulate human iPSC-derived astrocyte reactivity,
2. To trial CBD as a potential agent capable of modulating reactivity in human iPSC-derived astrocytes.

The hypothesis pertaining to these aims are that FGF2 and CBD will be capable of modulating astrocyte reactivity. It is expected that FGF2 will reduce expression of reactive astrocyte markers, and CBD will reduce expression of pro-inflammatory and immune related reactivity markers, e.g. *IL1β*, *ICAM1*, and *CXCL10*.

5.2 Materials and Methods

5.2.1 Cell lines

Human iPSC homozygous for APOE3 and APOE4 were used in this study to generate astrocytes and subsequently reactive astrocytes.

5.2.2 Astrocyte progenitor cell culture and terminal differentiation

Human *E3E3* and *E4E4* iPSC were patterned towards a neural fate and subsequently differentiated along a glial lineage as described in sections 3.2.3 and 3.2.5.

5.2.3 Astrocyte stimulation to examine the effect of FGF2 on astrocyte reactivity

Astrocytes were stimulated with inflammatory microglial factors IL1α (3 ng/mL), TNFα (30 ng/mL) and C1q (400 ng/mL) for 24 h, as per Liddelow *et al*., 2017 in order to induce reactivity. A 10-factor dilution of these concentrations was also used; IL1α (0.3 ng/mL), TNFα (3 ng/mL) and C1q (40 ng/mL). These treatments are denoted as "Factors High" and "Factors Low" where appropriate. Astrocytes were treated with FGF2 (50 ng/mL; PeproTech, UK) alone and in combination with both concentrations of factors for 24 h in order to assess its ability to modulate the astrocyte response to inflammatory insult (Figure 5.2.1). Post stimulation, media was collected and stored at -20˚C. Cells were prepared for qPCR (Section 2.4.1 – main methods).

FGF2 concentration was chosen based on that used by Roybon *et al*. They found that 50 ng/mL of FGF2 aided in the maturation of quiescent astrocytes in their astrocyte differentiation protocol (Roybon *et al.*, 2013).

5.2.4 Astrocyte stimulation to examine the effect of CBD on astrocyte reactivity

Astrocytes were stimulated with inflammatory cytokines IL1α (0.3 ng/mL) and TNFα (3 ng/mL) and treated with CBD (0.1, 1, 5 and 10 μM; Tocris, UK) for 24 h (Figure 5.2.1). Cytokines were chosen because they have previously been shown to induce a reactive phenotype in astrocytes, and CBD has been shown to counteract the effect of these inflammatory mediators in other cell types (Khaksar & Bigdeli, 2017; Chiricosta *et al.*, 2019). A range of CBD concentrations were chosen to trial as per the literature (Petrosino

et al., 2018; Fitzpatrick *et al.*, 2020). Post stimulation, media was collected and stored at -20˚C. Cells were prepared for qPCR (Section 2.4 – main methods).

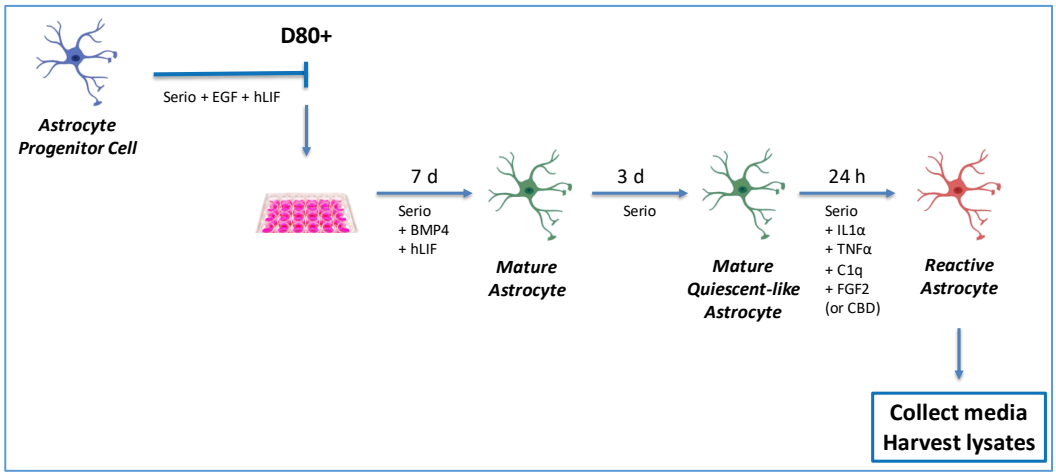


Figure 5.2.1. Experimental timeline to test the effect of immunomodulatory agents on astrocyte reactivity.

Astrocyte progenitor cells were expanded in Serio media supplemented with EGF and hLIF. From D80 APC were plated and terminally differentiated for 7 d, followed by 3 d in Serio media without factors to ensure a quiescent-like astrocyte at time of stimulation. Astrocytes were stimulated for 24 h in order to generate a reactive astrocyte and assess the ability of FGF2 or CBD to modulate reactivity. Media and lysates were harvested to examine the reactive astrocyte profile.

5.2.5 Analysis of astrocyte reactivity by qPCR

mRNA was isolated from human cortical astrocyte lysates. Total mRNA was reverse transcribed into cDNA. The expression of 10 genes (*ICAM1*, *IL1β*, *LCN2*, *PTX3*, *C3*, *CXCL10*, *GFAP*, *SERPINA3*, *VIM* and *IL6*) was assessed by qPCR (Table 5.2.1). Gene expression concentrations were analysed using the comparative Ct method. The target genes from each sample were compared with GAPDH, which acted as an endogenous control. The Ct values of each target gene and control gene were compared and expressed as a ratio known as RQ. The full qPCR protocol is described in detail in the main methods section of this thesis (Section 2.4.1).

Gene	Cat No.	Gene Code
C3	4453320	Hs00163811_m1
CXCL10	4453320	Hs00171042_m1
GFAP	4453320	Hs00909233_m1
ICAM1	4453320	Hs00164932_m1
IL1B	4453320	Hs01555410_m1
IL6	4453320	Hs00174131_m1
LCN2	4453320	Hs01008571_m1
PTX3	4453320	Hs00173615_m1
SERPINA3	4453320	Hs00153674_m1
VIM	4448892	Hs00958111_m1

Table 5.2.1. Target genes used for qPCR analysis of E4E4 astrocyte reactivity profile.

5.2.6 Analysis of astrocyte reactivity by ELISA

The levels of IL6 secretion in human cortical astrocytes was determined via ELISA in order to assess whether or not FGF2 (or CBD) had an effect on IL6 protein secretion following administration of an inflammatory signal. The full ELISA protocol is described in detail in the main methods section of this thesis (Section 2.5.1).

5.2.7 Statistical analysis

Data is expressed as mean ± SEM. At least three neural induction and astrocyte differentiations (N) were performed per iPSC line. 'n' values denote experimental or biological replicates and are representative of different thaws or passage numbers, while 'reps' denotes technical replicates within each experimental group, i.e. cells from the same plate but separate wells.

Two-way ANOVA was used for statistical analysis of the effect of factors and FGF2 on astrocytes, followed by Bonferroni *post hoc* if significance was inferred. One-way ANOVA was used to assess the effect of two concentrations of CBD on basal reactivity in astrocytes, with Newman-Keuls *post hoc* if significance was inferred. One-way ANOVA was used to determine whether CBD at four concentrations significantly attenuated inflammatory cytokine induced reactivity in astrocytes, with Tukey *post hoc*. Significance was set at $p < 0.05$. Statistical analysis was performed using GraphPad Prism 8 (GraphPad Software).

5.3 Results

Part 1 – Effect of FGF2 on astrocyte reactivity

Recently FGF2 was demonstrated to reduce astrocyte reactivity and redirect mature astrocytes towards a more quiescent phenotype (Roybon *et al.*, 2013). If FGF2 was capable of maintaining a quiescent phenotype in astrocytes following inflammatory insult, this could be extremely beneficial for modulating reactive astrogliosis in neurodegenerative diseases such as AD. FGF2 (50 ng/mL) was administered alone or in combination with microglial factors at both a high (3 ng/mL of IL1α, 30 ng/mL of TNFα and 400 ng/mL of C1q) and low concentration (0.3 ng/mL of IL1α, 3 ng/mL of TNFα and 40 ng/mL of C1q) to investigate whether is attenuate expression of reactive astrocyte markers in *E3E3* and *E4E4* astrocytes.

5.3.1 FGF2 does not alter IL6 secretion and expression in *E3E3* astrocytes

IL6 is regarded as the primary cytokine secreted by astrocytes in response to injury, disease or stress, and is significantly up-regulated in our reactive astrocyte model, therefore a therapeutic treatment that would reduce both its expression and secretion would be extremely beneficial for CNS disorders. To explore the effects of FGF2 on IL6 expression and secretion in reactive astrocytes, human cortical *E3E3* astrocytes were stimulated ± inflammatory microglial factors and ± FGF2.

FGF2 had no significant effect on the factors induced expression of *IL6* (Figure 5.3.1. A). Similarly, the significant increase in IL6 secretion as a result of stimulation ($p < 0.01$) was not attenuated by FGF2 (Figure 5.3.1. B). FGF2 did however tend to decrease *IL6* expression and secretion, therefore warranting further investigation into the potential modulatory effects of this growth factor.

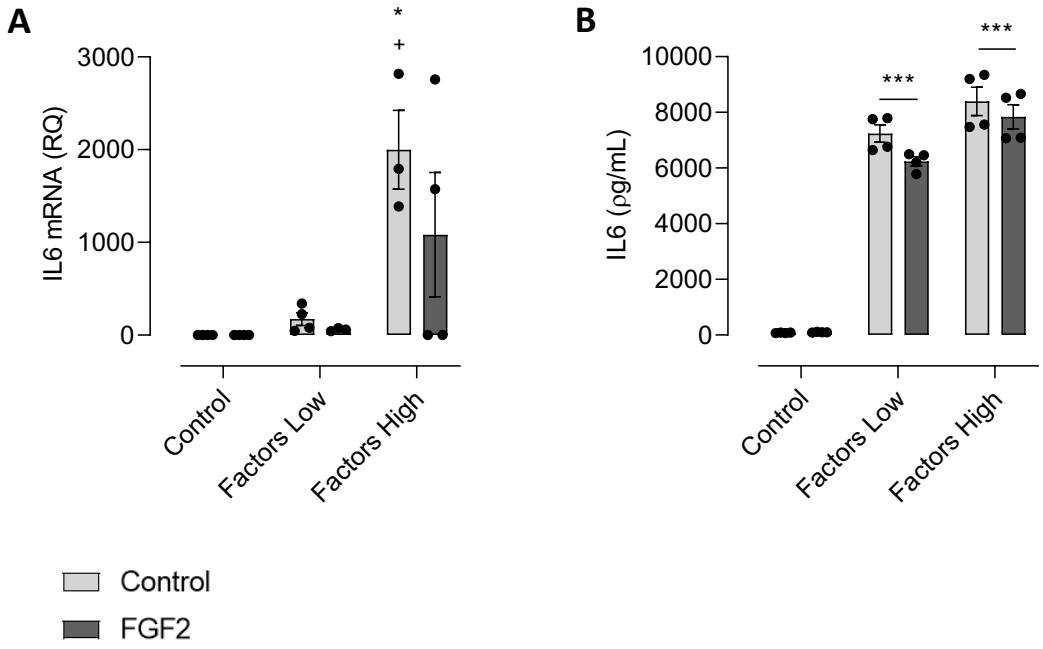


Figure 5.3.1. FGF2 does not significantly attenuate the microglial factors induced expression and secretion of IL6 in E3E3 astrocytes.

*FGF2 does not affect the inflammatory microglial factors induced expression (A) and secretion (B) of IL6. Data expressed as mean ± SEM (N=3, n=3-4). * $p < 0.05$, *** $p < 0.001$ vs control; $^{+}$ $p < 0.05$ vs factors low. IL6 mRNA effect of factors $F(2, 16) = 12.78$, $p = 0.0005$; effect of FGF2 $F(1, 16) = 1.556$, $p = 0.2302$; interaction effect $F(2, 16) = 1.088$, $p = 0.3605$. IL6 secretion effect of factors $F(2, 18) = 386.3$, $p = < 0.0001$; effect of FGF2 $F(1, 18) = 4.140$, $p = 0.0569$; interaction effect $F(2, 18) = 1.381$, $p = 0.2768$ (Two-Way ANOVA with Bonferroni post hoc).*

5.3.2 FGF2 significantly attenuates the microglial factors induced expression of reactive astrocyte markers in *E3E3* astrocytes

To explore the effects of FGF2 on astrocyte reactivity, human cortical *E3E3* astrocytes were stimulated ± inflammatory microglial factors and ± FGF2. The reactive astrocyte gene expression profile was used as an indicator of any modulatory effect of FGF2.

Consistent with results previously presented, inflammatory microglial factors IL1α, TNFα and C1q significantly increased mRNA expression of a number of reactivity markers, including *CXCL10*, *LCN2*, *ICAM1 IL1β* and *PTX3*. FGF2 significantly attenuated this microglial factor induced increase in mRNA expression of *CXCL10* ($p < 0.001$), *LCN2* ($p < 0.001$), *ICAM1* ($p < 0.05$), *SERPINA3* ($p < 0.01$) and *C3* ($p < 0.001$) (Figure 5.3.2. A-E). FGF2 also significantly decreased basal mRNA expression of *GFAP* ($p < 0.001$, Figure 5.3.2. F). The remaining inflammatory markers assessed, *IL1β*, *PTX3* and *VIM*, were unaffected by FGF2, although the attenuation of *PTX3* almost reached significance ($p = 0.06$) (Figure 5.3.3).

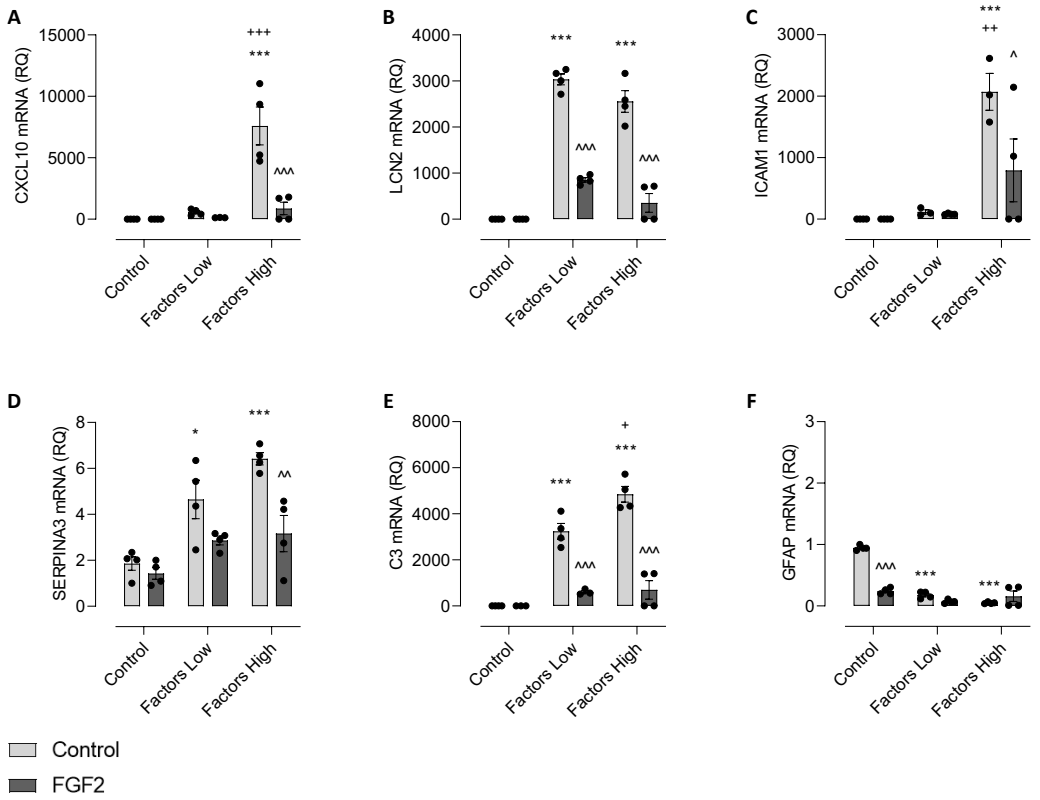


Figure 5.3.2. FGF2 significantly attenuates the microglial factors induced expression of reactive astrocyte markers in E3E3 astrocytes.

*FGF2 significantly attenuates the microglial factors induced expression of CXCL10 (A), LCN2 (B), ICAM1 (C), SERPINA3 (D) and C3 (E). FGF2 significantly decreases basal expression of GFAP (F). Data expressed as mean ± SEM (N=3, n=3-4). * p < 0.05, *** p < 0.001 vs control; $^{+}$ p < 0.05, $^{++}$ p < 0.01, $^{+++}$ p < 0.001 vs factors low; ^ p < 0.05, ^^ p < 0.01, ^^^ p < 0.001 vs without FGF2. CXCL10 mRNA effect of factors F(2, 17) = 23.04, p = < 0.0001; effect of FGF2 F(1, 17) = 17.13, p = 0.0007; interaction effect F(2, 17) = 14.72, p = 0.0002. LCN2 mRNA effect of factors F(2, 18) = 107.7, p = < 0.0001; effect of FGF2 F(1, 18) = 168.8, p = < 0.0001; interaction effect F(2, 18) = 42.17, p < 0.0001. ICAM1 mRNA effect of factors F(2, 16) = 19.64, p = < 0.0001; effect of FGF2 F(1, 16) = 4.510, p = 0.0496; interaction effect F(2, 16) = 4.067, p = 0.0373. SERPINA3 mRNA effect of factors F(2, 18) = 19.52, p = < 0.0001; effect of FGF2 F(1, 18) = 19.52, p = < 0.0001; interaction effect F(2, 18) = 3.783, p = 0.0425. C3 mRNA effect of factors F(2, 16) = 49.42, p = < 0.0001; effect of FGF2 F(1, 16) = 93.48, p = < 0.0001; interaction effect F(2, 16) = 27.17, p = < 0.0001. GFAP mRNA effect of factors F(2, 18) = 98.48, p = < 0.0001; effect of FGF2 F(1, 18) = 52.95, p = < 0.0001; interaction effect F(2, 18) = 56.93, p = < 0.0001 (Two-Way ANOVA with Bonferroni post hoc).*

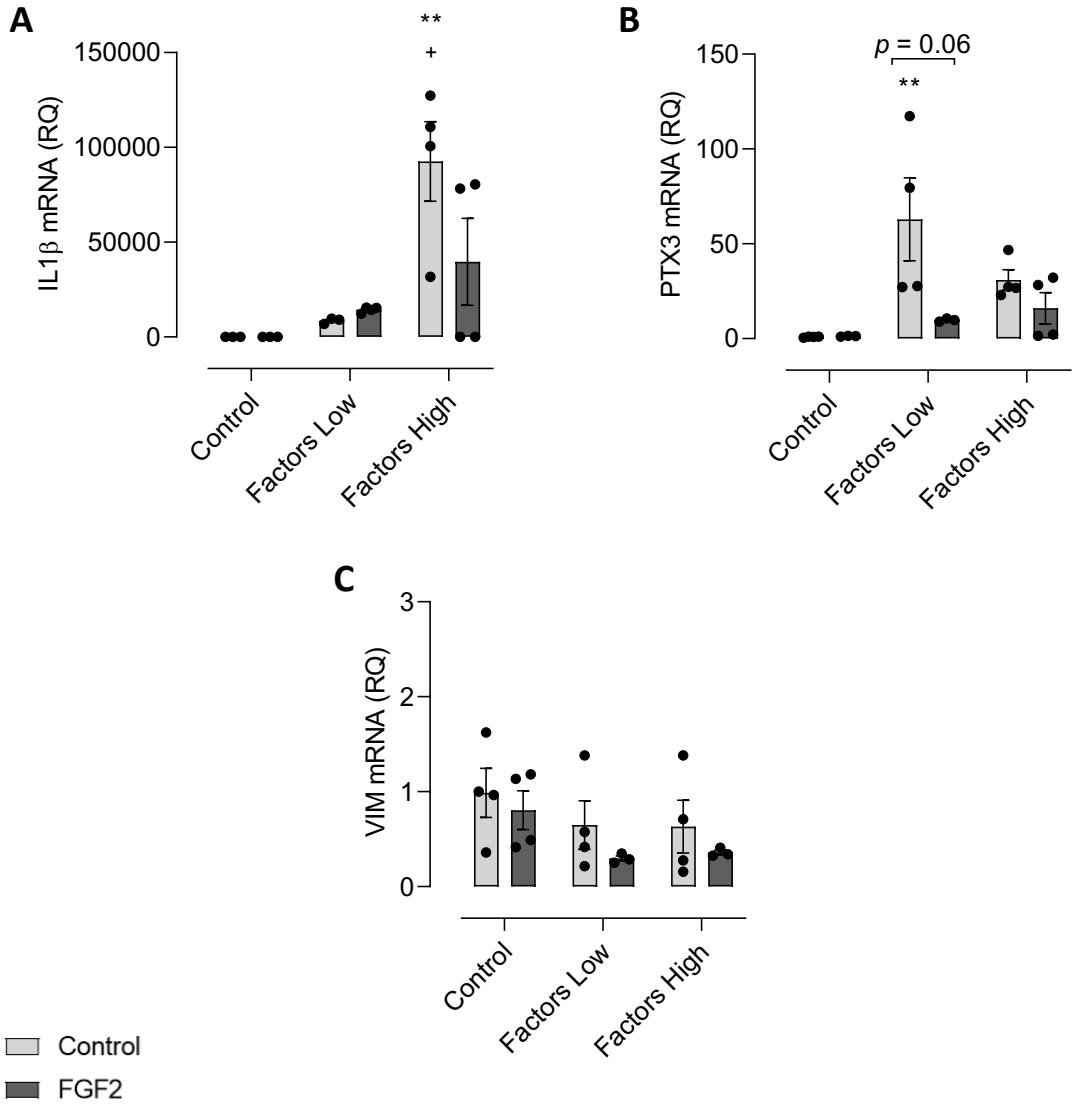


Figure 5.3.3. FGF2 does not affect mRNA expression of inflammatory astrocyte markers IL1β, PTX3 and VIM in E3E3 astrocytes.

*FGF2 does not affect the inflammatory microglial factors induced mRNA expression of IL1β (A) and PTX3 (B). FGF2 has no effect on VIM mRNA expression (C). Data expressed as mean ± SEM (N=3, n=3-4). ** $p < 0.01$ vs control; $^{+}$ $p < 0.05$ vs factors low. IL1β mRNA effect of factors $F(2, 15) = 11.74$, $p = < 0.0009$; effect of FGF2 $F(1, 15) = 1.636$, $p = 0.2202$; interaction effect $F(2, 15) = 2.512$, $p = 0.1146$. PTX3 mRNA effect of factors $F(2, 16) = 5.076$, $p = 0.0196$; effect of FGF2 $F(1, 16) = 6.371$, $p = 0.0226$; interaction effect $F(2, 16) = 3.037$, $p = 0.0762$. VIM mRNA effect of factors $F(2, 16) = 2.284$, $p = 0.1341$; effect of FGF2 $F(1, 16) = 2.075$, $p = 0.1690$; interaction effect $F(2, 16) = 0.07107$, $p = 0.9317$ (Two-Way ANOVA with Bonferroni post hoc).*

5.3.3 FGF2 significantly attenuates the microglial factors induced expression of reactive astrocyte markers in *E4E4* astrocytes

To further explore the effects of FGF2 on IL6 in reactive astrocytes, human cortical *E4E4* astrocytes were stimulated ± inflammatory microglial factors and ± FGF2. FGF2 exacerbated the increase in *IL6* mRNA expression following stimulation with inflammatory microglial factors at a high dose ($p < 0.01$; Figure 5.3.1. A). As with *E3E3* astrocytes, the significant increase in IL6 secretion as a result of stimulation ($p < 0.01$) was not attenuated by FGF2 (Figure 5.3.4. B).

FGF2 had no effect on *ICAM1* mRNA expression in *E4E4* astrocytes (Figure 5.3.4. C) but resulted in significantly increased *IL1β* mRNA expression following inflammatory insult compared to stimulation alone ($p < 0.001$; Figure 5.3.4. D). This may point to a synergistic interaction between FGF2 and IL1β, which interestingly was not the case in *E3E3* astrocytes.

Similar to the effects found in *E3E3* astrocytes, FGF2 significantly attenuated the microglial factor induced increase in mRNA expression of *CXCL10* ($p < 0.001$), *C3* ($p < 0.05$), *LCN2* ($p < 0.001$) and *PTX3* ($p < 0.001$) (Figure 5.3.5. A-D). FGF2 also significantly decreased basal expression of *GFAP* ($p < 0.001$, Figure 5.3.5. E).

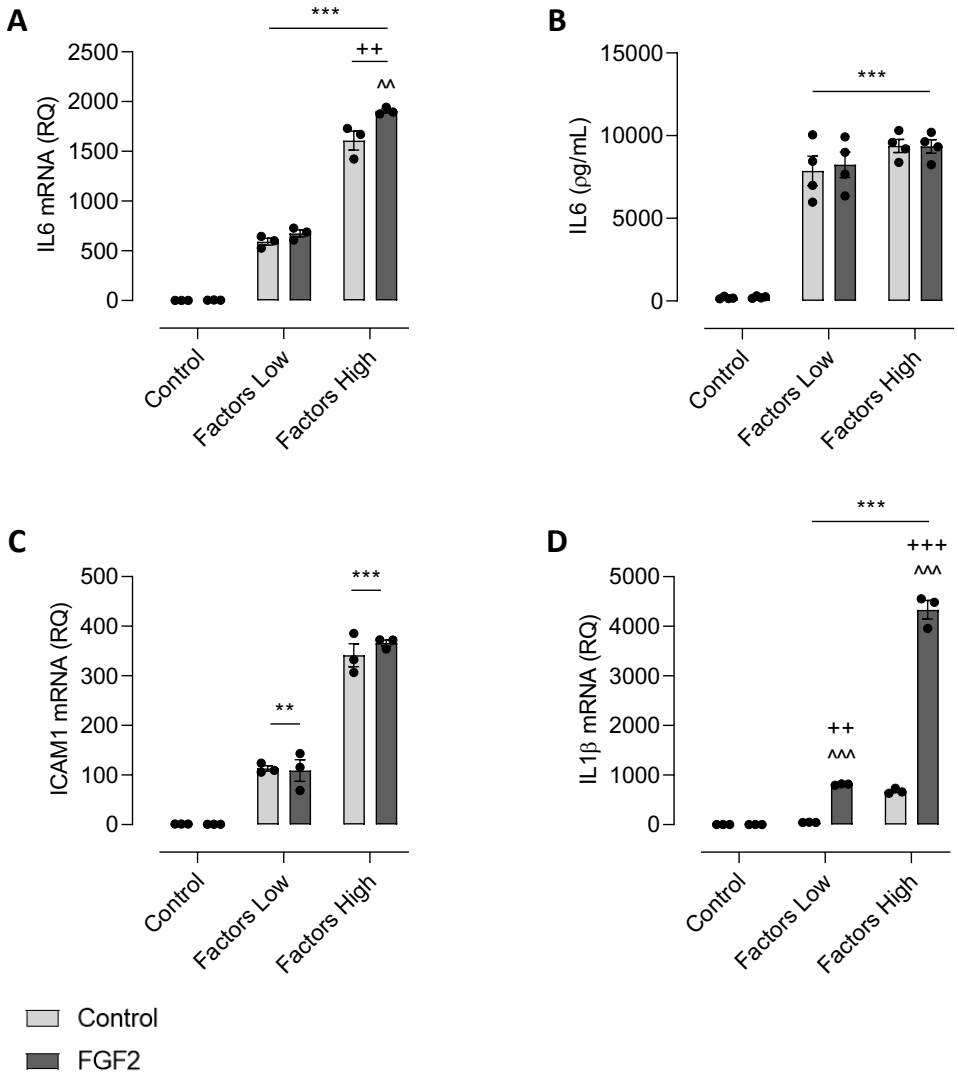


Figure 5.3.4. FGF2 significantly increases IL6 and IL1β mRNA expression in E4E4 reactive astrocytes.

*FGF2 significantly increases the IL6 mRNA response to stimulation with a high concentration of inflammatory microglial factors (A), but has no effect on IL6 secretion (B). FGF2 has no effect on ICAM1 mRNA expression (C). FGF2 affects IL1β expression in E4E4 astrocytes resulting in significantly increased expression in response to inflammatory insult (D). Data expressed as mean ± SEM (N=3, n=3). ** p < 0.01 vs control, *** p < 0.001; ++ p < 0.01, +++ p < 0.001 vs factors low; ^^ p < 0.01, ^^^ p < 0.001 vs without FGF2. IL6 mRNA effect of factors F(2, 12) = 805.9, p = < 0.0001; effect of FGF2 F(1, 12) = 12.59, p = 0.0040; interaction effect F(2, 12) = 5.879, p = 0.0166. IL6 secretion effect of factors F(2, 18) = 171.5, p = < 0.0001; effect of FGF2 F(1, 18) = 0.08824; p = 0.7698, interaction effect F(2, 18) = 0.07708, p = 0.9261. ICAM1 mRNA effect of factors F(2, 12) = 362.5, p = < 0.0001; effect of FGF2 F(1, 12) = 0.3643, p = 0.5574; interaction effect F2, 12) = 0.6693, p = 0.5302.IL1β mRNA effect of factors F(2, 12) = 592.8, p = < 0.0001; effect of FGF2 F(1, 12) = 538.7, p = < 0.0001; interaction effect F(2, 12) = 307.8, p = < 0.0001 (Two-way ANOVA with Bonferroni post hoc).*

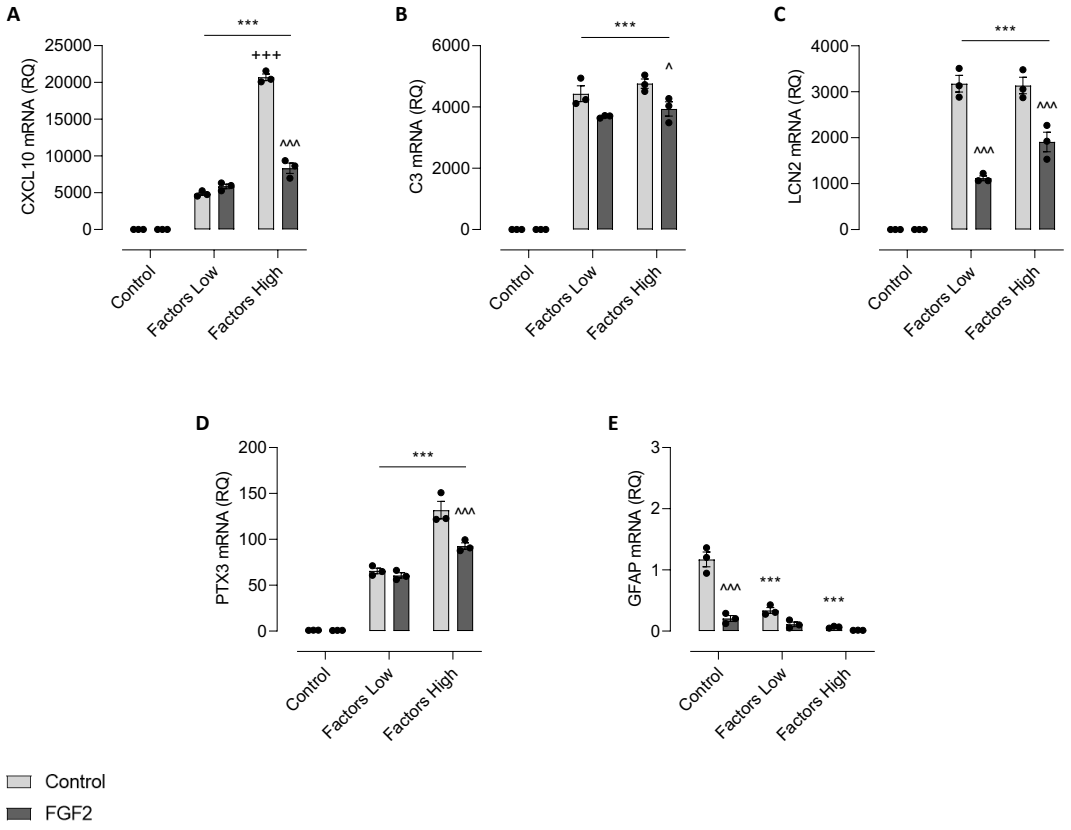


Figure 5.3.5. FGF2 significantly attenuates inflammatory microglial factor induced expression of reactivity markers CXCL10, C3, LCN2 and PTX3 in E4E4 astrocytes.

*FGF2 significantly decreases mRNA expression of CXCL10 (A), C3 (B), LCN2 (C), and PTX3 (D) following inflammatory insult. FGF2 significantly decreases control levels of GFAP mRNA expression (E) but has no effect on GFAP following stimulation with inflammatory microglial factors. Data expressed as mean ± SEM (N=3, n=3). *** p < 0.001 vs control; $^{+++}$ p < 0.001 vs factors low; ^ p < 0.05, ^^ p < 0.01, ^^^ p < 0.001 vs without FGF2. CXCL10 mRNA effect of factors F(2, 12) = 767.9, p = < 0.0001; effect of FGF2 F(1, 12) = 153.5, p = < 0.0001; interaction effect F2, 12) = 197.7, p = < 0.0001. C3 mRNA effect of factors F(2, 12) = 489.0, p = < 0.0001; effect of FGF2 F(1, 12) = 17.07, p = 0.0014; interaction effect F(2, 12) = 4.292, p = 0.0393. LCN2 mRNA effect of factors F(2, 12) = 195.3, p = < 0.0001; effect of FGF2 F(1, 12) = 95.19, p = < 0.0001; interaction effect F(2, 12) = 28.28, p = < 0.0001. PTX3 mRNA effect of factors F(2, 12) = 308.8, p = < 0.0001; effect of FGF2 F(1, 12) = 16.11, p = 0.0017; interaction effect F(2, 12) = 11.21, p = 0.0018. GFAP mRNA effect of factors F(2, 12) = 64.87, p = < 0.0001; effect of FGF2 F(1, 12) = 74.58, p = < 0.0001; interaction effect F(2, 12) = 34.02, p = < 0.0001 (Two-way ANOVA with Bonferroni post hoc).*

Part 2 – Effect of CBD on astrocyte reactivity

CBD has been shown to modulate inflammation with respect to immune cells of the periphery, is approved as a treatment for spasticity in the inflammatory disorder MS, and currently under investigation for further potential therapeutic uses. As a lipophilic compound CBD readily crosses the BBB and as such is likely to evoke effects on cells of the CNS. With this in mind it was postulated that CBD may be capable of modulating reactivity in astrocytes following inflammatory insult and thereby present viable therapeutic potential for modulating neuroinflammation. The ability of CBD (0.1, 1, 5 and 10 µM) to modulate astrocyte reactivity was investigated in iPSC-derived astrocytes in their quiescent-like state as well as following inflammatory insult with cytokines IL1α (0.3 ng/mL) and TNFα (3 ng/mL).

5.3.4 CBD has varied effects on astrocyte basal reactivity

It was first established whether CBD had any effect on basal reactivity in iPSC-derived astrocytes. CBD marginally increased *IL6* mRNA expression although marginally decreased IL6 secretion (Figure 5.3.6. A, B). CBD had no significant effect on *IL1β*, *C3* or *CXCL10* mRNA expression although CBD tended to decrease *IL1β* mRNA expression at a dose of 10 µM, and *CXCL10* mRNA expression at a dose of 5 µM (Figure 5.3.6. C-E). CBD significantly decreases basal *GFAP* mRNA expression ($p < 0.05$) at a dose of 10 µM (Figure 5.3.6. F). Taken together this data indicates that CBD does not significantly affect basal reactivity in astrocytes but if anything marginally reduces expression of reactive astrocyte markers. However, CBD significantly increased mRNA expression of *LCN2* ($p < 0.001$), *ICAM1* ($p < 0.05$) and *PTX3* ($p < 0.001$) at both doses and 10 µM respectively (Figure 5.3.6. G-I). This indicates that CBD might increase reactivity in human iPSC-derived astrocytes.

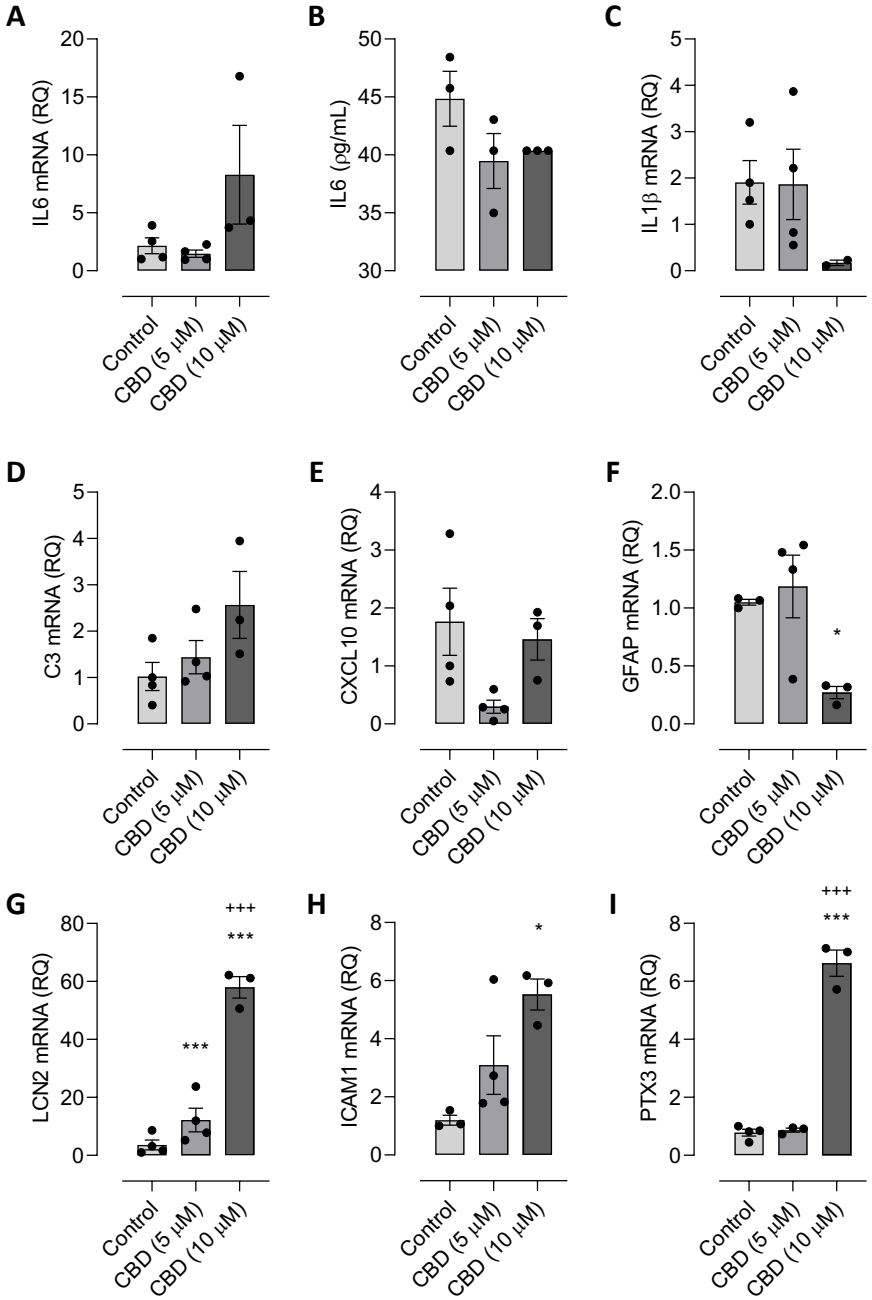


Figure 5.3.6. Effect of CBD on baseline reactivity in iPSC-derived astrocytes.

*CBD does not affect basal mRNA expression (A) or secretion (B) of IL6. CBD does not affect basal mRNA expression IL1β (C), C3 (D) and CXCL10 (E). CBD decreases basal GFAP mRNA expression at a dose of 10 μM. CBD increases basal mRNA expression of LCN2 (G) at 5 and 10 μM, and ICAM1 (H) and PTX3 (I) at 10 μM. Data expressed as mean ± SEM (N=3, n=3-4). * $p < 0.05$, *** $p < 0.001$ vs control; $^{+++}$ $p < 0.001$ vs CBD (5 μM). IL6 mRNA $F(2, 8) = 3.191$, $p = 0.0597$; IL6 secretion $F(2, 6) = 2.214$, $p = 0.1904$; IL1β $F(2, 7) = 1.720$, $p = 0.2469$; C3 $F(2, 8) = 2.960$, $p = 0.1091$; CXCL10 $F(2, 8) = 3.799$, $p = 0.0692$; GFAP $F(2, 7) = 6.151$, $p = 0.0287$; LCN2 $F(2, 8) = 70.34$, $p = < 0.0001$; ICAM1 $F(2, 7) = 7.021$, $p = 0.0212$; PTX3 $F(2, 7) = 174.9$, $p = < 0.0001$ (One-way ANOVA with Newman-Keuls post hoc).*

5.3.5 CBD tends to reduce astrocyte reactivity following inflammatory insult

After establishing that CBD had an effect on basal reactivity in human astrocytes, particularly at the higher dose of 10 µM, it was next determined whether CBD was capable of modulating astrocyte response to inflammatory insult. Inflammatory insult was delivered via cytokines IL1α (0.3 ng/mL) and TNFα (3 ng/mL), the effects of which CBD has previously been shown to counteract in human mesenchymal stem cells and a mouse model of MS (Khaksar & Bigdeli, 2017; Chiricosta *et al.*, 2019). CBD was trialled at four doses; 0.1, 1, 5 and 10 µM.

Inflammatory cytokines induced a significant increase in *IL6* mRNA expression ($p < 0.05$) and IL6 secretion ($p < 0.001$), and CBD significantly attenuated this increase in IL6 secretion ($p < 0.001$) at a dose of 10 µM (Figure 5.3.7. A, B). Inflammatory cytokines significantly induced *CXCL10* ($p < 0.05$) and *C3* ($p < 0.01$) mRNA expression which tended to be attenuated by CBD in a dose dependent manner (Figure 5.3.7. C, D). Inflammatory cytokines significantly induced mRNA expression of *LCN2* ($p < 0.01$), *ICAM1* ($p < 0.05$), and *PTX3* ($p < 0.001$). While CBD tended to attenuate *LCN2* the effect was not significant and CBD had no effect on *ICAM1* or *PTX3* mRNA expression (Figure 5.3.8). Stimulation with inflammatory factors significantly decreased *GFAP* mRNA expression ($p < 0.001$), while CBD had no significant effect it tended to further decrease *GFAP* mRNA expression at a dose of 10 µM (Figure 5.3.9. A). Inflammatory factors tend to increase *IL1β* mRNA expression but not significantly, CBD had no effect (Figure 5.3.9. B). Taken together this data provides some preliminary insights into the effect of CBD on astrocytes and their reactivity state.

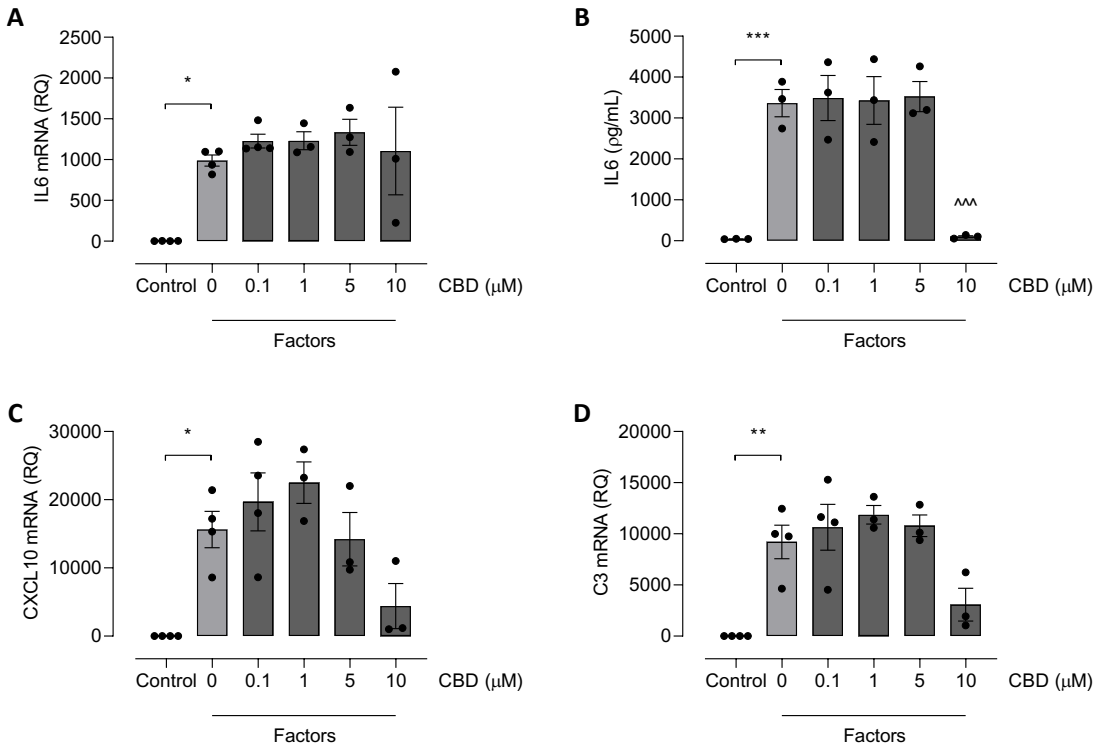


Figure 5.3.7. CBD tends to decrease reactive markers IL6, CXCL10 and C3 in iPSC-derived reactive astrocytes.

*Inflammatory factors significantly increase mRNA expression and secretion of IL6. CBD has no significant effect on IL6 mRNA (A), but IL6 secretion is attenuated by CBD at 10 μM (B). Inflammatory factors significantly increase mRNA expression of CXCL10 (C) and C3 (D) but CBD has no significant effect. Data expressed as mean ± SEM (N=3, n=3-4). * $p < 0.05$, ** $p < 0.01$, *** $p < 0.001$ vs control; ^^^ $p < 0.001$ vs stimulation with factors only. IL6 mRNA $F(5, 15) = 6.665$, $p = 0.0019$; IL6 secretion $F(5, 12) = 20.51$, $p = < 0.0001$; CXCL10 $F(5, 15) = 7.992$, $p = 0.0008$; C3 $F(5, 15) = 10.68$, $p = 0.0002$ (One-way ANOVA with Tukey post hoc).*

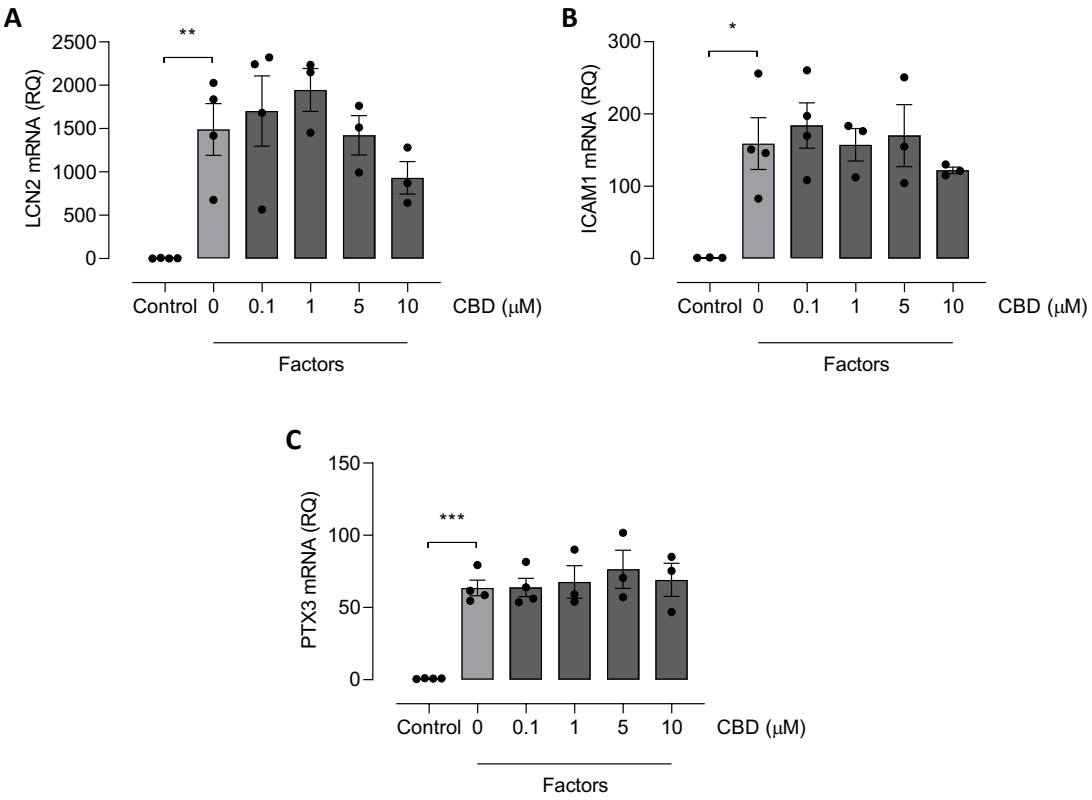


Figure 5.3.8. CBD does not affect mRNA expression of reactive markers LCN2, ICAM1 and PTX3 in iPSC-derived reactive astrocytes.

*Inflammatory factors significantly increase mRNA expression of LCN2 (A), ICAM1 (B) and PTX3 (C) while CBD has no effect. Data expressed as mean ± SEM (N=3, n=3-4). * p < 0.05, ** p < 0.01, *** p < 0.001 vs control. LCN2 F(5, 15) = 6.953, p = 0.0015; ICAM1 F(5, 14) = 4.803, p = 0.0091; PTX3 F(5, 15) = 12.94, p = < 0.0001 (One-way ANOVA with Tukey post hoc).*

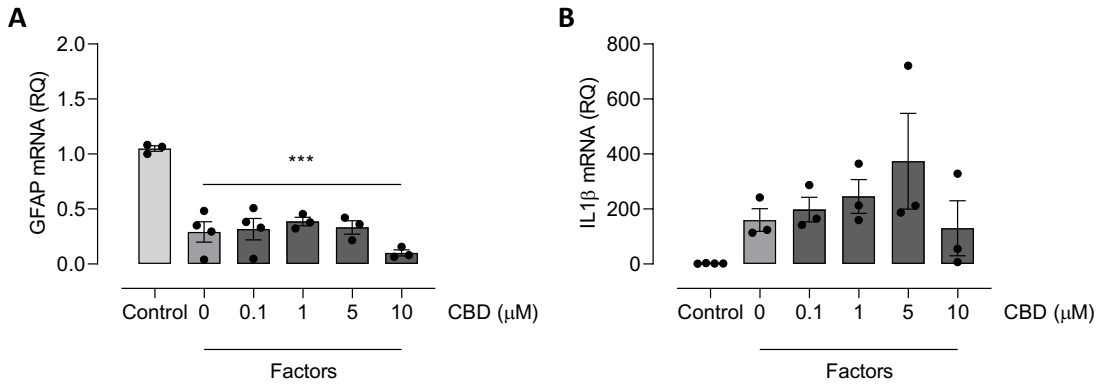


Figure 5.3.9. CBD does not affect mRNA expression of reactive markers GFAP and IL1β in iPSC-derived reactive astrocytes.

*Stimulation with inflammatory factors significantly decreased GFAP mRNA expression while CBD had no significant effect (A). Inflammatory factors tend to increase IL1β mRNA expression but not significantly, CBD had no effect (B). Data expressed as mean ± SEM (N=3, n=3-4). *** p < 0.001 vs control. GFAP F(5, 14) = 17.62, p = < 0.0001; IL1β F(5, 13) = 2.369, p = 0.0976 (One-way ANOVA with Tukey post hoc).*

5.4 Discussion

Reactivity in astrocytes was previously characterised in terms of protein secretion, gene expression and morphology changes. It was further demonstrated that reactive astrocytes are detrimental to neurons via a conditioned media study and that APOE genotype might predispose astrocytes to becoming reactive following inflammatory insult. Following on from this, it was the objective of this study to investigate a number of potential immunomodulatory agents on reactivity in iPSC-derived *E3E3* and *E4E4* astrocytes.

FGF2 was chosen as it has previously be used in astrocyte maturation protocols to generate mature quiescent astrocytes (Roybon *et al.*, 2013) and has been demonstrated to supress reactive astrogliosis (Kang *et al.*, 2014b). FGF2 is endogenously produced within the CNS and has important roles in neural development, however importantly it has been demonstrated that exogenous FGF2 is capable of crossing the BBB (Deguchi *et al.*, 2000).

CBD was also investigated due to the abundance of literature pertaining to its anti-inflammatory effects. Given that CBD and other cannabinoids are readily available as treatments for MS (Fitzpatrick & Downer, 2017), and have shown promise in models of inflammatory disorders (Ceprian *et al.*, 2017; Al-Ghezi *et al.*, 2019), we were interested to determine whether their anti-inflammatory effect extended to astrocytes in a neurodegeneration model.

5.4.1 FGF2 holds promise as a modulator of astrocyte reactivity

Several studies have demonstrated *in vitro* and *in vivo* that FGF2 has the ability to ameliorate astrocyte reactivity. Interesting research carried out by Kang and colleagues revealed that FGF signalling could suppress astrocyte activation in both the healthy and injured brain (Kang *et al.*, 2014b). This study revealed that FGF signalling was required in order to maintain astrocytes in a quiescent state in the unperturbed adult neocortex. It was further shown that FGF signalling delayed astrocyte response as well as aiding quick return to their resting state. Lastly, astrocytic FGF receptors were disrupted which resulted in decreased glial scar area without compromising neuronal survival (Kang *et al.*, 2014b). The FGF2-FGFR1 pathway has also been implicated as having inhibitory effects on astrocyte-regulated neuroinflammation caused by infrasound CNS injury (Shi *et al.*,

2018). As such FGF2 was selected to test as a potential modulator of astrocyte reactivity in our iPSC-derived reactive astrocyte model.

5.4.1.1 FGF2 has no effect on cytokine secretion

Pro-inflammatory cytokines have many roles, including attracting leukocytes to inflammation sites, stimulating leukocyte proliferation, inducing cytotoxicity, stimulating release of proteolytic enzymes and producing prostaglandins and secondary cytokines. Activated astrocytes, along with microglia, are the primary sources of cytokine production within the CNS (Singhal *et al.*, 2014), with IL6 considered the main astroglial cytokine (Van Wagoner & Benveniste, 1999). IL6 is considered both a pro- and anti-inflammatory cytokine as it plays a key role in both the homeostasis of neural tissue, acts as a neurotrophic factor for differentiating oligodendrocytes and regenerating peripheral nerves (Rothaug *et al.*, 2016), however is also involved in the pathogenesis of various inflammatory disorders including MS, PD and AD (Gonzalez-Reyes *et al.*, 2017; Green *et al.*, 2019; von Essen *et al.*, 2019). These pro- and anti-inflammatory characteristics of IL6 have been attributed to its signalling where classical signalling via the membrane bound IL6R is usually associated with anti-inflammatory processes important for bacterial defence, while trans-signalling occurs through the soluble IL6R and is associated with pro-inflammatory processes such as neurodegeneration (Rothaug *et al.*, 2016).

It was previously established that IL6 mRNA and protein expression is significantly increased in the presented model of reactive astrocytes. Therefore it was of interest to examine where FGF2 was capable of modulating this cytokine. The effect of FGF2 on astrocyte IL6 production and secretion was examined and it was found to have no effect at the mRNA or protein level. IL6 mRNA expression and protein secretion was significantly elevated upon stimulation with inflammatory microglial factors, but FGF2 failed to attenuate this response. FGF2 increased *IL6* mRNA expression in *E4E4* astrocytes when combined with a high dose of microglial factors, an effect which did not occur in *E3E3* astrocytes. A link between APOE and FGF has already been established in AD, where concurrent expression of *APOE4* and *FGF1* was linked to episodic memory impairment in AD patients (Chang *et al.*, 2019). It has also been reported that FGF1 up-regulates synthesis and secretion of APOE protein in cultured astrocytes following injury (Tada *et al.*, 2004; Ito *et al.*, 2005). It is interesting to find that a link between APOE4 and FGF2 might also exist in astrocytes in response to insult.

IL6 is downstream of numerous signalling cascades including the MyD88-dependent TLR4 signalling pathway (Nyati *et al.*, 2017; Zhang *et al.*, 2018a). It may well be the case that FGF2 acts independently from one or more these pathways and thus cannot alter IL6. This theory contradicts that of Ye and colleagues who showed a decrease in the expression of inflammatory cytokines IL6 and TNFα in rats following treatment with exogenous FGF2 via regulation of the upstream TLR4/NF-κB signalling pathway (Ye *et al.*, 2015). Interestingly, they found that low concentrations of FGF2 (10-50 ng/mL) induced activation of astrocytes while higher concentrations (100-200 ng/mL) attenuated astrocyte activation. The concentration of FGF2 used in the present study was 50 ng/mL which might explain the different results and furthermore the FGF2 induced increase in *IL6* mRNA.

FGF2 has previously been shown to modulate microglial activation. In an LPS-induced model of depression, exogenous FGF2 infusions counteracted the effect of LPS by decreasing levels of pro-inflammatory cytokines IL1β, IL6 and TNFα, and increasing levels of anti-inflammatory cytokine IL10 resulting in reversal of depressive-like behaviour in treated animals (Tang *et al.*, 2018). By inhibiting microglial activation, FGF2 may be in turn more effective at modulating astrocyte activation as reactive microglia have been shown to induce astrocyte activation (Liddelow *et al.*, 2017). A more complex model system utilising 3D-organoid structures with iPSC-derived microglia introduced to the system would allow for the study of the effect of FGF2 on microglia-astrocyte interactions.

While FGF2 failed to significantly attenuate IL6 expression and secretion in reactive astrocytes, analysis of expression of reactive astrocyte markers provided some interesting results.

5.4.1.2 FGF2 attenuates expression of reactive astrocyte genes

In this study, FGF2 significantly attenuated mRNA expression of *CXCL10*, *LCN2*, *ICAM1*, *SERPINA3* and *C3* in *E3E3* reactive astrocytes. This result followed through to the *E4E4* astrocytes with regards to *CXCL10*, *C3* and *LCN2*, and also included attenuation of *PTX3* expression. This data indicates that while FGF2 does not affect IL6 at the protein level, it still appears to have the ability to modulate astrocyte reactivity via other mechanisms.

CXCL10 mRNA expression was significantly up-regulated following inflammatory insult in *E3E3* and *E4E4* astrocytes, FGF2 treatment was able to subsequently decrease this up-regulation. Given the role of CXCL10 as a chemokine involved in the recruitment of T cells

into the CNS it follows that its expression would be increased after inflammatory insult. It has been shown that CXCL10 is strongly induced by INFγ and acts by binding to the G-protein coupled receptor CXCR3 (Koper *et al.*, 2018). In a study which aimed to investigate the potential use of cytokine patterns to differentiate CNS infections from other CNS disorders, it was discovered that CNS infections can be identified by significantly higher concentrations of CXCL10 in the CSF compared to non-infectious disorders (Fortuna *et al.*, 2018). Excessive levels of CXCL10 has also been linked to MS, as concentrations of CXCL10 and CXCR3 were found to be elevated in active MS lesion sites and actually co-localised with the lesions (Sorensen *et al.*, 2002). It is thought that CXCL10 may play a role in AD as CSF concentrations of the chemokine are significantly higher in AD patients, as well as in patients with mild-cognitive impairment, compared to the controls. For this reason it is hypothesised that it may be involved in early stages of AD when inflammation is elevated (Koper *et al.*, 2018).

FGF2 significantly attenuated the factor induced mRNA expression of *LCN2* in *E3E3* and *E4E4* reactive astrocytes. LCN2 is an acute phase protein with multiple functions, expressed and produced by reactive astrocytes in response to infection, inflammation or injury (Jha *et al.*, 2015). *LCN2*, along with *SERPINA3*, has been labelled a marker for reactive astrocytes in mouse (Zamanian *et al.*, 2012). In a study using transgenic rats, LCN2 was found to be an inducible factor released by reactive astrocytes and selectively neurotoxic towards neurons (Bi *et al.*, 2013). The authors concluded that during neuronal death and neurodegeneration, dying neurons communicate with and activate quiescent astrocytes resulting in astrocyte activation and secretion of LCN2 which acts as a potent neurotoxic mediator and further propagates neuronal death (Bi *et al.*, 2013). *LCN2* expression has been shown to be increased in various pathologies including cancer, neuroinflammatory conditions, neurodegeneration, brain injury and schizophrenia (Jha *et al.*, 2015). *LCN2* gene expression is thought to be regulated cooperatively by a network of different transcription factors including NF-κB and CCAAT/enhancer binding protein (Sunil *et al.*, 2007). The fact that FGF2 was able to significantly decrease expression of this reactivity gene in our reactive astrocyte model suggests a possibly promising role for FGF2 in the modulation of astrocyte reactivity.

When stimulated with inflammatory microglial factors *ICAM1* mRNA expression was significantly up-regulated and FGF2 treatment was able to significantly attenuate this up-regulation in *E3E3* astrocytes. Following injury, astrocytes have been shown to express many adhesion molecules, including ICAM1. ICAM1 is an immunoglobulin protein

expressed on the cell surface of leukocytes and endothelial cells (Pflugfelder *et al.*, 2017). ICAM1 can bind to leukocyte β-2 integrins as well as plasma fibrinogen and subsequently becomes activated (Turowski *et al.*, 2005). It is thought that adhesion molecules like ICAM1 may aid in astrocyte-lymphocyte communications and the recruitment of immune cells into the CNS (Liddelow & Hoyer, 2016). Many diseases such as MS, AD and PD have a neuroinflammatory component in their pathology which requires the migration of leukocytes from the blood, across the BBB into the neural parenchyma, a process in which ICAM1 plays a key role. As a result of this central role in leukocyte migration, ICAM1 is considered an attractive target for the development of anti-inflammatory drugs (Turowski *et al.*, 2005). Considering the effect FGF2 had on ICAM1 expression, this could lead to progressions in the production of drugs which target this gene.

SERPINA3 mRNA expression was significantly up-regulated following inflammatory insult with microglial factors in *E3E3* astrocytes and FGF2 significantly attenuated this response. SERPINA3 functions as a secreted peptidase inhibitor. Its expression has been shown to be up-regulated after inflammation and nerve injury (Gesase & Kiyama, 2007), as well as in neurodegenerative disorders including ALS (Fukada *et al.*, 2007). In a study carried out in the MCAO mouse model of ischaemic stroke and the LPS mouse model of neuroinflammation, SERPINA3 was identified as a marker of early phase reactive astrogliosis (Zamanian *et al.*, 2012). A role for SERPINA3 has also been implicated in tumour progression as the cytokine has been found to be overexpressed in many different tumour types (Li *et al.*, 2018). *SERPINA3* expression has been shown to strongly correlate with glioma invasion and may play a role in the initiation or progression of these common brain tumours (Li *et al.*, 2018).

Complement component C3 is the pivotal protein in the complement cascade which plays a major role in the immune system. C3 carries out many immunological roles including triggering phagocytosis or cell lysis (Shi *et al.*, 2017a), however abnormal initiation of the complement system has been shown to contribute to some CNS disorders. An example of this may be complement overexpression, which has been linked to AD, HD and acute brain injury. C3 concentrations in CSF functions as a stage-biomarker of AD (Nitkiewicz *et al.*, 2017). It has also been shown, using mouse models of AD, that C3 released from astrocytes binds to microglial C3a receptors in order to modulate neuroinflammation and β-amyloid pathology, which ultimately contributes to disrupting cognitive function in AD (Lian *et al.*, 2016). In a 2017 study using C3 as a marker for reactive astrogliosis, $C3^+$ immunostaining was found in post-mortem brain slices from patients with the

neurodegenerative disorders AD, PD, HD and ALS (Liddelow *et al.*, 2017). The ability of FGF2 to attenuate C3 expression following stimulation with inflammatory factors highlights the potential of FGF2 to modulate astrocyte reactivity.

PTX3 is an acute phase protein which has both neuroprotective and detrimental effects in CNS disorders (Rajkovic *et al.*, 2016). PTX3 is undetectable in the brain under normal physiological conditions but becomes significantly up-regulated in neuropathology and the precise role of PTX3 in the CNS is still largely unknown (Rajkovic *et al.*, 2016). It has been uncovered that reactive astrocytes are the primary source of PTX3 in the brain (Polentarutti *et al.*, 2000), therefore it is considered a potential marker for reactive astrogliosis (Zamanian *et al.*, 2012). A link has previously been investigated between PTX3 and FGF2 in the context of cancer therapy which identified PTX3 as a potential therapeutic. PTX3 was shown to inhibit angiogenesis and tumorigenesis by interfering with FGF2 which promotes these processes in cancers (Ronca *et al.*, 2015). It is interesting that in the context of our reactive astrocyte model, FGF2 down-regulates *PTX3* mRNA expression and thus appears to have an anti-inflammatory effect.

Interestingly, FGF2 tended to decrease *IL1β* mRNA expression in *E3E3* astrocytes but further increased *IL1β* mRNA expression in *E4E4* astrocytes when in conjunction with microglial factors. IL1β was successfully up-regulated following stimulation with microglial factors but FGF2-treatment was unsuccessful in significantly decreasing this pro-inflammatory cytokine, in fact FGF2 further increased levels of *IL1β* expressed by *E4E4* reactive astrocytes. IL1β is a pro-inflammatory cytokine which has been implicated in numerous CNS diseases, including traumatic brain injury, and neurodegenerative diseases such as MS and AD (Licastro *et al.*, 2000). IL1β has already been identified as a promising therapeutic target for neuroinflammatory conditions ranging from neurodegenerative diseases to traumatic brain injury and diabetic retinopathy (DR) following promising blockade of IL1β in DR patients with canakinumab, an IgG1 antibody against IL1β (Stahel *et al.*, 2016; Mendiola & Cardona, 2018). Increased expression of the transcription factor NF-κB has been seen following astrocytic activation, which in turn elevates levels of IL6 and IL1β (Singh *et al.*, 2011). IL1β contributes to neuronal injury and death by inducing the production of neurotoxic molecules such as nitric oxide and TNFα through MAPK pathways in glial cells (Temporin *et al.*, 2008). It has also been uncovered that IL1β increases BBB permeability through the suppression of astrocytic SHH production (Wang *et al.*, 2014), a morphogenic factor released from astrocytes which up-regulates the production of tight junction proteins in endothelial cells and in turn

promotes BBB formation and maintenance (Alvarez *et al.*, 2011). IL1β may be produced following activation of the NLRP3 inflammasome – a protein complex which activates caspase-1, which in turn cleaves the precursor proteins of several pro-inflammatory cytokines, including IL1β, into their active forms (Singhal *et al.*, 2014). It is likely that FGF2 does not interact with the inflammasome and therefore cannot down-regulate IL1β production via this mechanism. The surprising increase in IL1β following FGF2 treatment is potentially explained by the fact that both IL1β and FGF2 are capable of activating the MAPK signalling pathways. FGF2 signalling is initiated upon the molecule binding to its receptor tyrosine kinase, which activates its downstream signal ERK1/2, a member of the MAPK family (Johnson-Farley *et al.*, 2007). A synergistic effect of IL1β and FGF2 has previously been described in fibroblasts with regards to S100A8 expression, this effect was attributed to their converging signalling, i.e. MAPK signalling (Rahimi *et al.*, 2005).

FGF2 significantly reduced baseline expression of *GFAP* in both *E3E3* and *E4E4* astrocytes. The intermediate filament protein GFAP is expressed almost exclusively by adult CNS astrocytes and is widely used as an astrocyte marker (Gruol, 2016). It is believed that GFAP functions include providing mechanical strength, contributing to the BBB, suppressing neuronal proliferation in the mature brain and supporting myelination (Brenner, 2014). GFAP expression is highly regulated by the GFAP promotor and is induced by numerous factors, including brain injury and disease (Eng *et al.*, 2000). As a result it is sometimes considered a reactive astrocyte marker, however there is still some debate among the community as to how effective a marker it is and there are some issues with reproducibility. The results of our study complement that of a 2015 study in rats which revealed that exogenous FGF2 attenuated astrocyte activation by reducing GFAP expression following inflammatory insult with LPS (Ye *et al.*, 2015). Ye *et al*. also found that FGF2 reduced expression of vimentin and neurocan in LPS-treated astrocytes. While *VIM* mRNA expression was also analysed in our study, FGF2 had no effect on its expression. Vimentin is another major intermediate filament protein expressed by astrocytes (Middeldorp & Hol, 2011), with functions including organising several critical proteins which are involved in cell signalling, attachment and cell migration (Sun & Jakobs, 2012). Vimentin has been described as a reactive astrocyte marker but this characteristic does not present in our human astrocyte model.

Taken together, this data indicates that FGF2 is capable of modulating aspects of astrocyte reactivity and should be taken under consideration for further study.

5.4.2 The ability of CBD to modulate reactivity in astrocytes warrants further investigation

CBD, the non-psychoactive component of cannabis, is currently available on prescription as Sativex® for the treatment of symptoms associated with MS (Fitzpatrick & Downer, 2017). It has also shown promise in preclinical and clinical studies for the management of PD and L-DOPA induced dyskinesia (Junior *et al.*, 2020). Given that CBD is a highly lipophilic compound therefore readily crosses the BBB (Cabral & Jamerson, 2014; Aparicio-Blanco *et al.*, 2019), and cannabinoid receptors are highly expressed within the CNS (Kozela *et al.*, 2017) it is now of interest to determine whether CBD may be useful in modulating the neuroinflammation which is associated with many neurodegenerative diseases, including AD (Kim *et al.*, 2019; Schubert *et al.*, 2019).

In a rodent model of neonatal ischemic brain damage, CBD was shown to be neuroprotective by inhibiting astrogliosis and microglial activation (Ceprian *et al.*, 2017). Therefore it was of interest to determine whether CBD might modulate astrocyte reactivity in our human iPSC-derived model system. Inflammatory insult was delivered via cytokines IL1α (0.3 ng/mL) and TNFα (3 ng/mL), the effects of which CBD has previously been shown to counteract (Khaksar & Bigdeli, 2017; Chiricosta *et al.*, 2019). The concentrations of CBD to be trialled were chosen from the literature, with 10 µM previously attenuating activation of peripheral immune cells (Fitzpatrick *et al.*, 2020). It was decided to also include some lower doses to examine any dose response of CBD.

It was first determined whether CBD (5 and 10 µM) had any effect on expression of reactive astrocyte markers in quiescent-like astrocytes. CBD had no effect on basal IL6 mRNA expression or secretion and no effect on *IL1β*, *C3* or *CXCL10* mRNA expression. CBD significantly decreased basal *GFAP* mRNA but significantly increased mRNA expression of *LCN2*, *ICAM1* and *PTX3*. This data indicates that CBD has varied effects on reactivity markers and is therefore not an all-encompassing inhibitor of pro-inflammatory mediators. Astrocytes were subsequently stimulated and four doses of CBD (0.1, 1, 5, and 10 µM) were trialled for their ability to modulate reactive astrocyte markers. This again generated some mixed results. IL6 mRNA expression and secretion as well as *CXCL10*, *C3* and *LCN2* mRNA expression data indicate that CBD may be capable of modulating these inflammatory markers, although only IL6 secretion was significantly attenuated by CBD at 10 µM. Data pertaining to mRNA expression of *ICAM1*, *PTX3*, *GFAP* and *IL1β* indicate that CBD is not modulating astrocyte reactivity.

Von Widdern and colleagues also found mixed effects of CBD in an *in vitro* LPS model of neuroinflammation using rodent astrocyte-microglia co-cultures. CBD attenuated the LPS-induced production of TNFα and nitrite but not IL6. The study reported some interesting effects of mono- versus co-cultures, where pro-inflammatory mediators were more highly induced in co-cultures versus astrocyte monocultures and only TNFα was attenuated by CBD in isolated astrocytes (Cardinal von Widdern *et al.*, 2020). The anti-inflammatory effects of CBD may predominantly act via microglia-mediated mechanisms with a limited direct effect on astrocytes, this would explain the lack of positive results found in this study. Similarly, CBD has been shown to be neuroprotective in rodent models of newborn hypoxic-ischemic brain damage and adult stroke. CBD administered following MCAO in neonatal rats proved beneficial by reducing perilesional gliosis, and preserving astrocyte function by inhibiting astrogliosis and microglial activation (Ceprian *et al.*, 2017). Again perhaps CBD affected the interplay between microgliosis and astrogliosis to induce its effect.

With regards to a lack of effect on *IL1β* expression following insult, this contrasts a study carried out in human mesenchymal stem cells which found that CBD suppresses activation of the NLRP3 inflammasome and subsequently inhibit release of its downstream products IL18 and IL1β (Libro *et al.*, 2016). CBD was also found to suppress IL1β expression and secretion in a mouse model of AD, this was coupled with inhibition of GFAP mRNA and protein expression, and impairment of *iNOS* expression and NO release (Esposito *et al.*, 2007). In an experimental autoimmune encephalomyelitis mouse model of MS, combination therapy with THC and CBD reduced neuroinflammation by decreasing levels of pro-inflammatory molecules such as IL17, TNFα and IL6 as well as increasing levels of anti-inflammatory molecules such as IL4, IL10, and TGFβ (Al-Ghezi *et al.*, 2019). Notably, neither THC nor CBD alone provided these anti-inflammatory effects suggesting that combination therapy is required to significantly reduce neuroinflammation. It has been suggested that the combination of CBD with THC shows better therapeutic potential compared to the actions of each cannabinoid component alone (Russo & Guy, 2006; Aso *et al.*, 2015).

CBD significantly increased basal expression of *ICAM1*, *LCN2* and *PTX3*, a surprising result considering its widely accepted anti-inflammatory effects. Cannabinoids have previously been shown to promote expression of ICAM1 in lung cancer cells. CBD evoked ICAM1 expression resulted in adhesion of cancer cells to lymphokine-activated killer cells and their subsequent lysis, in this case CBD exerts anti-invasive and antimetastatic actions

(Haustein *et al.*, 2014). At the time of writing, no literature linking CBD or cannabinoids and PTX3 or LCN2 could be found, therefore the finding that CBD increases basal LCN2 and PTX3 mRNA expression appears to be novel.

Although this study provided no conclusive findings, this data provides some preliminary insights into the effect of CBD on astrocyte reactivity state.

5.4.3 Concluding remarks

This study provided some insight into the ability of FGF2 and CBD to modulate reactivity in iPSC-derived astrocytes. FGF2 shows promise as an agent capable of modulating reactivity in astrocytes while data pertaining to CBD indicates that it requires further investigation, perhaps taking advantage of the latest in iPSC technology where microglia may be incorporated in to organoids (Raja *et al.*, 2016; Lin *et al.*, 2018).

Chapter 6

Glutamate dynamics in human iPSC-derived astrocytes is affected by APOE genotype

6. Glutamate dynamics in human iPSC-derived astrocytes is affected by APOE genotype

6.1 Introduction

6.1.1 Glutamate homeostasis – one of the key functions of astrocytes

Astrocytes provide physical and metabolic support for neurons, and along with pericytes and vascular endothelium they make up the BBB. Astrocytes exhibit an ever increasing amount of functions at the synapse (Khakh & Sofroniew, 2015). They respond to and modulate neuronal excitation via gliotransmitters such as glutamate and ATP, they regulate synaptic remodeling as well as synaptic [K^+] and [Ca^{2+}] levels (Benarroch, 2016; Verkhratsky *et al.*, 2019). At a higher level, this enables astrocytes to regulate processes including breathing and memory (Bliss & Collingridge, 1993).

A primary role for astrocytes in the CNS is the removal of excess glutamate from the extracellular space, particularly the synaptic cleft in order to maintain optimal neuronal functioning (Mark *et al.*, 2001) (Figure 6.1.1). Glutamate is the main excitatory neurotransmitter in the CNS, and while this is considered its major function it has many other fates in the CNS. Glutamate may be used as a precursor for glutamine, GABA and glutathione, it can be oxidised and used for energy production or incorporated into proteins (McKenna, 2007). Glutamate as a neurotransmitter has far reaching effects owing to the fact that almost all neurons in the CNS express the NMDA receptor (Hynd *et al.*, 2004) and are therefore sensitive to changes in extracellular glutamate. Therefore, it is vital that glutamate homeostasis be maintained.

When glutamate is not effectively and efficiently buffered away from the synapse, excessive activation of NMDA receptors leads to large influxes of Ca^{2+} in postsynaptic neurons which in turn activates enzymes such as phospholipases (Lazarewicz *et al.*, 1990; Conway, 2020), resulting in the eventual degeneration of brain cells (Figure 6.1.1). Such mechanisms of neurodegeneration are implicated in AD pathology and may explain the specific loss of glutamatergic neurons in cortical layers III and IV during AD pathogenesis (Hynd *et al.*, 2004).

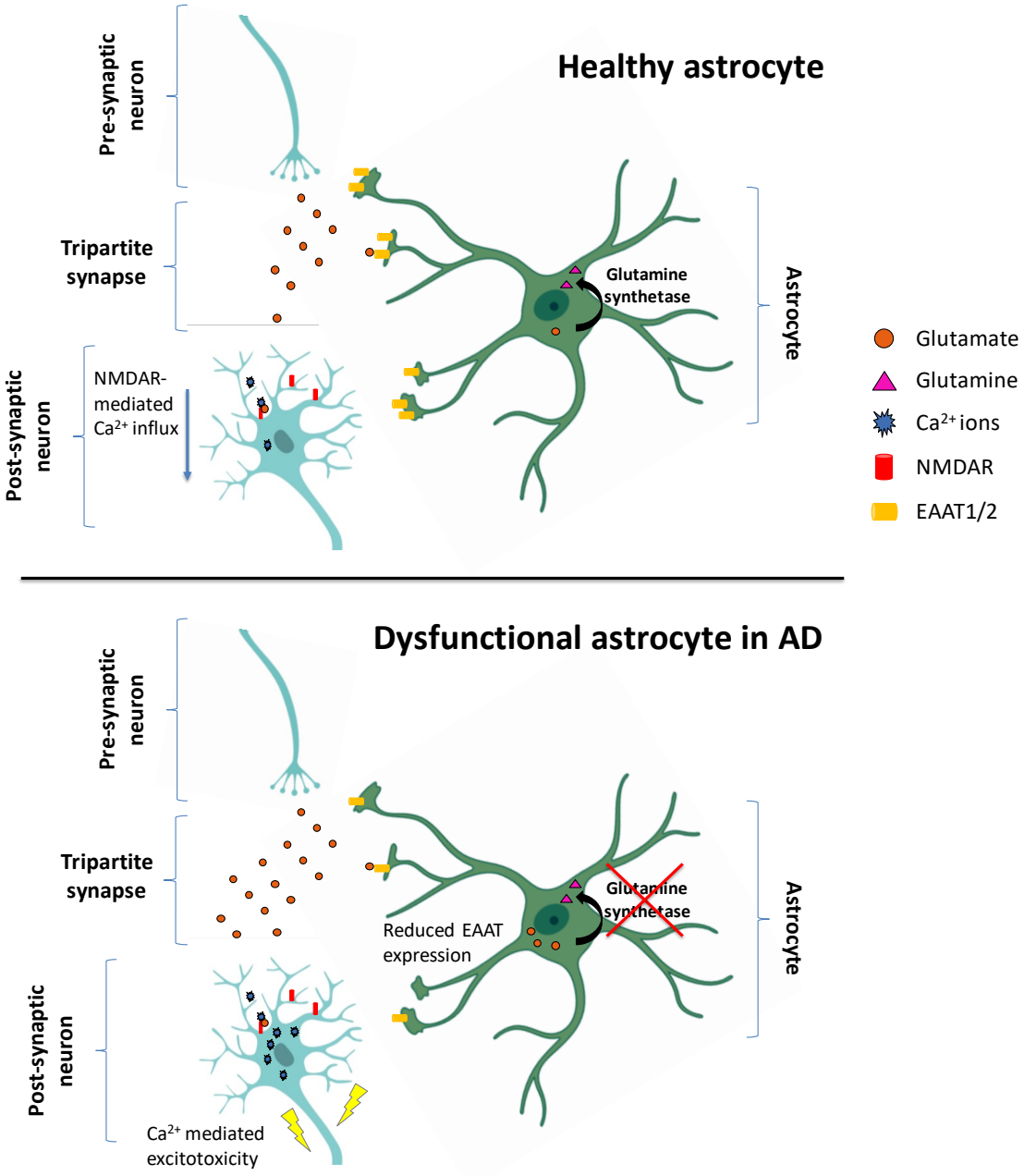


Figure 6.1.1. Healthy and dysfunctional astrocytes in AD.

Astrocytes maintain glutamate homeostasis by buffering synaptic glutamate levels thereby preventing glutamate reaching excitotoxic levels. Glutamate is then converted to glutamine by glutamine synthetase (GS) which can be recycled by neurons. In AD, calcium-mediated excitotoxicity can occur when glutamate homeostasis is dysregulated. Proposed mechanisms include reduced EAAT expression and GS activity.

6.1.2 Glutamate Transporters

Glutamate transporters can be broadly characterised as Na^+-independent and Na^+-dependent glutamate uptake transporters. Na^+-dependent glutamate uptake transporters include the already mentioned EAAT glutamate transporters of which there are five. EAAT1 and EAAT2 are expressed by astrocytes within the CNS, and are responsible for up to 90% of glutamate uptake within the CNS (Mahmoud *et al.*, 2019). EAAT3 is expressed by neurons and is a means of glutamate sequestration by presynaptic neurons (Kanai & Hediger, 1992). EAAT4 and EAAT5 are expressed by purkinje cells (Fairman *et al.*, 1995), and by retinal cells (Arriza *et al.*, 1997) respectively, and are minimally involved in CNS glutamate homeostasis.

6.1.2.1 Excitatory amino acids transporters 1 and 2

EAAT1 and EAAT2 have a similar structure and share 65% homology at the amino acid level (Gegelashvili & Schousboe, 1997). Functionally, EAAT1 and EAAT2 have the same affinity for glutamate. EAAT1 has a glutamate Km value of 10-77 µM, while EAAT2 has a Km of 36-97 µM (Arriza *et al.*, 1994). As such, both are capable of reducing extracellular glutamate to the same level (Table 6.1.1).

EAAT1/GLAST expression has been detected in radial glial cells and immature astrocytes of the forebrain and cerebellum in postnatal mice (Shibata *et al.*, 1997). In the adult brain, EAAT1/GLAST is predominately expressed by mature astrocytes (Schmitt *et al.*, 1997; Lehre & Danbolt, 1998), and to a lesser extent by oligodendrocytes and microglia (Kondo *et al.*, 1995), suggesting that glutamate uptake is not an essential function of these cells. In the adult CNS, EAAT1 expression is highest in the cerebellum (Rothstein *et al.*, 1994; Lehre & Danbolt, 1998), but it is also expressed in areas such as the retina (Derouiche & Rauen, 1995) and in cochlear glial cells (Glowatzki *et al.*, 2006). EAAT1 expression in the forebrain is limited (Mahmoud *et al.*, 2019). In contrast to EAAT1, EAAT2/GLT-1 is not detected in postnatal rat CNS but only at 3-5 weeks of age (Furuta *et al.*, 1997). In the mature CNS, EAAT2 is the major glutamate transporter expressed by mature astrocytes in most regions however there are some regions where EAAT1 dominates (Rothstein *et al.*, 1994). EAAT expression in astrocytes is associated with clustering of both EAAT1 and EAAT2 on perisynaptic processes proximal to active glutamatergic synapses (Minelli *et al.*, 2001; Zhou & Sutherland, 2004). EAAT1 and EAAT2 are expressed on cortical astrocytes, as determined by electron microscopy of human post-mortem brain samples (Roberts *et*

al., 2014). Interestingly, EAAT1 expression is relatively constant in the adult CNS, while EAAT2 expression appears to be dependent on synaptic activity (Swanson *et al.*, 1997). EAAT2 up-regulation is associated with increased glutamate release from neighbouring glutamatergic neurons (Schlag *et al.*, 1998; Poitry-Yamate *et al.*, 2002).

Several mechanisms are involved in the regulation of transcription, translation, post-translational modification, and activity of EAAT1 and EAAT2 glutamate transporters. The extracellular concentration of glutamate has been shown to increase protein expression of GLAST/EAAT1 in rats (Gegelashvili *et al.*, 1996; Duan *et al.*, 1999). Glutamate receptor stimulation has also been demonstrated to affect transporter expression. Activation of group II mGluRs enhance GLAST via ERK/P13K/NF-κB, activation of group I mGluRs inhibit GLAST and GLT-1 expression via the same pathway (Aronica *et al.*, 2003; Lin *et al.*, 2014), and activation of iGluRs down-regulate GLAST expression (Lopez-Bayghen *et al.*, 2003). Cell culture conditions, growth factors such as EGF and FGF, hormones including oestrogen and glucocorticoids, and constitutively active GSK3β are all important in controlling the expression of functional glutamate transporters on the plasma membrane (Jimenez *et al.*, 2014).

	EAAT1	**EAAT2**	**Reference**
Structure	Share 65% homology		(Gegelashvili & Schousboe, 1997)
Glutamate Affinity (K_m)	10 to 77 µM	36 to 97 µM	(Arriza *et al.*, 1994; Gegelashvili & Schousboe, 1997; Mahmoud *et al.*, 2019)
Expression after birth	High	Low	(Furuta *et al.*, 1997; Shibata *et al.*, 1997)
Expression in adulthood	High in specific regions	High	(Rothstein *et al.*, 1994; Lehre & Danbolt, 1998)
Expression in CNS	Constant	Changes as a function of synaptic activity	(Swanson *et al.*, 1997)

Table 6.1.1. Comparison of excitatory amino acid transporters 1 and 2.

EAAT1 and EAAT2 have similar structure and affinity to glutamate while their expression levels vary throughout the lifespan and CNS.

6.1.2.2 Glutamate dynamics in astrocytes

Glutamate is the primary excitatory neurotransmitter of the CNS. It mediates neuron-to-neuron signalling at the synapse as well as astrocyte-to-neuron signalling and large-scale processes like plasticity and memory (Khakh & Sofroniew, 2015). Excessive release of transmitter in glutamatergic circuits, or insufficient removal of glutamate from the synapse can result in excitotoxicity-induced cell death. Glutamatergic neurotoxicity is suspected to play a role in neurodegenerative diseases such as AD (Shigeri *et al.*, 2004). To avoid this, and to terminate the excitatory signal, the CNS relies primarily on astrocytes and specifically astrocytic EAAT1 and EAAT2 to remove excess glutamate from the synapse (Shigeri *et al.*, 2004).

6.1.2.3 Mechanisms of glutamate uptake in astrocytes

Glutamate uptake from the extracellular space involves inward transport of glutamate, along with three Na^+ ions and one H^+ ion, coupled with the outward transport of two K^+ ions. These ions move along their concentration gradients while glutamate moves against its concentration gradient – µM in extracellular space versus mM intracellularly (Mahmoud *et al.*, 2019). As a result, glutamate uptake is one of the highest energy consuming processes in the CNS as more than one molecule of ATP is required per glutamate molecule (Sibson *et al.*, 1998).

6.1.2.4 Mechanisms of glutamate release in astrocytes

In addition to glutamate uptake, astrocytes are also capable of releasing glutamate which may provide a mechanism for astrocytic modulation of neuronal activity. Six possible mechanisms of glutamate release by astrocytes have been described, including (i) reverse glutamate uptake by glutamate transporters, (ii) opening of anion channels induced by cell swelling, (iii) Ca^{2+}-dependent exocytosis, (iv) glutamate exchange via the cysteine-glutamate antiporter, (v) glutamate release through ionotropic purinergic receptors, and (vi) functional unpaired connexin “hemichannels” on the cell surface (Malarkey & Parpura, 2008). Although these various pathways have been defined, it is not clear how often and to what extent astrocytes employ them. It will be necessary to determine whether the same glutamate release mechanisms that operate under physiological

conditions operate during pathological conditions or whether there are specific release mechanisms that operate under specific conditions.

6.1.3 Glutamate metabolism in astrocytes

Once released into the synaptic cleft, glutamate can bind to ionotropic glutamate receptors (e.g. AMPA, NMDA, and kainate) and metabotropic glutamate receptors (i.e. mGluR1-8) localised to plasma membranes of neurons and glial cells, initiating various responses (Nicoletti *et al.*, 2011; Popoli *et al.*, 2011; Charsouei *et al.*, 2020). Excess glutamate is then cleared from the synapse. In astrocytes, glutamate may be broken down to glutamine by glutamine synthetase (GS) and released into the synapse for uptake by neurons where it is used to resynthesise glutamate. This process is known as the glutamate-glutamine cycle. Alternatively, glutamate can be oxidised to yield α-ketoglutarate which can then be utilised in the tricarboxylic acid (TCA) cycle to produce ATP. The determining factor for which pathway is used to metabolise glutamate within astrocytes is extracellular glutamate concentrations. Glutamine cycling is favoured when the extracellular concentration is less than 0.2 mM in order to provide glutamine to neurons, while oxidative metabolism of glutamate is favoured when extracellular glutamate is greater than 0.2 mM in order to generate the energy required for glutamate uptake (McKenna *et al.*, 1996).

6.1.3.1 Glutamate-glutamine cycle

The majority of glutamate enters the glutamate-glutamine cycle to be converted to glutamine. Upon glutamate uptake by the astrocyte, GS catalyses the conversion of glutamate to glutamine (Figure 6.1.2). Glutamine is released into the extracellular space via system N transporters, electroneutral Na^+-dependent transporters. Glutamine is then taken up by neurons via system A transporters (Popoli *et al.*, 2011). In neurons, glutamine is used to synthesise the neurotransmitters glutamate or GABA, for synaptic transmission (Mahmoud *et al.*, 2019). Glutamate metabolism further supports the astrocytes role as a regulator of homeostasis as activated GS breaks down ammonia and ammonium to prevent against ammonium neurotoxicity.

6.1.3.2 Tricarboxylic acid cycle

Glutamate may be oxidized to α-ketoglutarate which serves as a substrate to ATP production in the TCA cycle (Figure 6.1.2). This oxidative metabolism of glutamate is mediated by the mitochondrial enzyme glutamate dehydrogenase (Mahmoud *et al.*, 2019). Partial oxidation of glutamate can also be achieved with the enzymes aspartate aminotransferase, alanine aminotransferase and branched chain aminotransferase via the process of transamination (Popoli *et al.*, 2011).

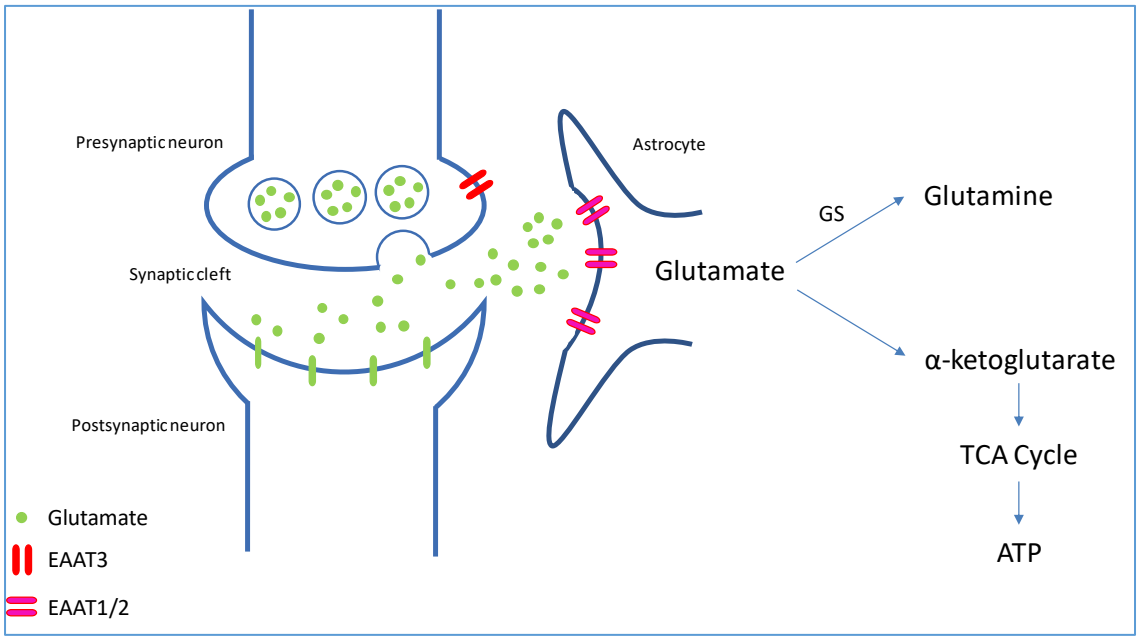


Figure 6.1.2. Glutamate uptake and metabolism by astrocytes.

Glutamate uptake by astrocytes – After release of glutamate from the presynaptic neuron, only 20% of glutamate is taken up by post-synaptic glutamate receptors to transmit excitatory impulses, while astrocytes uptake most of the remaining glutamate via the glutamate uptake transporters, EAAT1 and EAAT2, expressed on the surface of the astrocytic perisynaptic processes. Glutamate metabolism in astrocytes – In astrocytes, glutamate can be metabolised to glutamine by glutamine synthetase (GS), then glutamine is released to the extracellular space to be taken up by neurons and used to resynthesise glutamate or GABA. Alternatively, glutamate may be oxidatively metabolised to α-ketoglutarate, which is used in ATP synthesis. Figure modified from (Mahmoud et al., 2019).

6.1.4 Dysfunctional glutamate cycling and excitotoxicity in Alzheimer's disease

In healthy astrocytes, glutamate is sequestered from the synapse via glutamate transporters EAAT1 and EAAT2, then converted to glutamine by GS for return to the neuron. GS activity is decreased in the AD brain (Butterfield *et al.*, 1997), potentially as a result of oxidative modification (Castegna *et al.*, 2002). Additionally, altered expression of glutamate transporters has also been noted in the brains of AD patients (Jacob *et al.*, 2007). This may cause a build-up of glutamate in the synapse, activating NMDA receptors on the post synaptic neuron and resulting in excess Ca^{2+} influx (Figure 6.1.3). Increased Ca^{2+} is associated with membrane permeabilisation, and cytochrome c release, which actives caspase 9 and sequentially caspase-3 resulting in apoptosis (Brustovetsky *et al.*, 2002; Yoon *et al.*, 2003; Madeddu *et al.*, 2004).

Neuroinflammation may contribute to the excitotoxic neurodegeneration characteristic of AD. It has been shown that TNFα stimulates extensive glutamate release from microglia in an autocrine manner by up-regulating glutaminase (Takeuchi *et al.*, 2006). TNFα has also been shown to affect EAAT expression. Wang and colleagues demonstrated that TNFα reduces the expression of EAAT1 and EAAT2 in human astrocytes (Wang *et al.*, 2003). There is also evidence that reactive oxygen species (ROS) contribute to the reduction in GS-dependent breakdown of glutamate, reinforcing glutamate neurotoxicity (Castegna *et al.*, 2002).

Interestingly, there is some evidence that APP cleavage products are protective against excitotoxicity, raising the possibility that increased Aβ production stems from an attempt at alleviating pathology initiated by excitotoxicity. This may result in a positive-feedback mechanism whereby Aβ renders neurons susceptible to glutamatergic cytotoxicity (Mattson *et al.*, 1993). The role of APOE in this pathologic pathway in AD has not been properly explored. Loss of ability to buffer glutamate should now be seriously considered as an adjunct to rectifying mechanisms of excitotoxic neurodegeneration in AD.

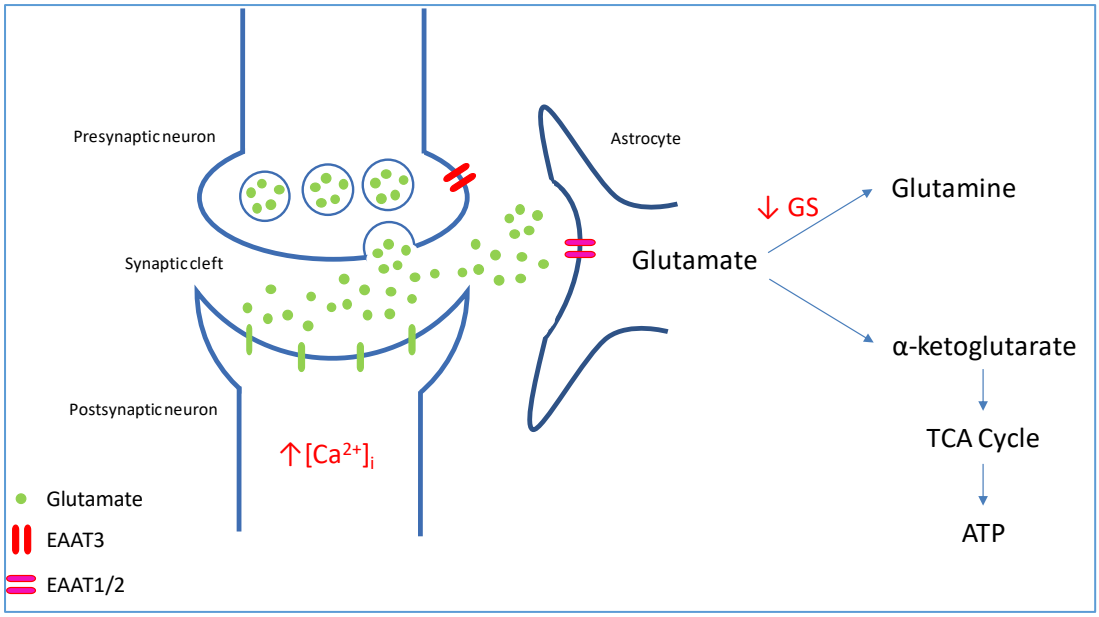


Figure 6.1.3. Dysfunctional glutamate cycling in Alzheimer's disease results in excitotoxicity.
Reduced EAAT expression alters glutamate uptake dynamics in astrocytes in the AD brain This coupled with decreased glutamine synthetase (GS) activity results in compromised glutamate cycling. Excess synaptic glutamate leads to increased intracellular [Ca^{2+}] in the post-synaptic neuron, excitotoxicity and ultimately neuronal cell death.

6.1.5 Role of APOE in astrocyte glutamate handling

Several reports indicate reduction in EAAT levels, down-regulation of NMDA receptors (Jacob *et al.*, 2007; Hoshi *et al.*, 2018), and loss of glutamate receptor proteins in the AD brain as a result of APOE genotype (Chen *et al.*, 2010). APOE4 genotype also facilitates excessive long-term potentiation via stabilisation of NMDA receptors (Chen *et al.*, 2010). Together, these reports suggest that glutamate uptake and breakdown are hindered in the AD brain and that APOE may play a role. However, there appears to be a gap in the literature pertaining to a link between APOE genotype and glutamate dynamics. Given that APOE4 is the single greatest genetic risk factor associated with AD and that excitotoxicity has been proposed as one of the initiating steps in AD pathology (Zoltowska *et al.*, 2018), it is not a far reach to suggest that APOE4 genotype may predispose astrocytes to mishandle glutamate. iPSC provide a valuable model system suited to examining the effect of genotype on functionality in human cells.

6.1.6 Aims

The objectives of this chapter can be separated into three primary aims:

1. To investigate levels of glutamate transporter expression at the RNA (*SLC1A3*, *SLC1A2*) and protein level (EAAT1, EAAT2) in *E3E3* and *E4E4* astrocytes,
2. To elucidate any effect of APOE genotype and astrocyte reactivity state on glutamate transporter expression,
3. To delineate any effect of APOE genotype and astrocyte reactivity state on functionality of glutamate transporters.

The hypothesis pertaining to these aims are that APOE genotype and astrocyte reactivity state will affect glutamate transporter expression and subsequently glutamate dynamics. There are some limitations in the current literature but the information put out so far would indicate that APOE genotype and astrocyte reactivity negatively impact glutamate homeostasis. Therefore, we hypothesise that glutamate transporter expression will be reduced in *E4E4* and reactive astrocytes. It is expected that *E4E4* and reactive astrocytes will have a compromised ability to uptake glutamate from the extracellular environment.

6.2 Materials and Methods

6.2.1 Cell lines

Human iPSC homozygous for APOE3 and APOE4 were used in this study to generate astrocytes and subsequently reactive astrocytes.

6.2.2 Astrocyte progenitor cell culture and terminal differentiation

Human *E3E3* and *E4E4* iPSC were patterned towards a neural fate and subsequently differentiated along a glial lineage as described in sections 3.2.3 and 3.2.5.

6.2.3 Astrocyte stimulation to examine the effect of astrocyte reactivity on glutamate dynamics

Astrocytes were stimulated with inflammatory microglial factors IL1α (3 ng/mL; PeproTech, UK), TNFα (30 ng/mL; Cell Signalling Technology, USA) and C1q (400 ng/mL; MyBioSource, USA) for 24 h as per Liddelow *et al*., 2017 to generate reactive astrocytes in order to determine whether astrocyte reactivity state affected glutamate transporter expression and glutamate dynamics. A 10-factor dilution of these concentrations was also used. These treatments are denoted as "Factors High" and "Factors Low" where appropriate. Post stimulation, cells were lysed as appropriate for qPCR and Western blotting analysis of glutamate transporter expression. Alternatively, media and cell lysates were collected, snap frozen in liquid nitrogen and stored at -80˚C for later analysis of extracellular and intracellular glutamate concentrations via glutamate assay (Figure 6.2.1).

To further assess the efficacy of glutamate transport in the astrocytes, and any effect of reactivity state, extracellular glutamate was altered. Serio media components Advanced DMEM and NEAA contain L-glutamic acid at a concentration of 50 µM and 10 µM respectively. GlutaMAX contains L-alanyl-L-glutamine dipeptide at a concentration of 2 mM that is broken down by cells to release L-glutamine as needed. By removing GlutaMAX and NEAA the extracellular concentration of glutamate was reduced to approximately 50 µM. This reduced glutamate media (Serio media minus GlutaMAX and NEAA) was applied to astrocytes for 3 h prior to stimulation. Astrocytes were then stimulated with inflammatory microglial factors at low and high concentrations for 24 h, astrocytes were maintained in reduced glutamate media for this time. Post stimulation,

media and cell lysates were collected, snap frozen in liquid nitrogen and stored at -80˚C for later analysis of extracellular and intracellular glutamate concentrations via glutamate assay (Figure 6.2.1).

6.2.4 Astrocyte stimulation to examine the effect of FGF2 on glutamate transporter expression in iPSC-derived astrocytes

Astrocytes were stimulated with inflammatory microglial factors IL1α, TNFα and C1q at high and low concentrations for 24 h as described above. Astrocytes were treated with FGF2 (50 ng/mL; PeproTech, UK) alone and in combination with both concentrations of factors in order to assess its ability to modulate glutamate transporter expression. Post stimulation, cells were lysed as appropriate for qPCR and Western blotting analysis of glutamate transporter expression (Figure 6.2.1).

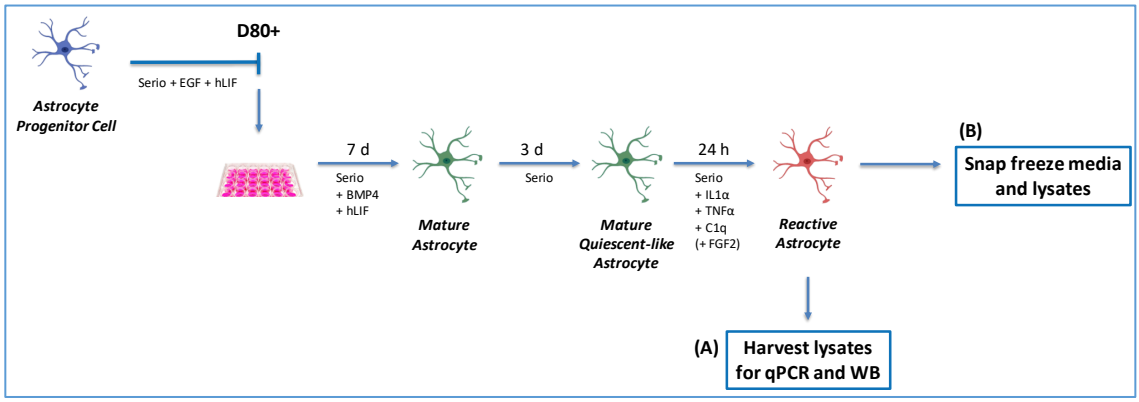


Figure 6.2.1. Experimental timeline to test the effect of astrocyte reactivity on glutamate transporter expression and glutamate dynamics.

Astrocyte progenitor cells were expanded in Serio media supplemented with EGF and hLIF. From D80 APC are plated and terminally differentiated for 7 d, followed by 3 d in Serio media without factors to ensure a quiescent-like astrocyte at time of stimulation. Astrocytes are stimulated for 24 h in order to assess the effect of reactivity (±FGF2) on glutamate dynamics. Cell lysates were harvested for qPCR and Western blotting (WB) analysis of glutamate transporter expression (A). Media and cell lysates were harvested for analysis of $[glutamate]_i$ *and* $[glutamate]_e$ *(B).*

6.2.5 Analysis of glutamate transporter mRNA expression by qPCR

The mRNA expression of *SLC1A3*, *SLC1A2* and *GLUL* which encode the proteins EAAT1, EAAT2 and GS respectfully were assessed by qPCR (Table 6.2.1). Gene expression concentrations were analysed using the comparative Ct method. The target genes from each sample were compared with GAPDH, which acted as an endogenous control. The Ct values of each target gene and control gene were compared and expressed as RQ ratio. The full qPCR protocol is described in detail in the main methods section of this thesis (Section 2.4.1).

Gene	Primer Code
SLC1A3	Hs00904823_g1
SLC1A2	Hs01102423_m1
GLUL	Hs00365928_g1

Table 6.2.1. Target genes used for qPCR analysis of glutamate transporter and glutamine synthetase expression.

6.2.6 Analysis of glutamate transporter protein expression by Western blotting

The protein expression of EAAT1 was assessed by Western blotting (Table 6.2.2). Densitometry analysis was carried out on protein bands using Image Studio Lite (v 5.2) with β-actin acting as a loading control. Densitometry signals for EAAT1 were divided by β-actin signals and normalised to control in order to present data as fold change. The full Western blotting protocol is described in detail in the main methods section of this thesis (Section 2.5.3).

Antibody	Dilution Factor	Manufacturer
Rabbit anti-EAAT1	1:1000	Novus Biologicals, USA
Mouse anti-β-actin	1:2000	Sigma-Aldrich, USA
Goat anti-rabbit HRP-conjugated	1:2000	Thermo Scientific, USA
Goat anti-mouse HRP-conjugated	1:2000	Thermo Scientific, USA

Table 6.2.2. Antibodies used for Western blotting analysis of EAAT1 expression.

6.2.7 Glutamate assay

The glutamate assay kit (fluorometric, ab138883, Abcam, UK) takes advantage of the reaction between L-glutamic acid and $NADP^+$, which results in the production of NADPH. Assuming that the samples/standards are the source of glutamate, the reaction mix contains $NADP^+$, an enzyme mix to catalyse the reaction and an NADPH sensor. During the reaction, a red fluorescence product is produced (NADPH + sensor) which can be detected at Ex/Em = 540/590 nm (Figure 6.2.2). The fluorescence reading is then used to infer the concentration of glutamate in the samples via a standard curve. The protocol states that the assay can detect as little as 1 µM glutamic acid.

6.2.7.1 Sample preparation

Following stimulation, supernatant was removed and snap frozen in liquid nitrogen to preserve protein content. Cells were lysed by incubation in 5X Mammalian cell Lysis Buffer diluted to 1X in dH_2O (100 uL, 20 min, RT; Abcam, UK). Cells were abraded, lysates collected and snap frozen in liquid nitrogen. A sample of Serio media and 1X lysis buffer not exposed to cells were also snap frozen for use as negative controls. Samples were stored at -80^oC until assaying.

6.2.7.2 Glutamate assay procedure

Glutamate concentrations in media and lysate samples were determined using a glutamate assay kit (Abcam, UK) as per the manufacturer's instructions. Preparation of the kit prior to its first use involved reconstitution of the glutamic acid standard by addition of dilution buffer (200 µL) to generate a 100 mM stock solution. This was subsequently aliquoted and stored at -20^oC protected from the light. A 50X enzyme mixture stock was prepared with the addition of dH_2O (200 µL) and the stock aliquoted and stored at -20^oC. A 200X $NADP^+$ stock solution was prepared by the addition of dilution buffer (100 µL) to the stock vial provided and subsequently aliquoted and stored at -20^oC protected from light.

On the day of assaying all samples and reaction components were thawed on ice. Glutamic acid standards were prepared by first diluting the stock to a 300 µM top standard followed by serial dilution (300-1 µM) in dilution buffer. Dilution buffer was used as a blank. Reaction mix was prepared by combining $NADP^+$ (0.25 µL per reaction), enzyme

mix (1 µL per reaction) and assay buffer (48.75 µL per reaction). Lysate samples were diluted (1:2) in dilution buffer to ensure their glutamate concentration fell within the standard curve. Samples and standards were loaded (50 µL) onto a 96-well black-walled clear-bottomed plate. Reaction mix (50 µL) was loaded to begin the redox reaction between glutamate and $NADP^+$, the plate was shaken on an orbital shaker to mix and then incubated (1 h, RT, protected from light). The fluorescence of each sample was measured on a Spectramax M3 microplate reader (Molecular Devices, USA) with SoftMax Pro (6.2.1) software at Ex/Em = 540/590 nm. The glutamate concentration of each sample was determined from the standard curve produced. Glutamate concentration in the media was considered a measure of extracellular glutamate, while glutamate concentration in the cell lysates was considered a measure of intracellular glutamate.

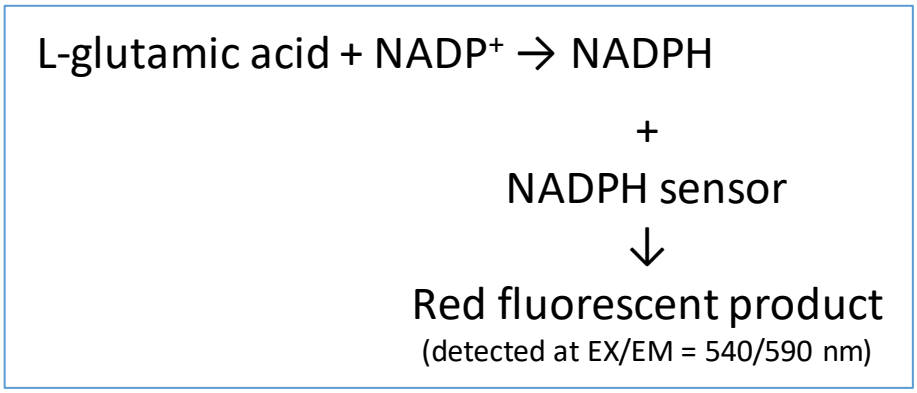


Figure 6.2.2. Glutamate assay mechanism.

The reaction between L-glutamic acid and $NADP^+$ results in the production of NADPH. The glutamate assay uses a reaction mix containing $NADP^+$, an enzyme mix to catalyse the reaction and an NADPH sensor, with the samples and standards providing the L-glutamic acid. The red fluorescent product produced (NADPH + sensor) can be detected at Ex/Em = 540/590nm.

6.2.8 Statistical analysis

Data is expressed as mean ± SEM. At least three neural induction and astrocyte differentiations (N) were performed per iPSC line. 'n' values denote experimental or biological replicates and are representative of different thaws or passage numbers, while 'reps' denotes technical replicates within each experimental group, i.e. cells from the same plate but separate wells.

An unpaired t-test was used to analyse baseline expression of glutamate transporters in *E3E3* and *E4E4* astrocytes, as well as analysing expression of EAAT1 versus EAAT2. One-way ANOVA was used to analyse the effect of microglial factors. Two-way ANOVA was used for statistical analysis of two variables, i.e. APOE genotype and microglial factors, and FGF2 and microglial factors, followed by Bonferroni *post hoc* if significance was inferred. Three-way ANOVA was used to analyse the interaction of APOE genotype, microglial factors and FGF2, followed by Bonferroni *post hoc*. Significance was set at $p < 0.05$. Statistical analysis was performed using GraphPad Prism 8 (GraphPad Software).

6.3 Results

A central task of astrocytes in the CNS is to maintain homeostatic concentrations of the neurotransmitter glutamate in the extracellular space. There is evidence that this function is compromised in the AD brain. Here, we investigated whether APOE genotype influences glutamate dynamics in astrocytes, and whether inflammatory insult impacted glutamate dynamics. Glutamate transporter expression were examined at mRNA and protein levels, via qPCR and Western blotting. Glutamate dynamics was assessed using a glutamate assay.

6.3.1 APOE3 and APOE4 homozygous astrocytes show differential expression of glutamate transporters, EAAT1 and EAAT2

In order to ascertain whether APOE genotype had any effect on EAAT expression, levels of the major glutamate transporters EAAT1 and EAAT2 were assessed in iPSC-derived astrocytes by carrying out qPCR analysis on their respective genes, *SLC1A3* and *SLC1A2*. *SLC1A3* showed greater levels of mRNA expression in both APOE3 ($p < 0.001$; Figure 6.3.1. A) and APOE4 ($p < 0.001$; Figure 6.3.1. B) homozygous astrocytes as compared to *SLC1A2*, indicating that EAAT1 is more highly expressed in these cells. When transporter expression was expressed as a ratio of *SLC1A3:SLC1A2* (*SLC1A3* RQ ÷ *SLC1A2* RQ) it could be determined that *E3E3* astrocytes have significantly greater overall transporter expression compared to *E4E4* astrocytes ($p < 0.05$). *E3E3* astrocytes have a ratio of approximately 140:1, while *E4E4* astrocytes have a ratio of approximately 60:1 (Figure 6.3.1. C). Baseline mRNA expression levels of *SLC1A3* are greater in *E3E3* astrocytes compared to *E4E4* astrocytes ($p < 0.001$; Figure 6.3.2. A), with the same trend holding for *SLC1A2* expression ($p < 0.01$; Figure 6.3.2. B). These trends indicate that APOE genotype affects transporter expression. This reduced *SLC1A3* expression in *E4E4* astrocytes did not translate to reduced EAAT1 protein when assessed by Western blotting (Figure 6.3.2. C).

Taken together this data indicates that APOE genotype impacts glutamate transporter expression at the mRNA level. Having examined baseline expression of glutamate transporters, we next examined EAAT expression in astrocytes following inflammatory insult.

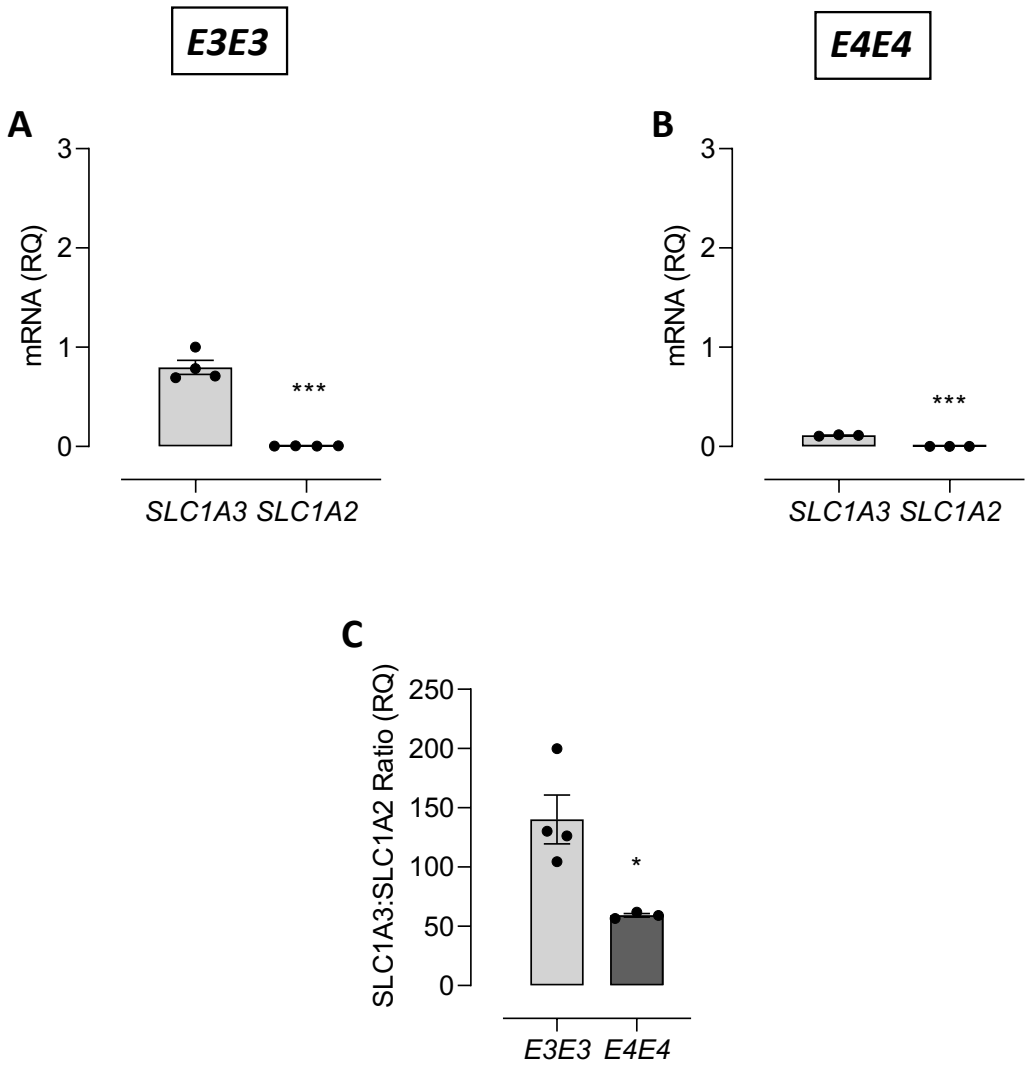


Figure 6.3.1. SLC1A3 expression is greater than SLC1A2 mRNA expression in E3E3 and E4E4 astrocytes.

*SLC1A2 mRNA expression is significantly lower than SLC1A3 expression in E3E3 (A) and E4E4 (B) astrocytes. The SLC1A3:SLC1A2 ratio is significantly reduced in E4E4 astrocytes compared to E3E3 astrocytes (C). Data expressed as mean ± SEM (N=3, n=3-4). * p < 0.05, *** p < 0.001 vs E3E3. E3E3 t = 11.23, df = 6, p = < 0.0001. E4E4 t = 26.70, df = 4, p = < 0.0001. Ratio t = 3.310, df = 5, p = 0.0212 (Unpaired t-test).*

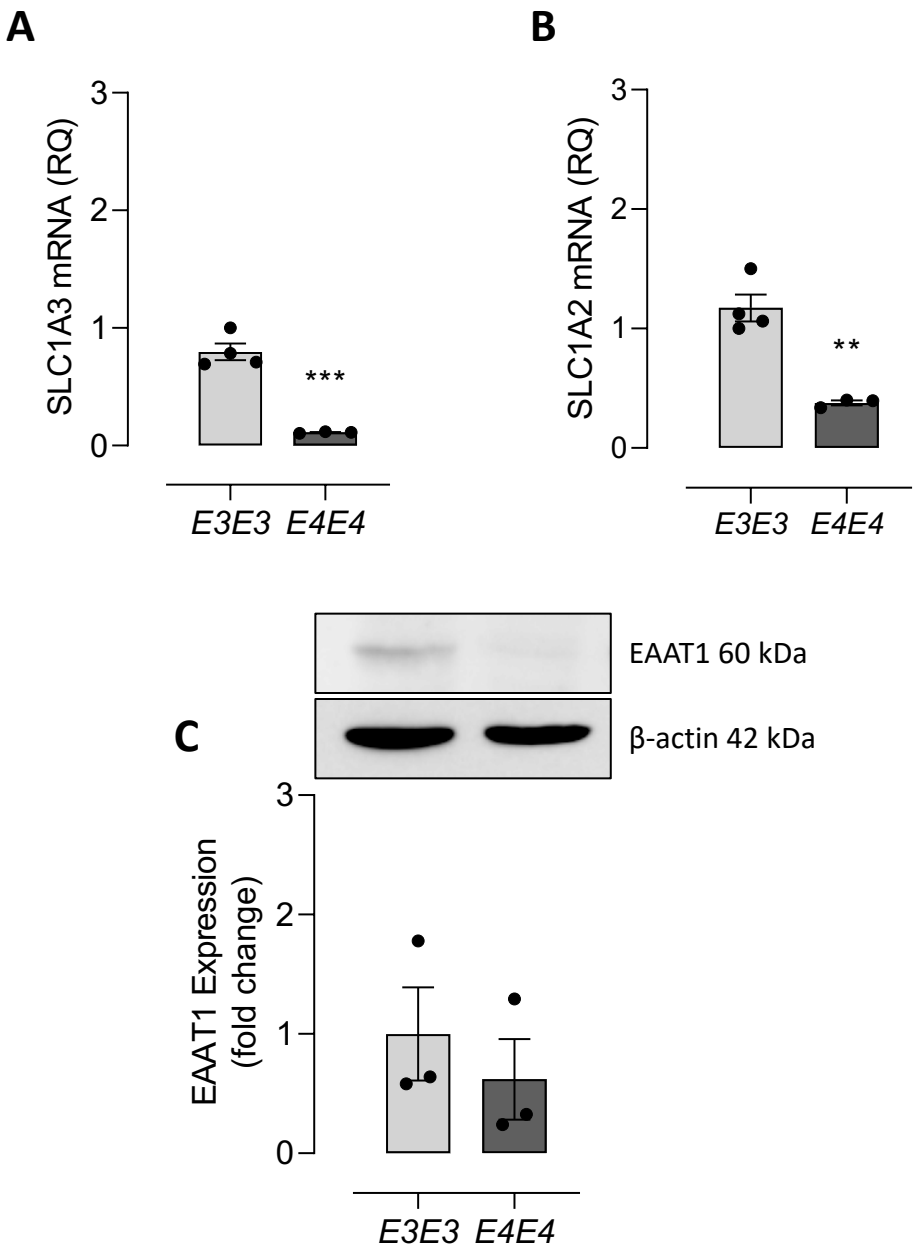


Figure 6.3.2. E4E4 astrocytes have significantly reduced glutamate transporter mRNA expression but no change in EAAT1 protein expression.

*E4E4 astrocytes have significantly less baseline mRNA expression of glutamate transporters SLC1A3 (A) and SLC1A2 (B) compared to E3E3 astrocytes. EAAT1 transporter expression does not significantly differ between E3E3 and E4E4 astrocytes (C). Data expressed as mean ± SEM (N=3, n=3-4). ** p < 0.01, *** p < 0.001 vs E3E3. SLC1A3 t = 8.214, df = 5, p = 0.0004; SCL1A2 t = 5.914, df = 5, p = 0.0020; EAAT1 t = 0.7381, df = 4, p = 0.5014 (Unpaired t-test).*

6.3.2 Inflammatory insult affects glutamate transporter expression

Given that astrocyte reactivity state has previously been shown to impact glutamate transporter expression in rodents, levels of EAAT1 and EAAT2 were examined following inflammatory insult delivered via microglial factors IL1α, TNFα and C1q.

Initial one-way ANOVA analysis carried out to assess the effect of inflammatory factors on *SLC1A3* and *SLC1A2* mRNA expression independently from genotype indicated that astrocyte reactivity increased transporter expression. In *E3E3* astrocytes, *SLC1A3* was not affected (Figure 6.3.3. A) but *SLC1A2* mRNA expression significantly increased following inflammatory insult ($p < 0.001$; Figure 6.3.3. B). In *E4E4* astrocytes, both *SLC1A3* and *SLC1A2* mRNA expression was increased in reactive astrocytes ($p < 0.001$; Figure 6.3.3. C-D). When the combined impact of APOE genotype and astrocyte reactivity state were examined by the more powerful two-way ANOVA, the effect of inflammatory insult on *SLC1A3* mRNA expression is lost (Figure 6.3.4. A). However astrocyte reactivity significantly increases *SLC1A2* mRNA expression in both *E3E3* and *E4E4* astrocytes ($p < 0.001$; Figure 6.3.4. B). Analysis of EAAT1 at the protein level showed no effect of reactivity on transporter expression in *E3E3* or *E4E4* astrocytes (Figure 6.3.5).

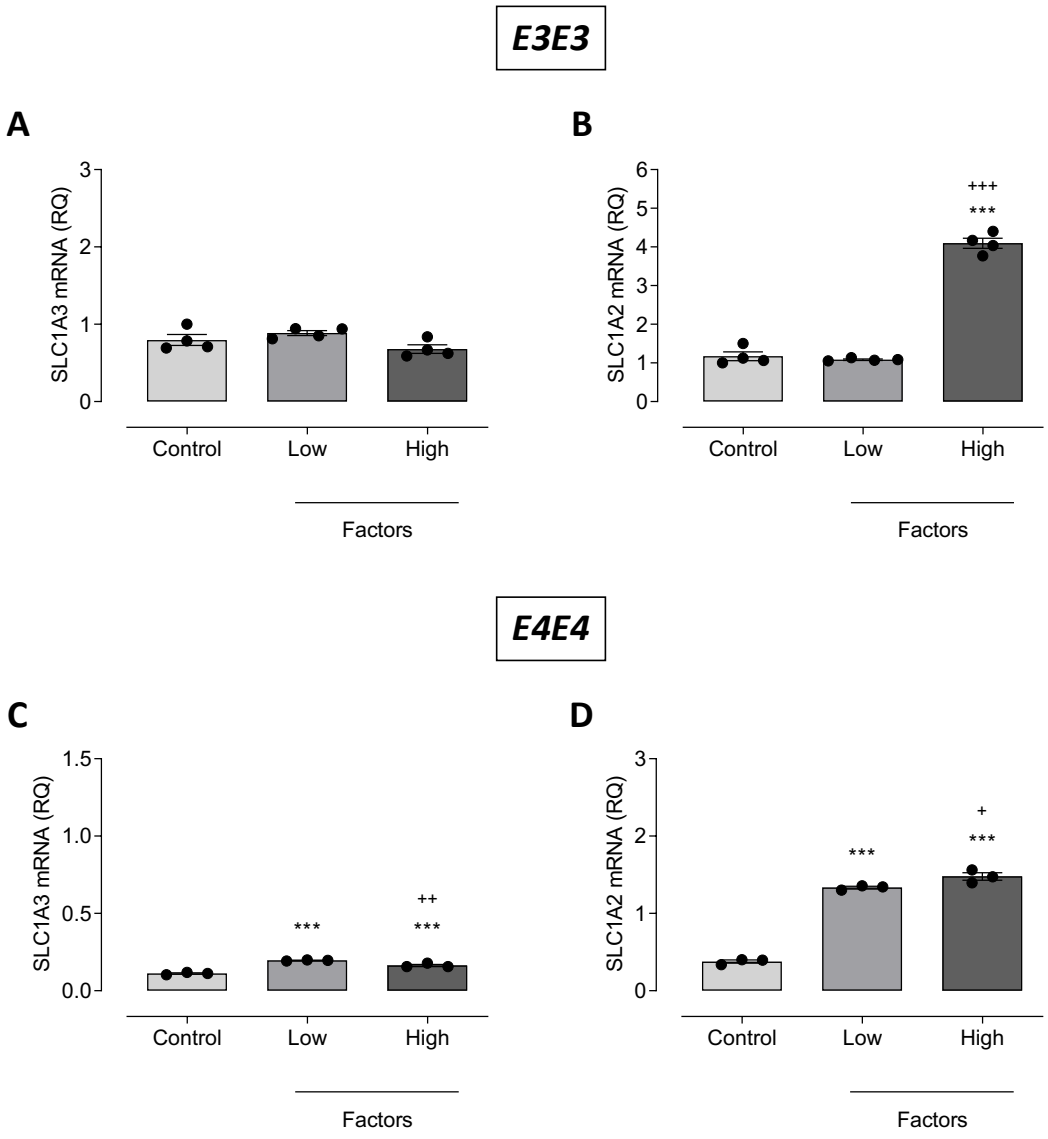


Figure 6.3.3. Inflammatory microglial factors affect SLC1A3 and SLC1A2 mRNA expression in E3E3 and E4E4 astrocytes.

*Inflammatory microglial factors do not affect SLC1A3 mRNA expression in E3E3 astrocytes (A) but significantly increase SLC1A2 mRNA expression at a high dose (B). Inflammatory microglial factors significantly increase SLC1A3 (C) and SLC1A2 (D) mRNA expression in E4E4 astrocytes. Data expressed as mean ± SEM (N=3, n=3-4). *** p < 0.001 vs control; $^{+}$ p < 0.05, $^{++}$ p < 0.01, $^{+++}$ p < 0.001 vs factors low. E3E3 SLC1A3 F(2, 9) = 3.563, p = 0.0725; SLC1A2 F(2, 9) = 287.7, p = < 0.0001. E4E4 SLC1A3 F(2, 6) = 75.07, p < 0.0001; SLC1A2 F(2, 6) = 350.5, p < 0.0001 (One-way ANOVA with Newman-Keuls post hoc).*

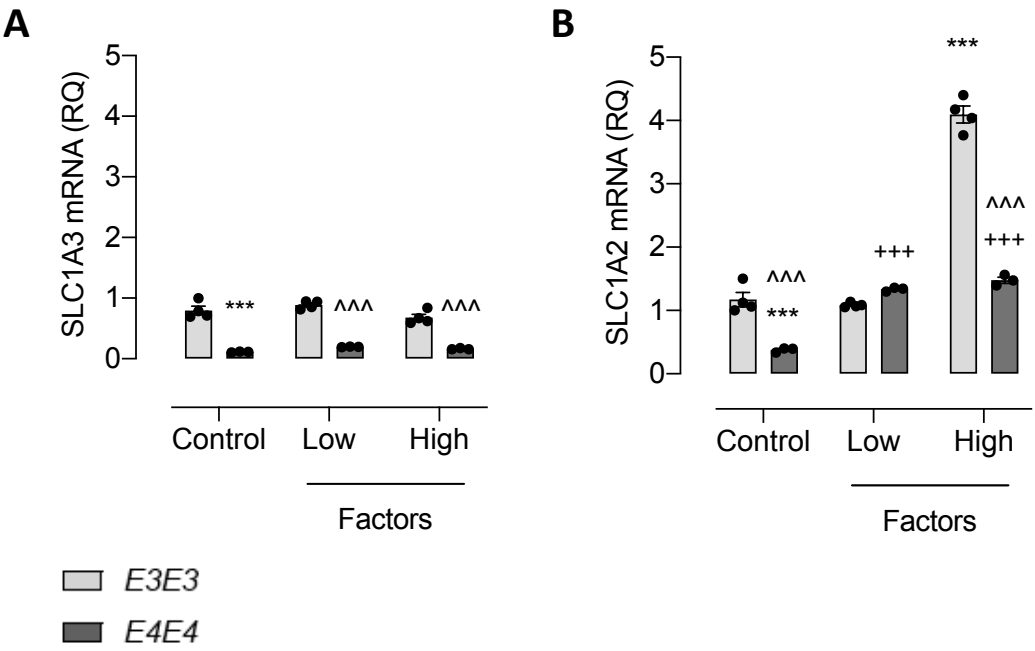


Figure 6.3.4. Inflammatory microglial factors do not affect SLC1A3 mRNA expression but significantly increase SLC1A2 mRNA expression in E3E3 and E4E4 astrocytes.

*SLC1A3 mRNA expression is unchanged following stimulation with inflammatory microglial factors but is significantly reduced in E4E4 astrocytes compared to E3E3 astrocytes (A). SLC1A2 mRNA expression is significantly increased following stimulation with inflammatory microglial factors in both E3E3 and E4E4 astrocytes (B). Data expressed as mean ± SEM (N=3, n=3-4). *** $p < 0.001$ vs E3E3 control; $^{+++}$ $p < 0.001$ vs E4E4 control; ^^^ $p < 0.001$ vs E3E3 genotype. SLC1A3 genotype effect $F(1, 15) = 281.2$, $p = < 0.0001$; effect of factors $F(2, 15) = 3.606$, $p = 0.0527$; Interaction effect $F(2, 15) = 2.320$, $p = 0.1325$. SLC1A2 genotype effect $F(1, 15) = 222.3$, $p = < 0.0001$; effect of factors $F(2, 15) = 298.8$, $p = < 0.0001$; Interaction effect $F(2, 15) = 140.3$, $p = < 0.0001$ (Two-way ANOVA with Bonferroni post hoc).*

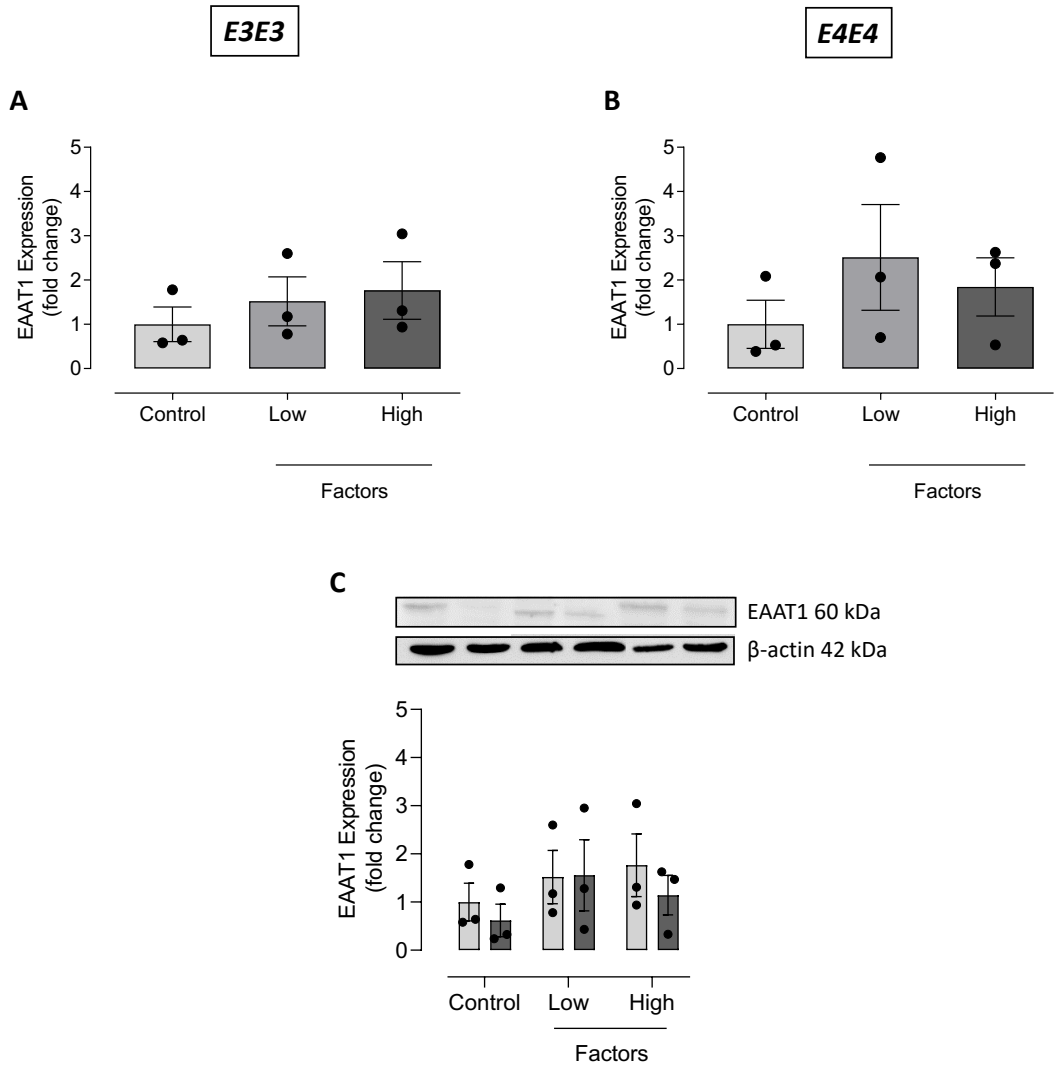


Figure 6.3.5. EAAT1 protein expression in E3E3 and E4E4 astrocytes following inflammatory insult.

Inflammatory microglial factors do not effect EAAT1 expression in E3E3 (A) or E4E4 (B) astrocytes. APOE genotype does not impact the effect of factors on EAAT1 protein expression (C). Data expressed as mean ± SEM (N=3, n=3). E3E3 F(2, 6) = 0.5209, p = 0.6186; E4E4 F(2, 6) = 0.7983, p = 0.4927 (One-way ANOVA). Genotype effect F(1, 12) = 0.5459, p = 0.4746; Factor effect F(2, 12) = 1.116, p = 0.3593; Interaction effect F(2, 12) =0.1952, p = 0.8252 (Two-way ANOVA).

6.3.3 FGF2 decreases glutamate transporter expression

In the previous chapter, FGF2 was presented as a potential modulator of astrocyte reactivity having attenuated mRNA expression of some reactive astrocyte markers following inflammatory insult. As such, we next aimed to assess the effect of FGF2 on glutamate transporter expression to determine whether it might affect glutamate dynamics in astrocytes. FGF2 (50 ng/mL) was co-administered with microglial factors at both a high (3 ng/mL IL1α, 30 ng/mL TNFα and 400 ng/mL C1q) and low concentration (0.3 ng/mL IL1α, 3 ng/mL TNFα and 40 ng/mL C1q).

FGF2 significantly decreased baseline *SLC1A3* ($p < 0.01$) and *SLC1A2* ($p < 0.001$) mRNA expression in both *E3E3* and *E4E4* astrocytes (Figure 6.3.6). Further to this, FGF2 tends to counteract the increase in transporter mRNA expression induced by inflammatory microglial factors (Figure 6.3.7). The effect of FGF2 on *SLC1A3* mRNA expression remains when a more powerful three-way ANOVA is used to examine all three variables. Interestingly the effect of APOE4 genotype ($p < 0.001$) also persists (Figure 6.3.8). However the effect of FGF2 and APOE genotype on *SLC1A2* mRNA is lost when the more powerful statistical analysis is applied (Figure 6.3.9).

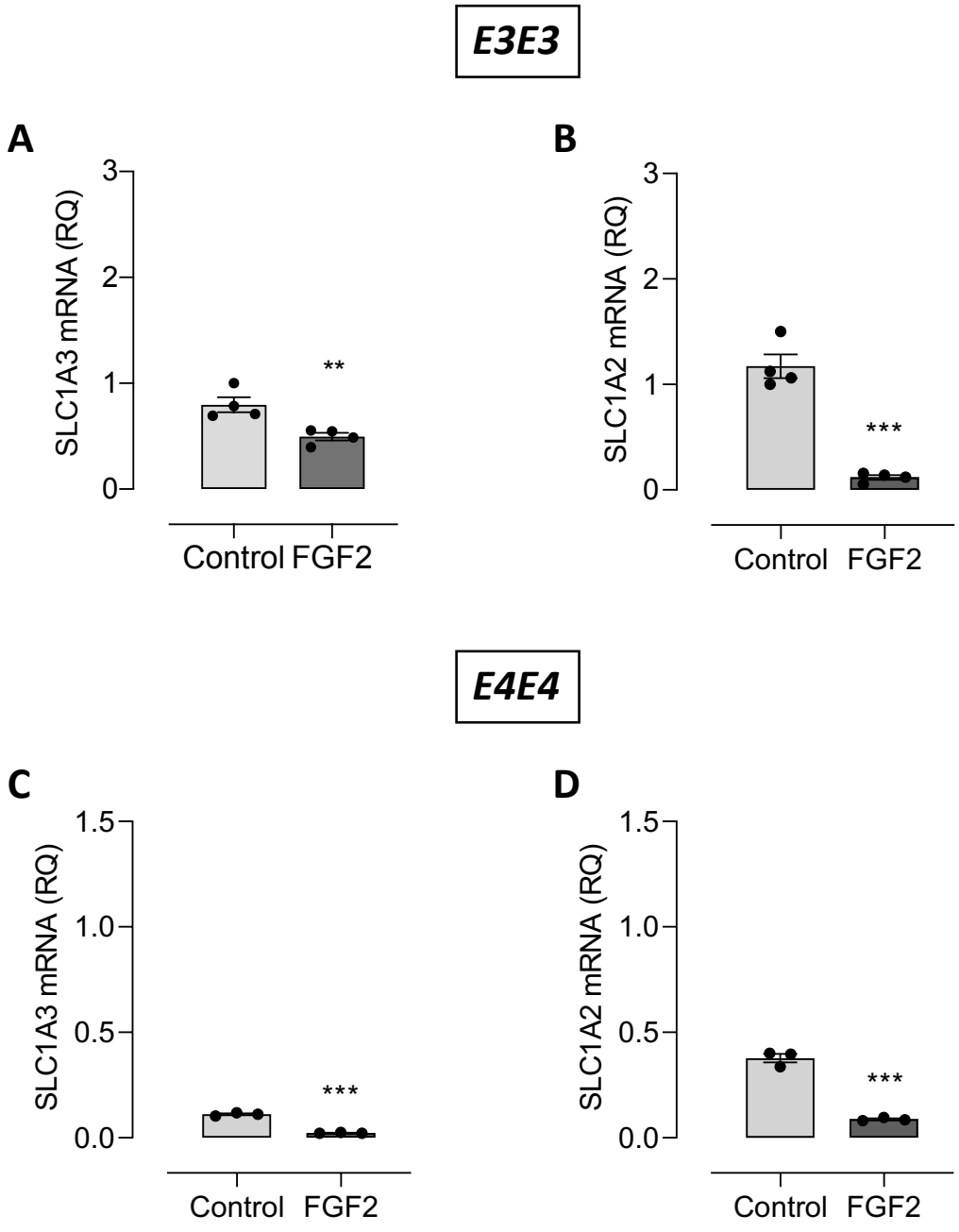


Figure 6.3.6. FGF2 significantly decreases SLC1A3 and SLC1A2 mRNA expression in E3E3 and E4E4 astrocytes.

*FGF2 significantly reduced baseline SLC1A3 (A) and SLC1A2 (B) mRNA expression in E3E3 astrocytes. FGF2 significantly reduced baseline mRNA levels of SLC1A3 (C) and SLC1A2 (D) in E4E4 astrocytes. Data expressed as mean ± SEM (N=3, n=3-4). ** $p < 0.01$, *** $p < 0.001$ vs control. E3E3 SLC1A3 $t = 3.803$, $df = 6$, $p = 0.0089$; SLC1A2 $t = 9.176$, $df = 6$, $p < 0.0001$. E4E4 SLC1A3 $t = 20.46$, $df = 4$, $p < 0.0001$; SLC1A2 $t = 13.71$, $df = 4$, $p = 0.0002$ (Unpaired t-test).*

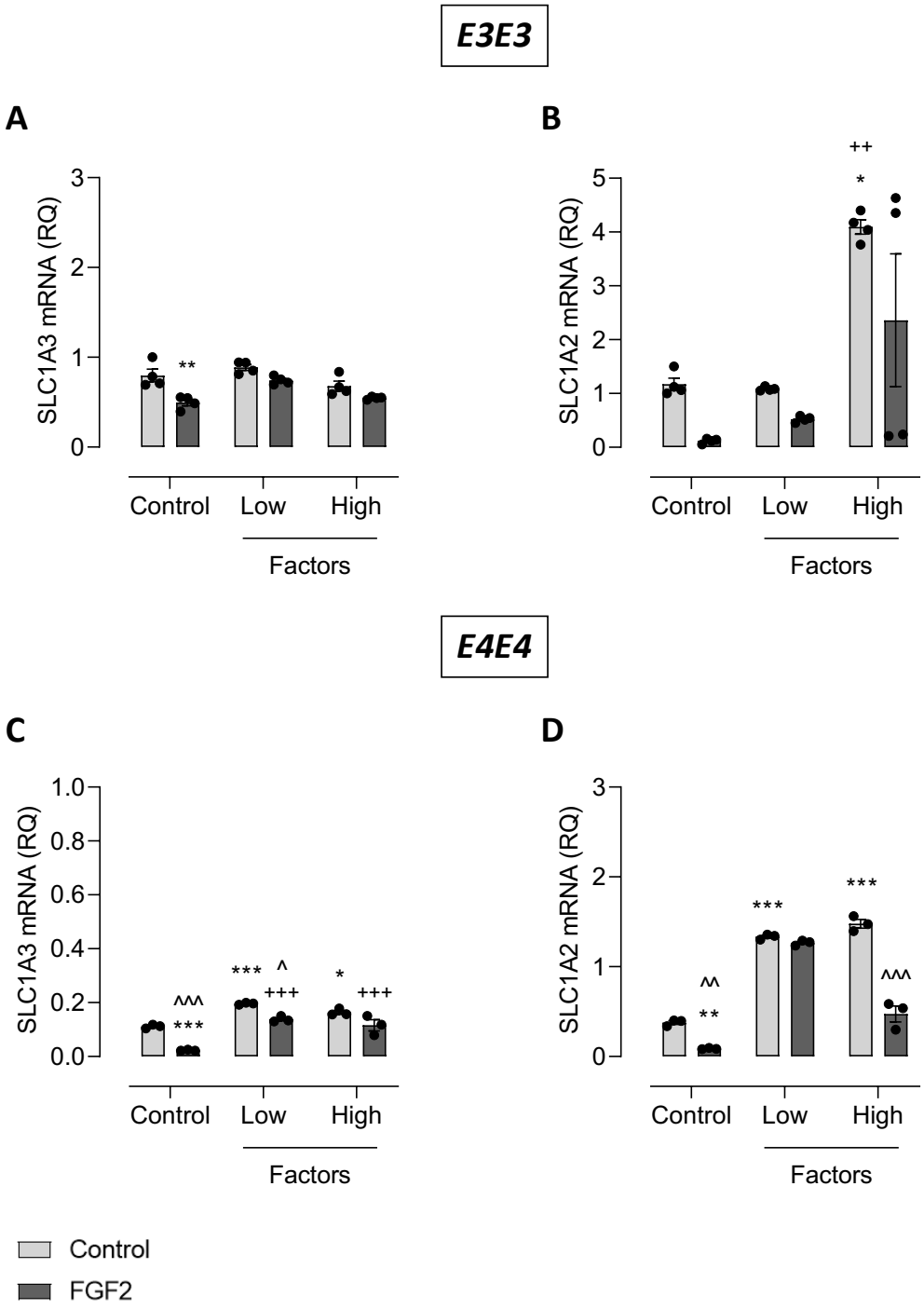


Figure 6.3.7. FGF2 significantly reduces the factor-induced up-regulation of SLC1A3 and SLC1A2. *FGF2 significantly reduces baseline expression of SLC1A3 in E3E3 astrocytes (A). FGF2 tends to decrease SLC1A2 expression in E3E3 astrocytes but does not counteract the factor-induced increase (B). FGF2 counteracts the factor-induced increase in SLC1A3 (C) and SLC1A2 (D) expression in E4E4 astrocytes. Data expressed as mean ± SEM (N=3, n=3-4). * P < 0.05, ** p < 0.01, *** p < 0.001 vs control; $^{++}$ p < 0.01, $^{+++}$ p < 0.001 vs FGF2 control; ^ p < 0.05, ^^ p < 0.01, ^^^ p < 0.001 vs without FGF2. E3E3 SLC1A3 FGF2 effect F(1, 18) = 30.84, p = < 0.0001; effect of factors F(2, 18) = 12.71, p = 0.0004; Interaction effect F(2, 18) = 2.419, p = 0.1174. SLC1A2 FGF2 effect F(1, 18) = 7.231, p =*

0.0150; effect of factors F(2, 18) = 16.18, p = < 0.0001; Interaction effect F(2, 18) = 0.6696, p = 0.5242. E4E4 SLC1A3 FGF2 effect F(1, 12) = 69.51, p = < 0.0001; effect of factors F(2, 12) = 58.95, p = < 0.0001; Interaction effect F(2, 12) = 2.515, p = 0.1224. SLC1A2 FGF2 effect F(1, 12) = 165.6, p = < 0.0001; effect of factors F(2, 12) = 320.9, p = < 0.0001; Interaction effect F(2, 12) = 64.27, p = < 0.0001. (Two-way ANOVA with Bonferroni post hoc).

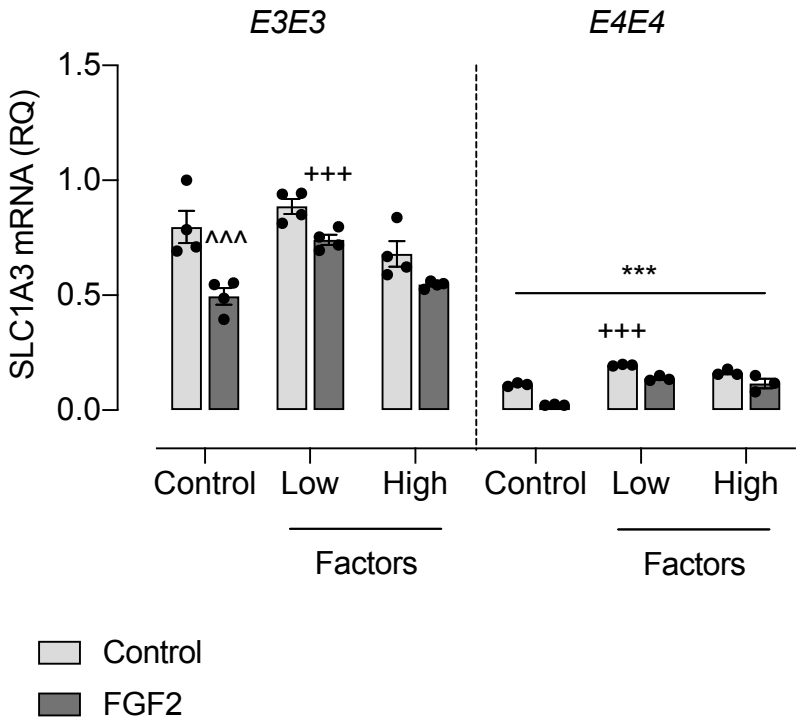


Figure 6.3.8. APOE genotype, astrocyte reactivity state and FGF2 treatment affects SLC1A3 expression.

*Astrocytes were treated with FGF2 (50 ng/mL) either alone or in combination with inflammatory microglial factors (IL1α, TNFα and C1q) at two doses for 24 h. FGF2 significantly reduced SLC1A3 mRNA expression at baseline in E3E3 astrocytes. Stimulation with a low concentration of inflammatory microglial factors increased SLC1A3 mRNA expression, which was attenuated by FGF2 treatment. Overall, E4E4 astrocytes expressed significantly less SLC1A3 compared to E3E3 astrocytes. Data expressed as mean ± SEM (N=3, n=3-4). *** p < 0.001 denotes significant effect of APOE genotype; $^{+++}$ p < 0.001 denotes significant effect of factors; ^^^ p < 0.001 denotes significant effect of FGF2. Effect of factors F(2, 30) = 15.94, p = < 0.0001; effect of APOE genotype F(1, 30) = 734.1, p = < 0.0001; effect of FGF2 F(1, 30) = 38.24, p = < 0.0001; interaction effect F(2, 30) = 1.021, p = 0.3723. (Three-way ANOVA with Bonferroni post hoc). Full three-way ANOVA readout and Bonferroni post hoc can be found in Appendix 6.*

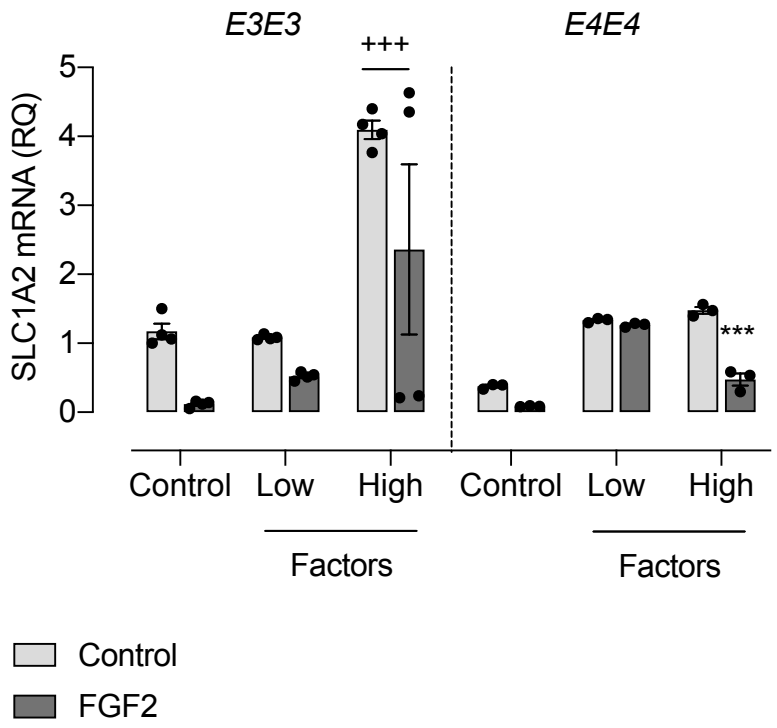


Figure 6.3.9. FGF2 treatment does not alter SLC1A2 expression.

*Astrocytes were treated for 24 h with FGF2 (50 ng/mL) either alone or in combination with inflammatory microglial factors (IL1α, TNFα and C1q) at two doses. FGF2 tends to decrease SLC1A2 expression in E3E3 and E4E4 astrocytes but does not counteract the factor-induced increase. Data expressed as mean ± SEM (N=3, n=3-4). *** p < 0.001 denotes significant effect of APOE genotype; $^{+++}$ p < 0.001 denotes significant effect of factors; ^^^ p < 0.001 denotes significant effect of FGF2. Effect of factors F(2, 30) = 15.54, p = < 0.0001; effect of APOE genotype F(1, 30) = 8.608, p = 0.0064; effect of FGF2 F(1, 30) = 10.18, p = 0.0033; interaction effect F(2, 30) = 0.02959, p = 0.9709. (Three-way ANOVA with Bonferroni post hoc). Full three-way ANOVA readout and Bonferroni post hoc can be found in Appendix 6.*

6.3.4 APOE4 astrocytes show altered glutamate dynamics

Uptake of glutamate from the extracellular space is an important physiological function of astrocytes which is key to maintaining low glutamate levels at the synapse and to preventing excitotoxicity. An investigation was carried out to see if a difference in glutamate uptake existed between the APOE genotypes in hiPSC-derived astrocytes which may contribute to increased AD risk for *APOE4* carriers.

E3E3 and *E4E4* astrocytes show significantly different glutamate dynamics. In terms of glutamate release into the culture medium, *E3E3* astrocytes have a net negative glutamate efflux of approximately 100 µM indirectly indicating glutamate uptake. In contrast, *E4E4* astrocytes have a net positive glutamate efflux of approximately 200 µM suggesting glutamate release into the extracellular environment. This suggests a significant difference in glutamate release between genotypes ($p < 0.05$; Figure 6.3.10. A-B). Glutamate uptake (as assessed from cell lysates) is also significantly different between genotypes with *E3E3* astrocytes taking up approximately 120 µM of glutamate compared to 30 µM taken up by *E4E4* astrocytes ($p < 0.001$; Figure 6.3.10. C-D).

Reducing extracellular concentrations of glutamate did not alter this genotype-dependent effect on glutamate dynamics. This reduction in extracellular glutamate was achieved by removing the glutamic acid containing media ingredients GlutaMAX and non-essential amino acids for 24 h, and successfully reduced extracellular glutamate from approximately 200 µM to 100 µM. The same trend in glutamate release remained with *E3E3* astrocytes presenting a net negative glutamate release of 50 µM and *E4E4* astrocytes had a net positive glutamate release of 20 µM ($p < 0.001$; Figure 6.3.11. A-B). As before, *E3E3* astrocytes had significantly greater glutamate uptake of 250 µM compared to 20 µM in *E4E4* astrocytes ($p < 0.05$; Figure 6.3.11. C-D).

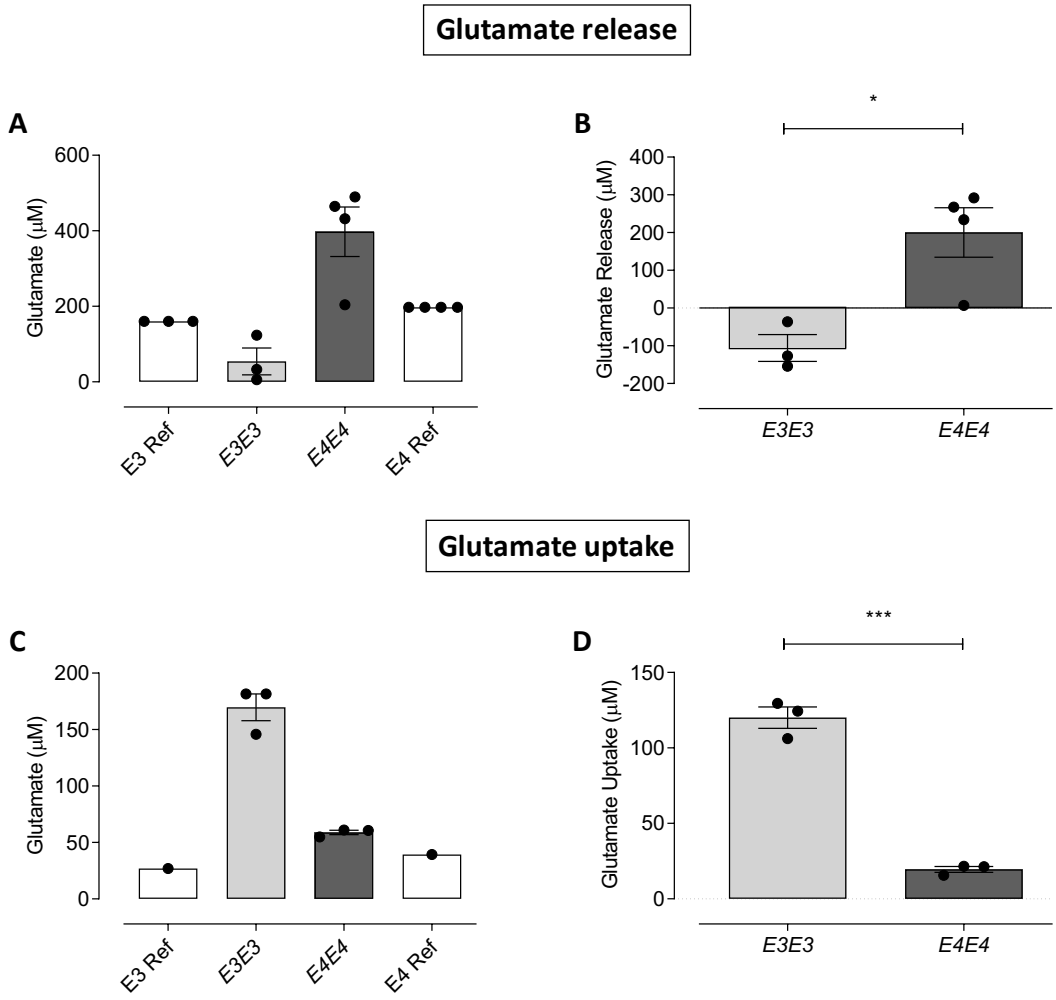


Figure 6.3.10. APOE genotype affects glutamate dynamics in iPSC-derived astrocytes.

*Glutamate is taken up from media by E3E3 astrocytes while E4E4 astrocytes release glutamate (A, B). E4E4 astrocytes have reduced glutamate uptake compared to E3E3 astrocytes (C, D). Data expressed as mean ± SEM (N=3, n=3-4). * $p < 0.05$, *** $p < 0.001$ vs control. Glutamate release $t = 3.689$, $df = 5$, $p = 0.0142$; glutamate uptake $t = 13.66$, $df = 4$, $p = 0.0002$ (Unpaired t-test).*

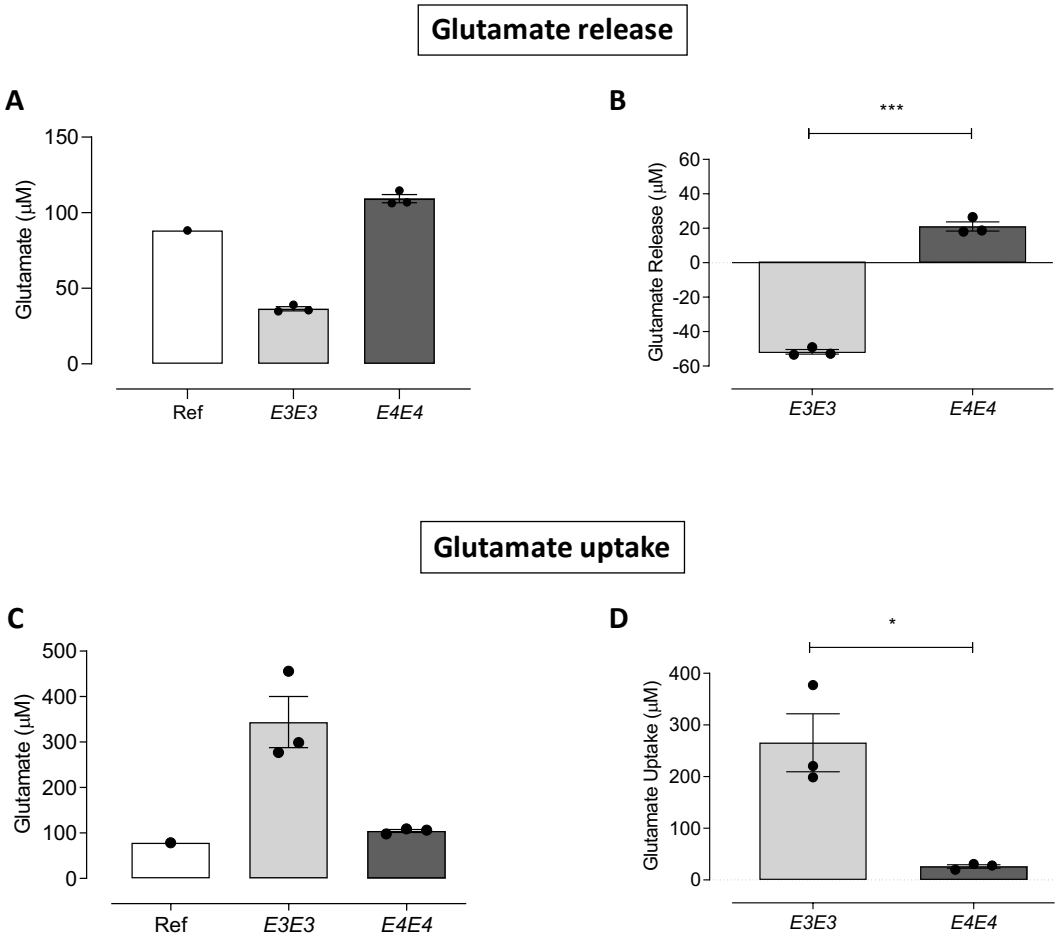


Figure 6.3.11. Reducing extracellular glutamate does not alter the genotype effect on glutamate dynamics.

*There is a net glutamate uptake from media by E3E3 astrocytes while E4E4 astrocytes release glutamate (A, B). E4E4 astrocytes have significantly reduced glutamate uptake compared to E3E3 astrocytes (C, D). Data expressed as mean ± SEM (N=3, n=3-4). * $p < 0.05$, *** $p < 0.001$ vs control. Glutamate release $t = 24.24$, $df = 4$, $p = < 0.0001$; glutamate uptake $t = 4.251$, $df = 4$, $p = 0.0132$ (Unpaired t-test).*

6.3.5 Astrocyte reactivity state does not affect glutamate dynamics

In AD, high extracellular levels of glutamate have been reported in conjunction with alterations in astrocytic glutamate transporters EAAT1 and EAAT2 believed to have an important role. The role of neuroinflammation in altering glutamate transport in human iPSC-derived APOE3 and APOE4 homozygous astrocytes has yet to be established. In order to determine whether astrocyte reactivity state leads to a functional change in glutamate dynamics on iPSC-derived astrocytes, the astrocytes were stimulated with inflammatory microglial factors IL1α, TNFα and C1q. Media and lysates were then collected to read extracellular and intracellular glutamate concentration respectively.

Astrocyte reactivity did not alter glutamate dynamics in *E3E3* or *E4E4* astrocytes with no discernible change in extracellular glutamate concentration across treatment groups. However, *E3E3* astrocytes were clearly taking up glutamate from the media while the *E4E4* astrocytes released glutamate into the media (Figure 6.3.12. A, C). There was a trend for reactivity to increase glutamate uptake in both *E3E3* and *E4E4* astrocytes but this did not translate to a significant effect of stimulation (Figure 6.3.12. B, D). There was no significant interaction of astrocyte reactivity state with APOE genotype, that is to say that APOE genotype did not affect glutamate dynamics as a function of exposure to inflammatory microglial factors. The levels of glutamate in the media of *E3E3* and *E4E4* astrocytes suggested that the *E3E3* astrocytes were again removing considerably more glutamate compared to their *E4E4* counterparts. Analysis inferred that altered glutamate dynamics in *E4E4* astrocytes is as a function of APOE genotype and independent of reactivity state ($p < 0.001$; Figure 6.3.13).

Extracellular glutamate concentration was reduced in an attempt to tease out any effect astrocyte reactivity state may be having on glutamate dynamics. As before *E3E3* astrocytes removed glutamate from the media while *E4E4* astrocytes effluxed glutamate into the media (Figure 6.3.14 A, C) but this did not change as a function of reactivity state. Both genotypes had some level of glutamate uptake, as determined from cell lysates, but with no significant effect of stimulation (Figure 6.3.14. B, D). Overall the data confirms the previous result that altered glutamate dynamics in *E4E4* astrocytes compared to *E3E3* astrocytes is a genotype-specific effect and independent of inflammatory insult ($p < 0.001$; Figure 6.3.15).

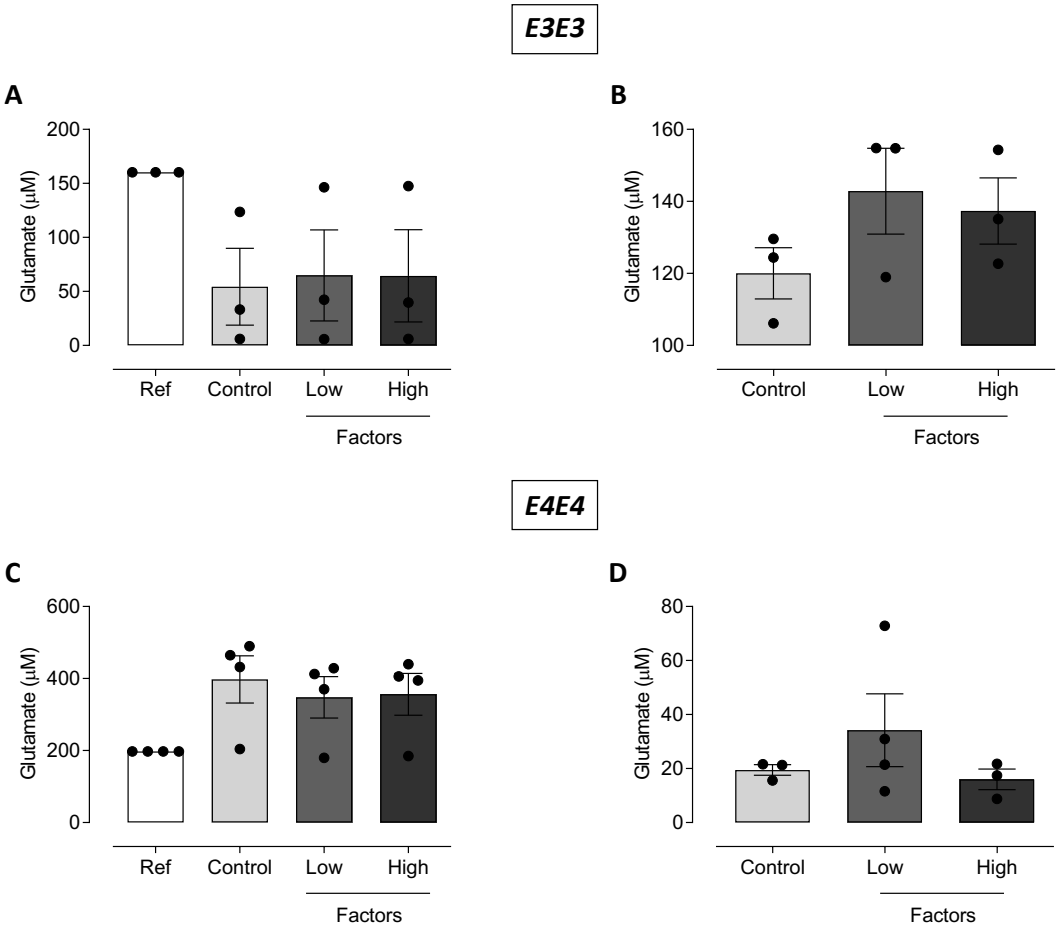


Figure 6.3.12. Inflammatory microglial factors do not affect glutamate dynamics in iPSC-derived astrocytes.

Stimulation with inflammatory microglial factors did not alter glutamate release (A) or uptake (B) in E3E3 astrocytes, as determined from media and lysates respectively. There was a net decrease in glutamate concentration compared to the reference media sample (A). Inflammatory microglial factors did not affect glutamate release (C) or uptake (D) in E4E4 astrocytes compared to control. There was a net increase in media glutamate concentrations from these astrocytes compared to the reference media sample. Data expressed as mean ± SEM (N=3, n=3-4). E3E3 glutamate release $F(3, 8) = 2.039$, $p = 0.1870$; glutamate uptake $F(2, 6) = 1.530$, $p = 0.2904$. E4E4 glutamate release $F(3, 12) = 2.806$, $p = 0.0849$; glutamate uptake $F(2, 7) = 1.023$, $p = 0.4075$ (One-way ANOVA).

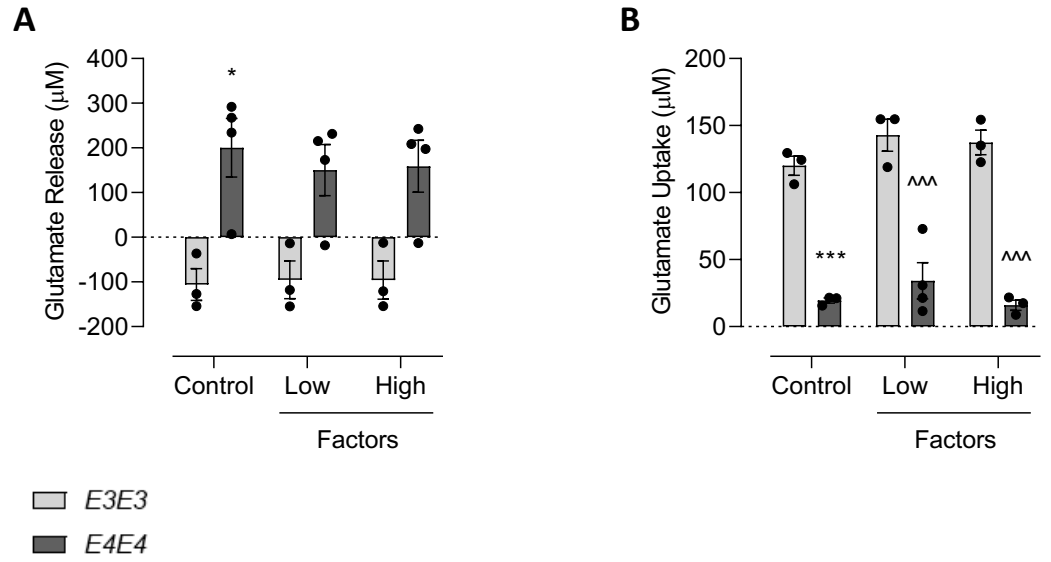


Figure 6.3.13. Glutamate dynamics which are altered in E4E4 astrocytes is independent of reactivity state.

*E3E3 astrocytes show net glutamate uptake while E4E4 astrocytes show net glutamate release as determined from extracellular media glutamate concentrations (A). E4E4 astrocytes show reduced glutamate uptake compared to E3E3 astrocytes, as determined from intracellular glutamate concentrations (B). Data expressed as mean ± SEM (N=3, n=3-4). * p < 0.05, *** p < 0.001 vs E3E3 control; ^^^ p < 0.001 vs E3E3 genotype. Glutamate release effect of factors F(2, 15) = 0.06909, p = 0.9335; effect of genotype F(1, 15) = 34.73, p = < 0.0001; interaction effect F(2, 15) = 0.1702, p = 0.8451. Glutamate uptake effect of factors F(2, 13) = 1.917, p = 0.1864; effect of genotype F(1, 13) = 187.6, p = < 0.0001; interaction effect F(2, 13) = 0.5426, p = 0.5939 (Two-way ANOVA with Bonferroni post hoc).*

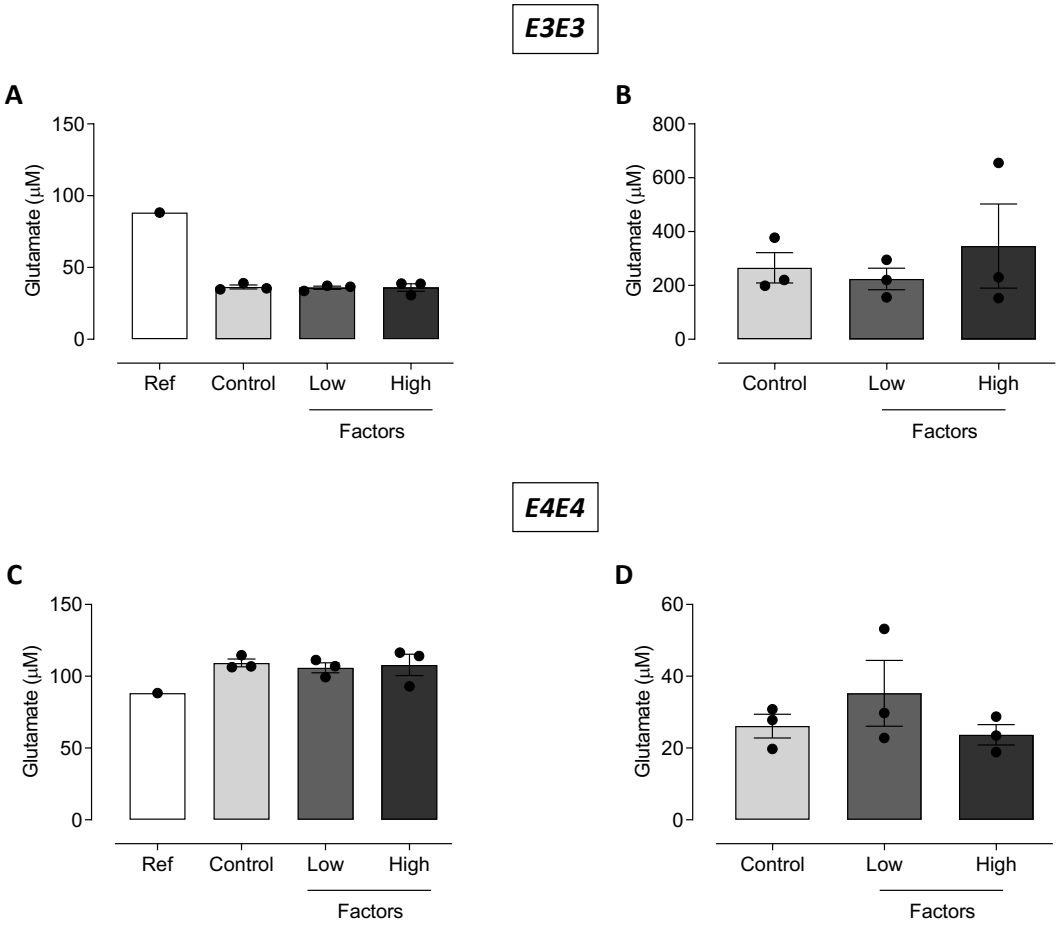


Figure 6.3.14. Reducing extracellular glutamate does not alter the effect of inflammatory microglial factors on glutamate dynamics in iPSC-derived astrocytes.

Reducing extracellular glutamate concentration prior to stimulation with inflammatory microglial factors does not alter glutamate dynamics in iPSC-derived E3E3 and E4E4 astrocytes. Stimulation with inflammatory microglial factors does not affect glutamate release (A) or uptake (B) in E3E3 astrocytes, as determined from media and lysates respectively. There was a net decrease in glutamate concentration compared to the reference media sample (A). Inflammatory microglial factors did not affect glutamate release (C) or uptake (D) in E4E4 astrocytes compared to control. There was a net increase in media glutamate concentrations from these astrocytes compared to the reference media sample. Data expressed as mean ± SEM (N=3, n=3-4). E3E3 glutamate release $F(3, 6) = 81.20$, $p = < 0.0001$; glutamate uptake $F(2, 6) = 0.3956$, $p = 0.6896$. E4E4 glutamate release $F(3, 6) = 1.602$, $p = 0.2849$; glutamate uptake $F(2, 6) = 1.077$, $p = 0.3984$ (One-way ANOVA).

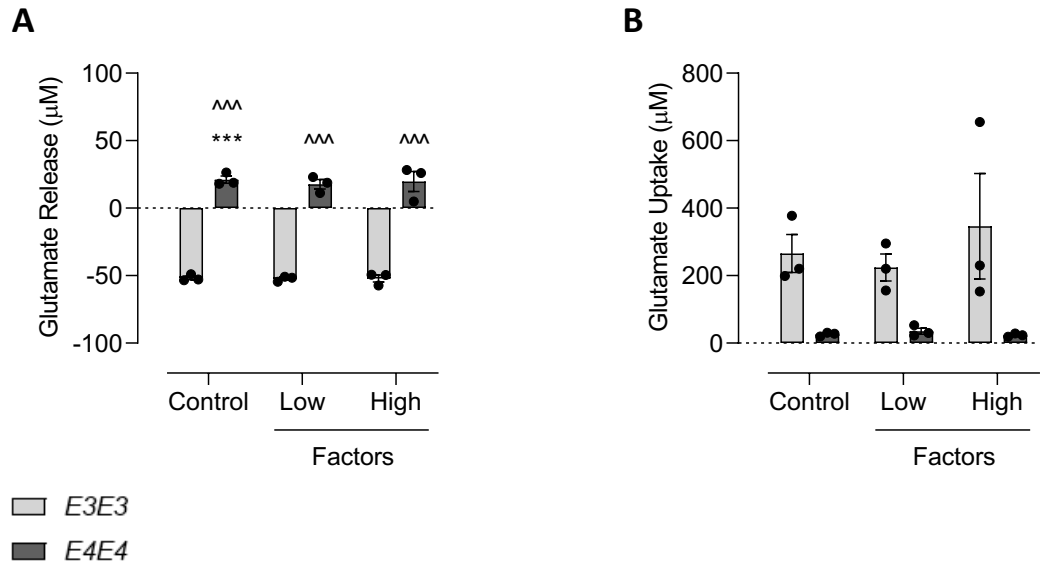


Figure 6.3.15. Reducing extracellular glutamate does not alter the APOE dependent effect on glutamate dynamics.

*E3E3 astrocytes show net glutamate uptake while E4E4 astrocytes show net glutamate release, as determined from extracellular media glutamate concentrations (A). E4E4 astrocytes show reduced glutamate uptake compared to E3E3 astrocytes as determined from intracellular glutamate concentrations (B). Data expressed as mean ± SEM (N=3, n=3-4). *** p < 0.001 vs E3E3 control; ^^^ p < 0.001 vs E3E3 genotype. Glutamate release effect of factors F(2, 12) = 0.1413, p = 0.8697; effect of genotype F(1, 12) = 543.4, p = < 0.0001; interaction effect F(2, 12) = 0.07042, p = 0.9324. Glutamate uptake effect of factors F(2, 12) = 0.3302, p = 0.7251; effect of genotype F(1, 12) = 19.23, p = < 0.0009; interaction effect F(2, 12) = 0.4658, p = 0.6385 (Two-way ANOVA with Bonferroni post hoc).*

6.3.6 *GLUL* expression in *E3E3* and *E4E4* astrocytes

With *E3E3* and *E4E4* astrocytes displaying a striking difference in glutamate dynamics we were interested to further investigate the glutamate-glutamine cycle in these cells. Once glutamate is taken up by the astrocyte it is converted to glutamine by the enzyme glutamine synthetase so *GLUL* mRNA expression was examined in our astrocytes. Baseline expression of *GLUL* mRNA was significantly greater in *E4E4* astrocytes compared to *E3E3* astrocytes ($p < 0.001$; Figure 6.3.16).

In order to examine whether astrocyte reactivity state may also affect *GLUL* mRNA expression we examined *GLUL* levels in astrocytes following stimulation with the inflammatory microglial factors IL1α, TNFα and C1q. Indeed reactivity had the effect of increasing *GLUL* mRNA expression in both *E3E3* and *E4E4* astrocytes ($p < 0.001$; Figure 6.3.18. A-B) and to a greater extent in the *E4E4* astrocytes when compared statistically by a two-way ANOVA ($p < 0.05$; Figure 6.3.17. C).

Given that FGF2 had the effect of reducing glutamate transporter mRNA expression its effect on *GLUL* was also assessed. FGF2 tended to increase baseline *GLUL* in *E3E3* astrocytes but significantly decreased baseline *GLUL* in *E4E4* astrocytes ($p < 0.01$; Figure 6.3.18. A-B). FGF2 opposed the factor induced increase in *GLUL* expression in both *E3E3* and *E4E4* astrocytes ($p < 0.05$; Figure 6.3.18. C-D). This effect of factors and FGF2 on *GLUL* mRNA expression remains when the more powerful three-way ANOVA analysis is applied in order to account for all three variables; APOE genotype, reactivity state and FGF2 treatment (Figure 6.3.19).

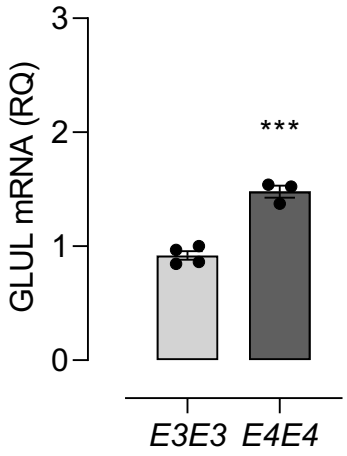


Figure 6.3.16. E4E4 astrocytes have significantly increased baseline GLUL mRNA expression compared to E3E3 astrocytes.

*APOE genotype affects GLUL baseline mRNA with expression significantly greater in E4E4 astrocytes compared to E3E3 astrocytes. Data expressed as mean ± SEM (N=3, n=3-4). *** p < 0.001 vs E3E3; t = 8.849, df = 5, p = 0.0003 (Unpaired t-test).*

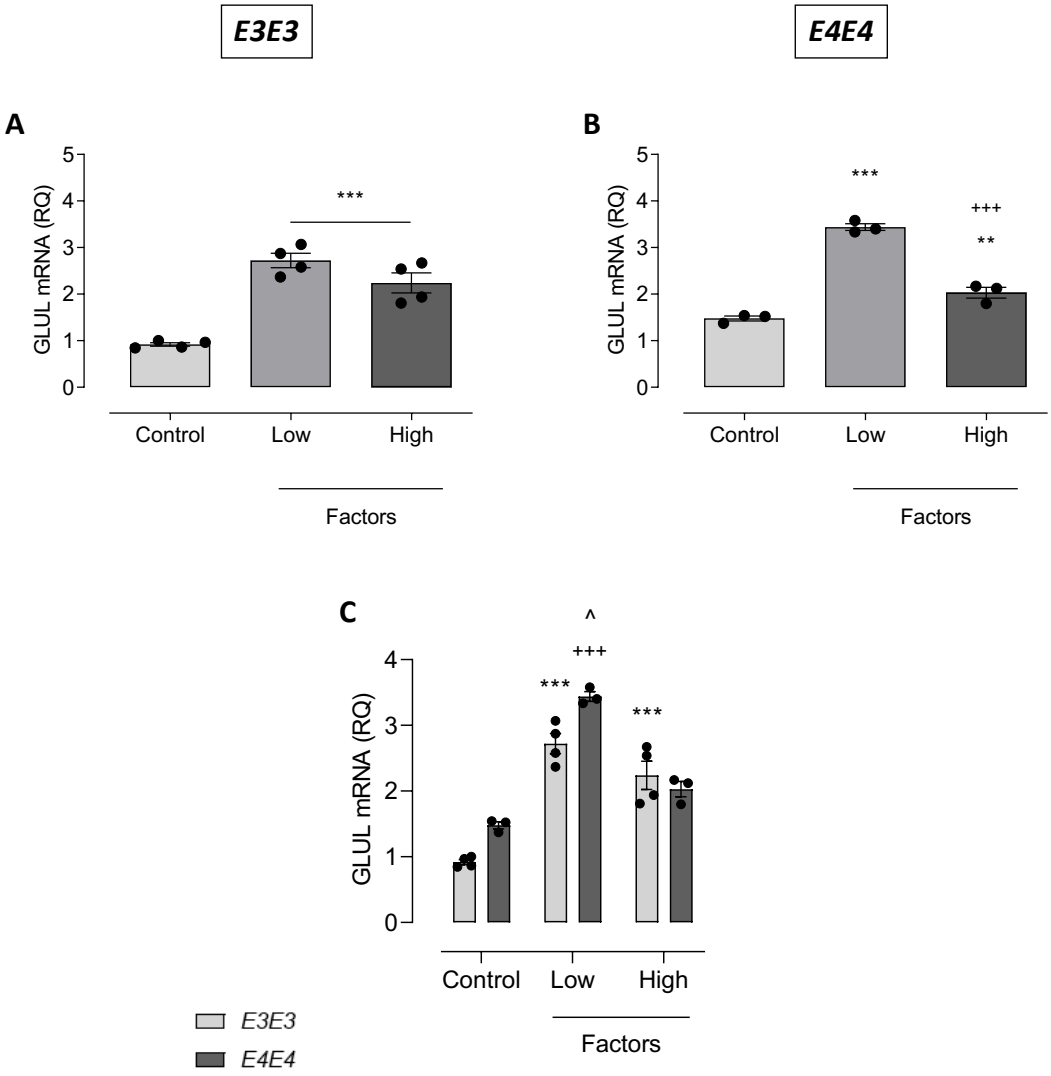


Figure 6.3.17. Inflammatory microglial factors significantly increase GLUL mRNA expression in E3E3 and E4E4 astrocytes.

*Stimulation with inflammatory microglial factors increased GLUL mRNA expression in both E3E3 (A) and E4E4 astrocytes (B). This reactivity induced increase in GLUL expression is comparable across both genotypes (C). Data expressed as mean ± SEM (N=3, n=3-4). ** p < 0.01, *** p < 0.001 vs control/ E3E3 control; $^{+++}$ p < 0.001 vs factors low/E4E4 control; ^ p < 0.05 vs E3E3 genotype. E3E3 F(2, 9) = 36.57, p = < 0.0001; E4E4 F(2, 6) = 141.8, p < 0.0001 (One-way ANOVA with Newman-Keuls post hoc). Genotype effect F(1, 15) = 9.880, p = 0.0067; effect of factors F(2, 15) = 92.22, p = < 0.001; Interaction effect F(2, 15) = 6.421, p = 0.0097 (Two-way ANOVA with Bonferroni post hoc).*

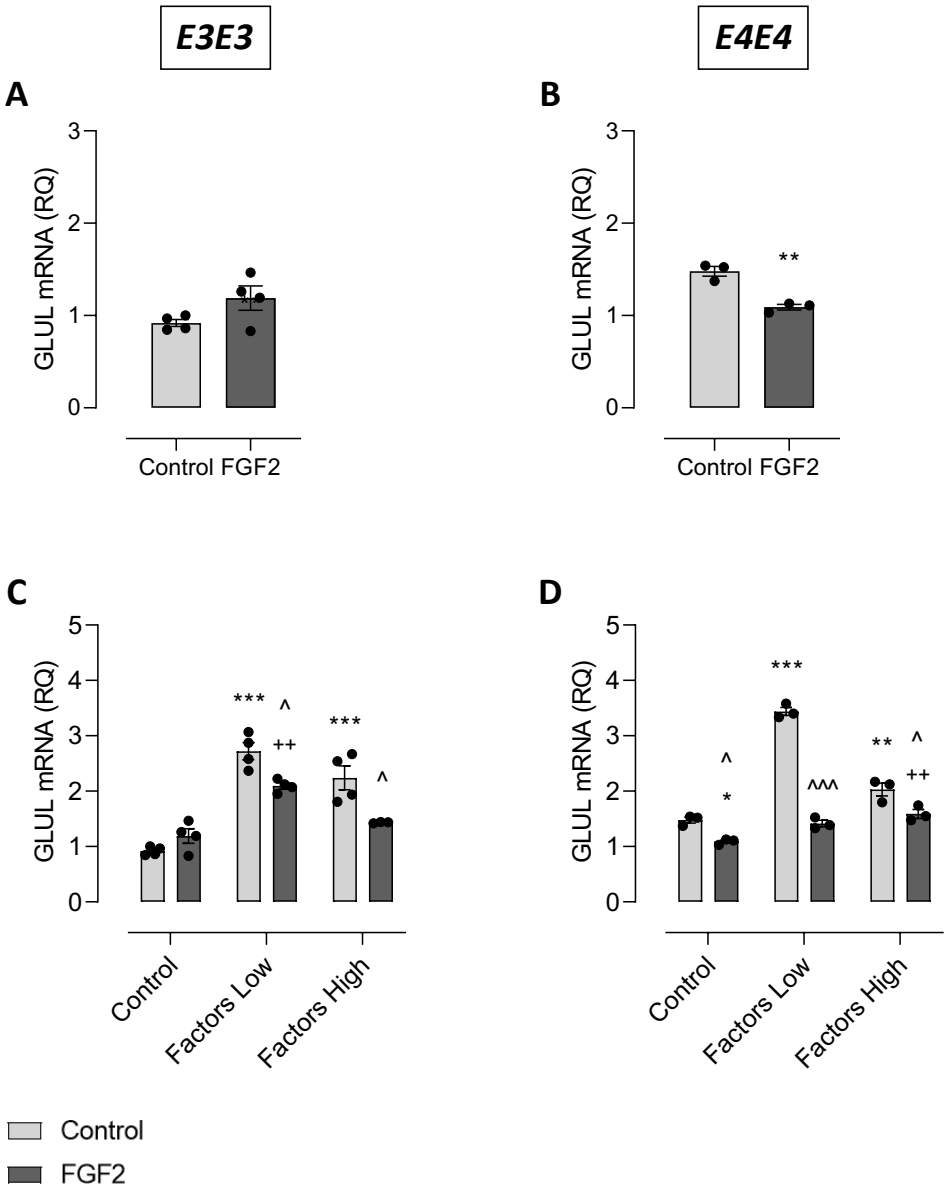


Figure 6.3.18. FGF2 attenuates the effect of reactivity on GLUL expression in iPSC-derived astrocytes.

*FGF2 tends to increase GLUL mRNA expression in E3E3 astrocytes (A), but decrease GLUL in E4E4 astrocytes (B). FGF2 opposes the factor induced increase in GLUL expression in E3E3 astrocytes (C). FGF2 returns GLUL expression levels to control following stimulation with factors in E4E4 astrocytes (D). Data expressed as mean ± SEM (N=3, n=3-4). * p < 0.05, ** p < 0.01, *** p < 0.001 vs control; ++ p < 0.001 vs FGF2 control; ^ p < 0.05, ^^^ p < 0.001 vs without FGF2. E3E3 GLUL t = 1.957, df = 6, p = 0.0981; E4E4 GLUL t = 6.382, df = 4, p = 0.0031 (Unpaired t-test). E3E3 FGF2 effect F(1, 17) = 13.23, p = 0.0020; effect of factors F(2, 17) = 56.81, p = < 0.0001; Interaction effect F(2, 17) = 9.819, p = 0.0015. E4E4 FGF2 effect F(1, 12) = 253.4, p = < 0.0001; effect of factors F(2, 12) = 122.2, p = < 0.0001; Interaction effect F(2, 12) = 80.68, p = < 0.0001.*

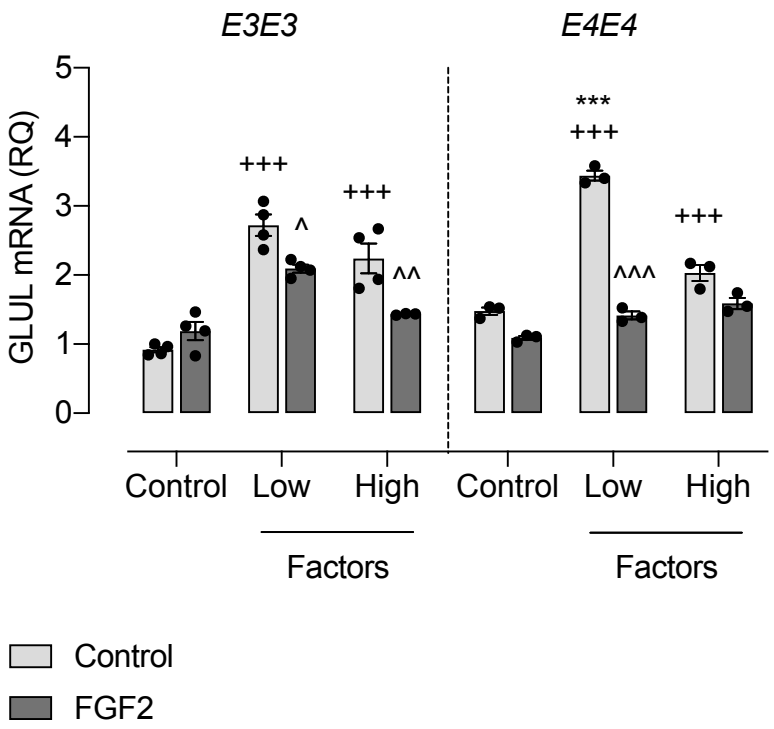


Figure 6.3.19. FGF2 tends to attenuate the factor induced increase in GLUL mRNA expression.

*Astrocytes were treated for 24 h with FGF2 (50 ng/mL) either alone or in combination with inflammatory microglial factors (IL1α, TNFα and C1q) at two doses. FGF2 attenuates the factor induced increase in GLUL mRNA expression in E3E3 and E4E4 astrocytes. Data expressed as mean ± SEM (N=3, n=3-4). *** $p < 0.001$ denotes significant effect of APOE genotype; $^{+++}$ $p < 0.001$ denotes significant effect of factors; ^ $p < 0.05$, ^^ $p < 0.001$; ^^^ $p < 0.001$ denotes significant effect of FGF2. Effect of factors $F(2, 29) = 119.4$, $p = < 0.0001$; effect of APOE genotype $F(1, 29) = 1.246$, $p = 0.2735$; effect of FGF2 $F(1, 29) = 100.8$, $p = < 0.0001$; interaction effect $F(2, 29) = 14.43$, $p = < 0.0001$. (Three-way ANOVA with Bonferroni post hoc). Full three-way ANOVA readout and Bonferroni post hoc can be found in Appendix 6.*

6.4 Discussion

Alzheimer's disease is a complex condition with several areas of neural homeostatic control becoming prone to dysregulation, dysfunction and leading to widespread cell death. Despite AD being the focus of intense research over recent decades, it has proven difficult to disentangle the mechanisms underlying its many pathological processes, including Aβ and tau deposition, neuroinflammation and excitotoxicity. The human *APOE4* gene is one of the major genetic risk factors for sporadic AD, but the reason why remains poorly understood. In this study we aimed to elucidate the relationship between APOE genotype, astrocyte reactivity state, glutamate transporter expression and glutamate dynamics in human iPSC-astrocytes. We investigated whether astrocytic expression levels of the most important glutamate transporters and glutamate dynamics are modulated by APOE genotype and whether this changes with exposure to inflammatory insult. Data from this study indicates that astrocyte reactivity state has no effect on glutamate handling while APOE genotype impacts glutamate transporter expression levels and glutamate dynamics, when assessed by qPCR, Western blotting and glutamate assay. This genotype effect on glutamate dynamics may be a significant contributing factor to APOE dependent AD pathology.

6.4.1 EAAT1 is more highly expressed than EAAT2 in human iPSC-derived astrocytes

E3E3 and *E4E4* iPSC-derived astrocytes express greater levels of EAAT1 compared to EAAT2, as assessed at the mRNA level. *E3E3* astrocytes had significantly greater glutamate transporter expression overall with a *SLC1A3:SLC1A2* ratio of 140:1, while *E4E4* astrocytes had a *SLC1A3:SLC1A2* ratio of 60:1. It is well documented that cultured astrocytes predominantly express EAAT1 (Kondo *et al.*, 1995; Pathmajeyan *et al.*, 2011; Mahmoud *et al.*, 2019) with minimal expression of EAAT2, unless co-cultured with neurons. It is likely that the neuron-derived peptide pituitary adenylate cyclase-activating polypeptide, or PACAP, accounts for this difference (Figiel & Engele, 2000). Thus a limiting factor of monoculture experiments like the one presented here is that the results are more indicative of EAAT1 behaviour, than both EAAT1 and EAAT2. EAAT1 dysregulation is thought to contribute to the pathogenesis of many neurological disorders including schizophrenia, traumatic brain injury and AD (Shan *et al.*, 2013; Karki *et al.*, 2018; Parkin

et al., 2018). Consequently, the use of monocultures may be ideal for teasing out the underlying mechanisms of this dysfunction.

6.4.2 APOE4 astrocytes have reduced glutamate transporter expression and altered glutamate dynamics

APOE4 is one of the largest genetic risk factors for developing sporadic AD, and compromised glutamate dynamics are suspected to contribute to AD pathology (Hynd *et al.*, 2004; Walton & Dodd, 2007; Tampellini, 2015). Altered expression of glutamate transporters is reported to provoke amyloid pathology and cognitive decline in transgenic mouse models of AD (Zoltowska *et al.*, 2018). Based on this, it was thought that APOE may modulate expression of the astrocytic glutamate transporters, EAAT1 and EAAT2.

6.4.2.1 E3E3 and E4E4 astrocytes differ significantly in their glutamate transporter expression

It was found that astrocytes derived from human iPSC homozygous for APOE3 and APOE4 have different expression levels of EAAT1 and EAAT2 at mRNA level as well as EAAT1 at protein level. *E4E4* astrocytes had significantly reduced mRNA expression of *SLC1A3* and *SLC1A2* compared to *E3E3* astrocytes. *E4E4* astrocytes also tended to express lower levels of EAAT1 protein compared to *E3E3* astrocytes. Taking *E3E3* astrocytes as healthy control and *E4E4* astrocytes as high risk for AD, this data complements that of Hoshi and colleagues who found reduced EAAT2 immunoreactivity in the temporal cortex of AD patient brain slices compared to control individuals (Hoshi *et al.*, 2018). Jacob and colleagues also found impaired EAAT gene and protein expression in the hippocampus and gyrus frontalis medialis, but interestingly increased EAAT in the cerebellum of sporadic AD patients (Jacob *et al.*, 2007). Reduced EAAT expression has also been linked to AD with cerebral amyloid angiopathy (CAA), where expression of perivascular EAAT2 was reduced in cortical astrocytes of AD cases with CAA compared to cases lacking CAA and healthy controls (Thal *et al.*, 2010). To this author's knowledge, this data is the first to present glutamate transporter expression as a function of APOE genotype in an iPSC-derived model.

6.4.2.2 E3E3 and E4E4 astrocytes differ significantly in their glutamate dynamics

Analysis of glutamate uptake in *E3E3* astrocytes indicated that approximately 100 µM glutamate was removed from the cell culture media that was applied to astrocytes. Assuming that not all glutamate is immediately recycled to glutamine within the astrocyte, it would be expected that intracellular glutamate would mirror this finding. Indeed it was found that this perceived glutamate uptake was accounted for in the cell lysates where 120-140 µM glutamate was detected. Taken together these two readings indicate that *E3E3* astrocytes are functionally capable of glutamate uptake. In contrast, *E4E4* astrocytes appear to have compromised glutamate uptake and are, in fact, secreting glutamate. The extracellular glutamate as determined from culture media applied to astrocytes indicated a glutamate efflux by *E4E4* astrocytes of about 200 µM. This is surprising given an extracellular concentration of glutamate of 150 µM is well within physiological limits and a saturation point would not be expected at these levels (Yao *et al.*, 2014). This is coupled with a small uptake of 20-40 µM as measured from cell lysates. This discrepancy between APOE genotypes shows that altered transporter expression is having a marked effect on glutamate uptake.

In order to try and tease this out further, the study was repeated with altered extracellular glutamate by removing two sources of L-glutamic acid (GlutaMAX and NEAA) from the media recipe. Advanced DMEM and NEAA contain L-glutamic acid at concentrations of 50 µM and 10 µM respectively. GlutaMAX contains L-alanyl-L-glutamine dipeptide at a concentration of 2 mM, which is broken down by cells to release L-glutamine as needed. By removing NEAA and GlutaMAX from the Serio media recipe the extracellular concentration of glutamate was reduced to approximately 50 µM. *E3E3* astrocytes removed approximately 50 µM glutamate from the media which could be detected in the intracellular lysate samples. *E4E4* astrocytes again showed glutamate efflux about 20 µM, coupled with a small uptake of approximately 20 µM as measured from cell lysates. Taken together this data indicates that APOE4 homozygous astrocytes have compromised glutamate dynamics.

Comparing these values to other studies is difficult owing to a wide discrepancy in the literature regarding normal extracellular and intracellular concentrations of glutamate in and outside the astrocyte cell body. For extracellular concentrations, levels ranging from 40 nM to 10 µM are recorded for resting states and up to 1 mM may be expected at the time of neuron firing which is rapidly returned to the nanomolar range (Hynd *et al.*, 2004;

McKenna, 2007; Romanos *et al.*, 2019). Astrocytes have been shown to successfully buffer extracellular concentrations of glutamate from 5-400 µM in culture (Yao *et al.*, 2014). Homeostatic intracellular glutamate concentrations can lie in the millimolar range, as such glutamate uptake requires active transport of glutamate against its concentration gradient (Erecinska & Silver, 1990; Attwell *et al.*, 2010; Mahmoud *et al.*, 2019). These values give context to those presented in this study, and confirm that the concentrations of glutamate to which astrocytes were exposed are within physiological ranges and should therefore be within the functional capacity of astrocytes to buffer. This indicates that the reduced ability of *E4E4* astrocytes to uptake glutamate compared to *E3E3* astrocytes is not due to glutamate overload or toxic levels, and therefore must be intrinsic.

Again considering *E3E3* astrocytes as controls, and *E4E4* astrocytes as AD-like, this data complements the literature pertaining to compromised glutamate cycling in AD. Initial indications for altered glutamate dynamics in AD came from observations of reduced aspartate uptake, another amino acid transported by EAAT (Cowburn *et al.*, 1988; Masliah *et al.*, 1996). Liang and colleagues found reduced glutamate uptake in cultured human astrocytes derived from the cortex of AD patients (Liang *et al.*, 2002). In the AβPP23 transgenic mouse model of AD, decreased expression of glutamate transporters GLAST and GLT-1 was coupled with decreased glutamate reuptake in the hippocampus and cortex (Schallier *et al.*, 2011). The same deficits in glutamate neurotransmission have also been reported in 3×Tg-AD mice (Cassano *et al.*, 2012). Altered glutamate transport is proposed to have important consequences for memory and cognition. In agreement with this, EAAT1 knock-out mice display memory impairment (Chen *et al.*, 2011c). Excessive glutamate at the synapse results in over activation of glutamate receptors on the postsynaptic neuron which in turn causes excessive Ca^{2+} influx and activation of a cascade leading to apoptotic or necrotic death of neurons (Fontana, 2015). This explains why memantine, an FDA approved AD treatment, offers some efficiency for cognition as it prevents excessive activation of NMDA receptors caused by increased glutamate at the synapse (Okada *et al.*, 2019; Torrez *et al.*, 2019). It would be interesting to examine the efficacy of memantine in AD cohorts of known APOE genotype.

Taken together, the transporter expression and glutamate uptake data presented in this study provides preliminary evidence that APOE genotype affects glutamate transporters and subsequently glutamate dynamics. This finding that APOE has a genotype dependent effect on glutamate dynamics in astrocytes has potentially serious implications in AD

pathogenesis and highlights it as a target for future therapeutic strategies attempting to combat AD.

6.4.2.3 Possible mechanisms for altered glutamate dynamics in APOE4 astrocytes

EAAT transporters are central to maintaining glutamate homeostasis in the CNS (Shigeri *et al.*, 2004), and have exhibited the capacity to uptake and also efflux glutamate from astrocytes (Helms *et al.*, 2012). This study shows that glutamate uptake and efflux from iPSC-derived astrocytes is dependent on APOE genotype, the following are some potential mechanisms via which APOE may influence EAAT function and subsequently glutamate dynamics.

APOE genotype may impact post-translational modifications of glutamate transporters. For example, N-glycosylation has been shown to be critical for localisation of EAAT1 and EAAT2 to the plasma membrane and for increased stability of the transporters at the plasma membrane (Bauer *et al.*, 2010). Disruptions of glycosylation have been implicated in AD with decreased glycosylation linked to decreased capacity for glutamate uptake (Bauer *et al.*, 2010; Parkin *et al.*, 2018). Perhaps this is dependent on APOE. Phosphorylation is another post-translational modification with implications for EAAT function (Spencer & Kalivas, 2017). EAAT in rats is known to be inhibited by phosphorylation, for example by PKC (Conradt & Stoffel, 1997). There is evidence for altered PKC dynamics in *APOE4*-expressing human SH-SY5Y neuroblastoma cells and fibroblasts. This coincides with increased translocation to the membrane (Cedazo-Mínguez *et al.*, 2001) where it could affect function of membrane bound EAAT transporters. Calmodulin-dependent protein kinase II (CaMKII)-dependent phosphorylation is also important for constitutive transporter activity (Chawla *et al.*, 2017). Furthermore, EAAT2 is compartmentalised into endosomes following activation of the CaMKII pathway which itself is up-regulated by PKC activation (Underhill *et al.*, 2015). In contrast, pharmacological inhibition of CaMKII reduces glutamate uptake mediated by EAAT1 in HEK293T cells (Chawla *et al.*, 2017) and cortical astrocytes (Ashpole *et al.*, 2013). Another reason to suspect endocytosis plays a role in *APOE*-dependent EAAT inhibition is that APOE4 causes disruption in endocytosis pathways in astrocytes (Cataldo *et al.*, 2000) which may also affect metabolism of Aβ.

Arachidonic acid (AA) is an omega-6 polyunsaturated fatty acid. Present in phospholipids of cellular membranes, AA is highly expressed within the CNS and has functions including that of a second messenger (Rapoport, 2008; Tallima & El Ridi, 2018). AA has been shown to reduce EAAT1 affinity for glutamate by up to 30% while increasing the affinity of EAAT2 (Zerangue *et al.*, 1995). AA can facilitate prolonged reduction in glial glutamate buffering which was demonstrated using synaptosomes and cultured astrocytes from rat cerebral cortex (Volterra *et al.*, 1992). AA has also been shown to modulate NMDA receptor activity and support long term potentiation at synapses, possibly promoting glutamate-mediated excitotoxicity (Ramakers & Storm, 2002). One way in which *APOE4* may affect glutamate dynamics is by modulation of levels of AA in the CNS. AA has been shown to have increased and altered distribution in *APOE4* brain tissue (Abdullah *et al.*, 2017). As such endogenous or exogenous imbalance of AA in *APOE4* cell populations may manifest as dysregulated glutamate dynamics. Similar to AA, oxidative stress is known to affect EAAT function (Trotti *et al.*, 1997). Oxidative stress has also been observed to be higher in isogenic E4 astrocytes compared to E3 astrocytes (Jofre-Monseny *et al.*, 2008) suggesting a potential link to transporter dysfunction.

Using isogenic human iPSC-derived astrocytes, it has been demonstrated that APOE4 astrocytes express and secrete lower levels of APOE protein compared to APOE3 astrocytes (Lin *et al.*, 2018). Given the role of APOE as a cholesterol transporter, this results in altered cholesterol metabolism and higher cholesterol accumulation and secretion in APOE4 astrocytes (Lin *et al.*, 2018). It has been suggested that this in turn affects plasma membrane composition and subsequently stability. In agreement with this, cholesterol levels in the cell membranes of AD patients are decreased compared to control (Zhao *et al.*, 2017). This altered plasma membrane composition may play a key role in glutamate transport by affecting expression and function of EAAT1 and EAAT2 at the level of the astrocyte plasma membrane. Cholesterol-rich lipid raft micro-domains are crucial to trafficking of EAAT to the membrane, transporter localisation and function (Butchbach *et al.*, 2004). Furthermore, association of EAAT2 with lipid rafts is disrupted in AD brains (Tian *et al.*, 2010). It is possible that in APOE4-expressing astrocytes, lipid raft micro-domains are disrupted due to increased cholesterol secretion and altered plasma membrane composition. This may make EAAT1 and EAAT2 prone to dissociation from the membrane thereby disrupt transporter expression and function, in turn leading to impaired glutamate uptake and leaving the CNS more susceptible to excitotoxicity-induced damage.

6.4.3 Reactive astrocytes display altered glutamate transporter expression which does not impact glutamate dynamics

As APOE4 is inherently pro-inflammatory (Theendakara *et al.*, 2016), and *E4E4* astrocytes were found to express higher levels of certain astrocyte reactivity markers compared to *E3E3* astrocytes, it is natural to suspect a role for APOE4 in modulating glutamate dynamics. Astrocyte reactivity state has previously been shown to impact glutamate transporter expression in rodents, thus levels of EAAT1 and EAAT2 were examined in our model system following inflammatory insult delivered via microglial factors IL1α, TNFα and C1q. Subsequently glutamate dynamics were investigated as a function of astrocyte reactivity.

6.4.3.1 Glutamate transporter expression is not altered by inflammatory insult

Inflammatory microglial factors do not affect *SLC1A3* mRNA expression but significantly increase *SLC1A2* mRNA expression in *E3E3* and *E4E4* astrocytes. Further to this EAAT1 protein expression was not significantly affected by inflammatory insult as assessed by Western blotting. There may be a trend for inflammatory microglia factors to increase EAAT1 protein expression, which would contradict the theory that reactive astrocytes lead to neuronal excitotoxicity. However whole cell lysates were used for this experiment therefore it is not possible to discern whether the EAAT1 was membrane bound or intracellular, perhaps it is membrane bound but dysfunctional or the transporters have been endocytosed. Fractioning the cell lysates would allow for this to be clarified.

Lee and colleagues also found no change in *SLC1A3* and *SLC1A2* mRNA expression or EAAT1/2 protein expression in rat cultured astrocytes stimulated with TNFα and IL1β for 24 h. However stimulation with pro-inflammatory cytokines for 48 h resulted in significant reduction in glutamate transporter expression (Lee *et al.*, 2017). Perhaps sustained inflammation is required to significantly alter glutamate transporter expression at both mRNA and protein level.

Much of the literature pertaining to the effect of inflammation on EAAT expression supports an impact of inflammation on EAAT and glutamate uptake. A study carried out by the Volsky laboratory reported a reduction in EAAT1/2 protein and RNA expression in human primary astrocytes (foetal astrocytes of gestational week 18) following exposure to TNFα (Wang *et al.*, 2003). TNFα has also been shown to potentiate motoneuron death in a rat spinal cord organotypic model of chronic glutamate excitotoxicity, an effect which

was found to be reversible upon inhibition of NF-κB (Tolosa *et al.*, 2011). The Cavalla laboratory correlated activated microglia infiltration into cortical MS lesion sites with a focal loss of EAAT1, EAAT2 and synaptophysin as well as increased neuronal pJNK, which is involved in the neuronal response to excitotoxic injury (Vercellino *et al.*, 2007). Infiltrating peripheral immune cells, such as IL17 secreting Th17 cells, have also been shown to promote glutamate excitotoxicity by reducing GLT-1 and GLAST expression in primary rat astrocytes (Kostic *et al.*, 2017). The working theory in the literatutre is that inflammation results in a loss of functional neurotrophic support in astrocytes, e.g. glutamate homeostasis, and that this loss of homeostatic functioning might be due to down-regulation of glutamate transporters. However, we found no evidence to support this claim. The inflammatory insult exposure time could be prolonged to examine the effects of a sustained inflammatory state on glutamate transporter expression, for example 48 h (Lee *et al.*, 2017).

6.4.3.2 Glutamate dynamics are not affected by astrocyte reactivity state

The effect of inflammatory insult on glutamate transporter mRNA expression did not translate to protein expression or altered glutamate dynamics in our reactive astrocyte model. We found that astrocyte reactivity state did not significantly alter glutamate dynamics in either *E3E3* or *E4E4* astrocytes. Previous reports vary widely and often contradict each other with regards to the effect of inflammation on glutamate dynamics. Some studies report reduced glutamate uptake following IL1β exposure in human astrocytes (Hu *et al.*, 2009) and TNFα exposure in rat astrocytes (Zou *et al.*, 2019), or a combination of both in iPSC-derived astrocytes (Hyvarinen *et al.*, 2019). While TNFα insult has also been shown to increase glutamate uptake in rat astrocytes (Romera *et al.*, 2004). Another study reported glutamate efflux following LPS insult in human astrocytes (Bal-Price & Brown, 2001). It seems quite possible that the reason for these divergent results are a function of subtle differences, perhaps relating to species differences in rodent and human glutamate transporters or in the reactive profiles prompted by different inflammatory factors.

Glutamate uptake has been shown to be comprimised in AD pathology (Hynd *et al.*, 2004), although to this author's knowledge the only post-mortem study to correlate EAAT expression with AD pathology found that the two did not correlate (Beckstrøm *et al.*, 1999). One of the proposed mechanisms for compromised glutamate uptake in

neuroinflammation is the 'collusion' hypothesis which is based on data indicating that activated microglia down-regulate EAAT via release of glutamate leading to subsequent increased intracellular astrocytic glutamate (Takaki *et al.*, 2012). Though it is unclear how increased intracellular glutamate affects EAAT expression, it is possible that mGluR are involved due to their role in the regulation of EAAT transcription (Aronica *et al.*, 2003). This raises the possibilty that glutamate dynamics are altered by factors other than expression of EAAT. One prominent possibility is that glutamate transporter expression remains constant while transporter function is compromised by exposure to inflammatory factors. It is reasonable that EAAT could be inhibited by allosteric modulation of the receptors (Conradt & Stoffel, 1997), or by means of transporter internalisation (Gosselin *et al.*, 2013) for example. As discussed above, our data provides evidence that EAAT and glutamate dynamics are affected more by APOE genotype than exposure to inflammatory factors.

6.4.4 FGF2 affects glutamate transporter expression

Having shown that FGF2 modulates aspects of astrocyte reactivity we were interested to examine any effect of this growth factor on glutamate transporters and dynamics. FGF2 was found to actively decrease glutamate transporter expression at the mRNA level as determined by qPCR analysis of *SLC1A3* and *SLC1A2* expression. The literature pertaining to FGF2 and EAAT is largely based on studies carried out in rodent models and shows conflicting evidence for and against a positive effect of FGF2 on glutamate transporter expression and function.

Glial glutamate transporter expression has been found to be regulated by growth factors including EGF and FGF (Casper & Blum, 1995; Figiel *et al.*, 2003). It has been found in a rat model of stress that FGF2 alleviates GLT-1 and GLAST dysfunction and behavioural symptoms by restoring GLAST function via the JAK/STAT signalling pathway (Feng *et al.*, 2015). The Engele laboratory found that FGF2 promoted GLT-1, but not GLAST expression and did not affect glutamate uptake. This effect was only seen with simultaneous inhibition of ERK signalling (Figiel *et al.*, 2003). Liu and colleagues found that FGF2 up-regulated the cysteine/glutamate antiporter on astrocytes thereby increasing cysteine uptake and glutamate release. In mixed neuronal and glial cultures derived from foetal mouse cortex, this resulted in neuronal death by AMPA receptor-mediated excitotoxicity supporting a negative impact of FGF2 on glutamate transporters (Liu *et al.*, 2014).

Exposure to FGF1 for 7 days resulted in up-regulation of glutamate transporters, coupled with a 2-fold increase in glutamate transport (Roybon *et al.*, 2013). Savchenko and colleagues demonstrated that while short-term FGF2 treatment (24 h) resulted in reduced expression of *SLC1A2*, long-term FGF2 treatment increased GLT-1 levels in astrocytes (Savchenko *et al.*, 2019). Feng and colleagues also found that FGF2 administered for 48 h alleviated symptoms in a rat model of post-traumatic stress disorder by restoring GLAST/GLT-1 dysfunction (Feng *et al.*, 2015). Taken together, this would indicate that the ability of FGF2 to increase glutamate transporter expression is time sensitive.

There are a number of other factors presented in the literature which display beneficial modulation of EAAT expression including arundic acid, TGFα and β-lactam antibiotics. A 2018 study found that arundic acid up-regulated EAAT1 expression and enhanced transporter function via the Akt, ERK, and NF-κB signalling pathways in human H4 astrocytes as well as primary human astrocytes (Karki *et al.*, 2018). In human promoter constructs, db-cAMP, PACAP, EGF, and TGFα represent potent stimulators of endogenous EAAT1 expression (Unger *et al.*, 2012). Pharmacological agents such as β-lactam antibiotics, selective oestrogen receptor modulators, growth factors, histone deacetylase inhibitors, and translational activators have been shown to enhance the expression and function of GLAST/GLT-1 and glutamate uptake both *in vitro* and *in vivo* (Pajarillo *et al.*, 2019). Further to this memantine, a glutamatergic NMDA receptor channel blocker, has been shown to mediate astrocytic response to excitotoxicity in a rat model of tauopathy (Torrez *et al.*, 2019). These agents might be better suited to modulate the compromised glutamate dynamics we found in *E4E4* astrocytes.

6.4.5 *GLUL* expression is increased in APOE4 and reactive astrocytes

Glutamine synthetase (GS) is an enzyme which plays a crucial role in the metabolism of nitrogen by catalysing the condensation of glutamate and ammonia to yield glutamine. Within the CNS, GS is predominantly expressed by astrocytes, in order to carry out the essential buffering of extracellular ammonia and glutamate. In healthy astrocytes, GS catalyses the rapid amidation of glutamate to form the non-neurotoxic amino acid, glutamine. Through this conversion, GS helps maintain the correct level of glutamate and ammonia, preventing excitotoxicity (Castegna *et al.*, 2002).

In an attempt to elucidate the underpinning mechanisms for altered glutamate dynamics as a function of APOE genotype, GS expression was assessed by probing for the *GLUL* gene via qPCR. At baseline, *E4E4* astrocytes had significantly higher *GLUL* mRNA expression. This was increased upon stimulation with inflammatory microglial factors and then returned to approximate baseline levels when FGF2 was applied. This contrasts a study carried out using APOE-targeted replacement mice where no difference was found in *GLUL* levels between APOE3 and APOE4 genotypes (Dumanis *et al.*, 2013). And further, a study showing decreased GS expression in astrocytes derived from iPSC of sporadic AD patients compared to healthy controls (Jones *et al.*, 2017). An inflammatory environment, induced by ischemia, resulted in increased GS levels (Petito *et al.*, 1992) which corresponds to the effect of inflammatory microglial factors found in this study. The effect of FGF2 on *GLUL* mRNA expression corresponds with the results of a study carried out on a chick neural retina tissue. Treatment with exogenous FGF2 resulted in a significant decrease in *GLUL* mRNA expression due to inhibition of hormonal induction of GS (Kruchkova *et al.*, 2001).

Assuming that the *GLUL* mRNA translates to functional protein then the observed up-regulation of *GLUL* may represent a compensatory mechanism of rapid conversion of glutamate to glutamine in E4E4 astrocytes in an attempt to balance reduced transporter expression. The *E4E4* astrocytes may be capable of quicker conversion of glutamate to glutamine which is one explanation for the decreased intracellular glutamate detected in *E4E4* astrocytes compared to their *E3E3* counterparts. One means of testing this theory is by the addition of the GS inhibitor methionine sulfoximine in order to give a measure of glutamate uptake without conversion (Ghoddoussi *et al.*, 2010). An alternative method to analyse GS would be to measure protein expression by Western blotting for example, or isolate the protein and assess its enzymatic activity (Kingdon *et al.*, 1968; Bender *et al.*, 1977; Harth *et al.*, 1994). The conversion of glutamate to glutamine does not however account for the fact that *E4E4* astrocytes were releasing glutamate into the media which in an *in vivo* scenario would lead to increased extracellular glutamate and potential excitotoxicity. This supports the idea that the APOE4 genotype predisposes astrocytes to altered glutamate handling.

6.4.6 Concluding remarks

The data presented in this chapter indicate that APOE4 homozygous astrocytes have altered glutamate transporter expression and glutamate dynamics compared to APOE3 homozygous astrocytes. We have also provided evidence against modulation of astrocytic EAAT expression and glutamate dynamics as a function of exposure to inflammatory microglial factors. Data from this study has for the first time, to this author's knowledge, definitively demonstrated that APOE4 results in considerable loss of glutamate buffering function in human astrocytes *in vitro* using an iPSC-derived model. It represents an important breakthrough in this field and suggests that ameliorating glutamate transport is an important therapeutic target, and sheds further light on the mechanisms of APOE dependent pathology in AD.

Chapter 7

Final Discussion

7. Final discussion

Alzheimer's diease is the leading cause of dementia world wide and the current therapies available manage symptoms but fail to prevent diease progression. Therefore more research is required to fully elucidate the mechanisms of this devasting neurodegenerative disorder to alleviate impact on patients, their carers and the economy. The *APOE4* isoform has been identified as the leading genetic risk factor for sporadic AD. Furthermore astrocytes have been seen to be key players in AD pathology by responding to changes in the micro-environment and becoming reactive and involved in neuroinflammatory process. With that in mind, the overarching aims of this study were to build on prior research into the role of astrocytes and APOE genotype in AD pathology. Taking advantage of the latest PSC technologies, iPSC of known APOE genotypes (APOE3 and APOE4 homozygous) were used to generate astrocytes in order to investigate the interplay between neuroinflammation and APOE genotype on astrocyte reactivity and functionality.

7.1.1 Summary of findings

Human iPSC-derived *E3E3* "control" astrocytes were first used to generate a profile of astrocyte reactivity. Inflammatory insult was delivered in the form of microglial factors IL1α, TNFα and C1q. These factors have previously been shown to be secreted by activated microglia and subsequently induce reactivity in astrocytes (Liddelow *et al.*, 2017). Reactive astrocytes were characterised in terms of morphology, cytokine secretion and gene expression. It was found that reactive astrocytes had altered morphology compared to their quiescent-like counterparts. They also secreted significantly higher levels of pro-inflammatory cytokines IL6 and GM-CSF, and chemokine RANTES, as well as showing up-regulation of expression of reactive astrocyte markers, including *C3*, *CXCL10*, *LCN2* and *ICAM1*.

Having characterised reactive astrocytes in our iPSC-derived model it was next examined how APOE4 genotype affected reactivity. Basal levels of reactive astrocyte markers were examined in *E3E3* and *E4E4* astrocytes with *E4E4* astrocytes showing increased base line reactivity. Following stimulation, *E4E4* reactive astrocytes showed an enhanced response in terms of expression of reactive markers *C3*, *CXCL10* and *ICAM1*. This data indicated an APOE genotype effect on astrocyte reactivity. This study was followed up by trialling two compounds, FGF2 and CBD, as modulators of astrocyte reactivity. Both of these

compounds showed promise in their ability to attenuate astrocyte reactivity, however further research into the mechanisms would be advised.

Finally, functionality of iPSC-derived astrocytes was examined. iPSC-derived astrocyte functionality is largely understudied, and furthermore the effect of APOE genotype on astrocytic functions. Therefore, the final chapter of this thesis presented an investigation into the interplay between APOE genotype and reactivity on glutamate dynamics. Glutamate transporter expression was decreased in *E4E4* astrocytes, which was accompanied by impaired glutamate transport. Astrocyte reactivity had no effect on glutamate dynamics but the effect of APOE genotype persisted following stimulation indicating a strong APOE4-dependent effect on glutamate transport.

Overall, this thesis identifies increased expression of *IL6*, *C3* and *CXCL10*, as well as impaired glutamate dynamics in APOE4 homozygous astrocytes. These represent potential mechanisms which may contribute to increased AD risk in *APOE4* carriers, and suggests these areas as targets for future therapies aiming to combat AD.

7.1.2 APOE4: Loss or Gain of Function?

A major question currently unanswered in the literature is whether APOE4 results in a loss or gain of function.

Zhao and colleagues found that APOE4 astrocytes presented with a loss of neurotrophic function. iPSC-derived APOE4 astrocytes had a reduced capacity to support synapse formation in neurons compared to APOE3 astrocytes (Zhao *et al.*, 2017). This finding was in "healthy" astrocytes without insult or injury, therefore indicates an intrinsic loss of function in APOE4 astrocytes. A recent study by Wang and colleagues correlated *APOE4* genotype with a gain of toxic function in iPSC-derived neurons. It was found that *APOE4*-expressing neurons had greater levels of tau phosphorylation, increased Aβ production and GABAergic degeneration. These effects were attributed to the APOE4 genotype as converting *APOE4* to *APOE3* was protective. Furthermore, neurons lacking APOE behaved much like APOE3 neurons indicating a gain of toxic function in APOE4 neurons (Wang *et al.*, 2018).

The data presented in this thesis indicates that there is an interplay between both. The reactivity profile characterised is indicative of a gain of toxic function in response to inflammatory insult, whereas the investigation into glutamate handling indicates a clear

loss of homeostatic function in APOE4 homozygous astrocytes. Future therapies should address both gain and loss of function in astrocytes in AD.

7.1.3 Limitations

iPSC technology has offered unprecedented insights into cell-type specific pathology through the generation of disease- and patient-specific *in vitro* models. And, as applied in this study, is an invaluable model system for investigating the impact of genotype on cell phenotype. However, this study like most comes with some limitations.

7.1.3.1 Small sample size, timepoints and lack of APOE2 genotype

iPSC-derived reactive astrocytes were generated by stimulation with inflammatory microglial factors IL1α, TNFα and C1q. These reactive astrocytes were then characterised in terms of morphology, secretion of inflammatory mediators and expression of genes to confirm reactivity. However, a single timepoint of 24 h was used to induce this reactive phenotype and therefore is perhaps more representative of acute inflammation. Additional timepoints such as 48/72 h or 7 days for example may be more representative of chronic inflammation and chronic astrogliosis as is the case in neurodegenerative diseases.

It would have been interesting to expand this study to also include representatives of the APOE2 genotype. APOE2 is reported to protect against AD risk with individuals expressing at least one APOE2 isoform having an estimated 40% reduced risk of developing AD (Belloy *et al.*, 2019). However the mechanisms underlying this protective effect of APOE2 genotype are unknown. Unfortunately its low prevalence in the population means it is a difficult genotype to acquire, although iPSC banks are now becoming more common which provide a sources for purchasing this genotype.

7.1.3.2 Isogenic iPSC lines will facilitate confirmation of genotype effects on glutamate dynamics

This thesis provides evidence that APOE genotype affects astrocyte reactivity, glutamate transporter expression and subsequently glutamate dynamics. However it must be noted that the *E3E3* and *E4E4* astrocyte cell lines utilised in this project were derived from different individuals and therefore there is no knowing what background genetics may be

influencing the results. The results presented here may be consolidated with the use of isogenic controls, whereby APOE3 may be genetically edited to APOE4 in the *E3E3* astrocytes and vice versa for the *E4E4* astrocytes. Numerous gene editing techniques have been applied in the literature for this purpose.

Wang and colleagues applied gene editing and a structural corrector to *APOE4*-expressing neurons and found that conversion of APOE4 to APOE3 counteracted the AD pathology found in APOE4 neurons (tau phosphorylation, Aβ production and degeneration) (Wang *et al.*, 2018). In the first instance, they used Zinc Finger Nuclease (ZFN)-mediated gene editing. A specific ZFN was manufactured to target and cut the region of the *APOE4* gene which contains Arg112, while donor *APOE3* DNA replaced this cut section (Fong *et al.*, 2013). In the second instance, they utilised the small molecule structure corrector PH002. PH002 is a phthalazinone derivative that directly binds the amino-terminal region of APOE4 thereby blocking intramolecular domain interactions. In both cases, *APOE4*-expressing neurons were altered to an APOE3-like phenotype. Since this small molecule is available from Sigma-Aldrich (Merck Millipore) it would be possible to purchase and use it in further studies to validate the APOE model presented in this thesis.

The combined use of clustered regularly-interspaced short palindromic repeat (CRISPR) sequences and CRISPR-associated (Cas) proteins represent a major breakthrough in gene editing technology. For many years it was considered a specialist technique applied only in fields such as microbiology, until in 2012 it was demonstrated that this technology may be applied to gene modification in almost any organism (Mojica & Montoliu, 2016). CRISPR/Cas9 gene editing allows for editing of single nucleotides. With Cas9 acting as a guide, a specific sequence in the genetic code can be targeted, cut and removed from the genome, thereby allowing space for this section to be replaced, i.e. edited. In this manner APOE4 has been targeted and altered to APOE3 to facilitate research into mechanisms associated with AD risk in APOE4 carriers. This technology has already been applied by several labs to elucidate the role of APOE4 genotype on cellular function. The Tsai laboratory applied CRISPR/Cas9 to generate isogenic controls for iPSC lines with APOE3 and APOE4 homozygous genotypes. They showed that APOE4 neurons secreted greater levels of $A\beta_{42}$, APOE4 astrocytes had impaired Aβ clearance, and APOE4 microglia had increased inflammatory gene expression. They further demonstrated via isogenic controls that altered function in these cells types was a direct result of APOE genotype and not due to confounding factors (Lin *et al.*, 2018).

It is of interest to point out that the Caldwell laboratory have acquired isogenic iPSC from the Tsai laboratory with a view to further investigate the impact of APOE4 genotype on glutamate dynamics. Four iPSC lines have been acquired including an APOE4 homozygous iPSC line derived from a sporadic AD patient and its APOE3 homozygous isogenic control, as well as an APOE3 homozygous iPSC line with the APOE4 homozygous condition introduced as per the above mentioned protocol (Lin *et al.*, 2018). It is our aim to consolidate the findings of this study by ruling out confounding effects of other polymorphisms present in our iPSC-derived astrocytes, such as glutamate transporter polymorphisms (rs4354668 and rs27731880) which directly affect glutamate transport (Spangaro *et al.*, 2014). At the time of writing, these iPSC have been expanded in the feeder system using mouse embryonic fibroblasts as the feeder layer to generate a stock. iPSC have further been transitioned into the feeder-free mTeSR system and subsequently patterned towards a cortical fate to generate β-tubulin III^{+} TBR1^{+} neural progenitors (Figure 7.1.1) which will be used to derive astrocytes as per the protocol laid out in Chapter 3.

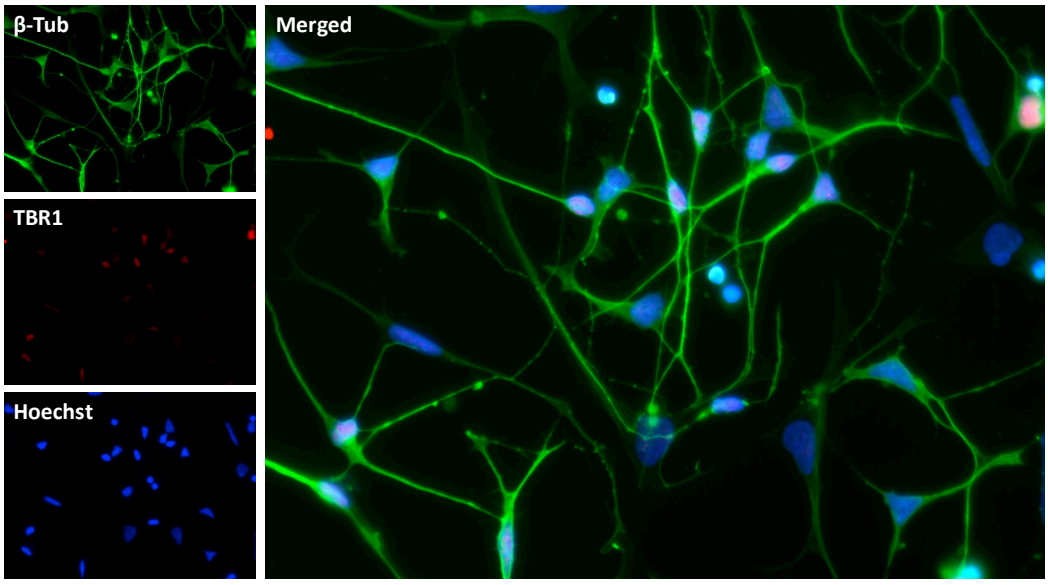


Figure 7.1.1. Characterisation of isogenic iPSC-derived neural progenitors.

iPSC-derived neural progenitors (E3E3 parental line) are positive for classical neuronal marker β-tubulin III (green) and cortical marker TBR1 (red). Nuclei are counterstained with hoechst (blue). Images were taken at x40 magnification.

7.1.3.3 Monolayer cultures versus neurospheres and 3D organoids

Monolayer cultures lend themselves to efficient differentiation of defined populations allowing for analysis of cell type specific responses. However they are not a true representation of the 3D environment of the CNS consisting of multiple heterogeneous populations of cells. Organoids provide a means to replicate the 3D nature of the CNS.

In capturing the complex structural arrangement present in the CNS, brain organoids provide a more realistic model system to facilitate investigation of intercellular relationships and also provide greater translational value to therapies (Lancaster *et al.*, 2013; Gabriel & Gopalakrishnan, 2017). Lin and colleagues applied this technology to generate APOE4-organoids. They found that APOE4-organoids accumulated Aβ and phosphorylated tau much like the AD brain. Furthermore, iPSC-derived organoids first differentiate NPC, then neurons, with astrocytes developing later, which is representative of embryonic development (Raja *et al.*, 2016; Lin *et al.*, 2018). With respect to the data presented in this thesis, brain organoids would facilitate analysis of the effect of altered glutamate dynamics in *E4E4* astrocytes on activity at the tripartite synapse and the postsynaptic neuron itself. Furthermore, protein aggregates may be introduced into the culture system to represent the microenvironment of the AD brain. This *in vitro* model may provide unprecedented insight into the inner workings of the AD brain.

7.1.3.4 iPSC lack age-associated molecular signatures

iPSC are somatic cells which have been forced back into a primordial state. They behave much like ESC and therefore do not possess age-associated molecular signatures such as telomere shortening and cellular senescence (Rohani *et al.*, 2014). Given that the major risk factor for AD is age itself, it would be beneficial if this factor could also be represented in the model system. Since aged astrocytes also generally have a reactive phenotype (Clarke *et al.*, 2018) it is important that age signature be considered in modelling of AD and other age-associated diseases.

There is much literature pertaining to protocols for the generation of induced-NPC and induced-neurons (Lee *et al.*, 2018; Xiao *et al.*, 2018; Yavarpour-Bali *et al.*, 2020). By avoiding the iPSC step, the parent cells maintain their age signature (Mertens *et al.*, 2015; Mertens *et al.*, 2016). It is also possible to directly reprogram adult cells into astrocytes (Caiazzo *et al.*, 2015; Tian *et al.*, 2016). The gene expression profiles and functional assays of induced-astrocytes are comparable to primary astrocytes.

It would be interesting to apply these protocols, generate directly induced-astrocytes and compare their age signatures to that of our iPSC-derived astrocytes much like the study Mertens and colleagues carried out using induced-neurons.

7.1.4 Data presented in this thesis may contribute to future therapeutic strategies

The data presented in this thesis, coupled with the existing literature pertaining to the detrimental effect of APOE4 genotype, present APOE4 as an attractive therapeutic target. By reducing APOE4 expression it may be possible to alleviate the associated AD risk.

The effect of APOE absence has previously been examined in a patient with homozygous APOE deficiency. Whole-exome sequencing identified an ablative APOE mutation (c.291del, p.E97fs) as the root cause of APOE deficiency. Cognitive testing confirmed that in spite of the APOE deficiency the patient had normal cognition, normal neurological and retinal function, as well as normal ranges of Aβ and tau proteins in the CSF. Together this indicated no profound CNS defects. Peripherally, APOE deficiency resulted in severe dysbetalipoproteinemia characterised by elevated serum levels of both cholesterol and triglyceride, indicating a profound effect on lipid metabolism. The authors concluded that APOE functions in the CNS may have compensatory mechanisms, and therefore targeted knockdown of APOE may be a viable therapeutic target (Mak *et al.*, 2014). However, they did not comment on the increased risk of cardiovascular disease that the patient is exposed to as a result of elevated serum cholesterol and triglyceride. Separately, APOE deficiency has been shown to result in oxidative stress and endothelial dysfunction in the mouse retina (Zadeh *et al.*, 2019). Therefore APOE targeted knockdown does not pose a viable therapeutic target given the data associated with APOE deficiency. However, a means of correcting the APOE4 defect may generate more satisfactory results. Small-molecule structure correctors have shown promise in *in vitro* validation of concept studies, and CRISPR/Cas9 has been posed as a potential gene therapy although requires significant development (Prendecki *et al.*, 2020).

The small-molecule structure corrector, PH002, has shown success *in vitro* by rendering APOE4 APOE3-like both structurally and functionally and in turn rescuing the AD-like pathology associated with APOE4 neurons (Wang *et al.*, 2018). Interestingly, the efficacy of PH002 was shown to be dependent on the presence of APOE4, with no effect on APOE null cells pointing to its specificity. The small-molecule structure correctors GIND25 and

PH002 have also been applied to correct defects in *APOE4*-expressing Neuro-2A cells associated with secretory pathways (Brodbeck *et al.*, 2011). Chen and colleagues carried out a proof of concept study with the small-molecule structure corrector CB9032258. They found that CB9032258 restored mitochondrial and neurite outgrowth impairments in *APOE4*-expressing neuronal cells and proposed APOE4 structure correctors as a therapeutic means to rectify APOE4 defects in the treatment of AD (Chen *et al.*, 2012). APOE4 structure correctors have also attenuated APOE4-induced Aβ production in neuroblastoma cells (Ye *et al.*, 2005). Small-molecule structure correctors provide a means to restore proper 3D-structure and thereby function to defective proteins. In this way, gene editing can be avoided and so too the risk of off-target effects. Structure corrector-based therapies could prove effective for modulating APOE4-associated AD risk, and furthermore could be applied to many disorders associated with protein misfolding.

7.1.5 Concluding remarks

The findings presented in this thesis indicate that human iPSC-derived astrocytes are capable of responding to inflammatory insult and producing a reactive phenotype, therefore provide a useful model system of astrogliosis. *E3E3* and *E4E4* astrocytes have a distinct basal reactive profile which translates to some interesting genotype related differences following insult, with APOE4 genotype resulting in some enhanced responses. Furthermore, APOE genotype appears to have a profound effect on glutamate transport in iPSC-derived astrocytes. With APOE4 astrocytes showing marked impairments in glutamate uptake. This strong genotype effect may be an underlying mechanism by which APOE4 affects AD risk. In conclusion, this thesis presents APOE4 as an attractive therapeutic target for managing AD risk and highlights the need for further investigation of APOE-based therapies.

Chapter 8

Appendices

8. Appendices

8.1 Appendix 1 – iPSC Characterisation

E4E4 homozygous astrocytes were derived from dermal fibroblasts by episomal plasmid vector. This work was carried out by Dr Lucy Crompton in the University of Bristol as part of the BRACE project. Details of iPSC generation and characterisation are depicted in figure 8.1.1. iPSC were characterised by immunostaining for pluripotency markers TRA-1-60 and SSEA4; original images of this iPSC characterisation is shown in figure 8.1.2. Two iPSC clones were generated, denoted as E4E4A and E4E4B. The E4E4B clone was used in the experiments described in this thesis.

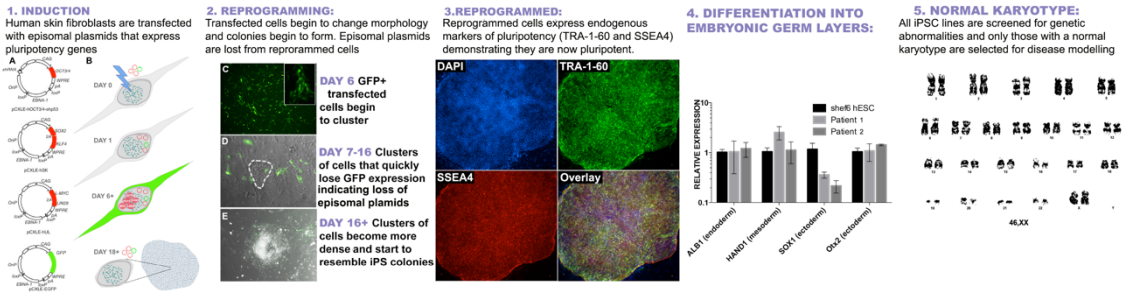


Figure 8.1.1. Generation of iPSC from E4E4 homozygous dermal fibroblasts and subsequent characterisation.

Data and figure was produced by Dr Lucy Crompton.

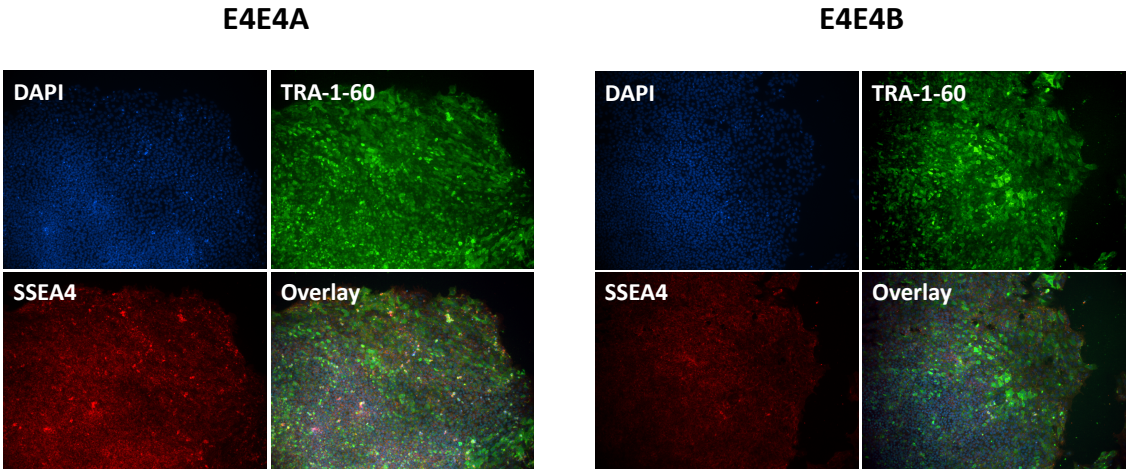


Figure 8.1.2. Characterisation of E4E4 iPSC.

E4E4 iPSC are positive for pluripotency markers TRA-1-60 (green) and SSEA4 (red).

8.2 Appendix 2 – Materials

8.2.1 Molecular biology

Reagent	Manufacturer	Catalogue Number
C3	Applied BioSciences	Hs00163811_m1
cDNA manufacture kit	Applied BioSciences	4368814
CXCL10	Applied BioSciences	Hs00171042_m1
dNTP Mix 100 mM	Applied BioSciences	4367381
GAPDH (VIC)	Applied BioSciences	Hs02786624_g1
GFAP	Applied BioSciences	Hs00164932_m1
GLUL	Applied BioSciences	Hs00365928_g1
ICAM1	Applied BioSciences	Hs00164932_m1
IL1β	Applied BioSciences	Hs01555410_m1
IL6	Applied BioSciences	Hs00174131_m1
LCN2	Applied BioSciences	Hs01008571_m1
MicroAmp™ Fast Optical 96-Well Plate	Applied BioSciences	4346906
MultiScribe Reverse Transcriptase	Applied BioSciences	4311235
NucleoSpin RNA Isolation kit	Macherey Nagel Bioanalysis	740955.50
PCR Plate Adhesive Film	Applied BioSciences	4311971
PTX3	Applied BioSciences	Hs00173615_m1
RNAse Away	VWR International	732-2271
RNAse-free water	Fisher Scientific Ltd	10192813
SERPINA3	Applied BioSciences	Hs00153674_m1
SLC1A2	Applied BioSciences	Hs01102423_m1
SLC1A3	Applied BioSciences	Hs00904823_g1
Taqman Mastermix	Applied BioSciences	4444557
VIM	Applied BioSciences	Hs00958111_m1

8.2.2 Cell culture reagents

Reagent	Manufacturer	Catalogue Number
Accutase	Thermo Fisher Scientific	A11105-01
Advanced DMEM/F-12	Thermo Fisher Scientific	12634010
B27	Thermo Fisher Scientific	17504-044
Bone morphogenic protein 4	Bio-Techne	314-BP-010
Cryo canes, aluminium	Thermo Scientific Nalgene	10100341
Cryo straws	Fisher Scientific	11734673
CryoStor CS10	Sigma-Aldrich	C2874
Dimethyl sulfoxide	Molecular Probes	D12345
DMEM/F-12 + GlutaMAX	Thermo Fisher Scientific	31331028
Epidermal growth factor	Sigma-Aldrich	E9644
Essential 8™ Flex Medium Kit	Thermo Fisher Scientific	A2858501
Ethylenediaminetetraacetic acid	Thermo Fisher Scientific	15575-020

Geltrex	Thermo Fisher Scientific	A1413302
GlutaMAX	Thermo Fisher Scientific	35050-038
Human leukemia inhibitory factor	PeproTech	167300-05-B
Insulin	Sigma-Aldrich	I4011
Laminin	Sigma-Aldrich	L2020
LDN193189	Sigma-Aldrich	SML0559
N2	Thermo Fisher Scientific	17502-048
Neurobasal Medium SFM	Thermo Fisher Scientific	21103-049
Non-essential amino acids	Thermo Fisher Scientific	11140-035
Pen/Strep	Sigma-Aldrich	P4333
Polyornithine	Sigma-Aldrich	P3655
RevitaCell	Thermo Fisher Scientific	A26445-01
SB431542	Bio-Techne (Tocris Bioscience)	1614/1 or 1614/10
Vitronectin	Thermo Fisher Scientific	A14700
Y-27632	Axon Medchem	1683
β-mercaptoethanol	Invitrogen	31350-010

8.2.3 Primary and secondary antibodies for immunocytochemistry

Product	**Manufacturer**	**Catalogue Number**
Chicken anti-GFAP	Abcam	ab4674
Donkey anti-mouse Alexa 488	Invitrogen	A21202
Goat anti-chicken IgG Alexa Fluor 488	Life Technology	
Goat anti-rabbit IgG Alexa Fluor 555	Invitrogen (Thermo Fisher Scientific)	A21428
Hoescht	Cell Signalling Technology	H33342
Mouse anti-S100β	Sigma-Aldrich	S2532
Mouse anti-β-tubulin III	Merck Millipore	
Rabbit anti-Connexin-43	Sigma-Aldrich	C6219
Rabbit anti-EAAT1	Novus Biologicals	NBPI-20135
Rabbit anti-TBR1	Abcam	ab31940

8.2.4 Experimental treatments

Reagent	**Manufacturer**	**Catalogue Number**
C1q	MyBioScource	MBS143105
Cannabidiol	Tocris	-
FGF2	PeproTech	100-18B
IL1α	PeproTech	200-01A
TNFα	Cell Signaling Technology	8902

8.2.5 Biological assays, chemicals and reagents

Reagent	Manufacturer	Catalogue Number
Chicken anti-GFAP	Abcam	ab4674
Donkey anti-mouse Alexa 488	Invitrogen	A21202
Goat anti-chicken IgG Alexa Fluor 488	Life Technology	
Goat anti-rabbit IgG Alexa Fluor 555	Invitrogen (Thermo Fisher Scientific)	A21428
Hoescht	Cell Signalling Technology	H33342
Mouse anti-S100β	Sigma-Aldrich	S2532
Mouse anti-β-tubulin III	Merck Millipore	
Rabbit anti-Connexin-43	Sigma-Aldrich	C6219
Rabbit anti-EAAT1	Novus Biologicals	NBPI-20135
Rabbit anti-TBR1	Abcam	ab31940

8.2.6 Laboratory equipment and consumables

Product	Manufacturer	Catalogue Number
1 mL cryovials	Nunc	377267K
1.5 mL eppendorfs	VWR International	211-0015
10 mL pipettes	VWR International	612-3700
12-well cell culture plates	Corning	10253041
15 mL falcon tubes	Sarstedt Ltd	62.554.002
24-well cell culture plates	Corning	10732552
24-well cell culture plates	Sarstedt Ltd Ireland	83.3922
25 mL pipettes	VWR International	612-3698
5 mL pipettes	VWR International	612-3702
50 mL falcon tubes	Sarstedt Ltd	62.547.004
50 mL pipettes	VWR International	612-3696
6-well cell culture plates	Corning	10578911
6-well cell culture plates	Nunc	140675
Coverslips	VWR International	631-1578
Cryo 1°C freezing container	Nalgene	10110051
CryoPure Tube, 2.0ml	Sarstedt Ltd Ireland	72.380.002
ELISA plate covers	Greiner, Cruinn Diagnostics Ltd	676001
ELISA plates	Nunc, Bio-Sciences Ltd	442404
Filter	Millipore (UK) Limited	SLGP033RS
Glass slides	VWR International	631-1551
Nalgene Cryovial 1.2ml Sterile	Analab Limited	CRY8200
P10 filter tips	Medical Supply Co. Ltd	311-4050
P1000 filter tips	Medical Supply Co. Ltd	361-4050
P1000 pipette tips	Sarstedt Ltd	70.762
P2 pipette tips	Greiner	771290
P20 filter tips	Medical Supply Co. Ltd	341-4050
P20 pipette tips	Greiner	739290
P200 filter tips	Medical Supply Co. Ltd	351-4050
P200 pipette tips	Sarstedt Ltd	70.760.002

PCR MicroTubes, 0.2 mL	VWR International	7324836
Syringe - 20 mL	Fisher Scientific Ltd	10569215
T25 flask	Sigma-Aldrich	CLS3289-200EA
Transfer pipettes	VWR International	612-1685
Virkon	VWR International	115-0020

8.3 Appendix 3 – Media Recipes

Neural maintenance media (50 mL)

- DMEM/F-12 + GlutaMax: 25 mL
- Neurobasal medium:25 mL
- NEAA: 500 µL
- GlutaMax: 250 µL
- Pen/Strep: 500 µL
- N2: 250 µL
- B27: 500 µL
- B-mercaptoethanol (50 mM): 75 µL
- Insulin (20 ng/µL): 50 µL

Serio media (50 mL)

- Advanced DMEM/F-12: 49 mL
- NEAA: 500 µL
- GlutaMax: 500 µL
- Pen/Strep: 500 µL
- N2: 500 µL
- B27: 100 µL

Serio EL (50 mL)

- Serio media: 50 mL
- EGF (20 ng/µL stock): 50 µL
- hLIF (20 ng/µL stock): 50 µL

Serio BMP4 hLIF (50 mL)

- Serio media: 50 mL
- BMP4 (20 ng/µL stock): 50 µL
- hLIF (20 ng/µL stock): 50 µL

Reduced glutamate media (50 mL)

- Advanced DMEM/F-12: 49 mL
- Pen/Strep: 500 µL
- N2: 500 µL
- B27: 100 µL

8.4 Appendix 4 – Solutions and Buffers

8.4.1 Solutions for general lab use

Phosphate-buffered saline (PBS; 1 L)

- dH_2O: 1 L
- PBS tablets: 5 tablets

8.4.2 ELISA solutions

Reagent diluent (1% BSA)

- PBS: 100 mL
- BSA: 1 g
- Filter sterilised with 0.1 µm filter

Wash buffer (0.05% Tween-20)

- PBS: 500 mL
- Tween-20: 250 µL

8.4.3 Western blotting buffers

PBS-T (0.05%)

- PBS: 100 mL
- Tween-20: 50 µL

Running buffer (1X)

- Tris base (250 mM): 3 g
- Glycine (1.92 M): 14.4 g
- SDS: 1 g
- dH_2O: 800 mL
- Make up to 1 L with dH_2O

Transfer buffer (1X)

- Tris base: 0.606 g
- Glycine: 0.3 g
- dH_2O: 80 mL
- Methanol: 20 mL

4% stacking gel

- dH_2O: 1.525 mL
- Acrylamide: 0.325 mL
- Tris-HCl (pH 8.8): 0.625 mL
- SDS: 25 µL
- APS: 12.5 µL
- TEMED: 4 µL

10% resolving gel

- dH_2O: 2.01 mL
- Acrylamide: 1.665 mL
- Tris-HCl (pH 8.8): 1.25 mL
- SDS: 50 µL
- APS: 25 µL
- TEMED: 3 µL

Ammonium persulfate (APS, 10%)

- APS: 0.1 g
- dH_2O: 1 mL
- Make up fresh on the day

Sodium dodecyl sulfate (SDS, 10%)

- SDS: 0.1 g
- dH_2O: 1 mL
- Store at 4°C for up to 1 week

Tris-HCl (1 M), pH 6.8

- Tris base (1.5 M): 90.8 g
- SDS: 1 g
- dH_2O: 400 mL
- pH to 6.8 with HCl, bring up to 500 mL with dH_2O
- Store at 4°C

Tris-HCl, pH 8.8

- Tris base (1 M): 15.13 g
- SDS: 1 g
- Bromophenol blue: few granules
- dH_2O: 150 mL
- pH to 8.8 with HCL, bring up to 250ml with dH_2O
- Store at 4°C

Protein loading dye (5X)

- SDS: 4 g
- Glycerol: 20 mL
- Tris HCl (pH 8.8): 10 mL
- Bromophenol blue: 40 mg
- dH_2O: 10 mL

Sample buffer

- Protein loading dye (5X): 10 µL
- B-mercaptoethanol: 1 µL

Marvel Solution (5%)

- PBS-T: 50 mL
- Marvel original dried skimmed milk powder (Premier Foods, UK): 2.5 g

Stripping Buffer

- Glycine: 15 g
- SDS: 1 g
- Tween-20: 10 mL
- dH_2O: 990 mL
- pH to 2.2

8.4.4 Immunofluorescence buffers

Blocking Buffer

- Normal goat serum: 100 µL
- Triton-X (10%): 33 µL
- PBS: 867 µL

PTX wash buffer (0.02%)

- Triton-X (10%): 20 µL
- PBS: 10 mL

Triton-X (10%)

- Triton-X-100: 100 µL
- PBS: 900 µL

8.5 Appendix 5 – Cell Counting

Astrocytes were detached, centrifuged and the pellet resuspended in 1 mL Serio media for counting before seeding. Following resuspension, 10 µL of cell suspension was diluted in 40 µL of Serio media (1:5) and homogenised. 10 µL of the diluted cell suspension was added to 10 µL of trypan blue (1:2; Thermo Fisher Scientific, USA), a dye which stains dead cells. 10 µL of this mix was loaded onto a glass haemocytometer slide and examined under a light microscope at 10x magnification. After checking that cells were evenly dispersed across the 9 major grid boxes, the number of viable cells in 4 of the boxes (see Figure 9.4.1. for example) was counted using a handheld manual tally clicker and the average number of cells per major grid box was established (i.e. cells per µL). To calculate the number of cells/mL, the number of cells/µL was multiplied by 10, the dilution factor and 10^4, to account for the resuspension of the pellet in 1 mL of media. The desired cell count per well, e.g. 50,000 cells/well for ELISA, was then divided by the total number of cells/mL which determined the volume of cells to be added per well.

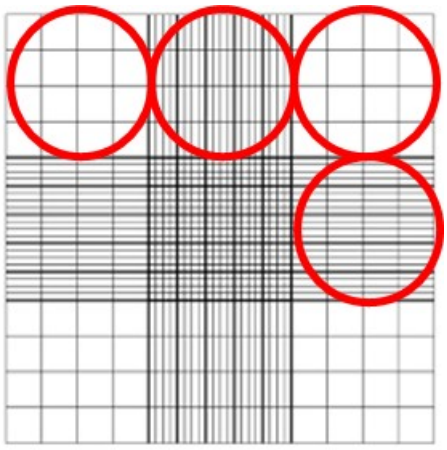


Figure 8.5.1. Diagram of a haemocytometer glass slide used to count cells.

Viable cells present in the four squares circled were counted.

8.6 Appendix 6 – Three-way ANOVA with Bonferroni *post hoc*

ANOVA table	F (DFn, DFd)	P value
Factors	F (2, 30) = 15.94	P<0.0001
APOE	F (1, 30) = 734.1	P<0.0001
FGF2	F (1, 30) = 38.24	P<0.0001
Factors x APOE	F (2, 30) = 5.845	P=0.0072
Factors x FGF2	F (2, 30) = 2.524	P=0.0970
APOE x FGF2	F (1, 30) = 9.546	P=0.0043
Factors x APOE x FGF2	F (2, 30) = 1.021	P=0.3723

Table 8.6.1. Three-way ANOVA analysis of SLC1A3 mRNA expression.

Bonferroni's multiple comparisons test	Summary	Adjusted P Value
Control:E3E3 - FGF2 vs. Control:E3E3 + FGF2	****	<0.0001
Control:E3E3 - FGF2 vs. Control:E4E4 - FGF2	****	<0.0001
Control:E3E3 - FGF2 vs. Control:E4E4 + FGF2	****	<0.0001
Control:E3E3 - FGF2 vs. Low:E3E3 - FGF2	ns	>0.9999
Control:E3E3 - FGF2 vs. Low:E3E3 + FGF2	ns	>0.9999
Control:E3E3 - FGF2 vs. Low:E4E4 - FGF2	****	<0.0001
Control:E3E3 - FGF2 vs. Low:E4E4 + FGF2	****	<0.0001
Control:E3E3 - FGF2 vs. High:E3E3 - FGF2	ns	>0.9999
Control:E3E3 - FGF2 vs. High:E3E3 + FGF2	***	0.0007
Control:E3E3 - FGF2 vs. High:E4E4 - FGF2	****	<0.0001
Control:E3E3 - FGF2 vs. High:E4E4 + FGF2	****	<0.0001
Control:E3E3 + FGF2 vs. Control:E4E4 - FGF2	****	<0.0001
Control:E3E3 + FGF2 vs. Control:E4E4 + FGF2	****	<0.0001
Control:E3E3 + FGF2 vs. Low:E3E3 - FGF2	****	<0.0001
Control:E3E3 + FGF2 vs. Low:E3E3 + FGF2	***	0.0009
Control:E3E3 + FGF2 vs. Low:E4E4 - FGF2	***	0.0001
Control:E3E3 + FGF2 vs. Low:E4E4 + FGF2	****	<0.0001
Control:E3E3 + FGF2 vs. High:E3E3 - FGF2	*	0.0335
Control:E3E3 + FGF2 vs. High:E3E3 + FGF2	ns	>0.9999
Control:E3E3 + FGF2 vs. High:E4E4 - FGF2	****	<0.0001
Control:E3E3 + FGF2 vs. High:E4E4 + FGF2	****	<0.0001
Control:E4E4 - FGF2 vs. Control:E4E4 + FGF2	ns	>0.9999
Control:E4E4 - FGF2 vs. Low:E3E3 - FGF2	****	<0.0001
Control:E4E4 - FGF2 vs. Low:E3E3 + FGF2	****	<0.0001

Control:E4E4 - FGF2 vs. Low:E4E4 - FGF2	ns	>0.9999
Control:E4E4 - FGF2 vs. Low:E4E4 + FGF2	ns	>0.9999
Control:E4E4 - FGF2 vs. High:E3E3 - FGF2	****	<0.0001
Control:E4E4 - FGF2 vs. High:E3E3 + FGF2	****	<0.0001
Control:E4E4 - FGF2 vs. High:E4E4 - FGF2	ns	>0.9999
Control:E4E4 - FGF2 vs. High:E4E4 + FGF2	ns	>0.9999
Control:E4E4 + FGF2 vs. Low:E3E3 - FGF2	****	<0.0001
Control:E4E4 + FGF2 vs. Low:E3E3 + FGF2	****	<0.0001
Control:E4E4 + FGF2 vs. Low:E4E4 - FGF2	ns	0.2360
Control:E4E4 + FGF2 vs. Low:E4E4 + FGF2	ns	>0.9999
Control:E4E4 + FGF2 vs. High:E3E3 - FGF2	****	<0.0001
Control:E4E4 + FGF2 vs. High:E3E3 + FGF2	****	<0.0001
Control:E4E4 + FGF2 vs. High:E4E4 - FGF2	ns	>0.9999
Control:E4E4 + FGF2 vs. High:E4E4 + FGF2	ns	>0.9999
Low:E3E3 - FGF2 vs. Low:E3E3 + FGF2	ns	0.2994
Low:E3E3 - FGF2 vs. Low:E4E4 - FGF2	****	<0.0001
Low:E3E3 - FGF2 vs. Low:E4E4 + FGF2	****	<0.0001
Low:E3E3 - FGF2 vs. High:E3E3 - FGF2	**	0.0092
Low:E3E3 - FGF2 vs. High:E3E3 + FGF2	****	<0.0001
Low:E3E3 - FGF2 vs. High:E4E4 - FGF2	****	<0.0001
Low:E3E3 - FGF2 vs. High:E4E4 + FGF2	****	<0.0001
Low:E3E3 + FGF2 vs. Low:E4E4 - FGF2	****	<0.0001
Low:E3E3 + FGF2 vs. Low:E4E4 + FGF2	****	<0.0001
Low:E3E3 + FGF2 vs. High:E3E3 - FGF2	ns	>0.9999
Low:E3E3 + FGF2 vs. High:E3E3 + FGF2	*	0.0181
Low:E3E3 + FGF2 vs. High:E4E4 - FGF2	****	<0.0001
Low:E3E3 + FGF2 vs. High:E4E4 + FGF2	****	<0.0001
Low:E4E4 - FGF2 vs. Low:E4E4 + FGF2	ns	>0.9999
Low:E4E4 - FGF2 vs. High:E3E3 - FGF2	****	<0.0001
Low:E4E4 - FGF2 vs. High:E3E3 + FGF2	****	<0.0001
Low:E4E4 - FGF2 vs. High:E4E4 - FGF2	ns	>0.9999
Low:E4E4 - FGF2 vs. High:E4E4 + FGF2	ns	>0.9999
Low:E4E4 + FGF2 vs. High:E3E3 - FGF2	****	<0.0001
Low:E4E4 + FGF2 vs. High:E3E3 + FGF2	****	<0.0001
Low:E4E4 + FGF2 vs. High:E4E4 - FGF2	ns	>0.9999
Low:E4E4 + FGF2 vs. High:E4E4 + FGF2	ns	>0.9999
High:E3E3 - FGF2 vs. High:E3E3 + FGF2	ns	0.5509
High:E3E3 - FGF2 vs. High:E4E4 - FGF2	****	<0.0001
High:E3E3 - FGF2 vs. High:E4E4 + FGF2	****	<0.0001

High:E3E3 + FGF2 vs. High:E4E4 - FGF2	****	<0.0001
High:E3E3 + FGF2 vs. High:E4E4 + FGF2	****	<0.0001
High:E4E4 - FGF2 vs. High:E4E4 + FGF2	ns	>0.9999

Table 8.6.2. Bonferroni post hoc of SLC1A3 mRNA expression.

ANOVA table	F (DFn, DFd)	P value
Factors	F (2, 30) = 15.54	P<0.0001
APOE	F (1, 30) = 8.608	P=0.0064
FGF2	F (1, 30) = 10.18	P=0.0033
Factors x APOE	F (2, 30) = 10.78	P=0.0003
Factors x FGF2	F (2, 30) = 1.583	P=0.2221
APOE x FGF2	F (1, 30) = 1.814	P=0.1881
Factors x APOE x FGF2	F (2, 30) = 0.02959	P=0.9709

Table 8.6.3. Three-way ANOVA analysis of SLC1A2 mRNA expression.

Bonferroni's multiple comparisons test	Summary	Adjusted P Value
Control:E3E3 - FGF2 vs. Control:E3E3 + FGF2	ns	>0.9999
Control:E3E3 - FGF2 vs. Control:E4E4 - FGF2	ns	>0.9999
Control:E3E3 - FGF2 vs. Control:E4E4 + FGF2	ns	>0.9999
Control:E3E3 - FGF2 vs. Low:E3E3 - FGF2	ns	>0.9999
Control:E3E3 - FGF2 vs. Low:E3E3 + FGF2	ns	>0.9999
Control:E3E3 - FGF2 vs. Low:E4E4 - FGF2	ns	>0.9999
Control:E3E3 - FGF2 vs. Low:E4E4 + FGF2	ns	>0.9999
Control:E3E3 - FGF2 vs. High:E3E3 - FGF2	***	0.0008
Control:E3E3 - FGF2 vs. High:E3E3 + FGF2	ns	>0.9999
Control:E3E3 - FGF2 vs. High:E4E4 - FGF2	ns	>0.9999
Control:E3E3 - FGF2 vs. High:E4E4 + FGF2	ns	>0.9999
Control:E3E3 + FGF2 vs. Control:E4E4 - FGF2	ns	>0.9999
Control:E3E3 + FGF2 vs. Control:E4E4 + FGF2	ns	>0.9999
Control:E3E3 + FGF2 vs. Low:E3E3 - FGF2	ns	>0.9999
Control:E3E3 + FGF2 vs. Low:E3E3 + FGF2	ns	>0.9999
Control:E3E3 + FGF2 vs. Low:E4E4 - FGF2	ns	>0.9999
Control:E3E3 + FGF2 vs. Low:E4E4 + FGF2	ns	>0.9999
Control:E3E3 + FGF2 vs. High:E3E3 - FGF2	****	<0.0001
Control:E3E3 + FGF2 vs. High:E3E3 + FGF2	*	0.0242
Control:E3E3 + FGF2 vs. High:E4E4 - FGF2	ns	>0.9999
Control:E3E3 + FGF2 vs. High:E4E4 + FGF2	ns	>0.9999
Control:E4E4 - FGF2 vs. Control:E4E4 + FGF2	ns	>0.9999
Control:E4E4 - FGF2 vs. Low:E3E3 - FGF2	ns	>0.9999

Control:E4E4 - FGF2 vs. Low:E3E3 + FGF2	ns	>0.9999
Control:E4E4 - FGF2 vs. Low:E4E4 - FGF2	ns	>0.9999
Control:E4E4 - FGF2 vs. Low:E4E4 + FGF2	ns	>0.9999
Control:E4E4 - FGF2 vs. High:E3E3 - FGF2	****	<0.0001
Control:E4E4 - FGF2 vs. High:E3E3 + FGF2	ns	0.1710
Control:E4E4 - FGF2 vs. High:E4E4 - FGF2	ns	>0.9999
Control:E4E4 - FGF2 vs. High:E4E4 + FGF2	ns	>0.9999
Control:E4E4 + FGF2 vs. Low:E3E3 - FGF2	ns	>0.9999
Control:E4E4 + FGF2 vs. Low:E3E3 + FGF2	ns	>0.9999
Control:E4E4 + FGF2 vs. Low:E4E4 - FGF2	ns	>0.9999
Control:E4E4 + FGF2 vs. Low:E4E4 + FGF2	ns	>0.9999
Control:E4E4 + FGF2 vs. High:E3E3 - FGF2	****	<0.0001
Control:E4E4 + FGF2 vs. High:E3E3 + FGF2	*	0.0476
Control:E4E4 + FGF2 vs. High:E4E4 - FGF2	ns	>0.9999
Control:E4E4 + FGF2 vs. High:E4E4 + FGF2	ns	>0.9999
Low:E3E3 - FGF2 vs. Low:E3E3 + FGF2	ns	>0.9999
Low:E3E3 - FGF2 vs. Low:E4E4 - FGF2	ns	>0.9999
Low:E3E3 - FGF2 vs. Low:E4E4 + FGF2	ns	>0.9999
Low:E3E3 - FGF2 vs. High:E3E3 - FGF2	***	0.0005
Low:E3E3 - FGF2 vs. High:E3E3 + FGF2	ns	>0.9999
Low:E3E3 - FGF2 vs. High:E4E4 - FGF2	ns	>0.9999
Low:E3E3 - FGF2 vs. High:E4E4 + FGF2	ns	>0.9999
Low:E3E3 + FGF2 vs. Low:E4E4 - FGF2	ns	>0.9999
Low:E3E3 + FGF2 vs. Low:E4E4 + FGF2	ns	>0.9999
Low:E3E3 + FGF2 vs. High:E3E3 - FGF2	****	<0.0001
Low:E3E3 + FGF2 vs. High:E3E3 + FGF2	ns	0.1690
Low:E3E3 + FGF2 vs. High:E4E4 - FGF2	ns	>0.9999
Low:E3E3 + FGF2 vs. High:E4E4 + FGF2	ns	>0.9999
Low:E4E4 - FGF2 vs. Low:E4E4 + FGF2	ns	>0.9999
Low:E4E4 - FGF2 vs. High:E3E3 - FGF2	**	0.0051
Low:E4E4 - FGF2 vs. High:E3E3 + FGF2	ns	>0.9999
Low:E4E4 - FGF2 vs. High:E4E4 - FGF2	ns	>0.9999
Low:E4E4 - FGF2 vs. High:E4E4 + FGF2	ns	>0.9999
Low:E4E4 + FGF2 vs. High:E3E3 - FGF2	**	0.0037

Low:E4E4 + FGF2 vs. High:E3E3 + FGF2	ns	>0.9999
Low:E4E4 + FGF2 vs. High:E4E4 - FGF2	ns	>0.9999
Low:E4E4 + FGF2 vs. High:E4E4 + FGF2	ns	>0.9999
High:E3E3 - FGF2 vs. High:E3E3 + FGF2	ns	0.2714
High:E3E3 - FGF2 vs. High:E4E4 - FGF2	**	0.0099
High:E3E3 - FGF2 vs. High:E4E4 + FGF2	****	<0.0001
High:E3E3 + FGF2 vs. High:E4E4 - FGF2	ns	>0.9999
High:E3E3 + FGF2 vs. High:E4E4 + FGF2	ns	0.2572
High:E4E4 - FGF2 vs. High:E4E4 + FGF2	ns	>0.9999

Table 8.6.4. Bonferroni post hoc of SLC1A2 mRNA expression.

ANOVA table	F (DFn, DFd)	P value
Factors	F (2, 29) = 119.4	P<0.0001
APOE Genotype	F (1, 29) = 1.246	P=0.2735
FGF2	F (1, 29) = 100.8	P<0.0001
Factors x APOE Genotype	F (2, 29) = 1.425	P=0.2569
Factors x FGF2	F (2, 29) = 30.83	P<0.0001
APOE Genotype x FGF2	F (1, 29) = 17.73	P=0.0002
Factors x APOE Genotype x FGF2	F (2, 29) = 14.43	P<0.0001

Table 8.6.5. Three-way ANOVA analysis of GLUL mRNA expression.

Bonferroni's multiple comparisons test	Summary	Adjusted P Value
Control:E3E3 - FGF2 vs. Control:E3E3 + FGF2	ns	>0.9999
Control:E3E3 - FGF2 vs. Control:E4E4 - FGF2	ns	0.1104
Control:E3E3 - FGF2 vs. Control:E4E4 + FGF2	ns	>0.9999
Control:E3E3 - FGF2 vs. Low:E3E3 - FGF2	****	<0.0001
Control:E3E3 - FGF2 vs. Low:E3E3 + FGF2	****	<0.0001
Control:E3E3 - FGF2 vs. Low:E4E4 - FGF2	****	<0.0001
Control:E3E3 - FGF2 vs. Low:E4E4 + FGF2	ns	0.3053
Control:E3E3 - FGF2 vs. High:E3E3 - FGF2	****	<0.0001
Control:E3E3 - FGF2 vs. High:E3E3 + FGF2	ns	0.2328
Control:E3E3 - FGF2 vs. High:E4E4 - FGF2	****	<0.0001
Control:E3E3 - FGF2 vs. High:E4E4 + FGF2	*	0.0180
Control:E3E3 + FGF2 vs. Control:E4E4 - FGF2	ns	>0.9999
Control:E3E3 + FGF2 vs. Control:E4E4 + FGF2	ns	>0.9999
Control:E3E3 + FGF2 vs. Low:E3E3 - FGF2	****	<0.0001
Control:E3E3 + FGF2 vs. Low:E3E3 + FGF2	****	<0.0001
Control:E3E3 + FGF2 vs. Low:E4E4 - FGF2	****	<0.0001
Control:E3E3 + FGF2 vs. Low:E4E4 + FGF2	ns	>0.9999
Control:E3E3 + FGF2 vs. High:E3E3 - FGF2	****	<0.0001
Control:E3E3 + FGF2 vs. High:E3E3 + FGF2	ns	>0.9999
Control:E3E3 + FGF2 vs. High:E4E4 - FGF2	***	0.0009
Control:E3E3 + FGF2 vs. High:E4E4 + FGF2	ns	>0.9999
Control:E4E4 - FGF2 vs. Control:E4E4 + FGF2	ns	>0.9999
Control:E4E4 - FGF2 vs. Low:E3E3 - FGF2	****	<0.0001

Control:E4E4 - FGF2 vs. Low:E3E3 + FGF2	*	0.0453
Control:E4E4 - FGF2 vs. Low:E4E4 - FGF2	****	<0.0001
Control:E4E4 - FGF2 vs. Low:E4E4 + FGF2	ns	>0.9999
Control:E4E4 - FGF2 vs. High:E3E3 - FGF2	**	0.0038
Control:E4E4 - FGF2 vs. High:E3E3 + FGF2	ns	>0.9999
Control:E4E4 - FGF2 vs. High:E4E4 - FGF2	ns	0.2285
Control:E4E4 - FGF2 vs. High:E4E4 + FGF2	ns	>0.9999
Control:E4E4 + FGF2 vs. Low:E3E3 - FGF2	****	<0.0001
Control:E4E4 + FGF2 vs. Low:E3E3 + FGF2	****	<0.0001
Control:E4E4 + FGF2 vs. Low:E4E4 - FGF2	****	<0.0001
Control:E4E4 + FGF2 vs. Low:E4E4 + FGF2	ns	>0.9999
Control:E4E4 + FGF2 vs. High:E3E3 - FGF2	****	<0.0001
Control:E4E4 + FGF2 vs. High:E3E3 + FGF2	ns	>0.9999
Control:E4E4 + FGF2 vs. High:E4E4 - FGF2	***	0.0005
Control:E4E4 + FGF2 vs. High:E4E4 + FGF2	ns	0.4845
Low:E3E3 - FGF2 vs. Low:E3E3 + FGF2	*	0.0152
Low:E3E3 - FGF2 vs. Low:E4E4 - FGF2	**	0.0079
Low:E3E3 - FGF2 vs. Low:E4E4 + FGF2	****	<0.0001
Low:E3E3 - FGF2 vs. High:E3E3 - FGF2	ns	0.2052
Low:E3E3 - FGF2 vs. High:E3E3 + FGF2	****	<0.0001
Low:E3E3 - FGF2 vs. High:E4E4 - FGF2	*	0.0120
Low:E3E3 - FGF2 vs. High:E4E4 + FGF2	****	<0.0001
Low:E3E3 + FGF2 vs. Low:E4E4 - FGF2	****	<0.0001
Low:E3E3 + FGF2 vs. Low:E4E4 + FGF2	*	0.0155
Low:E3E3 + FGF2 vs. High:E3E3 - FGF2	ns	>0.9999
Low:E3E3 + FGF2 vs. High:E3E3 + FGF2	*	0.0207
Low:E3E3 + FGF2 vs. High:E4E4 - FGF2	ns	>0.9999
Low:E3E3 + FGF2 vs. High:E4E4 + FGF2	ns	0.2655
Low:E4E4 - FGF2 vs. Low:E4E4 + FGF2	****	<0.0001
Low:E4E4 - FGF2 vs. High:E3E3 - FGF2	****	<0.0001
Low:E4E4 - FGF2 vs. High:E3E3 + FGF2	****	<0.0001
Low:E4E4 - FGF2 vs. High:E4E4 - FGF2	****	<0.0001
Low:E4E4 - FGF2 vs. High:E4E4 + FGF2	****	<0.0001
Low:E4E4 + FGF2 vs. High:E3E3 - FGF2	**	0.0013

Low:E4E4 + FGF2 vs. High:E3E3 + FGF2	ns	>0.9999
Low:E4E4 + FGF2 vs. High:E4E4 - FGF2	ns	0.0874
Low:E4E4 + FGF2 vs. High:E4E4 + FGF2	ns	>0.9999
High:E3E3 - FGF2 vs. High:E3E3 + FGF2	**	0.0017
High:E3E3 - FGF2 vs. High:E4E4 - FGF2	ns	>0.9999
High:E3E3 - FGF2 vs. High:E4E4 + FGF2	*	0.0244
High:E3E3 + FGF2 vs. High:E4E4 - FGF2	ns	0.1137
High:E3E3 + FGF2 vs. High:E4E4 + FGF2	ns	>0.9999
High:E4E4 - FGF2 vs. High:E4E4 + FGF2	ns	>0.9999

Table 8.6.6. Bonferroni post hoc of GLUL mRNA expression.

8.7 Appendix 7 – Presentations and publications

8.7.1 Presentations

McComish S.F., Caldwell M.A. The effect of inflammatory cytokines on astrocytes in a human induced pluripotent stem cell-derived *in vitro* model of neurodegeneration. ***Oral presentation at the Royal Academy of Medicine in Ireland, Biomedical Sciences Section Annual Meeting, Dublin, Ireland, June 2017.***

McComish S.F., Caldwell M.A. The effect of inflammatory cytokines on astrocytes in a human induced pluripotent stem cell-derived *in vitro* model of neurodegeneration. ***Poster presentation at the Neuroscience Ireland Conference, Galway, Ireland, August 2017.***

McComish S.F., Caldwell M.A. The effect of inflammatory cytokines on astrocytes in a human induced pluripotent stem cell-derived *in vitro* model of neurodegeneration. ***Oral presentation at the Neuroscience Ireland Conference, Galway, Ireland, August 2017.***

McComish S.F., Caldwell M.A. The effect of inflammatory cytokines on astrocytes in a human induced pluripotent stem cell-derived *in vitro* model of neurodegeneration. ***Oral presentation at the Network for European CNS Transplantation & Restoration (NECTAR) Annual Meeting, Dublin, Ireland, December 2017.***

McComish S.F., Crompton L.A., Lane J.D., Caldwell M.A. The effect of inflammatory microglial factors and Apolipoprotein E genotype on astrocytes in a human induced pluripotent stem cell-derived *in vitro* model of Alzheimer's disease. ***Oral presentation at the Network for European CNS Transplantation & Restoration (NECTAR) Annual Meeting, Paris, France, December 2018.***

McComish S.F., Haetzel L., Farrell C., Leavy E., O'Connor C., Boyle N., Crompton L.A., Lane J.D., Caldwell M.A. The effect of inflammatory insult and apolipoprotein E genotype on astrocytes in a human induced pluripotent stem cell-derived *in vitro* model of Alzheimer's disease. ***Poster presentation at the British Neuroscience Association and Neuroscience Ireland Conference and Festival of Neuroscience, Dublin, Ireland, April 2019.***

McComish S.F., Crompton L.A., Lane J.D., Caldwell M.A. The effect of inflammatory insult and apolipoprotein E genotype on astrocytes in a human induced pluripotent stem cell-derived *in vitro* model of Alzheimer's disease. ***Oral presentation at the Network for European CNS Transplantation & Restoration (NECTAR) Annual Meeting, Cardiff, Wales, November 2019.***

8.7.2 Publications

McComish SF & Caldwell MA. (2018). Generation of defined neural populations from pluripotent stem cells. *Philos Trans R Soc Lond B Biol Sci* **373**.

Hawkins SJ, Crompton LA, Sood A, Saunders M, Boyle NT, Buckley A, Minogue AM, McComish SF, Jimenez-Moreno N, Cordero-Llana O, Stathakos P, Gilmore CE, Kelly S, Lane JD, Case CP & Caldwell MA. (2018). Nanoparticle-induced neuronal toxicity across placental barriers is mediated by autophagy and dependent on astrocytes. *Nat Nanotechnol* **13**, 427-433.

Chapter 9

Bibliography

9. Bibliography

(2020). 2020 Alzheimer's disease facts and figures. *Alzheimers Dement*.

Abbott NJ, Rönnbäck L & Hansson E. (2006). Astrocyte-endothelial interactions at the blood-brain barrier. *Nat Rev Neurosci* **7,** 41-53.

Abdullah L, Crawford F, Tsolaki M, Borjesson-Hanson A, Olde Rikkert M, Pasquier F, Wallin A, Kennelly S, Ait-Ghezala G, Paris D, Hendrix S, Blennow K, Lawlor B & Mullan M. (2020). The Influence of Baseline Alzheimer's Disease Severity on Cognitive Decline and CSF Biomarkers in the NILVAD Trial. *Front Neurol* **11,** 149.

Abdullah L, Evans JE, Emmerich T, Crynen G, Shackleton B, Keegan AP, Luis C, Tai L, LaDu MJ & Mullan M. (2017). APOE ε4 specific imbalance of arachidonic acid and docosahexaenoic acid in serum phospholipids identifies individuals with preclinical Mild Cognitive Impairment/Alzheimer's Disease. *Aging (Albany NY)* **9,** 964.

Abraham JA, Whang JL, Tumolo A, Mergia A, Friedman J, Gospodarowicz D & Fiddes JC. (1986). Human basic fibroblast growth factor: nucleotide sequence and genomic organization. *Embo j* **5,** 2523-2528.

Abramov AY, Canevari L & Duchen MR. (2003). Changes in intracellular calcium and glutathione in astrocytes as the primary mechanism of amyloid neurotoxicity. *J Neurosci* **23,** 5088-5095.

Abu-Remaileh M, Gerson A, Farago M, Nathan G, Alkalay I, Zins Rousso S, Gur M, Fainsod A & Bergman Y. (2010). Oct-3/4 regulates stem cell identity and cell fate decisions by modulating Wnt/beta-catenin signalling. *Embo j* **29,** 3236-3248.

Agulhon C, Sun MY, Murphy T, Myers T, Lauderdale K & Fiacco TA. (2012). Calcium Signaling and Gliotransmission in Normal vs. Reactive Astrocytes. *Front Pharmacol* **3,** 139.

Al-Ghezi ZZ, Miranda K, Nagarkatti M & Nagarkatti PS. (2019). Combination of Cannabinoids, Delta9- Tetrahydrocannabinol and Cannabidiol, Ameliorates Experimental Multiple Sclerosis by Suppressing Neuroinflammation Through Regulation of miRNA-Mediated Signaling Pathways. *Front Immunol* **10,** 1921.

Allen NJ. (2014). Astrocyte regulation of synaptic behavior. *Annu Rev Cell Dev Biol* **30,** 439-463.

Almad AA, Doreswamy A, Gross SK, Richard JP, Huo Y, Haughey N & Maragakis NJ. (2016). Connexin 43 in astrocytes contributes to motor neuron toxicity in amyotrophic lateral sclerosis. *Glia* **64,** 1154-1169.

Aloisi F, Care A, Borsellino G, Gallo P, Rosa S, Bassani A, Cabibbo A, Testa U, Levi G & Peschle C. (1992). Production of hemolymphopoietic cytokines (IL-6, IL-8, colony-stimulating factors) by normal human astrocytes in response to IL-1 beta and tumor necrosis factor-alpha. *J Immunol* **149,** 2358-2366.

Alvarez JI, Dodelet-Devillers A, Kebir H, Ifergan I, Fabre PJ, Terouz S, Sabbagh M, Wosik K, Bourbonniere L, Bernard M, van Horssen J, de Vries HE, Charron F & Prat A. (2011). The Hedgehog pathway promotes blood-brain barrier integrity and CNS immune quiescence. *Science* **334,** 1727-1731.

Anderson MA, Ao Y & Sofroniew MV. (2014). Heterogeneity of reactive astrocytes. *Neurosci Lett* **565,** 23-29.

Anderson MA, Burda JE, Ren Y, Ao Y, O'Shea TM, Kawaguchi R, Coppola G, Khakh BS, Deming TJ & Sofroniew MV. (2016). Astrocyte scar formation aids central nervous system axon regeneration. *Nature* **532,** 195-200.

Angelova PR & Abramov AY. (2014). Interaction of neurons and astrocytes underlies the mechanism of Abeta-induced neurotoxicity. *Biochem Soc Trans* **42,** 1286-1290.

Aparicio-Blanco J, Romero IA, Male DK, Slowing K, Garcia-Garcia L & Torres-Suarez AI. (2019). Cannabidiol Enhances the Passage of Lipid Nanocapsules across the Blood-Brain Barrier Both in Vitro and in Vivo. *Mol Pharm* **16,** 1999-2010.

Araki R, Uda M, Hoki Y, Sunayama M, Nakamura M, Ando S, Sugiura M, Ideno H, Shimada A, Nifuji A & Abe M. (2013). Negligible immunogenicity of terminally differentiated cells derived from induced pluripotent or embryonic stem cells. *Nature* **494,** 100-104.

Araque A, Sanzgiri RP, Parpura V & Haydon PG. (1999). Astrocyte-induced modulation of synaptic transmission. *Can J Physiol Pharmacol* **77,** 699-706.

Arber C, Precious SV, Cambray S, Risner-Janiczek JR, Kelly C, Noakes Z, Fjodorova M, Heuer A, Ungless MA, Rodriguez TA, Rosser AE, Dunnett SB & Li M. (2015). Activin A directs striatal projection neuron differentiation of human pluripotent stem cells. *Development* **142,** 1375-1386.

Armbruster M, Hanson E & Dulla CG. (2016). Glutamate Clearance Is Locally Modulated by Presynaptic Neuronal Activity in the Cerebral Cortex. *J Neurosci* **36,** 10404-10415.

Aronica E, Gorter JA, Ijlst-Keizers H, Rozemuller AJ, Yankaya B, Leenstra S & Troost D. (2003). Expression and functional role of mGluR3 and mGluR5 in human astrocytes and glioma cells: opposite regulation of glutamate transporter proteins. *European Journal of Neuroscience* **17,** 2106-2118.

Arriza JL, Eliasof S, Kavanaugh MP & Amara SG. (1997). Excitatory amino acid transporter 5, a retinal glutamate transporter coupled to a chloride conductance. *Proc Natl Acad Sci U S A* **94,** 4155-4160.

Arriza JL, Fairman WA, Wadiche JI, Murdoch GH, Kavanaugh MP & Amara SG. (1994). Functional comparisons of three glutamate transporter subtypes cloned from human motor cortex. *J Neurosci* **14,** 5559-5569.

Arsenijevic Y, Weiss S, Schneider B & Aebischer P. (2001). Insulin-like growth factor-I is necessary for neural stem cell proliferation and demonstrates distinct actions of epidermal growth factor and fibroblast growth factor-2. *J Neurosci* **21,** 7194-7202.

Ashpole NM, Chawla AR, Martin MP, Brustovetsky T, Brustovetsky N & Hudmon A. (2013). Loss of calcium/calmodulin-dependent protein kinase II activity in cortical astrocytes decreases glutamate uptake and induces neurotoxic release of ATP. *J Biol Chem* **288,** 14599-14611.

Aso E, Sanchez-Pla A, Vegas-Lozano E, Maldonado R & Ferrer I. (2015). Cannabis-based medicine reduces multiple pathological processes in AbetaPP/PS1 mice. *J Alzheimers Dis* **43,** 977-991.

Association As. (2015). 2015 Alzheimer's disease facts and figures. *Alzheimers Dement* **11,** 332-384.

Attwell D, Buchan AM, Charpak S, Lauritzen M, Macvicar BA & Newman EA. (2010). Glial and neuronal control of brain blood flow. *Nature* **468,** 232-243.

Avior Y, Sagi I & Benvenisty N. (2016). Pluripotent stem cells in disease modelling and drug discovery. *Nat Rev Mol Cell Biol* **17,** 170-182.

Azevedo FA, Carvalho LR, Grinberg LT, Farfel JM, Ferretti RE, Leite RE, Jacob Filho W, Lent R & Herculano-Houzel S. (2009). Equal numbers of neuronal and nonneuronal cells make the human brain an isometrically scaled-up primate brain. *J Comp Neurol* **513,** 532-541.

Bachmeier C, Shackleton B, Ojo J, Paris D, Mullan M & Crawford F. (2014). Apolipoprotein E isoform-specific effects on lipoprotein receptor processing. *Neuromolecular Med* **16,** 686-696.

Bagheri-Fam S, Sim H, Bernard P, Jayakody I, Taketo MM, Scherer G & Harley VR. (2008). Loss of Fgfr2 leads to partial XY sex reversal. *Dev Biol* **314,** 71-83.

Bagyinszky E, Youn YC, An SS & Kim S. (2014). The genetics of Alzheimer's disease. *Clin Interv Aging* **9,** 535-551.

Baitsch D, Bock HH, Engel T, Telgmann R, Muller-Tidow C, Varga G, Bot M, Herz J, Robenek H, von Eckardstein A & Nofer JR. (2011). Apolipoprotein E induces antiinflammatory phenotype in macrophages. *Arterioscler Thromb Vasc Biol* **31,** 1160-1168.

Bal-Price A & Brown GC. (2001). Inflammatory neurodegeneration mediated by nitric oxide from activated glia-inhibiting neuronal respiration, causing glutamate release and excitotoxicity. *Journal of Neuroscience* **21,** 6480-6491.

Baldwin KT & Eroglu C. (2017). Molecular mechanisms of astrocyte-induced synaptogenesis. *Curr Opin Neurobiol* **45,** 113-120.

Barage SH & Sonawane KD. (2015). Amyloid cascade hypothesis: Pathogenesis and therapeutic strategies in Alzheimer's disease. *Neuropeptides* **52,** 1-18.

Barateiro A, Domingues HS, Fernandes A, Relvas JB & Brites D. (2014). Rat cerebellar slice cultures exposed to bilirubin evidence reactive gliosis, excitotoxicity and impaired myelinogenesis that is prevented by AMPA and TNF-alpha inhibitors. *Mol Neurobiol* **49,** 424-439.

Barger SW & Harmon AD. (1997). Microglial activation by Alzheimer amyloid precursor protein and modulation by apolipoprotein E. *Nature* **388,** 878-881.

Barnes DA, Huston M, Holmes R, Benveniste EN, Yong VW, Scholz P & Perez HD. (1996). Induction of RANTES expression by astrocytes and astrocytoma cell lines. *J Neuroimmunol* **71,** 207-214.

Batarseh YS, Duong QV, Mousa YM, Al Rihani SB, Elfakhri K & Kaddoumi A. (2016). Amyloid-beta and Astrocytes Interplay in Amyloid-beta Related Disorders. *Int J Mol Sci* **17,** 338.

Bauer D, Haroutunian V, Meador-Woodruff JH & McCullumsmith RE. (2010). Abnormal glycosylation of EAAT1 and EAAT2 in prefrontal cortex of elderly patients with schizophrenia. *Schizophr Res* **117,** 92-98.

Becerra-Calixto A & Cardona-Gomez GP. (2017). The Role of Astrocytes in Neuroprotection after Brain Stroke: Potential in Cell Therapy. *Front Mol Neurosci* **10,** 88.

Beckstrøm H, Julsrud L, Haugeto Ø, Dewar D, Graham DI, Lehre KP, Storm-Mathisen J & Danbolt NC. (1999). Interindividual differences in the levels of the glutamate transporters GLAST and GLT, but no clear correlation with Alzheimer's disease. *Journal of neuroscience research* **55,** 218-229.

Bedogni F, Hodge RD, Elsen GE, Nelson BR, Daza RA, Beyer RP, Bammler TK, Rubenstein JL & Hevner RF. (2010). Tbr1 regulates regional and laminar identity of postmitotic neurons in developing neocortex. *Proc Natl Acad Sci U S A* **107,** 13129-13134.

Beecham GW, Hamilton K, Naj AC, Martin ER, Huentelman M, Myers AJ, Corneveaux JJ, Hardy J, Vonsattel JP, Younkin SG, Bennett DA, De Jager PL, Larson EB, Crane PK, Kamboh MI, Kofler JK, Mash DC, Duque L, Gilbert JR, Gwirtsman H, Buxbaum JD, Kramer P, Dickson DW, Farrer LA, Frosch MP, Ghetti B, Haines JL, Hyman BT, Kukull WA, Mayeux RP, Pericak-Vance MA, Schneider JA, Trojanowski JQ, Reiman EM, Schellenberg GD & Montine TJ. (2014). Genome-wide association meta-analysis of neuropathologic features of Alzheimer's disease and related dementias. *PLoS Genet* **10,** e1004606.

Belinsky GS, Sirois CL, Rich MT, Short SM, Moore AR, Gilbert SE & Antic SD. (2013). Dopamine receptors in human embryonic stem cell neurodifferentiation. *Stem Cells Dev* **22,** 1522-1540.

Bell RD, Winkler EA, Singh I, Sagare AP, Deane R, Wu Z, Holtzman DM, Betsholtz C, Armulik A, Sallstrom J, Berk BC & Zlokovic BV. (2012). Apolipoprotein E controls cerebrovascular integrity via cyclophilin A. *Nature* **485,** 512-516.

Belloy ME, Napolioni V & Greicius MD. (2019). A Quarter Century of APOE and Alzheimer's Disease: Progress to Date and the Path Forward. *Neuron* **101,** 820-838.

Ben Haim L, Carrillo-de Sauvage MA, Ceyzeriat K & Escartin C. (2015). Elusive roles for reactive astrocytes in neurodegenerative diseases. *Front Cell Neurosci* **9,** 278.

Ben Halima S, Mishra S, Raja KMP, Willem M, Baici A, Simons K, Brüstle O, Koch P, Haass C, Caflisch A & Rajendran L. (2016). Specific Inhibition of β-Secretase Processing of the Alzheimer Disease Amyloid Precursor Protein. *Cell Rep* **14,** 2127-2141.

Benarroch EE. (2008). Brain cholesterol metabolism and neurologic disease. *Neurology* **71,** 1368-1373.

Benarroch EE. (2016). Astrocyte signaling and synaptic homeostasis: II: Astrocyte-neuron interactions and clinical correlations. *Neurology* **87,** 726-735.

Bender RA, Janssen KA, Resnick AD, Blumenberg M, Foor F & Magasanik B. (1977). Biochemical parameters of glutamine synthetase from Klebsiella aerogenes. *J Bacteriol* **129,** 1001-1009.

Benito C, Kim WK, Chavarria I, Hillard CJ, Mackie K, Tolon RM, Williams K & Romero J. (2005). A glial endogenous cannabinoid system is upregulated in the brains of macaques with simian immunodeficiency virus-induced encephalitis. *J Neurosci* **25,** 2530-2536.

Benveniste EN, Sparacio SM, Norris JG, Grenett HE & Fuller GM. (1990). Induction and regulation of interleukin-6 gene expression in rat astrocytes. *J Neuroimmunol* **30,** 201-212.

Bertram L, Lange C, Mullin K, Parkinson M, Hsiao M, Hogan MF, Schjeide BM, Hooli B, Divito J, Ionita I, Jiang H, Laird N, Moscarillo T, Ohlsen KL, Elliott K, Wang X, Hu-Lince D, Ryder M, Murphy A, Wagner SL, Blacker D, Becker KD & Tanzi RE. (2008). Genome-wide association analysis reveals putative Alzheimer's disease susceptibility loci in addition to APOE. *Am J Hum Genet* **83,** 623-632.

Besusso D, Schellino R, Boido M, Belloli S, Parolisi R, Conforti P, Faedo A, Cernigoj M, Campus I, Laporta A, Bocchi VD, Murtaj V, Parmar M, Spaiardi P, Talpo F, Maniezzi C, Toselli MG, Biella G, Moresco RM, Vercelli A, Buffo A & Cattaneo E. (2020). Stem Cell-Derived Human Striatal Progenitors Innervate Striatal Targets and Alleviate Sensorimotor Deficit in a Rat Model of Huntington Disease. *Stem Cell Reports*.

Bi F, Huang C, Tong J, Qiu G, Huang B, Wu Q, Li F, Xu Z, Bowser R, Xia XG & Zhou H. (2013). Reactive astrocytes secrete lcn2 to promote neuron death. *Proc Natl Acad Sci U S A* **110,** 4069-4074.

Bilican B, Serio A, Barmada SJ, Nishimura AL, Sullivan GJ, Carrasco M, Phatnani HP, Puddifoot CA, Story D, Fletcher J, Park IH, Friedman BA, Daley GQ, Wyllie DJ, Hardingham GE, Wilmut I, Finkbeiner S, Maniatis T, Shaw CE & Chandran S. (2012). Mutant induced pluripotent stem cell lines recapitulate aspects of TDP-43 proteinopathies and reveal cell-specific vulnerability. *Proc Natl Acad Sci U S A* **109,** 5803-5808.

Bissonnette CJ, Lyass L, Bhattacharyya BJ, Belmadani A, Miller RJ & Kessler JA. (2011). The controlled generation of functional basal forebrain cholinergic neurons from human embryonic stem cells. *Stem Cells* **29,** 802-811.

Bliss TV & Collingridge GL. (1993). A synaptic model of memory: long-term potentiation in the hippocampus. *Nature* **361,** 31-39.

Boisvert MM, Erikson GA, Shokhirev MN & Allen NJ. (2018). The Aging Astrocyte Transcriptome from Multiple Regions of the Mouse Brain. *Cell Rep* **22,** 269-285.

Bonham LW, Desikan RS & Yokoyama JS. (2016). The relationship between complement factor C3, APOE epsilon4, amyloid and tau in Alzheimer's disease. *Acta Neuropathol Commun* **4,** 65.

Booz GW. (2011). Cannabidiol as an emergent therapeutic strategy for lessening the impact of inflammation on oxidative stress. *Free Radic Biol Med* **51,** 1054-1061.

Bowman GL, Dayon L, Kirkland R, Wojcik J, Peyratout G, Severin IC, Henry H, Oikonomidi A, Migliavacca E, Bacher M & Popp J. (2018). Blood-brain barrier breakdown, neuroinflammation, and cognitive decline in older adults. *Alzheimers Dement* **14,** 1640-1650.

Braak H, Rub U, Schultz C & Del Tredici K. (2006). Vulnerability of cortical neurons to Alzheimer's and Parkinson's diseases. *J Alzheimers Dis* **9,** 35-44.

Brecht WJ, Harris FM, Chang S, Tesseur I, Yu GQ, Xu Q, Dee Fish J, Wyss-Coray T, Buttini M, Mucke L, Mahley RW & Huang Y. (2004). Neuron-specific apolipoprotein e4 proteolysis is associated with increased tau phosphorylation in brains of transgenic mice. *J Neurosci* **24,** 2527-2534.

Brenner M. (2014). Role of GFAP in CNS injuries. *Neurosci Lett* **565,** 7-13.

Brodbeck J, McGuire J, Liu Z, Meyer-Franke A, Balestra ME, Jeong DE, Pleiss M, McComas C, Hess F, Witter D, Peterson S, Childers M, Goulet M, Liverton N, Hargreaves R, Freedman S, Weisgraber KH, Mahley RW & Huang Y. (2011). Structure-dependent impairment of intracellular apolipoprotein E4 trafficking and its detrimental effects are rescued by small-molecule structure correctors. *J Biol Chem* **286,** 17217-17226.

Brouwers N, Van Cauwenberghe C, Engelborghs S, Lambert JC, Bettens K, Le Bastard N, Pasquier F, Montoya AG, Peeters K, Mattheijssens M, Vandenberghe R, Deyn PP, Cruts M, Amouyel P, Sleegers K & Van Broeckhoven C. (2012). Alzheimer risk associated with a copy number variation in the complement receptor 1 increasing C3b/C4b binding sites. *Mol Psychiatry* **17,** 223-233.

Brown AM & Ransom BR. (2007). Astrocyte glycogen and brain energy metabolism. *Glia* **55,** 1263-1271.

Brown RC, Mark KS, Egleton RD, Huber JD, Burroughs AR & Davis TP. (2003). Protection against hypoxia-induced increase in blood-brain barrier permeability: role of tight junction proteins and NFkappaB. *J Cell Sci* **116,** 693-700.

Brustovetsky N, Brustovetsky T, Jemmerson R & Dubinsky JM. (2002). Calcium-induced cytochrome c release from CNS mitochondria is associated with the permeability transition and rupture of the outer membrane. *J Neurochem* **80,** 207-218.

Bu G. (2009). Apolipoprotein E and its receptors in Alzheimer's disease: pathways, pathogenesis and therapy. *Nat Rev Neurosci* **10,** 333-344.

Burdine RD, Chen EB, Kwok SF & Stern MJ. (1997). egl-17 encodes an invertebrate fibroblast growth factor family member required specifically for sex myoblast migration in Caenorhabditis elegans. *Proc Natl Acad Sci U S A* **94,** 2433-2437.

Burkert K, Moodley K, Angel CE, Brooks A & Graham ES. (2012). Detailed analysis of inflammatory and neuromodulatory cytokine secretion from human NT2 astrocytes using multiplex bead array. *Neurochem Int* **60,** 573-580.

Burstein S. (2015). Cannabidiol (CBD) and its analogs: a review of their effects on inflammation. *Bioorg Med Chem* **23,** 1377-1385.

Butchbach ME, Tian G, Guo H & Lin CL. (2004). Association of excitatory amino acid transporters, especially EAAT2, with cholesterol-rich lipid raft microdomains: importance for excitatory amino acid transporter localization and function. *J Biol Chem* **279,** 34388-34396.

Butterfield DA, Hensley K, Cole P, Subramaniam R, Aksenov M, Aksenova M, Bummer PM, Haley BE & Carney JM. (1997). Oxidatively induced structural alteration of glutamine synthetase assessed by analysis of spin label incorporation kinetics: relevance to Alzheimer's disease. *J Neurochem* **68,** 2451-2457.

Byun YG & Chung WS. (2018). A Novel In Vitro Live-imaging Assay of Astrocyte-mediated Phagocytosis Using pH Indicator-conjugated Synaptosomes. *J Vis Exp*.

Cabral GA & Jamerson M. (2014). Marijuana use and brain immune mechanisms. *Int Rev Neurobiol* **118,** 199-230.

Cahoy JD, Emery B, Kaushal A, Foo LC, Zamanian JL, Christopherson KS, Xing Y, Lubischer JL, Krieg PA, Krupenko SA, Thompson WJ & Barres BA. (2008). A transcriptome database for astrocytes, neurons, and oligodendrocytes: a new resource for understanding brain development and function. *J Neurosci* **28,** 264-278.

Caiazzo M, Giannelli S, Valente P, Lignani G, Carissimo A, Sessa A, Colasante G, Bartolomeo R, Massimino L, Ferroni S, Settembre C, Benfenati F & Broccoli V. (2015). Direct conversion of fibroblasts into functional astrocytes by defined transcription factors. *Stem Cell Reports* **4,** 25-36.

Campbell NK, Fitzgerald HK, Fletcher JM & Dunne A. (2019). Plant-Derived Polyphenols Modulate Human Dendritic Cell Metabolism and Immune Function via AMPK-Dependent Induction of Heme Oxygenase-1. *Front Immunol* **10,** 345.

Campbell NK, Fitzgerald HK, Malara A, Hambly R, Sweeney CM, Kirby B, Fletcher JM & Dunne A. (2018). Naturally derived Heme-Oxygenase 1 inducers attenuate inflammatory responses in human dendritic cells and T cells: relevance for psoriasis treatment. *Sci Rep* **8,** 10287.

Capani F, Quarracino C, Caccuri R & Sica RE. (2016). Astrocytes As the Main Players in Primary Degenerative Disorders of the Human Central Nervous System. *Front Aging Neurosci* **8,** 45.

Cardinal von Widdern J, Hohmann T & Dehghani F. (2020). Abnormal Cannabidiol Affects Production of Pro-Inflammatory Mediators and Astrocyte Wound Closure in Primary Astrocytic-Microglial Cocultures. *Molecules* **25**.

Carrera I, Etcheverría I, Li Y, Fernández-Novoa L, Lombardi V, Vigo C, Palacios HH, Benberin VV, Cacabelos R & Aliev G. (2013). Immunocytochemical characterization of Alzheimer disease hallmarks in APP/PS1 transgenic mice treated with a new anti-amyloid-β vaccine. *Biomed Res Int* **2013,** 709145.

Carrier EJ, Auchampach JA & Hillard CJ. (2006). Inhibition of an equilibrative nucleoside transporter by cannabidiol: a mechanism of cannabinoid immunosuppression. *Proc Natl Acad Sci U S A* **103,** 7895-7900.

Casper D & Blum M. (1995). Epidermal growth factor and basic fibroblast growth factor protect dopaminergic neurons from glutamate toxicity in culture. *J Neurochem* **65,** 1016-1026.

Cassano T, Calcagnini S, Pace L, De Marco F, Romano A & Gaetani S. (2017). Cannabinoid Receptor 2 Signaling in Neurodegenerative Disorders: From Pathogenesis to a Promising Therapeutic Target. *Front Neurosci* **11,** 30.

Cassano T, Serviddio G, Gaetani S, Romano A, Dipasquale P, Cianci S, Bellanti F, Laconca L, Romano AD, Padalino I, LaFerla FM, Nicoletti F, Cuomo V & Vendemiale G. (2012). Glutamatergic alterations and mitochondrial impairment in a murine model of Alzheimer disease. *Neurobiol Aging* **33,** 1121.e1121-1112.

Casse F, Richetin K & Toni N. (2018). Astrocytes' Contribution to Adult Neurogenesis in Physiology and Alzheimer's Disease. *Front Cell Neurosci* **12,** 432.

Castegna A, Aksenov M, Aksenova M, Thongboonkerd V, Klein JB, Pierce WM, Booze R, Markesbery WR & Butterfield DA. (2002). Proteomic identification of oxidatively modified proteins in Alzheimer's disease brain. Part I: creatine kinase BB, glutamine synthase, and ubiquitin carboxy-terminal hydrolase L-1. *Free Radical Biology and Medicine* **33,** 562-571.

Castellano JM, Kim J, Stewart FR, Jiang H, DeMattos RB, Patterson BW, Fagan AM, Morris JC, Mawuenyega KG, Cruchaga C, Goate AM, Bales KR, Paul SM, Bateman RJ & Holtzman DM. (2011). Human apoE isoforms differentially regulate brain amyloid-beta peptide clearance. *Sci Transl Med* **3,** 89ra57.

Castillo A, Tolon MR, Fernandez-Ruiz J, Romero J & Martinez-Orgado J. (2010). The neuroprotective effect of cannabidiol in an in vitro model of newborn hypoxic-ischemic brain damage in mice is mediated by CB(2) and adenosine receptors. *Neurobiol Dis* **37,** 434-440.

Cataldo AM, Peterhoff CM, Troncoso JC, Gomez-Isla T, Hyman BT & Nixon RA. (2000). Endocytic pathway abnormalities precede amyloid β deposition in sporadic Alzheimer's disease and Down syndrome: differential effects of APOE genotype and presenilin mutations. *The American journal of pathology* **157,** 277-286.

Cedazo-Mínguez A, Wiehager B, Winblad B, Hüttinger M & Cowburn RF. (2001). Effects of apolipoprotein E (apoE) isoforms, β-amyloid (Aβ) and apoE/Aβ complexes on Protein Kinase C-α (PKC-α) translocation and amyloid precursor protein (APP) processing in human SH-SY5Y neuroblastoma cells and fibroblasts. *Neurochemistry international* **38,** 615-625.

Ceprian M, Jimenez-Sanchez L, Vargas C, Barata L, Hind W & Martinez-Orgado J. (2017). Cannabidiol reduces brain damage and improves functional recovery in a neonatal rat model of arterial ischemic stroke. *Neuropharmacology* **116,** 151-159.

Ceyzeriat K, Ben Haim L, Denizot A, Pommier D, Matos M, Guillemaud O, Palomares MA, Abjean L, Petit F, Gipchtein P, Gaillard MC, Guillermier M, Bernier S, Gaudin M, Auregan G, Josephine C, Dechamps N, Veran J, Langlais V, Cambon K, Bemelmans AP, Baijer J, Bonvento G, Dhenain M, Deleuze JF, Oliet SHR, Brouillet E, Hantraye P, Carrillo-de Sauvage MA, Olaso R, Panatier A & Escartin C. (2018). Modulation of astrocyte reactivity improves functional deficits in mouse models of Alzheimer's disease. *Acta Neuropathol Commun* **6,** 104.

Chai M & Kohyama J. (2019). Non-Cell-Autonomous Neurotoxicity in Parkinson's Disease Mediated by Astroglial alpha-Synuclein. *Stem Cell Reports* **12,** 183-185.

Chambers SM, Fasano CA, Papapetrou EP, Tomishima M, Sadelain M & Studer L. (2009). Highly efficient neural conversion of human ES and iPS cells by dual inhibition of SMAD signaling. *Nat Biotechnol* **27,** 275-280.

Chandra G, Rangasamy SB, Roy A, Kordower JH & Pahan K. (2016). Neutralization of RANTES and Eotaxin Prevents the Loss of Dopaminergic Neurons in a Mouse Model of Parkinson Disease. *J Biol Chem* **291,** 15267-15281.

Chandrasekaran A, Avci HX, Leist M, Kobolák J & Dinnyés A. (2016). Astrocyte Differentiation of Human Pluripotent Stem Cells: New Tools for Neurological Disorder Research. *Front Cell Neurosci* **10,** 215.

Chang YT, Kazui H, Ikeda M, Huang CW, Huang SH, Hsu SW, Chang WN & Chang CC. (2019). Genetic Interaction of APOE and FGF1 is Associated with Memory Impairment and Hippocampal Atrophy in Alzheimer's Disease. *Aging Dis* **10,** 510-519.

Chappell J & Dalton S. (2013). Roles for MYC in the establishment and maintenance of pluripotency. *Cold Spring Harb Perspect Med* **3,** a014381.

Charsouei S, Jabalameli MR & Karimi-Moghadam A. (2020). Molecular insights into the role of AMPA receptors in the synaptic plasticity, pathogenesis and treatment of epilepsy: therapeutic potentials of perampanel and antisense oligonucleotide (ASO) technology. *Acta Neurol Belg*.

Chawla AR, Johnson DE, Zybura AS, Leeds BP, Nelson RM & Hudmon A. (2017). Constitutive regulation of the glutamate/aspartate transporter EAAT1 by Calcium-Calmodulin-Dependent Protein Kinase II. *J Neurochem* **140,** 421-434.

Chen G, Gulbranson DR, Hou Z, Bolin JM, Ruotti V, Probasco MD, Smuga-Otto K, Howden SE, Diol NR, Propson NE, Wagner R, Lee GO, Antosiewicz-Bourget J, Teng JM & Thomson JA. (2011a). Chemically defined conditions for human iPSC derivation and culture. *Nat Methods* **8,** 424-429.

Chen HK, Ji ZS, Dodson SE, Miranda RD, Rosenblum CI, Reynolds IJ, Freedman SB, Weisgraber KH, Huang Y & Mahley RW. (2011b). Apolipoprotein E4 domain interaction mediates detrimental effects on mitochondria and is a potential therapeutic target for Alzheimer disease. *J Biol Chem* **286,** 5215-5221.

Chen HK, Liu Z, Meyer-Franke A, Brodbeck J, Miranda RD, McGuire JG, Pleiss MA, Ji ZS, Balestra ME, Walker DW, Xu Q, Jeong DE, Budamagunta MS, Voss JC, Freedman

SB, Weisgraber KH, Huang Y & Mahley RW. (2012). Small molecule structure correctors abolish detrimental effects of apolipoprotein E4 in cultured neurons. *J Biol Chem* **287,** 5253-5266.

Chen KH, Reese EA, Kim HW, Rapoport SI & Rao JS. (2011c). Disturbed neurotransmitter transporter expression in Alzheimer's disease brain. *J Alzheimers Dis* **26,** 755-766.

Chen Y, Durakoglugil MS, Xian X & Herz J. (2010). ApoE4 reduces glutamate receptor function and synaptic plasticity by selectively impairing ApoE receptor recycling. *Proceedings of the National Academy of Sciences* **107,** 12011-12016.

Chiricosta L, Silvestro S, Pizzicannella J, Diomede F, Bramanti P, Trubiani O & Mazzon E. (2019). Transcriptomic Analysis of Stem Cells Treated with Moringin or Cannabidiol: Analogies and Differences in Inflammation Pathways. *Int J Mol Sci* **20**.

Chiurchiu V, Lanuti M, De Bardi M, Battistini L & Maccarrone M. (2015). The differential characterization of GPR55 receptor in human peripheral blood reveals a distinctive expression in monocytes and NK cells and a proinflammatory role in these innate cells. *Int Immunol* **27,** 153-160.

Choi SS, Lee HJ, Lim I, Satoh J & Kim SU. (2014). Human astrocytes: secretome profiles of cytokines and chemokines. *PLoS One* **9,** e92325.

Chou SY, Weng JY, Lai HL, Liao F, Sun SH, Tu PH, Dickson DW & Chern Y. (2008). Expanded-polyglutamine huntingtin protein suppresses the secretion and production of a chemokine (CCL5/RANTES) by astrocytes. *J Neurosci* **28,** 3277-3290.

Chun H & Lee CJ. (2018). Reactive astrocytes in Alzheimer's disease: A double-edged sword. *Neurosci Res* **126,** 44-52.

Chung J, Zhang X, Allen M, Wang X, Ma Y, Beecham G, Montine TJ, Younkin SG, Dickson DW, Golde TE, Price ND, Ertekin-Taner N, Lunetta KL, Mez J, Mayeux R, Haines JL, Pericak-Vance MA, Schellenberg G, Jun GR & Farrer LA. (2018). Genome-wide pleiotropy analysis of neuropathological traits related to Alzheimer's disease. *Alzheimers Res Ther* **10,** 22.

Chung WS, Clarke LE, Wang GX, Stafford BK, Sher A, Chakraborty C, Joung J, Foo LC, Thompson A, Chen C, Smith SJ & Barres BA. (2013). Astrocytes mediate synapse elimination through MEGF10 and MERTK pathways. *Nature* **504,** 394-400.

Chung WS, Verghese PB, Chakraborty C, Joung J, Hyman BT, Ulrich JD, Holtzman DM & Barres BA. (2016). Novel allele-dependent role for APOE in controlling the rate of synapse pruning by astrocytes. *Proc Natl Acad Sci U S A* **113,** 10186-10191.

Ciammola A, Sassone J, Cannella M, Calza S, Poletti B, Frati L, Squitieri F & Silani V. (2007). Low brain-derived neurotrophic factor (BDNF) levels in serum of Huntington's disease patients. *Am J Med Genet B Neuropsychiatr Genet* **144b,** 574-577.

Ciccarelli R, Di Iorio P, Ballerini P, Ambrosini G, Giuliani P, Tiboni GM & Caciagli F. (1994). Effects of exogenous ATP and related analogues on the proliferation rate of dissociated primary cultures of rat astrocytes. *J Neurosci Res* **39,** 556-566.

Clarke LE & Barres BA. (2013). Emerging roles of astrocytes in neural circuit development. *Nat Rev Neurosci* **14,** 311-321.

Clarke LE, Liddelow SA, Chakraborty C, Munch AE, Heiman M & Barres BA. (2018). Normal aging induces A1-like astrocyte reactivity. *Proc Natl Acad Sci U S A* **115,** E1896-e1905.

Colvin JS, Green RP, Schmahl J, Capel B & Ornitz DM. (2001). Male-to-female sex reversal in mice lacking fibroblast growth factor 9. *Cell* **104,** 875-889.

Conradt M & Stoffel W. (1997). Inhibition of the high-affinity brain glutamate transporter GLAST-1 via direct phosphorylation. *Journal of neurochemistry* **68,** 1244-1251.

Console-Bram L, Marcu J & Abood ME. (2012). Cannabinoid receptors: nomenclature and pharmacological principles. *Prog Neuropsychopharmacol Biol Psychiatry* **38,** 4-15.

Conway ME. (2020). Alzheimer's disease: targeting the glutamatergic system. *Biogerontology*.

Corder EH, Saunders AM, Risch NJ, Strittmatter WJ, Schmechel DE, Gaskell PC, Jr., Rimmler JB, Locke PA, Conneally PM, Schmader KE & et al. (1994). Protective effect of apolipoprotein E type 2 allele for late onset Alzheimer disease. *Nat Genet* **7,** 180-184.

Corder EH, Saunders AM, Strittmatter WJ, Schmechel DE, Gaskell PC, Small GW, Roses AD, Haines JL & Pericak-Vance MA. (1993). Gene dose of apolipoprotein E type 4 allele and the risk of Alzheimer's disease in late onset families. *Science* **261,** 921-923.

Cordero-Llana O, Scott SA, Maslen SL, Anderson JM, Boyle J, Chowhdury RR, Tyers P, Barker RA, Kelly CM, Rosser AE, Stephens E, Chandran S & Caldwell MA. (2011). Clusterin secreted by astrocytes enhances neuronal differentiation from human neural precursor cells. *Cell Death Differ* **18,** 907-913.

Cornell-Bell AH, Finkbeiner SM, Cooper MS & Smith SJ. (1990). Glutamate induces calcium waves in cultured astrocytes: long-range glial signaling. *Science* **247,** 470-473.

Costa B, Giagnoni G, Franke C, Trovato AE & Colleoni M. (2004). Vanilloid TRPV1 receptor mediates the antihyperalgesic effect of the nonpsychoactive cannabinoid, cannabidiol, in a rat model of acute inflammation. *Br J Pharmacol* **143,** 247-250.

Costello DA, Carney DG & Lynch MA. (2015). α-TLR2 antibody attenuates the Aβ-mediated inflammatory response in microglia through enhanced expression of SIGIRR. *Brain Behav Immun* **46,** 70-79.

Cowburn R, Hardy J, Roberts P & Briggs R. (1988). Presynaptic and postsynaptic glutamatergic function in Alzheimer's disease. *Neurosci Lett* **86,** 109-113.

Crompton LA, Byrne ML, Taylor H, Kerrigan TL, Bru-Mercier G, Badger JL, Barbuti PA, Jo J, Tyler SJ, Allen SJ, Kunath T, Cho K & Caldwell MA. (2013). Stepwise, non-adherent differentiation of human pluripotent stem cells to generate basal forebrain cholinergic neurons via hedgehog signaling. *Stem Cell Res* **11,** 1206-1221.

Crompton LA, Cordero-Llana O & Caldwell MA. (2017). Astrocytes in a dish: Using pluripotent stem cells to model neurodegenerative and neurodevelopmental disorders. *Brain Pathol* **27,** 530-544.

Cunningham C, Wilcockson DC, Campion S, Lunnon K & Perry VH. (2005). Central and systemic endotoxin challenges exacerbate the local inflammatory response and increase neuronal death during chronic neurodegeneration. *J Neurosci* **25,** 9275-9284.

Davies G, Martin TA, Ye L, Lewis-Russell JM, Mason MD & Jiang WG. (2008). Phospholipase-C gamma-1 (PLCgamma-1) is critical in hepatocyte growth factor induced in vitro invasion and migration without affecting the growth of prostate cancer cells. *Urol Oncol* **26,** 386-391.

De Strooper B & Karran E. (2016). The Cellular Phase of Alzheimer's Disease. *Cell* **164,** 603-615.

Deguchi Y, Naito T, Yuge T, Furukawa A, Yamada S, Pardridge WM & Kimura R. (2000). Blood-brain barrier transport of 125I-labeled basic fibroblast growth factor. *Pharm Res* **17,** 63-69.

Derouiche A & Rauen T. (1995). Coincidence of L-glutamate/L-aspartate transporter (GLAST) and glutamine synthetase (GS) immunoreactions in retinal glia: evidence for coupling of GLAST and GS in transmitter clearance. *J Neurosci Res* **42,** 131-143.

Devine MJ, Ryten M, Vodicka P, Thomson AJ, Burdon T, Houlden H, Cavaleri F, Nagano M, Drummond NJ, Taanman JW, Schapira AH, Gwinn K, Hardy J, Lewis PA & Kunath T. (2011). Parkinson's disease induced pluripotent stem cells with triplication of the alpha-synuclein locus. *Nat Commun* **2,** 440.

Devinsky O, Patel AD, Cross JH, Villanueva V, Wirrell EC, Privitera M, Greenwood SM, Roberts C, Checketts D, VanLandingham KE & Zuberi SM. (2018). Effect of Cannabidiol on Drop Seizures in the Lennox-Gastaut Syndrome. *N Engl J Med* **378,** 1888-1897.

Dhandapani KM, Hadman M, De Sevilla L, Wade MF, Mahesh VB & Brann DW. (2003). Astrocyte protection of neurons: role of transforming growth factor-beta signaling via a c-Jun-AP-1 protective pathway. *J Biol Chem* **278,** 43329-43339.

Di Bona D, Plaia A, Vasto S, Cavallone L, Lescai F, Franceschi C, Licastro F, Colonna-Romano G, Lio D, Candore G & Caruso C. (2008). Association between the interleukin-1beta polymorphisms and Alzheimer's disease: a systematic review and meta-analysis. *Brain Res Rev* **59,** 155-163.

di Domenico A, Carola G, Calatayud C, Pons-Espinal M, Munoz JP, Richaud-Patin Y, Fernandez-Carasa I, Gut M, Faella A, Parameswaran J, Soriano J, Ferrer I, Tolosa E, Zorzano A, Cuervo AM, Raya A & Consiglio A. (2019). Patient-Specific iPSC-Derived Astrocytes Contribute to Non-Cell-Autonomous Neurodegeneration in Parkinson's Disease. *Stem Cell Reports* **12,** 213-229.

Di Giammartino DC, Kloetgen A, Polyzos A, Liu Y, Kim D, Murphy D, Abuhashem A, Cavaliere P, Aronson B, Shah V, Dephoure N, Stadtfeld M, Tsirigos A & Apostolou E. (2019). KLF4 is involved in the organization and regulation of pluripotency-associated three-dimensional enhancer networks. *Nat Cell Biol* **21,** 1179-1190.

Di Giorgio FP, Boulting GL, Bobrowicz S & Eggan KC. (2008). Human embryonic stem cell-derived motor neurons are sensitive to the toxic effect of glial cells carrying an ALS-causing mutation. *Cell Stem Cell* **3,** 637-648.

Di Giorgio FP, Carrasco MA, Siao MC, Maniatis T & Eggan K. (2007). Non-cell autonomous effect of glia on motor neurons in an embryonic stem cell-based ALS model. *Nat Neurosci* **10,** 608-614.

Diniz LP, Almeida JC, Tortelli V, Vargas Lopes C, Setti-Perdigao P, Stipursky J, Kahn SA, Romao LF, de Miranda J, Alves-Leon SV, de Souza JM, Castro NG, Panizzutti R & Gomes FC. (2012). Astrocyte-induced synaptogenesis is mediated by transforming growth factor beta signaling through modulation of D-serine levels in cerebral cortex neurons. *J Biol Chem* **287,** 41432-41445.

Dong XX, Wang Y & Qin ZH. (2009). Molecular mechanisms of excitotoxicity and their relevance to pathogenesis of neurodegenerative diseases. *Acta Pharmacol Sin* **30,** 379-387.

Dorey E, Chang N, Liu QY, Yang Z & Zhang W. (2014). Apolipoprotein E, amyloid-beta, and neuroinflammation in Alzheimer's disease. *Neurosci Bull* **30,** 317-330.

Du ZW, Chen H, Liu H, Lu J, Qian K, Huang CL, Zhong X, Fan F & Zhang SC. (2015). Generation and expansion of highly pure motor neuron progenitors from human pluripotent stem cells. *Nat Commun* **6,** 6626.

Duan L, Bhattacharyya BJ, Belmadani A, Pan L, Miller RJ & Kessler JA. (2014). Stem cell derived basal forebrain cholinergic neurons from Alzheimer's disease patients are more susceptible to cell death. *Mol Neurodegener* **9,** 3.

Duan S, Anderson CM, Stein BA & Swanson RA. (1999). Glutamate induces rapid upregulation of astrocyte glutamate transport and cell-surface expression of GLAST. *J Neurosci* **19,** 10193-10200.

Dumanis SB, DiBattista AM, Miessau M, Moussa CE & Rebeck GW. (2013). APOE genotype affects the pre-synaptic compartment of glutamatergic nerve terminals. *J Neurochem* **124,** 4-14.

Elder GA, Gama Sosa MA, De Gasperi R, Dickstein DL & Hof PR. (2010). Presenilin transgenic mice as models of Alzheimer's disease. *Brain Struct Funct* **214,** 127-143.

Emdad L, D'Souza SL, Kothari HP, Qadeer ZA & Germano IM. (2012). Efficient differentiation of human embryonic and induced pluripotent stem cells into functional astrocytes. *Stem Cells Dev* **21,** 404-410.

Eng LF, Ghirnikar RS & Lee YL. (2000). Glial fibrillary acidic protein: GFAP-thirty-one years (1969-2000). *Neurochem Res* **25,** 1439-1451.

Erecinska M & Silver IA. (1990). Metabolism and role of glutamate in mammalian brain. *Prog Neurobiol* **35,** 245-296.

Eroglu C & Barres BA. (2010). Regulation of synaptic connectivity by glia. *Nature* **468,** 223-231.

Esposito G, De Filippis D, Maiuri MC, De Stefano D, Carnuccio R & Iuvone T. (2006). Cannabidiol inhibits inducible nitric oxide synthase protein expression and nitric

oxide production in beta-amyloid stimulated PC12 neurons through p38 MAP kinase and NF-kappaB involvement. *Neurosci Lett* **399,** 91-95.

Esposito G, Scuderi C, Savani C, Steardo L, Jr., De Filippis D, Cottone P, Iuvone T, Cuomo V & Steardo L. (2007). Cannabidiol in vivo blunts beta-amyloid induced neuroinflammation by suppressing IL-1beta and iNOS expression. *Br J Pharmacol* **151,** 1272-1279.

Essayan-Perez S, Zhou B, Nabet AM, Wernig M & Huang YA. (2019). Modeling Alzheimer's disease with human iPS cells: advancements, lessons, and applications. *Neurobiol Dis* **130,** 104503.

Faideau M, Kim J, Cormier K, Gilmore R, Welch M, Auregan G, Dufour N, Guillermier M, Brouillet E, Hantraye P, Deglon N, Ferrante RJ & Bonvento G. (2010). In vivo expression of polyglutamine-expanded huntingtin by mouse striatal astrocytes impairs glutamate transport: a correlation with Huntington's disease subjects. *Hum Mol Genet* **19,** 3053-3067.

Fairman WA, Vandenberg RJ, Arriza JL, Kavanaugh MP & Amara SG. (1995). An excitatory amino-acid transporter with properties of a ligand-gated chloride channel. *Nature* **375,** 599-603.

Fan J, Fong T, Chen X, Chen C, Luo P & Xie H. (2018). Glia maturation factor-beta: a potential therapeutic target in neurodegeneration and neuroinflammation. *Neuropsychiatr Dis Treat* **14,** 495-504.

Farfel JM, Yu L, De Jager PL, Schneider JA & Bennett DA. (2016). Association of APOE with tau-tangle pathology with and without beta-amyloid. *Neurobiol Aging* **37,** 19-25.

Farrell B & Breeze AL. (2018). Structure, activation and dysregulation of fibroblast growth factor receptor kinases: perspectives for clinical targeting. *Biochem Soc Trans* **46,** 1753-1770.

Fassbender K, Walter S, Kühl S, Landmann R, Ishii K, Bertsch T, Stalder AK, Muehlhauser F, Liu Y, Ulmer AJ, Rivest S, Lentschat A, Gulbins E, Jucker M, Staufenbiel M, Brechtel K, Walter J, Multhaup G, Penke B, Adachi Y, Hartmann T & Beyreuther K. (2004). The LPS receptor (CD14) links innate immunity with Alzheimer's disease. *FASEB J* **18,** 203-205.

Feldman B, Poueymirou W, Papaioannou VE, DeChiara TM & Goldfarb M. (1995). Requirement of FGF-4 for postimplantation mouse development. *Science* **267,** 246-249.

Feng D, Guo B, Liu G, Wang B, Wang W, Gao G, Qin H & Wu S. (2015). FGF2 alleviates PTSD symptoms in rats by restoring GLAST function in astrocytes via the JAK/STAT pathway. *Eur Neuropsychopharmacol* **25,** 1287-1299.

Ferguson SA, Sarkar S & Schmued LC. (2013). Longitudinal behavioral changes in the APP/PS1 transgenic Alzheimer's disease model. *Behav Brain Res* **242,** 125-134.

Fernandez CG, Hamby ME, McReynolds ML & Ray WJ. (2019). The Role of APOE4 in Disrupting the Homeostatic Functions of Astrocytes and Microglia in Aging and Alzheimer's Disease. *Front Aging Neurosci* **11,** 14.

Ferreira-Vieira TH, Guimaraes IM, Silva FR & Ribeiro FM. (2016). Alzheimer's disease: Targeting the Cholinergic System. *Curr Neuropharmacol* **14,** 101-115.

Figiel M & Engele J. (2000). Pituitary adenylate cyclase-activating polypeptide (PACAP), a neuron-derived peptide regulating glial glutamate transport and metabolism. *J Neurosci* **20,** 3596-3605.

Figiel M, Maucher T, Rozyczka J, Bayatti N & Engele J. (2003). Regulation of glial glutamate transporter expression by growth factors. *Exp Neurol* **183,** 124-135.

Fitzpatrick JK & Downer EJ. (2017). Toll-like receptor signalling as a cannabinoid target in Multiple Sclerosis. *Neuropharmacology* **113,** 618-626.

Fitzpatrick JM, Minogue E, Curham L, Tyrrell H, Gavigan P, Hind W & Downer EJ. (2020). MyD88-dependent and -independent signalling via TLR3 and TLR4 are differentially modulated by Delta(9)-tetrahydrocannabinol and cannabidiol in human macrophages. *J Neuroimmunol* **343,** 577217.

Fleetwood AJ, Cook AD & Hamilton JA. (2005). Functions of granulocyte-macrophage colony-stimulating factor. *Crit Rev Immunol* **25,** 405-428.

Fleisher AS, Chen K, Liu X, Ayutyanont N, Roontiva A, Thiyyagura P, Protas H, Joshi AD, Sabbagh M, Sadowsky CH, Sperling RA, Clark CM, Mintun MA, Pontecorvo MJ, Coleman RE, Doraiswamy PM, Johnson KA, Carpenter AP, Skovronsky DM & Reiman EM. (2013). Apolipoprotein E epsilon4 and age effects on florbetapir positron emission tomography in healthy aging and Alzheimer disease. *Neurobiol Aging* **34,** 1-12.

Fong H, Wang C, Knoferle J, Walker D, Balestra ME, Tong LM, Leung L, Ring KL, Seeley WW, Karydas A, Kshirsagar MA, Boxer AL, Kosik KS, Miller BL & Huang Y. (2013). Genetic correction of tauopathy phenotypes in neurons derived from human induced pluripotent stem cells. *Stem Cell Reports* **1,** 226-234.

Fontana AC. (2015). Current approaches to enhance glutamate transporter function and expression. *J Neurochem* **134,** 982-1007.

Ford-Perriss M, Abud H & Murphy M. (2001). Fibroblast growth factors in the developing central nervous system. *Clin Exp Pharmacol Physiol* **28,** 493-503.

Fortuna D, Hooper DC, Roberts AL, Harshyne LA, Nagurney M & Curtis MT. (2018). Potential role of CSF cytokine profiles in discriminating infectious from non-infectious CNS disorders. *PLoS One* **13,** e0205501.

Fourgeaud L & Boulanger LM. (2007). Synapse remodeling, compliments of the complement system. *Cell* **131,** 1034-1036.

Fukada Y, Yasui K, Kitayama M, Doi K, Nakano T, Watanabe Y & Nakashima K. (2007). Gene expression analysis of the murine model of amyotrophic lateral sclerosis: studies of the Leu126delTT mutation in SOD1. *Brain Res* **1160,** 1-10.

Furuta A, Rothstein JD & Martin LJ. (1997). Glutamate transporter protein subtypes are expressed differentially during rat CNS development. *J Neurosci* **17,** 8363-8375.

Gabriel E & Gopalakrishnan J. (2017). Generation of iPSC-derived Human Brain Organoids to Model Early Neurodevelopmental Disorders. *J Vis Exp*.

Gadea A, Schinelli S & Gallo V. (2008). Endothelin-1 regulates astrocyte proliferation and reactive gliosis via a JNK/c-Jun signaling pathway. *J Neurosci* **28,** 2394-2408.

Gage FH. (2000). Mammalian neural stem cells. *Science* **287,** 1433-1438.

Gagne SJ, Stout JM, Liu E, Boubakir Z, Clark SM & Page JE. (2012). Identification of olivetolic acid cyclase from Cannabis sativa reveals a unique catalytic route to plant polyketides. *Proc Natl Acad Sci U S A* **109,** 12811-12816.

Galimberti D, Schoonenboom N, Scarpini E & Scheltens P. (2003). Chemokines in serum and cerebrospinal fluid of Alzheimer's disease patients. *Ann Neurol* **53,** 547-548.

Galimberti D, Schoonenboom N, Scheltens P, Fenoglio C, Bouwman F, Venturelli E, Guidi I, Blankenstein MA, Bresolin N & Scarpini E. (2006). Intrathecal chemokine synthesis in mild cognitive impairment and Alzheimer disease. *Arch Neurol* **63,** 538-543.

Galimberti D, Venturelli E, Fenoglio C, Lovati C, Guidi I, Scalabrini D, Mariani C, Bresolin N & Scarpini E. (2007). IP-10 serum levels are not increased in mild cognitive impairment and Alzheimer's disease. In *Eur J Neurol*, pp. e3-4. England.

Games D, Adams D, Alessandrini R, Barbour R, Berthelette P, Blackwell C, Carr T, Clemens J, Donaldson T & Gillespie F. (1995). Alzheimer-type neuropathology in transgenic mice overexpressing V717F beta-amyloid precursor protein. *Nature* **373,** 523-527.

Garwood CJ, Pooler AM, Atherton J, Hanger DP & Noble W. (2011). Astrocytes are important mediators of Abeta-induced neurotoxicity and tau phosphorylation in primary culture. *Cell Death Dis* **2,** e167.

Gaspard N, Bouschet T, Hourez R, Dimidschstein J, Naeije G, van den Ameele J, Espuny-Camacho I, Herpoel A, Passante L, Schiffmann SN, Gaillard A & Vanderhaeghen P. (2008). An intrinsic mechanism of corticogenesis from embryonic stem cells. *Nature* **455,** 351-357.

Gegelashvili G, Civenni G, Racagni G, Danbolt NC, Schousboe I & Schousboe A. (1996). Glutamate receptor agonists up-regulate glutamate transporter GLAST in astrocytes. *Neuroreport* **8,** 261-265.

Gegelashvili G & Schousboe A. (1997). High affinity glutamate transporters: regulation of expression and activity. *Mol Pharmacol* **52,** 6-15.

Genin E, Hannequin D, Wallon D, Sleegers K, Hiltunen M, Combarros O, Bullido MJ, Engelborghs S, De Deyn P, Berr C, Pasquier F, Dubois B, Tognoni G, Fievet N, Brouwers N, Bettens K, Arosio B, Coto E, Del Zompo M, Mateo I, Epelbaum J, Frank-Garcia A, Helisalmi S, Porcellini E, Pilotto A, Forti P, Ferri R, Scarpini E, Siciliano G, Solfrizzi V, Sorbi S, Spalletta G, Valdivieso F, Vepsalainen S, Alvarez V, Bosco P, Mancuso M, Panza F, Nacmias B, Bossu P, Hanon O, Piccardi P, Annoni G, Seripa D, Galimberti D, Licastro F, Soininen H, Dartigues JF, Kamboh MI, Van Broeckhoven C, Lambert JC, Amouyel P & Campion D. (2011). APOE and Alzheimer disease: a major gene with semi-dominant inheritance. *Mol Psychiatry* **16,** 903-907.

Gesase AP & Kiyama H. (2007). Peripheral nerve injury induced expression of mRNA for serine protease inhibitor 3 in the rat facial and hypoglossal nuclei but not in the spinal cord. *Ital J Anat Embryol* **112,** 157-168.

Geula C. (1998). Abnormalities of neural circuitry in Alzheimer's disease: hippocampus and cortical cholinergic innervation. *Neurology* **51,** S18-29; discussion S65-17.

Ghanavatinejad F, Fard Tabrizi ZP, Omidghaemi S, Sharifi E, Moller SG & Jami MS. (2019). Protein biomarkers of neural system. *J Otol* **14,** 77-88.

Ghoddoussi F, Galloway MP, Jambekar A, Bame M, Needleman R & Brusilow WS. (2010). Methionine sulfoximine, an inhibitor of glutamine synthetase, lowers brain glutamine and glutamate in a mouse model of ALS. *J Neurol Sci* **290,** 41-47.

Glowatzki E, Cheng N, Hiel H, Yi E, Tanaka K, Ellis-Davies GC, Rothstein JD & Bergles DE. (2006). The glutamate-aspartate transporter GLAST mediates glutamate uptake at inner hair cell afferent synapses in the mammalian cochlea. *J Neurosci* **26,** 7659-7664.

Goldshmit Y, Sztal TE, Jusuf PR, Hall TE, Nguyen-Chi M & Currie PD. (2012). Fgf-dependent glial cell bridges facilitate spinal cord regeneration in zebrafish. *J Neurosci* **32,** 7477-7492.

Gomes WA, Mehler MF & Kessler JA. (2003). Transgenic overexpression of BMP4 increases astroglial and decreases oligodendroglial lineage commitment. *Dev Biol* **255,** 164-177.

Gonzalez-Reyes RE, Nava-Mesa MO, Vargas-Sanchez K, Ariza-Salamanca D & Mora-Munoz L. (2017). Involvement of Astrocytes in Alzheimer's Disease from a Neuroinflammatory and Oxidative Stress Perspective. *Front Mol Neurosci* **10,** 427.

Gordon GR, Mulligan SJ & MacVicar BA. (2007). Astrocyte control of the cerebrovasculature. *Glia* **55,** 1214-1221.

Gosselin R-D, Meylan P & Decosterd I. (2013). Extracellular microvesicles from astrocytes contain functional glutamate transporters: regulation by protein kinase C and cell activation. *Frontiers in cellular neuroscience* **7,** 251.

Gray CW & Patel AJ. (1992). Characterization of a neurotrophic factor produced by cultured astrocytes involved in the regulation of subcortical cholinergic neurons. *Brain Res* **574,** 257-265.

Green HF, Khosousi S & Svenningsson P. (2019). Plasma IL-6 and IL-17A Correlate with Severity of Motor and Non-Motor Symptoms in Parkinson's Disease. *J Parkinsons Dis* **9,** 705-709.

Griffin WS & Mrak RE. (2002). Interleukin-1 in the genesis and progression of and risk for development of neuronal degeneration in Alzheimer's disease. *J Leukoc Biol* **72,** 233-238.

Griffin WS, Nicoll JA, Grimaldi LM, Sheng JG & Mrak RE. (2000). The pervasiveness of interleukin-1 in alzheimer pathogenesis: a role for specific polymorphisms in disease risk. *Exp Gerontol* **35,** 481-487.

Groom JR & Luster AD. (2011). CXCR3 ligands: redundant, collaborative and antagonistic functions. *Immunol Cell Biol* **89,** 207-215.

Gruol DL. (2016). Impact of Increased Astrocyte Expression of IL-6, CCL2 or CXCL10 in Transgenic Mice on Hippocampal Synaptic Function. *Brain Sci* **6**.

Gu XL, Long CX, Sun L, Xie C, Lin X & Cai H. (2010). Astrocytic expression of Parkinson's disease-related A53T alpha-synuclein causes neurodegeneration in mice. *Mol Brain* **3,** 12.

Guerreiro R, Wojtas A, Bras J, Carrasquillo M, Rogaeva E, Majounie E, Cruchaga C, Sassi C, Kauwe JS, Younkin S, Hazrati L, Collinge J, Pocock J, Lashley T, Williams J, Lambert JC, Amouyel P, Goate A, Rademakers R, Morgan K, Powell J, St George-Hyslop P, Singleton A & Hardy J. (2013). TREM2 variants in Alzheimer's disease. *N Engl J Med* **368,** 117-127.

Guillemot F & Zimmer C. (2011). From cradle to grave: the multiple roles of fibroblast growth factors in neural development. *Neuron* **71,** 574-588.

Guo L, LaDu MJ & Van Eldik LJ. (2004). A dual role for apolipoprotein e in neuroinflammation: anti- and pro-inflammatory activity. *J Mol Neurosci* **23,** 205-212.

Gupta K, Patani R, Baxter P, Serio A, Story D, Tsujita T, Hayes JD, Pedersen RA, Hardingham GE & Chandran S. (2012). Human embryonic stem cell derived astrocytes mediate non-cell-autonomous neuroprotection through endogenous and drug-induced mechanisms. *Cell Death Differ* **19,** 779-787.

Haddick PC, Larson JL, Rathore N, Bhangale TR, Phung QT, Srinivasan K, Hansen DV, Lill JR, Pericak-Vance MA, Haines J, Farrer LA, Kauwe JS, Schellenberg GD, Cruchaga C, Goate AM, Behrens TW, Watts RJ, Graham RR, Kaminker JS & van der Brug M. (2017). A Common Variant of IL-6R is Associated with Elevated IL-6 Pathway Activity in Alzheimer's Disease Brains. *J Alzheimers Dis* **56,** 1037-1054.

Haenseler W, Sansom SN, Buchrieser J, Newey SE, Moore CS, Nicholls FJ, Chintawar S, Schnell C, Antel JP, Allen ND, Cader MZ, Wade-Martins R, James WS & Cowley SA. (2017). A Highly Efficient Human Pluripotent Stem Cell Microglia Model Displays a Neuronal-Co-culture-Specific Expression Profile and Inflammatory Response. *Stem Cell Reports* **8,** 1727-1742.

Halassa MM, Fellin T & Haydon PG. (2007a). The tripartite synapse: roles for gliotransmission in health and disease. *Trends Mol Med* **13,** 54-63.

Halassa MM, Fellin T, Takano H, Dong JH & Haydon PG. (2007b). Synaptic islands defined by the territory of a single astrocyte. *J Neurosci* **27,** 6473-6477.

Hallmann AL, Arauzo-Bravo MJ, Mavrommatis L, Ehrlich M, Ropke A, Brockhaus J, Missler M, Sterneckert J, Scholer HR, Kuhlmann T, Zaehres H & Hargus G. (2017). Astrocyte pathology in a human neural stem cell model of frontotemporal dementia caused by mutant TAU protein. *Sci Rep* **7,** 42991.

Hamby ME, Coppola G, Ao Y, Geschwind DH, Khakh BS & Sofroniew MV. (2012). Inflammatory mediators alter the astrocyte transcriptome and calcium signaling elicited by multiple G-protein-coupled receptors. *J Neurosci* **32,** 14489-14510.

Harris FM, Brecht WJ, Xu Q, Mahley RW & Huang Y. (2004). Increased tau phosphorylation in apolipoprotein E4 transgenic mice is associated with activation of extracellular signal-regulated kinase: modulation by zinc. *J Biol Chem* **279,** 44795-44801.

Hart KC, Robertson SC & Donoghue DJ. (2001). Identification of tyrosine residues in constitutively activated fibroblast growth factor receptor 3 involved in mitogenesis, Stat activation, and phosphatidylinositol 3-kinase activation. *Mol Biol Cell* **12,** 931-942.

Harth G, Clemens DL & Horwitz MA. (1994). Glutamine synthetase of Mycobacterium tuberculosis: extracellular release and characterization of its enzymatic activity. *Proc Natl Acad Sci U S A* **91,** 9342-9346.

Hartmann K, Sepulveda-Falla D, Rose IVL, Madore C, Muth C, Matschke J, Butovsky O, Liddelow S, Glatzel M & Krasemann S. (2019). Complement 3(+)-astrocytes are highly abundant in prion diseases, but their abolishment led to an accelerated disease course and early dysregulation of microglia. *Acta Neuropathol Commun* **7,** 83.

Hashimoto T, Serrano-Pozo A, Hori Y, Adams KW, Takeda S, Banerji AO, Mitani A, Joyner D, Thyssen DH, Bacskai BJ, Frosch MP, Spires-Jones TL, Finn MB, Holtzman DM & Hyman BT. (2012). Apolipoprotein E, especially apolipoprotein E4, increases the oligomerization of amyloid beta peptide. *J Neurosci* **32,** 15181-15192.

Hashioka S, Klegeris A, Qing H & McGeer PL. (2011). STAT3 inhibitors attenuate interferon-gamma-induced neurotoxicity and inflammatory molecule production by human astrocytes. *Neurobiol Dis* **41,** 299-307.

Hatters DM, Peters-Libeu CA & Weisgraber KH. (2006). Apolipoprotein E structure: insights into function. *Trends Biochem Sci* **31,** 445-454.

Hauser PS & Ryan RO. (2013). Impact of apolipoprotein E on Alzheimer's disease. *Curr Alzheimer Res* **10,** 809-817.

Haustein M, Ramer R, Linnebacher M, Manda K & Hinz B. (2014). Cannabinoids increase lung cancer cell lysis by lymphokine-activated killer cells via upregulation of ICAM-1. *Biochem Pharmacol* **92,** 312-325.

Hawkins SJ, Crompton LA, Sood A, Saunders M, Boyle NT, Buckley A, Minogue AM, McComish SF, Jimenez-Moreno N, Cordero-Llana O, Stathakos P, Gilmore CE, Kelly S, Lane JD, Case CP & Caldwell MA. (2018). Nanoparticle-induced neuronal toxicity across placental barriers is mediated by autophagy and dependent on astrocytes. *Nat Nanotechnol* **13,** 427-433.

Haynes LW. (1988). Fibroblast (heparin-binding) growing factors in neuronal development and repair. *Mol Neurobiol* **2,** 263-289.

Heidary M, Rakhshi N, Pahlevan Kakhki M, Behmanesh M, Sanati MH, Sanadgol N, Kamaladini H & Nikravesh A. (2014). The analysis of correlation between IL-1B gene expression and genotyping in multiple sclerosis patients. *J Neurol Sci* **343,** 41-45.

Heimann G & Sirko S. (2019). Investigating Age-Related Changes in Proliferation and the Cell Division Repertoire of Parenchymal Reactive Astrocytes. *Methods Mol Biol* **1938,** 277-292.

Heinrich PC, Behrmann I, Muller-Newen G, Schaper F & Graeve L. (1998). Interleukin-6-type cytokine signalling through the gp130/Jak/STAT pathway. *Biochem J* **334 (Pt 2),** 297-314.

Helms HC, Madelung R, Waagepetersen HS, Nielsen CU & Brodin B. (2012). In vitro evidence for the brain glutamate efflux hypothesis: Brain endothelial cells cocultured with astrocytes display a polarized brain-to-blood transport of glutamate. *Glia* **60,** 882-893.

Hennessy E, Griffin EW & Cunningham C. (2015). Astrocytes Are Primed by Chronic Neurodegeneration to Produce Exaggerated Chemokine and Cell Infiltration Responses to Acute Stimulation with the Cytokines IL-1beta and TNF-alpha. *J Neurosci* **35,** 8411-8422.

Hernandez DG, Reed X & Singleton AB. (2016). Genetics in Parkinson disease: Mendelian versus non-Mendelian inheritance. *J Neurochem* **139 Suppl 1,** 59-74.

Herrero-Gonzalez S, Valle-Casuso JC, Sanchez-Alvarez R, Giaume C, Medina JM & Tabernero A. (2009). Connexin43 is involved in the effect of endothelin-1 on astrocyte proliferation and glucose uptake. *Glia* **57,** 222-233.

Hertz L & Chen Y. (2016). Importance of astrocytes for potassium ion (K(+)) homeostasis in brain and glial effects of K(+) and its transporters on learning. *Neurosci Biobehav Rev* **71,** 484-505.

Hoffmann O, Braun JS, Becker D, Halle A, Freyer D, Dagand E, Lehnardt S & Weber JR. (2007). TLR2 mediates neuroinflammation and neuronal damage. *J Immunol* **178,** 6476-6481.

Hol EM & Pekny M. (2015). Glial fibrillary acidic protein (GFAP) and the astrocyte intermediate filament system in diseases of the central nervous system. *Curr Opin Cell Biol* **32,** 121-130.

Hollingworth P, Harold D, Sims R, Gerrish A, Lambert JC, Carrasquillo MM, Abraham R, Hamshere ML, Pahwa JS, Moskvina V, Dowzell K, Jones N, Stretton A, Thomas C, Richards A, Ivanov D, Widdowson C, Chapman J, Lovestone S, Powell J, Proitsi P, Lupton MK, Brayne C, Rubinsztein DC, Gill M, Lawlor B, Lynch A, Brown KS, Passmore PA, Craig D, McGuinness B, Todd S, Holmes C, Mann D, Smith AD, Beaumont H, Warden D, Wilcock G, Love S, Kehoe PG, Hooper NM, Vardy ER, Hardy J, Mead S, Fox NC, Rossor M, Collinge J, Maier W, Jessen F, Ruther E, Schurmann B, Heun R, Kolsch H, van den Bussche H, Heuser I, Kornhuber J, Wiltfang J, Dichgans M, Frolich L, Hampel H, Gallacher J, Hull M, Rujescu D, Giegling I, Goate AM, Kauwe JS, Cruchaga C, Nowotny P, Morris JC, Mayo K, Sleegers K, Bettens K, Engelborghs S, De Deyn PP, Van Broeckhoven C, Livingston G, Bass NJ, Gurling H, McQuillin A, Gwilliam R, Deloukas P, Al-Chalabi A, Shaw CE, Tsolaki M, Singleton AB, Guerreiro R, Muhleisen TW, Nothen MM, Moebus S, Jockel KH, Klopp N, Wichmann HE, Pankratz VS, Sando SB, Aasly JO, Barcikowska M, Wszolek ZK, Dickson DW, Graff-Radford NR, Petersen RC, van Duijn CM, Breteler MM, Ikram MA, DeStefano AL, Fitzpatrick AL, Lopez O, Launer LJ, Seshadri S, Berr C, Campion D, Epelbaum J, Dartigues JF, Tzourio C, Alperovitch A, Lathrop M, Feulner TM, Friedrich P, Riehle C, Krawczak M, Schreiber S, Mayhaus M, Nicolhaus S, Wagenpfeil S, Steinberg S, Stefansson H, Stefansson K, Snaedal J, Bjornsson S, Jonsson PV, Chouraki V, Genier-Boley B, Hiltunen M, Soininen H, Combarros O, Zelenika D, Delepine M, Bullido MJ, Pasquier F, Mateo I, Frank-Garcia A, Porcellini E, Hanon O, Coto E, Alvarez V, Bosco P, Siciliano G, Mancuso M, Panza F, Solfrizzi V, Nacmias B, Sorbi S, Bossu P, Piccardi P, Arosio B, Annoni G, Seripa D, Pilotto A, Scarpini E, Galimberti D, Brice A, Hannequin D, Licastro F, Jones L, Holmans PA, Jonsson T, Riemenschneider M, Morgan K, Younkin SG, Owen MJ, O'Donovan M, Amouyel P & Williams J. (2011). Common variants at ABCA7, MS4A6A/MS4A4E, EPHA1, CD33 and CD2AP are associated with Alzheimer's disease. *Nat Genet* **43,** 429-435.

Holtzman DM, Herz J & Bu G. (2012). Apolipoprotein E and apolipoprotein E receptors: normal biology and roles in Alzheimer disease. *Cold Spring Harb Perspect Med* **2,** a006312.

Hong S, Beja-Glasser VF, Nfonoyim BM, Frouin A, Li S, Ramakrishnan S, Merry KM, Shi Q, Rosenthal A, Barres BA, Lemere CA, Selkoe DJ & Stevens B. (2016). Complement and microglia mediate early synapse loss in Alzheimer mouse models. *Science* **352,** 712-716.

Honig LS, Vellas B, Woodward M, Boada M, Bullock R, Borrie M, Hager K, Andreasen N, Scarpini E, Liu-Seifert H, Case M, Dean RA, Hake A, Sundell K, Poole Hoffmann V, Carlson C, Khanna R, Mintun M, DeMattos R, Selzler KJ & Siemers E. (2018). Trial of Solanezumab for Mild Dementia Due to Alzheimer's Disease. *N Engl J Med* **378,** 321-330.

Hopkins PC, Sainz-Fuertes R & Lovestone S. (2011). The impact of a novel apolipoprotein E and amyloid-beta protein precursor-interacting protein on the production of amyloid-beta. *J Alzheimers Dis* **26,** 239-253.

Hoshi A, Tsunoda A, Yamamoto T, Tada M, Kakita A & Ugawa Y. (2018). Altered expression of glutamate transporter-1 and water channel protein aquaporin-4 in human temporal cortex with Alzheimer's disease. *Neuropathol Appl Neurobiol* **44,** 628-638.

Hsiao K, Chapman P, Nilsen S, Eckman C, Harigaya Y, Younkin S, Yang F & Cole G. (1996). Correlative memory deficits, Abeta elevation, and amyloid plaques in transgenic mice. *Science* **274,** 99-102.

Hu BY, Du ZW & Zhang SC. (2009). Differentiation of human oligodendrocytes from pluripotent stem cells. *Nat Protoc* **4,** 1614-1622.

Huang Y & Mahley RW. (2014). Apolipoprotein E: Structure and Function in Lipid Metabolism, Neurobiology, and Alzheimer's Diseases. *Neurobiol Dis* **72PA,** 3-12.

Huang YA, Zhou B, Wernig M & Sudhof TC. (2017). ApoE2, ApoE3, and ApoE4 Differentially Stimulate APP Transcription and Abeta Secretion. *Cell* **168,** 427-441.e421.

Hughes MM, Field RH, Perry VH, Murray CL & Cunningham C. (2010). Microglia in the degenerating brain are capable of phagocytosis of beads and of apoptotic cells, but do not efficiently remove PrPSc, even upon LPS stimulation. *Glia* **58,** 2017-2030.

Hunter JM, Cirrito JR, Restivo JL, Kinley RD, Sullivan PM, Holtzman DM, Koger D, Delong C, Lin S, Zhao L, Liu F, Bales K & Paul SM. (2012). Emergence of a seizure phenotype in aged apolipoprotein epsilon 4 targeted replacement mice. *Brain Res* **1467,** 120-132.

Hynd MR, Scott HL & Dodd PR. (2004). Glutamate-mediated excitotoxicity and neurodegeneration in Alzheimer's disease. *Neurochemistry international* **45,** 583-595.

Hyvarinen T, Hagman S, Ristola M, Sukki L, Veijula K, Kreutzer J, Kallio P & Narkilahti S. (2019). Co-stimulation with IL-1beta and TNF-alpha induces an inflammatory reactive astrocyte phenotype with neurosupportive characteristics in a human pluripotent stem cell model system. *Sci Rep* **9,** 16944.

Ideguchi M, Palmer TD, Recht LD & Weimann JM. (2010). Murine embryonic stem cell-derived pyramidal neurons integrate into the cerebral cortex and appropriately project axons to subcortical targets. *J Neurosci* **30,** 894-904.

Ifergan I, Davidson TS, Kebir H, Xu D, Palacios-Macapagal D, Cann J, Rodgers JM, Hunter ZN, Pittet CL, Beddow S, Jones CA, Prat A, Sleeman MA & Miller SD. (2017). Targeting the GM-CSF receptor for the treatment of CNS autoimmunity. *J Autoimmun* **84,** 1-11.

Ilieva H, Polymenidou M & Cleveland DW. (2009). Non-cell autonomous toxicity in neurodegenerative disorders: ALS and beyond. *J Cell Biol* **187,** 761-772.

Ito J, Nagayasu Y, Lu R, Kheirollah A, Hayashi M & Yokoyama S. (2005). Astrocytes produce and secrete FGF-1, which promotes the production of apoE-HDL in a manner of autocrine action. *J Lipid Res* **46,** 679-686.

Itoh N. (2007). The Fgf families in humans, mice, and zebrafish: their evolutional processes and roles in development, metabolism, and disease. *Biol Pharm Bull* **30,** 1819-1825.

Itoh N & Ornitz DM. (2004). Evolution of the Fgf and Fgfr gene families. *Trends Genet* **20,** 563-569.

Iuvone T, Esposito G, Esposito R, Santamaria R, Di Rosa M & Izzo AA. (2004). Neuroprotective effect of cannabidiol, a non-psychoactive component from Cannabis sativa, on beta-amyloid-induced toxicity in PC12 cells. *J Neurochem* **89,** 134-141.

Jacob C, Koutsilieri E, Bartl J, Neuen-Jacob E, Arzberger T, Zander N, Ravid R, Roggendorf W, Riederer P & Grünblatt E. (2007). Alterations in expression of glutamatergic transporters and receptors in sporadic Alzheimer's disease. *Journal of Alzheimer's Disease* **11,** 97-116.

Jana M, Palencia CA & Pahan K. (2008). Fibrillar amyloid-beta peptides activate microglia via TLR2: implications for Alzheimer's disease. *J Immunol* **181,** 7254-7262.

Janeczko K. (1993). Co-expression of GFAP and vimentin in astrocytes proliferating in response to injury in the mouse cerebral hemisphere. A combined autoradiographic and double immunocytochemical study. *Int J Dev Neurosci* **11,** 139-147.

Janelidze S, Mattsson N, Stomrud E, Lindberg O, Palmqvist S, Zetterberg H, Blennow K & Hansson O. (2018). CSF biomarkers of neuroinflammation and cerebrovascular dysfunction in early Alzheimer disease. *Neurology* **91,** e867-e877.

Jankovic J. (2008). Parkinson's disease: clinical features and diagnosis. *J Neurol Neurosurg Psychiatry* **79,** 368-376.

Jellinger KA. (2002). Alzheimer disease and cerebrovascular pathology: an update. *J Neural Transm (Vienna)* **109,** 813-836.

Jensen CJ, Massie A & De Keyser J. (2013). Immune players in the CNS: the astrocyte. *J Neuroimmune Pharmacol* **8,** 824-839.

Jeong W, Lee H, Cho S & Seo J. (2019). ApoE4-Induced Cholesterol Dysregulation and Its Brain Cell Type-Specific Implications in the Pathogenesis of Alzheimer's Disease. *Mol Cells* **42,** 739-746.

Jha MK, Lee S, Park DH, Kook H, Park KG, Lee IK & Suk K. (2015). Diverse functional roles of lipocalin-2 in the central nervous system. *Neurosci Biobehav Rev* **49,** 135-156.

Ji ZS, Brecht WJ, Miranda RD, Hussain MM, Innerarity TL & Mahley RW. (1993). Role of heparan sulfate proteoglycans in the binding and uptake of apolipoprotein E-enriched remnant lipoproteins by cultured cells. *J Biol Chem* **268,** 10160-10167.

Jimenez E, Nunez E, Ibanez I, Draffin JE, Zafra F & Gimenez C. (2014). Differential regulation of the glutamate transporters GLT-1 and GLAST by GSK3beta. *Neurochem Int* **79,** 33-43.

Jo S, Yarishkin O, Hwang YJ, Chun YE, Park M, Woo DH, Bae JY, Kim T, Lee J, Chun H, Park HJ, Lee DY, Hong J, Kim HY, Oh SJ, Park SJ, Lee H, Yoon BE, Kim Y, Jeong Y, Shim I, Bae YC, Cho J, Kowall NW, Ryu H, Hwang E, Kim D & Lee CJ. (2014). GABA from reactive astrocytes impairs memory in mouse models of Alzheimer's disease. *Nat Med* **20,** 886-896.

Jofre-Monseny L, Minihane AM & Rimbach G. (2008). Impact of apoE genotype on oxidative stress, inflammation and disease risk. *Molecular nutrition & food research* **52,** 131-145.

Johann S, Heitzer M, Kanagaratnam M, Goswami A, Rizo T, Weis J, Troost D & Beyer C. (2015). NLRP3 inflammasome is expressed by astrocytes in the SOD1 mouse model of ALS and in human sporadic ALS patients. *Glia* **63,** 2260-2273.

John Lin CC, Yu K, Hatcher A, Huang TW, Lee HK, Carlson J, Weston MC, Chen F, Zhang Y, Zhu W, Mohila CA, Ahmed N, Patel AJ, Arenkiel BR, Noebels JL, Creighton CJ & Deneen B. (2017). Identification of diverse astrocyte populations and their malignant analogs. *Nat Neurosci* **20,** 396-405.

Johnson-Farley NN, Patel K, Kim D & Cowen DS. (2007). Interaction of FGF-2 with IGF-1 and BDNF in stimulating Akt, ERK, and neuronal survival in hippocampal cultures. *Brain Res* **1154,** 40-49.

Jones VC, Atkinson-Dell R, Verkhratsky A & Mohamet L. (2017). Aberrant iPSC-derived human astrocytes in Alzheimer's disease. *Cell Death Dis* **8,** e2696.

Jonsson T, Stefansson H, Steinberg S, Jonsdottir I, Jonsson PV, Snaedal J, Bjornsson S, Huttenlocher J, Levey AI, Lah JJ, Rujescu D, Hampel H, Giegling I, Andreassen OA, Engedal K, Ulstein I, Djurovic S, Ibrahim-Verbaas C, Hofman A, Ikram MA, van Duijn CM, Thorsteinsdottir U, Kong A & Stefansson K. (2013). Variant of TREM2 associated with the risk of Alzheimer's disease. *N Engl J Med* **368,** 107-116.

Junior NCF, Dos-Santos-Pereira M, Guimaraes FS & Del Bel E. (2020). Cannabidiol and Cannabinoid Compounds as Potential Strategies for Treating Parkinson's Disease and L-DOPA-Induced Dyskinesia. *Neurotox Res* **37,** 12-29.

Kamakura S, Oishi K, Yoshimatsu T, Nakafuku M, Masuyama N & Gotoh Y. (2004). Hes binding to STAT3 mediates crosstalk between Notch and JAK-STAT signalling. *Nat Cell Biol* **6,** 547-554.

Kanai Y & Hediger MA. (1992). Primary structure and functional characterization of a high-affinity glutamate transporter. *Nature* **360,** 467-471.

Kanazawa M, Ninomiya I, Hatakeyama M, Takahashi T & Shimohata T. (2017). Microglia and Monocytes/Macrophages Polarization Reveal Novel Therapeutic Mechanism against Stroke. *Int J Mol Sci* **18**.

Kang K, Lee SW, Han JE, Choi JW & Song MR. (2014a). The complex morphology of reactive astrocytes controlled by fibroblast growth factor signaling. *Glia* **62,** 1328-1344.

Kang SS, Ren Y, Liu CC, Kurti A, Baker KE, Bu G, Asmann Y & Fryer JD. (2018). Lipocalin-2 protects the brain during inflammatory conditions. *Mol Psychiatry* **23,** 344-350.

Kang W, Balordi F, Su N, Chen L, Fishell G & Hébert JM. (2014b). Astrocyte activation is suppressed in both normal and injured brain by FGF signaling. *Proc Natl Acad Sci U S A* **111,** E2987-2995.

Kantarci K, Lowe V, Przybelski SA, Weigand SD, Senjem ML, Ivnik RJ, Preboske GM, Roberts R, Geda YE, Boeve BF, Knopman DS, Petersen RC & Jack CR, Jr. (2012). APOE modifies the association between Abeta load and cognition in cognitively normal older adults. *Neurology* **78,** 232-240.

Karki P, Hong P, Johnson J, Jr., Pajarillo E, Son DS, Aschner M & Lee EY. (2018). Arundic Acid Increases Expression and Function of Astrocytic Glutamate Transporter EAAT1 Via the ERK, Akt, and NF-kappaB Pathways. *Mol Neurobiol* **55,** 5031-5046.

Karran E & De Strooper B. (2016). The amyloid cascade hypothesis: are we poised for success or failure? *J Neurochem* **139 Suppl 2,** 237-252.

Kaur G & Dufour JM. (2012). Cell lines: Valuable tools or useless artifacts. *Spermatogenesis* **2,** 1-5.

Kawabata S, Takano M, Numasawa-Kuroiwa Y, Itakura G, Kobayashi Y, Nishiyama Y, Sugai K, Nishimura S, Iwai H, Isoda M, Shibata S, Kohyama J, Iwanami A, Toyama Y, Matsumoto M, Nakamura M & Okano H. (2016). Grafted Human iPS Cell-Derived Oligodendrocyte Precursor Cells Contribute to Robust Remyelination of Demyelinated Axons after Spinal Cord Injury. *Stem Cell Reports* **6,** 1-8.

Kempuraj D, Thangavel R, Natteru PA, Selvakumar GP, Saeed D, Zahoor H, Zaheer S, Iyer SS & Zaheer A. (2016). Neuroinflammation Induces Neurodegeneration. *J Neurol Neurosurg Spine* **1**.

Khakh BS & Sofroniew MV. (2015). Diversity of astrocyte functions and phenotypes in neural circuits. *Nature Neuroscience* **18,** 942.

Khaksar S & Bigdeli MR. (2017). Intra-cerebral cannabidiol infusion-induced neuroprotection is partly associated with the TNF-alpha/TNFR1/NF-small ka, CyrillicB pathway in transient focal cerebral ischaemia. *Brain Inj* **31,** 1932-1943.

Kim J, Basak JM & Holtzman DM. (2009). The role of apolipoprotein E in Alzheimer's disease. *Neuron* **63,** 287-303.

Kim SH, Yang JW, Kim KH, Kim JU & Yook TH. (2019). A Review on Studies of Marijuana for Alzheimer's Disease - Focusing on CBD, THC. *J Pharmacopuncture* **22,** 225-230.

Kingdon HS, Hubbard JS & Stadtman ER. (1968). Regulation of glutamine synthetase. XI. The nature and implications of a lag phase in the Escherichia coli glutamine synthetase reaction. *Biochemistry* **7,** 2136-2142.

Kinney JW, Bemiller SM, Murtishaw AS, Leisgang AM, Salazar AM & Lamb BT. (2018). Inflammation as a central mechanism in Alzheimer's disease. *Alzheimers Dement (N Y)* **4,** 575-590.

Klegeris A, Giasson BI, Zhang H, Maguire J, Pelech S & McGeer PL. (2006). Alpha-synuclein and its disease-causing mutants induce ICAM-1 and IL-6 in human astrocytes and astrocytoma cells. *Faseb j* **20,** 2000-2008.

Klein RC, Mace BE, Moore SD & Sullivan PM. (2010). Progressive loss of synaptic integrity in human apolipoprotein E4 targeted replacement mice and attenuation by apolipoprotein E2. *Neuroscience* **171,** 1265-1272.

Kondo K, Hashimoto H, Kitanaka J, Sawada M, Suzumura A, Marunouchi T & Baba A. (1995). Expression of glutamate transporters in cultured glial cells. *Neurosci Lett* **188,** 140-142.

Kondo T, Asai M, Tsukita K, Kutoku Y, Ohsawa Y, Sunada Y, Imamura K, Egawa N, Yahata N, Okita K, Takahashi K, Asaka I, Aoi T, Watanabe A, Watanabe K, Kadoya C, Nakano R, Watanabe D, Maruyama K, Hori O, Hibino S, Choshi T, Nakahata T, Hioki H, Kaneko T, Naitoh M, Yoshikawa K, Yamawaki S, Suzuki S, Hata R, Ueno S, Seki T, Kobayashi K, Toda T, Murakami K, Irie K, Klein WL, Mori H, Asada T, Takahashi R, Iwata N, Yamanaka S & Inoue H. (2013). Modeling Alzheimer's disease with iPSCs reveals stress phenotypes associated with intracellular Abeta and differential drug responsiveness. *Cell Stem Cell* **12,** 487-496.

Koper OM, Kaminska J, Sawicki K & Kemona H. (2018). CXCL9, CXCL10, CXCL11, and their receptor (CXCR3) in neuroinflammation and neurodegeneration. *Adv Clin Exp Med* **27,** 849-856.

Kostic M, Zivkovic N, Cvetanovic A, Stojanovic I & Colic M. (2017). IL-17 signalling in astrocytes promotes glutamate excitotoxicity: Indications for the link between inflammatory and neurodegenerative events in multiple sclerosis. *Multiple sclerosis and related disorders* **11,** 12-17.

Koudinov AR & Koudinova NV. (2002). Cholesterol's role in synapse formation. *Science* **295,** 2213.

Kouhara H, Hadari YR, Spivak-Kroizman T, Schilling J, Bar-Sagi D, Lax I & Schlessinger J. (1997). A lipid-anchored Grb2-binding protein that links FGF-receptor activation to the Ras/MAPK signaling pathway. *Cell* **89,** 693-702.

Kozela E, Juknat A & Vogel Z. (2017). Modulation of Astrocyte Activity by Cannabidiol, a Nonpsychoactive Cannabinoid. *Int J Mol Sci* **18**.

Krencik R, Weick JP, Liu Y, Zhang ZJ & Zhang SC. (2011). Specification of transplantable astroglial subtypes from human pluripotent stem cells. *Nat Biotechnol* **29,** 528-534.

Kriks S, Shim JW, Piao J, Ganat YM, Wakeman DR, Xie Z, Carrillo-Reid L, Auyeung G, Antonacci C, Buch A, Yang L, Beal MF, Surmeier DJ, Kordower JH, Tabar V & Studer L. (2011). Dopamine neurons derived from human ES cells efficiently engraft in animal models of Parkinson's disease. *Nature* **480,** 547-551.

Krimbou L, Denis M, Haidar B, Carrier M, Marcil M & Genest J, Jr. (2004). Molecular interactions between apoE and ABCA1: impact on apoE lipidation. *J Lipid Res* **45,** 839-848.

Kruchkova Y, Ben-Dror I, Herschkovitz A, David M, Yayon A & Vardimon L. (2001). Basic fibroblast growth factor: a potential inhibitor of glutamine synthetase expression in injured neural tissue. *J Neurochem* **77,** 1641-1649.

Kuhn HG, Dickinson-Anson H & Gage FH. (1996). Neurogenesis in the dentate gyrus of the adult rat: age-related decrease of neuronal progenitor proliferation. *J Neurosci* **16,** 2027-2033.

Kunkle BW, Grenier-Boley B, Sims R, Bis JC, Damotte V, Naj AC, Boland A, Vronskaya M, van der Lee SJ, Amlie-Wolf A, Bellenguez C, Frizatti A, Chouraki V, Martin ER, Sleegers K, Badarinarayan N, Jakobsdottir J, Hamilton-Nelson KL, Moreno-Grau S, Olaso R, Raybould R, Chen Y, Kuzma AB, Hiltunen M, Morgan T, Ahmad S, Vardarajan BN, Epelbaum J, Hoffmann P, Boada M, Beecham GW, Garnier JG, Harold D, Fitzpatrick AL, Valladares O, Moutet ML, Gerrish A, Smith AV, Qu L, Bacq D, Denning N, Jian X, Zhao Y, Del Zompo M, Fox NC, Choi SH, Mateo I, Hughes JT, Adams HH, Malamon J, Sanchez-Garcia F, Patel Y, Brody JA, Dombroski BA, Naranjo MCD, Daniilidou M, Eiriksdottir G, Mukherjee S, Wallon D, Uphill J, Aspelund T, Cantwell LB, Garzia F, Galimberti D, Hofer E, Butkiewicz M, Fin B, Scarpini E, Sarnowski C, Bush WS, Meslage S, Kornhuber J, White CC, Song Y, Barber RC, Engelborghs S, Sordon S, Voijnovic D, Adams PM, Vandenberghe R, Mayhaus M, Cupples LA, Albert MS, De Deyn PP, Gu W, Himali JJ, Beekly D, Squassina A, Hartmann AM, Orellana A, Blacker D, Rodriguez-Rodriguez E, Lovestone S, Garcia ME, Doody RS, Munoz-Fernadez C, Sussams R, Lin H, Fairchild TJ, Benito YA, Holmes C, Karamujic-Comic H, Frosch MP, Thonberg H, Maier W, Roshchupkin G, Ghetti B, Giedraitis V, Kawalia A, Li S, Huebinger RM, Kilander L, Moebus S, Hernandez I, Kamboh MI, Brundin R, Turton J, Yang Q, Katz MJ, Concari L, Lord J, Beiser AS, Keene CD, Helisalmi S, Kloszewska I, Kukull WA, Koivisto AM, Lynch A, Tarraga L, Larson EB, Haapasalo A, Lawlor B, Mosley TH, Lipton RB, Solfrizzi V, Gill M, Longstreth WT, Jr., Montine TJ, Frisardi V, Diez-Fairen M, Rivadeneira F, Petersen RC, Deramecourt V, Alvarez I, Salani F, Ciaramella A,

Boerwinkle E, Reiman EM, Fievet N, Rotter JI, Reisch JS, Hanon O, Cupidi C, Andre Uitterlinden AG, Royall DR, Dufouil C, Maletta RG, de Rojas I, Sano M, Brice A, Cecchetti R, George-Hyslop PS, Ritchie K, Tsolaki M, Tsuang DW, Dubois B, Craig D, Wu CK, Soininen H, Avramidou D, Albin RL, Fratiglioni L, Germanou A, Apostolova LG, Keller L, Koutroumani M, Arnold SE, Panza F, Gkatzima O, Asthana S, Hannequin D, Whitehead P, Atwood CS, Caffarra P, Hampel H, Quintela I, Carracedo A, Lannfelt L, Rubinsztein DC, Barnes LL, Pasquier F, Frolich L, Barral S, McGuinness B, Beach TG, Johnston JA, Becker JT, Passmore P, Bigio EH, Schott JM, Bird TD, Warren JD, Boeve BF, Lupton MK, Bowen JD, Proitsi P, Boxer A, Powell JF, Burke JR, Kauwe JSK, Burns JM, Mancuso M, Buxbaum JD, Bonuccelli U, Cairns NJ, McQuillin A, Cao C, Livingston G, Carlson CS, Bass NJ, Carlsson CM, Hardy J, Carney RM, Bras J, Carrasquillo MM, Guerreiro R, Allen M, Chui HC, Fisher E, Masullo C, Crocco EA, DeCarli C, Bisceglio G, Dick M, Ma L, Duara R, Graff-Radford NR, Evans DA, Hodges A, Faber KM, Scherer M, Fallon KB, Riemenschneider M, Fardo DW, Heun R, Farlow MR, Kolsch H, Ferris S, Leber M, Foroud TM, Heuser I, Galasko DR, Giegling I, Gearing M, Hull M, Geschwind DH, Gilbert JR, Morris J, Green RC, Mayo K, Growdon JH, Feulner T, Hamilton RL, Harrell LE, Drichel D, Honig LS, Cushion TD, Huentelman MJ, Hollingworth P, Hulette CM, Hyman BT, Marshall R, Jarvik GP, Meggy A, Abner E, Menzies GE, Jin LW, Leonenko G, Real LM, Jun GR, Baldwin CT, Grozeva D, Karydas A, Russo G, Kaye JA, Kim R, Jessen F, Kowall NW, Vellas B, Kramer JH, Vardy E, LaFerla FM, Jockel KH, Lah JJ, Dichgans M, Leverenz JB, Mann D, Levey AI, Pickering-Brown S, Lieberman AP, Klopp N, Lunetta KL, Wichmann HE, Lyketsos CG, Morgan K, Marson DC, Brown K, Martiniuk F, Medway C, Mash DC, Nothen MM, Masliah E, Hooper NM, McCormick WC, Daniele A, McCurry SM, Bayer A, McDavid AN, Gallacher J, McKee AC, van den Bussche H, Mesulam M, Brayne C, Miller BL, Riedel-Heller S, Miller CA, Miller JW, Al-Chalabi A, Morris JC, Shaw CE, Myers AJ, Wiltfang J, O'Bryant S, Olichney JM, Alvarez V, Parisi JE, Singleton AB, Paulson HL, Collinge J, Perry WR, Mead S, Peskind E, Cribbs DH, Rossor M, Pierce A, Ryan NS, Poon WW, Nacmias B, Potter H, Sorbi S, Quinn JF, Sacchinelli E, Raj A, Spalletta G, Raskind M, Caltagirone C, Bossu P, Orfei MD, Reisberg B, Clarke R, Reitz C, Smith AD, Ringman JM, Warden D, Roberson ED, Wilcock G, Rogaeva E, Bruni AC, Rosen HJ, Gallo M, Rosenberg RN, Ben-Shlomo Y, Sager MA, Mecocci P, Saykin AJ, Pastor P, Cuccaro ML, Vance JM, Schneider JA, Schneider LS, Slifer S, Seeley WW, Smith AG, Sonnen JA, Spina S, Stern RA, Swerdlow RH, Tang M, Tanzi RE, Trojanowski JQ, Troncoso JC, Van Deerlin VM, Van Eldik LJ, Vinters HV, Vonsattel JP, Weintraub S, Welsh-Bohmer KA, Wilhelmsen KC, Williamson J, Wingo TS, Woltjer RL, Wright CB, Yu CE, Yu L, Saba Y, Pilotto A, Bullido MJ, Peters O, Crane PK, Bennett D, Bosco P, Coto E, Boccardi V, De Jager PL, Lleo A, Warner N, Lopez OL, Ingelsson M, Deloukas P, Cruchaga C, Graff C, Gwilliam R, Fornage M, Goate AM, Sanchez-Juan P, Kehoe PG, Amin N, Ertekin-Taner N, Berr C, Debette S, Love S, Launer LJ, Younkin SG, Dartigues JF, Corcoran C, Ikram MA, Dickson DW, Nicolas G, Campion D, Tschanz J, Schmidt H, Hakonarson H, Clarimon J, Munger R, Schmidt R, Farrer LA, Van Broeckhoven C, M COD, DeStefano AL, Jones L, Haines JL, Deleuze JF, Owen MJ, Gudnason V, Mayeux R, Escott-Price V, Psaty BM, Ramirez A, Wang LS, Ruiz A, van Duijn CM, Holmans PA, Seshadri S, Williams J, Amouyel P, Schellenberg GD, Lambert JC & Pericak-Vance MA. (2019a). Genetic meta-analysis of diagnosed Alzheimer's disease identifies new risk loci and implicates Abeta, tau, immunity and lipid processing. *Nat Genet* **51,** 414-430.

Kunkle BW, Grenier-Boley B, Sims R, Bis JC, Damotte V, Naj AC, Boland A, Vronskaya M, van der Lee SJ, Amlie-Wolf A, Bellenguez C, Frizatti A, Chouraki V, Martin ER, Sleegers K, Badarinarayan N, Jakobsdottir J, Hamilton-Nelson KL, Moreno-Grau S, Olaso R, Raybould R, Chen Y, Kuzma AB, Hiltunen M, Morgan T, Ahmad S, Vardarajan BN, Epelbaum J, Hoffmann P, Boada M, Beecham GW, Garnier JG, Harold D, Fitzpatrick AL, Valladares O, Moutet ML, Gerrish A, Smith AV, Qu L, Bacq D, Denning N, Jian X, Zhao Y, Del Zompo M, Fox NC, Choi SH, Mateo I, Hughes JT, Adams HH, Malamon J, Sanchez-Garcia F, Patel Y, Brody JA, Dombroski BA, Naranjo MCD, Daniilidou M, Eiriksdottir G, Mukherjee S, Wallon D, Uphill J, Aspelund T, Cantwell LB, Garzia F, Galimberti D, Hofer E, Butkiewicz M, Fin B, Scarpini E, Sarnowski C, Bush WS, Meslage S, Kornhuber J, White CC, Song Y, Barber RC, Engelborghs S, Sordon S, Voijnovic D, Adams PM, Vandenberghe R, Mayhaus M, Cupples LA, Albert MS, De Deyn PP, Gu W, Himali JJ, Beekly D, Squassina A, Hartmann AM, Orellana A, Blacker D, Rodriguez-Rodriguez E, Lovestone S, Garcia ME, Doody RS, Munoz-Fernadez C, Sussams R, Lin H, Fairchild TJ, Benito YA, Holmes C, Karamujic-Comic H, Frosch MP, Thonberg H, Maier W, Roshchupkin G, Ghetti B, Giedraitis V, Kawalia A, Li S, Huebinger RM, Kilander L, Moebus S, Hernandez I, Kamboh MI, Brundin R, Turton J, Yang Q, Katz MJ, Concari L, Lord J, Beiser AS, Keene CD, Helisalmi S, Kloszewska I, Kukull WA, Koivisto AM, Lynch A, Tarraga L, Larson EB, Haapasalo A, Lawlor B, Mosley TH, Lipton RB, Solfrizzi V, Gill M, Longstreth WT, Jr., Montine TJ, Frisardi V, Diez-Fairen M, Rivadeneira F, Petersen RC, Deramecourt V, Alvarez I, Salani F, Ciaramella A, Boerwinkle E, Reiman EM, Fievet N, Rotter JI, Reisch JS, Hanon O, Cupidi C, Uitterlinden AGA, Royall DR, Dufouil C, Maletta RG, de Rojas I, Sano M, Brice A, Cecchetti R, George-Hyslop PS, Ritchie K, Tsolaki M, Tsuang DW, Dubois B, Craig D, Wu CK, Soininen H, Avramidou D, Albin RL, Fratiglioni L, Germanou A, Apostolova LG, Keller L, Koutroumani M, Arnold SE, Panza F, Gkatzima O, Asthana S, Hannequin D, Whitehead P, Atwood CS, Caffarra P, Hampel H, Quintela I, Carracedo A, Lannfelt L, Rubinsztein DC, Barnes LL, Pasquier F, Frolich L, Barral S, McGuinness B, Beach TG, Johnston JA, Becker JT, Passmore P, Bigio EH, Schott JM, Bird TD, Warren JD, Boeve BF, Lupton MK, Bowen JD, Proitsi P, Boxer A, Powell JF, Burke JR, Kauwe JSK, Burns JM, Mancuso M, Buxbaum JD, Bonuccelli U, Cairns NJ, McQuillin A, Cao C, Livingston G, Carlson CS, Bass NJ, Carlsson CM, Hardy J, Carney RM, Bras J, Carrasquillo MM, Guerreiro R, Allen M, Chui HC, Fisher E, Masullo C, Crocco EA, DeCarli C, Bisceglio G, Dick M, Ma L, Duara R, Graff-Radford NR, Evans DA, Hodges A, Faber KM, Scherer M, Fallon KB, Riemenschneider M, Fardo DW, Heun R, Farlow MR, Kolsch H, Ferris S, Leber M, Foroud TM, Heuser I, Galasko DR, Giegling I, Gearing M, Hull M, Geschwind DH, Gilbert JR, Morris J, Green RC, Mayo K, Growdon JH, Feulner T, Hamilton RL, Harrell LE, Drichel D, Honig LS, Cushion TD, Huentelman MJ, Hollingworth P, Hulette CM, Hyman BT, Marshall R, Jarvik GP, Meggy A, Abner E, Menzies GE, Jin LW, Leonenko G, Real LM, Jun GR, Baldwin CT, Grozeva D, Karydas A, Russo G, Kaye JA, Kim R, Jessen F, Kowall NW, Vellas B, Kramer JH, Vardy E, LaFerla FM, Jockel KH, Lah JJ, Dichgans M, Leverenz JB, Mann D, Levey AI, Pickering-Brown S, Lieberman AP, Klopp N, Lunetta KL, Wichmann HE, Lyketsos CG, Morgan K, Marson DC, Brown K, Martiniuk F, Medway C, Mash DC, Nothen MM, Masliah E, Hooper NM, McCormick WC, Daniele A, McCurry SM, Bayer A, McDavid AN, Gallacher J, McKee AC, van den Bussche H, Mesulam M, Brayne C, Miller BL, Riedel-Heller S, Miller CA, Miller JW, Al-Chalabi A, Morris JC, Shaw CE, Myers AJ, Wiltfang J, O'Bryant S, Olichney JM, Alvarez V, Parisi JE, Singleton AB, Paulson HL, Collinge J, Perry WR, Mead S, Peskind E, Cribbs DH, Rossor M, Pierce A, Ryan NS,

Poon WW, Nacmias B, Potter H, Sorbi S, Quinn JF, Sacchinelli E, Raj A, Spalletta G, Raskind M, Caltagirone C, Bossu P, Orfei MD, Reisberg B, Clarke R, Reitz C, Smith AD, Ringman JM, Warden D, Roberson ED, Wilcock G, Rogaeva E, Bruni AC, Rosen HJ, Gallo M, Rosenberg RN, Ben-Shlomo Y, Sager MA, Mecocci P, Saykin AJ, Pastor P, Cuccaro ML, Vance JM, Schneider JA, Schneider LS, Slifer S, Seeley WW, Smith AG, Sonnen JA, Spina S, Stern RA, Swerdlow RH, Tang M, Tanzi RE, Trojanowski JQ, Troncoso JC, Van Deerlin VM, Van Eldik LJ, Vinters HV, Vonsattel JP, Weintraub S, Welsh-Bohmer KA, Wilhelmsen KC, Williamson J, Wingo TS, Woltjer RL, Wright CB, Yu CE, Yu L, Saba Y, Alzheimer Disease Genetics C, European Alzheimer's Disease I, Cohorts for Heart and Aging Research in Genomic Epidemiology C, Genetic and Environmental Risk in Ad/Defining Genetic PaERfAsDC, Pilotto A, Bullido MJ, Peters O, Crane PK, Bennett D, Bosco P, Coto E, Boccardi V, De Jager PL, Lleo A, Warner N, Lopez OL, Ingelsson M, Deloukas P, Cruchaga C, Graff C, Gwilliam R, Fornage M, Goate AM, Sanchez-Juan P, Kehoe PG, Amin N, Ertekin-Taner N, Berr C, Debette S, Love S, Launer LJ, Younkin SG, Dartigues JF, Corcoran C, Ikram MA, Dickson DW, Nicolas G, Campion D, Tschanz J, Schmidt H, Hakonarson H, Clarimon J, Munger R, Schmidt R, Farrer LA, Van Broeckhoven C, O'Donovan MC, DeStefano AL, Jones L, Haines JL, Deleuze JF, Owen MJ, Gudnason V, Mayeux R, Escott-Price V, Psaty BM, Ramirez A, Wang LS, Ruiz A, van Duijn CM, Holmans PA, Seshadri S, Williams J, Amouyel P, Schellenberg GD, Lambert JC & Pericak-Vance MA. (2019b). Author Correction: Genetic meta-analysis of diagnosed Alzheimer's disease identifies new risk loci and implicates Abeta, tau, immunity and lipid processing. In *Nat Genet*, pp. 1423-1424. United States.

Lai MI, Wendy-Yeo WY, Ramasamy R, Nordin N, Rosli R, Veerakumarasivam A & Abdullah S. (2011). Advancements in reprogramming strategies for the generation of induced pluripotent stem cells. *J Assist Reprod Genet* **28,** 291-301.

Lambert JC, Ibrahim-Verbaas CA, Harold D, Naj AC, Sims R, Bellenguez C, DeStafano AL, Bis JC, Beecham GW, Grenier-Boley B, Russo G, Thorton-Wells TA, Jones N, Smith AV, Chouraki V, Thomas C, Ikram MA, Zelenika D, Vardarajan BN, Kamatani Y, Lin CF, Gerrish A, Schmidt H, Kunkle B, Dunstan ML, Ruiz A, Bihoreau MT, Choi SH, Reitz C, Pasquier F, Cruchaga C, Craig D, Amin N, Berr C, Lopez OL, De Jager PL, Deramecourt V, Johnston JA, Evans D, Lovestone S, Letenneur L, Moron FJ, Rubinsztein DC, Eiriksdottir G, Sleegers K, Goate AM, Fievet N, Huentelman MW, Gill M, Brown K, Kamboh MI, Keller L, Barberger-Gateau P, McGuiness B, Larson EB, Green R, Myers AJ, Dufouil C, Todd S, Wallon D, Love S, Rogaeva E, Gallacher J, St George-Hyslop P, Clarimon J, Lleo A, Bayer A, Tsuang DW, Yu L, Tsolaki M, Bossu P, Spalletta G, Proitsi P, Collinge J, Sorbi S, Sanchez-Garcia F, Fox NC, Hardy J, Deniz Naranjo MC, Bosco P, Clarke R, Brayne C, Galimberti D, Mancuso M, Matthews F, Moebus S, Mecocci P, Del Zompo M, Maier W, Hampel H, Pilotto A, Bullido M, Panza F, Caffarra P, Nacmias B, Gilbert JR, Mayhaus M, Lannefelt L, Hakonarson H, Pichler S, Carrasquillo MM, Ingelsson M, Beekly D, Alvarez V, Zou F, Valladares O, Younkin SG, Coto E, Hamilton-Nelson KL, Gu W, Razquin C, Pastor P, Mateo I, Owen MJ, Faber KM, Jonsson PV, Combarros O, O'Donovan MC, Cantwell LB, Soininen H, Blacker D, Mead S, Mosley TH, Jr., Bennett DA, Harris TB, Fratiglioni L, Holmes C, de Bruijn RF, Passmore P, Montine TJ, Bettens K, Rotter JI, Brice A, Morgan K, Foroud TM, Kukull WA, Hannequin D, Powell JF, Nalls MA, Ritchie K, Lunetta KL, Kauwe JS, Boerwinkle E, Riemenschneider M, Boada M, Hiltuenen M, Martin ER, Schmidt R, Rujescu D, Wang LS, Dartigues JF, Mayeux R,

Tzourio C, Hofman A, Nothen MM, Graff C, Psaty BM, Jones L, Haines JL, Holmans PA, Lathrop M, Pericak-Vance MA, Launer LJ, Farrer LA, van Duijn CM, Van Broeckhoven C, Moskvina V, Seshadri S, Williams J, Schellenberg GD & Amouyel P. (2013). Meta-analysis of 74,046 individuals identifies 11 new susceptibility loci for Alzheimer's disease. *Nat Genet* **45,** 1452-1458.

Lancaster MA, Renner M, Martin CA, Wenzel D, Bicknell LS, Hurles ME, Homfray T, Penninger JM, Jackson AP & Knoblich JA. (2013). Cerebral organoids model human brain development and microcephaly. *Nature* **501,** 373-379.

Lane-Donovan C & Herz J. (2017). ApoE, ApoE Receptors, and the Synapse in Alzheimer's Disease. *Trends Endocrinol Metab* **28,** 273-284.

Lanfranco MF, Mocchetti I, Burns MP & Villapol S. (2017). Glial- and Neuronal-Specific Expression of CCL5 mRNA in the Rat Brain. *Front Neuroanat* **11,** 137.

Lasiene J & Yamanaka K. (2011). Glial cells in amyotrophic lateral sclerosis. *Neurol Res Int* **2011,** 718987.

Lautner R, Palmqvist S, Mattsson N, Andreasson U, Wallin A, Palsson E, Jakobsson J, Herukka SK, Owenius R, Olsson B, Hampel H, Rujescu D, Ewers M, Landen M, Minthon L, Blennow K, Zetterberg H & Hansson O. (2014). Apolipoprotein E genotype and the diagnostic accuracy of cerebrospinal fluid biomarkers for Alzheimer disease. *JAMA Psychiatry* **71,** 1183-1191.

Lawlor B, Segurado R, Kennelly S, Olde Rikkert MGM, Howard R, Pasquier F, Borjesson-Hanson A, Tsolaki M, Lucca U, Molloy DW, Coen R, Riepe MW, Kalman J, Kenny RA, Cregg F, O'Dwyer S, Walsh C, Adams J, Banzi R, Breuilh L, Daly L, Hendrix S, Aisen P, Gaynor S, Sheikhi A, Taekema DG, Verhey FR, Nemni R, Nobili F, Franceschi M, Frisoni G, Zanetti O, Konsta A, Anastasios O, Nenopoulou S, Tsolaki-Tagaraki F, Pakaski M, Dereeper O, de la Sayette V, Senechal O, Lavenu I, Devendeville A, Calais G, Crawford F & Mullan M. (2018). Nilvadipine in mild to moderate Alzheimer disease: A randomised controlled trial. *PLoS Med* **15,** e1002660.

Lazarewicz JW, Wroblewski JT & Costa E. (1990). N-methyl-D-aspartate-sensitive glutamate receptors induce calcium-mediated arachidonic acid release in primary cultures of cerebellar granule cells. *J Neurochem* **55,** 1875-1881.

Lee C, Robinson M & Willerth SM. (2018). Direct Reprogramming of Glioblastoma Cells into Neurons Using Small Molecules. *ACS Chem Neurosci* **9,** 3175-3185.

Lee DH, Seubert S, Huhn K, Brecht L, Rotger C, Waschbisch A, Schlachetzki J, Klausmeyer A, Melms A, Wiese S, Winkler J & Linker RA. (2017). Fingolimod effects in

neuroinflammation: Regulation of astroglial glutamate transporters? *PLoS One* **12,** e0171552.

Lee H, Shamy GA, Elkabetz Y, Schofield CM, Harrsion NL, Panagiotakos G, Socci ND, Tabar V & Studer L. (2007). Directed differentiation and transplantation of human embryonic stem cell-derived motoneurons. *Stem Cells* **25,** 1931-1939.

Lee S, Jha MK & Suk K. (2015). Lipocalin-2 in the Inflammatory Activation of Brain Astrocytes. *Crit Rev Immunol* **35,** 77-84.

Lee S, Park JY, Lee WH, Kim H, Park HC, Mori K & Suk K. (2009). Lipocalin-2 is an autocrine mediator of reactive astrocytosis. *J Neurosci* **29,** 234-249.

Lee SC, Liu W, Brosnan CF & Dickson DW. (1994). GM-CSF promotes proliferation of human fetal and adult microglia in primary cultures. *Glia* **12,** 309-318.

Lee SJ, Drabik K, Van Wagoner NJ, Lee S, Choi C, Dong Y & Benveniste EN. (2000). ICAM-1-induced expression of proinflammatory cytokines in astrocytes: involvement of extracellular signal-regulated kinase and p38 mitogen-activated protein kinase pathways. *J Immunol* **165,** 4658-4666.

Lehre KP & Danbolt NC. (1998). The number of glutamate transporter subtype molecules at glutamatergic synapses: chemical and stereological quantification in young adult rat brain. *J Neurosci* **18,** 8751-8757.

Li AW & Murphy PR. (2000). Expression of alternatively spliced FGF-2 antisense RNA transcripts in the central nervous system: regulation of FGF-2 mRNA translation. *Mol Cell Endocrinol* **170,** 233-242.

Li L, Donly C, Li Q, Willis LG, Keddie BA, Erlandson MA & Theilmann DA. (2002). Identification and genomic analysis of a second species of nucleopolyhedrovirus isolated from Mamestra configurata. *Virology* **297,** 226-244.

Li XJ, Du ZW, Zarnowska ED, Pankratz M, Hansen LO, Pearce RA & Zhang SC. (2005). Specification of motoneurons from human embryonic stem cells. *Nat Biotechnol* **23,** 215-221.

Li Y, Dong X, Cai J, Yin S, Sun Y, Yang D & Jiang C. (2018). SERPINA3 induced by astroglia/microglia co-culture facilitates glioblastoma stem-like cell invasion. *Oncol Lett* **15,** 285-291.

Lian H, Litvinchuk A, Chiang AC, Aithmitti N, Jankowsky JL & Zheng H. (2016). Astrocyte-Microglia Cross Talk through Complement Activation Modulates Amyloid Pathology in Mouse Models of Alzheimer's Disease. *J Neurosci* **36,** 577-589.

Liang Z, Valla J, Sefidvash-Hockley S, Rogers J & Li R. (2002). Effects of estrogen treatment on glutamate uptake in cultured human astrocytes derived from cortex of Alzheimer's disease patients. *J Neurochem* **80,** 807-814.

Liao MC, Muratore CR, Gierahn TM, Sullivan SE, Srikanth P, De Jager PL, Love JC & Young-Pearse TL. (2016). Single-Cell Detection of Secreted Abeta and sAPPalpha from Human IPSC-Derived Neurons and Astrocytes. *J Neurosci* **36,** 1730-1746.

Libro R, Scionti D, Diomede F, Marchisio M, Grassi G, Pollastro F, Piattelli A, Bramanti P, Mazzon E & Trubiani O. (2016). Cannabidiol Modulates the Immunophenotype and Inhibits the Activation of the Inflammasome in Human Gingival Mesenchymal Stem Cells. *Front Physiol* **7,** 559.

Licastro F, Pedrini S, Caputo L, Annoni G, Davis LJ, Ferri C, Casadei V & Grimaldi LM. (2000). Increased plasma levels of interleukin-1, interleukin-6 and alpha-1-antichymotrypsin in patients with Alzheimer's disease: peripheral inflammation or signals from the brain? *J Neuroimmunol* **103,** 97-102.

Liddelow S & Hoyer D. (2016). Astrocytes: Adhesion Molecules and Immunomodulation. *Curr Drug Targets* **17,** 1871-1881.

Liddelow SA & Barres BA. (2017). Reactive Astrocytes: Production, Function, and Therapeutic Potential. *Immunity* **46,** 957-967.

Liddelow SA, Guttenplan KA, Clarke LE, Bennett FC, Bohlen CJ, Schirmer L, Bennett ML, Münch AE, Chung WS, Peterson TC, Wilton DK, Frouin A, Napier BA, Panicker N, Kumar M, Buckwalter MS, Rowitch DH, Dawson VL, Dawson TM, Stevens B & Barres BA. (2017). Neurotoxic reactive astrocytes are induced by activated microglia. *Nature* **541,** 481-487.

Lin CH, Jackson AL, Guo J, Linsley PS & Eisenman RN. (2009). Myc-regulated microRNAs attenuate embryonic stem cell differentiation. *Embo j* **28,** 3157-3170.

Lin CH, You JR, Wei KC & Gean PW. (2014). Stimulating ERK/PI3K/NFkappaB signaling pathways upon activation of mGluR2/3 restores OGD-induced impairment in glutamate clearance in astrocytes. *Eur J Neurosci* **39,** 83-96.

Lin YT, Seo J, Gao F, Feldman HM, Wen HL, Penney J, Cam HP, Gjoneska E, Raja WK, Cheng J, Rueda R, Kritskiy O, Abdurrob F, Peng Z, Milo B, Yu CJ, Elmsaouri S, Dey D, Ko T, Yankner BA & Tsai LH. (2018). APOE4 Causes Widespread Molecular and Cellular

Alterations Associated with Alzheimer's Disease Phenotypes in Human iPSC-Derived Brain Cell Types. *Neuron* **98,** 1294.

Linetti A, Fratangeli A, Taverna E, Valnegri P, Francolini M, Cappello V, Matteoli M, Passafaro M & Rosa P. (2010). Cholesterol reduction impairs exocytosis of synaptic vesicles. *J Cell Sci* **123,** 595-605.

Linton MF, Gish R, Hubl ST, Butler E, Esquivel C, Bry WI, Boyles JK, Wardell MR & Young SG. (1991). Phenotypes of apolipoprotein B and apolipoprotein E after liver transplantation. *J Clin Invest* **88,** 270-281.

Litvinchuk A, Wan YW, Swartzlander DB, Chen F, Cole A, Propson NE, Wang Q, Zhang B, Liu Z & Zheng H. (2018). Complement C3aR Inactivation Attenuates Tau Pathology and Reverses an Immune Network Deregulated in Tauopathy Models and Alzheimer's Disease. *Neuron* **100,** 1337-1353.e1335.

Liu CC, Kanekiyo T, Xu H & Bu G. (2013). Apolipoprotein E and Alzheimer disease: risk, mechanisms and therapy. In *Nat Rev Neurol*, pp. 106-118. England.

Liu CC, Zhao N, Fu Y, Wang N, Linares C, Tsai CW & Bu G. (2017). ApoE4 Accelerates Early Seeding of Amyloid Pathology. *Neuron* **96,** 1024-1032.e1023.

Liu RX, Huang C, Bennett DA, Li H & Wang R. (2016). The characteristics of astrocyte on Abeta clearance altered in Alzheimer's disease were reversed by anti-inflammatory agent (+)-2-(1-hydroxyl-4-oxocyclohexyl) ethyl caffeate. *Am J Transl Res* **8,** 4082-4094.

Liu S, Liu Y, Hao W, Wolf L, Kiliaan AJ, Penke B, Rübe CE, Walter J, Heneka MT, Hartmann T, Menger MD & Fassbender K. (2012). TLR2 is a primary receptor for Alzheimer's amyloid β peptide to trigger neuroinflammatory activation. *J Immunol* **188,** 1098-1107.

Liu X, Albano R & Lobner D. (2014). FGF-2 induces neuronal death through upregulation of system xc. *Brain Res* **1547,** 25-33.

Liu Y, Walter S, Stagi M, Cherny D, Letiembre M, Schulz-Schaeffer W, Heine H, Penke B, Neumann H & Fassbender K. (2005). LPS receptor (CD14): a receptor for phagocytosis of Alzheimer's amyloid peptide. *Brain* **128,** 1778-1789.

Liu Z & Chopp M. (2016). Astrocytes, therapeutic targets for neuroprotection and neurorestoration in ischemic stroke. *Prog Neurobiol* **144,** 103-120.

Liu Z, Xu J, Colvin JS & Ornitz DM. (2002). Coordination of chondrogenesis and osteogenesis by fibroblast growth factor 18. *Genes Dev* **16,** 859-869.

Lobsiger CS & Cleveland DW. (2007). Glial cells as intrinsic components of non-cell-autonomous neurodegenerative disease. *Nat Neurosci* **10,** 1355-1360.

Lok K, Zhao H, Shen H, Wang Z, Gao X, Zhao W & Yin M. (2013). Characterization of the APP/PS1 mouse model of Alzheimer's disease in senescence accelerated background. *Neurosci Lett* **557 Pt B,** 84-89.

Long EO. (2011). ICAM-1: getting a grip on leukocyte adhesion. *J Immunol* **186,** 5021-5023.

Loo BM, Kreuger J, Jalkanen M, Lindahl U & Salmivirta M. (2001). Binding of heparin/heparan sulfate to fibroblast growth factor receptor 4. *J Biol Chem* **276,** 16868-16876.

Lopez-Bayghen E, Espinoza-Rojo M & Ortega A. (2003). Glutamate down-regulates GLAST expression through AMPA receptors in Bergmann glial cells. *Brain Res Mol Brain Res* **115,** 1-9.

Lynch JR, Tang W, Wang H, Vitek MP, Bennett ER, Sullivan PM, Warner DS & Laskowitz DT. (2003). APOE genotype and an ApoE-mimetic peptide modify the systemic and central nervous system inflammatory response. *J Biol Chem* **278,** 48529-48533.

Madeddu F, Naska S & Bozzi Y. (2004). BDNF down-regulates the caspase 3 pathway in injured geniculo-cortical neurones. *Neuroreport* **15,** 2045-2049.

Madill M, McDonagh K, Ma J, Vajda A, McLoughlin P, O'Brien T, Hardiman O & Shen S. (2017). Amyotrophic lateral sclerosis patient iPSC-derived astrocytes impair autophagy via non-cell autonomous mechanisms. *Mol Brain* **10,** 22.

Maezawa I, Maeda N, Montine TJ & Montine KS. (2006). Apolipoprotein E-specific innate immune response in astrocytes from targeted replacement mice. *J Neuroinflammation* **3,** 10.

Magistretti PJ & Pellerin L. (1999). Astrocytes Couple Synaptic Activity to Glucose Utilization in the Brain. *News Physiol Sci* **14,** 177-182.

Mahley RW. (1988). Apolipoprotein E: cholesterol transport protein with expanding role in cell biology. *Science* **240,** 622-630.

Mahmoud S, Gharagozloo M, Simard C & Gris D. (2019). Astrocytes Maintain Glutamate Homeostasis in the CNS by Controlling the Balance between Glutamate Uptake and Release. *Cells* **8**.

Majumder A, Dhara SK, Swetenburg R, Mithani M, Cao K, Medrzycki M, Fan Y & Stice SL. (2013). Inhibition of DNA methyltransferases and histone deacetylases induces astrocytic differentiation of neural progenitors. *Stem Cell Res* **11,** 574-586.

Mak AC, Pullinger CR, Tang LF, Wong JS, Deo RC, Schwarz JM, Gugliucci A, Movsesyan I, Ishida BY, Chu C, Poon A, Kim P, Stock EO, Schaefer EJ, Asztalos BF, Castellano JM, Wyss-Coray T, Duncan JL, Miller BL, Kane JP, Kwok PY & Malloy MJ. (2014). Effects of the absence of apolipoprotein e on lipoproteins, neurocognitive function, and retinal function. *JAMA Neurol* **71,** 1228-1236.

Malarkey EB & Parpura V. (2008). Mechanisms of glutamate release from astrocytes. *Neurochem Int* **52,** 142-154.

Mangia S, Simpson IA, Vannucci SJ & Carruthers A. (2009). The in vivo neuron-to-astrocyte lactate shuttle in human brain: evidence from modeling of measured lactate levels during visual stimulation. *J Neurochem* **109 Suppl 1,** 55-62.

Marchetto MC, Muotri AR, Mu Y, Smith AM, Cezar GG & Gage FH. (2008). Non-cell-autonomous effect of human SOD1 G37R astrocytes on motor neurons derived from human embryonic stem cells. *Cell Stem Cell* **3,** 649-657.

Mark LP, Prost RW, Ulmer JL, Smith MM, Daniels DL, Strottmann JM, Brown WD & Hacein-Bey L. (2001). Pictorial review of glutamate excitotoxicity: fundamental concepts for neuroimaging. *American journal of neuroradiology* **22,** 1813-1824.

Martin-Moreno AM, Reigada D, Ramirez BG, Mechoulam R, Innamorato N, Cuadrado A & de Ceballos ML. (2011). Cannabidiol and other cannabinoids reduce microglial activation in vitro and in vivo: relevance to Alzheimer's disease. *Mol Pharmacol* **79,** 964-973.

Martinez-Morillo E, Hansson O, Atagi Y, Bu G, Minthon L, Diamandis EP & Nielsen HM. (2014). Total apolipoprotein E levels and specific isoform composition in cerebrospinal fluid and plasma from Alzheimer's disease patients and controls. *Acta Neuropathol* **127,** 633-643.

Masliah E, Alford M, DeTeresa R, Mallory M & Hansen L. (1996). Deficient glutamate transport is associated with neurodegeneration in Alzheimer's disease. *Ann Neurol* **40,** 759-766.

Masvekar R, Wu T, Kosa P, Barbour C, Fossati V & Bielekova B. (2019). Cerebrospinal fluid biomarkers link toxic astrogliosis and microglial activation to multiple sclerosis severity. *Mult Scler Relat Disord* **28,** 34-43.

Mathys H, Davila-Velderrain J, Peng Z, Gao F, Mohammadi S, Young JZ, Menon M, He L, Abdurrob F, Jiang X, Martorell AJ, Ransohoff RM, Hafler BP, Bennett DA, Kellis M & Tsai LH. (2019). Single-cell transcriptomic analysis of Alzheimer's disease. *Nature* **570,** 332-337.

Matias I, Morgado J & Gomes FCA. (2019). Astrocyte Heterogeneity: Impact to Brain Aging and Disease. *Front Aging Neurosci* **11,** 59.

Mattson MP, Cheng B, Culwell AR, Esch FS, Lieberburg I & Rydel RE. (1993). Evidence for excitoprotective and intraneuronal calcium-regulating roles for secreted forms of the β-amyloid precursor protein. *Neuron* **10,** 243-254.

Matyash V & Kettenmann H. (2010). Heterogeneity in astrocyte morphology and physiology. *Brain Res Rev* **63,** 2-10.

McComish SF & Caldwell MA. (2018). Generation of defined neural populations from pluripotent stem cells. *Philos Trans R Soc Lond B Biol Sci* **373**.

McGeer PL & McGeer EG. (2008). Glial reactions in Parkinson's disease. *Mov Disord* **23,** 474-483.

McGonigle P & Ruggeri B. (2014). Animal models of human disease: challenges in enabling translation. *Biochem Pharmacol* **87,** 162-171.

McKenna MC. (2007). The glutamate-glutamine cycle is not stoichiometric: Fates of glutamate in brain. *Journal of neuroscience research* **85,** 3347-3358.

McKenna MC, Sonnewald U, Huang X, Stevenson J & Zielke HR. (1996). Exogenous glutamate concentration regulates the metabolic fate of glutamate in astrocytes. *J Neurochem* **66,** 386-393.

Mecha M, Feliu A, Inigo PM, Mestre L, Carrillo-Salinas FJ & Guaza C. (2013). Cannabidiol provides long-lasting protection against the deleterious effects of inflammation in a viral model of multiple sclerosis: a role for A2A receptors. *Neurobiol Dis* **59,** 141-150.

Mendiola AS & Cardona AE. (2018). The IL-1beta phenomena in neuroinflammatory diseases. *J Neural Transm (Vienna)* **125,** 781-795.

Mertens J, Marchetto MC, Bardy C & Gage FH. (2016). Evaluating cell reprogramming, differentiation and conversion technologies in neuroscience. *Nat Rev Neurosci* **17,** 424-437.

Mertens J, Paquola ACM, Ku M, Hatch E, Bohnke L, Ladjevardi S, McGrath S, Campbell B, Lee H, Herdy JR, Goncalves JT, Toda T, Kim Y, Winkler J, Yao J, Hetzer MW & Gage FH. (2015). Directly Reprogrammed Human Neurons Retain Aging-Associated Transcriptomic Signatures and Reveal Age-Related Nucleocytoplasmic Defects. *Cell Stem Cell* **17,** 705-718.

Meyer-Franke A, Kaplan MR, Pfrieger FW & Barres BA. (1995). Characterization of the signaling interactions that promote the survival and growth of developing retinal ganglion cells in culture. *Neuron* **15,** 805-819.

Middeldorp J & Hol EM. (2011). GFAP in health and disease. *Prog Neurobiol* **93,** 421-443.

Mignatti P, Morimoto T & Rifkin DB. (1992). Basic fibroblast growth factor, a protein devoid of secretory signal sequence, is released by cells via a pathway independent of the endoplasmic reticulum-Golgi complex. *J Cell Physiol* **151,** 81-93.

Mills CD, Kincaid K, Alt JM, Heilman MJ & Hill AM. (2000). M-1/M-2 macrophages and the Th1/Th2 paradigm. *J Immunol* **164,** 6166-6173.

Min H, Danilenko DM, Scully SA, Bolon B, Ring BD, Tarpley JE, DeRose M & Simonet WS. (1998). Fgf-10 is required for both limb and lung development and exhibits striking functional similarity to Drosophila branchless. *Genes Dev* **12,** 3156-3161.

Minelli A, Barbaresi P, Reimer RJ, Edwards RH & Conti F. (2001). The glial glutamate transporter GLT-1 is localized both in the vicinity of and at distance from axon terminals in the rat cerebral cortex. *Neuroscience* **108,** 51-59.

Mocchetti I & Wrathall JR. (1995). Neurotrophic factors in central nervous system trauma. *J Neurotrauma* **12,** 853-870.

Mojica FJM & Montoliu L. (2016). On the Origin of CRISPR-Cas Technology: From Prokaryotes to Mammals. *Trends Microbiol* **24,** 811-820.

Morizane A. (2019). [Cell therapy for Parkinson's disease with induced pluripotent stem cells]. *Rinsho Shinkeigaku* **59,** 119-124.

Morrison RS, Sharma A, de Vellis J & Bradshaw RA. (1986). Basic fibroblast growth factor supports the survival of cerebral cortical neurons in primary culture. *Proc Natl Acad Sci U S A* **83,** 7537-7541.

Mosser DM & Edwards JP. (2008). Exploring the full spectrum of macrophage activation. *Nat Rev Immunol* **8,** 958-969.

Mullett SJ & Hinkle DA. (2011). DJ-1 deficiency in astrocytes selectively enhances mitochondrial Complex I inhibitor-induced neurotoxicity. *J Neurochem* **117,** 375-387.

Murphy KR, Landau SM, Choudhury KR, Hostage CA, Shpanskaya KS, Sair HI, Petrella JR, Wong TZ & Doraiswamy PM. (2013). Mapping the effects of ApoE4, age and cognitive status on 18F-florbetapir PET measured regional cortical patterns of beta-amyloid density and growth. *Neuroimage* **78,** 474-480.

Murray PJ, Allen JE, Biswas SK, Fisher EA, Gilroy DW, Goerdt S, Gordon S, Hamilton JA, Ivashkiv LB, Lawrence T, Locati M, Mantovani A, Martinez FO, Mege JL, Mosser DM, Natoli G, Saeij JP, Schultze JL, Shirey KA, Sica A, Suttles J, Udalova I, van Ginderachter JA, Vogel SN & Wynn TA. (2014). Macrophage activation and polarization: nomenclature and experimental guidelines. *Immunity* **41,** 14-20.

Naj AC, Jun G, Beecham GW, Wang LS, Vardarajan BN, Buros J, Gallins PJ, Buxbaum JD, Jarvik GP, Crane PK, Larson EB, Bird TD, Boeve BF, Graff-Radford NR, De Jager PL, Evans D, Schneider JA, Carrasquillo MM, Ertekin-Taner N, Younkin SG, Cruchaga C, Kauwe JS, Nowotny P, Kramer P, Hardy J, Huentelman MJ, Myers AJ, Barmada MM, Demirci FY, Baldwin CT, Green RC, Rogaeva E, St George-Hyslop P, Arnold SE, Barber R, Beach T, Bigio EH, Bowen JD, Boxer A, Burke JR, Cairns NJ, Carlson CS, Carney RM, Carroll SL, Chui HC, Clark DG, Corneveaux J, Cotman CW, Cummings JL, DeCarli C, DeKosky ST, Diaz-Arrastia R, Dick M, Dickson DW, Ellis WG, Faber KM, Fallon KB, Farlow MR, Ferris S, Frosch MP, Galasko DR, Ganguli M, Gearing M, Geschwind DH, Ghetti B, Gilbert JR, Gilman S, Giordani B, Glass JD, Growdon JH, Hamilton RL, Harrell LE, Head E, Honig LS, Hulette CM, Hyman BT, Jicha GA, Jin LW, Johnson N, Karlawish J, Karydas A, Kaye JA, Kim R, Koo EH, Kowall NW, Lah JJ, Levey AI, Lieberman AP, Lopez OL, Mack WJ, Marson DC, Martiniuk F, Mash DC, Masliah E, McCormick WC, McCurry SM, McDavid AN, McKee AC, Mesulam M, Miller BL, Miller CA, Miller JW, Parisi JE, Perl DP, Peskind E, Petersen RC, Poon WW, Quinn JF, Rajbhandary RA, Raskind M, Reisberg B, Ringman JM, Roberson ED, Rosenberg RN, Sano M, Schneider LS, Seeley W, Shelanski ML, Slifer MA, Smith CD, Sonnen JA, Spina S, Stern RA, Tanzi RE, Trojanowski JQ, Troncoso JC, Van Deerlin VM, Vinters HV, Vonsattel JP, Weintraub S, Welsh-Bohmer KA, Williamson J, Woltjer RL, Cantwell LB, Dombroski BA, Beekly D, Lunetta KL, Martin ER, Kamboh MI, Saykin AJ, Reiman EM, Bennett DA, Morris JC, Montine TJ, Goate AM, Blacker D, Tsuang DW, Hakonarson H, Kukull WA, Foroud TM, Haines JL, Mayeux R, Pericak-Vance MA, Farrer LA & Schellenberg GD. (2011). Common variants at MS4A4/MS4A6E, CD2AP, CD33 and EPHA1 are associated with late-onset Alzheimer's disease. *Nat Genet* **43,** 436-441.

National Academies of Sciences EaM, Health and Medicine D, Board on Health Sciences P & Forum on Neurosciences and Nervous System D. (2017). The National Academies Collection: Reports funded by National Institutes of Health. In *Therapeutic Development in the Absence of Predictive Animal Models of Nervous System Disorders: Proceedings of a Workshop*. National Academies Press (US)

Copyright 2017 by the National Academy of Sciences. All rights reserved., Washington (DC).

Neumann M, Muller V, Gorner K, Kretzschmar HA, Haass C & Kahle PJ. (2004). Pathological properties of the Parkinson's disease-associated protein DJ-1 in alpha-synucleinopathies and tauopathies: relevance for multiple system atrophy and Pick's disease. *Acta Neuropathol* **107,** 489-496.

Nichols J, Zevnik B, Anastassiadis K, Niwa H, Klewe-Nebenius D, Chambers I, Scholer H & Smith A. (1998). Formation of pluripotent stem cells in the mammalian embryo depends on the POU transcription factor Oct4. *Cell* **95,** 379-391.

Nickerson DA, Taylor SL, Fullerton SM, Weiss KM, Clark AG, Stengard JH, Salomaa V, Boerwinkle E & Sing CF. (2000). Sequence diversity and large-scale typing of SNPs in the human apolipoprotein E gene. *Genome Res* **10,** 1532-1545.

Nicoleau C, Varela C, Bonnefond C, Maury Y, Bugi A, Aubry L, Viegas P, Bourgois-Rocha F, Peschanski M & Perrier AL. (2013). Embryonic stem cells neural differentiation qualifies the role of Wnt/beta-Catenin signals in human telencephalic specification and regionalization. *Stem Cells* **31,** 1763-1774.

Nicoletti F, Bockaert J, Collingridge GL, Conn PJ, Ferraguti F, Schoepp DD, Wroblewski JT & Pin JP. (2011). Metabotropic glutamate receptors: from the workbench to the bedside. *Neuropharmacology* **60,** 1017-1041.

Nieweg K, Schaller H & Pfrieger FW. (2009). Marked differences in cholesterol synthesis between neurons and glial cells from postnatal rats. *J Neurochem* **109,** 125-134.

Nilbratt M, Porras O, Marutle A, Hovatta O & Nordberg A. (2010). Neurotrophic factors promote cholinergic differentiation in human embryonic stem cell-derived neurons. *J Cell Mol Med* **14,** 1476-1484.

Nishitsuji K, Hosono T, Nakamura T, Bu G & Michikawa M. (2011). Apolipoprotein E regulates the integrity of tight junctions in an isoform-dependent manner in an in vitro blood-brain barrier model. *J Biol Chem* **286,** 17536-17542.

Nistor PA, May PW, Tamagnini F, Randall AD & Caldwell MA. (2015). Long-term culture of pluripotent stem-cell-derived human neurons on diamond--A substrate for neurodegeneration research and therapy. *Biomaterials* **61,** 139-149.

Nitkiewicz J, Borjabad A, Morgello S, Murray J, Chao W, Emdad L, Fisher PB, Potash MJ & Volsky DJ. (2017). HIV induces expression of complement component C3 in astrocytes by NF-kappaB-dependent activation of interleukin-6 synthesis. *J Neuroinflammation* **14,** 23.

Nolbrant S, Heuer A, Parmar M & Kirkeby A. (2017). Generation of high-purity human ventral midbrain dopaminergic progenitors for in vitro maturation and intracerebral transplantation. *Nat Protoc* **12,** 1962-1979.

Nortley R & Attwell D. (2017). Control of brain energy supply by astrocytes. *Curr Opin Neurobiol* **47,** 80-85.

Numakawa T, Nakajima S, Yamamoto N, Ooshima Y, Odaka H, Hashido K, Adachi N & Kunugi H. (2015). Basic fibroblast growth factor induces miR-134 upregulation in astrocyte for cell maturation. *Biochem Biophys Res Commun* **456,** 465-470.

Nyati KK, Masuda K, Zaman MM, Dubey PK, Millrine D, Chalise JP, Higa M, Li S, Standley DM, Saito K, Hanieh H & Kishimoto T. (2017). TLR4-induced NF-kappaB and MAPK signaling regulate the IL-6 mRNA stabilizing protein Arid5a. *Nucleic Acids Res* **45,** 2687-2703.

O'Neill E, Chiara Goisis R, Haverty R & Harkin A. (2019). L-alpha-aminoadipic acid restricts dopaminergic neurodegeneration and motor deficits in an inflammatory model of Parkinson's disease in male rats. *J Neurosci Res* **97,** 804-816.

Oberheim NA, Goldman SA & Nedergaard M. (2012). Heterogeneity of astrocytic form and function. *Methods Mol Biol* **814,** 23-45.

Oberheim NA, Takano T, Han X, He W, Lin JH, Wang F, Xu Q, Wyatt JD, Pilcher W, Ojemann JG, Ransom BR, Goldman SA & Nedergaard M. (2009). Uniquely hominid features of adult human astrocytes. *J Neurosci* **29,** 3276-3287.

Ohbayashi N, Shibayama M, Kurotaki Y, Imanishi M, Fujimori T, Itoh N & Takada S. (2002). FGF18 is required for normal cell proliferation and differentiation during osteogenesis and chondrogenesis. *Genes Dev* **16,** 870-879.

Ojala J, Alafuzoff I, Herukka SK, van Groen T, Tanila H & Pirttila T. (2009). Expression of interleukin-18 is increased in the brains of Alzheimer's disease patients. *Neurobiol Aging* **30,** 198-209.

Okada M, Fukuyama K, Kawano Y, Shiroyama T & Ueda Y. (2019). Memantine protects thalamocortical hyper-glutamatergic transmission induced by NMDA receptor antagonism via activation of system xc<sup/>. *Pharmacol Res Perspect* **7,** e00457.

Okada S, Nakamura M, Katoh H, Miyao T, Shimazaki T, Ishii K, Yamane J, Yoshimura A, Iwamoto Y, Toyama Y & Okano H. (2006). Conditional ablation of Stat3 or Socs3 discloses a dual role for reactive astrocytes after spinal cord injury. *Nat Med* **12,** 829-834.

Okita K, Matsumura Y, Sato Y, Okada A, Morizane A, Okamoto S, Hong H, Nakagawa M, Tanabe K, Tezuka K, Shibata T, Kunisada T, Takahashi M, Takahashi J, Saji H & Yamanaka S. (2011). A more efficient method to generate integration-free human iPS cells. *Nat Methods* **8,** 409-412.

Olivares D, Deshpande VK, Shi Y, Lahiri DK, Greig NH, Rogers JT & Huang X. (2012). N-methyl D-aspartate (NMDA) receptor antagonists and memantine treatment for Alzheimer's disease, vascular dementia and Parkinson's disease. *Curr Alzheimer Res* **9,** 746-758.

Olsen SK, Ibrahimi OA, Raucci A, Zhang F, Eliseenkova AV, Yayon A, Basilico C, Linhardt RJ, Schlessinger J & Mohammadi M. (2004). Insights into the molecular basis for fibroblast growth factor receptor autoinhibition and ligand-binding promiscuity. *Proc Natl Acad Sci U S A* **101,** 935-940.

Ornitz DM & Itoh N. (2001). Fibroblast growth factors. *Genome Biol* **2,** Reviews3005.

Osborn LM, Kamphuis W, Wadman WJ & Hol EM. (2016). Astrogliosis: An integral player in the pathogenesis of Alzheimer's disease. *Prog Neurobiol* **144,** 121-141.

Osera C, Pascale A, Amadio M, Venturini L, Govoni S & Ricevuti G. (2012). Pentraxins and Alzheimer's disease: at the interface between biomarkers and pharmacological targets. *Ageing Res Rev* **11,** 189-198.

Pajarillo E, Rizor A, Lee J, Aschner M & Lee E. (2019). The role of astrocytic glutamate transporters GLT-1 and GLAST in neurological disorders: Potential targets for neurotherapeutics. *Neuropharmacology* **161,** 107559.

Palm T, Bolognin S, Meiser J, Nickels S, Trager C, Meilenbrock RL, Brockhaus J, Schreitmuller M, Missler M & Schwamborn JC. (2015). Rapid and robust generation of long-term self-renewing human neural stem cells with the ability to generate mature astroglia. *Sci Rep* **5,** 16321.

Palop JJ & Mucke L. (2010). Amyloid-beta-induced neuronal dysfunction in Alzheimer's disease: from synapses toward neural networks. *Nat Neurosci* **13,** 812-818.

Panatier A, Vallee J, Haber M, Murai KK, Lacaille JC & Robitaille R. (2011). Astrocytes are endogenous regulators of basal transmission at central synapses. *Cell* **146,** 785-798.

Parajuli B, Sonobe Y, Kawanokuchi J, Doi Y, Noda M, Takeuchi H, Mizuno T & Suzumura A. (2012). GM-CSF increases LPS-induced production of proinflammatory mediators via upregulation of TLR4 and CD14 in murine microglia. *J Neuroinflammation* **9,** 268.

Park JY, Kim SK, Woo DH, Lee EJ, Kim JH & Lee SH. (2009). Differentiation of neural progenitor cells in a microfluidic chip-generated cytokine gradient. *Stem Cells* **27,** 2646-2654.

Parkin GM, Udawela M, Gibbons A & Dean B. (2018). Glutamate transporters, EAAT1 and EAAT2, are potentially important in the pathophysiology and treatment of schizophrenia and affective disorders. *World J Psychiatry* **8,** 51-63.

Parkinson J. (2002). An essay on the shaking palsy. 1817. *J Neuropsychiatry Clin Neurosci* **14,** 223-236; discussion 222.

Pathmajeyan MS, Patel SA, Carroll JA, Seib T, Striebel JF, Bridges RJ & Chesebro B. (2011). Increased excitatory amino acid transport into murine prion protein knockout astrocytes cultured in vitro. *Glia* **59,** 1684-1694.

Pauklin S & Vallier L. (2015). Activin/Nodal signalling in stem cells. *Development* **142,** 607-619.

Paulson OB & Newman EA. (1987). Does the release of potassium from astrocyte endfeet regulate cerebral blood flow? *Science* **237,** 896-898.

Pazos MR, Mohammed N, Lafuente H, Santos M, Martinez-Pinilla E, Moreno E, Valdizan E, Romero J, Pazos A, Franco R, Hillard CJ, Alvarez FJ & Martinez-Orgado J. (2013). Mechanisms of cannabidiol neuroprotection in hypoxic-ischemic newborn pigs: role of 5HT(1A) and CB2 receptors. *Neuropharmacology* **71,** 282-291.

Pekny M, Wilhelmsson U & Pekna M. (2014). The dual role of astrocyte activation and reactive gliosis. *Neurosci Lett* **565,** 30-38.

Penney J, Ralvenius WT & Tsai LH. (2020). Modeling Alzheimer's disease with iPSC-derived brain cells. *Mol Psychiatry* **25,** 148-167.

Perego C, Vanoni C, Bossi M, Massari S, Basudev H, Longhi R & Pietrini G. (2000). The GLT-1 and GLAST glutamate transporters are expressed on morphologically distinct astrocytes and regulated by neuronal activity in primary hippocampal cocultures. *J Neurochem* **75,** 1076-1084.

Perez-Nievas BG & Serrano-Pozo A. (2018). Deciphering the Astrocyte Reaction in Alzheimer's Disease. *Front Aging Neurosci* **10,** 114.

Petito CK, Chung MC, Verkhovsky LM & Cooper AJ. (1992). Brain glutamine synthetase increases following cerebral ischemia in the rat. *Brain Res* **569,** 275-280.

Petros TJ, Tyson JA & Anderson SA. (2011). Pluripotent stem cells for the study of CNS development. *Front Mol Neurosci* **4,** 30.

Petrosino S, Verde R, Vaia M, Allara M, Iuvone T & Di Marzo V. (2018). Anti-inflammatory Properties of Cannabidiol, a Nonpsychotropic Cannabinoid, in Experimental Allergic Contact Dermatitis. *J Pharmacol Exp Ther* **365,** 652-663.

Pflugfelder SC, Stern M, Zhang S & Shojaei A. (2017). LFA-1/ICAM-1 Interaction as a Therapeutic Target in Dry Eye Disease. *J Ocul Pharmacol Ther* **33,** 5-12.

Poirier J, Davignon J, Bouthillier D, Kogan S, Bertrand P & Gauthier S. (1993). Apolipoprotein E polymorphism and Alzheimer's disease. *Lancet* **342,** 697-699.

Poitry-Yamate CL, Vutskits L & Rauen T. (2002). Neuronal-induced and glutamate-dependent activation of glial glutamate transporter function. *J Neurochem* **82,** 987-997.

Polentarutti N, Bottazzi B, Di Santo E, Blasi E, Agnello D, Ghezzi P, Introna M, Bartfai T, Richards G & Mantovani A. (2000). Inducible expression of the long pentraxin PTX3 in the central nervous system. *J Neuroimmunol* **106,** 87-94.

Popoli M, Yan Z, McEwen BS & Sanacora G. (2011). The stressed synapse: the impact of stress and glucocorticoids on glutamate transmission. *Nat Rev Neurosci* **13,** 22-37.

Porter JT & McCarthy KD. (1996). Hippocampal astrocytes in situ respond to glutamate released from synaptic terminals. *J Neurosci* **16,** 5073-5081.

Prah J, Winters A, Chaudhari K, Hersh J, Liu R & Yang SH. (2019). A Novel Serum Free Primary Astrocyte Culture Method that Mimic Quiescent Astrocyte Phenotype. *J Neurosci Methods*.

Prat A, Biernacki K, Wosik K & Antel JP. (2001). Glial cell influence on the human blood-brain barrier. *Glia* **36,** 145-155.

Prendecki M, Kowalska M, Toton E & Kozubski W. (2020). Genetic Editing and Pharmacogenetics in Current And Future Therapy Of Neurocognitive Disorders. *Curr Alzheimer Res*.

Prokosch V, Brockhaus K, Anders F, Liu H, Mercieca K, Gericke A, Melkonyan H & Thanos S. (2019). Elevated intraocular pressure induces neuron-specific beta-III-tubulin expression in non-neuronal vascular cells. *Acta Ophthalmol*.

Purves-Tyson TD, Weber-Stadlbauer U, Richetto J, Rothmond DA, Labouesse MA, Polesel M, Robinson K, Shannon Weickert C & Meyer U. (2019). Increased levels of midbrain immune-related transcripts in schizophrenia and in murine offspring after maternal immune activation. *Mol Psychiatry*.

Qin N, Neeper MP, Liu Y, Hutchinson TL, Lubin ML & Flores CM. (2008). TRPV2 is activated by cannabidiol and mediates CGRP release in cultured rat dorsal root ganglion neurons. *J Neurosci* **28,** 6231-6238.

Rabchevsky AG, Weinitz JM, Coulpier M, Fages C, Tinel M & Junier MP. (1998). A role for transforming growth factor alpha as an inducer of astrogliosis. *J Neurosci* **18,** 10541-10552.

Raffai RL, Dong LM, Farese RV, Jr. & Weisgraber KH. (2001). Introduction of human apolipoprotein E4 "domain interaction" into mouse apolipoprotein E. *Proc Natl Acad Sci U S A* **98,** 11587-11591.

Raffioni S, Thomas D, Foehr ED, Thompson LM & Bradshaw RA. (1999). Comparison of the intracellular signaling responses by three chimeric fibroblast growth factor receptors in PC12 cells. *Proc Natl Acad Sci U S A* **96,** 7178-7183.

Rahimi F, Hsu K, Endoh Y & Geczy CL. (2005). FGF-2, IL-1beta and TGF-beta regulate fibroblast expression of S100A8. *Febs j* **272,** 2811-2827.

Rai KS, Hattiangady B & Shetty AK. (2007). Enhanced production and dendritic growth of new dentate granule cells in the middle-aged hippocampus following intracerebroventricular FGF-2 infusions. *Eur J Neurosci* **26,** 1765-1779.

Raja WK, Mungenast AE, Lin YT, Ko T, Abdurrob F, Seo J & Tsai LH. (2016). Self-Organizing 3D Human Neural Tissue Derived from Induced Pluripotent Stem Cells Recapitulate Alzheimer's Disease Phenotypes. *PLoS One* **11,** e0161969.

Rajkovic I, Denes A, Allan SM & Pinteaux E. (2016). Emerging roles of the acute phase protein pentraxin-3 during central nervous system disorders. *J Neuroimmunol* **292,** 27-33.

Ramakers GM & Storm JF. (2002). A postsynaptic transient K+ current modulated by arachidonic acid regulates synaptic integration and threshold for LTP induction in hippocampal pyramidal cells. *Proceedings of the National Academy of Sciences* **99,** 10144-10149.

Ramsauer M, Krause D & Dermietzel R. (2002). Angiogenesis of the blood-brain barrier in vitro and the function of cerebral pericytes. *Faseb j* **16,** 1274-1276.

Raponi E, Agenes F, Delphin C, Assard N, Baudier J, Legraverend C & Deloulme JC. (2007). S100B expression defines a state in which GFAP-expressing cells lose their neural stem cell potential and acquire a more mature developmental stage. *Glia* **55,** 165-177.

Rapoport SI. (2008). Arachidonic acid and the brain. *J Nutr* **138,** 2515-2520.

Reale M, Kamal MA, Velluto L, Gambi D, Di Nicola M & Greig NH. (2012). Relationship between inflammatory mediators, Abeta levels and ApoE genotype in Alzheimer disease. *Curr Alzheimer Res* **9,** 447-457.

Reed-Geaghan EG, Savage JC, Hise AG & Landreth GE. (2009). CD14 and toll-like receptors 2 and 4 are required for fibrillar A{beta}-stimulated microglial activation. *J Neurosci* **29,** 11982-11992.

Reilly JF & Kumari VG. (1996). Alterations in fibroblast growth factor receptor expression following brain injury. *Exp Neurol* **140,** 139-150.

Reuss B & von Bohlen und Halbach O. (2003). Fibroblast growth factors and their receptors in the central nervous system. *Cell Tissue Res* **313,** 139-157.

Richard KL, Filali M, Préfontaine P & Rivest S. (2008). Toll-like receptor 2 acts as a natural innate immune receptor to clear amyloid beta 1-42 and delay the cognitive decline in a mouse model of Alzheimer's disease. *J Neurosci* **28,** 5784-5793.

Ricklin D, Reis ES, Mastellos DC, Gros P & Lambris JD. (2016). Complement component C3 - The "Swiss Army Knife" of innate immunity and host defense. *Immunol Rev* **274,** 33-58.

Rinaldi F & Caldwell MA. (2013). Modeling astrocytic contribution toward neurodegeneration with pluripotent stem cells: focus on Alzheimer's and Parkinson's diseases. *Neuroreport* **24,** 1053-1057.

Rius-Perez S, Tormos AM, Perez S & Talens-Visconti R. (2018). Vascular pathology: Cause or effect in Alzheimer disease? *Neurologia* **33,** 112-120.

Roberts RC, Roche JK & McCullumsmith RE. (2014). Localization of excitatory amino acid transporters EAAT1 and EAAT2 in human postmortem cortex: a light and electron microscopic study. *Neuroscience* **277,** 522-540.

Rodriguez-Grande B, Swana M, Nguyen L, Englezou P, Maysami S, Allan SM, Rothwell NJ, Garlanda C, Denes A & Pinteaux E. (2014). The acute-phase protein PTX3 is an essential mediator of glial scar formation and resolution of brain edema after ischemic injury. *J Cereb Blood Flow Metab* **34,** 480-488.

Rohani L, Johnson AA, Arnold A & Stolzing A. (2014). The aging signature: a hallmark of induced pluripotent stem cells? *Aging Cell* **13,** 2-7.

Romanos J, Benke D, Saab AS, Zeilhofer HU & Santello M. (2019). Differences in glutamate uptake between cortical regions impact neuronal NMDA receptor activation. *Commun Biol* **2,** 127.

Romera C, Hurtado O, Botella SH, Lizasoain I, Cárdenas A, Fernández-Tomé P, Leza JC, Lorenzo P & Moro MA. (2004). In vitro ischemic tolerance involves upregulation of glutamate transport partly mediated by the TACE/ADAM17-tumor necrosis factor-α pathway. *Journal of Neuroscience* **24,** 1350-1357.

Ronca R, Giacomini A, Di Salle E, Coltrini D, Pagano K, Ragona L, Matarazzo S, Rezzola S, Maiolo D, Torrella R, Moroni E, Mazzieri R, Escobar G, Mor M, Colombo G & Presta M. (2015). Long-Pentraxin 3 Derivative as a Small-Molecule FGF Trap for Cancer Therapy. *Cancer Cell* **28,** 225-239.

Rossi D, Brambilla L, Valori CF, Roncoroni C, Crugnola A, Yokota T, Bredesen DE & Volterra A. (2008). Focal degeneration of astrocytes in amyotrophic lateral sclerosis. *Cell Death Differ* **15,** 1691-1700.

Rothaug M, Becker-Pauly C & Rose-John S. (2016). The role of interleukin-6 signaling in nervous tissue. *Biochim Biophys Acta* **1863,** 1218-1227.

Rothstein JD, Martin L, Levey AI, Dykes-Hoberg M, Jin L, Wu D, Nash N & Kuncl RW. (1994). Localization of neuronal and glial glutamate transporters. *Neuron* **13,** 713-725.

Rothstein JD, Van Kammen M, Levey AI, Martin LJ & Kuncl RW. (1995). Selective loss of glial glutamate transporter GLT-1 in amyotrophic lateral sclerosis. *Ann Neurol* **38,** 73-84.

Rovere P, Peri G, Fazzini F, Bottazzi B, Doni A, Bondanza A, Zimmermann VS, Garlanda C, Fascio U, Sabbadini MG, Rugarli C, Mantovani A & Manfredi AA. (2000). The long pentraxin PTX3 binds to apoptotic cells and regulates their clearance by antigen-presenting dendritic cells. *Blood* **96,** 4300-4306.

Roybon L, Lamas NJ, Garcia-Diaz A, Yang EJ, Sattler R, Jackson-Lewis V, Kim YA, Kachel CA, Rothstein JD, Przedborski S, Wichterle H & Henderson CE. (2013). Human stem cell-derived spinal cord astrocytes with defined mature or reactive phenotypes. *Cell Rep* **4,** 1035-1048.

Ruiz J, Kouiavskaia D, Migliorini M, Robinson S, Saenko EL, Gorlatova N, Li D, Lawrence D, Hyman BT, Weisgraber KH & Strickland DK. (2005). The apoE isoform binding properties of the VLDL receptor reveal marked differences from LRP and the LDL receptor. *J Lipid Res* **46,** 1721-1731.

Russo E & Guy GW. (2006). A tale of two cannabinoids: the therapeutic rationale for combining tetrahydrocannabinol and cannabidiol. *Med Hypotheses* **66,** 234-246.

Saito H, Dhanasekaran P, Nguyen D, Baldwin F, Weisgraber KH, Wehrli S, Phillips MC & Lund-Katz S. (2003). Characterization of the heparin binding sites in human apolipoprotein E. *J Biol Chem* **278,** 14782-14787.

Sanal MG. (2011). Future of liver transplantation: non-human primates for patient-specific organs from induced pluripotent stem cells. *World J Gastroenterol* **17,** 3684-3690.

Sanfilippo C, Longo A, Lazzara F, Cambria D, Distefano G, Palumbo M, Cantarella A, Malaguarnera L & Di Rosa M. (2017). CHI3L1 and CHI3L2 overexpression in motor cortex and spinal cord of sALS patients. *Mol Cell Neurosci* **85,** 162-169.

Santos R, Vadodaria KC, Jaeger BN, Mei A, Lefcochilos-Fogelquist S, Mendes APD, Erikson G, Shokhirev M, Randolph-Moore L, Fredlender C, Dave S, Oefner R, Fitzpatrick C, Pena M, Barron JJ, Ku M, Denli AM, Kerman BE, Charnay P, Kelsoe JR, Marchetto MC & Gage FH. (2017). Differentiation of Inflammation-Responsive Astrocytes from Glial Progenitors Generated from Human Induced Pluripotent Stem Cells. *Stem Cell Reports* **8,** 1757-1769.

Satoh J, Tabunoki H, Ishida T, Saito Y & Arima K. (2013). Accumulation of a repulsive axonal guidance molecule RGMa in amyloid plaques: a possible hallmark of regenerative failure in Alzheimer's disease brains. *Neuropathol Appl Neurobiol* **39,** 109-120.

Savchenko E, Teku GN, Boza-Serrano A, Russ K, Berns M, Deierborg T, Lamas NJ, Wichterle H, Rothstein J, Henderson CE, Vihinen M & Roybon L. (2019). FGF family members differentially regulate maturation and proliferation of stem cell-derived astrocytes. *Sci Rep* **9,** 9610.

Schallier A, Smolders I, Van Dam D, Loyens E, De Deyn PP, Michotte A, Michotte Y & Massie A. (2011). Region- and age-specific changes in glutamate transport in the AbetaPP23 mouse model for Alzheimer's disease. *J Alzheimers Dis* **24,** 287-300.

Scheller J, Chalaris A, Schmidt-Arras D & Rose-John S. (2011). The pro- and anti-inflammatory properties of the cytokine interleukin-6. *Biochim Biophys Acta* **1813,** 878-888.

Schlag BD, Vondrasek JR, Munir M, Kalandadze A, Zelenaia OA, Rothstein JD & Robinson MB. (1998). Regulation of the glial Na+-dependent glutamate transporters by cyclic AMP analogs and neurons. *Mol Pharmacol* **53,** 355-369.

Schmitt A, Asan E, Puschel B & Kugler P. (1997). Cellular and regional distribution of the glutamate transporter GLAST in the CNS of rats: nonradioactive in situ hybridization and comparative immunocytochemistry. *J Neurosci* **17,** 1-10.

Schubert D, Kepchia D, Liang Z, Dargusch R, Goldberg J & Maher P. (2019). Efficacy of Cannabinoids in a Pre-Clinical Drug-Screening Platform for Alzheimer's Disease. *Mol Neurobiol* **56,** 7719-7730.

Serio A, Bilican B, Barmada SJ, Ando DM, Zhao C, Siller R, Burr K, Haghi G, Story D, Nishimura AL, Carrasco MA, Phatnani HP, Shum C, Wilmut I, Maniatis T, Shaw CE, Finkbeiner S & Chandran S. (2013). Astrocyte pathology and the absence of non-cell autonomy in an induced pluripotent stem cell model of TDP-43 proteinopathy. *Proc Natl Acad Sci U S A* **110,** 4697-4702.

Serrano-Pozo A, Gomez-Isla T, Growdon JH, Frosch MP & Hyman BT. (2013). A phenotypic change but not proliferation underlies glial responses in Alzheimer disease. *Am J Pathol* **182,** 2332-2344.

Serrano-Pozo A, Qian J, Monsell SE, Betensky RA & Hyman BT. (2015). APOEepsilon2 is associated with milder clinical and pathological Alzheimer disease. *Ann Neurol* **77,** 917-929.

Shaltouki A, Peng J, Liu Q, Rao MS & Zeng X. (2013). Efficient generation of astrocytes from human pluripotent stem cells in defined conditions. *Stem Cells* **31,** 941-952.

Shan D, Lucas EK, Drummond JB, Haroutunian V, Meador-Woodruff JH & McCullumsmith RE. (2013). Abnormal expression of glutamate transporters in temporal lobe areas in elderly patients with schizophrenia. *Schizophr Res* **144,** 1-8.

Sharma M, Fitzpatrick AL, Arnold AM, Chi G, Lopez OL, Jenny NS & DeKosky ST. (2016). Inflammatory Biomarkers and Cognitive Decline: The Ginkgo Evaluation of Memory Study. *J Am Geriatr Soc* **64,** 1171-1177.

Shen T, Pu J, Zheng T & Zhang B. (2015). Induced neural stem/precursor cells for fundamental studies and potential application in neurodegenerative diseases. *Neurosci Bull* **31,** 589-600.

Sheng JG, Bora SH, Xu G, Borchelt DR, Price DL & Koliatsos VE. (2003). Lipopolysaccharide-induced-neuroinflammation increases intracellular accumulation of amyloid precursor protein and amyloid β peptide in APPswe transgenic mice. *Neurobiology of disease* **14,** 133-145.

Shi G & Jin Y. (2010). Role of Oct4 in maintaining and regaining stem cell pluripotency. *Stem Cell Res Ther* **1,** 39.

Shi Q, Chowdhury S, Ma R, Le KX, Hong S, Caldarone BJ, Stevens B & Lemere CA. (2017a). Complement C3 deficiency protects against neurodegeneration in aged plaque-rich APP/PS1 mice. *Sci Transl Med* **9**.

Shi Y, Kirwan P & Livesey FJ. (2012). Directed differentiation of human pluripotent stem cells to cerebral cortex neurons and neural networks. *Nat Protoc* **7,** 1836-1846.

Shi Y, Yamada K, Liddelow SA, Smith ST, Zhao L, Luo W, Tsai RM, Spina S, Grinberg LT & Rojas JC. (2017b). ApoE4 markedly exacerbates tau-mediated neurodegeneration in a mouse model of tauopathy. *Nature* **549,** 523.

Shi Y, Yamada K, Liddelow SA, Smith ST, Zhao L, Luo W, Tsai RM, Spina S, Grinberg LT, Rojas JC, Gallardo G, Wang K, Roh J, Robinson G, Finn MB, Jiang H, Sullivan PM, Baufeld C, Wood MW, Sutphen C, McCue L, Xiong C, Del-Aguila JL, Morris JC, Cruchaga C, Fagan AM, Miller BL, Boxer AL, Seeley WW, Butovsky O, Barres BA, Paul SM & Holtzman DM. (2017c). ApoE4 markedly exacerbates tau-mediated neurodegeneration in a mouse model of tauopathy. *Nature* **549,** 523-527.

Shi YJ, Shi M, Xiao LJ, Li L, Zou LH, Li CY, Zhang QJ, Zhou LF, Ji XC, Huang H, Xi Y, Liu L, Zhang HY, Zhao G & Ma L. (2018). Inhibitive Effects of FGF2/FGFR1 Pathway on Astrocyte-Mediated Inflammation in vivo and in vitro After Infrasound Exposure. *Front Neurosci* **12,** 582.

Shibata K, Sato K, Shirai R, Seki T, Okano T, Yamashita T, Koide A, Mitsuboshi M, Mori Y, Hirano T & Watanabe T. (2020). Lipocalin-2 exerts pro-atherosclerotic effects as evidenced by in vitro and in vivo experiments. *Heart Vessels*.

Shibata T, Yamada K, Watanabe M, Ikenaka K, Wada K, Tanaka K & Inoue Y. (1997). Glutamate transporter GLAST is expressed in the radial glia-astrocyte lineage of developing mouse spinal cord. *J Neurosci* **17,** 9212-9219.

Shigeri Y, Seal RP & Shimamoto K. (2004). Molecular pharmacology of glutamate transporters, EAATs and VGLUTs. *Brain Research Reviews* **45,** 250-265.

Shigetomi E, Saito K, Sano F & Koizumi S. (2019). Aberrant Calcium Signals in Reactive Astrocytes: A Key Process in Neurological Disorders. *Int J Mol Sci* **20**.

Shin JY, Fang ZH, Yu ZX, Wang CE, Li SH & Li XJ. (2005). Expression of mutant huntingtin in glial cells contributes to neuronal excitotoxicity. *J Cell Biol* **171,** 1001-1012.

Shohami E, Cohen-Yeshurun A, Magid L, Algali M & Mechoulam R. (2011). Endocannabinoids and traumatic brain injury. *Br J Pharmacol* **163,** 1402-1410.

Shrikant P, Chung IY, Ballestas ME & Benveniste EN. (1994). Regulation of intercellular adhesion molecule-1 gene expression by tumor necrosis factor-alpha, interleukin-1 beta, and interferon-gamma in astrocytes. *J Neuroimmunol* **51,** 209-220.

Sibson NR, Dhankhar A, Mason GF, Rothman DL, Behar KL & Shulman RG. (1998). Stoichiometric coupling of brain glucose metabolism and glutamatergic neuronal activity. *Proc Natl Acad Sci U S A* **95,** 316-321.

Simonovitch S, Schmukler E, Bespalko A, Iram T, Frenkel D, Holtzman DM, Masliah E, Michaelson DM & Pinkas-Kramarski R. (2016). Impaired Autophagy in APOE4 Astrocytes. *J Alzheimers Dis* **51,** 915-927.

Singh S, Swarnkar S, Goswami P & Nath C. (2011). Astrocytes and microglia: responses to neuropathological conditions. *Int J Neurosci* **121,** 589-597.

Singh VK, Kalsan M, Kumar N, Saini A & Chandra R. (2015). Induced pluripotent stem cells: applications in regenerative medicine, disease modeling, and drug discovery. *Front Cell Dev Biol* **3,** 2.

Singhal G, Jaehne EJ, Corrigan F, Toben C & Baune BT. (2014). Inflammasomes in neuroinflammation and changes in brain function: a focused review. *Front Neurosci* **8,** 315.

Skelly DT, Hennessy E, Dansereau MA & Cunningham C. (2013). A systematic analysis of the peripheral and CNS effects of systemic LPS, IL-1beta, [corrected] TNF-alpha and IL-6 challenges in C57BL/6 mice. *PLoS One* **8,** e69123.

Sofroniew MV & Vinters HV. (2010). Astrocytes: biology and pathology. *Acta Neuropathol* **119,** 7-35.

Sorensen TL, Trebst C, Kivisakk P, Klaege KL, Majmudar A, Ravid R, Lassmann H, Olsen DB, Strieter RM, Ransohoff RM & Sellebjerg F. (2002). Multiple sclerosis: a study of CXCL10 and CXCR3 co-localization in the inflamed central nervous system. *J Neuroimmunol* **127,** 59-68.

Spangaro M, Bosia M, Zanoletti A, Bechi M, Mariachiara B, Pirovano A, Lorenzi C, Bramanti P, Smeraldi E & Cavallaro R. (2014). Exploring effects of EAAT polymorphisms on cognitive functions in schizophrenia. *Pharmacogenomics* **15,** 925-932.

Spencer S & Kalivas PW. (2017). Glutamate Transport: A New Bench to Bedside Mechanism for Treating Drug Abuse. *Int J Neuropsychopharmacol* **20,** 797-812.

Sriram K, Benkovic SA, Hebert MA, Miller DB & O'Callaghan JP. (2004). Induction of gp130-related cytokines and activation of JAK2/STAT3 pathway in astrocytes precedes up-regulation of glial fibrillary acidic protein in the 1-methyl-4-phenyl-1,2,3,6-tetrahydropyridine model of neurodegeneration: key signaling pathway for astrogliosis in vivo? *J Biol Chem* **279,** 19936-19947.

Stahel M, Becker M, Graf N & Michels S. (2016). SYSTEMIC INTERLEUKIN 1beta INHIBITION IN PROLIFERATIVE DIABETIC RETINOPATHY: A Prospective Open-Label Study Using Canakinumab. *Retina* **36,** 385-391.

Stranahan AM & Mattson MP. (2010). Selective vulnerability of neurons in layer II of the entorhinal cortex during aging and Alzheimer's disease. *Neural Plast* **2010,** 108190.

Strittmatter WJ, Saunders AM, Goedert M, Weisgraber KH, Dong LM, Jakes R, Huang DY, Pericak-Vance M, Schmechel D & Roses AD. (1994). Isoform-specific interactions of apolipoprotein E with microtubule-associated protein tau: implications for Alzheimer disease. *Proc Natl Acad Sci U S A* **91,** 11183-11186.

Strittmatter WJ, Saunders AM, Schmechel D, Pericak-Vance M, Enghild J, Salvesen GS & Roses AD. (1993). Apolipoprotein E: high-avidity binding to beta-amyloid and increased frequency of type 4 allele in late-onset familial Alzheimer disease. *Proc Natl Acad Sci U S A* **90,** 1977-1981.

Sun D & Jakobs TC. (2012). Structural remodeling of astrocytes in the injured CNS. *Neuroscientist* **18,** 567-588.

Sun X, Meyers EN, Lewandoski M & Martin GR. (1999). Targeted disruption of Fgf8 causes failure of cell migration in the gastrulating mouse embryo. *Genes Dev* **13,** 1834-1846.

Sunil VR, Patel KJ, Nilsen-Hamilton M, Heck DE, Laskin JD & Laskin DL. (2007). Acute endotoxemia is associated with upregulation of lipocalin 24p3/Lcn2 in lung and liver. *Exp Mol Pathol* **83,** 177-187.

Sutherland D, Samakovlis C & Krasnow MA. (1996). branchless encodes a Drosophila FGF homolog that controls tracheal cell migration and the pattern of branching. *Cell* **87,** 1091-1101.

Swanson RA, Liu J, Miller JW, Rothstein JD, Farrell K, Stein BA & Longuemare MC. (1997). Neuronal regulation of glutamate transporter subtype expression in astrocytes. *J Neurosci* **17,** 932-940.

Szekely CA, Breitner JC, Fitzpatrick AL, Rea TD, Psaty BM, Kuller LH & Zandi PP. (2008). NSAID use and dementia risk in the Cardiovascular Health Study: role of APOE and NSAID type. *Neurology* **70,** 17-24.

Tada T, Ito J, Asai M & Yokoyama S. (2004). Fibroblast growth factor 1 is produced prior to apolipoprotein E in the astrocytes after cryo-injury of mouse brain. *Neurochem Int* **45,** 23-30.

Tai LM, Ghura S, Koster KP, Liakaite V, Maienschein-Cline M, Kanabar P, Collins N, Ben-Aissa M, Lei AZ, Bahroos N, Green SJ, Hendrickson B, Van Eldik LJ & LaDu MJ. (2015). APOE-modulated Abeta-induced neuroinflammation in Alzheimer's disease: current landscape, novel data, and future perspective. *J Neurochem* **133,** 465-488.

Takahashi K, Tanabe K, Ohnuki M, Narita M, Ichisaka T, Tomoda K & Yamanaka S. (2007). Induction of pluripotent stem cells from adult human fibroblasts by defined factors. *Cell* **131,** 861-872.

Takahashi K & Yamanaka S. (2006). Induction of pluripotent stem cells from mouse embryonic and adult fibroblast cultures by defined factors. *Cell* **126,** 663-676.

Takaki J, Fujimori K, Miura M, Suzuki T, Sekino Y & Sato K. (2012). L-glutamate released from activated microglia downregulates astrocytic L-glutamate transporter expression in neuroinflammation: the 'collusion'hypothesis for increased

extracellular L-glutamate concentration in neuroinflammation. *Journal of neuroinflammation* **9,** 275.

Takeuchi H, Jin S, Wang J, Zhang G, Kawanokuchi J, Kuno R, Sonobe Y, Mizuno T & Suzumura A. (2006). Tumor necrosis factor-alpha induces neurotoxicity via glutamate release from hemichannels of activated microglia in an autocrine manner. *J Biol Chem* **281,** 21362-21368.

Talantova M, Sanz-Blasco S, Zhang X, Xia P, Akhtar MW, Okamoto S, Dziewczapolski G, Nakamura T, Cao G, Pratt AE, Kang YJ, Tu S, Molokanova E, McKercher SR, Hires SA, Sason H, Stouffer DG, Buczynski MW, Solomon JP, Michael S, Powers ET, Kelly JW, Roberts A, Tong G, Fang-Newmeyer T, Parker J, Holland EA, Zhang D, Nakanishi N, Chen HS, Wolosker H, Wang Y, Parsons LH, Ambasudhan R, Masliah E, Heinemann SF, Pina-Crespo JC & Lipton SA. (2013). Abeta induces astrocytic glutamate release, extrasynaptic NMDA receptor activation, and synaptic loss. *Proc Natl Acad Sci U S A* **110,** E2518-2527.

Tallima H & El Ridi R. (2018). Arachidonic acid: Physiological roles and potential health benefits - A review. *J Adv Res* **11,** 33-41.

Tampellini D. (2015). Synaptic activity and Alzheimer's disease: a critical update. *Front Neurosci* **9,** 423.

Tang MM, Lin WJ, Pan YQ & Li YC. (2018). Fibroblast Growth Factor 2 Modulates Hippocampal Microglia Activation in a Neuroinflammation Induced Model of Depression. *Front Cell Neurosci* **12,** 255.

Tang P, Chong L, Li X, Liu Y, Liu P, Hou C & Li R. (2014). Correlation between serum RANTES levels and the severity of Parkinson's disease. *Oxid Med Cell Longev* **2014,** 208408.

Tarassishin L, Suh HS & Lee SC. (2014). LPS and IL-1 differentially activate mouse and human astrocytes: role of CD14. *Glia* **62,** 999-1013.

Tarkowski E, Wallin A, Regland B, Blennow K & Tarkowski A. (2001). Local and systemic GM-CSF increase in Alzheimer's disease and vascular dementia. *Acta Neurol Scand* **103,** 166-174.

Tchieu J, Calder EL, Guttikonda SR, Gutzwiller EM, Aromolaran KA, Steinbeck JA, Goldstein PA & Studer L. (2019). NFIA is a gliogenic switch enabling rapid derivation of functional human astrocytes from pluripotent stem cells. *Nat Biotechnol* **37,** 267-275.

Tcw J, Liang SA, Qian L, Pipalia NH, Chao MJ, Shi Y, Bertelsen SE, Kapoor M, Marcora E, Sikora E, Holtzman DM, Maxfield FR, Zhang B, Wang M, Poon WW & Goate AM.

Teh DBL, Prasad A, Jiang W, Ariffin MZ, Khanna S, Belorkar A, Wong L, Liu X & All AH. (2017). Transcriptome Analysis Reveals Neuroprotective aspects of Human Reactive Astrocytes induced by Interleukin 1beta. *Sci Rep* **7,** 13988.

Teismann P & Schulz JB. (2004). Cellular pathology of Parkinson's disease: astrocytes, microglia and inflammation. *Cell Tissue Res* **318,** 149-161.

Temporin K, Tanaka H, Kuroda Y, Okada K, Yachi K, Moritomo H, Murase T & Yoshikawa H. (2008). Interleukin-1 beta promotes sensory nerve regeneration after sciatic nerve injury. *Neurosci Lett* **440,** 130-133.

Thal DR, Papassotiropoulos A, Saido TC, Griffin WS, Mrak RE, Kolsch H, Del Tredici K, Attems J & Ghebremedhin E. (2010). Capillary cerebral amyloid angiopathy identifies a distinct APOE epsilon4-associated subtype of sporadic Alzheimer's disease. *Acta Neuropathol* **120,** 169-183.

Theendakara V, Peters-Libeu CA, Bredesen DE & Rao RV. (2018). Transcriptional Effects of ApoE4: Relevance to Alzheimer's Disease. *Mol Neurobiol* **55,** 5243-5254.

Theendakara V, Peters-Libeu CA, Spilman P, Poksay KS, Bredesen DE & Rao RV. (2016). Direct Transcriptional Effects of Apolipoprotein E. *J Neurosci* **36,** 685-700.

Tian E, Sun G, Chao J, Ye P, Warden C, Riggs AD & Shi Y. (2016). Small-Molecule-Based Lineage Reprogramming Creates Functional Astrocytes. *Cell Rep* **16,** 781-792.

Tian G, Kong Q, Lai L, Ray-Chaudhury A & Lin CL. (2010). Increased expression of cholesterol 24S-hydroxylase results in disruption of glial glutamate transporter EAAT2 association with lipid rafts: a potential role in Alzheimer's disease. *J Neurochem* **113,** 978-989.

Tokami H, Ago T, Sugimori H, Kuroda J, Awano H, Suzuki K, Kiyohara Y, Kamouchi M & Kitazono T. (2013). RANTES has a potential to play a neuroprotective role in an autocrine/paracrine manner after ischemic stroke. *Brain Res* **1517,** 122-132.

Tokuda T, Calero M, Matsubara E, Vidal R, Kumar A, Permanne B, Zlokovic B, Smith JD, Ladu MJ, Rostagno A, Frangione B & Ghiso J. (2000). Lipidation of apolipoprotein E influences its isoform-specific interaction with Alzheimer's amyloid beta peptides. *Biochem J* **348 Pt 2,** 359-365.

Tolosa L, Caraballo-Miralles V, Olmos G & Llado J. (2011). TNF-alpha potentiates glutamate-induced spinal cord motoneuron death via NF-kappaB. *Mol Cell Neurosci* **46,** 176-186.

Tong J, Ang LC, Williams B, Furukawa Y, Fitzmaurice P, Guttman M, Boileau I, Hornykiewicz O & Kish SJ. (2015). Low levels of astroglial markers in Parkinson's disease: relationship to alpha-synuclein accumulation. *Neurobiol Dis* **82,** 243-253.

Tong J, Borbat PP, Freed JH & Shin YK. (2009). A scissors mechanism for stimulation of SNARE-mediated lipid mixing by cholesterol. *Proc Natl Acad Sci U S A* **106,** 5141-5146.

Tornero D, Wattananit S, Gronning Madsen M, Koch P, Wood J, Tatarishvili J, Mine Y, Ge R, Monni E, Devaraju K, Hevner RF, Brustle O, Lindvall O & Kokaia Z. (2013). Human induced pluripotent stem cell-derived cortical neurons integrate in stroke-injured cortex and improve functional recovery. *Brain* **136,** 3561-3577.

Torrez VR, Zimmer ER, Kalinine E, Haas CB, Zenki KC, Muller AP, Souza DO & Portela LV. (2019). Memantine mediates astrocytic activity in response to excitotoxicity induced by PP2A inhibition. *Neurosci Lett* **696,** 179-183.

Trepanier MO, Hopperton KE, Mizrahi R, Mechawar N & Bazinet RP. (2016). Postmortem evidence of cerebral inflammation in schizophrenia: a systematic review. *Mol Psychiatry* **21,** 1009-1026.

Trias E, Barbeito L & Yamanaka K. (2018). Phenotypic heterogeneity of astrocytes in motor neuron disease. *Clin Exp Neuroimmunol* **9,** 225-234.

Trindade P, Loiola EC, Gasparotto J, Ribeiro CT, Cardozo PL, Devalle S, Salerno JA, Ornelas IM, Ledur PF, Ribeiro FM, Ventura ALM, Moreira JCF, Gelain DP, Porciuncula LO & Rehen SK. (2020). Short and long TNF-alpha exposure recapitulates canonical astrogliosis events in human-induced pluripotent stem cells-derived astrocytes. *Glia*.

Trotti D, Rizzini BL, Rossi D, Haugeto O, Racagni G, Danbolt NC & Volterra A. (1997). Neuronal and glial glutamate transporters possess an SH-based redox regulatory mechanism. *European Journal of Neuroscience* **9,** 1236-1243.

Tsui-Pierchala BA, Encinas M, Milbrandt J & Johnson EM, Jr. (2002). Lipid rafts in neuronal signaling and function. *Trends Neurosci* **25,** 412-417.

Turner CA, Watson SJ & Akil H. (2012). The fibroblast growth factor family: neuromodulation of affective behavior. *Neuron* **76,** 160-174.

Turowski P, Adamson P & Greenwood J. (2005). Pharmacological targeting of ICAM-1 signaling in brain endothelial cells: potential for treating neuroinflammation. *Cell Mol Neurobiol* **25,** 153-170.

Tyzack G, Lakatos A & Patani R. (2016). Human Stem Cell-Derived Astrocytes: Specification and Relevance for Neurological Disorders. *Curr Stem Cell Rep* **2,** 236-247.

Tyzack GE, Hall CE, Sibley CR, Cymes T, Forostyak S, Carlino G, Meyer IF, Schiavo G, Zhang SC, Gibbons GM, Newcombe J, Patani R & Lakatos A. (2017). A neuroprotective astrocyte state is induced by neuronal signal EphB1 but fails in ALS models. *Nat Commun* **8,** 1164.

Udan ML, Ajit D, Crouse NR & Nichols MR. (2008). Toll-like receptors 2 and 4 mediate Abeta(1-42) activation of the innate immune response in a human monocytic cell line. *J Neurochem* **104,** 524-533.

Underhill SM, Wheeler DS & Amara SG. (2015). Differential regulation of two isoforms of the glial glutamate transporter EAAT2 by DLG1 and CaMKII. *Journal of Neuroscience* **35,** 5260-5270.

Unger T, Lakowa N, Bette S & Engele J. (2012). Transcriptional regulation of the GLAST/EAAT-1 gene in rat and man. *Cell Mol Neurobiol* **32,** 539-547.

Van Wagoner NJ & Benveniste EN. (1999). Interleukin-6 expression and regulation in astrocytes. *J Neuroimmunol* **100,** 124-139.

Van Wagoner NJ, Oh JW, Repovic P & Benveniste EN. (1999). Interleukin-6 (IL-6) production by astrocytes: autocrine regulation by IL-6 and the soluble IL-6 receptor. *J Neurosci* **19,** 5236-5244.

Vance JE. (2012). Dysregulation of cholesterol balance in the brain: contribution to neurodegenerative diseases. *Dis Model Mech* **5,** 746-755.

Vandebroek A & Yasui M. (2020). Regulation of AQP4 in the Central Nervous System. *Int J Mol Sci* **21**.

Vasile F, Dossi E & Rouach N. (2017). Human astrocytes: structure and functions in the healthy brain. *Brain Struct Funct* **222,** 2017-2029.

Vercellino M, Merola A, Piacentino C, Votta B, Capello E, Mancardi GL, Mutani R, Giordana MT & Cavalla P. (2007). Altered glutamate reuptake in relapsing-remitting and secondary progressive multiple sclerosis cortex: correlation with microglia

infiltration, demyelination, and neuronal and synaptic damage. *J Neuropathol Exp Neurol* **66,** 732-739.

Verghese PB, Castellano JM, Garai K, Wang Y, Jiang H, Shah A, Bu G, Frieden C & Holtzman DM. (2013). ApoE influences amyloid-beta (Abeta) clearance despite minimal apoE/Abeta association in physiological conditions. *Proc Natl Acad Sci U S A* **110,** E1807-1816.

Verkhratsky A, Parpura V, Vardjan N & Zorec R. (2019). Physiology of Astroglia. *Adv Exp Med Biol* **1175,** 45-91.

Vinores SA, Derevjanik NL, Mahlow J, Hackett SF, Haller JA, deJuan E, Frankfurter A & Campochiaro PA. (1995). Class III beta-tubulin in human retinal pigment epithelial cells in culture and in epiretinal membranes. *Exp Eye Res* **60,** 385-400.

Volterra A, Trotti D, Cassutti P, Tromba C, Salvaggio A, Melcangi RC & Racagni G. (1992). High sensitivity of glutamate uptake to extracellular free arachidonic acid levels in rat cortical synaptosomes and astrocytes. *Journal of neurochemistry* **59,** 600-606.

von Essen MR, Sondergaard HB, Petersen ERS & Sellebjerg F. (2019). IL-6, IL-12, and IL-23 STAT-Pathway Genetic Risk and Responsiveness of Lymphocytes in Patients with Multiple Sclerosis. *Cells* **8**.

Waak J, Weber SS, Waldenmaier A, Gorner K, Alunni-Fabbroni M, Schell H, Vogt-Weisenhorn D, Pham TT, Reumers V, Baekelandt V, Wurst W & Kahle PJ. (2009). Regulation of astrocyte inflammatory responses by the Parkinson's disease-associated gene DJ-1. *Faseb j* **23,** 2478-2489.

Wahrle SE, Jiang H, Parsadanian M, Legleiter J, Han X, Fryer JD, Kowalewski T & Holtzman DM. (2004). ABCA1 is required for normal central nervous system ApoE levels and for lipidation of astrocyte-secreted apoE. *J Biol Chem* **279,** 40987-40993.

Wakabayashi K, Hayashi S, Yoshimoto M, Kudo H & Takahashi H. (2000). NACP/alpha-synuclein-positive filamentous inclusions in astrocytes and oligodendrocytes of Parkinson's disease brains. *Acta Neuropathol* **99,** 14-20.

Walter S, Letiembre M, Liu Y, Heine H, Penke B, Hao W, Bode B, Manietta N, Walter J, Schulz-Schuffer W & Fassbender K. (2007). Role of the toll-like receptor 4 in neuroinflammation in Alzheimer's disease. *Cell Physiol Biochem* **20,** 947-956.

Walton HS & Dodd PR. (2007). Glutamate-glutamine cycling in Alzheimer's disease. *Neurochem Int* **50,** 1052-1066.

Walz W & Lang MK. (1998). Immunocytochemical evidence for a distinct GFAP-negative subpopulation of astrocytes in the adult rat hippocampus. *Neurosci Lett* **257,** 127-130.

Wan Q, Liu ZY, Yang YP & Liu SM. (2016). Effect of curcumin on inhibiting atherogenesis by down-regulating lipocalin-2 expression in apolipoprotein E knockout mice. *Biomed Mater Eng* **27,** 577-587.

Wang C, Najm R, Xu Q, Jeong DE, Walker D, Balestra ME, Yoon SY, Yuan H, Li G, Miller ZA, Miller BL, Malloy MJ & Huang Y. (2018). Gain of toxic apolipoprotein E4 effects in human iPSC-derived neurons is ameliorated by a small-molecule structure corrector. *Nat Med* **24,** 647-657.

Wang F, Kan M, Xu J, Yan G & McKeehan WL. (1995). Ligand-specific structural domains in the fibroblast growth factor receptor. *J Biol Chem* **270,** 10222-10230.

Wang H, Sui H, Zheng Y, Jiang Y, Shi Y, Liang J & Zhao L. (2019). Curcumin-primed exosomes potently ameliorate cognitive function in AD mice by inhibiting hyperphosphorylation of the Tau protein through the AKT/GSK-3beta pathway. *Nanoscale* **11,** 7481-7496.

Wang JK, Xu H, Li HC & Goldfarb M. (1996). Broadly expressed SNT-like proteins link FGF receptor stimulation to activators of Ras. *Oncogene* **13,** 721-729.

Wang JZ, Xia YY, Grundke-Iqbal I & Iqbal K. (2013). Abnormal hyperphosphorylation of tau: sites, regulation, and molecular mechanism of neurofibrillary degeneration. *J Alzheimers Dis* **33 Suppl 1,** S123-139.

Wang Y, Jin S, Sonobe Y, Cheng Y, Horiuchi H, Parajuli B, Kawanokuchi J, Mizuno T, Takeuchi H & Suzumura A. (2014). Interleukin-1beta induces blood-brain barrier disruption by downregulating Sonic hedgehog in astrocytes. *PLoS One* **9,** e110024.

Wang Z, Pekarskaya O, Bencheikh M, Chao W, Gelbard HA, Ghorpade A, Rothstein JD & Volsky DJ. (2003). Reduced expression of glutamate transporter EAAT2 and impaired glutamate transport in human primary astrocytes exposed to HIV-1 or gp120. *Virology* **312,** 60-73.

Watanabe K, Ueno M, Kamiya D, Nishiyama A, Matsumura M, Wataya T, Takahashi JB, Nishikawa S, Muguruma K & Sasai Y. (2007). A ROCK inhibitor permits survival of dissociated human embryonic stem cells. *Nat Biotechnol* **25,** 681-686.

Webster SJ, Bachstetter AD & Van Eldik LJ. (2013). Comprehensive behavioral characterization of an APP/PS-1 double knock-in mouse model of Alzheimer's disease. *Alzheimers Res Ther* **5,** 28.

Weisgraber KH, Rall SC, Jr. & Mahley RW. (1981). Human E apoprotein heterogeneity. Cysteine-arginine interchanges in the amino acid sequence of the apo-E isoforms. *J Biol Chem* **256,** 9077-9083.

Wells A. (2000). Tumor invasion: role of growth factor-induced cell motility. *Adv Cancer Res* **78,** 31-101.

Werner S, Unsicker K & von Bohlen und Halbach O. (2011). Fibroblast growth factor-2 deficiency causes defects in adult hippocampal neurogenesis, which are not rescued by exogenous fibroblast growth factor-2. *J Neurosci Res* **89,** 1605-1617.

Whiting PF, Wolff RF, Deshpande S, Di Nisio M, Duffy S, Hernandez AV, Keurentjes JC, Lang S, Misso K, Ryder S, Schmidlkofer S, Westwood M & Kleijnen J. (2015). Cannabinoids for Medical Use: A Systematic Review and Meta-analysis. *Jama* **313,** 2456-2473.

Wilsie LC & Orlando RA. (2003). The low density lipoprotein receptor-related protein complexes with cell surface heparan sulfate proteoglycans to regulate proteoglycan-mediated lipoprotein catabolism. *J Biol Chem* **278,** 15758-15764.

Wilson PA & Hemmati-Brivanlou A. (1995). Induction of epidermis and inhibition of neural fate by Bmp-4. *Nature* **376,** 331-333.

Winter CG, Saotome Y, Levison SW & Hirsh D. (1995). A role for ciliary neurotrophic factor as an inducer of reactive gliosis, the glial response to central nervous system injury. *Proc Natl Acad Sci U S A* **92,** 5865-5869.

Wyss MT, Jolivet R, Buck A, Magistretti PJ & Weber B. (2011). In vivo evidence for lactate as a neuronal energy source. *J Neurosci* **31,** 7477-7485.

Xia MQ, Bacskai BJ, Knowles RB, Qin SX & Hyman BT. (2000). Expression of the chemokine receptor CXCR3 on neurons and the elevated expression of its ligand IP-10 in reactive astrocytes: in vitro ERK1/2 activation and role in Alzheimer's disease. *J Neuroimmunol* **108,** 227-235.

Xiao D, Liu X, Zhang M, Zou M, Deng Q, Sun D, Bian X, Cai Y, Guo Y, Liu S, Li S, Shiang E, Zhong H, Cheng L, Xu H, Jin K & Xiang M. (2018). Direct reprogramming of fibroblasts into neural stem cells by single non-neural progenitor transcription factor Ptf1a. *Nat Commun* **9,** 2865.

Xie Z, Morgan TE, Rozovsky I & Finch CE. (2003). Aging and glial responses to lipopolysaccharide in vitro: greater induction of IL-1 and IL-6, but smaller induction of neurotoxicity. *Exp Neurol* **182,** 135-141.

Yamaguchi H, Sugihara S, Ogawa A, Saido TC & Ihara Y. (1998). Diffuse plaques associated with astroglial amyloid beta protein, possibly showing a disappearing stage of senile plaques. *Acta Neuropathol* **95,** 217-222.

Yamamizu K, Iwasaki M, Takakubo H, Sakamoto T, Ikuno T, Miyoshi M, Kondo T, Nakao Y, Nakagawa M, Inoue H & Yamashita JK. (2017). In Vitro Modeling of Blood-Brain Barrier with Human iPSC-Derived Endothelial Cells, Pericytes, Neurons, and Astrocytes via Notch Signaling. *Stem Cell Reports* **8,** 634-647.

Yamanaka K, Chun SJ, Boillee S, Fujimori-Tonou N, Yamashita H, Gutmann DH, Takahashi R, Misawa H & Cleveland DW. (2008). Astrocytes as determinants of disease progression in inherited amyotrophic lateral sclerosis. *Nat Neurosci* **11,** 251-253.

Yan JW, Tan TY & Huang QL. (2013). Protective effect of astrocyte-conditioned medium on neurons following hypoxia and mechanical injury. *Chin J Traumatol* **16,** 3-9.

Yan Y, Song L, Madinya J, Ma T & Li Y. (2018). Derivation of Cortical Spheroids from Human Induced Pluripotent Stem Cells in a Suspension Bioreactor. *Tissue Eng Part A* **24,** 418-431.

Yang H, Zhou J & Lehmann C. (2016a). GPR55 - a putative "type 3" cannabinoid receptor in inflammation. *J Basic Clin Physiol Pharmacol* **27,** 297-302.

Yang HM, Do HJ, Kim DK, Park JK, Chang WK, Chung HM, Choi SY & Kim JH. (2007). Transcriptional regulation of human Oct4 by steroidogenic factor-1. *J Cell Biochem* **101,** 1198-1209.

Yang J, Li S, He XB, Cheng C & Le W. (2016b). Induced pluripotent stem cells in Alzheimer's disease: applications for disease modeling and cell-replacement therapy. *Mol Neurodegener* **11,** 39.

Yang Y, Ge W, Chen Y, Zhang Z, Shen W, Wu C, Poo M & Duan S. (2003). Contribution of astrocytes to hippocampal long-term potentiation through release of D-serine. *Proc Natl Acad Sci U S A* **100,** 15194-15199.

Yao PS, Kang DZ, Lin RY, Ye B, Wang W & Ye ZC. (2014). Glutamate/glutamine metabolism coupling between astrocytes and glioma cells: neuroprotection and inhibition of glioma growth. *Biochem Biophys Res Commun* **450,** 295-299.

Yavarpour-Bali H, Ghasemi-Kasman M & Shojaei A. (2020). Direct reprogramming of terminally differentiated cells into neurons: A novel and promising strategy for Alzheimer's disease treatment. *Prog Neuropsychopharmacol Biol Psychiatry* **98,** 109820.

Ye L, Yang Y, Zhang X, Cai P, Li R, Chen D, Wei X, Xu H, Xiao J, Li X, Lin L & Zhang H. (2015). The Role of bFGF in the Excessive Activation of Astrocytes Is Related to the Inhibition of TLR4/NFkappaB Signals. *Int J Mol Sci* **17**.

Ye Q, Wu Y, Wu J, Zou S, Al-Zaazaai AA, Zhang H, Shi H, Xie L, Liu Y, Xu K, He H, Zhang F, Ji Y, He Y & Xiao J. (2018). Neural Stem Cells Expressing bFGF Reduce Brain Damage and Restore Sensorimotor Function after Neonatal Hypoxia-Ischemia. *Cell Physiol Biochem* **45,** 108-118.

Ye S, Huang Y, Mullendorff K, Dong L, Giedt G, Meng EC, Cohen FE, Kuntz ID, Weisgraber KH & Mahley RW. (2005). Apolipoprotein (apo) E4 enhances amyloid beta peptide production in cultured neuronal cells: apoE structure as a potential therapeutic target. *Proc Natl Acad Sci U S A* **102,** 18700-18705.

Yoon WJ, Won SJ, Ryu BR & Gwag BJ. (2003). Blockade of ionotropic glutamate receptors produces neuronal apoptosis through the Bax-cytochrome C-caspase pathway: the causative role of Ca2+ deficiency. *J Neurochem* **85,** 525-533.

Yoshida M, Saito H & Katsuki H. (1995). Neurotrophic effects of conditioned media of astrocytes isolated from different brain regions on hippocampal and cortical neurons. *Experientia* **51,** 133-136.

Youmans KL, Tai LM, Nwabuisi-Heath E, Jungbauer L, Kanekiyo T, Gan M, Kim J, Eimer WA, Estus S, Rebeck GW, Weeber EJ, Bu G, Yu C & Ladu MJ. (2012). APOE4-specific changes in Abeta accumulation in a new transgenic mouse model of Alzheimer disease. *J Biol Chem* **287,** 41774-41786.

Yu J, Vodyanik MA, Smuga-Otto K, Antosiewicz-Bourget J, Frane JL, Tian S, Nie J, Jonsdottir GA, Ruotti V, Stewart R, Slukvin, II & Thomson JA. (2007). Induced pluripotent stem cell lines derived from human somatic cells. *Science* **318,** 1917-1920.

Zadeh JK, Zhutdieva MB, Laspas P, Yuksel C, Musayeva A, Pfeiffer N, Brochhausen C, Oelze M, Daiber A, Xia N, Li H & Gericke A. (2019). Apolipoprotein E Deficiency Causes Endothelial Dysfunction in the Mouse Retina. *Oxid Med Cell Longev* **2019,** 5181429.

Zaheer A, Zaheer S, Sahu SK, Knight S, Khosravi H, Mathur SN & Lim R. (2007). A novel role of glia maturation factor: induction of granulocyte-macrophage colony-stimulating factor and pro-inflammatory cytokines. *J Neurochem* **101,** 364-376.

Zamanian JL, Xu L, Foo LC, Nouri N, Zhou L, Giffard RG & Barres BA. (2012). Genomic analysis of reactive astrogliosis. *J Neurosci* **32,** 6391-6410.

Zerangue N, Arriza JL, Amara SG & Kavanaugh MP. (1995). Differential modulation of human glutamate transporter subtypes by arachidonic acid. *Journal of Biological Chemistry* **270,** 6433-6435.

Zhang B, Gaiteri C, Bodea LG, Wang Z, McElwee J, Podtelezhnikov AA, Zhang C, Xie T, Tran L, Dobrin R, Fluder E, Clurman B, Melquist S, Narayanan M, Suver C, Shah H, Mahajan M, Gillis T, Mysore J, MacDonald ME, Lamb JR, Bennett DA, Molony C, Stone DJ, Gudnason V, Myers AJ, Schadt EE, Neumann H, Zhu J & Emilsson V. (2013). Integrated systems approach identifies genetic nodes and networks in late-onset Alzheimer's disease. *Cell* **153,** 707-720.

Zhang M, Wang C, Wu J, Ha X, Deng Y, Zhang X, Wang J, Chen K, Feng J, Zhu J, Xie J & Zhang J. (2018a). The Effect and Mechanism of KLF7 in the TLR4/NF-kappaB/IL-6 Inflammatory Signal Pathway of Adipocytes. *Mediators Inflamm* **2018,** 1756494.

Zhang P, Andrianakos R, Yang Y, Liu C & Lu W. (2010). Kruppel-like factor 4 (Klf4) prevents embryonic stem (ES) cell differentiation by regulating Nanog gene expression. *J Biol Chem* **285,** 9180-9189.

Zhang SC, Barclay C, Alexander LA, Geldenhuys L, Porter GA, Casson AG & Murphy PR. (2007). Alternative splicing of the FGF antisense gene: differential subcellular localization in human tissues and esophageal adenocarcinoma. *J Mol Med (Berl)* **85,** 1215-1228.

Zhang W, Jiao B, Zhou M, Zhou T & Shen L. (2016a). Modeling Alzheimer's Disease with Induced Pluripotent Stem Cells: Current Challenges and Future Concerns. *Stem Cells Int* **2016,** 7828049.

Zhang X, Lao K, Qiu Z, Rahman MS, Zhang Y & Gou X. (2019). Potential Astrocytic Receptors and Transporters in the Pathogenesis of Alzheimer's Disease. *J Alzheimers Dis* **67,** 1109-1122.

Zhang X, Wan JQ & Tong XP. (2018b). Potassium channel dysfunction in neurons and astrocytes in Huntington's disease. *CNS Neurosci Ther*.

Zhang X, Zhang J, Wang T, Esteban MA & Pei D. (2008). Esrrb activates Oct4 transcription and sustains self-renewal and pluripotency in embryonic stem cells. *J Biol Chem* **283,** 35825-35833.

Zhang Y, Chen K, Sloan SA, Bennett ML, Scholze AR, O'Keeffe S, Phatnani HP, Guarnieri P, Caneda C, Ruderisch N, Deng S, Liddelow SA, Zhang C, Daneman R, Maniatis T, Barres BA & Wu JQ. (2014). An RNA-sequencing transcriptome and splicing database of glia, neurons, and vascular cells of the cerebral cortex. *J Neurosci* **34,** 11929-11947.

Zhang Y, Li P, Feng J & Wu M. (2016b). Dysfunction of NMDA receptors in Alzheimer's disease. *Neurol Sci* **37,** 1039-1047.

Zhang Y, Sloan SA, Clarke LE, Caneda C, Plaza CA, Blumenthal PD, Vogel H, Steinberg GK, Edwards MS, Li G, Duncan JA, 3rd, Cheshier SH, Shuer LM, Chang EF, Grant GA, Gephart MG & Barres BA. (2016c). Purification and Characterization of Progenitor and Mature Human Astrocytes Reveals Transcriptional and Functional Differences with Mouse. *Neuron* **89,** 37-53.

Zhao J, Davis MD, Martens YA, Shinohara M, Graff-Radford NR, Younkin SG, Wszolek ZK, Kanekiyo T & Bu G. (2017). APOE epsilon4/epsilon4 diminishes neurotrophic function of human iPSC-derived astrocytes. *Hum Mol Genet* **26,** 2690-2700.

Zhao N, Liu CC, Qiao W & Bu G. (2018). Apolipoprotein E, Receptors, and Modulation of Alzheimer's Disease. *Biol Psychiatry* **83,** 347-357.

Zhao T, Zhang ZN, Rong Z & Xu Y. (2011). Immunogenicity of induced pluripotent stem cells. *Nature* **474,** 212-215.

Zhou J & Sutherland ML. (2004). Glutamate transporter cluster formation in astrocytic processes regulates glutamate uptake activity. *J Neurosci* **24,** 6301-6306.

Zhu Y, Nwabuisi-Heath E, Dumanis SB, Tai LM, Yu C, Rebeck GW & LaDu MJ. (2012). APOE genotype alters glial activation and loss of synaptic markers in mice. *Glia* **60,** 559-569.

Zoltowska KM, Maesako M, Meier J & Berezovska O. (2018). Novel interaction between Alzheimer's disease-related protein presenilin 1 and glutamate transporter 1. *Sci Rep* **8,** 8718.

Zou LH, Shi YJ, He H, Jiang SM, Huo FF, Wang XM, Wu F & Ma L. (2019). Effects of FGF2/FGFR1 Pathway on Expression of A1 Astrocytes After Infrasound Exposure. *Front Neurosci* **13,** 429.

Zuliani G, Ranzini M, Guerra G, Rossi L, Munari MR, Zurlo A, Volpato S, Atti AR, Ble A & Fellin R. (2007). Plasma cytokines profile in older subjects with late onset Alzheimer's disease or vascular dementia. *J Psychiatr Res* **41,** 686-693.